Introduction to

Engineering Mechanics

A Continuum Approach

Second Edition

Jenn Stroud Rossmann
Clive L. Dym
Lori Bassman

CRC Press
Taylor & Francis Group

Introduction to
Engineering Mechanics

A Continuum Approach

Second Edition

Introduction to
Engineering
Mechanics

A Continuum Approach

Second Edition

Jenn Stroud Rossmann
Clive L. Dym
Lori Bassman

Contents

Preface

> If science teaches us anything, it's to accept our failures, as well as our successes, with quiet dignity and grace.
>
> **Gene Wilder**,
> *Young Frankenstein, 1974*

This book is intended to provide a unified introduction to solid and fluid mechanics, and to convey the underlying principles of continuum mechanics to undergraduates. We assume that the students using this book have taken courses in calculus, physics, and vector analysis. By demonstrating both the connections and the distinctions between solid and fluid mechanics, this book will prepare students for further study in either field or in fields such as bioengineering that blur traditional disciplinary boundaries.

The use of a continuum approach to make connections between solid and fluid mechanics is typically provided only to advanced undergraduates and graduate students. This book *introduces* the concepts of stress and strain in the continuum context, showing the relationships between solid and fluid behavior and the mathematics that describe them. It is an introductory textbook in strength of materials and in fluid mechanics and also includes the mathematical connective tissue between these fields. We have decided to begin with the aha! of continuum mechanics rather than requiring students to wait for it.

This approach was first developed for a sophomore-level course called Continuum Mechanics at Harvey Mudd College (HMC). The broad, unspecialized engineering program at HMC requires that faculty developing the curriculum ask themselves, What specific knowledge is essential for an engineer who may practice, or continue study, in one of a wide variety of fields? This course was our answer to the question, What *engineering mechanics* knowledge is essential for a broadly educated engineer?

An engineer of any type, we felt, should have an understanding of how materials respond to loading: how solids deform and incur stress and how fluids flow. We conceived of a spectrum of material behavior, with the idealizations of Hookean solids and Newtonian fluids at the extremes. Most modern engineering materials—biological materials, for example—lie between these two extremes, and we believe that students who are aware of the entire spectrum from their first introduction to engineering mechanics will be well prepared to understand this complex middle ground of nonlinearity and viscoelasticity.

Our integrated introduction to the mechanics of solids and fluids has evolved. As initially taught by Clive L. Dym, the HMC course emphasized the underlying principles from a mathematical, applied mechanics perspective. This focus on the structure of elasticity problems made it difficult for students to relate formulation to applications. In subsequent offerings, Jenn Stroud Rossmann chose to embed continuum concepts and mathematics into introductory problems and to build the strain and stress tensors gradually. We now establish a "continuum checklist"—compatibility [kinematics of deformation], constitutive law relating deformation to stress, and equilibrium—that we return repeatedly.

This checklist provides a framework for a wide variety of problems in solid and fluid mechanics.

We have found this approach effective at Harvey Mudd and Lafayette Colleges and were gratified by the adoption of the first edition at a wide variety of institutions. For the second edition, we have persuaded our colleague and friend Lori Bassman, who has taught the HMC course for 10 years, to join us as a coauthor, and her perspective has improved many aspects of the book. Bassman's enthusiasm for real-world applications, from plant biomechanics to the material behavior of candy, enriched the relevance of our approach, and readers may soon learn to recognize which of the examples and problems here bear her hallmarks of elegance and fun.

We make the necessary definitions and present the template for our continuum approach in Chapter 1. In Chapter 2, we introduce strain and stress in one dimension, develop a constitutive law, and apply these concepts to the simple case of an axially loaded bar. In Chapter 4, we extend these concepts to higher dimensions by introducing the Poisson's ratio and strain and stress tensors. In Chapters 5 through 11 we apply our continuum sense of solid mechanics to problems including torsion, pressure vessels, beams, and columns. In Chapter 13, we make connections between solid and fluid mechanics, introducing properties of fluids and strain *rate* tensor. Chapter 16 addresses fluid statics. Applications in fluid mechanics are considered in Chapters 18 and 20. We develop the governing equations in both control volume and differential forms. In Chapter 22, we see that the equations for solid *dynamics* strongly resemble the ones, what we have used to study fluid dynamics. Throughout, we emphasize real-world design applications. We maintain a continuum "big picture" approach, tempered with worked examples, problems, and a set of case studies. The second edition significantly includes more of these examples, problems, and case studies than the first edition.

The 10 case studies included in this book (an increase from the six in the first edition) illustrate important applications of the concepts. In some cases, students' knowledge with understanding of solid and fluid mechanics will help them to understand what went wrong in famous failures; in others, students will see how the textbook theories can be extended and applied in other fields, such as bioengineering. The essence of continuum mechanics, the internal response of materials to external loading, is often obscured by the complex mathematics of its formulation. By gradually building the formulations from one-dimensional to two- and three-dimensional, and by including these illustrative real-world case studies, we hope to help students develop physical intuition for solid and fluid behavior.

We have written this book for our students, and we hope that reading this book is very much like sitting in our classes. We have tried to keep the tone conversational, and we have included many asides that describe the historical context for the ideas we describe and hints at how some concepts may become even more useful later on.

Authors

Jenn Stroud Rossmann is an associate professor of mechanical engineering at Lafayette College. She earned a BS and PhD at the University of California, Berkeley. Her research interests include the study of blood flow in vessels affected by atherosclerosis and aneurysms. She has a strong commitment to teaching engineering methods and values to non-engineers, and she has developed several courses and workshops for liberal arts majors.

Clive L. Dym served as a Fletcher Jones Professor of Engineering Design for 21 years, and is now Professor Emeritus of Engineering, at Harvey Mudd College. He earned a BS at Cooper Union and a PhD at Stanford University. His primary interests are in engineering design and structural mechanics. He is the author of eighteen books and has edited eleven others; his two most recent books are *Engineering Design: A Project-Based Introduction* (with Patrick Little and Elizabeth Orwin), 4th Edition, John Wiley, 2013; and *Analytical Estimates of Structural Behavior* (with Harry Williams), CRC Press, 2012. Among his awards are the Merryfield Design Award (ASEE, 2002), the Spira Outstanding Design Educator Award (ASME, 2004), and the Gordon Prize (NAE, 2012). He is a Fellow of the ASCE, ASME, and ASEE.

Lori Bassman is a professor of engineering and a director of the Laspa Fellowship Program in applied mechanics at Harvey Mudd College. She earned a BSE at Princeton University and a PhD at Stanford. Through a visiting appointment at the University of New South Wales in Australia, she pursues her research in physical metallurgy, and her other research interests include computational modeling of bird flight biomechanics.

1

Introduction

Mechanics is the study of the motion or equilibrium of matter and the forces that cause such motion or equilibrium. We are generally familiar with the sort of "billiard ball" mechanics formulated in physics courses; for example, when two such billiard balls collide, applying Newton's second law would help us to calculate the velocities of both balls after the collision. *Engineering mechanics* asks that we also consider how the impact will affect the balls: Will they deform or even crack? How many such collisions can they sustain? How does the material chosen for their construction affect both these answers? What design decisions will optimize the strength, cost, or other properties of the balls?

Recall that in our first set of examinations of billiard balls collision, we assumed that they were absolutely rigid, that is, undeformable. Now we will take a *continuum* approach to engineering mechanics: we want to consider what is going on inside the billiard balls if we recognize that they are not rigid. We want to quantify the *internal response* to external loading.

In this book, we will introduce the mechanics of both solids and fluids and will emphasize both distinctions and connections between these fields. We will see that the material behaviors of ideal solids and fluids are at the far ends of a *spectrum* of material behavior and that many materials of interest to modern engineers—particularly biomaterials—lie between these two extremes, combining elements of both "solid" and "fluid" behavior.

Our objectives are to learn how to formulate problems in mechanics and how to reduce vague questions and ideas into precise mathematical statements. The floor of a building may be strong enough to support us, our furniture, and even the occasional fatiguing dance party without collapsing, but if not designed carefully, the floor may deflect considerably and sag. By learning how to predict the effects of forces, stresses, and strains, we will become better designers and better engineers.

1.1 A Motivating Example: Remodeling an Underwater Structure

Underwater rigs, such as the one shown in Figure 1.1, are commonly used by the petroleum industry to harvest offshore oil. Over the life of a structure, many sea creatures and plants attach themselves to the rig's supporting structures. When wells have dried up, the underwater structures can be removed in manageable segments and towed to shore. However, this process results in the loss of both the reef dwellers attached to the platform's trusses and the larger fish who feed there. Corporations often abandon their rigs rather than incur the financial and environmental expense of removal. An engineering firm would like to make use of a decommissioned rig by redesigning it to serve as an artificial reef that would provide a hospitable sea habitat. This firm must find ways to strengthen the supports and to affix the reef components to sustain the sea life.

South pass   Block 77
"D" structure

Water depth 180′
No. of well slots 24

Approx. steel weight		(tons)
Jacket	=	3400
Piling	=	4100
Decks	=	900
Total	=	8400

Waterline

Mudline

84″ O.D. piling

144″ O.D. piling

12–24″ O.D. conductors
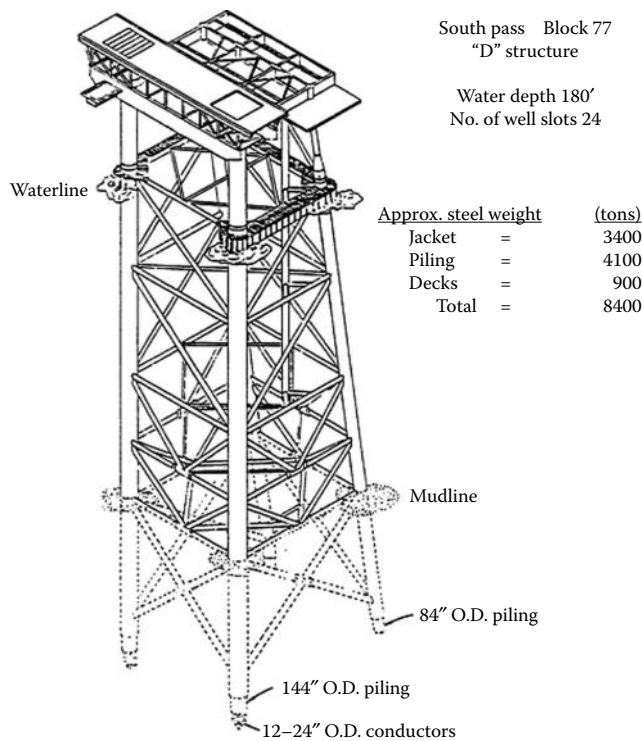
FIGURE 1.1
Mud-slide-type platform. (From the Committee on Techniques for Removing Fixed Offshore Structures and the Marine Board Commission on Engineering and Technical Systems, National Research Council, *An Assessment of Techniques for Removing Offshore Structures*, Washington, DC: National Academy Press, 1996. With permission.)

The rig support structure was initially designed to support the drilling platform above the water level. As the oil drill itself was mobile, the structure was built so that it could remain balanced, without listing, under dynamic loading. In its new life as the support for an artificial reef, this structure must continue to withstand the weight of the platform and the changing loads of wind and sea currents, and it must also support the additional loading of concrete "reef balls" and other reef-mimicking assemblies (Figure 1.2), as well as the weight of the reef dwellers.

To remodel the underwater rig, a team of engineers must dive below the water surface to attach the necessary reef balls and other attachments. The reef balls themselves may be lowered using a crane. A conceptualization of this is shown in Figure 1.3.

Among the factors that must be considered in the redesign process are the structural performance of the modified structure and its ability to withstand the required loading. An additional challenge to the engineering firm is the undersea location of the structure. What materials should be chosen so that the structure remains sound? How should the additional supports and reef assemblies be added? What precautions must engineers and fabricators take when they work underwater? What effects will the exposure to the ocean environment have on their structure, equipment, and bodies? We address many of these issues in this book. Throughout, we return to this problem to demonstrate the utility of various theoretical results, and we rely on first principles that look familiar.

FIGURE 1.2
Concrete reef ball. (Courtesy of the Reef Ball Foundation, Athens, GA. With permission.)
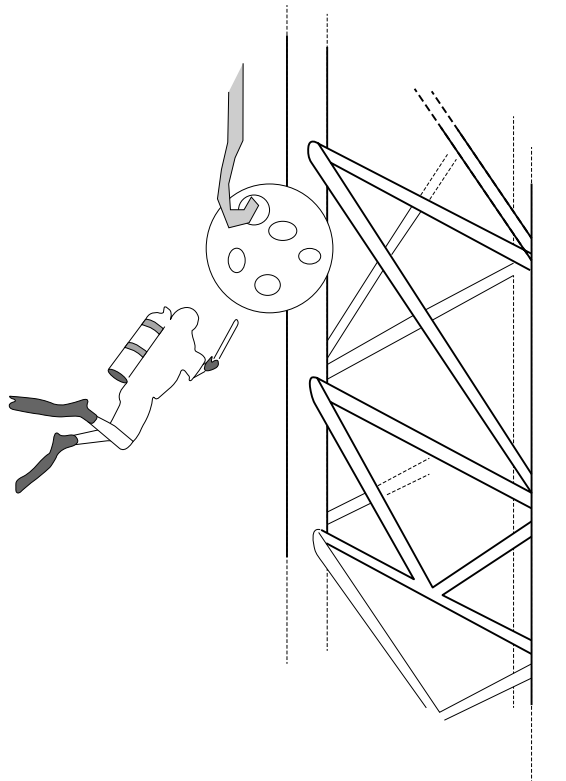
FIGURE 1.3
Rendering of scuba diver at work remodeling underwater rig structure.

1.2 Newton's Laws: The First Principles of Mechanics

Newton's laws provide us with the *first principles* that, along with conservation equations, guide the work we do in continuum mechanics. These laws were formulated by Sir Isaac Newton (1642–1727), based on his own experimental work and on the observations of

others, including Galileo Galilei (1564–1642). Many of the equations we use in problem solving are directly descended from Newton's elegant statements, which are expressed as follows:

Newton's first law: A body remains at rest or moves in a straight line with a constant velocity if there is no unbalanced force acting on it.

Newton's second law: The time rate of change of momentum of a body is equal to (and in the same direction as) the resultant of the forces acting on it:

$$\sum \mathbf{F} = \frac{d}{dt}(m\,\mathbf{V}).$$ (1.1)

When the mass of the body of interest is constant, this has the form

$$\sum \mathbf{F} = m\,\mathbf{a}.$$ (1.2)

When $\mathbf{a} = 0$, we have

$$\sum \mathbf{F} = \mathbf{0}.$$ (1.3)

The class of problems governed by Equation 1.3 is called *statics*.

Newton's third law: To every action, there is an equal and opposite reaction. That is, the forces of action and reaction between the interacting bodies are equal in magnitude and exactly opposite in direction.

Forces always occur, according to Newton's third law, in pairs of equal and opposite forces. The downward force exerted on the desk by the pencil is accompanied by an upward force of equal magnitude exerted on the pencil by the desk.

1.3 Equilibrium

We have alluded to the concept of equilibrium (also known as *static* equilibrium) in our discussion of Newton's second law. To be in equilibrium, a three-dimensional object must satisfy six equations. In Cartesian coordinates, these are as follows:

$$\sum F_x = 0,$$
$$\sum F_y = 0,$$ (1.4a)
$$\sum F_z = 0,$$
$$\sum M_x = 0,$$
$$\sum M_y = 0,$$ (1.4b)
$$\sum M_z = 0.$$

These equations can be written more concisely in the vector form as

$$\sum \mathbf{F} = \mathbf{0}, \tag{1.5}$$

$$\sum \mathbf{M} = \mathbf{0}, \tag{1.6}$$

and represent the statements "the sum of forces equals zero" and "the sum of moments equals zero." One advantage of writing these equations in the vector form is that we do not have to specify a coordinate system.

For planar (two-dimensional) situations or models, equilibrium requires the satisfaction of only three equations, typically in the xy-plane:

$$\sum F_x = 0, \tag{1.7a}$$

$$\sum F_y = 0, \tag{1.7b}$$

$$\sum M_z = 0. \tag{1.7c}$$

These equations essentially state that the object is neither translating (in the x- or y-directions) nor rotating (about the z-axis) in the xy-plane as a result of applied forces.

It is useful to distinguish between forces that act externally and those that act internally. *External* loads are applied to a structure by, for example, gravity or wind. Reaction forces are also external: They occur at supports and at points where the structure is prevented from moving in response to the external loads. These supports may be surfaces, rollers, or hinges that restrict both deflections and rotations. Internal forces, on the other hand, result from the applied external loads and are what we are concerned with when we study continuum mechanics. These are forces that act within a body as a result of all external forces. Chapter 2 shows how the principle of equilibrium helps us calculate these internal forces.

1.4 Definition of a Continuum

In elementary physics, we concerned ourselves with particles and bodies that behaved like inert, rigid billiard balls: bouncing off each other and interacting without deformation or other changes. In continuum mechanics, we consider the effects of deformation, of internal forces within bodies, to obtain a fuller sense of how bodies react to external forces.

We would like to be able to consider these bodies as whole entities and not have to account for each individual particle composing each body. It would be much more convenient for us to treat the properties (e.g., density, momentum, forces) of such bodies as continuous functions. We may do this if the body in question is modeled as a *continuum*.

We may treat a body as a continuum if we believe that the ensemble of particles making up the body—in other words, the body as a whole—acts like a continuum, that is, more like a single body than a lot of independent bodies. We may then consider average or *bulk* properties of the body and may ignore the details of any individual particle dynamics. This means that when we assume or model a body as a continuum and then look at a very small chunk of the body, that chunk will have the same properties (e.g., density) as the rest of the body.
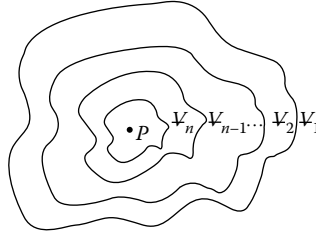
FIGURE 1.4
Volumes $\mathcal{V}_i$ surrounding a point P.

Mathematically, we define a continuum as a continuous distribution of matter in space and time. For a mass m_n contained in a small volume of space $\mathcal{V}_n$, surrounding a point P, as in Figure 1.4, we can define a mass density ρ:

$$\rho(P) = \lim_{\substack{n \to \infty \\ \mathcal{V}_n \to 0}} \frac{m_n}{\mathcal{V}_n}. \tag{1.8}$$

So, a material continuum is a material for which density (of mass, momentum, or energy) exists in a mathematical sense. We define its properties as continuous functions and neglect what is happening on the microscopic, molecular level in favor of the macroscopic, bulk behaviors.

Note that materials will not satisfy this equation if $\mathcal{V}_n$ truly goes to zero. If the volume goes to zero, it will not have a chance to enclose any atoms—so naturally, the density will be undefined. Yet we still think of these materials as continua. So physically, our definition of a continuum is a material for which

$$\left| \rho - \frac{m_n}{\mathcal{V}_n} \right| < \varepsilon \quad \text{as } n \to \infty. \tag{1.9}$$

Here, ε represents a *very* small number approaching zero, indicating that the mathematical definition of density approaches a usable value ρ.

Sometimes, it is easier to get a grasp on what is not a continuum than on what is. Almost all solids satisfy the definition handily, in part because the intermolecular forces are greater in solids and solids are generally denser than fluids. Because fluids can be liquids or gases, it is harder to pin down a "density" when the molecules get sparse and the intermolecular forces are much smaller. It would surely be a stretch of our definition of a continuum to apply it to interstellar space, for example, where the objects of interest (planets and asteroids, for example) are not much farther apart than the molecules of the interstellar medium. Fortunately, there is another test for continuity, and it is especially applicable to fluids.

That additional test is expressed in terms of the dimensionless Knudsen* number, *Kn*:

$$Kn = \frac{\lambda}{L}. \tag{1.10}$$

---

* The Knudsen number is named after Martin Hans Christian Knudsen (1871–1949), Professor at the University of Copenhagen and author of *The Kinetic Theory of Gases* (London, 1934). In physical gas dynamics, the Knudsen number defines the extent to which a gas behaves like a collection of independent particles ($Kn \gg 1$) or like a viscous fluid ($Kn \ll 1$).

Here L is a problem-specific characteristic length, such as a diameter or width, and λ is the material's mean free path, or average distance between particle collisions, which is calculated as

$$\lambda = 0.225 \frac{m}{\rho d^2}, \tag{1.11}$$

where m is the mass of a particle, ρ is its density, and d is the effective diameter of the particle. We would then say that a fluid, be it a liquid or a gas, may be called a *continuum* if its *Kn* is less than 0.1.

For example, for air $m = 4.8 \times 10^{-26}$ kg, $d = 3.7 \times 10^{-10}$ m, and at atmospheric conditions λ is approximately 6×10^{-6} cm; at an altitude of 100 km, it is 10 cm; and at 160 km, it is 5000 cm. In order for the Knudsen number to justify the continuum assumption, our length scales of interest (e.g., the diameter of a baseball, or the wing chord length of an aircraft or spacecraft) must be more than 10 times greater than these mean free paths. So at higher altitudes, the continuum assumption is unacceptable and the molecular dynamics must be considered in the governing equations.

The ease with which we can define density, and thus continuity, is not the only difference between solids and fluids. A *solid* is a three-dimensional continuum that supports both tensile and shear forces and stresses. The atoms making up a solid have a fixed spatial arrangement—often a crystal lattice structure—in which atoms are able to vibrate and spin and their electrons can fly and dance around, but the internal structure is basically fixed. Because of this, although it is possible to distort or destroy the shape taken by a solid, it is generally said that a solid object retains its own shape. For solids, we will be able to relate *stresses* (the internal distribution of forces over areas, resulting from external forces on the body) to *strains* (the descriptors of the resulting changes in lengths and angles in the body) by a *constitutive law* (containing material constants that reflect the interatomic or intra-molecular forces binding the atoms into the solid).

A *fluid*, be it a liquid or a gas, cannot support a shear force: Under the slightest shearing force, a fluid will flow or deform continuously. We see that when liquids assume the shapes of their containers, and when gases expand to fill their containers. This is because the interatomic or intramolecular forces in a fluid are not spatially constrained like those in a solid. Also, a fluid typically cannot support tensile forces or stresses. For fluids, we will be able to relate stresses to *strain rates* (the time rate of change of the strains) by a constitutive law.

We note that the distinction between solid and fluid behavior is not always clear-cut; there are classes of materials whose behavior situates them in a sort of middle ground. We explore this middle ground further in Chapter 14. The existence of this middle ground provides us with more motivation to understand the broad field of continuum mechanics and the connections between solid and fluid behavior.

In this text, we are interested in how Newton's laws apply to continua. Some of the relevant consequences of Newton's laws, which we discuss in more detail later, are as follows:

Momentum is always conserved, in both solids and fluids. *Equilibrium* equations (see Section 1.3) are mathematical expressions of the conservation of momentum.

Equilibrium must apply both to entire bodies *and* to sections of, or particles within, those bodies. This is one of the reasons why free-body diagrams (FBDs) are so valuable: They illustrate the equilibrium of a section of a larger body or system. This is also why we will introduce control volumes to analyze fluid flows.

Mass is conserved.

Area is a *vector* because it has both a magnitude (size) and a direction that is defined by a unit vector normal to the area. That unit normal vector is designated as positive when it is directed outward from the free body or section of interest.

Forces produce changes in shape and geometry, which we will characterize in terms of *strains* for solids and *strain rates* for fluids.

In the real world, material objects are subjected to *body* forces (e.g., gravitational and electromagnetic forces), which do not require direct contact, and *surface* forces (e.g., atmospheric pressure, wind and rain, burdens to be carried), which do. We want to know how the material in the body reacts to external forces. To do this, we will need to (1) characterize the deformation of a continuous material, (2) define the internal loading, (3) relate this to the body's deformation, and (4) make sure that the body is in equilibrium. This is what continuum mechanics is all about.

1.5 Some Mathematical Basics: Scalars and Vectors

The familiar distinction between scalars and vectors is that a vector, unlike a scalar, has direction as well as magnitude. Examples of scalar quantities include time, volume, density, speed, energy, and mass. Velocity, acceleration, force, and momentum are vectors and thus contain additional directional information. We denote vectors with a bold font. Unit vectors are indicated with hats, as in the following equations.

A vector $\mathbf{V}$ may be expressed mathematically by multiplying its magnitude, V, by a unit vector $\hat{\mathbf{n}}$ (i.e., $|\hat{\mathbf{n}}| = 1$), where the direction of $\hat{\mathbf{n}}$ coincides with that of $\mathbf{V}$:

$$\mathbf{V} = V\hat{\mathbf{n}}. \tag{1.12}$$

We may also write a vector $\mathbf{V}$ in terms of its components along the primary directions, whether these are the Cartesian (x, y, z) directions or cylindrical (r, θ, z) or another set. In Cartesian coordinates, the vector is simply written as

$$\mathbf{V} = V_x\hat{\mathbf{i}} + V_y\hat{\mathbf{j}} + V_z\hat{\mathbf{k}}, \tag{1.13}$$

based on a situation like that shown in Figure 1.5. In general, in coordinates (x_1, x_2, x_3) with unit vectors $\hat{\mathbf{e}}_1, \hat{\mathbf{e}}_2, \hat{\mathbf{e}}_3$, we will be able to write any vector $\mathbf{V}$ as

$$\mathbf{V} = V_1\hat{\mathbf{e}}_1 + V_2\hat{\mathbf{e}}_2 + V_3\hat{\mathbf{e}}_3, \tag{1.14}$$

or as the triplet (V_1, V_2, V_3) that is called a column vector in linear algebra.* We recall that the magnitude of $\mathbf{V}$ can be obtained as

$$V = |\mathbf{V}| = \sqrt{V_1^2 + V_2^2 + V_3^2}, \tag{1.15}$$

so $V = 0$ if, and only if, $V_1 = V_2 = V_3 = 0$.

---

* We have written the column vector of components of $\mathbf{V}$ as a row vector to save space.
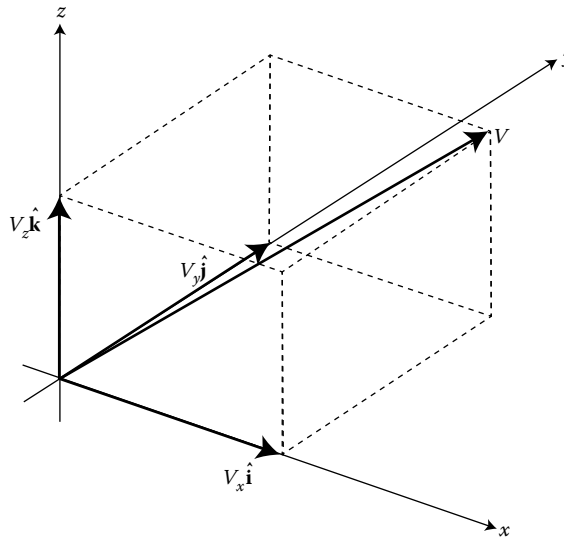
FIGURE 1.5
Decomposition of vector $\mathbf{V}$ in x, y, z coordinates.

The calculated scalar (dot) and vector (cross) products are also of interest. Remember that the result of taking a dot product between two vectors is a *scalar* and that the result of a cross product is a *vector*. Thus,

$$\mathbf{u} \cdot \mathbf{v} = |\mathbf{u}||\mathbf{v}| \cos \theta, \tag{1.16}$$

where θ is the angle between vectors $\mathbf{u}$ and $\mathbf{v}$, and $0 \leq \theta \leq \pi$. (Remember that two intersecting lines form a plane and that θ is the angle between the two lines.) In terms of components,

$$\mathbf{u} = u_1 \hat{\mathbf{e}}_1 + u_2 \hat{\mathbf{e}}_2 + u_3 \hat{\mathbf{e}}_3, \tag{1.17}$$

$$\mathbf{v} = v_1 \hat{\mathbf{e}}_1 + v_2 \hat{\mathbf{e}}_2 + v_3 \hat{\mathbf{e}}_3, \tag{1.18}$$

$$\mathbf{u} \cdot \mathbf{v} = u_1 v_1 + u_2 v_2 + u_3 v_3. \tag{1.19}$$

The cross product results in a vector that is perpendicular to both $\mathbf{u}$ and $\mathbf{v}$:

$$\mathbf{u} \times \mathbf{v} = \mathbf{w}, \tag{1.20}$$

where

$$\mathbf{w} = \hat{\mathbf{n}}|\mathbf{u}||\mathbf{v}| \sin \theta, \tag{1.21}$$

with unit vector $\hat{\mathbf{n}}$ being in the direction perpendicular to both $\mathbf{u}$ and $\mathbf{v}$, and

$$\mathbf{u} \times \mathbf{v} = (u_2 v_3 - u_3 v_2)\hat{\mathbf{e}}_1 + (u_3 v_1 - u_1 v_3)\hat{\mathbf{e}}_2 + (u_1 v_2 - u_2 v_1)\hat{\mathbf{e}}_3 . \tag{1.22}$$

We notice that this has the form of a determinant:

$$\mathbf{u} \times \mathbf{v} = \begin{vmatrix} \hat{\mathbf{e}}_1 & \hat{\mathbf{e}}_2 & \hat{\mathbf{e}}_3 \\ u_1 & u_2 & u_3 \\ v_1 & v_2 & v_3 \end{vmatrix}. \tag{1.23}$$

When we work with vectors, we may find ourselves getting stuck carrying around a lot of variables distinguished by their various subscripts: $x_1, x_2, \ldots, x_n$. This can become unwieldy, and so we use a shortcut known as *index notation*. Using this shortcut, we write those variables as x_i, $i = 1, 2, \ldots, n$, and call i the *index*. For example, the vectors in Equations 1.17 and 1.18 can be written as

$$\mathbf{u} = \sum_{i=1}^{3} u_i \hat{\mathbf{e}}_i \quad \text{and} \quad \mathbf{v} = \sum_{j=1}^{3} v_j \hat{\mathbf{e}}_j. \tag{1.24}$$

We may further simplify life by introducing a very efficient shortcut known as the *summation convention*: The repetition of the index (or subscript) represents summation with respect to that index over its range, which in our continuum mechanics work will always be 1 to 3 and thus will not require specification. Using index notation and the summation convention, we can rewrite Equation 1.24 as

$$\mathbf{u} = u_i \hat{\mathbf{e}}_i \quad \text{and} \quad \mathbf{v} = v_j \hat{\mathbf{e}}_j. \tag{1.25}$$

Note that in Equation 1.25, we have used different letters for the repeated subscripts. In fact, the repeated subscripts in the summation are often referred to as dummy variables because it does not matter whether we call them i or j or k, or a or b or c. The reason that we have used different dummy variables in Equation 1.25 is that we frequently confront situations where there may be more than one dummy variable. For example, how would we express the scalar (dot) product in Equation 1.19? If we were to spell out all the details, we would start with Equation 1.24 and first write that

$$\mathbf{u} \cdot \mathbf{v} = \sum_{i=1}^{3} u_i \hat{\mathbf{e}}_i \cdot \sum_{j=1}^{3} v_j \hat{\mathbf{e}}_j = u_i \hat{\mathbf{e}}_i \cdot v_j \hat{\mathbf{e}}_j = u_i v_j \left(\hat{\mathbf{e}}_i \cdot \hat{\mathbf{e}}_j \right). \tag{1.26}$$

We invoked the summation convention twice, once for each of the two dummy variables i and j, and then we appropriately re-ordered the respective scalar and vector components. To further clarify the right-most term of Equation 1.26, we expand the summation terms to make them explicit while noting that $\hat{\mathbf{e}}_i \cdot \hat{\mathbf{e}}_j = 0$ for $i \neq j$ assuming the unit vectors form an orthogonal set. Then of nine terms, three remain:

$$u_i v_j \left(\hat{\mathbf{e}}_i \cdot \hat{\mathbf{e}}_j \right) = u_1 v_1 \left(\hat{\mathbf{e}}_1 \cdot \hat{\mathbf{e}}_1 \right) + u_2 v_2 \left(\hat{\mathbf{e}}_2 \cdot \hat{\mathbf{e}}_2 \right) + u_3 v_3 \left(\hat{\mathbf{e}}_3 \cdot \hat{\mathbf{e}}_3 \right). \tag{1.27}$$

Now $\hat{\mathbf{e}}_i \cdot \hat{\mathbf{e}}_j = 1$ for $i = j$, that is, $\left(\hat{\mathbf{e}}_1 \cdot \hat{\mathbf{e}}_1 \right) = \left(\hat{\mathbf{e}}_2 \cdot \hat{\mathbf{e}}_2 \right) = \left(\hat{\mathbf{e}}_3 \cdot \hat{\mathbf{e}}_3 \right) = 1$. Thus, we can combine Equations 1.26 and 1.27 to find that

$$\mathbf{u} \cdot \mathbf{v} = u_i v_j \left(\hat{\mathbf{e}}_i \cdot \hat{\mathbf{e}}_j \right) = u_1 v_1 + u_2 v_2 + u_3 v_3 = u_i v_i. \tag{1.28}$$

There are a couple more pieces of shorthand notation that we will use later on, but can introduce now. We have noted that $\hat{\mathbf{e}}_i \cdot \hat{\mathbf{e}}_j = 1$ for $i = j$ and $\hat{\mathbf{e}}_i \cdot \hat{\mathbf{e}}_j = 0$ for $i \neq j$. We now define the Kronecker delta as

$$\delta_{ij} = \begin{cases} 0, & \text{when } i \neq j, \\ 1, & \text{when } i = j. \end{cases} \tag{1.29}$$

Then we can easily abbreviate an effective definition of our unit vectors as

$$\hat{\mathbf{e}}_i \cdot \hat{\mathbf{e}}_j = \delta_{ij}. \tag{1.30}$$

We understand a scalar to contain only one piece of information—a magnitude—while a vector contains more information—a magnitude and a direction—and can be manipulated in more ways. This raises the provocative question of what might contain even more information than a vector. Both scalars and vectors are, in fact, subclasses of quantities we call tensors, which we will use in Chapter 5 to describe stress and strain in three dimensions. The notation and shorthand we have just described will be useful there as well. We will consider points in rectangular coordinate systems (x, y, z) that displace very small amounts (u, v, w). In index or subscripted notation, we would consider the coordinates as (x_1, x_2, x_3) and the displacements as (u_1, u_2, u_3). In Chapter 5, we will define normal and shear strains that we write here in both "regular" Cartesian and index notation as

$$
\begin{aligned}
\varepsilon_{xx} &= \frac{\partial u}{\partial x} = \frac{\partial u_1}{\partial x_1} = \frac{1}{2}\left(\frac{\partial u_1}{\partial x_1} + \frac{\partial u_1}{\partial x_1}\right) = \varepsilon_{11}, \\
\varepsilon_{xy} &= \frac{1}{2}\left(\frac{\partial u}{\partial y} + \frac{\partial v}{\partial x}\right) = \frac{1}{2}\left(\frac{\partial u_1}{\partial x_2} + \frac{\partial u_2}{\partial x_1}\right) = \varepsilon_{12}.
\end{aligned}
\tag{1.31}
$$

The physical and mathematical meanings of these expressions will be discussed in more detail in Chapter 5. However, now we can use these expressions to illustrate another bit of notation: a comma denotes a partial derivative with respect to the index that follows. That is,

$$\frac{\partial(\ )}{\partial x_i} \equiv (\ )_{,i}. \tag{1.32}$$

So we can further simplify Equation 1.31 as

$$
\begin{aligned}
\varepsilon_{11} &= \frac{1}{2}\left(\frac{\partial u_1}{\partial x_1} + \frac{\partial u_1}{\partial x_1}\right) = \frac{1}{2}\left(u_{1,1} + u_{1,1}\right) = u_{1,1}, \\
\varepsilon_{12} &= \frac{1}{2}\left(\frac{\partial u_1}{\partial x_2} + \frac{\partial u_2}{\partial x_1}\right) = \frac{1}{2}\left(u_{1,2} + u_{2,1}\right).
\end{aligned}
\tag{1.33}
$$

1.6 Problem Solving

Any reader, of your solution to a given problem, should be able to follow the reasoning behind it. To test yourself, you may find a stranger on the street and ask whether your logic is clear, or you may simply make sure that you have included each of the following steps:

1. *State what is given*: A major league pitcher throws a ball at a speed of 132 fps (or 90 mph), and the distance from the pitcher's mound to home plate, 60 feet 6 inches is also given.
2. *State what is sought*: Find the time a batter has to react to an incoming pitch.

3. *Draw relevant sketches or pictures*: In particular, isolate the body (or relevant control volume) to see the forces involved, by means of an FBD.

4. *State the simplifying assumptions*: What assumptions will you make, and how can you justify them based on what is known?

5. *Identify the governing principles*: For example, Newton's second law.

6. *Start the relevant calculations*: Write the final formulas in symbolic terms (e.g., $v = d/t$).

7. *Check the physical dimensions of the answer*: Does the answer have dimensions of time? If it looks like it will be a length, go back.

8. *Complete relevant calculations*: Substitute in numbers—but wait as long as possible to plug in numbers. This provides time to perform a dimensional check and to think about whether the dependencies found make sense (should the answer depend on the pitcher's wingspan?), and it allows the reuse of the model for similar problems that may arise in the future.

9. State answers and conclusions.

We will follow these steps in the worked example problems that follow each chapter in this book.

1.7 Examples

EXAMPLE 1.1

A force **F** with magnitude $100\,\text{N}$ points from point $(1,2,1)$ toward $(3,-2,2)$, where the coordinates are in meters. Determine: (a) the magnitudes of the x, y, and z scalar components of **F**; (b) the moment of **F** about the origin; and (c) the moment of **F** about the point $(2,0.3,1)$.

Given: Force vector.

Find: Components of vector and moment of vector about two points.

Assume: No assumptions are necessary.

Solution

We can obtain a solution using either a holistic "vector approach" or a piece-by-piece "component approach." We will demonstrate both approaches.
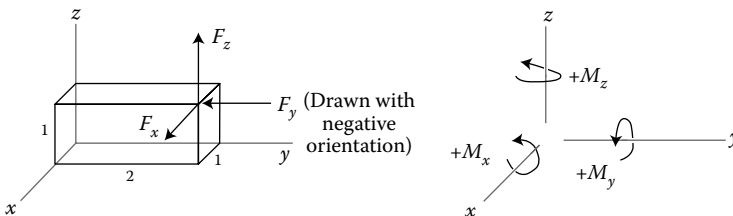
Vector Approach

a. The force can be written as $\mathbf{F} = F\hat{\mathbf{n}}$, where $\hat{\mathbf{n}}$ is the unit vector in the direction of the force:

$$\hat{\mathbf{n}} = \frac{2\hat{\mathbf{i}} - 4\hat{\mathbf{j}} + 1\hat{\mathbf{k}}}{\sqrt{2^2 + (-4)^2 + 1^2}} = 0.436\hat{\mathbf{i}} - 0.873\hat{\mathbf{j}} + 0.218\hat{\mathbf{k}},$$

$$\mathbf{F} = 100\hat{\mathbf{n}} = 43.6\hat{\mathbf{i}} - 87.3\hat{\mathbf{j}} + 21.8\hat{\mathbf{k}} \text{ N}.$$

The scalar components of $\mathbf{F}$ are thus

$$(F_x, F_y, F_z) = (43.6, -87.3, 21.8) \text{ N}.$$

b. The moment of $\mathbf{F}$ about the origin is found using $\mathbf{M}_0 = \mathbf{r}_0 \times \mathbf{F}$, where $\mathbf{r}$ is a vector from the origin to any point on the line of action of $\mathbf{F}$. With $\mathbf{r}_0 = 1\hat{\mathbf{i}} + 2\hat{\mathbf{j}} + 1\hat{\mathbf{k}}$ m, the moment can be written as a determinant:

$$\mathbf{M}_0 = \begin{vmatrix} \hat{\mathbf{i}} & \hat{\mathbf{j}} & \hat{\mathbf{k}} \\ r_x & r_y & r_z \\ F_x & F_y & F_z \end{vmatrix} = \begin{vmatrix} \hat{\mathbf{i}} & \hat{\mathbf{j}} & \hat{\mathbf{k}} \\ 1 & 2 & 1 \\ 43.6 & -87.3 & 21.8 \end{vmatrix} \text{ N m}$$

$$= \left[2(21.8) - 1(-87.3)\right]\hat{\mathbf{i}} + \left[1(43.6) - 1(21.8)\right]\hat{\mathbf{j}} + \left[1(-87.3) - 2(43.6)\right]\hat{\mathbf{k}}$$

$$= 130.9\hat{\mathbf{i}} + 21.8\hat{\mathbf{j}} - 174.5\hat{\mathbf{k}} \text{ N m}.$$

c. A vector $\mathbf{r}$ is needed from the point $P(2, 0.3, 1)$ to any point on the line of action of $\mathbf{F}$. We see that $\mathbf{r}_P = -1\hat{\mathbf{i}} + 1.7\hat{\mathbf{j}} + 0\hat{\mathbf{k}}$, going to the point $(1, 2, 1)$, is such a vector. Then $\mathbf{M}_P = \mathbf{r}_P \times \mathbf{F}$ yields

$$\mathbf{M}_P = \begin{vmatrix} \hat{\mathbf{i}} & \hat{\mathbf{j}} & \hat{\mathbf{k}} \\ r_x & r_y & r_z \\ F_x & F_y & F_z \end{vmatrix} = \begin{vmatrix} \hat{\mathbf{i}} & \hat{\mathbf{j}} & \hat{\mathbf{k}} \\ -1 & 1.7 & 0 \\ 43.6 & -87.3 & 21.8 \end{vmatrix} \text{ N m}$$

$$= 37.1\hat{\mathbf{i}} + 21.8\hat{\mathbf{j}} + 13.2\hat{\mathbf{k}} \text{ N m}.$$

Scalar (Components) Approach

a. The length of the segment from $(1, 2, 1)$ to $(3, -2, 2)$ is

$$\sqrt{(3-1)^2 + (-2-2)^2 + (2-1)^2} = \sqrt{2^2 + (-4)^2 + 1^2} = \sqrt{21}.$$

Direction cosines	Then
$l = 2/\sqrt{21} = 0.436$	$F_x = 100(0.436) = 43.6 \text{ N}$
$m = -4/\sqrt{21} = -0.873$	$F_y = -100(0.873) = -87.3 \text{ N}$
$n = 1/\sqrt{21} = 0.218$	$F_z = 100(0.218) = 21.8 \text{ N}$

b. As described, the force $\mathbf{F}$ is applied at $(1, 2, 1)$. The moments about the x-, y-, and z-axes through the origin are

$$M_{0x} = 1(87.3) + 2(21.8) = 130.9 \text{ N m}.$$

Note that F_x is parallel to the x-axis and thus does not have a moment about the x-axis. Similarly,

$$M_{0y} = 1(43.6) - 1(21.8) = 21.8\,\text{N m},$$

$$M_{0z} = -2(43.6) - 1(87.3) = -174.5\,\text{N m}.$$

c. Use the same procedure as part (b). In this case, the distances required are from the point of action of the force to the point $P(2, 0.3, 1)$, and we choose $(1, 2, 1)$ as before:

$$M_{Px} = (1 - 1)(87.3) + (2 - 0.3)(21.8) = 37.1\,\text{N m},$$

$$M_{Py} = (1 - 1)(43.6) + (2 - 1)(21.8) = 21.8\,\text{N m},$$

$$M_{Pz} = -(2 - 0.3)(43.6) + (2 - 1)(87.3) = 13.2\,\text{N m}.$$

EXAMPLE 1.2

Given the three vectors $\mathbf{r}_1 = a\hat{\mathbf{i}}$, $\mathbf{r}_2 = b\hat{\mathbf{j}}$, and $\mathbf{r}_3 = c\hat{\mathbf{k}}$, (a) determine how the vector product $\mathbf{r}_1 \cdot \mathbf{r}_2 \times \mathbf{r}_3$ should be evaluated and explain why; and (b) explain the results to (a) in physical terms.

Given: Three line vectors.

Find: The meaning and value of the vector product $\mathbf{r}_1 \cdot \mathbf{r}_2 \times \mathbf{r}_3$.

Assume: No assumptions are necessary.

Solution

a. There are two ways in which the given vector product can be evaluated because there are only two choices about the order in which the individual products are performed:

$$P_1 = (\mathbf{r}_1 \cdot \mathbf{r}_2) \times \mathbf{r}_3,$$

$$P_2 = \mathbf{r}_1 \cdot (\mathbf{r}_2 \times \mathbf{r}_3).$$

The first of these has no meaning because it requires the cross product of a scalar $(\mathbf{r}_1 \cdot \mathbf{r}_2)$ with a vector. The second evaluation does produce a meaningful result whose value is a scalar:

$$P_2 = a\hat{\mathbf{i}} \cdot \begin{vmatrix} \hat{\mathbf{i}} & \hat{\mathbf{j}} & \hat{\mathbf{k}} \\ 0 & b & 0 \\ 0 & 0 & c \end{vmatrix} = a\hat{\mathbf{i}} \cdot \left[bc\hat{\mathbf{i}} + 0\hat{\mathbf{j}} + 0\hat{\mathbf{k}} \right] = abc.$$

b. The scalar resulting from the *scalar triple product* $\mathbf{r}_1 \cdot \mathbf{r}_2 \times \mathbf{r}_3$ is the volume of the rectangular parallelepiped defined by (or contained within) the original vectors given.

EXAMPLE 1.3

Consider the three two-dimensional vectors:

$$\mathbf{r}_1 = \cos\alpha\hat{\mathbf{i}} + \sin\alpha\hat{\mathbf{j}}, \quad \mathbf{r}_2 = \cos\beta\hat{\mathbf{i}} - \sin\beta\hat{\mathbf{j}}, \quad \text{and} \quad \mathbf{r}_3 = \cos\beta\hat{\mathbf{i}} + \sin\beta\hat{\mathbf{j}}.$$

Use the definition (Equation 1.21) of the cross product to find formulas for $\sin(\alpha + \beta)$ and $\sin(\alpha - \beta)$.

Given: Three line vectors and two angles $(\alpha, \pm\beta)$.

Find: Formulas for the sines of the angles $\alpha \pm \beta$.

Assume: No assumptions are necessary.

Solution

Note that each of the three vectors given is a *unit* vector. It then follows from the definition of the cross product that

$$\mathbf{r}_1 \times \mathbf{r}_2 = \begin{vmatrix} \hat{\mathbf{i}} & \hat{\mathbf{j}} & \hat{\mathbf{k}} \\ \cos\alpha & \sin\alpha & 0 \\ \cos\beta & -\sin\beta & 0 \end{vmatrix} = -(\sin\alpha\cos\beta + \cos\alpha\sin\beta)\hat{\mathbf{k}}.$$

But from the definition (Equation 1.21), it is also true that

$$\mathbf{r}_1 \times \mathbf{r}_2 = -|\mathbf{r}_1||\mathbf{r}_2|\sin(\alpha + \beta)\hat{\mathbf{k}}.$$

When we equate these two results, we find

$$\sin(\alpha + \beta) = \sin\alpha\cos\beta + \cos\alpha\sin\beta.$$

In exactly the same way, we can see that

$$\mathbf{r}_1 \times \mathbf{r}_3 = -|\mathbf{r}_1||\mathbf{r}_3|\sin(\alpha - \beta)\hat{\mathbf{k}},$$

and

$$\mathbf{r}_1 \times \mathbf{r}_3 = \begin{vmatrix} \hat{\mathbf{i}} & \hat{\mathbf{j}} & \hat{\mathbf{k}} \\ \cos\alpha & \sin\alpha & 0 \\ \cos\beta & \sin\beta & 0 \end{vmatrix} = -(\sin\alpha\cos\beta - \cos\alpha\sin\beta)\hat{\mathbf{k}}.$$

So just as before, we find the difference formula

$$\sin(\alpha - \beta) = \sin\alpha\cos\beta - \cos\alpha\sin\beta.$$

EXAMPLE 1.4

A clever student wants to weigh himself using only a scale with a capacity of $500\,\text{N}$ and a small $80\,\text{N}$ spring dynamometer. With the rig shown, he discovers that when he exerts a pull on the rope so that the dynamometer registers $76\,\text{N}$, the scale reads $454\,\text{N}$. What are his correct weight and mass?
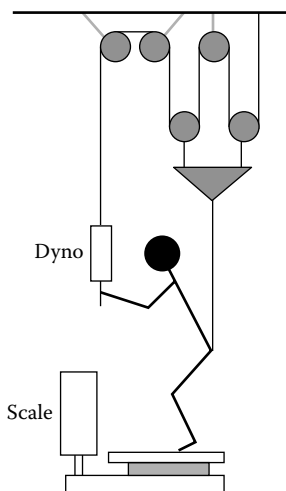
Given: Geometry of problem, weight indicated on scale, and tension registered on dynamometer.

Find: True weight and mass of the student.

Assume: This is a planar *statics* problem. Also, assume that the tension in the rope is constant, the masses of the pulleys are negligible, and static equilibrium.

Governing principles: Newton's second and third laws, as reflected in Equation 1.7.

Solution

The relevant FBDs are those of the two lower pulleys (circles) and of the student (at right figure):
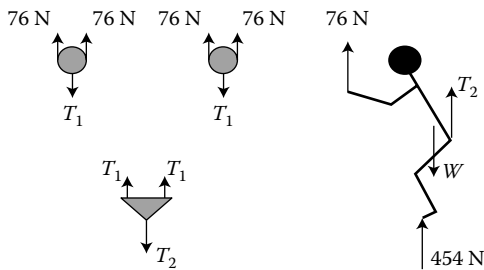
Next, we ensure that $\sum F_y = 0$ holds for each FBD, that is, that the two pulleys and the student are each in equilibrium. From the pulleys,

$$T_1 = 76\,\text{N} + 76\,\text{N} = 152\,\text{N}.$$

Similarly, from the remaining FBDs, we obtain

$$T_2 = T_1 + T_1 = 304\,\text{N},$$
$$W = 454\,\text{N} + 76\,\text{N} + T_2 = 834\,\text{N}.$$

So, the student's mass is

$$\frac{834\,\text{N}}{9.8\,\text{m/s}^2} = 85\,\text{kg}.$$

EXAMPLE 1.5

Determine the force(s) and moment(s) required to keep the tree shown from falling down the hill:

Given: The tree shown.

Find: The system of force(s) and moment(s) needed to equilibrate the tree.

Assume: The tree lies in a plane so that Equation 1.7 may be used (i.e., this is a planar statics problem). In addition, assume that the ground around the tree is level (i.e., ignore the slope appearing in the photo).

Governing principles: Newton's second and third laws, as reflected in Equation 1.7.

Solution

In principle, a horizontal force **H**, a vertical force **V**, and a moment **M** are needed at the base of the tree to support it. They are shown in the FBDs. These three elements are provided by the interaction between the tree's root system and the soil at the tree's base. Then we apply the equations of equilibrium (1.7), summing forces, and summing counterclockwise moments about the base of the tree. First consider the weight of the tree, inclined at an angle θ from the ground, modeled as a constant distributed load q_0 per unit length (as in the left FBD), with s representing the position along the length of the tree.

$$\sum \mathbf{F}_x = H\hat{\mathbf{i}} = 0 \;\Rightarrow\; H = 0,$$

$$\sum \mathbf{F}_y = V\hat{\mathbf{j}} - q_0 L\hat{\mathbf{j}} = 0 \;\Rightarrow\; V = q_0 L,$$

$$\sum \mathbf{M}_z = M\hat{\mathbf{k}} + \int\limits_{0}^{L} (-s\cos\theta\hat{\mathbf{i}}) \times -(q_0 ds\hat{\mathbf{j}}) = 0$$

$$\Rightarrow M = -\frac{q_0 \cos\theta L^2}{2}.$$
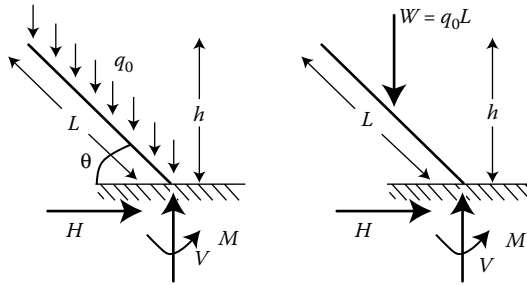
If the tree weight is modeled as a concentrated load at its center of mass (as in the right FBD), halfway up the trunk, only the moment equilibrium equation changes:

$$\sum \mathbf{M}_z = M\hat{\mathbf{k}} + [(-(L/2)\cos\theta)\hat{\mathbf{i}} \times -q_0 L\hat{\mathbf{j}}] = 0$$

$$\Rightarrow M = -\frac{q_0 \cos\theta L^2}{2}.$$

Not surprisingly, we get the same result.

EXAMPLE 1.6

Determine the forces required to maintain equilibrium and support the load W in the plank shown. Then, find expressions for the *internal* force and moment required at any position along the left side of the plank.
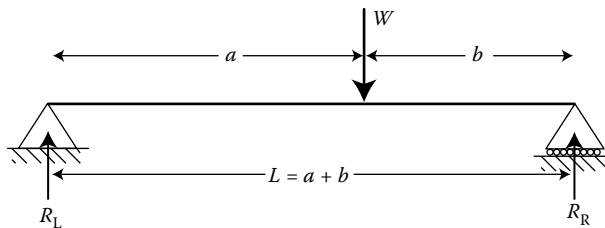
Given: The loaded plank shown.

Find: The system of force(s) and moment(s) needed to equilibrate the plank and support the load W.

Assume: This is a planar statics problem.

Governing principles: Newton's second and third laws, as reflected in Equation 1.7.

Solution

Since this is a planar statics problem, we can dispense with some of the vector formalism simply by recognizing that all of the loads are in the vertical direction (i.e., $\hat{\mathbf{j}}$) and all of the coordinate measurements are in the horizontal direction (i.e., $\hat{\mathbf{i}}$), so that all moments or couples are out-of-plane vectors (i.e., $\hat{\mathbf{k}}$). Then summing forces in the vertical (y) direction (see figure in Example 1.6) shows that

$$\sum F_y = R_\mathrm{L} + R_\mathrm{R} - W = 0 \;\Rightarrow\; R_\mathrm{L} + R_\mathrm{R} = W.$$

By summing moments about the left support, taking counterclockwise as positive, we see that

$$\sum M_{R_\mathrm{L}} = a\,W - R_\mathrm{R}L = 0 \;\Rightarrow\; R_\mathrm{R} = \frac{a\,W}{L}.$$

When we combine these two results, we find

$$R_\mathrm{L} = \frac{b\,W}{L} \quad\text{and}\quad R_\mathrm{R} = \frac{a\,W}{L}.$$

We now look at a *section* or piece of the beam as shown in the figure below and ask, What is needed there, in the beam at coordinate x, in order to maintain equilibrium? Clearly a vertical internal reaction there would still leave a moment or couple that would serve to spin that section as a rigid body. Thus, since vertical equilibrium requires a downward shear force $V_\mathrm{L} = -R_\mathrm{L}$ there, the plank must develop an internal moment to maintain equilibrium:

$$M_\mathrm{L} = -R_\mathrm{L}x = -\frac{Wbx}{L}.$$

The negative signs here indicate that in our FBD, we have assumed the incorrect sense of the force V_L and moment M_L. This is not a case of bad judgment, but our attempt to follow the sign convention for positive internal forces and moments that we will continue to use for the more complex loading we encounter in Chapter 11.
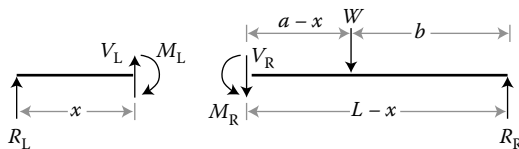
A similar examination of the right-hand section of the plank shows that

$$V_\mathrm{R} = R_\mathrm{R} - W = (W - R_\mathrm{L}) - W = -R_\mathrm{L},$$

and

$$M_\mathrm{R} = -R_\mathrm{R}(L - x) + W(a - x) = -W\left(\frac{a}{L}\right)(L - x) + W(a - x) = -W\left(\frac{bx}{L}\right).$$

Again, our use of the standard sign convention for internal moment has led us to negative answers, representing a force and a moment that are in the opposite directions from those drawn in our FBD.

Importantly, we see that at the cut itself we have equilibrium in accord with Newton's third law, that is, while accounting for signs and the directions drawn:

$$V_L - V_R = 0 \quad \text{and} \quad M_R - M_L = 0.$$

This simple example presages some very important concepts to which we will return. First, we have briefly introduced the *method of sections* by dividing the plank into contiguous pieces and applying Newton's third law. We will do that a lot in what follows. Second, we have seen that even a simple plank or *beam* must somehow develop an internal moment to support an external vertical force. We will develop the theory of beams extensively in Chapters 11 and 16.

EXAMPLE 1.7

Determine the forces in the truss members *AB* and *AC* in the truss structure shown and use them to show that the truss as a whole *bends* (i.e., provides an internal moment or couple) as it supports the load *W*:
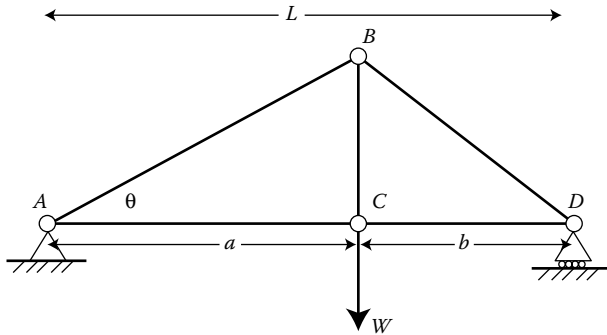
Given: The truss shown.

Find: The bar forces needed to illustrate how the truss supports the load.

Assume: This is a planar statics problem.

Governing principles: Newton's second and third laws, as reflected in Equation 1.7.

Solution

Again, we skip the vector formalism and start by noting that a truss is made up of one-dimensional elements that: (a) are loaded only by forces applied at the ends of each bar, and (b) cannot have any loads applied along and normal to their axis. Having said this, we will quickly see that taken in its entirety, the truss supports and transmits forces rather like a beam. Each individual bar is assumed to be in tension, with positive force and indicated by an arrow directed outward from the joint.

We apply the method of sections, here taking a section at coordinate *x*, as shown. At the section we see that the individual bar forces also reflect Newton's third law about action and reactions. Then we apply the *method of joints* by summing forces in both vertical (*y*) and horizontal (*x*) directions for the joint *A* on the left:

$$\sum F_y = R_L + F_{AB} \sin\theta = 0 \quad \Rightarrow \quad F_{AB} = -\frac{R_L}{\sin\theta},$$

$$\sum F_x = F_{AC} + F_{AB} \cos\theta = 0 \quad \Rightarrow \quad F_{AC} = -F_{AB}\cos\theta = R_L \cot\theta.$$
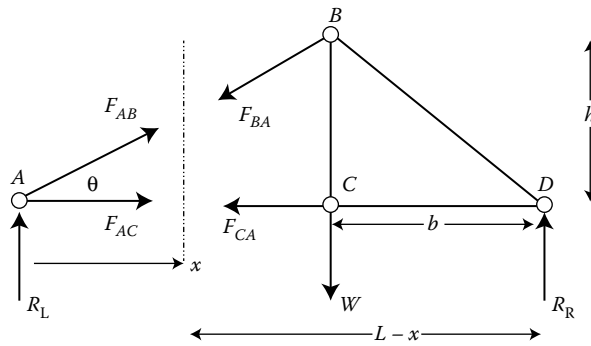
We now take a look at the right-hand section of the truss (see below figure). We see that the horizontal component of the bar force F_{ABx} is a compressive (remember, $F_{AB} < 0$) force acting on joint B with magnitude

$$F_{ABx} = -\left(\frac{R_L}{\sin\theta}\right)\cos\theta = -R_L\cot\theta = -F_{AC}.$$
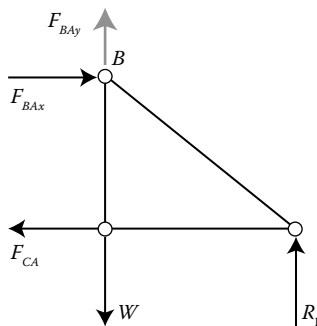
Thus, F_{ABx} and F_{AC} form a couple or moment of magnitude hF_{ABx}, which allows us to say that the truss as a whole acts like the plank or beam in Example 1.6.

PROBLEMS

1.1 The premixed concrete in a cement truck can be treated as a fluid continuum when it is poured into a mold. Sand flowing from a large bucket can also be considered a fluid. Describe three other examples in which an aggregate of solid objects flows likes a fluid continuum.

1.2 Investigate the reef balls used to create artificial reef environments. What are the most important parameters for the successful maintenance of a stable marine environment?

1.3 Use the dot product to find the angle θ between the two vectors $\mathbf{F}_1 = 4\hat{\mathbf{i}} + 3\hat{\mathbf{j}}$ and $\mathbf{F}_2 = 1\hat{\mathbf{i}} + 7\hat{\mathbf{j}}$.

1.4 Find and sketch the cross product of the two vectors $\mathbf{F}_1 = -5\hat{\mathbf{i}} + 3\hat{\mathbf{j}}$ and $\mathbf{F}_2 = 1\hat{\mathbf{i}} - 4\hat{\mathbf{j}}$.

1.5 Generalize the results of Example 1.2 to show that for three arbitrary vectors (i.e., not each collinear with one axis), the scalar triple product $\mathbf{r}_1 \cdot (\mathbf{r}_2 \times \mathbf{r}_3)$ produces the volume of the parallelepiped whose sides are, respectively, given by $\mathbf{r}_1$, $\mathbf{r}_2$, and $\mathbf{r}_3$.

1.6 Using the generalized vectors of Problem 1.5, show that

$$\mathbf{r}_1 \cdot \mathbf{r}_2 \times \mathbf{r}_3 = \mathbf{r}_2 \cdot \mathbf{r}_3 \times \mathbf{r}_1 = \mathbf{r}_3 \cdot \mathbf{r}_1 \times \mathbf{r}_2.$$

1.7 Use vector representations of the sides of the triangle below to demonstrate the *law of sines*. (Hint: Note that in vector arithmetic, $\mathbf{r}(C/A) = \mathbf{r}(B/A) + \mathbf{r}(C/B)$, where, for example, $\mathbf{r}(C/A)$ is the position of C relative to A.)
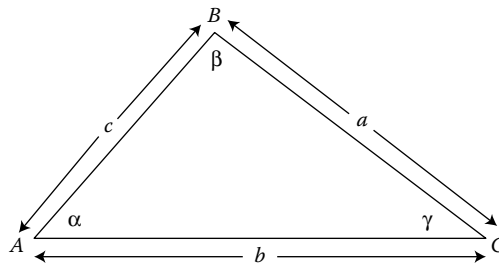
1.8 Use vector representations of the sides of the triangle in Problem 1.7 to demonstrate the *law of cosines*. (Hint: Note that in vector arithmetic, $\mathbf{r}(C/A) = \mathbf{r}(B/A) + \mathbf{r}(C/B)$, where, for example, $\mathbf{r}(C/A)$ is the position of C relative to A.)

1.9 Show that the included angle $\angle APB$ in the triangle shown below is a right angle (i.e., $\angle APB = \pi/2$). (Hint: Note that with vector arithmetic, $\mathbf{r}(P/A) = R\hat{\mathbf{i}} + \mathbf{r}(P/O)$.)
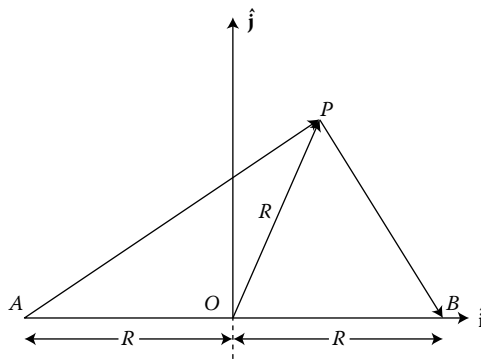
1.10 For the triangle in Problem 1.9 show that $\angle BOP = 2\angle AOP$. (Hint: Note that $R\hat{\mathbf{i}} = \mathbf{r}(P/O) + \mathbf{r}(B/P)$.)

1.11 Find an expression for the force F required (as a function of the angle θ) to keep the pulley system shown in static equilibrium.
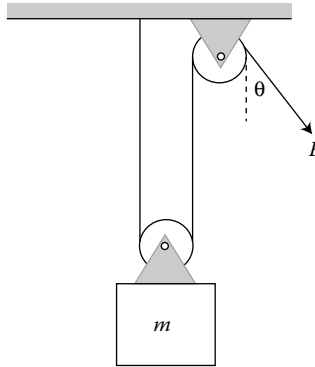
1.12 A force **F** acts on a uniform pendulum as shown. Find the reaction forces at the pin connection and the angle θ, letting $F = 100\,\text{N}$, $d = 1.6\,\text{m}$, and $W = 300\,\text{N}$.
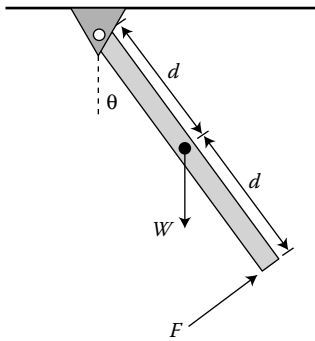
1.13 Suppose the tree considered in Example 1.5 is subjected to a fierce wind (blowing left to right) that produces pressure p_w that acts on the projected area of the tree. Assuming the tree trunk is a circular cylinder of radius r, calculate the forces and moment at the base of the tree.

1.14 Calculate the forces and moment required to support the same tree if the slope on which it stands is considered, and we would like to know the forces parallel and normal to the ground. Assume the slope is at an angle α.

1.15 For the truss shown, find the bar forces at the section indicated.
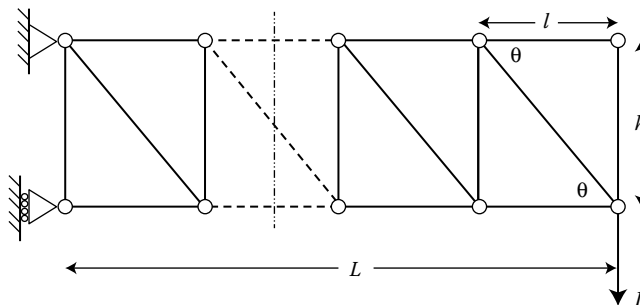
1.16 Determine the effective moment and vertical shear force that would be required to replicate the effect of the three bar forces in Problem 1.15.

1.17 For the truss shown, find the bar forces at the section indicated.
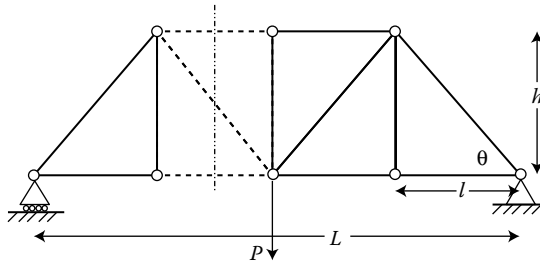
1.18 Determine the effective moment and vertical shear force that would be required to replicate the effect of the three bar forces in Problem 1.17.

1.19 A 15 m tall utility pole is located at a $40°$ bend in a set of power lines. The tension in each line is 15 kN, and due to sag of the lines, the tension forces act along directions $10°$ below horizontal. A guy wire has been installed, as shown in the photo and the top-view sketch, to keep the pole upright. What should be the tension in the guy wire to minimize the magnitude of the moment reaction required from the ground at the bottom of the pole? With that tension, what are the reaction forces and moments required at the ground? Assume that the forces from the guy wire and all incoming and outgoing lines act at a single point on the top of the pole itself.
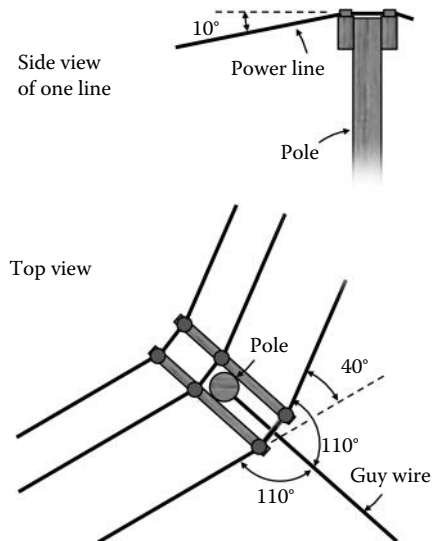
2

Strain and Stress in One Dimension

In Chapter 1, we stated that in order to study continuum mechanics, that is, to characterize the response of a continuous material to external loading, we must (1) characterize the material's deformation, (2) define its internal loading, and (3) relate this to its deformation, and (4) ensure that the body is in equilibrium.* We will begin by considering the deformation of a material under loading.

Returning to our example of the remodeling of an underwater oil rig as an artificial reef, we want to examine the trusses of the existing rig. As we have seen (Figures 1.1 and 1.3), the rig is composed of many slender steel bars that must withstand the cyclic loading of ocean currents, as well as other loads. Each bar may be pulled or pushed along its axis, as in Figure 2.1, and by isolating each bar, we can begin to determine whether the bars can withstand this loading.

This raises the question of what it means to "withstand" a load. Is it sufficient for the bar to sustain the load without incurring damage or breaking, or is it necessary for it to sustain the load without deforming or bending?

You may have noticed that a standard office table or desk can support far more weight or force than it does when serving as a writing table or computer desk and that some chairs can support the weight of several people without breaking. These are not examples of wasteful or inefficient designs. In fact, these products have been designed for *stiffness* rather than for *strength*. Instead of merely building a chair strong enough to hold a person, designers have chosen to make the chair stiff enough that its deflections can be limited to some small amount, under a load much larger than it is expected to typically carry. Under normal use, therefore, the chair should not deflect perceptibly. Designing for stiffness means minimizing or limiting deflections, and it is generally a much more restrictive proposition than designing purely for strength. In this chapter, we will discover ways of characterizing the stiffness and strength of materials and structures.

In order to begin to design for stiffness by minimizing deflection, we must understand how to characterize the deformation a loaded body will undergo.

2.1 Kinematics: Strain

In continuum mechanics, we want to characterize how bodies respond to the effects of external loading, and how these responses are distributed through the bodies. One way a body responds to external loads is by deforming. We will develop a way of quantifying its deformation relative to its initial size and shape, and we will call this relative deformation *strain*.

---

* Otherwise, more generally, that Newton's second law is satisfied.
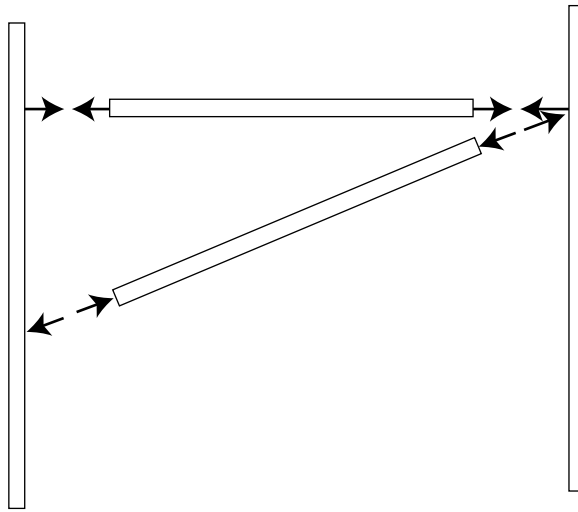
FIGURE 2.1
Isolated bars of underwater structure.

2.1.1 Normal Strain

When an axial force is applied to a body, the distance between any two points *A* and *B* along the body changes. We call the initial, undeformed length between two points *A* and *B* the *gage length* (or *gauge length*). During a tensile experiment such as the one sketched in Figure 2.2, we may measure the change in gage length as a function of applied force. What interests us is how much this gage length changes, relative to its initial value, or, in other words, the *intensity of deformation*.

In Figure 2.2, the bar is acted on, or loaded, at its ends by two equal and opposite axial forces. (An axial force is one that coincides with the *longitudinal* axis of the bar and acts through the centroid of the cross section.) These forces, called *tensile* forces, tend to stretch or elongate the bar. We say that such a bar is in tension.

If L_0 is the initial gage length and L is the observed length of the same segment under an applied load, the gage elongation is $\Delta L = L - L_0$. The elongation per unit of initial gage length, or "deformation intensity," ε is then

$$\varepsilon = \frac{L - L_0}{L_0} = \frac{\Delta L}{L_0}. \tag{2.1}$$

This expression for epsilon defines the macroscopic extensional strain.

It is also possible for this apparatus to load a bar with two equal and opposite forces directed toward each other, as in the sketch in Figure 2.3. These forces, called *compressive* forces, tend to shorten or compress the bar. We say that such a bar is in compression. Note that for compressive loading $\Delta L < 0$, the strain as calculated from Equation 2.1 is negative.

Both tensile (tending to elongate) and compressive (tending to shorten) deformations result in *normal strain*, defined as the change in length of our material relative to its initial undeformed length. Normal strain is a dimensionless quantity, but is often represented as having dimensions of length/length, or units of in/in, m/m, or mm/mm. Sometimes it is given as a percentage.
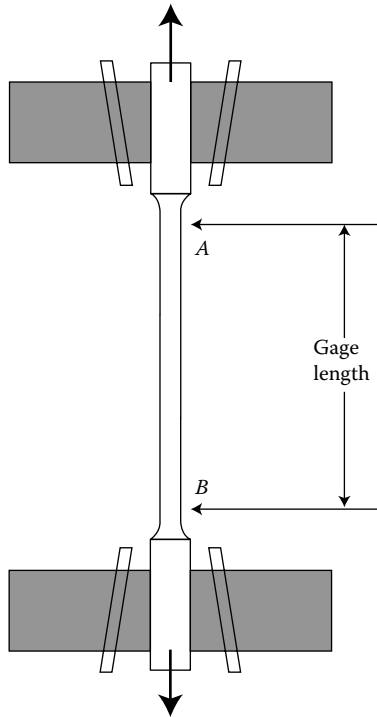
FIGURE 2.2
Tension specimen.

In some applications, we will use a slightly more careful definition of strain. This is sometimes called the *natural* or *true strain* as distinct from the *engineering strain* defined by Equation 2.1. In this *true strain* definition, a strain increment $d\varepsilon$ is integrated over the bar:

$$\bar{\varepsilon} = \int_{L_0}^{L} d\varepsilon = \int_{L_0}^{L} \frac{dL}{L} = \ln\left(\frac{L}{L_0}\right) = \ln(1 + \varepsilon). \qquad (2.2)$$

For very small strains, this natural strain is coincident with the engineering normal strain ε. This book focuses on problems for which such a small strain assumption is reasonable.

In a third definition of strain, we consider that each and every planar section normal to the longitudinal axis moves a distance along the axis $u(x)$. We assume here that each planar section remains planar. An element of the bar that was originally of length dx is thus stretched to a new length, $dx + u(x + dx) - u(x)$. This is illustrated in Figure 2.4.
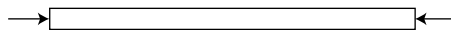
FIGURE 2.3
Bar in compression.
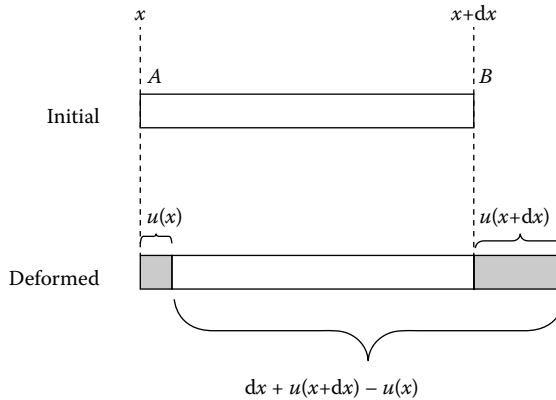
FIGURE 2.4
One-dimensional stretching of a bar.

For this longitudinal deformation, we define strain—in the same spirit as the first definition—as

$$\varepsilon = \frac{\text{change in length}}{\text{original length}} = \frac{\left[dx + u(x + dx) - u(x)\right] - dx}{dx}, \qquad (2.3)$$

or, retaining only the first-order term in a Taylor series expansion of $u(x + dx)$, we find

$$\varepsilon \approx \frac{\left[u(x) + (du/dx)\,dx - u(x)\right]}{dx} = \frac{du}{dx}, \qquad (2.4)$$

In Section 2.8, we use Equation 2.4 to express equilibrium in terms of the displacement $u(x)$, to illustrate where the concept of compatibility is applied and to obtain a classic result for the extension of an axially loaded bar.

2.1.2 Shear Strain

Bodies may experience both normal and *shear* deformations, and hence normal and shear strains. When an axial tensile load is applied to a body, it causes elongation. Similarly, an axial compressive load will cause shortening. When a shear force is applied to a body, it will cause an angular deformation. The intensity of this deformation is *shear strain*.

To visualize the effect of shear strain, consider a motor mount as shown in Figure 2.5a. The motor mount is composed of a block of elastic material (our "body") with attachments to allow for connection to the base of the motor and the support structure. A force P is applied at the top of the block, and the support structure resists with an equal and opposite force P. This subjects the block/body (of initial height L) to a pair of shear forces, as shown in Figure 2.5b. If we imagine that the block is composed of many thin layers and that each layer will slide slightly with respect to its neighbor, we may visualize how the angular distortion of the block will develop, resulting in maximum displacement Δ_s at the top of the block.

As for normal strain, several definitions of shear strain exist. The *engineering* shear deformation incurred is ϕ, the *change* in an initially right angle, as shown in Figure 2.5b. This is
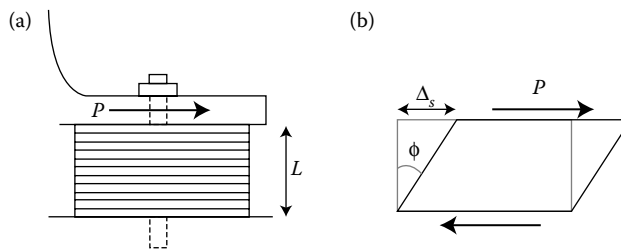
FIGURE 2.5
Shear strain. (a) Motor mount. (b) Motor mount distorted in shear.

the formal definition of shear strain: the change in the angle between two initially perpendicular planes. It is measured in radians and hence, like normal strain, is dimensionless. However, it is often difficult to take precise measurements of these angular changes, especially for very small deformations. For small deformations, the tangent of the angle ϕ will closely approximate ϕ itself, so that we can approximate the shear strain gamma by:

$$\gamma = \phi \approx \tan \phi = \frac{\Delta_s}{L}. \tag{2.5}$$

With normal and shear strain defined, we are equipped to address the kinematics of deformation of continuous materials due to loading. In Section 2.2, we will then move on to the second item on our checklist: the internal forces developed in response to external loading. First, we will consider how to measure the small deformations of interest.

2.1.3 Measurement of Strain

Until 1930, normal strain was commonly measured indirectly, using extensometers that measured the displacement ΔL over some initial gage length L to allow strain to be calculated using the equations we have just discussed. An extensometer system typically included a mechanical or optical lever system. In 1931, the first electrical strain gage demonstrated that strain could also be measured directly. Most modern strain gages are resistive electrical meters.

In 1856, Lord Kelvin demonstrated that the resistances of copper and iron wires changed when the wires were stretched, compressed, or otherwise deformed. This concept is at the heart of the electrical strain gages first implemented by Roy Carlson in 1931 and Edward Simmons in 1938.* Advances in materials and fabrication techniques have since refined the design of the resistive strain gage, whose general construction is shown in Figure 2.6.

When the resistance element, typically a thin wire array etched in a metal foil, is attached to a loaded (and thus deformed) body in such a way that the wire will also be deformed, the measured change in resistance may be calibrated in terms of strain in the direction aligned with the long wire segments. Important parameters in the design and performance of a strain gage are: (1) the material used for the wires or foil, and to a lesser extent, the backing and bonding materials; (2) protection of the gage; and (3) electrical circuitry, typically involving a Wheatstone bridge. The wires should have a large change in resistance

---

* Carlson was a civil engineer investigating California dams; Simmons was an electrical engineer who first developed a way to manufacture a bonded wire strain gage and patented his design—though it took an 11-year court battle for him to win the patent rights for himself and not for Caltech, where he had been educated and continued to work.
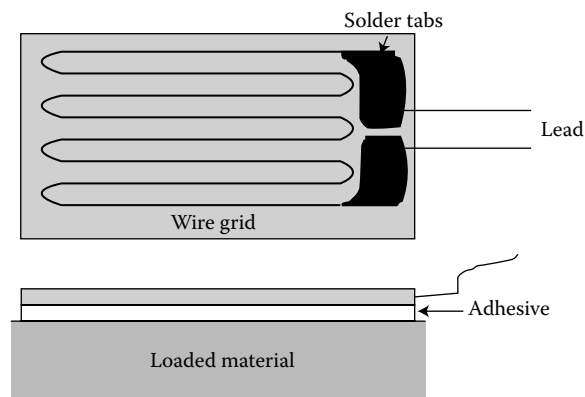
FIGURE 2.6
Construction of a bonded-wire strain gage.

corresponding to the strains expected (sometimes called the wire material's *gage factor*), a high electrical resistivity, a low-temperature sensitivity*, and a good corrosion resistance, among other properties. Mounting a strain gage is straightforward (though not always easy) as long as the surface of the body in question is extremely clean, and as long as the manufacturer's installation procedures are followed carefully.

2.2 The Method of Sections and Stress

We now want to consider the forces *within* a body that balances the effect of externally applied forces. In order to do this, we must prepare a FBD that shows all the external forces acting on the body at their respective points of application (Figure 2.7a). All of the forces acting on a body, including reactive forces caused by supports and the weight of the body itself (sometimes assumed negligible and not included if much smaller than the applied loads), are considered external forces. This view is valuable, but does not allow us to visualize the internal forces we are interested in, so we imagine slicing open our body (Figure 2.7b and c). Then the former internal forces at the slice become external forces on each section and so must be included in the separate FBDs. Each sliced section must be in equilibrium, just as the larger body is in equilibrium. The fundamental statement of this concept is that: *the externally applied forces on one side of an arbitrary cut through a body must be balanced by the internal forces developed at the cut*. We may use this principle to solve for the internal forces of interest, and the name given to this technique is the *method of sections*.

These internal forces revealed by the method of sections are vectors, with magnitude and direction. In a solid, these forces determine the solid's resistance to deformations and to external forces.

Physically, these internal forces are the ones that hold the body together: they are the resultants of intermolecular forces, or chemical bonds. The application of an external force changes the distances between the atoms (i.e. deformation) by changing the forces exerted

---

* Temperature considerations are important because the wires' electrical properties may be temperature-dependent, and also because temperature itself can result in deformation, as will be quantified in Section 2.10.
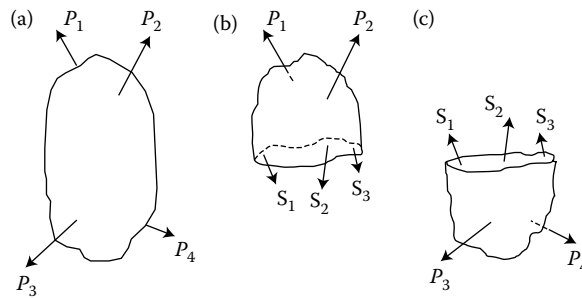
FIGURE 2.7
The method of sections. (a) Equilibrium of entire body. (b, c) Equilibrium of sections created by arbitrary cut through body.

by these bonds. We *could* model the individual internal atomic forces, and this is in fact done for atomistic simulations of very small numbers of atoms, but for engineering-scale questions the bookkeeping, associated with so many force vectors and complex atomic arrangements, is prohibitive. In addition, dealing with *continuous* materials was supposed to get us off the hook from having to worry about individual atoms, anyway. So, we tend to consider one distributed internal force, and stress as the intensity of that distributed force.

In general, *stress* is a force per unit area, or the intensity of the force, with typical units [N/m^2 or Pa] or [lb/in^2 or psi]. This indicates that we should divide the force **P** by the area **A** on which it acts, but remember that both **P** and **A** are vectors.* The stress depends on the orientations of both **P** and **A**, as we will see in Chapter 4. It will be useful for us to resolve the internal force **P** into its components perpendicular and parallel to the section of interest.

Interestingly, it took a long time for engineers and scientists to conceptualize stress as we now understand it. While this was partly due to the susceptibility of scientific progress to fads and biases, and the tyranny of Isaac Newton as a trendsetter (more on this later), it was also a result of researchers focusing on whole structures and not "looking inside" the body as the method of section demands. Instead, as J. E. Gordon notes, "all through the eighteenth century and well into the nineteenth, very clever men, such as Leonhard Euler and Thomas Young, performed what must appear to the modern engineer to be the most incredible intellectual contortions"[†] in order to characterize material behavior without the modern notion of stress.

It was Augustin Cauchy who first conceptualized stress and strain as we now understand them, in 1822. J. E. Gordon again: "Cauchy perceived that...the 'stress' in a solid is rather like the 'pressure' in a liquid or a gas. It is a measure of how hard the atoms and molecules which make up the material are being pushed together or pulled apart as a result of external forces."

2.2.1 Normal Stresses

By using the method of sections in one-dimensional loading cases, we can identify two different types of stresses. Consider a straight bar acted on at its ends by two equal and

---

* The vector **A** is $\hat{n}A$, where $\hat{n}$ is the outward normal unit vector of the area with magnitude *A*.
[†] From Gordon's illuminating *Structures, or Why Things Don't Fall Down*, 1978.
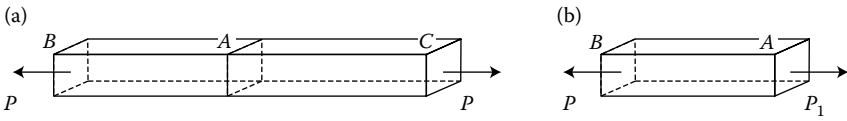
FIGURE 2.8
Bar in tension. (a) Bar BC. (b) Free body BA.
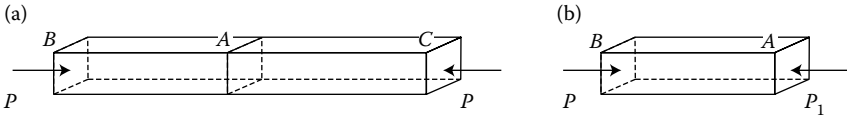
FIGURE 2.9
Bar in compression. (a) Bar BC. (b) Free body BA.

opposite forces, as in Figure 2.8a. Remember that these external forces are called tensile forces. Similarly, the bar in Figure 2.9a is acted on by two equal and opposite forces, directed toward each other; these forces are compressive forces. If we make an imaginary cut through each bar and consider the left-hand segment as a free body, as in Figure 2.8b and 2.9b, we see that for each bar to be in equilibrium, a force $\mathbf{P}_1$, equal and opposite to external force $\mathbf{P}$, must exist. This force $\mathbf{P}_1$ is actually an internal force in the original bar that resists the action of force $\mathbf{P}$. Also, we assume that the internal resisting force is uniformly distributed over the cross section of the bar. This force-per-area (the magnitude of the internal force divided by the cross-sectional area) is what we call *normal stress*.

The tensile forces in Figure 2.8 produce internal tensile stresses, and the compressive forces in Figure 2.9 produce internal compressive stresses. By convention, tensile stresses are positive, and compressive stresses are negative. (This sign convention has to do with the outward normal vector of surface *A*, as will be discussed in Chapter 4.) Tensile and compressive stresses are developed by forces perpendicular (normal) to the surfaces on which they act, hence the term normal stresses. As we understand that the direction of the vector **A** is also perpendicular to the surface, that is, the vectors are parallel to each other, in this one-dimensional case, we can work with the scalar magnitudes *P* and *A*. We use the Greek letter sigma to represent normal stress, and we write

$$\sigma \equiv \frac{P}{A}. \tag{2.6}$$

2.2.2 Shear Stresses

The other type of stress, called *shear stress* (sometimes *tangential* stress), is developed in a direction parallel to the surface on which it acts. An example is shown in Figure 2.10. When equal and opposite forces with magnitude *P* are applied to two flat plates bonded together by adhesive, the contact (shaded) surface is subjected to a shearing action. In the absence of the adhesive, the two surfaces would slide past one another. The shear force is assumed to be uniformly distributed across the contact area. As a result, the shear stress, defined as the shearing force divided by the contact area, is developed. Shear stress can also develop within a single body, when various layers of the material resist sliding with respect to each other.
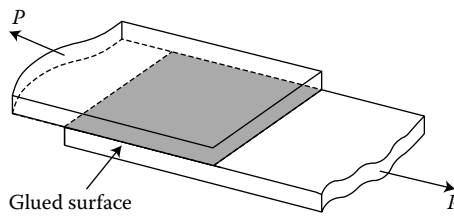
FIGURE 2.10
Shear between two bodies.

Again, stress is the intensity of the internal force, and in this case its magnitude is once again P/A, where A is the magnitude of the area of the glued surface; however, for shear stresses, the vector **A** is oriented perpendicular to the force vector **P**. We use the Greek letter tau to represent shear stress:

$$\tau \equiv \frac{P}{A_s}. \tag{2.7}$$

We have included a subscript on the area to remind ourselves that the force and area in this expression are magnitudes of vectors that are not parallel to each other. Now that we have defined both strain (kinematics) and stress, we must consider the relationship between them.

2.3 Stress–Strain Relationships

We will see that different materials respond differently to loads. In some materials (e.g., rubber), small loads produce relatively large deformations. Other engineering materials, such as steel, undergo smaller deformations; however, it is still important to consider the effects of such changes. Even very rigid materials, when subjected to a load, will experience a small deformation. Instead of characterizing a material's behavior in terms of loads and deformations, we will do so in terms of stresses and strains, defining the material's *constitutive law*.

For most engineering materials, a simple relationship exists between stress and strain. For each increment in stress, there is a proportional increase in strain, provided that a certain limit of stress is not exceeded. If the induced stress exceeds the limiting value, the strain will no longer be linearly proportional to the stress. This limiting value is called the *proportional limit*.

Most of the behavior we will consider occurs below the proportional limit, in the regime where stress and strain enjoy a linearly proportional relationship. If we subject a material in this regime to a tensile load P_A, producing a stress σ_A and a strain ε_A, then subject it to a tensile load P_B, producing a stress σ_B and a strain ε_B, and then we plot the stresses and strains to see a linear relationship between stress and strain, as shown in Figure 2.11.[*]

This linear relationship between load and deformation was first stated by Robert Hooke in 1678, and became known as *Hooke's law*: *Ut tensio, sic vis*. This Latin phrase—in the form

---

[*] Such experiments were performed by Jacob Bernoulli (1654–1705) and J. V. Poncelet (1788–1867) in the quest to understand materials' responses to loading.
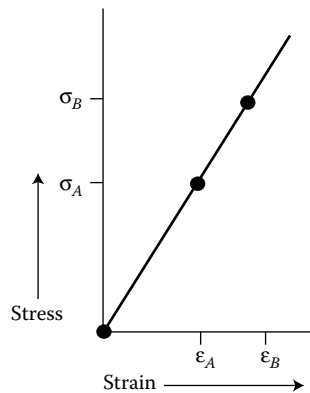
FIGURE 2.11
Linear relationship between stress and strain.

of an anagram, *ceiiinosssttuv*—was how Robert Hooke* summed up his finding, which he first applied to the extension of a spring. It translates: "as is the extension, so is the force." We are familiar with his law in this form:

$$F = kx, \tag{2.8}$$

and have called k the spring constant or *stiffness* of the spring in question. Figure 2.12 shows a representative spring.

The stress–strain diagram is another example of a force (stress being a force per area) being linearly proportional to an extension (strain being extension per initial length). It is too the Hooke's law: *Ut tensio, sic vis*. It too contains a linear constant of proportionality, a *stiffness*.

The ratio of change in stress to change in strain, which is also the slope of the line joining these two data points, is constant for loading below the material's proportional limit. This constant is now known as the elastic modulus (sometimes *modulus of elasticity*) or *Young's modulus*, after Thomas Young, who defined it in 1807. (Young's definition was somewhat awkward and ungainly, since Cauchy had yet to clearly define stress. It was not until 1826 that Claude Navier defined the elastic modulus as we are about to.) The

---

* Hooke (1635–1703) has never received due recognition for his scientific achievements. In addition to craft-ing what we know as Hooke's law, Hooke was an architect and geologist whose studies of microorganisms (using his friend Anton van Leeuwenhoek's newfangled microscopes) and fossils were seminal. Hooke's rela-tive obscurity is largely a result of the efforts of his vindictive contemporary, Sir Isaac Newton, who used his own fame and influence to diminish Hooke's accomplishments; it was his fear that Newton would steal or diminish "ut tensio, sic vis" that led Hooke to publish only his encrypted anagram for Hooke's law. He and Newton had had a feud over the inverse-square law of planetary motion, and Newton was so perturbed by it that he removed all traces of Hooke from his *Principia*. Hooke had even been prescient enough to anticipate the application of his observation of springs to material behavior, having stated that every kind of solid changes its shape when a mechanical force is applied, and that it is this deformation which enables the solid to do what Gordon calls "the pushing back." In so observing, Hooke anticipated the fields of continuum mechanics and elasticity. However, his intellectual heirs Young and Euler were denied their inheritance by Newton, and Hooke remained obscure. Furthermore, we do not know what Hooke looked like, perhaps because—as he is often described as a "lean, bent, and ugly man"—he was unwilling to sit for a portrait.
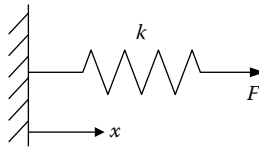
FIGURE 2.12
Linear (Hookean) spring.

elastic modulus for bodies in tension or compression is usually represented by the symbol E and is expressed as

$$E = \frac{\text{Normal stress}}{\text{Normal strain}} = \frac{\sigma}{\varepsilon}, \tag{2.9}$$

where it is understood that this refers to a change in normal stress divided by a change in normal strain. Since strain is a dimensionless quantity (length divided by length), E has the same units as stress: either N/m^2 or Pascals (Pa) in SI units, or lb/in^2 (psi) in U.S. customary units. Table 2.1 shows the values of E for several engineering materials.

Unlike the case of the spring constant k, the elastic modulus does not depend on the geometry of a body; it is the physical stiffness of the material itself. A material's stiffness may be defined as the property that enables the material to withstand stress without great strain, in other words, the material's resistance to deformation.

In the Hookean regime, both springs and solid materials are *linearly elastic*. In the presence of an applied load, stress is linearly related to strain. If an applied load is removed, both stress and strain decrease linearly to zero. However, if a material's proportional limit is exceeded due to an applied load, this is no longer true. In this case, the removal of the applied load causes both stress and strain to decrease linearly, along a line parallel to the linear portion of the stress–strain curve, as shown in Figure 2.13. The strain does not return to zero. By exceeding its proportional limit, the material has undergone a permanent *plastic* deformation. Plastic, as opposed to elastic, deformation represents a permanent set of materials as you likely have observed when bending a paper clip too far. For most materials, the degree of plastic deformation depends on both the maximum stress value reached and the time elapsed before the load is removed. The time-dependent part of plastic deformation, which can also be influenced by temperature, is known as *creep*.

TABLE 2.1

Approximate Design Values of Elastic and Shear Moduli for General Material Categories, in Linear Regimes (SI)

Material	Elastic Modulus, E (GPa)	Shear Modulus, G (GPa)
Steel	200	79
Aluminum alloy	70	26
Glass	65–75	26–31
Rubber	0.001–0.1	0.0003–0.03
Other polymers	0.2–5	0.08–1.5
Concrete	30	13
Bone	1–21	
Wood	8–14	
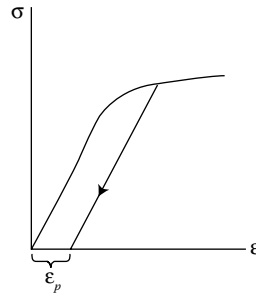
FIGURE 2.13
Plastic deformation incurred when proportional limit is exceeded.

A change in shear stress is also proportional to a change in shear strain, as long as the stress is below the proportional limit for that mode of loading. The constant of shear proportionality is known as the *shear modulus* or the *modulus of rigidity*. It is represented by G and expressed as:

$$G = \frac{\text{Shear stress}}{\text{Shear strain}} = \frac{\tau}{\gamma}. \tag{2.10}$$

Average values of the shear modulus for some common materials are given in Table 2.1. Note that the elastic and shear moduli differ significantly for each material.

It is interesting to observe the consistency of the ratio of E to G, despite the diversity of materials represented in Table 2.1. In Section 4.1, we will further reflect on the relationship between E and G, representing a material's resistance to axial deformation relative to its resistance to shear. Values for more specific materials are in Appendix C.

We now have two additional forms of Hooke's law, the constitutive law for linear elastic materials and likenesses of $F = kx$ for one-dimensional loading:

$$\sigma = E\varepsilon, \tag{2.11}$$

$$\tau = G\gamma. \tag{2.12}$$

In modeling our material body as a linear spring, we are making the assumption of linearity: that we are in the Hookean regime of the material's stress–strain curve and also that we have small deformations.

This model incorporates three further assumptions that thus represent limitations—albeit broad ones—on the kinds of materials it can represent. One assumption is that the material is *homogeneous*, by which we mean the material constants (e.g., the elastic modulus) do not vary from point to point, that is, are *not* functions of the coordinates. The second assumption is that the material is *isotropic*, by which we mean that the elastic properties are invariant with respect to any rotation of the coordinate axes. In other words, no matter of which axis we align with the loading, we see the same material behavior. (Note that the bone and wood listed in Table 2.1 are not isotropic, so that the range of material values given in Table 2.1 reflects different moduli in different directions, as well as variation among different materials in these categories.) The third assumption is that there is no apparent effect of temperature. We will incorporate the effects of temperature in Section 2.10.

Each material has its own characteristic stress–strain curve that illustrates its constitutive law. The extreme values of strain that materials can withstand or vary widely, as do
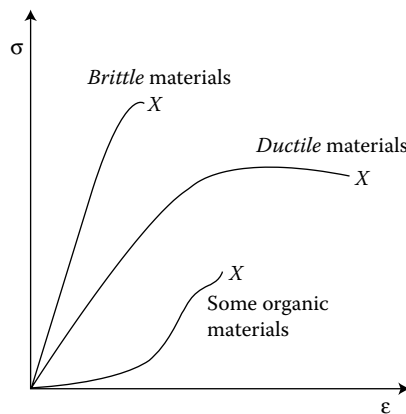
FIGURE 2.14
Schematic of typical stress–strain diagrams.

the slopes of the Hookean portions of their curves, as shown in Figure 2.14. The terminal point on a stress–strain diagram represents the complete failure (rupture or fracture) of the specimen. Materials that are capable of withstanding large plastic strains before they fail are called *ductile* materials. Low-carbon steels, most polymers, and skin are examples of ductile materials. *Brittle* materials, on the other hand, fail abruptly after a small amount of plastic deformation. Cast iron, glass, ceramics, concrete, and bone are examples of brittle materials. Further discussion of material properties is available in Section 2.13.

For the most part, we will be considering homogenous, isotropic materials—materials whose behavior does not depend on the direction of loading. Many engineering materials such as metals and ceramics may be readily modeled this way; however, we have seen that some materials, like wood and bone, have different properties in different directions. Wood is strongest against loading along its grain, and is much easier to break with loads applied across the grain; compact bone is strongest along its long axis to resist compressive loading. For the time being, we will neglect such variations and cling to the assumptions of homogeneity and isotropy, but we will keep in mind that for truly anisotropic materials the results of our calculations will be limited approximations.

2.4 Limiting Behavior

Let's look more closely at an idealized stress–strain diagram (Figure 2.15). This diagram represents the behavior of mild steel, a ductile material. Hooke's law, as we already know, governs the low-strain regime of the diagram, where stress and strain are linearly related. But what's going on at higher stress and strain, as the curve bends and ultimately terminates?

The point at which the curve is no longer linear, often a plateau on the stress–strain diagram, is called the material's *yield point*, defining a *yield strength* (or *yield stress*). Generally, beyond the yield point, it takes much less stress to cause much higher strains than in the Hookean region, and, of course the relationship between stress and strain is no longer linear. In some materials, a maximum stress may be reached just before fracture. This is
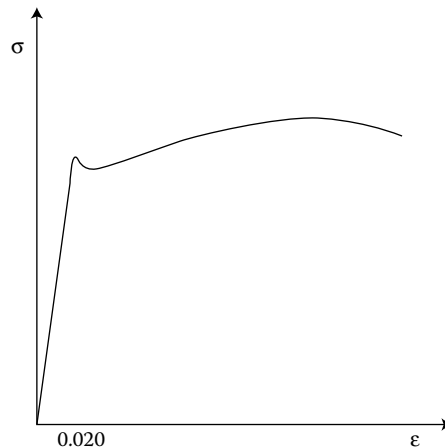
FIGURE 2.15
Idealized stress–strain diagram for mild steel (ductile).

called the *ultimate strength* (or *ultimate stress*) of the material. Finally, we see that the curve ends abruptly at a certain stress point. This point represents the stress that would cause the material to rupture or fracture. From Figure 2.14, we observe that ductile materials can withstand much more strain than brittle materials. We classify materials as *ductile* or *brittle* based on their behavior at room temperature; at elevated temperatures, an otherwise brittle material may behave more like a ductile one, while at lowered temperatures, a ductile material may behave like a brittle one.*

Stress–strain curves for various materials are obtained through rigorous testing of the materials' behaviors in tensile, compressive, and bending tests. The tensile tests are performed in a setup like that shown in Figure 2.2. Near the breaking point, a specimen of mild steel may resemble the sketch in Figure 2.16. The narrowing of the specimen at its midpoint is called "necking." Although the overall cross section of a bar in tension will narrow during elastic deformation (as we will learn in Section 4.1), the dramatic localized necking is plastic deformation.

Necking occurs in ductile materials, or in materials in ductile states. Figure 2.17 contains photographs of a ductile material undergoing necking (Figure 2.17a) and after failure (Figure 2.17b). Brittle materials, such as cast iron, glass, and stone, experience rupture without any observable change in deformation rate, and no necking. A photograph of a brittle material after failure is shown in Figure 2.17c.

The testing, necking phenomenon, and modulus values discussed here are all uniaxial, or one-dimensional, in nature. Values for elastic modulus, yield strength, and ultimate tensile strength are obtained by stretching a specimen until it fails. Values for shear modulus and ultimate shear strength are obtained by applying purely shearing deformations to a specimen. We are beginning to realize that real-world loading is not as simple as these testing conditions. Because of the complexities of real loading and real materials, various

---

* One example of each of these transitions has achieved notoriety. Combustion heating of the steel support members of the World Trade Center (2001) caused the steel to become more ductile and lose strength, contributing to the progressive failure of the towers. Also, the infamous O-ring seal on the Space Shuttle Challenger (1986) became brittle due to cold weather, and allowed hot gas to escape from the Solid Rocket Booster, leading to the destruction of the vehicle.

Original diameter of the specimen
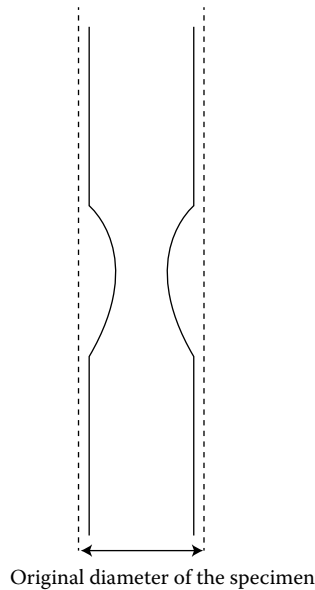
FIGURE 2.16
Necking of a ductile material during tensile testing.

criteria are used to predict failure of structures. In Section 5.4, we will develop such criteria, but for now we will keep this need for reliable predictors of structural failure in mind as we continue our study of continuum mechanics.

The yield and ultimate strengths of a range of engineering materials are shown in Appendix C. Brittle materials do not have meaningful yield strengths, so only ultimate strengths are listed. Note that while different related alloys (e.g., different steels) have similar elastic moduli, they may have very different strengths.

The fracture strength of a solid depends on the strength of intermolecular bonds in the material. Based on this reasoning, the theoretical cohesive strength of a brittle elastic solid can be estimated to be approximately one-tenth the value of E. However, experimentally determined fracture strengths of most engineering materials lie between 10 and 1000 times below this theoretical value. In the 1920s, A. A. Griffith proposed an explanation for this discrepancy that has now become widely accepted: the presence of microscopic flaws or

(a) (b) (c)
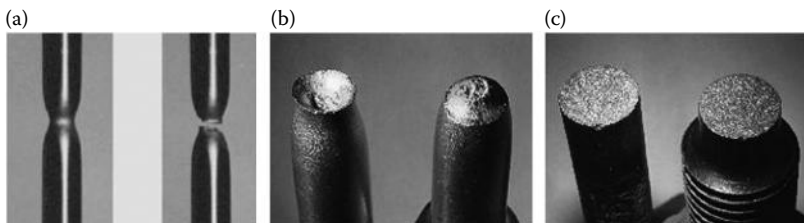
FIGURE 2.17
Ductile material (a) experiencing necking and (b) after failure, and (c) brittle material after failure, in uniaxial tension test. (http://www.hsc.csu.edu.au/engineering_studies/application/lift/3210/index.html. With permission.)

cracks that exist under normal conditions on surfaces and within a body of material reduce a material's overall strength due to stress concentration (as we will learn in Section 2.11). The local amplification of stress accelerates the growth of the crack, accelerating the material's failure. Using strain energy analysis (as in Section 2.12), Griffith showed that the critical stress required for crack propagation in a brittle material depends on the material's elastic modulus and the specific surface energy, and is inversely proportional to the initial size of the crack. A study of materials science would address the microscopic issues involved in stress concentration and crack propagation; in this text, we are concerned with the macroscopic implications for our structures. In particular, brittle materials have different strengths in tension and compression, as tension opens and propagates cracks, while compression tends to close them. Ductile materials, in which plastic deformation at a crack tip reduces stress, are more likely to have the same strengths in tension and compression.

Engineers include *safety factors* in designs. A safety factor is a margin of insurance against unforeseen conditions, material imperfections, fabrication errors, and other uncertainties. The allowable (actually induced) stress in a design must be less than the failure strength or (more conservatively) the yield strength. The safety factor is simply the ratio of failure (or yield) strength to the allowable stress in the current loading conditions (a limit determined from several factors, including material properties, confidence in load prediction, type of loading, possible deterioration, and design life of the structure). Although different applications have different established values, safety factors should have values over 2.0 in robust designs. That is, our analysis should assure us that the allowed stress will never exceed half of the reference (failure or yield) value. For higher-risk applications, we may prefer to use higher safety factors, which can reduce the risk but also increase costs, requiring engineers to use their judgment to make ethical and judicious tradeoffs.

2.5 Equilibrium

We recall our checklist of what is needed to apply continuum mechanics to understand the response of a body to external loading: we must (1) characterize the deformation of a continuous material, (2) define the internal loading, (3) relate this to the body's deformation, and (4) make sure that the body is in equilibrium. We have accomplished the first three items in the list, and now understand that in doing so we have constructed (1) a kinematic description of deformation, or strain; (2) a definition of stress; and (3) a constitutive law relating stress and strain. The last item in our list, (4) equilibrium, is addressed by the method of sections, but we can also consider it in a more rigorous manner.

We have used equilibrium and the method of sections to apply Newton's second law on a "macroscopic" basis. Now we will do a "microscopic" equilibrium analysis in terms of the stress resultants at an arbitrary point in the bar, an infinitesimal element of length dx, and of volume $d\mathcal{V} = A(x)\,dx$, as shown in Figure 2.18. Since the point we have chosen is arbitrary, this analysis is valid at *every* point in the bar, and also for the entire bar.

Because the loading is spread along the bar, the internal axial force $N(x)$ is different at each section. At the point $x + dx$, we represent this force using the first terms in the Taylor-series expansion of $N(x + dx)$. Summing forces in the x-direction on this uniaxially loaded element, we see that the internal axial force $N(x)$ balances both the external axial load $q(x)$,
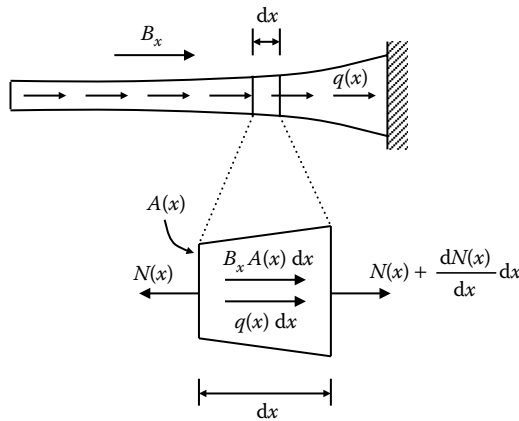
FIGURE 2.18
Equilibrium of an infinitesimal element in one dimension: internal axial force $N(x)$ balances applied axial load $q(x)$ and body force B_x.

a *distributed* axial load per unit length of the bar (a force per length, having units of N/m or lb/ft), and an axial *body force* B_x (a force per volume):

$$\left(N(x) + \frac{dN(x)}{dx}dx\right) - N(x) + q(x)\,dx + B_x A(x)\,dx = 0. \tag{2.13}$$

The load per length $q(x)$ might represent, for example, friction forces distributed on the outer surface of the bar. The volumetrically distributed constant body force per volume B_x allows us to include forces that depend on the intrinsic mass or volume, such as gravity or magnetic fields. For example, to consider the weight of a vertical element, we would use $B_x = \rho g$, if x points toward the center of the Earth. Equation 2.13 can then be simplified, yielding an ordinary differential equation of first order for the axial normal force resultant:

$$\frac{dN(x)}{dx} + q(x) + B_x A(x) = 0. \tag{2.14}$$

If loads are to be modeled as concentrated loads P_i located at coordinates x_i, the distributed load per length can be replaced by a discrete set of point loads with $q(x) = \sum_i P_i \delta(x - x_i)$, where $\delta(x - x_i)$ is the Dirac delta expression that equals 1 where $x = x_i$ and zero elsewhere. Then Equation 2.14 takes the form

$$\frac{dN(x)}{dx} + \sum_i P_i \delta(x - x_i) + B_x A(x) = 0. \tag{2.15}$$

In Section 2.8, we will see that microscopic and macroscopic equilibrium results are in agreement. Our checklist for continuum mechanics analysis is complete:

☑ Kinematics (strain)

☑ Definition of stress

☑ Constitutive law (stress–strain relationship)

☑ Equilibrium

Now that we have developed these four items for one-dimensional loading, we will see what they mean for an axially loaded bar like those in our underwater structure.

2.6 Stress in Axially Loaded Bars

Consider a steel ruler, a thin body made of a seemingly compliant material. We know that if we hold such a ruler by one end and push down on the other end (perpendicular to the ruler's broad surface), as in Figure 2.19a, the loaded end will be deflected significantly. In this case of loading, we call the system a cantilever *beam*. On the other hand, if we instead pull on the free end (parallel with the long axis of the ruler), as shown in Figure 2.19b, we would see very little movement. A system with this type of loading is called a *bar*. It is intriguing that the same body can experience such a dramatically different behavior due to differences in loading. We hope to be able to postulate and develop models to explain these different behaviors.

Once we remove either load from the ruler—once we stop pushing or pulling—the ruler returns to its original, planar shape. In this way, the ruler behaves like an elastic spring, just as Hooke suggested. In our "beam" and "bar" experiments, the different behavior of the ruler can be explained by its having a different stiffness depending on the loading. In Section 2.7, we will derive the bar stiffness, and then in Chapter 9 we will derive the different form of this structural stiffness for beams. We will see in detail that the beam stiffness is much less than the stiffness in the bar mode, which is why under similar applied forces we see greater movement or deflection when the ruler acts like a beam.

For now, the important lesson is that the effective stiffness (a measure of how much a body will resist being deflected by a load) of a structural element or mechanical device is dependent on several factors, including the nature of the loading, as well as the element's geometry and the material itself. Since we are interested in how bodies will react to external forces, this stiffness will provide us with a way to quantify their reactions.

Let us expand our ruler example of a bar in axial loading (Figure 2.20a). The bar is built in, or attached to a wall, at $x = 0$, and is subjected to a single external (applied) load P at $x = L$. The load P acts along the bar's axis. We know from Newton's second law that in order to keep the bar in static equilibrium, the attachment point or wall must exert an equal and opposite force P at the left end of the bar.

What we're interested in, to perhaps establish whether it is strong or stiff enough to meet our requirements, is what's happening *inside* the bar. We can use the method of sections
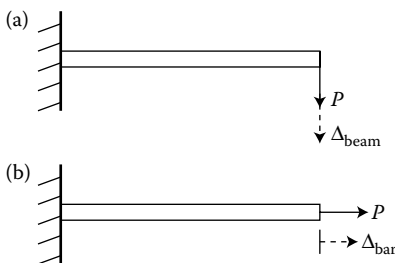
FIGURE 2.19
Steel ruler in (a) beam and (b) bar modes.
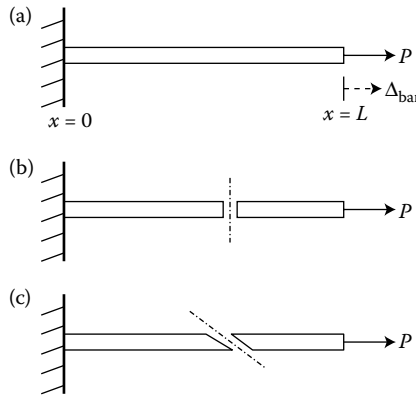
FIGURE 2.20
Stresses on sections of axially loaded bar. (a) An axially loaded bar. (b) Section cut normal to the bar's longitudinal axis. (c) Section cut at an angle θ.

to make an imaginary slice through the bar, exposing a cross section of area A. An FBD will show us that something must be happening on that area to exert a net tensile force P across A. And, if our slice is normal to the bar's axis (as in Figure 2.20b), the exposed area A is also normal to the axis, and we can define the normal stress σ acting on that area as $\sigma = P/A$.

If instead we make our section cut at an angle θ, then the picture will be different (Figure 2.20c). Now, the equilibrating force at the section surface has two components, as shown in Figure 2.21. The normal force component is $P \cos \theta$ and the shear component (parallel to the section surface) is $P \sin \theta$. (These components may be obtained by summing forces in the horizontal and vertical directions.)
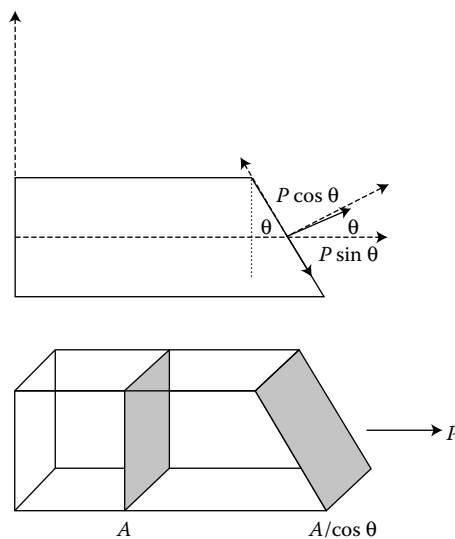
FIGURE 2.21
Sectioning of a bar at an angle θ.

The area of the inclined cross section is $A/\cos\theta$. From these values, we can calculate the magnitudes of normal stress σ_θ and shear stress τ_θ on this angled section by the following two equations*:

$$\sigma_\theta = \frac{\text{force}}{\text{area}} = \frac{P\cos\theta}{A/\cos\theta} = \frac{P}{A}\cos^2\theta, \tag{2.16a}$$

$$\tau_\theta = \frac{P\sin\theta}{A/\cos\theta} = \frac{P}{A}\sin\theta\cos\theta. \tag{2.16b}$$

Both normal and shear stresses will vary with the angle θ. Looking at the equation above for σ_θ, we see that it will reach its maximum value when $\theta = 0°$, that is, when the section is perpendicular to the axis of the bar (as in Figure 2.20b). The corresponding shear stress at $\theta = 0°$ would be zero. Hence we determine the maximum normal stress in an axially loaded bar:

$$\sigma_{\text{max}} = \frac{P}{A}. \tag{2.17}$$

A question to think about: What happens at $\theta = 90°$? Does this make sense?

If we differentiate the equation for shear stress with respect to the angle θ, and set it equal to zero, we should find the angle that produces the maximum value of τ_θ. We find that τ_θ has its maximum value when $\tan\theta = \pm 1$, leading us to the conclusion that τ_{max} occurs on planes of either $+45°$ or $-45°$ with the bar axis. If we substitute $\pm 45°$ into our equation, we find that

$$|\tau_{\text{max}}| = \frac{P}{2A} = \frac{\sigma_{\text{max}}}{2}. \tag{2.18}$$

Thus, the maximum shear stress in an axially loaded bar is only half as large as the maximum normal stress.

Note that as we consider different values for θ we are not changing the load the bar is subject to, but we are merely changing how we represent the stress that this load causes. When we consider applications including multi-dimensional loading in Chapter 5, we will find this concept to be quite important.

2.7 Deformation of Axially Loaded Bars

We have established expressions for stress, strain, and the elastic (Young's) modulus E. These may now be combined into a convenient expression to directly determine the total deformation ΔL for an axially loaded bar (Figure 2.20a). We begin with the definition of the elastic modulus, or Hooke's law, and substitute for stress and strain:

$$E = \frac{\sigma}{\varepsilon} = \frac{P/A}{\Delta L/L} = \frac{PL}{A\Delta L}. \tag{2.19}$$

---

* What we have done here is rotate our axes by the angle θ (we will do this a lot more in Chapter 5). You may have noticed that the shear force is pointing in a negative (rotated) direction, and in fact this stress is negative by the sign convention we will develop. We are only determining the magnitudes of the stress components at this time.

Then, solving for ΔL, we obtain

$$\Delta L = \frac{PL}{AE},$$ (2.20)

where ΔL is the total axial deformation, P the total applied external axial load, L the original length of the bar, A the cross-sectional area of the bar, and E the elastic modulus.

This expression is valid only when the stress in the bar does not exceed the proportional limit. This should make sense, as it is only below this limit that the bar's stress and strain will obey Hooke's law. Also, Equation 2.20 assumes that the force, area, and properties of the bar do not change along its length. For a more complex problem, where quantities vary along the bar's axis (here the x-axis), we can obtain a similar relationship that takes such variations into account:

$$\Delta L = \int_0^L \frac{N(x)}{A(x)E(x)} dx,$$ (2.21)

where $N(x)$ is the internal axial force as in Section 2.5.

We can cast Equation 2.20 in terms of the bar's *stiffness*, as discussed earlier. If we recall the form Hooke's law took for linear springs, $F = kx$, we can write P as a function of ΔL using Equation 2.20:

$$P = \frac{EA}{L}\Delta L.$$ (2.22)

Comparing Equation 2.22 with $F = kx$, we see that the axial deformation ΔL of this bar due to the axial load P depends on its *stiffness* EA/L. We can compare this spring stiffness to that for a beam, loaded as in Figure 2.19a, in Chapter 9.

2.8 Equilibrium of an Axially Loaded Bar

Now we want to combine our kinematics (Equation 2.4), constitutive (Equation 2.11), and equilibrium (Equation 2.15) models to characterize a uniaxially loaded bar. In principle, this is a system of three equations for three unknowns: the strain $\varepsilon(x)$, the stress $\sigma(x)$, and the axial displacement $u(x)$. However, we can simplify the mathematics by eliminating variables and reducing our system to a single differential equation. Since our system of equations includes two first-order differential equations (kinematics, equilibrium) and one algebraic equation (Hooke's law, our constitutive equation), we expect our single equation to be second-order. We achieve this result by writing the stress in terms of strain, and strain in terms of displacement. That is,

$$\sigma(x) = E\,\varepsilon(x) = E\left(\frac{du(x)}{dx}\right).$$ (2.23)

Second, we substitute Equation 2.23 into the equilibrium Equation 2.14 for the case of no distributed load $q(x)$, and with $\sigma(x) = N(x)/A$ to find, assuming that the area and elastic modulus are constant (i.e., they do not vary with the x-coordinate):

$$E\frac{d^2u(x)}{dx^2} + B_x = 0.$$ (2.24)

This is the second-order equation we expected. In the absence of body forces ($B_x = 0$), it is easily integrated, yielding

$$u(x) = C_1 x + C_2. \tag{2.25}$$

To determine the constants of integration in Equation 2.25, we must apply appropriate boundary conditions. As an example, we will solve for the displacement in the bar as is shown in Figure 2.20a. One boundary condition is clear: the displacement (or movement) of the bar is zero at the left end ($u(0) = 0$) because the bar is attached to the wall and restrained there. At the free end, $x = L$, we are pulling with a force P, so that we can express this boundary condition in terms of the strain as

$$\left.\frac{du}{dx}\right|_{x=L} = \varepsilon(L) = \frac{\sigma(L)}{E} = \frac{P}{EA}. \tag{2.26}$$

After applying our two boundary conditions, we find the solution (2.25) to be

$$u(x) = \frac{Px}{EA} + u(0) = \frac{Px}{EA}. \tag{2.27}$$

The net extension of an entire bar of length L is thus:

$$\Delta L = u(L) - u(0) = \frac{PL}{EA}, \tag{2.28}$$

which is in agreement with Equation 2.20, and from which we can recover the expression for the bar stiffness, EA/L, just as in Equation 2.22. We can also see from Equation 2.27 that the strain, as the derivative of $u(x)$, is constant; each section of the bar experiences the same stretch.

2.9 Statically Indeterminate Bars

For some structural systems, the equations for static equilibrium expressed in terms of forces are insufficient for determining reactions.* This may be because some of the reactions are superfluous or redundant for maintaining equilibrium. But even a redundant support feels reaction forces—forces we as engineers must calculate. However, regardless of how many extra support reaction forces there are in a system, we have a fixed number of independent equilibrium equations. Equilibrium equations may also be insufficient when some internal forces cannot be determined using the equations of statics alone. Both of these situations, called *statical indeterminacy*, may arise in axially loaded bar systems.

We can resolve statical indeterminacy by several methods. In all of the available methods, as in all of our mechanics problems, we must make sure of three things, in no prescribed order:

---

* If, instead, equilibrium is expressed in terms of displacements (as will be done in Section 4.6), the distinction between determinate and indeterminate problems vanishes, and we may apply the solution method developed in Section 2.8. However, it is useful to work out a technique to resolve the indeterminacy of problems expressed in terms of stresses.

- Equilibrium conditions for the system must be assured, both locally and globally.
- Geometric compatibility must be satisfied among deformed parts of the body, and at boundaries. This has to do with the kinematics of deformation.
- Constitutive relations such as Hooke's law must be obeyed by all materials of the system.

Of the available methods, the two most commonly used are: (1) the *force* method, in which we first remove, and then restore, a redundant reaction to develop a compatibility equation; and (2) the *displacement* method, in which we maintain compatibility of the displacements of adjoining bars and at the boundaries, and solution displacements are obtained from equilibrium equations.

The displacement method is the basis for most of the finite-element method (FEM) programs that are commonly used to analyze complex structures, and is better suited to large systems. Both methods make use of the analogy between the elastic (Young's) modulus E and the spring constant k. E and k each relate loading and deformation in a linear equation: $\sigma = E\varepsilon$ and $F = kx$. We have just seen that the stiffness of an axially loaded bar may be expressed as $k = EA/L$.

2.9.1 Force (Flexibility) Method

The force method is also sometimes called the force/flexibility method. We will be thinking of our indeterminate bars as elastic members of a system, each bar with a *flexibility* f defined as the reciprocal of k: $f = 1/k = \Delta L/P$, or $f_i = L_i/A_i E_i$. Note that f has physical dimensions of length/force, reciprocal dimensions of the stiffness k.

To illustrate the force method in the case where a compatibility equation cannot be written down directly, consider the following example: In Figure 2.22a, an axial force P is applied at point B of the varying-diameter bar ABC. This axial load leads to reactions R_1 and R_2 being developed at the ends, and the system deforms to the state seen in Figure 2.22b. The deformations shown are exaggerated.

Since only one nontrivial equation of statics is available ($\Sigma F_x = R_1 + R_2 + P = 0$, with two unknown R_i), this system is statically indeterminate to the first degree, meaning there is one more support reaction force than is needed for equilibrium. We will assume positive forces and deflections, so that any result with a negative sign will mean that the force or deflection in question is in the opposite direction from that drawn in Figure 2.22b. The force method tells us to "remove" one of the supports (in the same hypothetical sense that we "slice" bodies open to use the method of sections). We choose to remove the right-hand support with reaction R_2. This permits the system to deform as in Figure 2.22c.

We see that in Figure 2.22c, the same axial deformation Δ_0 occurs at B as at C—in the imagined absence of reaction R_2 (imposed by the right wall), the bar is free to deform in this way. Note that analysis by the method of sections shows that the bar BC is not loaded at all in this imagined situation. If the flexibilities of the elastic bars are f_{AB} and f_{BC}, then we can use the definition of flexibility to write

$$\Delta_0 = f_{AB}P + f_{BC}(0) = f_{AB}P = \frac{PL_{AB}}{A_{AB}E_{AB}}. \tag{2.29}$$

FIGURE 2.22
Force method for statically indeterminate bar ABC: (a) subjected to applied force P; (b) experiencing reactions and deformation; (c) with right support "removed"; and (d) subjected only to the support reactions.

But this deformation violates the geometric condition that is actually imposed at C: there is, truly, a wall that prevents a deflection of even Δ_0. To comply with geometric compatibility, we must find the deflection Δ_2 that would be caused by R_2 acting at C, as shown in Figure 2.22d. This deflection is caused by the stretching (if R_2 is in the direction shown; we might intuitively know that it must be in the other direction to cause compression, but assuming all unknown forces to be positive is a good strategy, and makes a negative result unambiguous) of both constituent bars. Thus,

$$\Delta_2 = (f_{AB} + f_{BC})R_2 = \frac{R_2 L_{AB}}{A_{AB} E_{AB}} + \frac{R_2 L_{BC}}{A_{BC} E_{BC}}. \tag{2.30}$$

We may then achieve compatibility by requiring that at C

$$\Delta_0 + \Delta_2 = 0. \tag{2.31}$$

That is, there is no net deformation of the actual bar system. From this expression, we find an expression for R_2:

$$R_2 = -\frac{f_{AB}}{f_{AB} + f_{BC}} P. \tag{2.32}$$

The negative sign here indicates that R_2 acts in the opposite direction from what we had assumed: the bar is in compression. (The same is true for the deflection, Δ_2. It is negative, reflecting the fact that bar BC is being compressed under this loading.) The original equilibrium equation may now be used to determine R_1. In this problem, it has a negative value, and thus is also pointing in the opposite direction from that assumed. With these reaction forces known, the method of sections provides the internal forces in the bars, tension in AB and compression in BC, as the initial figure suggests.

The idea of the force method is that the complete solution is the sum of the solutions shown in Figure 2.22c and d; the method is an application of the principle of *superposition*. Our premise is that the resultant stress or strain in a system due to several forces is the algebraic sum of these forces' effects when separately applied. This is *only true* if each effect is linearly related to the force causing it, that is, if we are in the Hookean range of behavior.

It may be useful to refer to the following steps of the force method in problem solving:

1. Determine the number of redundants, that is, the number of forces that cannot be determined from equilibrium alone. The number of forces needed to maintain equilibrium is equal to the number of equations of equilibrium, so any additional forces are redundant.

2. Determine *compatibility* equation(s) that describe geometric constraint(s). There should be one such equation for each redundant. In some cases, these may be immediately clear, and a complete set of equations is ready for solution without the following steps. In many cases, the method described above is required. In that case, choose reaction(s) to be the redundant(s) and remove them from the structure, thus temporarily producing a determinate structure. There is no formal method or set of criteria for making the choice, so convenience is the guiding principle for choosing redundants.

3. Calculate the displacements at the points from which redundants were removed, as produced by the actual (given) external loading.

4. Calculate the displacements at the points from which redundants were removed, but now as produced by the reapplied redundants only, without the given external loading.

5. Sum the two displacements at each point where a redundant has been removed, as calculated in the last two steps, that is, as displacement (step 3) + displacement (step 4). Applying superposition to this linear structure, we see that these must be added to equal the actual physical displacement at that point of the fully loaded, indeterminate structure. We then calculate the values for the redundant forces from these equations. (We are now enforcing compatibility or consistency of deformations.)

6. With the redundants determined in step 5 acting, determine the remaining support reactions of the fully loaded, indeterminate structure by applying equilibrium.

This procedure is very general; in practice, any number of axial loads, bar cross sections, material properties, and thermal effects (to be discussed in Section 2.10) on the length of a bar system may be included in your analyses. However, for very large systems, application of the force (flexibility) method is inefficient.

2.9.2 Displacement (Stiffness) Method

The displacement method is also known as the displacement/stiffness method. We remember that the stiffness of an axially loaded bar may be expressed as $k = EA/L$.

If we are presented with a statically indeterminate elastic axially loaded bar system (like that in Figure 2.23a), we may define the stiffness of each bar k_i as $E_i A_i / L_i$. An applied
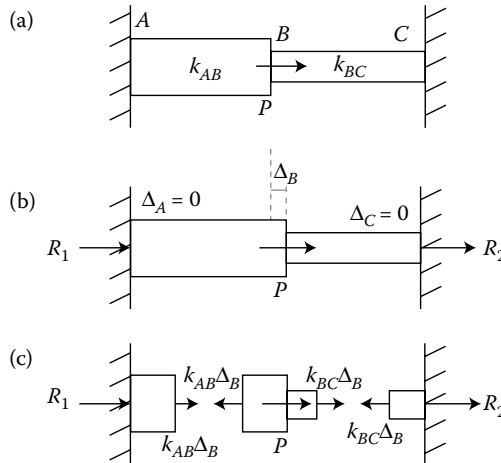
FIGURE 2.23
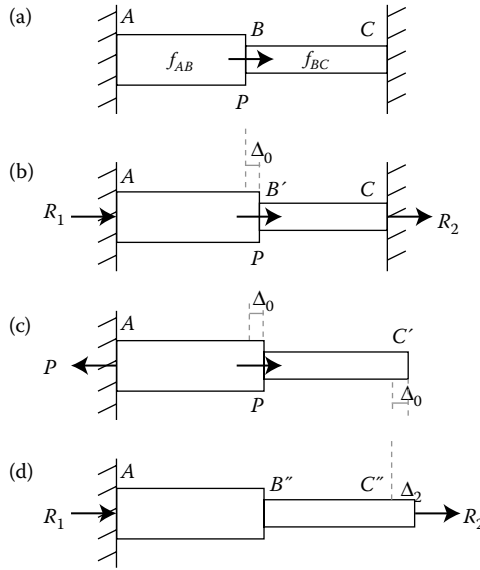Displacement method for a statically indeterminate bar ABC: (a) subjected to applied force P; (b) experiencing reactions and deformation; (c) with "cuts" in sections AB and BC to produce node FBDs.

force P at point B causes reactions R_1 and R_2. As before, these forces and the displacement Δ at B are considered positive when they act toward the right, and initially we assume them to have this sense as shown in Figure 2.23b.

Our objective is to determine the displacement Δ_B. (Since there is only one unknown Δ_B to be determined in this example, this problem is said to have one degree of kinematic indeterminacy, or one degree of freedom.) We also hope to find expressions for the reaction forces R_i.

In the problem considered here (Figure 2.23), the displacement Δ_B causes tension in bar AB and compression in bar BC. But if we had a more complex system and could not determine that through intuition, we could use the approach of assuming positive internal forces (tension) and understanding that final negative results indicate compression. With both external forces assumed positive (pointing to the right) and internal forces assumed positive (acting on bars in tension, whether that means drawing arrows to the left or right for a given bar*), we can produce isolated FBDs of each of the points, or *nodes*, A, B, and C as shown in Figure 2.23c.[†] Writing an equilibrium equation for the free body at node B, we have

$$-P_{AB} + P_{BC} + P = 0. \tag{2.33a}$$

---

* A bar in tension will pull on the nodes to which it is attached, and a bar in compression will push on them.

[†] You might be confused by the combination of sign conventions for external and internal forces. First, be clear that there are two different conventions for the two different types of forces. For external forces, the overall coordinate axes for the problem dictate signs. Typically, we choose pointing to the right and pointing up as positive directions. When we know the direction of a force, we draw it that way on our FBD, but when we do not know the real direction of an external force, we assume these positive directions and understand a negative result to mean the force points the opposite way. For internal forces, tension and compression dictate signs. We have established the convention of tension forces being positive. When we know the direction of a force, we draw it that way on our FBD, but when we do not know the real direction of an internal force, we assume it is pulling on the body (tension) and understand a negative result to indicate that it is actually pushing (compression).

We have more unknowns than equations, so we introduce additional information, the constitutive relation for each bar:

$$P_{AB} = k_{AB} (\Delta_B - \Delta_A) = k_{AB} \Delta_B, \tag{2.33b}$$

$$P_{BC} = k_{BC} (\Delta_C - \Delta_B) = -k_{BC} \Delta_B. \tag{2.33c}$$

Substituting these expressions into Equation 2.33a let us solve for the unknown displacement at node B, and then we can solve (2.33b) and (2.33c) for the unknown internal forces in each bar:

$$\Delta_B = \frac{P}{k_{AB} + k_{BC}}, \tag{2.33d}$$

$$P_{AB} = \frac{k_{AB}}{k_{AB} + k_{BC}} P \quad \text{and} \quad P_{BC} = -\frac{k_{BC}}{k_{AB} + k_{BC}} P. \tag{2.34}$$

Equilibrium for free bodies A and C gives us

$$R_1 = -P_{AB} = -\frac{k_{AB}}{k_{AB} + k_{BC}} P \quad \text{and} \quad R_2 = P_{BC} = -\frac{k_{BC}}{k_{AB} + k_{BC}} P. \tag{2.35}$$

Equation 2.35 tells us that both reaction forces are in directions opposite to those indicated in Figure 2.23b, as we could have expected, and the signs in Equation 2.34 indicate that AB is in tension and BC in compression.

It may be useful to refer to this sequence of steps for the displacement method:

1. Determine the number of redundants, that is, the number of forces that cannot be determined from equilibrium alone. Draw an FBD of the structure with unknown reaction forces pointed in positive coordinate directions.
2. Identify within the structure a number of nodes equal to the number of redundants, and for each of these points identify a nodal displacement of the structure.
3. Draw FBDs of these nodes, with unknown bar internal forces drawn in tension (positive) and sum all the forces at each node to enforce equilibrium.
4. Write internal bar forces in terms of displacements using constitutive laws.
5. Use the system of nodal equilibrium and constitutive equations to solve for unknown nodal displacements and unknown bar internal forces.
6. Determine the support reactions of the fully loaded, indeterminate structure by applying equilibrium.

2.10 Thermal Effects

So far, we have considered mechanical stress and externally applied loads as the only sources of strain in materials. However, solid bodies expand with increasing tempera-

ture and contract with decreasing temperature. These deformations can be represented as *thermal strains*. We define thermal strain ε_T in the following way:

$$\varepsilon_T = \alpha(T - T_0) = \alpha\Delta T, \tag{2.36}$$

where α is an experimentally determined coefficient of (linear) thermal expansion for a given material, and T_0 and T are the initial and final temperatures of our body of interest, respectively. The thermal expansion coefficient α measures dimensional change per degree of temperature change for a given material. Typical values for concrete, carbon steel, and aluminum, in SI units of $(m/m)/^\circ C$ or just $(^\circ C)^{-1}$, range from 9.9×10^{-6} for concrete to 11.7×10^{-6} for carbon steel to 23×10^{-6} for aluminum.

Thermal strain has no directional dependence; equal thermal strains develop in every direction for unconstrained homogeneous isotropic materials. For a body of length L subjected to a temperature change, the extensional deformation ΔL_T is

$$\Delta L_T = \alpha\Delta T L, \tag{2.37}$$

where ΔT is allowed to be positive or negative for increasing or decreasing temperature.

If the body in question is free to expand or contract (i.e., the body is not restrained), no stress is induced by these thermal effects. The dimensional change ΔL_T will simply occur, and the otherwise unloaded bar will continue to be in equilibrium. However, if the body is partially or fully restrained so as to inhibit or prevent this change ΔL_T, internal thermal stresses will develop, and the force/flexibility method of Section 2.9.1 is useful for solving the unknown forces as these are typically statically indeterminate situations.

The stresses and strains due to thermal effects may be combined with other stresses and strains in the same directions by straightforward superposition.

2.11 Saint-Venant's Principle and Stress Concentrations

In applying equations such as $\sigma = P/A$, we have assumed that forces and stresses are distributed uniformly across the surfaces on which they act. In ideal cases such as the axially loaded bars of the previous sections, this is very nearly the true situation. However, in more realistic scenarios, things are more complex. Fortunately for us, many researchers have performed detailed calculations of stress states, and have learned things from the distributions they found. We may benefit from their conclusions without performing arduous computations ourselves.

An exemplary result came from the analysis of an elastic block, acted on by concentrated forces at its ends, as shown in Figure 2.24a. (Of course, in the real world, a truly concentrated force such as this one is not even possible.) The calculated stress distributions at three incremental depths within the bar are shown in Figure 2.24b through d. Clearly, these are not uniform distributions across the cross section, but the stress as calculated by our formula $\sigma = P/A$ is in agreement with the averages of these more carefully obtained profiles.

The important fact to glean from these results is that the normal stresses are nearly uniform on a surface whose distance from the applied force is the same as the width of the body. (This is true despite the high spatial variation in stress at surfaces nearer to the force application.) This point illustrates *Saint-Venant's principle*, as first stated by the eponymous
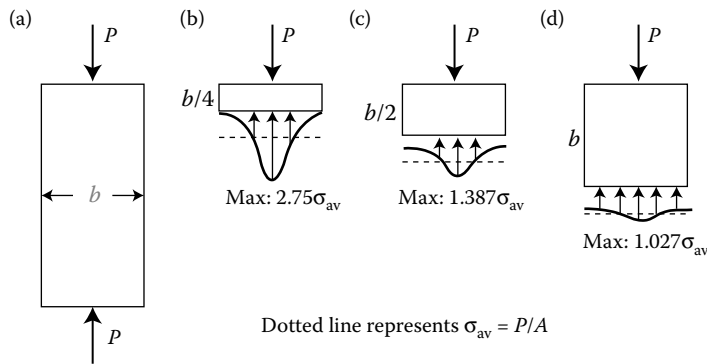
FIGURE 2.24
Stress distributions near concentrated force in a bar. (a) A bar of width b acted on by concentrated load P; and calculated stress distributions on "cut" sections (b) $b/4$; (c) $b/2$; and (d) b from the load application.

French elastician in 1855. It means that the manner of force application (point, or evenly distributed, or other) has a significant effect on the stress distribution *only* in the near vicinity of the force's application. We are applying this principle when we idealize our systems.

Highlighted in Figure 2.24b through d are the maximum normal stresses at each cut and their proportionality to the average stress. This maximum stress and its relation to average stress is a function of geometry. In particular, features such as holes and filleted edges cause areas of stress concentration, and ruin our idealization of uniform stress distribution. A formula is available for the calculation of maximum normal stress:

$$\sigma_{\max} = K\,\sigma_{av} = K\frac{P}{A}, \tag{2.38}$$

where K is an experimentally obtained *stress concentration factor* for the particular geometric feature in question. See Figure 2.25 for stress concentration factors for flat, axially loaded bars with three types of change in cross section.

Whether the area A used in Equation 2.38 is the original area (without a hole) or the reduced area can vary with researcher and data; this naturally affects the value of K. The data in Figure 2.25 are based on the reduced cross section. In cases not covered by the graph in Figure 2.25, another reference (such as *Peterson's Stress Concentration Factors*, by Walter Pilkey) or an online stress concentration calculator may prove useful.

In ductile materials, high stress concentration is not necessarily dangerous because these materials can accommodate high stresses through plastic yielding and subsequent stress redistribution. In brittle materials, cracks may occur in areas of high localized stress and lead to dramatic failure.

2.12 Strain Energy in One Dimension

Thanks to Robert Hooke, we have recognized that a solid material responds to loading in much the same way as a linear spring, as long as the material remains below its
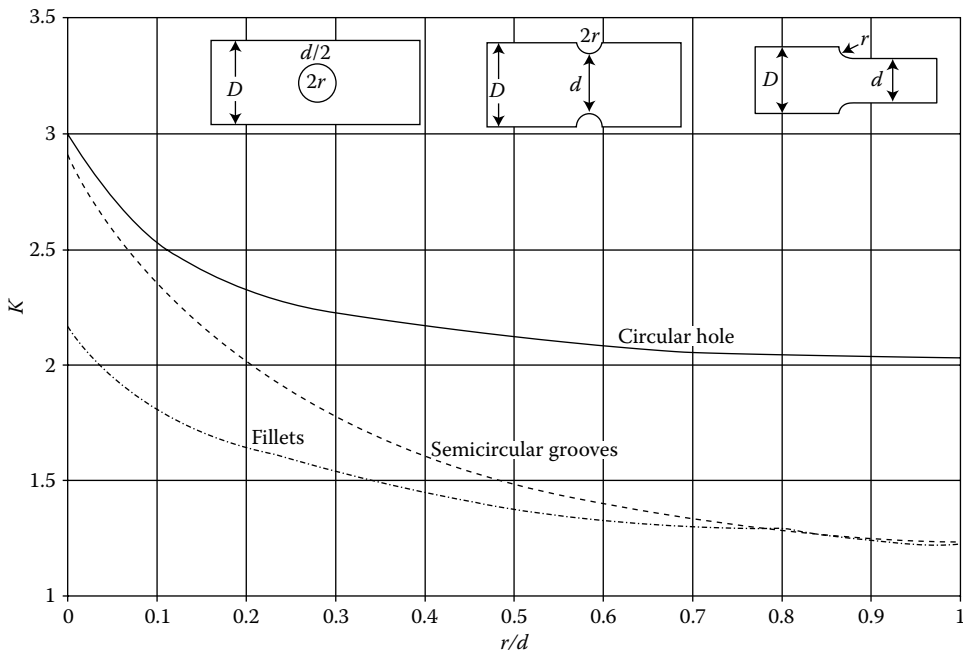
FIGURE 2.25
Stress concentration factors for flat bars. (After M. M. Frocht, Factors of Stress Concentration Photoelastically Determined, *ASME Journal of Applied Mechanics* 2:A67–A68 (1935).)

proportional limit. Recall that the linear elastic spring is an energy storage device for which we can calculate the stored energy as

$$U_{\text{spring}} = \int\limits_0^x F \, \mathrm{d}x = \int\limits_0^x kx \, \mathrm{d}x = \frac{1}{2}kx^2. \tag{2.39}$$

We can also calculate the strain energy stored in a deformed elastic solid. For the elementary one-dimensional Hooke's law, the *strain energy density U_0*, or strain energy per unit volume (check the dimensions), can be calculated as the work done by a stress state acting through its corresponding strain:

$$U_0 = \int\limits_0^\varepsilon \sigma \, \mathrm{d}\varepsilon = \int\limits_0^\varepsilon E\,\varepsilon \, \mathrm{d}\varepsilon = \frac{1}{2}E\,\varepsilon^2. \tag{2.40}$$

As with the comparable spring calculation, we recognize U_0 as the area below the stress–strain curve given by Hooke's law, as is shown in Figure 2.26. The concept of strain energy is the basis for several methods of analyzing displacements and forces in structures.
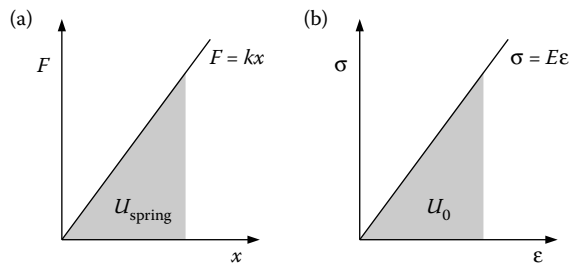
FIGURE 2.26
Constitutive relationships and (a) strain energy for a spring and (b) strain energy density for an elastic solid.

2.13 Properties of Engineering Materials

By performing a tension test, we obtain values for the proportional limit (the end of Hookean behavior), yield strength, and ultimate strength; we also determine the elastic modulus, percent elongation, and percent reduction in cross-sectional area. These values provide quantifiable definitions for the vocabulary generally used to discuss the way a material responds to loading and deformation.

- *Stiffness* is resistance to deformation. As we have seen, the stiffness of a material in the elastic range of deformation is indicated by its elastic modulus E or shear modulus G.

- *Strength* refers to the greatest stress a material can withstand before failure. This may be quantified by the proportional limit, which gives the yield strength (or yield stress), or the ultimate strength (ultimate stress), depending on the type of material and loading being considered.

- *Elasticity* is what enables a material to regain its original dimensions after a deforming load is removed. No known material is completely elastic in all ranges of stress. However, most engineering materials are elastic over large ranges of stress. Deformations beyond the elastic region are referred to as *plastic deformations*, and cannot be completely recovered.

- *Ductility* is what allows a material to undergo considerable plastic deformation under tensile load before final failure—to "bend before it breaks," or absorb energy by plastic deformation before fracturing. We can see this on the stress–strain curve for ductile materials (Figure 2.15): the curve features a sizeable, near-flat region beyond the Hookean limit, in which stress increases very little, while deformation increases. Ductility is characterized by the percent elongation of the specimen during the tensile test and by the percent reduction in area of the cross section (due to necking) at the plane of fracture. A high percent elongation indicates a highly ductile material; a material is considered ductile if its percent elongation before failure is greater than 5%. Many steels, aluminum alloys, and plastics are ductile. Often increasing a material's strength via chemical or thermomechanical means will decrease its ductility.

- *Brittleness* implies the absence of plastic deformation before abrupt failure. This is reflected in a stress–strain curve that ends rather suddenly after the proportional

limit. Brittle materials, such as cast iron, concrete, and stone, are relatively weak in tension and are usually tested and used in compression.

- *Malleability* is what enables a material to undergo considerable plastic deformation under compressive load before fracture. Most ductile materials are also quite malleable. When processing includes hammering or rolling of a metal, malleable materials are the best choice, because they are able to withstand the large compressive deformation that accompanies these processes.

- *Toughness* enables a material to endure high-impact loads or shock loads. In a high-impact load, some of the energy of the blow is transmitted to and absorbed by the body. Toughness is a measure of the energy required to crack the material. We can measure toughness by calculating the area under the entire stress–strain curve.

- *Resilience* enables a material to endure high-impact loads without inducing a stress above the elastic limit. In a resilient material, for example, rubber, the energy absorbed during the blow is stored and recovered when the body is unloaded. Resilient materials are well-suited to applications like baseball bats. We can measure resilience by calculating the area under the elastic portion of the stress–strain curve from the origin through the elastic limit. This is the strain energy density U_0, as we remember.

As has been suggested in the above descriptions of these properties, treatments or manufacturing techniques that change one of these properties will also affect the others. For example, quenching carbon steel makes it harder, but less tough and more brittle than it was before quenching. As designers, we must make tradeoffs and optimize the combination of material behaviors in our systems.

Many common materials may be categorized as metals, ceramics, and polymers, but there are natural and fabricated materials that fall outside these categories.

2.13.1 Metals

Metals are typically categorized as ferrous, meaning iron-containing, or nonferrous. Specific ferrous alloys are the primary metals currently used in civil engineering and other structures, as they are relatively inexpensive and easy to produce. The iron in ferrous metals must be extracted from the iron ores, which often contain impurities such as phosphorous and silica that must be removed during production. Steel and cast iron are the two most common forms of ferrous metals, and both are fundamentally iron–carbon alloys. Other elements such as manganese, nickel, and chromium are added to alter physical and mechanical properties.

Steel is an alloy consisting almost entirely of iron (less than 2%, and often less than 1%, carbon, and similar amounts of any other elements), and its properties may be changed dramatically by varying the composition through thermal and mechanical processing. Cast iron is a generic name for a group of alloys of carbon and silicon with iron. Most have at least 3% total carbon by weight. The graphite flakes in cast iron cause stress concentrations, making the cast iron as a whole fairly brittle.

The mechanical properties of the primary nonferrous metals depend on their principal element, the quantity and type of alloying element(s), on the method of manufacturing, and the heat-treating process.

Aluminum's basic raw material is bauxite ore. High-purity aluminum is soft, weak, and ductile. However, with the addition of small amounts of alloying elements such as

magnesium, silicon, and chromium, it becomes much stronger. As with steels, thermal and mechanical processing also have a large effect on properties. Aluminum alloys are lightweight, almost three times less dense than steel, and highly resistant to corrosion under most conditions. However, aluminum also has an elastic modulus that is approximately three times less than that of steel. It has good thermal conductivity and high electrical conductivity which are often useful properties, but it also has a high coefficient of thermal expansion, which can be a drawback.

Titanium and its alloys have attractive engineering properties. They are light, with densities between those of aluminum and steel, and also possess very high strength, up to twice that of aluminum. This combination of moderate weight and high strength gives titanium alloys the highest strength-to-weight ratio of any common structural metal. Titanium alloys also have excellent corrosion resistance, low coefficient of thermal expansion, high melting point, and high electrical resistivity. However, titanium's high cost has limited its utility and range of applications.

Copper's most significant properties are its high electrical conductivity, high thermal conductivity, good resistance to corrosion, and good malleability and strength. These properties are exploited in heat-exchange equipment and many other applications, but most of all in the electrical field. Brass, which is an alloy of copper and zinc, is the most common copper alloy. Bronzes are alloys of copper and, typically, tin or aluminum.

2.13.2 Ceramics

Ceramics are combinations of both metallic and nonmetallic elements, commonly oxygen, nitrogen, and carbon. They include traditional ceramics such as clays, glasses, and cements as well as advanced materials such as pure oxides, carbides, and nitrides. Ceramics are generally very stiff and hard, and are good thermal and electrical insulators. Traditional ceramics are typically brittle, but advanced materials have been developed to be more resistant to fracture.

A common engineering material, concrete consists mainly of a mixture of cement, fine and coarse aggregates (sand, gravel, crushed rock, etc.), and water to harden the mixture. The compressive strength of concrete is relatively high, but it is a fairly brittle material with low tensile strength. Steel reinforcing rods are often used in combination with concrete; the steel resists tension and the concrete resists compression. Please see Chapter 15 for more information about reinforced concrete and other composite materials.

2.13.3 Polymers

Polymers are a group of synthetic organic materials with chain-like structures created by a process called polymerization. They include plastics and rubbers, and a key quality is that they can easily be formed into complex shapes. A distinction is made between thermoplastic polymers, which can be repeatedly softened and made to flow by heating, and thermosetting polymers which have network structures and do not soften when heated. Most thermosetting plastics are relatively brittle, hard, and strong, while thermoplastics are typically ductile, low in strength, and resistant to impact. Exceptions are rubber materials, which are usually thermosetting polymers but are very resilient. Specific polymers have been developed to have desirable properties such as good chemical resistance, high electrical resistivity, high abrasion resistance, and low coefficient of friction.

2.13.4 Other Materials

Many materials do not fit neatly in the above categories. Some of these are natural materials such as wood and biomaterials, and others are engineered materials such as composites. As advanced materials such as semiconductors and nanomaterials of course obey the principles of continuum mechanics, we just need to employ sufficiently complex models (e.g., constitutive laws) to account for their specific structures.

Wood, one of the oldest natural construction materials, is a cellular organic material. We divide wood into two classes: hardwood and softwood. These are somewhat misleading terms in that there is no direct relationship between these designations and the actual hardness or softness of the wood. Softwood comes from conifers (trees with needle-like or scale-like leaves), and hardwood comes from deciduous trees. Mostly, the wood used in the United States for structural purposes is softwood, most often Douglas fir and southern pine. Allowable stresses for lumber must take into account species and grade (quality), as well as conditions under which the lumber is to be used, such as load duration and moisture conditions. Importantly, for our purposes, wood is not homogenous or isotropic. We will sometimes choose to apply the models that we are learning to wood materials, but we always remember that significant assumptions are being made. When needed, more complex models that account for anisotropy can be used.

The modern usage of the phrase "engineering materials" also includes both natural and synthetic biomaterials, whose properties can be quite complex. Please see Chapter 14 for a more involved discussion of the mechanics of biomaterials.

Engineered materials such as particle- and fiber-reinforced composites are multi-phase materials. They are composed of multiple components to produce properties that are superior to those of the individual components. Concrete, which was described in the ceramics section because of the nature of its components, is a particle-reinforced composite. Fiberglass and carbon-fiber materials are created from dissimilar materials: glass or carbon fibers imbedded in polymer. Like wood, these materials are not homogeneous or isotropic, and we must take care when making assumptions about their behaviors.

2.14 A Road Map for Strength of Materials

For one-dimensional loading, we have addressed the checklist for continuum mechanics, involving (1) kinematics, or description of deformation; (2) a definition of stress; (3) a relationship between stress and strain; and (4) equilibrium. We must next turn our attention to loading in multiple dimensions, so that we may model more realistic problems. If we look back at our modeling of stretched or compressed bars, we can discern a pattern of thought that serves as a road map for a more general approach to problems in strength of materials, structural analysis, and elasticity.

Our road map encompasses several major physical elements, beginning with the external loads—the applied loads on a solid. These loads or forces are the drivers of our analyses because, as engineers, we design structures and machine elements in order to support, guide, and contain the effects of the external loads. This was illustrated in our analysis of a long, thin bar that was being pulled (or pushed) by an axial force.

The reactions are external forces that support the loaded body and keep it from moving in response to the given applied loads. They are determined by requiring the body in its entirety to be in equilibrium under the given externally applied loads. There are many kinds of reactions. We needed only one axially directed support to ensure equilibrium for the stretched (or compressed) bar.

The internal forces $N(x)$ are the force distributions or resultants needed to maintain internal equilibrium. Stresses describe the distribution of the internal forces over planar sections drawn through the body's interior. They were defined as functions of the body's coordinates. So, although it seemed relatively straightforward to define a stress as the quotient $N(x)/A$, where A is the bar's cross-sectional area, we want to extend and generalize this simple definition.

The strains are measures of the deformation of the body that result from the applied forces. There are many definitions of strain, which we reviewed in Section 2.1. The mechanical strains are specifically related to the stresses by constitutive laws that describe the properties of the material of which the body is made (Section 2.3). Thermal strains were discussed in Section 2.10. The strains are required to be compatible, by which we mean that their point-by-point variation cannot produce holes in the continuous material of which the body is made, nor can they permit deformation that violates any geometrical constraints relative to the supports that keep the body in place. Simply put, we want our models to reflect "well-behaved" deformation that does not produce physically untenable results.

The displacements or the deflections are the (generally) more visible movements of the body. The strains are typically found by differentiating the displacements or deflections with respect to spatial coordinates, as we began to see in Section 2.1.1 and will further explore in Chapter 4. The deflections must also be compatible, that is, they must conform with the geometry of the body and its support constraints.

In the language of continuum mechanics, we can now restate our four-item checklist as three major physical considerations that must be applied:

- *Equilibrium* considerations relate external forces, reactions, internal forces, and stresses. That is, we apply Newton's second law to relate external loads to reactions; the method of sections to relate external forces and reactions to internal (resultant) forces; and consideration of areas on which forces act to relate internal forces to stresses. (This consideration comprises the second and fourth items on our checklist.)

- *Constitutive laws* relate stresses to strains. We invoke constitutive laws to describe the properties of the material of which a body is made. (This is the third on our four-item checklist.)

- *Compatibility* considerations relate strains to displacements and/or deflections, that is, kinematics. We pay attention to compatibility both when calculating movements and deflections and when ensuring consistency and continuity with respect to the geometry of the body and its support constraints. (This has been, so far, the first on our checklist: the kinematics of deformation.)

The order in which we apply these criteria, or in which we check off items on our checklist, is not important. The requirement is that our analyses include all of them, no matter the order.

2.15 Examples

EXAMPLE 2.1

Consider the given structure that might be part of an underwater oil rig-turned-artificial reef from Chapter 1. All bars of the truss pictured here have a cross-sectional area of $500\,\text{mm}^2$, and all the bolts and pin connectors have diameter 20 mm. Find the normal stresses in bars BC and DE.
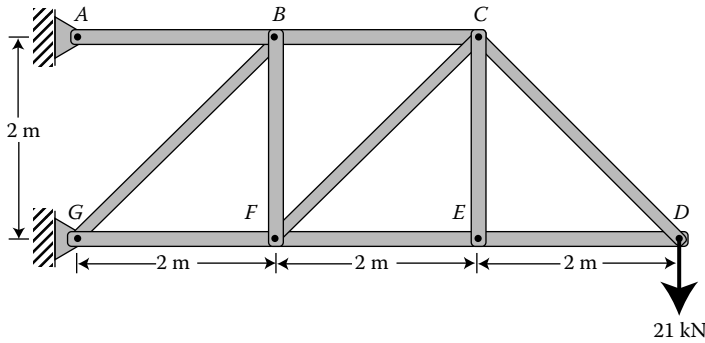
Given: Dimensions of and loading on truss system.

Find: Normal stresses in bars BC and DE.

Assume: Equilibrium; planar system; neglect weights of bars.

Solution

We first use the method of sections to examine an FBD of the joint at D:
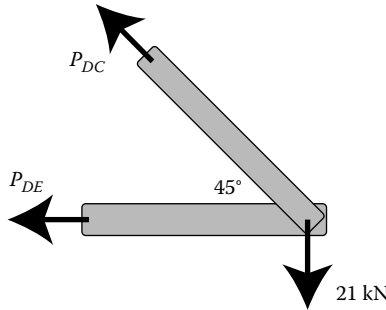
Note that we have assumed both bars DC and DE to be in tension; if we calculate negative values for either internal force, we will know that this assumption was incorrect and that the bar is in compression. Since the joint must be in equilibrium, we have

$$\sum F_y = 0 = P_{DC}\sin 45^\circ - 21\,\text{kN} \;\rightarrow\; P_{DC} = 29.7\,\text{kN},$$

$$\sum F_x = 0 = -P_{DE} - P_{DC}\cos 45^\circ \;\rightarrow\; P_{DE} = -21\,\text{kN}.$$

Using the definition of normal stress and the given cross-sectional area A, we have

$$\sigma_{DE} = \frac{P_{DE}}{A} = -42 \times 10^6\,\text{N/m}^2,$$

or

$$\sigma_{DE} = 42 \,\text{MPa compressive.}$$

In our next use of the method of sections, we make an imaginary cut between B and C, resulting in an FBD that includes the internal forces in three bars of the truss:
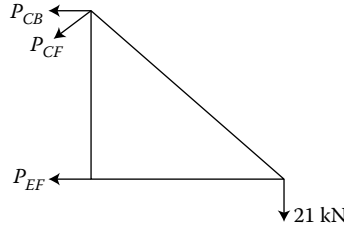
The force equilibrium equations are of course valid, but we cleverly find the bar force of interest directly by applying the third equilibrium equation, summing moments about point F, which is the intersection of the two bar forces that we are not asked to find. Point F is not even on our isolated section, but the moment about any and all points must be zero.

$$\sum M_F = 0 = P_{CB} \cdot (2\,\text{m}) - 21\,\text{kN} \cdot (4\,\text{m}) \;\rightarrow\; P_{CB} = 42\,\text{kN},$$

so that

$$\sigma_{CB} = \frac{P_{CB}}{A} = 84 \times 10^6 \,\text{N/m}^2,$$

$$\sigma_{CB} = 84 \,\text{MPa tensile.}$$

We may take this opportunity to check our intuition about this truss. The load, P, is pulling the structure down. Thus, the composite bar ABC should become longer, and $DEFG$ should become shorter. This would mean that bars on the top (like BC) would be in tension, and bars on the bottom (like DE) in compression. Our results are consistent with our physical intuition.

EXAMPLE 2.2

Consider again the truss from Example 2.1. Find the shear stress in the bolt at A if it is in double shear. A connection element (bolt or pin) is said to be in "single shear" if one cut between the bar and its support is sufficient to break the connection, as shown below on the left; "double shear" means that two cuts are needed to break the connection, as on the right.

Single shear   Double shear
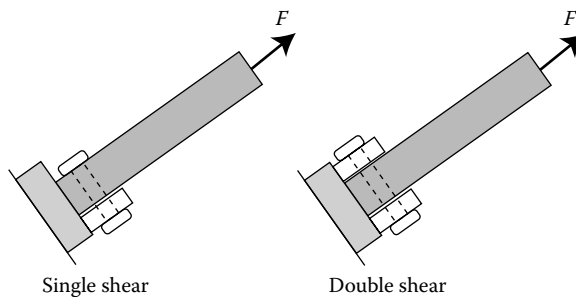
Given: Dimensions of and loading on truss system with connection bolt in double shear.

Find: Shear stress in the bolt in double shear.

Assume: Equilibrium; planar system; symmetric loading on bolt.

Solution

To find the reaction forces at the supports, we consider an FBD of the entire truss. Directions have been assumed for the unknown forces; any negative values in our results will indicate that the real direction is opposite of that assumed.
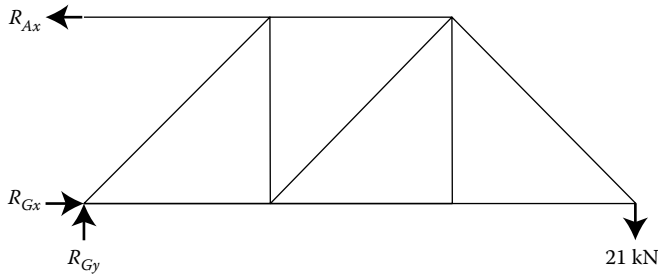
Summing moments about point G, since we are interested in the force at A, we have:

$$\sum M_G = 0 = R_{Ax} \cdot (2\,\text{m}) - 21\,\text{kN} \cdot (6\,\text{m}) \;\rightarrow\; R_{Ax} = 63\,\text{kN}.$$

Now, we draw an FBD of the bolt itself.
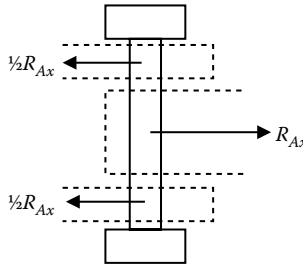
$\sum F_x = 0$ and the symmetry assumption lead to forces of $R_{Ax}/2$ in each support bracket. Using the method of sections, we see that this is also the maximum value of shear force in the bolt. So the shear stress in the bolt at A is

$$\tau_A = \frac{R_{Ax}/2}{A_\text{bolt}} = 100 \times 10^6\,\text{N/m}^2 = 100\,\text{MPa}.$$

EXAMPLE 2.3

An infinitesimal rectangle at a point in a reference state of a material becomes the parallelogram shown in a deformed state. Determine (a) the extensional strain in the $\text{d}L_1$ direction; (b) the extensional strain in the $\text{d}L_2$ direction; and (c) the shear strain corresponding to the $\text{d}L_1$ and $\text{d}L_2$ directions.

Reference state   Deformed state
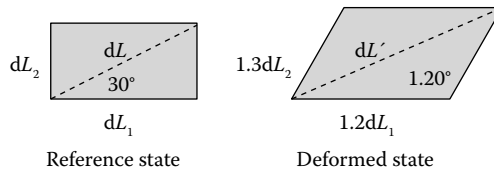
Given: Reference and deformed geometries of infinitesimal rectangle.

Find: Normal and shear components of strain.

Assume: Strain definitions are adequate; use of "true" strain integral is unnecessary.

Solution

a. Normal strain in dL_1 direction, $\varepsilon_1 = \dfrac{\Delta dL_1}{dL_1} = \dfrac{1.2dL_1 - dL_1}{dL_1} = 0.2$.

b. Normal strain in dL_2 direction, $\varepsilon_2 = \dfrac{\Delta dL_2}{dL_2} = \dfrac{1.3dL_2 - dL_2}{dL_2} = 0.3$.

c. Shear strain is the angular deformation, or change in angle between two reference lines. In the reference state, the angle between dL_1 and dL_2 is 90°, or $\pi/2$. In the deformed state, the angle between these lines is 60°, or $\pi/3$. The shear strain is thus:

$$\gamma_{12} = \frac{\pi}{6} = 0.52 \text{ rad}.$$

Note: If we tried to approximate shear strain by the tangent of this angular deformation instead of using the angle itself, we would obtain:

$$\gamma = \frac{1.3dL_2 \sin \pi/6}{dL_2} = 0.65 \text{ rad}.$$

This is close, but not *that* close, to 0.52 rad. The angular change in this problem is not sufficiently small to justify the use of the tangent in place of the angle itself.

EXAMPLE 2.4

Three metal balls are suspended by three wires of equal length arranged in sequence as shown. The masses of the balls, starting at the top, are 2, 4, and 3 kg. In the same order, beginning at the top, the wires have diameters 2, 1.5, and 1 mm, respectively. (a) Determine the most highly stressed wire, and (b) by changing the location of the balls, optimize the mass locations to achieve a system with minimum stresses.
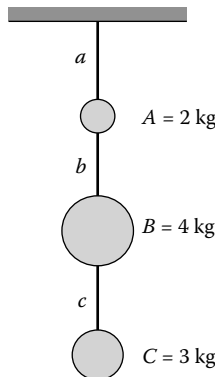
Given: Dimensions and arrangement of steel balls.

Find: Stresses in each wire; lowest stress configuration.

Assume: Neglect weights of wires.

Solution

a. We must find the internal force within each wire, then divide by the wire's cross-sectional area, to find the normal stress in each wire. For each wire, the internal force will equal the mass this wire must support times the acceleration of gravity. This can be found by using the method of sections by making an imaginary cut in a wire and drawing an FBD of the system below the cut. For example, the top wire, a, must support $(2 + 4 + 3)$ kg, so its internal axial force is 88.3 N. We tabulate these calculations:

	P_i(N)	A_i (m^2)	σ_i (MPa)
Wire a	88.3	3.14×10^{-6}	28.1
Wire b	68.7	1.77×10^{-6}	38.8
Wire c	29.4	0.79×10^{-6}	37.2

The wire subjected to the highest stress is wire b.

b. To achieve a minimum stress system, we recognize that stress is inversely proportional to cross-sectional area. Hence, since $A_a > A_b > A_c$, wire a should carry the largest load (which it must), and wire c should support as little load as possible. This leads us to the following configuration, with the maximum stress reduced by about 10 MPa:
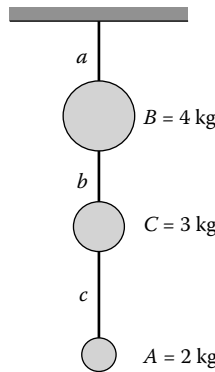
	σ_i (MPa)
Wire a	28.1
Wire b	27.7
Wire c	24.8

EXAMPLE 2.5

A steel bar of 10 m long used in a control mechanism must transmit a tensile force of 5 kN without stretching more than 3 mm, nor exceeding an allowable stress of 150 MPa. What must the diameter of the bar be? State your answer to the nearest millimeter, and use $E = 200$ GPa.

Given: Dimensions and loading on steel bar.

Find: Required bar diameter to nearest millimeter to meet stress and strain requirements.

Assume: Hooke's law applies.

Solution

We will impose both strength and stiffness constraints on the bar, and see which is the limiting case. Using the definition of normal stress, we must have

$$\sigma = \frac{P}{A} \leq 150 \, \text{MPa, or}$$

$$A \geq \frac{P}{150 \, \text{MN/m}^2} = \frac{5000 \, \text{N}}{150 \times 10^6 \, \text{N/m}^2} = 33.3 \times 10^{-6} \, \text{m}^2 = 33.3 \, \text{mm}^2.$$

If Hooke's law applies, as we have assumed it does, then $\Delta L = PL/AE$, and we must have

$$\frac{PL}{AE} \leq 3 \, \text{mm, or}$$

$$A \geq \frac{PL}{\Delta L E} = \frac{5000 \, \text{N} \cdot 10 \, \text{m}}{(0.003 \, \text{m})(200 \times 10^9 \, \text{N/m}^2)} = 83.3 \times 10^{-6} \, \text{m}^2 = 83.3 \, \text{mm}^2.$$

We see that the stiffness criterion produces the limiting case and that we must have a cross-sectional area greater than or equal to $83.3 \, \text{mm}^2$ to safely meet our constraint. This is all we need to find the required diameter of the steel bar:

$$\frac{\pi}{4} d^2 \geq 83.3 \, \text{mm}^2, \text{ so}$$

$$d \geq 10.3 \, \text{mm}.$$

So to the nearest millimeter, we must use an 11-mm diameter bar.

EXAMPLE 2.6

A solid bar 50 mm in diameter and 2000 mm in length consists of a steel and an aluminum section, as shown. When an axial force P is applied to the system, a strain gage attached to the aluminum indicates an axial strain of 873×10^{-6} m/m (also written as 873 µstrain). Determine the magnitude of applied force P.
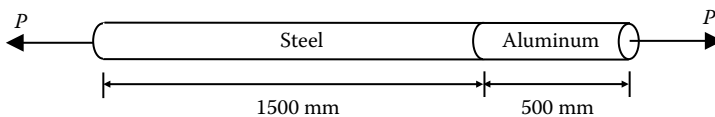
If the system behaves elastically, find the total elongation of the bar.

Given: Dimensions of composite bar, and measured normal strain.

Find: Applied force P, and elongation of bar, ΔL_{total}.

Assume: Hooke's law applies.

Solution

The diameter of the bar is 50 mm, so the cross-sectional areas of both parts are equal:

$$A_{St} = A_{Al} = \frac{\pi}{4}(0.05\,\text{m})^2 = 1.96 \times 10^{-3}\,\text{m}^2.$$

The elastic moduli for aluminum and steel may be looked up in Table 2.1 or in another reference.

$$E_{Al} = 70\,\text{GPa} \quad \text{and} \quad E_{St} = 200\,\text{GPa}.$$

If Hooke's law applies, we can relate the strain measured in the aluminum portion to the stress induced by P in that portion:

$$\varepsilon_{Al} = 873 \times 10^{-6} = \frac{\sigma_{Al}}{E_{Al}} = \frac{P/A_{Al}}{E_{Al}},$$

so

$$P = (873 \times 10^{-6})(70 \times 10^9\,\text{Pa})(1.96 \times 10^{-3}\,\text{m}^2) = 120\,\text{kN}.$$

We can exploit Hooke's law and superpose the displacements of both portions of the bar:

$$\Delta L_{\text{total}} = \sum \frac{PL}{AE} = \left(\frac{PL}{AE}\right)_{St} + \left(\frac{PL}{AE}\right)_{Al}$$

$$= \frac{120{,}000\,\text{N}}{1.96 \times 10^{-3}\,\text{m}^2}\left[\frac{1.5\,\text{m}}{200 \times 10^9\,\text{N/m}^2} + \frac{0.5\,\text{m}}{70 \times 10^9\,\text{N/m}^2}\right] = 896 \times 10^{-6}\,\text{m}.$$

$$\Delta L = 896\,\mu\text{m, or } 0.896\,\text{mm}.$$

Note: The aluminum section is only a third as long as the steel, but it deforms nearly as much.

EXAMPLE 2.7

If we would like to redesign the steel and aluminum bar from Example 2.6 to reduce its weight, we could reduce the diameter of the section that has a higher safety factor. If the bars are steel with an yield strength of 520 MPa and aluminum with an yield strength of 240 MPa, determine which section should be reduced and what the new diameter should be so that the safety factor for the whole system remains the same.

   Given: Dimensions of composite bar, and load computed in Example 2.6.

   Find: Reduction in diameter of one material so that both materials have the same safety factor.

   Assume: Hooke's law applies; neglect stress concentration that will be introduced by creating a stepped bar.

Solution

The safety factors are, for the specified common alloys of steel and aluminum,

$$\text{SF}_{Al} = \frac{\sigma_{Al_{\text{yield}}}}{\sigma_{Al}} = \frac{240\,\text{MPa}}{\sigma_{Al}} \quad \text{and} \quad \text{SF}_{St} = \frac{\sigma_{St_{\text{yield}}}}{\sigma_{St}} = \frac{520\,\text{MPa}}{\sigma_{St}}.$$

For the original bar with equal diameters, the stresses in the aluminum and steel are equal, so the steel has a factor of safety that is more than twice as large and it is this bar that should be reduced. The value of the safety factor in the aluminum for any value of load P (in N) is

$$SF_{Al} = \frac{240\,\text{MPa}}{P/((\pi/4)(0.05\,\text{m})^2)} = \frac{471 \times 10^3}{P}.$$

In order to match this for steel, we consider

$$SF_{St} = \frac{471 \times 10^3}{P} = \frac{520\,\text{MPa}}{P/((\pi/4)d_{St}^2)},$$

and solve for $d_{St} = 34\,\text{mm}$.

EXAMPLE 2.8

A load P is supported by a bar with a cross-sectional area A_B and elastic modulus E_B as well as a cylinder with a cross-sectional area A_C and elastic modulus E_C. The bar and the cylinder are of the same length L and the load P is applied to them via a rigid end plate. Determine expressions for (a) the stresses in the bar and the cylinder and (b) the total change in the length of the assembly.
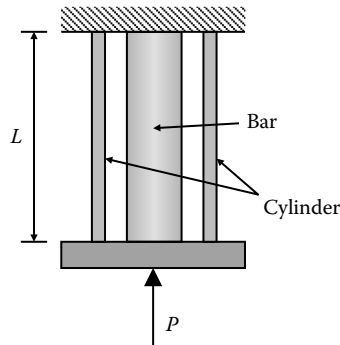
Given: Elastic and geometrical properties of the bar and cylinder system.

Find: Stress in each element and total length change.

Assume: Hooke's law applies. Neglect weight of the bar and the cylinder.

Solution

a. The first thing we need is an FBD, in particular, of the end plate because it is the element that is directly loaded by all forces in the problem.
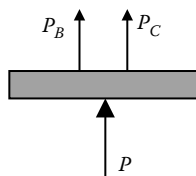
We ensure that this system is in equilibrium by stating

$$\sum F_y = 0 \quad \text{or} \quad P_B + P_C = -P.$$

This one equation contains two unknowns: the problem is statically indeterminate. We have two methods for solving such problems and both are suitable for this problem.

First, to use the force method, we must find the compatibility equation that describes the geometric constraints on the system. In this problem, the task is straightforward: the bar and the cylinder are of the same length and because the top plate is rigid, they experience the same change in length. So $\Delta L_B = \Delta L_C$.

Using Hooke's law, we can write these displacements as:

$$\Delta L_B = \frac{P_B L}{A_B E_B} \quad \text{and} \quad \Delta L_C = \frac{P_C L}{A_C E_C}.$$

So, imposing the geometric compatibility constraint, we have

$$\frac{P_B L}{A_B E_B} = \frac{P_C L}{A_C E_C},$$

or

$$P_B = \frac{A_B E_B}{A_C E_C} P_C.$$

The equilibrium equation has the same two unknowns, so we can solve these two equations to obtain the bar and cylinder forces. We then divide the internal forces by the cross-sectional areas they act on to obtain the normal stresses in both pieces:

$$P_B = -\frac{A_B E_B}{A_B E_B + A_C E_C} P \quad \text{and then} \quad \sigma_B = -\frac{E_B}{A_B E_B + A_C E_C} P,$$

$$P_C = -\frac{A_C E_C}{A_B E_B + A_C E_C} P \quad \text{and then} \quad \sigma_C = -\frac{E_C}{A_B E_B + A_C E_C} P.$$

These forces and stresses are compressive, as indicated by the negative signs.

b. The total change in length of the assembly may be calculated from either element:

$$\Delta L = \Delta L_B = -\frac{PL}{A_B E_B + A_C E_C}.$$

You may recognize these results as characteristic of solutions for springs in parallel. An alternate solution with the displacement method makes this explicit.

a. We start with the same single equation of equilibrium, developed from isolation of the node at point 2. We now introduce the constitutive relation for each element:
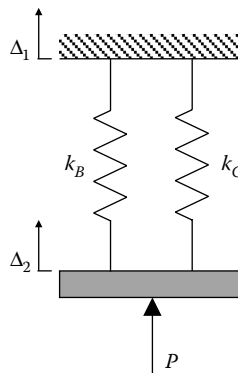
$$P_B = k_B \left(\Delta_2 - \Delta_1 \right) = k_B \Delta_2 = \frac{E_B A_B}{L} \Delta_2,$$

$$P_C = k_C \left(\Delta_2 - \Delta_1 \right) = k_C \Delta_2 = \frac{E_C A_C}{L} \Delta_2.$$

b. Substituting these expressions into the equilibrium equation let us solve for the unknown displacement at node 2, which is also the total change in length that we seek:

$$\frac{E_B A_B}{L} \Delta_2 + \frac{E_C A_C}{L} \Delta_2 = -P,$$

$$\Delta L = \Delta_2 = -\frac{PL}{E_B A_B + E_C A_C},$$

which is the same as the force method result. Replacing this in the constitutive equations gives us the same force expressions we found with the first method.

EXAMPLE 2.9

Each bar in the truss shown has a $2\,\text{in}^2$ cross-sectional area, elastic modulus $E = 14 \times 10^6$ psi, and coefficient of thermal expansion $\alpha = 11 \times 10^{-6}\,(^\circ\text{F})^{-1}$. If their temperature is increased by $40\,^\circ\text{F}$ from their initial temperature T, what is the resulting displacement of point A? What upward force must be applied to prevent this displacement?
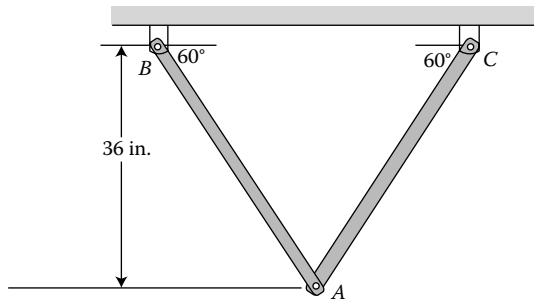
Given: Dimensions and properties of truss, imposed temperature change.

Find: Displacement of point A; force necessary to prevent this displacement.

Assume: Hooke's law applies. Neglect weight of bars.

Solution

The geometry of the problem allows us to find the original length of bars AB and AC. The change in the length of each bar due to the change in temperature ΔT is then

$$\Delta L_T = L \alpha \Delta T = (36\,\text{in}/\sin 60^\circ)(11 \times 10^{-6}\,(^\circ\text{F})^{-1})(40\,^\circ\text{F}) = 0.018\,\text{in}.$$

So, the new vertical distance from the fixed surface to point A is

$$(36\,\text{in}/\sin 60^\circ + 0.018) \cdot \sin 60^\circ = 36.008\,\text{in}.$$

The horizontal displacements of AB and AC will be equal and opposite, so the net displacement of point A is only vertical, and is 0.008 in.

The upward force applied to prevent this must induce a compressive axial load P in both bars to cause a change in length equal and opposite to ΔL_T. By Hooke's law,

$$\frac{PL}{AE} = -0.018\,\text{in, so } P = \frac{(-0.018\,\text{in})(14 \times 10^6\,\text{psi})(2\,\text{in}^2)}{36\,\text{in}/\sin 60°} = -12\,\text{kips.}$$

(1 kip = 1000 pounds). The negative sign indicates that the force is compressive. We construct an FBD and use equilibrium to find the force F necessary to induce this compressive load P in both bars. Because the loads P are known to be compressive, they are drawn in the correct direction.
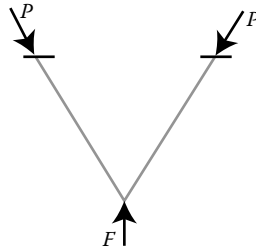
$$\sum F_y = 0 = F - 2P \sin 60° \quad \text{or} \quad F = 2P \sin 60°.$$

$$F = 21\,\text{kips.}$$

EXAMPLE 2.10

A steel railroad track ($E = 200\,\text{GPa}$, $\alpha = 11.7 \times 10^{-6}/°\text{C}$) was laid out at a temperature of $0°\text{C}$. Determine the normal stress in a rail when its temperature reaches $50°\text{C}$, assuming that the rails (a) are welded to form a continuous track, or (b) are 12 m long with 6 mm gaps between them.

Given: Geometry of problem, material properties, imposed temperature change.

Find: Normal stress when continuous or when gaps are left.

Assume: Hooke's law applies.

Solution

Based on our understanding of thermal stresses, we expect the stress calculated in part (b) to be lower than that in part (a): we have learned that thermal stresses are induced only when a part is prevented from experiencing its natural thermal deformation, so the space left to accommodate thermal expansion in part (b) should help relieve the induced stress. We will see whether this expectation is met.

A schematic of a segment of rail helps to illustrate the problem. In the final figure, we see forces P on the segment. The one equation of equilibrium that we have at our disposal confirms that these forces must be equal in magnitude, but it does not help us determine that magnitude. This is a statically indeterminate problem.
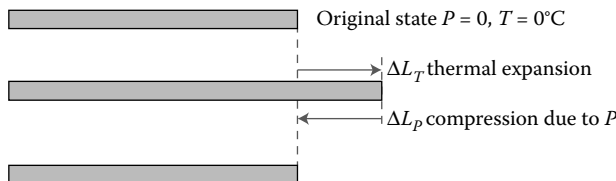
a. Using the force method, which is typically the more straightforward choice when thermal effects or gaps are involved, we imagine removing the redundant constraint (of the next segment of rail) on one end and calculate the displacement ΔL_T due to the temperature rise. We then consider the redundant constraint force re-applied as an external force $-P$ (negative since assumed compressive) and calculate the displacement ΔL_P. Note that although we have broken the problem into separate thermal and mechanical steps, physically these happen simultaneously to the bar and only one initial length is needed.

The total deformation of a steel track segment is zero, as the welding allows no net change to the length of the segments. Hence, we add the deformations due to thermal effects and compressive forces to obtain the compatibility equation that will let us solve for the unknown force:

$$\Delta L_T + \Delta L_P = 0,$$

$$\underset{\substack{\text{tends to} \\ \text{stretch}}}{\alpha(\Delta T)L} + \underset{\substack{\text{tends to} \\ \text{squash}}}{\frac{-PL}{AE}} = 0,$$

so

$$\alpha\Delta T = \frac{P}{AE} = \frac{\sigma}{E},$$

$$\sigma = \alpha\Delta T E = (11.7 \times 10^{-6}\,(°\text{C})^{-1})(50 - 0\,°\text{C})(200 \times 10^9\,\text{Pa}),$$

$$\sigma = 117\,\text{MPa (compressive due to assumed direction of } P\text{) when welded.}$$

b. If a gap of 6 mm is left between rails, we allow each segment a net extension of 6 mm, so our compatibility equation is revised to reflect this real total displacement:

$$\alpha(\Delta T)L - \frac{PL}{AE} = 0.006\,\text{m},$$

so

$$\sigma = \frac{\alpha\Delta T L - 0.006\,\text{m}}{L}E = \left(\frac{11.7 \times 10^{-6}\,(°\text{C})^{-1}(50\,°\text{C})(12\,\text{m}) - 0.006\,\text{m}}{12\,\text{m}}\right)(200 \times 10^9\,\text{Pa}),$$

$$\sigma = 17\,\text{MPa (compressive) when gap is left.}$$

EXAMPLE 2.11

If the railroad track of Example 2.10 is structural steel with a yield stress of 220 MPa, by how much is the safety factor increased by leaving the 6 mm gaps between the sections of rail?

Given: Geometry, material properties, imposed temperature change of Example 2.10.

Find: Safety factor without and with gaps between rails.

Assume: Hooke's law applies.

Solution

From Example 2.10, the stress in the rails due to an extreme 50°C temperature difference is 117 MPa with no gap and 17 MPa with a 6 mm gap. The safety factors are

$$SF_{\text{no gap}} = 220\,\text{MPa}/117\,\text{MPa} = 1.9,$$

$$SF_{\text{gap}} = 220\,\text{MPa}/17\,\text{MPa} = 13.$$

The gap changes this from a situation with a safety factor that is perhaps insufficient to one that is certainly more than is needed, in terms of failure by yielding. Note, however, that the long, slender rails would first fail by *buckling*, which we will learn about in Chapter 11, so this gap is not in fact excessively conservative.

EXAMPLE 2.12

A 6 mm by 75 mm plate, 600 mm long, has a circular hole of 25 mm diameter located at its center. Find the axial tensile force that can be applied to this plate in the longitudinal direction without exceeding an allowable stress of 220 MPa. How does the presence of the hole affect the strength of the plate?

   Given: Dimensions of plate, limiting normal stress.

   Find: Allowable axial load that can be applied to plate.

   Assume: Hole is only feature that causes a stress concentration.

Solution
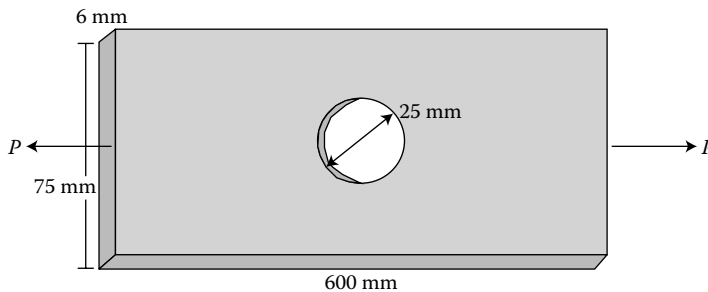
The cross-sectional area normal to an axial load P is $A_0 = 6\,\text{mm} \times 75\,\text{mm} = 450\,\text{mm}^2$. The average normal stress induced by such a load will be $\sigma_{\text{av}} = P/A_0$, and due to the presence of the hole we must consider the effects of stress concentration:

$$\sigma_{\max} = K\sigma_{\text{av}} = K\frac{P}{A_0}.$$

We can find K for this geometry using the graph in Figure 2.25:

$$\frac{r}{d} = \frac{(25\,\text{mm})/2}{75\,\text{mm} - 25\,\text{mm}} = \frac{1}{4},$$

$$K\left(\frac{r}{d} = 0.25\right) = 2.26,$$

so

$$\sigma_{\max} = K\frac{P}{A_0} = 2.26\frac{P}{450\,\text{mm}^2} = 0.005P,$$

we must have

$$220\,\text{MPa} \geq 0.005P,$$

$$P \leq 44\,\text{kN}.$$

Note: If there were no holes in this plate, we would simply have $\sigma_{\text{av}} = P/A_0$, and we could allow a force $P \leq 99\,\text{kN}$. So with the hole, we can permit only 44% of the load, we could have allowed without the hole.

PROBLEMS

2.1 In tissue engineering, biological materials are grown from seeded cells, so that artificial corneas, blood vessels, or other materials may be made from biological materials. Such materials are less likely than artificial parts made of plastic or metal to be rejected by the body. In order to engineer true replacement parts, it is necessary to understand the behavior of physiological systems, and to match material properties such as elastic and shear moduli. It is impractical to construct a tension specimen like that in Figure 2.2 from soft tissues such as muscles, tendons, or blood vessels. What would you do instead?

2.2 Concrete, rocks, and bone are strong in compression and are usually designed for compressive loading. To test their strength in compression, what sort of test specimen would be useful?

2.3 Suppose that a downward force is applied at point A of the truss, causing point A to move 0.360 in downward and 0.220 in to the left. If the resulting extensional strain ε_{AB} in the direction parallel to the axis of bar AB is uniform, what is ε_{AB}?
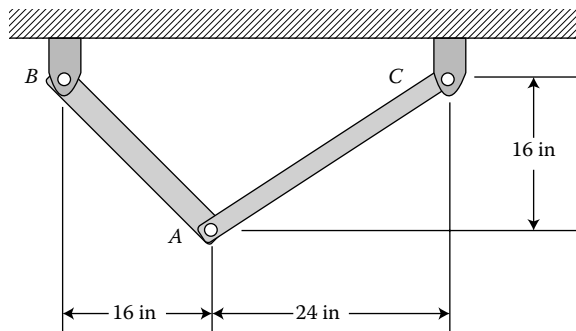
2.4 The tension in your Achilles tendon is considerable when you stand on tiptoe or poise for a jump. Design a tension gage that might be useful in measuring such tension, or the tension in a bow string or rubber slingshot.

Hint, after Y. C. Fung:
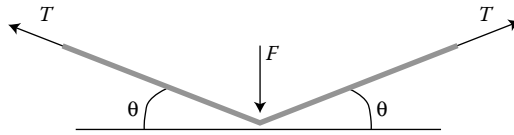
2.5 The top figure shows a diagram of the bones and biceps muscle of a person's arm supporting a mass. The lower figure shows a biomechanical model of the arm, in which the biceps muscle *AB* is represented by a bar with pin supports. The suspended mass is $m = 2$ kg, and the weight of the forearm is 9 N. If the cross-sectional area of the tendon connecting the biceps to the forearm at *A* is 28 mm^2, what is the average normal stress in the tendon? If the largest safe stress for the tendon is 10 MPa, what is the largest suspended mass that can be supported?
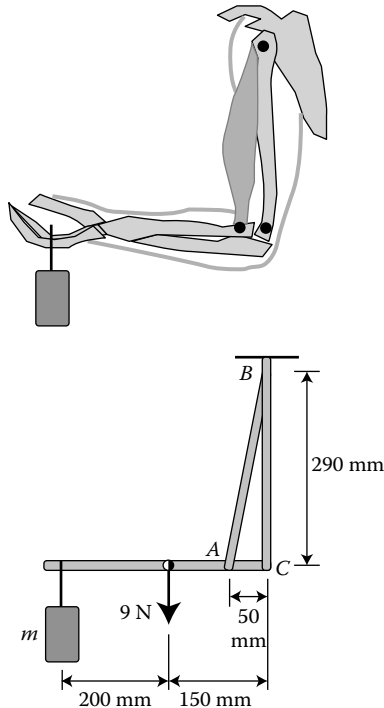
2.6 The bar shown has a solid circular cross section, with a 2-in radius. Determine the average normal stress at (a) plane P_1 and (b) plane P_2.
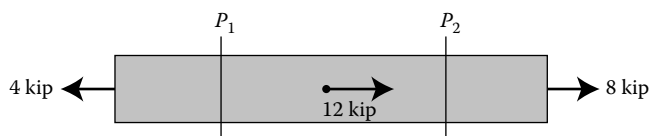
2.7 Your local lumber yard is providing a set of wooden 4 in × 4 in posts that you will mount on 6 in × 6 in concrete bases to support a section of roof. Handbooks provide the allowable compressive stresses: 1800 psi for wood and 1250 psi for concrete. The specific weight of concrete is also given as 150 lbf/ft^3, although the corresponding number for wood is not shown. For the post-support configuration shown, determine

    a. The specific weight of wood, given that a two-foot section of the post weighs 21 lb and knowing that a 4 in × 4 in post is actually 3.5 in × 3.5 in.

    b. The allowed load P when the weights of the support and post are included.

    c. The allowed load P when the weights of the support and post are not included.
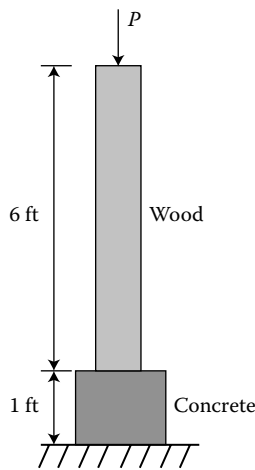
2.8 The jaws of the bolt cutter shown are connected by two links AB. The cross-sectional area of each link is 750 mm^2. (a) What average normal stress is induced in each link by the 90 N forces exerted on the handles? (b) The pins connecting the links AB to the jaws of the bolt cutter are 20 mm in diameter. What average shear stress is induced in the pins by the 90 N forces exerted on the handles?
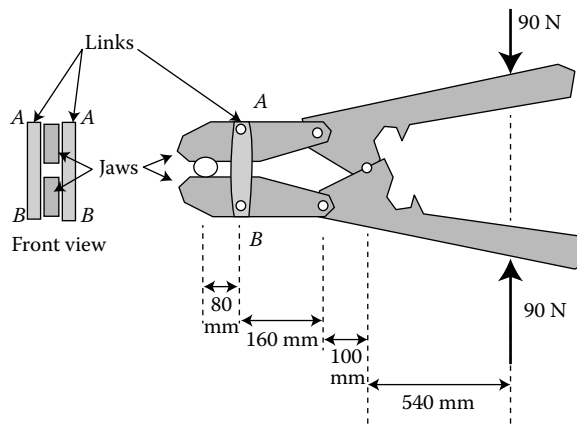
2.9 A prototype bolt shaft (assume a uniform cylinder) that is to be loaded in tension is
made of a stainless steel with a yield strength of 450 MPa and has a safety factor of 3
with respect to yielding for the maximum allowable loading. Find two ductile mate-
rials that could be used to replace the steel to make the bolt lighter while maintaining
the same safety factor. The new bolts will have the same length as the original but
may have different diameters. What is the percent weight savings with each of the
new materials? What other material properties might be important to consider before
a final choice is made?

2.10 For the wood block shown, the allowable shear stress parallel to the grain is $1\,MN/m^2$
and the maximum allowable compressive stress in any one direction is $4\,MN/m^2$.
Determine the maximum compressive force F that the block can support.
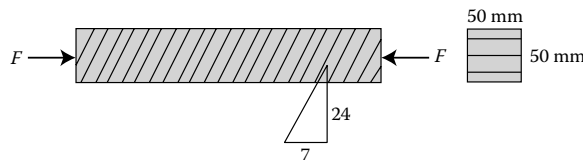
2.11 Determine the minimum allowable value of the force F if the tensile stress in segment
AB must be less than $150\,MN/m^2$. What are the changes in length of segment BC and
of the entire bar for this value of F? The bar's cross-sectional area is $50\,mm^2$, and the
bar is made of steel.
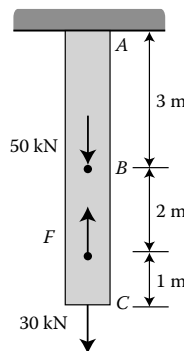
2.12 An electronic scoreboard is to be installed in a large stadium. Due to the design of the
roof structure, the suspending cables will have different lengths, as is shown below.
   a. Determine a suitable cross-sectional area for each cable so that the scoreboard
   will hang level, accounting for the stretch in each cable. Use the data in the figure
   and the requirement that the maximum stress allowed in the cable is 36 ksi. The
   elastic modulus for the cables is $E = 30,000\,ksi$, and the weight of the scoreboard
   is $W = 10\,k$. Remember, 1 kip (k) = 1000 pounds.
   b. The slope of the grain in the longer support cable has a maximum deviation from
   the cable's longitudinal axis of $15°$, and there is some concern that the relatively
   low shear strength of the cable material along its grain could cause problems.
   Calculate both normal and shear stresses along this grain.
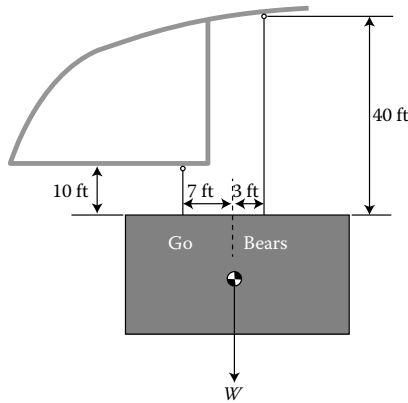
2.13 Oil drill pipes are long, heavy steel bars that deflect significantly hanging vertically under their own weight. Determine the movement Δ of the tip of a steel drill pipe (a) 3500 ft long, which is typical of Texas oil wells, and (b) 35,000 ft long, which was the depth of the ill-fated Deepwater Horizon well in the Gulf of Mexico. (Real drill pipes extend even more due to thermal expansion.)
Hint: you must take into account that the force on each section is a function of position.

2.14 Often we neglect the self-weight of elements in our structures because the stress due to this weight is much less than that caused by externally applied loads. However, if both are considered in the design of a circular cross section bar that is optimally shaped to vertically carry a point load and its own weight with constant stress, the radial profile of the bar is $r(z) = r_0 \exp(\rho g z / 2\sigma)$, where r_0 is the radius of the flat top of the bar, ρ is the mass density of the bar material, g is the acceleration due to gravity, and $\sigma = \sigma(0) = P/\pi r_0^2$ is the stress at the top of the bar. Show that this profile indeed produces constant stress σ along the length of the bar.
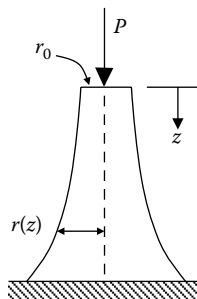
2.15 The bar shown has a constant cross section and is fixed rigidly at both walls. Determine the reactions at both walls for the given applied load P.
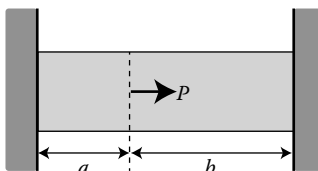
2.16 A rigid slab with mass $m = 15,000\,\text{kg}$ is supported by three columns, as shown below. Determine the compressive force in each of the columns. Each aluminum bar has twice the cross-sectional area of the steel bar.
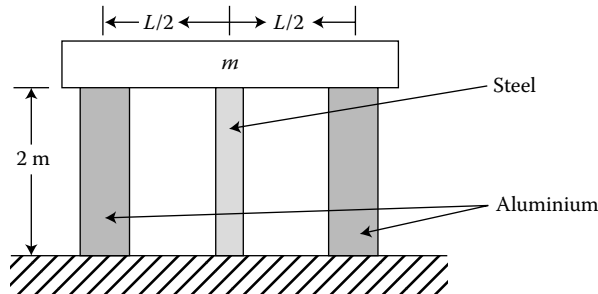
2.17 The bar shown has a varying cross section and is fixed rigidly at both walls. The cross-sectional area of the narrower section is A; the cross-sectional area of the wider section is larger by a factor of m, or $m\,A$. Using the force (flexibility) method, determine

  a. The reactions at both walls for the given applied load P.

  b. The displacement of the point D at which the load P acts.
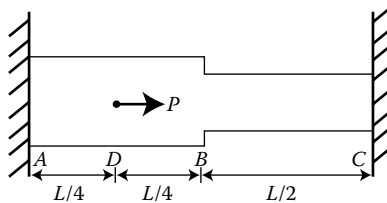
2.18 Considering again the bar of Problem 2.17, using the displacement (stiffness) method, determine

  a. The reactions at both walls for the given applied load P.

  b. The displacement of the point D at which the load P acts.

2.19 Two cylindrical bars with 30 mm diameters, one (ABC) made of yellow brass and the other (CDE) of stainless steel, are joined at C. End A of the composite bar is fixed, while there is a gap of 0.2 mm between the end E and a vertical wall. A force of magnitude 40 kN and directed to the right is applied at B. Determine

  a. The smallest force P needed at D to just close the gap without the steel bar exerting a force on the wall at E.

  b. The reactions at A and E if a 40 kN force directed to the right is applied at D.

  c. The reactions at A and E if force P is twice the value you calculated in part (a).
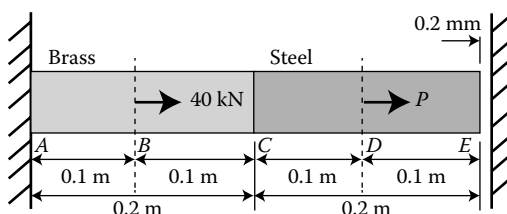
2.20 High-density polyethylene (HDPE; with an elastic modulus of 1.1 GPa, a coefficient of thermal expansion of $190 \times 10^{-6}/°C$, and a yield strength of 23 MPa) pipe was laid in a trench for the purpose of carrying water from an artesian bore to troughs for sheep in outback Australia. The pipe was straight when laid when the ambient temperature was 15°C and this photo was taken when it was 37°C. (a) By what percent has the length changed? (b) If the pipe had remained straight, would the yield stress have been exceeded?

(Courtesy of Rodney Shannon.)

2.21 An aluminum cylinder ($A_{Al} = 30\,\text{cm}^2$) is centered between two rigid end plates connected by two steel bolts (each $A_{St} = 1.0\,\text{cm}^2$). At 20°C, the bolts are just tight enough to hold the end plates against the cylinder and there are no axial loads in the cylinder or bolts. Find the stress in the steel bolts when the temperature is increased to 70°C. Do not include thermal expansion of the end plates in your solution.
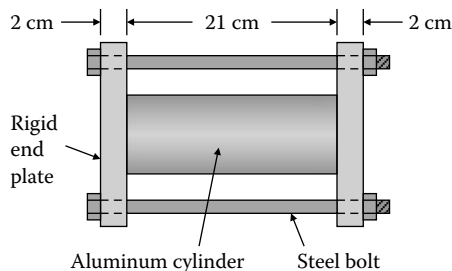
2.22 The stepped bar shown has a uniform thickness and can carry a certain axial load without yielding. We would like to drill a 0.2 in radius hole through the wider part of the bar, far from the fillet. Will this reduce its load-carrying capacity?

Original stepped bar   Proposed hole
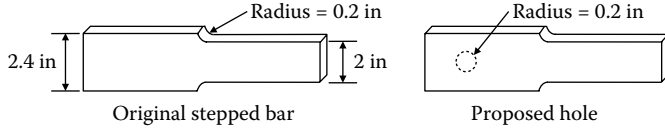
2.23 A bar consists of two portions BC and CD of the same material and of the same length L, but of different cross sections. Determine the strain energy of the bar when it is subjected to an axial load P, expressing the result in terms of P, L, E, the cross-sectional area A of portion CD, and the ratio n of the two diameters.
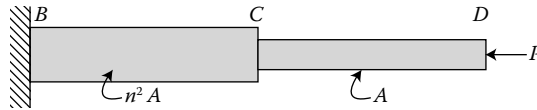
2.24 Kangaroo hopping is very efficient, because upon landing the kangaroo stores elastic strain energy in its tissues, which act as springs, and then recovers it in the next hop. The Achilles tendon (one of three major tendons in a kangaroo hindlimb) of a 40 kg kangaroo is 1 cm in diameter and 45 cm in length (human Achilles tendons have a smaller diameter and are about 15 cm long). If the Achilles tendon has an elastic modulus of 1.4 GPa and is loaded to 2% strain (below its elastic limit), how much strain energy (i.e., stored potential energy) would both Achilles tendons contain? Based strictly on energy considerations, how high could the amount of energy stored in just these tendons lift the kangaroo?

3

Case Study 1: Collapse of the Kansas City Hyatt Regency Walkways

On July 17, 1981, in the most damaging unforced structural failure in the history of the United States, two overhead walkways fell into the atrium lobby of the Hyatt Regency Hotel in Kansas City, Missouri. As a result of this collapse, 114 people died, and significant damage was sustained (Figure 3.1).

The failure derived, in large part, from a key aspect of modern engineering design, which is that engineering designers do not, typically, build what they design. Instead, they produce a *fabrication specification*, a detailed description of the designed object that allows its assembly or manufacture by others. Separating the "designing" from the "making" means that such fabrication specifications must be complete and unambiguous.

Fabrication specifications are presented in drawings (e.g., blueprints, circuit diagrams, flow charts) and in text (e.g., parts lists, materials specifications, assembly instructions). Such traditional specifications can be complete and sufficiently specific, but they may not capture the designer's intent—and this can lead to catastrophe. The suspended walkways in the Hyatt Regency Hotel in Kansas City collapsed because a contractor fabricated the connections for the walkways in a manner different from the original design.

In the original design, walkways at the second and fourth floors were hung from the same set of 24-ft-long threaded rods that would carry their weights and loads to a roof truss (Figure 3.2). The fabricator was unable to procure threaded rods sufficiently long to suspend the second-floor walkway from the roof truss, so instead, as shown in Figure 3.3, he hung it from the fourth-floor walkway using shorter rods. (The original design would not have been easy to implement because of the difficulty involved in screwing on bolts over such long hanger rods and attaching walkway support beams.) The support beams of the fourth-floor walkway were not designed to carry both the second-floor walkway and its own dead and live loads, resulting in the collapse. If the fabricator had understood the designer's intention to hang the second-floor walkway directly from the roof truss, this accident might have been avoided.

As Henry Petroski (1982) noted, the fabricator's redesign was akin to requiring that the lower of two climbers hanging independently from the same rope change his position so that he was grasping the feet of the climber above, causing the upper climber to carry the weights of both with respect to the rope. The redesigned supports for the second-floor walkway were configured similarly.

Figure 3.4 shows several sketches of the original design: (a) an elevation view of the second- and fourth-floor walkways, *each supported by the same pairs of hanger rods* (on east and west sides of the walkway) spaced at a distance L; and (b) an end view of the two walkways and FBDs of the supporting beam of each walkway. Consider now the lower, second-floor walkway. The load carried by each pair of its hanger rods can be estimated as the sum of the *dead load* of the walkway and its supporting beams and the *live load* of pedestrians likely to stand on walk across the walkways. Since the hanger rods are spaced

FIGURE 3.1
The lobby of the Kansas City Hyatt Regency Hotel after the collapse of the second- and fourth-floor walkways on July 17, 1981. The devastation is evident. (Courtesy of Lee Lowry, Kansas City, MO. Contribution of the National Institute of Standards and Technology. With permission.)

a distance L apart, we estimate the total force $2P$ needed to support a span of length $L/2$ on either side of a pair of hangers as

$$2P = (w + W)bL, \tag{3.1}$$

where w is the dead load per unit area, W the live load per unit area, and b the walkway width. In this instance, by both making calculations based on the design drawings and weighing pieces of the collapsed walkways, the engineers at the National Bureau of Standards (NBS)* who performed the forensic investigation of the walkway collapse determined that the combination of the dead and live loads, called the *design load*, was in this case $P = 90\,\text{kN}$ (20,300 lbf) per hanger rod. The analysis of the fourth-floor walkway based on the original design would be the same. Then the individual hanger rods needed to support both the second- and fourth-floor walkways as designed would each support a total load of $2P$ and would be sized accordingly.

On the other hand, the end views of the walkways as built and their corresponding FBDs (Figure 3.5) show that the rods would have to carry exactly the same loads at each level, that is, to support the lower walkway, each rod carries a load equal to P, while above the fourth floor each rod would have to carry a load of $2P$ to support both the second- and fourth-floor walkways. So the rods in both designs would have equivalent designs with

---

* Since 1988, has been called the National Institute of Science and Technology (NIST).
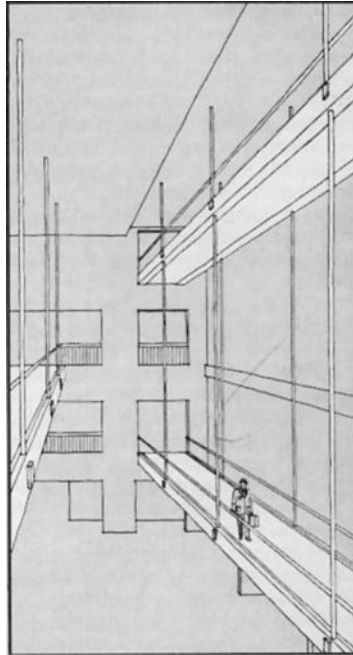
FIGURE 3.2
An artist's sketch of the second- and fourth-floor walkways across the west side of the atrium of the Kansas City Hyatt Regency Hotel. The view looks southward and also shows a separate third-floor walkway that did not collapse, but was taken down after a design review prompted by the collapse of the other two walkways on July 17, 1981. (From Pfrang and Marshall, *Civil Engineering*, pp. 65–68, July 1982. With permission.)

(a)   (b)

Original design   As built
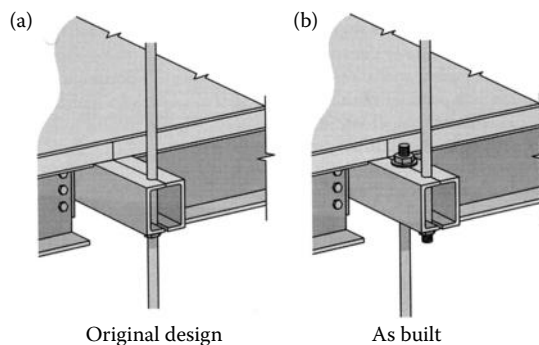
FIGURE 3.3
The two hanger connections at the fourth-floor walkway: (a) The left sketch shows the configuration as designed, wherein the hanger rods went straight through the fourth-floor connection, down to the second floor, which these rods also supported. (b) The right sketch shows the configuration as built, with the hanger rods supporting the second floor now hung from the box beams that hold up the fourth-floor walkway. (From Dym and Little, Engineering Design: A Project-Based Introduction, New York. 2008. Copyright Wiley-VCH Verlag GmbH & Co. KGaA. Reproduced with permission.)
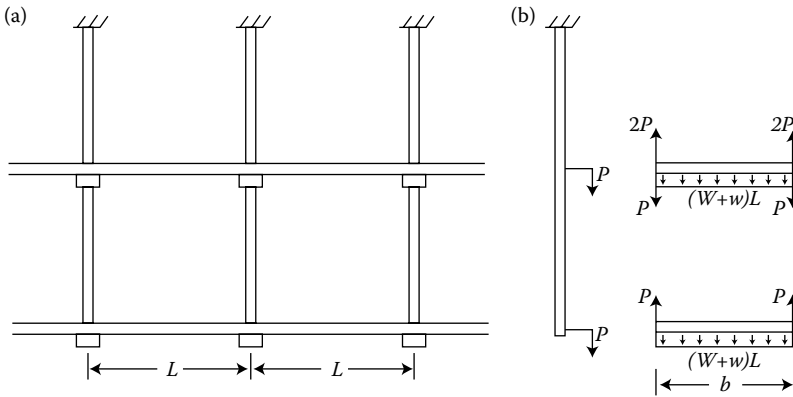
FIGURE 3.4
Building a model of the walkways and their supports: (a) an elevation of the second- and fourth-floor walkways as originally designed. (b) An end view and FBDs of the support beams. The forces carried by the hanger rods accumulate according to the number of walkways being supported below them.

the same area, determined by Equation 2.6,

$$A = \frac{2P}{\sigma_{\text{allow}}},\tag{3.2}$$

where σ_{allow} is the allowable stress in the rod. In terms of the rope analogy, the part of the rope above the two climbers has to support the weight of both: It does not care whether each hangs directly from the rope or one climber hangs from the other.

So, why did the walkways collapse? They failed because an unanticipated connection was inserted into the design and the connection was not properly designed (Figure 3.6). As noted by respected engineers E. O. Pfrang and R. Marshall (1982), "With this modification the design load to be supported by each second floor ... connection was unchanged ....
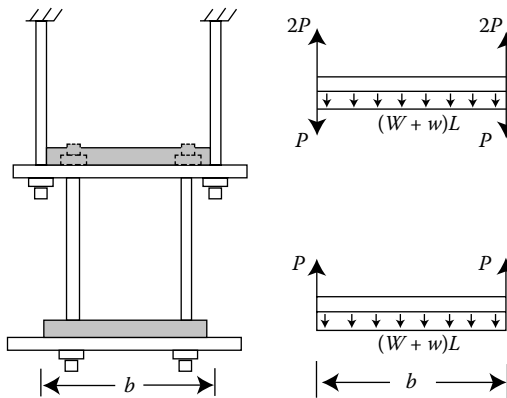
FIGURE 3.5
Extending the model of the walkways and their supports to reflect the redesign. An end view of the second- and fourth-floor walkways designed so that the second-floor walkway hangs from the fourth-floor supporting beams, and FBDs of a typical pair of supports. Note that the forces supported by the hanger rods are unchanged from the original design.
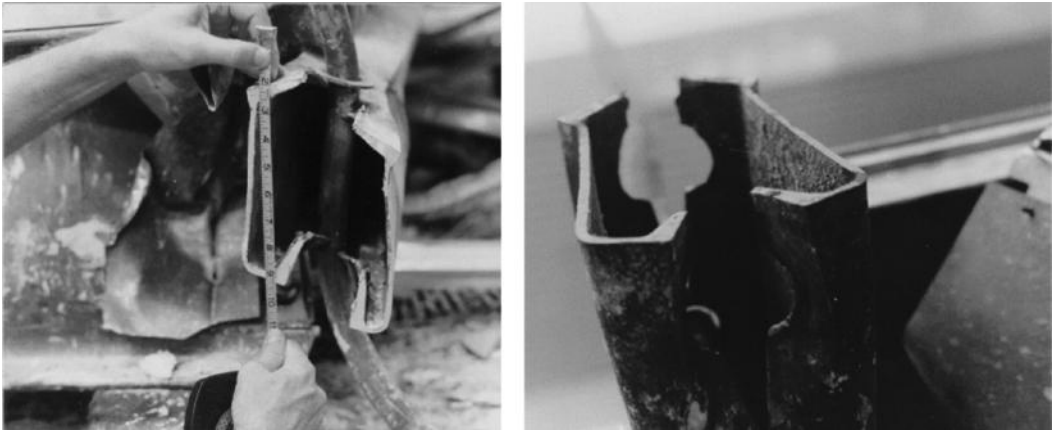
FIGURE 3.6
Photographs of the failed connections that led to the collapse of the two walkways in the Kansas City Hyatt Regency Hotel. Compare with Figure 3.3b and observe that the outboard connection (on the right-hand edge) failed because the threaded nut and washer that went underneath the box beam pulled right through the beam because that connection, designed originally to transmit a load of *P*, was actually carrying a load of 2*P*. (Courtesy of Lee Lowry, Kansas City, MO. Contribution of the National Institute of Standards and Technology. With permission.)

However, the load to be transferred from the fourth floor ... to the upper hanger rod under this arrangement was essentially doubled" (p. 68). Look again at the FBD in Figure 3.5: It shows that the redesign required the nut under the fourth-floor supporting beam and its connection with the beam itself to support the transfer of twice the load that would have been transferred in the original design—which the fabricator's redesigned connection did not.

Interestingly enough, it was also revealed in the subsequent forensic investigation that even the original design was only marginally safe. The NBS investigators found that the long-rod design would likely not have satisfied the Kansas City Building Code specifications. Further, it turned out that during construction, the building's construction workers had noticed that the walkways seemed flimsy and that they moved noticeably whenever workers moved wheelbarrows or other heavy objects across them. Their solution? Rather than report the problem and request a fix, they found other routes over which to transport their building materials!

The NBS official report issued in 1981 did not assign blame for this catastrophe. The essential problem was a lack of proper communication between the design engineers (Jack D. Gillum and Associates) and the manufacturers (Havens Steel). However, the NBS report's authors, Pfrang and Marshall, made it clear that responsibility lay primarily with the structural engineers. The Missouri licensing board and Court of Appeals agreed, finding that the design engineers should have noticed the difference between their design and what the contractor suggested, and should have analyzed the redesigned connection. Basic calculations should have demonstrated the flaws in both the original design and in what was ultimately built. The principal structural engineers lost their Missouri engineer's licenses, and the firm, Jack D. Gillum and Associates, dissolved. The Hyatt Regency Crown Center lobby in Kansas City today features only one walkway, which is not suspended from the roof but instead rests on sturdy-looking columns that transmit its loads to the atrium floor.

Sarah Pfatteicher (2010) has written about the implications of this case for the engineering profession and our codes of ethics. Gillum and the other engineers were the first American engineers to have their licenses revoked for "gross negligence." Pfatteicher has noted that after almost a century of industrialization and acknowledged acts of engineering heroism, this was "a disquieting admission" that "a good engineer could practice engineering badly." The catastrophe and investigations that followed also serve as object lessons in the challenges of managing complex projects among multiple organizations, and in the importance of communication to engineering projects. Because engineering is perpetually challenging limits and pushing boundaries of knowledge, and because in the modern world engineering projects are complex, interconnected systems, failures are "never desired, but never completely preventable."

Twenty years after the "Hyatt Horror," as the newspaper headlines called it, the American Society of Civil Engineers (ASCE) reflected upon its legacy in a special journal issue. The ASCE had rewritten its code of ethics in the 1970s, prioritizing its emphasis on public welfare, with the engineer's duty to "his client, employer, or employees," next, followed last by loyalty to his profession: a complete inversion of the previous version of the code. It was this sense that the engineer was accountable to the public that led to the initial revocation of the Hyatt engineers' licenses. In subsequent hearings, the ASCE reduced Gillum's punishment to a 3 year suspension, finding him "vicariously responsible . . . but not guilty of gross negligence nor of unprofessional conduct" (ASCE 1986). In a way, the most significant legacies of the disaster are the subsequent conversations among engineers about our responsibilities, to whom and for what we are accountable, and how we can uphold the values of our profession.

Our professional codes of ethics provide us with guidelines to follow; regulations, codes, and standards suggest appropriate parameters. Still, engineering inherently involves the risk of failure. We may strive to mitigate its catastrophic consequences, and to reduce the risks, and of course to communicate all of this clearly—but we should be prepared to learn from failure as well as from success.

PROBLEMS

3.1 If the Kansas City Building Code specified that a floor structure must support a live load of 4.79 kPa (100 psf), and if the walkway length $L = 9.1$ m $= 30.0$ ft and width $b = 2$ m $= 6.56$ ft, what contribution is made to the hanger rod load P?

3.2 If the design load is 90 kN (20,300 lbf), what is the dead load and what is the intensity of the dead load in the light of the live load calculation of Problem CS1.1?

3.3 Determine the specific weight of lightweight concrete and calculate its dead load intensity if it is used in an 80-mm (3.25-in) cover of a formed steel deck walkway. Compare this result with that found in Problem CS1.2 and explain any differences.

3.4 Determine the stress induced in hanger rods carrying a design load of 90 kN (20,300 lbf), if their diameter is 32 mm (1.26 in). Does that seem a reasonable stress level if the rods are made of mild steel? Explain your answer.

3.5 If the interfloor distance of the Hyatt Regency Hotel is 4.57 m (15 ft), how much does the second-floor walkway move down with respect to the fourth-floor walkway due to the design load?

References

ASCE Committee on Professional Conduct, "Disciplinary proceedings: Case of Mr. Jack D. Gillum, M. ASCE," Docket No. 1982–6, 1986.

National Bureau of Standards (NBS), Pfrang & Marshall, Eds., *Investigation of the Kansas City Hyatt Regency walkways collapse*, Science Series, 143, US Dept. of Commerce, Washington, DC, 1982.

Petroski, Henry, *To Engineer is Human*, Vintage Books, 1982.

Pfatteicher, Sarah, "The Hyatt Horror: Failure and Responsibility in American Engineering," *Journal of Performance of Constructed Facilities* **14**:62–66, 2000.

Pfatteicher, Sarah, *Lessons Amid the Rubble*, Johns Hopkins University Press, 2010.

4

Strain and Stress in Higher Dimensions

Now that we have constructed a foundation for our study of continuum mechanics, consisting of (1) kinematics or compatibility, (2) stress, (3) constitutive relationships, and (4) equilibrium, and have applied this to uniaxial loading and deformation, we are curious about the form this foundation will take in higher dimensions.

4.1 Poisson's Ratio

So far when we have discussed deformations of bodies in tension or compression, we have been referring to the deformation of a body in the direction of the applied uniaxial force. It is also true that in all solid materials, some deformation occurs along axes perpendicular to this force. That is, when a material is pulled along its axis, as shown in Figure 4.1a, it experiences some transverse (aka lateral) contraction. This is easily visualized by stretching a rubber band. When pushed, the material experiences transverse expansion (Figure 4.1b).

The deformations in Figure 4.1 are greatly exaggerated; in most engineering materials, this effect is small. One way to quantify material behavior, in fact, is to consider the relative *axial* and *lateral* strains due to axial loading. We do this by means of *Poisson's ratio*, first formulated by French scientist S. D. Poisson in 1828, and denoted by the Greek letter ν (nu):

$$\nu = -\frac{\text{lateral strain}}{\text{axial strain}}. \tag{4.1}$$

Poisson's ratio is a property of a material and can be found tabulated with other properties such as the elastic (Young's) modulus E, for example, in Appendix C of this book. Remember that the strains in question are caused by uniaxial stress only: by simple tension or compression. The value of ν varies for different materials; generally, it is on the order of 0.25–0.35, but can range from 0.1 (for some concretes) to 0.5 (for rubber).* Table 4.1 shows some of these values.

Note that the Poisson effect does not cause any additional stresses, unless the transverse deformation is inhibited or prevented. Incidentally, for isotropic Hookean solids, it is possible to relate the three material properties we have so far discussed (elastic modulus E, shear modulus G, and Poisson's ratio):

$$G = \frac{E}{2(1+\nu)}. \tag{4.2}$$

---

* An elegant demonstration of the Poisson's ratio effect can be seen by stretching a swatch of chicken wire (which is not a continuous material but is a fine demonstration): the wire mesh visibly expands in the direction you are pulling, and contracts in the transverse direction. Rod Lakes (*Science* **235**, 1038–1040 (1987)) has created polymer foams which exhibit *negative* Poisson's ratios: when pulled, they expand in the transverse direction as well as the axial. Some materials composed of fibrous networks (e.g., textiles, biomaterials) have also exhibited this "anti-rubber" or "auxetic" negative Poisson's behavior (Evans, K. E. *J. Phys. D* **22**, 1870–1876 (1989).).
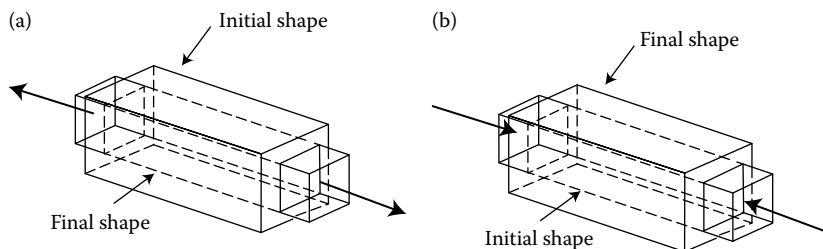
FIGURE 4.1
(a) Lateral contraction and (b) lateral expansion of solid bodies subjected to axial forces (Poisson effect).

TABLE 4.1

Typical Poisson's Ratio for Common Materials

Material	ν
Steel	0.27
Aluminum	0.35
Glass	0.23
Rubber	0.50
Concrete	0.20

What Poisson's ratio reminds us is that our ideal situation of one-dimensional strain, considered in the Chapter 2, is rarely physically realized. We must be conscious of a material's deformation in every dimension, even when loading is purely uniaxial. Although we will sometimes choose to neglect other dimensions, we should recognize that this is a choice to simplify our modeling, and that we are leaving something out of our analysis.

4.2 The Strain Tensor

The equations in Section 2.1 for strain as an average "percent deformation" are useful in a variety of straightforward loading conditions. However, in many cases, we will need to keep track of normal strains in multiple directions as well as shear strain. We can see how complicated the strain picture might become. There are three normal strains, in the *x*-, *y*-, and *z*-directions; and in addition six shear strains, a pair in each plane. That is nine strain components in all. All of these directions or senses of strain are contained quite elegantly in the *strain tensor*. This tensor can be represented as a 3×3 matrix, but it has special properties that we will examine more in Chapter 5.

Strain is a local property, and the values of each strain component may change dramatically within a material. And so we come to our mathematical definition of strain, which relates to relative deformations of an infinitesimal element.

If we consider the extensional strain in one direction of an original element *AB* with length Δx, as shown in Figure 4.2, we see that point *A* experiences a displacement *u*. This displacement is common to the whole element, a kind of "rigid-body displacement." A stretching Δu also takes place within the element, so that point *B* experiences a total displacement $u + \Delta u$.
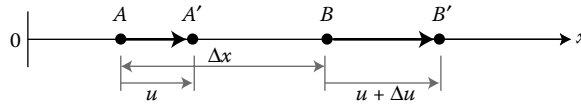
FIGURE 4.2
One-dimensional extensional strain.

Based on this situation, we define the extensional normal strain of this element as

$$\varepsilon = \lim_{\Delta x \to 0} \frac{\Delta u}{\Delta x} = \frac{du}{dx}, \tag{4.3}$$

taking the limit as $\Delta x \to 0$ so that the expression will apply to any length Δx of the element. We see that this definition is independent of whatever "rigid body displacement" occurred and recalls our third definition of normal strain, Equation 2.4, in Section 2.1.1.

If we extend our thinking to higher dimensions, as in Figure 4.3 for two dimensions, we see that we will now need to use subscripts to keep track of the components of strain; we will also need to use partial derivatives because, as we will understand fully when we discuss shear strains, displacement can vary in *all* directions as we consider a spatial element aligned in *any* direction.

And so, if u, v, and w are the three components of displacement **u** occurring in the x-, y-, and z-directions, and if we again take the limits as Δx, Δy, and Δz go to zero, we have three components[*] of normal strain:

$$\varepsilon_{xx} = \frac{\partial u}{\partial x}, \tag{4.4a}$$

$$\varepsilon_{yy} = \frac{\partial v}{\partial y}, \tag{4.4b}$$

$$\varepsilon_{zz} = \frac{\partial w}{\partial z}. \tag{4.4c}$$
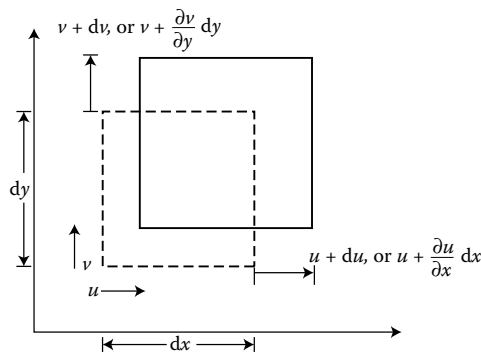
FIGURE 4.3
Two-dimensional normal strains.

---

[*] The subscripts on ε provide directional orientation. One subscript, j, tells us we are considering deformation in the j direction. The other subscript, i, tells us what to compare that deformation to. When $i = j$ this is normal strain: the deformation is in the reference direction, making strain a change in length with respect to a length in the same direction. For shear strain, $i \neq j$, and the displacement of interest is perpendicular to the reference direction.

The analysis here has shown that the three normal strains define the *change in size* of a rectangular parallelepiped with initial volume $dx\,dy\,dz$. Problem 4.1 will ask you to confirm that the normalized (meaning scaled by the original) change in volume of the rectangular parallelepiped $dx\,dy\,dz$ can be shown to be a function of the normal strains:

$$\frac{\Delta V}{V_0} = \varepsilon_{xx} + \varepsilon_{yy} + \varepsilon_{zz}. \tag{4.5}$$

In the normal strains of Equations 4.4a through 4.4c, we have the derivative of the displacement in each direction with respect to the spatial coordinate in the same direction. But why are the expressions written with partial derivatives? Because unlike in the one-dimensional case where the x-direction displacement u is simply $u(x)$, in multiple dimensions each displacement is a function of all spatial coordinates. That is, $\mathbf{u}$ is now $\mathbf{u}(x, y, z)$, meaning that the displacement in the x-direction can vary at different points in the body, whether they are located at different x positions or also different y or z positions. This is important to keep in mind as we learn about shear strains, as shown in Figure 4.4 for the two-dimensional case.

After straining, the initially horizontal side with initial length dx has slope $\partial v/\partial x$, and the initially vertical side with initial length dy has slope $\partial u/\partial y$. So, the initially right-angled ACB is reduced by the amount $\partial v/\partial x + \partial u/\partial y$. This is an angular deformation, or a shear strain, on the xy-plane, and like normal strain it is dimensionless. We have

$$\gamma_{xy} = \gamma_{yx} = \frac{\partial v}{\partial x} + \frac{\partial u}{\partial y}, \tag{4.6a}$$

$$\gamma_{xz} = \gamma_{zx} = \frac{\partial w}{\partial x} + \frac{\partial u}{\partial z}, \tag{4.6b}$$

$$\gamma_{yz} = \gamma_{zy} = \frac{\partial w}{\partial y} + \frac{\partial v}{\partial z}. \tag{4.6c}$$

We see that, as we learned in Section 2.1.2, the engineering shear strain is equal to the change in the right angle between the two axes denoted in the subscripts. Now we can
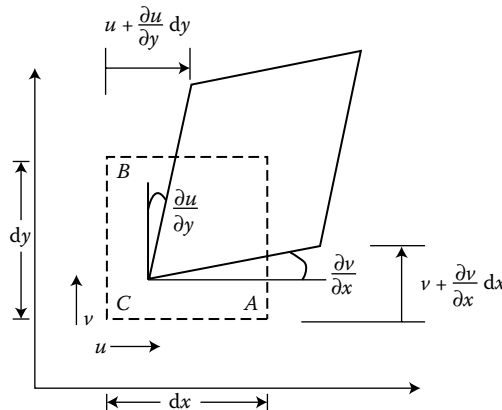
FIGURE 4.4
Shear strain in two dimensions.

think again about why partial derivatives are necessary: not only does the u displacement, for example, vary over an interval du, it also varies over dv and dw.

By considering all the possible deformations of our parallelepiped, we have identified nine total, and six unique, strain components: ε_{xx}, ε_{yy}, ε_{zz}, $\gamma_{xy} = \gamma_{yx}$, $\gamma_{xz} = \gamma_{zx}$, and $\gamma_{yz} = \gamma_{zy}$. Somehow, all of these components together represent the total state of strain for a point in our continuum. Strain is a *second-order tensor*, with one more level of sophistication than a vector.

Remember that we were able to write vectors, such as a force **P**, as column vectors:

$$\begin{pmatrix} P_x \\ P_y \\ P_z \end{pmatrix}.$$

In index notation, we can represent **P** as P_i where, as we recall from Section 1.5, it is implied that $i = 1, 2, 3$. There is no need to specify this range, and P_i indicates all three components of the vector **u**. A vector is also known as a first-order tensor. It contains information about both magnitude and direction. For strain, we have magnitudes and directions as well as directions relative to which strains are quantified. The normal strain component ε_{xx}, for example, represents the magnitude of deformation in the x-direction, relative to a reference length in the x-direction. We are able to write the nine components of strain as a 3×3 matrix, which is one way to represent a second-order tensor.

Although this definition is physically motivated and mathematically sound, these engineering shear strains are not exactly the shear components of the strain tensor. For a reason having to do with the fact that elements do not truly behave as rigid bodies, the strain tensor components are actually defined using a factor of $1/2$. This factor is necessary to make ε_{ij} behave mathematically as a proper tensor, as future study in continuum mechanics will show. We can write the strain tensor (using index notation*) as

$$\varepsilon_{kl} = \frac{1}{2}\left(\frac{\partial u_l}{\partial x_k} + \frac{\partial u_k}{\partial x_l}\right) = \frac{1}{2}\left(u_{l,k} + u_{k,l}\right). \tag{4.7}$$

Again we know that $k = 1, 2, 3$ and $l = 1, 2, 3$. Then u_k (and u_l) indicates all three components of the vector u, that is, the x-, y-, and z-direction displacements aka u, v, and w; and x_k (and x_l) indicates all three spatial coordinates. Therefore, Equation 4.7 defines nine terms, six unique, that form the components of a symmetric, second-order tensor. (*Symmetric* refers to the fact that each $\varepsilon_{ij} = \varepsilon_{ji}$; e.g., $\varepsilon_{xy} = \varepsilon_{yx}$, and of course also $\gamma_{xy} = \gamma_{yx}$.) Writing these out in long-hand notation, we obtain terms like

$$\varepsilon_{12} = \frac{1}{2}\left(\frac{\partial u_1}{\partial x_2} + \frac{\partial u_2}{\partial x_1}\right) = \frac{1}{2}\left(\frac{\partial u}{\partial y} + \frac{\partial v}{\partial x}\right) = \frac{1}{2}\gamma_{xy} = \varepsilon_{xy}, \tag{4.8}$$

$$\varepsilon_{11} = \frac{1}{2}\left(\frac{\partial u_1}{\partial x_1} + \frac{\partial u_1}{\partial x_1}\right) = \frac{1}{2}\left(\frac{\partial u}{\partial x} + \frac{\partial u}{\partial x}\right) = \frac{\partial u}{\partial x} = \varepsilon_{xx}. \tag{4.9}$$

---

* Also called Einstein notation because Albert Einstein introduced its use in his 1916 paper "The Foundation of the General Theory of Relativity."

Or we can write the strain tensor in its matrix form as

$$
\varepsilon = \begin{pmatrix} \varepsilon_{xx} & \varepsilon_{xy} & \varepsilon_{xz} \\ \varepsilon_{yx} & \varepsilon_{yy} & \varepsilon_{yz} \\ \varepsilon_{zx} & \varepsilon_{zy} & \varepsilon_{zz} \end{pmatrix} = \begin{pmatrix} \varepsilon_{xx} & \dfrac{\gamma_{xy}}{2} & \dfrac{\gamma_{xz}}{2} \\ \dfrac{\gamma_{yx}}{2} & \varepsilon_{yy} & \dfrac{\gamma_{yz}}{2} \\ \dfrac{\gamma_{zx}}{2} & \dfrac{\gamma_{zy}}{2} & \varepsilon_{zz} \end{pmatrix}
$$

$$
= \begin{pmatrix} \dfrac{\partial u}{\partial x} & \dfrac{1}{2}\left(\dfrac{\partial u}{\partial y} + \dfrac{\partial v}{\partial x}\right) & \dfrac{1}{2}\left(\dfrac{\partial u}{\partial z} + \dfrac{\partial w}{\partial x}\right) \\ \dfrac{1}{2}\left(\dfrac{\partial v}{\partial x} + \dfrac{\partial u}{\partial y}\right) & \dfrac{\partial v}{\partial y} & \dfrac{1}{2}\left(\dfrac{\partial v}{\partial z} + \dfrac{\partial w}{\partial y}\right) \\ \dfrac{1}{2}\left(\dfrac{\partial w}{\partial x} + \dfrac{\partial u}{\partial z}\right) & \dfrac{1}{2}\left(\dfrac{\partial w}{\partial y} + \dfrac{\partial v}{\partial z}\right) & \dfrac{\partial w}{\partial z} \end{pmatrix}. \tag{4.10}
$$

4.3 The Stress Tensor

We already understand stress as the intensity of an internal force, or force/area, but this division only makes sense while we are considering the uniaxial case and scalar values. We know that force **P** and the area **A** are, in fact, vectors (where the normal to the area defines its direction), and so when before we caculated P/A it was really $|\mathbf{P}|/|\mathbf{A}|$, where each was the component appropriate for a given calculation. This suggests to us that a full description of the stress distribution in a body will require a new notation and some careful bookkeeping.

As a starting point, we will consider a section of a loaded body, as shown in Figure 4.5. On that section, we identify a very small area $\Delta\mathbf{A}_n$ characterized by an outward normal $\hat{\mathbf{n}}$. This area contains the point O in which we are interested. We denote $\Delta\mathbf{P}$ as the net force acting on that small area, knowing that this is a contribution to the resultant force acting on the section in order to maintain equilibrium. (If we knew the particulars of the external loading on this body, we would have used the method of sections to calculate $\Delta\mathbf{P}$.)
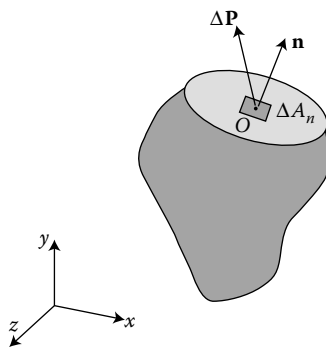
FIGURE 4.5
The stress vector on a planar section through point O with outward normal $\hat{\mathbf{n}}$.

Each of the vectors $\Delta\mathbf{P}$ and $\Delta\mathbf{A}_n$ may be written as the sum of components referred to a standard Cartesian system with unit vectors $(\hat{\mathbf{i}}, \hat{\mathbf{j}}, \hat{\mathbf{k}})$ in the (x, y, z) directions, respectively:

$$\Delta\mathbf{P} = \Delta P_x\hat{\mathbf{i}} + \Delta P_y\hat{\mathbf{j}} + \Delta P_z\hat{\mathbf{k}},$$
$$\Delta\mathbf{A}_n = \Delta A_x\hat{\mathbf{i}} + \Delta A_y\hat{\mathbf{j}} + \Delta A_z\hat{\mathbf{k}}.$$

(4.11)

Remember that in Chapter 2, we considered both normal and shear forces acting on an area and for each considered the stress (normal or shear) to be the intensity of the distribution of force over the area. Now consider that for each component of area, one component of force is a normal force. For example, on the area ΔA_x the force component ΔP_x is a normal force and ΔP_y and ΔP_z are shear forces. If we consider each component of the area vector, then there are nine different stresses we can define, three normal and six shear. Stress, like strain, is defined at a point, using an infinitesimal element. So we define each stress component as the point function yielded by a limit process in which we divide the force component ΔP_j acting at a point O by the area of the section ΔA_i at the point O, and then let the area become vanishingly small:

$$\sigma_{ij} \equiv \lim_{\Delta A_i \to 0} \frac{\Delta P_j}{\Delta A_i}.$$

(4.12)

With this we have characterized the entire stress state in one elegant package, using two subscripts, just as we did for multidimensional strain. For stress, the first subscript denotes the direction of the normal vector to the area component, while the second denotes the direction of the component of force measured on that plane. Thus, we will define stress components such as

$$\sigma_{12} \equiv \lim_{\Delta A_1 \to 0} \frac{\Delta P_2}{\Delta A_1} = \lim_{\Delta A_x \to 0} \frac{\Delta P_y}{\Delta A_x} \equiv \sigma_{xy},$$
$$\sigma_{11} \equiv \lim_{\Delta A_1 \to 0} \frac{\Delta P_1}{\Delta A_1} = \lim_{\Delta A_x \to 0} \frac{\Delta P_x}{\Delta A_x} \equiv \sigma_{xx},$$

(4.13)

as the resulting limits of forces in the y- and x-directions divided by the very small area normal to the x-axis. We recognize that when the area and force are in the same direction, so that the subscripts match, we have a normal stress component, and when they are in different directions and so the subscripts are mixed we have a shear stress component as illustrated in Figure 4.6.

The nine components can be displayed in the matrix form of the *stress tensor*:

$$\boldsymbol{\sigma} = \begin{pmatrix} \sigma_{xx} & \sigma_{xy} & \sigma_{xz} \\ \sigma_{yx} & \sigma_{yy} & \sigma_{yz} \\ \sigma_{zx} & \sigma_{zy} & \sigma_{zz} \end{pmatrix} = \begin{pmatrix} \sigma_{xx} & \tau_{xy} & \tau_{xz} \\ \tau_{yx} & \sigma_{yy} & \tau_{yz} \\ \tau_{zx} & \tau_{zy} & \sigma_{zz} \end{pmatrix}.$$

(4.14)

Sometimes, these components are cast in mixed-format symbols: σ_{xx} for components with repeated subscripts (normal stresses) and τ_{zx} for components with mixed subscripts (shear stresses). We mean the same thing by both of these representations.

This does get a bit simpler; it turns out that, like the strain tensor, the stress tensor is symmetric, that is, that $\sigma_{xy} = \sigma_{yx}$ or $\tau_{xy} = \tau_{yx}$. This is due to the need to maintain rotational equilibrium for the element we are considering. And, in many cases, we will only
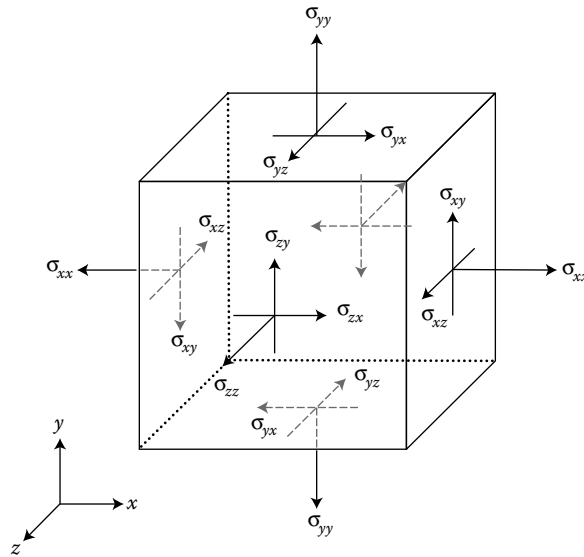
FIGURE 4.6
An infinitesimal element with a three-dimensional stress state.

speak of the average values over an area of a single component each of normal stress and shear stresses. However, it is useful to know the big picture.

The expressions that we have developed depend explicitly on the orientation of the (x, y, z) coordinate system chosen. With differently oriented unit vectors, we would find different values for stress and strain components to represent the same physical stress and strain. This is just the same as the case of first-order tensors, aka vectors. The vector representation has different scalar values for different choices of unit vectors.

There are some special coordinate system orientations that will allow us to understand key facts about a stress or strain state. Stress, strain, and also strain rate, which is relevant for time-dependent behavior in solids but which we will encounter when we begin to focus on fluids in Chapter 13, are all second-order tensors, and as such they exhibit some common properties about their respective *principal values*. These principal values have to do with extreme values of stress and strain on planes at different orientations through a given point. By considering the stresses on particular inclined sections of an axially loaded bar, as we did in Section 2.6, and maximizing normal stress we were taking a first step toward finding the *principal stresses* and the planes to which they corresponded. We also found the magnitude and plane of maximum shear stress. We will return to this issue in Section 5.3.

A note on sign conventions: normal stress is considered positive if it puts an element in tension, and negative if it puts an element in compression. The more general way to think about this is that positive normal stress arises when the force component acting on an area has the same direction as the normal to that area. Negative stress results when the force component is acting in a direction opposite to the area's normal. This is illustrated in Figure 4.7a. The convention for shear stress is exactly the same, and is illustrated in Figure 4.7b. On element faces with normals in positive directions, positively oriented shear forces produce positive stresses.
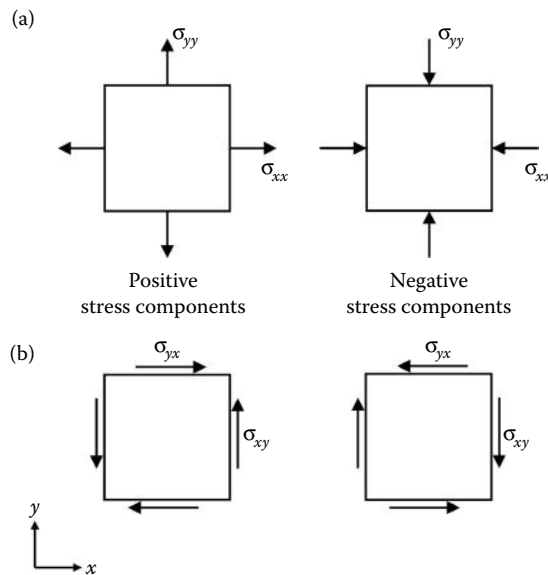
FIGURE 4.7
Sign convention for (a) normal and (b) shear stress.

In the light of our desire to know what is going on at any arbitrary point O within a loaded body—or, equivalently, at each and every point within the body—we now know that we can calculate the components of the forces on each of three perpendicular faces drawn through the point O. We now state the following (provable) mathematical assertion.

If we pass any three mutually orthogonal planes through a point O and find the stress components on each of three mutually perpendicular faces, then we have fully characterized the stress at point O.

If these faces or planes were themselves normal to the x-, y-, and z-axes, we would have found the stress components given in Equations 4.12 through 4.14. We are relieved to find that due to the symmetry of the stress tensor, we will only need six—not nine—components of the stress tensor to fully characterize stress at a point.

It bears repeating: *Stress represents the intensity of internal forces on surfaces within a body subjected to loads*. At an imaginary cut or section, a vector sum of these forces (sometimes called a stress resultant) keeps a body in equilibrium. The body we speak of could be a solid material, a liquid, or a gas. Although the internal forces in a gas more commonly arise from molecular collisions than from applied loads **P**, we can represent these forces by distributed loads in the same way we built up the stress tensor for our general body from Figure 4.5. This will be useful to us throughout our study of continuum mechanics.

4.4 Generalized Hooke's Law

Although we have discussed the fact that stress and strain are second-order tensors, we looked in Chapter 2 at one-dimensional loading, for which we considered only one scalar component of stress and strain at a time. We related stress to strain by the one-dimensional

form of Hooke's law, $\sigma = E\varepsilon$ for normal stress and strain or $\tau = G\gamma$ for shear stress and strain. We can also write a more general form of Hooke's law, relating stress and strain in three dimensions.

If we represent the stress and strain tensors as 3×3 matrices, the constant of proportionality between them is a rather bulky, multi-component construction. Remembering our index notation from Chapter 1, we write the general relation

$$\sigma_{ij} = C_{ijkm}\,\varepsilon_{km}. \tag{4.15}$$

C is an enormous, $3 \times 3 \times 3 \times 3$ tensor—a *fourth*-order tensor. In practice, **C** is known as a material's *stiffness matrix* and its inverse as the *compliance matrix*. It has 81 components. You may wonder why **C** is not simply another 3×3 tensor, as matrix multiplication rules would allow it to be. The reason is that the mechanical behavior **C** represents is complicated, in a way that we understand physically. Any one component of stress could contribute to any and all components of strain. As an example, think about the discussion of Poisson's ratio in Section 4.1: under the action of a single uniaxial applied force, there is deformation along that axis but also along axes perpendicular to the force. Fortunately, though, we do not need to deal with an 81-component tensor. Due to the symmetry of both stress and strain tensors, **C** is also symmetric, with only 36 independent components. The necessity of the existence of a strain energy function (U_0 from Chapter 2) adds some additional symmetry. Because of these symmetry conditions, there are only 21 independent constants (assuming material homogeneity) needed to fully represent a linear elastic solid. However, this most general case, referred to as *anisotropic elasticity*, is not needed for many, many practical materials,[*] and we will simplify further.

For these materials, Hooke's law can be written quite satisfactorily for the *isotropic* case, in which case the constants C_{ijkm} must be invariant with respect to coordinate rotations, that is, they will not change as we look in different directions. In this case, there are in fact only two elastic constants, E and G, although we will also make use of Poisson's ratio ν (not an independent constant; remember Equation 4.2) to keep expressions simple. Hooke's law for an isotropic elastic solid is written as

$$\varepsilon_{xx} = \frac{\sigma_{xx}}{E} - \nu\frac{\sigma_{yy}}{E} - \nu\frac{\sigma_{zz}}{E}, \tag{4.16a}$$

$$\varepsilon_{yy} = -\nu\frac{\sigma_{xx}}{E} + \frac{\sigma_{yy}}{E} - \nu\frac{\sigma_{zz}}{E}, \tag{4.16b}$$

$$\varepsilon_{zz} = -\nu\frac{\sigma_{xx}}{E} - \nu\frac{\sigma_{yy}}{E} + \frac{\sigma_{zz}}{E}, \tag{4.16c}$$

and

$$\gamma_{xy} = 2\varepsilon_{xy} = \frac{\sigma_{xy}}{G}, \tag{4.17a}$$

$$\gamma_{yz} = 2\varepsilon_{yz} = \frac{\sigma_{yz}}{G}, \tag{4.17b}$$

$$\gamma_{zx} = 2\varepsilon_{zx} = \frac{\sigma_{zx}}{G}. \tag{4.17c}$$

---

[*] One prominent exception to this optimistic assumption of homogeneity and isotropy arises in the consideration of biological materials. Arteries and other biological structures have varying properties in different directions, and this variation serves them well. (It also complicates the modeling and mimicking efforts of engineers and biologists.) Please see Chapter 14 for further discussion of the mechanics of biomaterials.

Please remember that the equations here apply only to homogeneous isotropic materials: materials that have the same properties at all points and in all directions. Note that even for these ideal, simplest case materials, the deformation in one direction depends on the normal stresses in all directions.

Finally, by noting the result in Equation 4.5 and summing Equations 4.16a through 4.16c, we find that

$$\frac{\Delta V}{V_0} = \varepsilon_{xx} + \varepsilon_{yy} + \varepsilon_{zz} = \frac{1 - 2\nu}{E}\left(\sigma_{xx} + \sigma_{yy} + \sigma_{zz}\right) = \frac{\sigma_{xx} + \sigma_{yy} + \sigma_{zz}}{3K}, \tag{4.18}$$

where K is known as the *bulk modulus* and the factor of 3 is introduced as part of its definition. Note that both G and K are defined in terms of E and ν, and that there are (still) only two independent constants for a homogeneous, linearly elastic, isotropic solid.

4.5 Equilibrium

We have now addressed the first three items in our continuum mechanics checklist. We have developed ways to talk about (1) deformation or strain, (2) stress, and (3) constitutive laws or stress–strain relationships in multiple dimensions. The fourth item that concerns us is equilibrium, our governing principle. Often, we will be able to tackle equilibrium using statics and the method of sections. Please see the worked examples in Section 4.7 for examples of this. It is also useful to recognize that we can formulate equilibrium as an *elasticity problem*.

4.5.1 Equilibrium Equations

Let's derive the equations of equilibrium for an infinitesimal element in three dimensions, starting with the six components that fully characterize stress at any arbitrary point (recall our assertion that the stress tensor is symmetric).

Consider an element of volume $dx\,dy\,dz$ in which we look at the changes in the stress as we sum forces in three independent directions (see Figure 4.8). We assume that the components of stress are known at the left, bottom, and rear faces, and use the first term of the Taylor expansion to approximate the values of these components at the right, top, and front faces, distances dx, dy, and dz away, as illustrated in Figure 4.8.

For example, forces in the x-direction result from stresses on all six faces (with each stress multiplied by the area on which it acts):

$$\left(\sigma_{xx} + \frac{\partial \sigma_{xx}}{\partial x}dx\right)dy\,dz - \sigma_{xx}\,dy\,dz + \left(\sigma_{yx} + \frac{\partial \sigma_{yx}}{\partial y}\,dy\right)dx\,dz - \sigma_{yx}\,dx\,dz$$

$$+ \left(\sigma_{zx} + \frac{\partial \sigma_{zx}}{\partial z}\,dz\right)dx\,dy - \sigma_{zx}\,dx\,dy + B_x\,dx\,dy\,dz = 0. \tag{4.19}$$
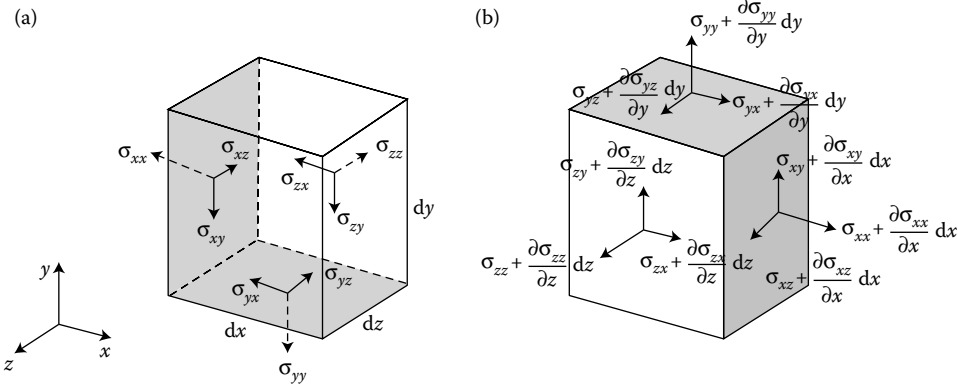
FIGURE 4.8
An element with a three-dimensional stress state. For clarity, stress components on three faces at a time are shown: (a) stress components on left, bottom, and rear faces; (b) stress components on right, top, and front faces.

In Equation 4.19, we have once again introduced a body force, per unit volume, whose x-component is B_x. After canceling terms appropriately and dividing through by the element volume, we find the following equation of equilibrium:

$$\frac{\partial \sigma_{xx}}{\partial x} + \frac{\partial \sigma_{yx}}{\partial y} + \frac{\partial \sigma_{zx}}{\partial z} + B_x = 0. \tag{4.20a}$$

Similarly, in the y- and z-directions,

$$\frac{\partial \sigma_{xy}}{\partial x} + \frac{\partial \sigma_{yy}}{\partial y} + \frac{\partial \sigma_{zy}}{\partial z} + B_y = 0, \tag{4.20b}$$

$$\frac{\partial \sigma_{xz}}{\partial x} + \frac{\partial \sigma_{yz}}{\partial y} + \frac{\partial \sigma_{zz}}{\partial z} + B_z = 0. \tag{4.20c}$$

Thus, Equations 4.20a through 4.20c represent three equations of equilibrium from which we must determine six components of stress. Interestingly, we reduced the number of stress unknowns to six from nine by effectively using three moment equilibrium equations that enforce the symmetry of the tensor.

We can also use indicial or index notation from Section 1.5 to write these equations in a very elegant form. Recalling the summation convention that a comma is used to denote partial differentiation and that the stress tensor is symmetric, the three equations of equilibrium can be written simply as

$$\sigma_{ij,j} + B_i = 0, \tag{4.21}$$

where σ is used for all stress components including shear stresses, and the range of the indices implied to be $i, j = 1, 2, 3$.

4.5.2 The Two-Dimensional State of Plane Stress

In many circumstances, we can simplify the analysis of stress by recognizing that a structure is thin in one dimension (e.g., the dimension along the z-axis) in comparison to its dimensions in the other two (x and y) directions, and the loading is essentially in the xy-plane. This class of problems is called *plane stress*, and it includes the analysis of aircraft
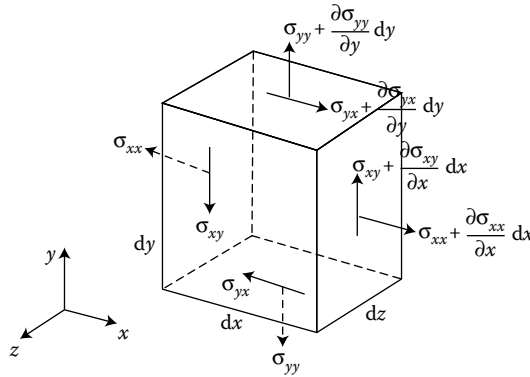
FIGURE 4.9
A three-dimensional element in plane stress.

and spacecraft structures, pressure vessels, and similar *thin-walled structures*. In this case, because we assume that

$$\sigma_{zz}, \sigma_{xz}, \sigma_{yz} \approx 0, \tag{4.22}$$

there are only three stress components to worry about: σ_{xx}, σ_{xy} and σ_{yy}.

In this context, we need to solve only two equilibrium equations (see also Figure 4.9):

$$\frac{\partial \sigma_{xx}}{\partial x} + \frac{\partial \sigma_{yx}}{\partial y} + B_x = 0,$$

$$\frac{\partial \sigma_{xy}}{\partial x} + \frac{\partial \sigma_{yy}}{\partial y} + B_y = 0. \tag{4.23}$$

It is important to note the following:

- Plane stress in the *z*-direction does *not* mean or imply that there are no loads applied in that direction. Indeed, the loads in the thickness- or *z*-direction in a thin-walled structure cause *membrane stresses* of significant magnitude in the *in-plane* directions. These stresses are significantly larger than the stress in the thickness direction. We will understand this more clearly when we study pressure vessels in Chapter 5.

- Plane stress in the *z*-direction does *not* mean or imply that the deflection (or displacement, w) is zero in that direction. For thin-walled structures, it is the deflection in the direction of the thickness that is usually the most prominent and visible deformation.

For the state of plane stress in the *z*-direction, as defined in Equation 4.23, the constitutive law, or appropriate form of generalized Hooke's law, for the remaining two normal stresses becomes

$$\sigma_{xx} = \frac{E}{1 - \nu^2} \left(\varepsilon_{xx} + \nu \varepsilon_{yy} \right),$$

$$\sigma_{yy} = \frac{E}{1 - \nu^2} \left(\nu \varepsilon_{xx} + \varepsilon_{yy} \right). \tag{4.24}$$

4.5.3 The Two-Dimensional State of Plane Strain

Problems in *plane strain* occur when there is reason to believe there is no appreciable variation or deformation in a direction. In such instances, the movement of any point is likely to be very small in that direction. Assuming that the loading doesn't vary appreciably along this direction, we could look at every plane perpendicular to this direction and expect to realize the same behavior in each plane. We realize plane strain in objects that are both very long in one direction and constrained (relatively) uniformly in that direction so that

$$\varepsilon_{zz} = \varepsilon_{xz} = \varepsilon_{yz} = 0. \tag{4.25}$$

Equation 4.25 indicates that when the conditions of plane strain are judged to apply, we simply set the corresponding strain components to zero. However, this does not mean that the corresponding stresses are zero. For the case of plane strain in the z-direction, as defined in Equation 4.25, the normal stress in the z-direction is not zero. In fact, it is the stress required to maintain the constraints that can be said to characterize plane strain. Re-arranging Equation 4.16c for the case of $\varepsilon_{zz} = 0$,

$$\sigma_{zz} = \nu \left(\sigma_{xx} + \sigma_{yy} \right) \neq 0, \tag{4.26}$$

so that the constitutive laws for plane strain become

$$\sigma_{xx} = \frac{E}{(1+\nu)(1-2\nu)} \left[(1-\nu)\varepsilon_{xx} + \nu\varepsilon_{yy} \right],$$

$$\sigma_{yy} = \frac{E}{(1+\nu)(1-2\nu)} \left[\nu\varepsilon_{xx} + (1-\nu)\varepsilon_{yy} \right]. \tag{4.27}$$

The in-plane equilibrium equations and the compatibility relations between strain and displacement are the same in both plane stress and plane strain.

4.6 Formulating Two-Dimensional Elasticity Problems

In this section, we briefly describe how a two-dimensional problem is formulated in the theory of elasticity. Bearing in mind the notation often used in structural mechanics, as we will do when we study beams in Chapters 7 and 9, we now place our problems in the (x, z)-plane, so that we are considering plane stress or plane strain in the y-direction.

The starting point is equilibrium, and the two-dimensional version (Equation 4.23) is repeated here with a body force due to gravity in the downward vertical or negative z-direction:

$$\frac{\partial \sigma_{xx}}{\partial x} + \frac{\partial \sigma_{zx}}{\partial z} = 0, \tag{4.28a}$$

$$\frac{\partial \sigma_{xz}}{\partial x} + \frac{\partial \sigma_{zz}}{\partial z} - \rho g = 0. \tag{4.28b}$$

If we were to integrate these partial differential equations, we could then algebraically calculate the corresponding strains, depending on which planar model we were applying.

For plane stress, for example, and from either Equations 4.16 or equivalently the inversion of Equations 4.27, we could find the engineering strains

$$\varepsilon_{xx} = \frac{1}{E}(\sigma_{xx} - \nu\sigma_{zz}), \tag{4.29a}$$

$$\varepsilon_{zz} = \frac{1}{E}(\sigma_{zz} - \nu\sigma_{xx}), \tag{4.29b}$$

$$\gamma_{xz} = \frac{\sigma_{xz}}{G}. \tag{4.29c}$$

Next we can determine the two meaningful displacements in this plane stress model, that is $u(x,z)$ and $w(x,z)$, by integrating the relevant strain–displacement equations (a subset of Equations 4.4 and 4.6),

$$\varepsilon_{xx} = \frac{\partial u}{\partial x}, \quad \varepsilon_{zz} = \frac{\partial w}{\partial z},$$

$$\gamma_{xz} = \left(\frac{\partial u}{\partial z} + \frac{\partial w}{\partial x}\right). \tag{4.30}$$

Summarizing what we have said so far for plane stress, in tabular form:

Equations	Number	Unknowns	Number
Equilibrium (4.28)	2	$\sigma_{xx}, \sigma_{zz}, \sigma_{xz}$	3
Hooke's law (4.29)	3	$\varepsilon_{xx}, \varepsilon_{zz}, \gamma_{xz}$	3
Strain–displacement (4.30)	3	$u(x,z), w(x,z)$	2
Total	8		8

On the surface, this seems copacetic: in Equations 4.28 through 4.30, we clearly have a *system* of eight equations involving eight unknowns. But some questions remain. First and foremost, are there ways to restructure the problem to make it seem less onerous? We espy a glimmer of hope, recalling that a footnote in Section 2.9 hinted that by formulating a problem in terms of displacements rather than stresses, we would be able to erode the distinction between statically indeterminate and determinate problems.

4.6.1 Equilibrium Expressed in Terms of Displacements

There are two ways to structure solution processes for elasticity problems, and choosing between the two depends on whether one wants to get directly to displacements or directly to stresses. The approach to calculating displacements directly requires a short chain of straightforward substitutions: First, Equations 4.29 is substituted into Equations 4.28 to cast equilibrium in terms of strain components. Second, the strain–displacement relations (4.30) are used to eliminate the strains from the intermediate results just found. As Problem 4.14 asks you to confirm, the equations of equilibrium cast in terms of displacements are, for plane stress:

$$G\nabla^2 u + \frac{1+\nu}{1-\nu}G\frac{\partial}{\partial x}\left(\frac{\partial u}{\partial x} + \frac{\partial w}{\partial z}\right) = 0,$$

$$G\nabla^2 w + \frac{1+\nu}{1-\nu}G\frac{\partial}{\partial z}\left(\frac{\partial u}{\partial x} + \frac{\partial w}{\partial z}\right) = \rho g. \tag{4.31}$$

This is a system of just two equations for the two unknown displacements, and an elegant system at that. Notice the symmetry of the differential operators* and of the groupings of elastic constants. In fact, Equations 4.31 are a subset (remember, we are talking about plane stress) of the well-known Navier equations of elasticity theory. In indicial notation, the three-dimensional Navier equations are

$$G\nabla^2 u_i + \frac{1}{1-2\nu}G\frac{\partial \varepsilon_{kk}}{\partial x_i} + B_i = 0, \tag{4.32}$$

where **B** is the net body force acting on the body—in very many cases, the only body force that comes into play is that due to gravity—with modulus G and Poisson's ratio ν. Of course with the summation convention ε_{kk} is the trace of the strain tensor. The parallels between Equations 4.31 and 4.32 are unmistakable. The difference in the elastic constants results from the plane stress assumption in Equation 4.31. Note, also, that both of Equation 4.31 include an abbreviated, two-dimensional version of the volume change, or *dilatation* (Equation 4.5):

$$\frac{\partial u}{\partial x} + \frac{\partial w}{\partial z} = \varepsilon_{xx} + \varepsilon_{zz}. \tag{4.33}$$

This term also clearly reflects the two-dimensional nature of this discussion.

4.6.2 Compatibility Expressed in Terms of Stress Functions

How would the solution process for the case of plane stress be different if we wanted to find stresses directly? It is a neat piece of arithmetic to show that if we can identify some function ϕ from which we can calculate the stress components by performing the following derivatives:

$$\sigma_{xx} = \frac{\partial^2 \phi}{\partial z^2},$$

$$\sigma_{zz} = \frac{\partial^2 \phi}{\partial x^2} + \rho g z, \tag{4.34}$$

$$\sigma_{xz} = -\frac{\partial^2 \phi}{\partial x \partial z}.$$

then these stress components will identically satisfy the two-dimensional equations of equilibrium. So, what is this function ϕ, and how do we find and calculate it?

The function ϕ is called a *potential function*, and in this instance it derives from the stress–strain and strain–displacement relations, Equations 4.29 and 4.30. Starting with Equation 4.30, we seem to have three strain–displacement relations for determining (only) two displacements. In fact, these three equations are themselves related, that is, they are not entirely independent. We can see this by eliminating the displacements u and w between the three Equation 4.30, that is, by noting that

$$\frac{\partial^2 \varepsilon_{xx}}{\partial z^2} + \frac{\partial^2 \varepsilon_{zz}}{\partial x^2} = \frac{\partial^3 u}{\partial x \partial z^2} + \frac{\partial^3 w}{\partial z \partial x^2} \equiv \frac{\partial^2 \gamma_{xz}}{\partial x \partial z},$$

---

* The del-squared ∇^2 operator, or Laplacian, is reviewed in Appendix B.

or

$$\frac{\partial^2 \varepsilon_{xx}}{\partial z^2} + \frac{\partial^2 \varepsilon_{zz}}{\partial x^2} = \frac{\partial^2 \gamma_{xz}}{\partial x \partial z}. \tag{4.35}$$

Equation 4.35 is a *compatibility condition* that the strains must satisfy in order that displacements obtained by integrating Equation 4.30 are continuous and single-valued. That compatibility condition can then be straightforwardly expressed in terms of the potential function—also called the *Airy stress function* after its originator—by substituting for the strains using the stress–strain law (Equation 4.29) and for the stresses from the definition of the potential function (Equation 4.34). Then, as Problem 4.15 asks you to confirm, the resulting form of the compatibility equation expressed in terms of the Airy stress function* is

$$\nabla^4 \phi = \nabla^2 \nabla^2 \phi = 0. \tag{4.36}$$

4.6.3 Some Remaining Pieces of the Puzzle of General Formulations

We can summarize our two formulations so far as follows. In the first instance, we used constitutive and kinematics relations to write equilibrium entirely in terms of displacements (see Equation 4.31). The solutions to these equations can be inspected to ensure that the resulting displacements are continuous, single-valued, and consistent with any constraints. From these displacements, we can calculate strain and then stress.

In the second instance, we used equilibrium and a constitutive law to write compatibility entirely in terms of a (single) Airy stress function (Equation 4.36). A solution to Equation 4.36 automatically satisfies equilibrium and will produce compatible displacements (although it is always a good idea to inspect displacement results).

How and where do the actual loads come into the picture? And, what are the correct boundary conditions corresponding to Equations 4.31 and 4.36? These two questions—and their answers —are related, in part because of issues raised in Chapter 2. Remember that there are two kinds of external or applied loads that are applied to solids or structures. One kind of applied load comes through *body forces* that typically reflect response on a specific, "per unit" basis to a field, such as gravity or electromagnetic radiation. As we have seen, body forces appear in our formulations of equilibrium. The second kind of external load results from *surface loading*, that is, the distribution of forces (and moments) on the surface of the solid or structure, including points on the solid's bounding surface at which the structure is supported (or grounded). Surface loads may appear in equations of equilibrium (as they did for axially loaded bars, and as they will in our discussion of beams in later chapters), as well as in appropriate boundary conditions, as we will now discuss.

We begin by introducing the idea of a *traction vector* as the point function resulting from a limit process in which we divide the net force $\Delta \mathbf{P}$ acting at a point O by the area of the section $\Delta \mathbf{A}_n$ at the point O, and then let the area become vanishingly small. This is the same process we used to define the stress tensor, but here we are going to group terms differently. Instead of breaking up the force and area each into three components and defining

---

* Again, the del-squared operator, or Laplacian, is reviewed in Appendix B. $\nabla^4 = \nabla^2 \nabla^2$ is called the biharmonic operator.

nine entries in the stress tensor, we will consider the total force acting on each component of area:

$$\mathbf{t}_x \equiv \lim_{\Delta A_x \to 0} \frac{\Delta P_x \hat{\mathbf{i}} + \Delta P_y \hat{\mathbf{j}} + \Delta P_z \hat{\mathbf{k}}}{\Delta A_x} = \sigma_{xx}\hat{\mathbf{i}} + \sigma_{xy}\hat{\mathbf{j}} + \sigma_{xz}\hat{\mathbf{k}}, \qquad (4.37a)$$

$$\mathbf{t}_y \equiv \lim_{\Delta A_y \to 0} \frac{\Delta P_x \hat{\mathbf{i}} + \Delta P_y \hat{\mathbf{j}} + \Delta P_z \hat{\mathbf{k}}}{\Delta A_y} = \sigma_{yx}\hat{\mathbf{i}} + \sigma_{yy}\hat{\mathbf{j}} + \sigma_{yz}\hat{\mathbf{k}}, \qquad (4.37b)$$

$$\mathbf{t}_z \equiv \lim_{\Delta A_z \to 0} \frac{\Delta P_x \hat{\mathbf{i}} + \Delta P_y \hat{\mathbf{j}} + \Delta P_z \hat{\mathbf{k}}}{\Delta A_z} = \sigma_{zx}\hat{\mathbf{i}} + \sigma_{zy}\hat{\mathbf{j}} + \sigma_{zz}\hat{\mathbf{k}}. \qquad (4.37c)$$

These components are truly vectors because in each we are looking at the vector force $\Delta \mathbf{P}$ acting on a scalar area.

Then, if we simply apply Equation 4.37 at points on a surface bounding the solid or structure of interest, with the various $\mathbf{t}$'s taken as *known* or *prescribed* forces, then Equation 4.37 serve as the boundary conditions on the corresponding stresses at those points on the surface. Written in indicial form, Equations 4.37 is the famous Cauchy equation of the theory of elasticity, relating traction vectors to the stress tensor:

$$t_i = \sigma_{ij} n_j, \qquad (4.38)$$

where n_j is the unit basis vectors. Of course, there are problems where we also know or prescribe the displacement(s) at points. These seem easier to express because we are simply equating displacement components to specified values or functions. However, it is also the case that we *cannot prescribe both a force and a displacement in the same direction at the same point*. We will see how that plays out in detail when we talk about engineering beam theory in Chapter 7. In the meantime, we leave it as an assertion that should have at least intuitive appeal. Would it make sense to prescribe the force we might apply to one end of a spring and, at the same time, prescribe independently how far that end should move?

Finally, we note that the above formulations of the plane stress problem can be duplicated for plane strain, although the final details may differ. Plane stress and plane strain are important concepts that find frequent use in elasticity theory and in structural mechanics. And while their mathematics may be quite similar, their applications are rather different. Thus, it is important to remember the domain of each. The plane stress model is valid for solids or structures that are both thin and only insignificantly loaded through the thickness, while the plane strain model is valid for a thin slice of a solid that is very long in one direction, along which there is no (or very little) variation in load or geometry.

This introduction to elasticity has been just that, an introduction. The important concepts here should not surprise you: kinematic description of displacements (strain), internal loading (stress), equilibrium, and compatibility. We have packed a full bag of mathematical tools for problems in continuum mechanics. In Chapter 5, we will investigate applications of these tools to problems in torsion and pressure vessels and return to the question of transforming coordinate systems in our descriptions of stress and strain.

4.7 Examples

EXAMPLE 4.1

Freshly cured concrete is cut with a saw to provide joints that allow for expansion and contraction to prevent random cracking. A flexible sealant is used to fill the gap between

concrete slabs. Consider a sealant joint that subsequently is subject to compression and shear forces P_n and P_s. Using the coordinate axes shown, write the strain tensor for a point in the sealant in terms of its elastic modulus E and Poisson's ratio ν; the height h, thickness t, and length L of the joint; and the force magnitudes.

Given: Geometry and loading on sealant.

Find: Strain tensor for the sealant.

Assume: Uniformly distributed loads; Hooke's law applies.

Solution

The sealant experiences one normal stress $\sigma_{yy} = P_n / hL$ which results in three normal strains.

$$\varepsilon_{yy} = \frac{\sigma_{yy}}{E} = \frac{P_n}{EhL} \quad \text{and} \quad \varepsilon_{xx} = \varepsilon_{zz} = -\nu\varepsilon_{yy} = -\frac{\nu P_n}{EhL}.$$

There is only one pair of nonzero shear stresses, $\sigma_{yz} = \sigma_{zy} = -P_s / hL$. Note that the negative sign indicates that the force is in the negative z-direction on the area with its normal in the positive y-direction. This results in one pair of normal strains.

$$\varepsilon_{yz} = \varepsilon_{zy} = \frac{1}{2}\gamma_{yz} = \frac{1}{2}\frac{\sigma_{yz}}{G} = \frac{1}{2}\frac{-P_s / hL}{E/2(1+\nu)} = -\frac{P_s(1+\nu)}{EhL}.$$

So the complete strain tensor is

$$\varepsilon = \begin{pmatrix} -\dfrac{\nu P_n}{EhL} & 0 & 0 \\[2ex] 0 & \dfrac{P_n}{EhL} & -\dfrac{P_s(1+\nu)}{EhL} \\[2ex] 0 & -\dfrac{P_s(1+\nu)}{EhL} & -\dfrac{\nu P_n}{EhL} \end{pmatrix}.$$

EXAMPLE 4.2

A rectangular copper alloy block as shown in the figure below has the following dimensions: $a = 200\,\text{mm}$, $b = 120\,\text{mm}$, and $c = 100\,\text{mm}$. This block is subjected to a tri-axial loading in equilibrium having the following magnitude: $\sigma_{xx} = +2.40\,\text{MPa}$, $\sigma_{yy} = -1.20\,\text{MPa}$, and $\sigma_{zz} = -2.0\,\text{MPa}$. Assuming that the applied forces are uniformly distributed on the respective faces, determine the size changes that take place along a, b, and c. Let $E = 140\,\text{GPa}$ and $\nu = 0.35$.
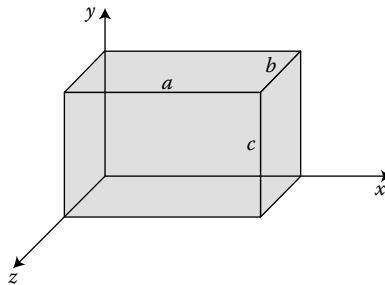
Given: Stress state, dimensions, and properties of the copper block.

Find: Size changes in each direction.

Assume: Homogeneous and isotropic; Hooke's law applies.

Solution

We will need the generalized form of Hooke's law, since we have stresses and deformations in multiple directions.

$$\varepsilon_{xx} = \frac{\sigma_{xx}}{E} - \nu\frac{\sigma_{yy}}{E} - \nu\frac{\sigma_{zz}}{E},$$

$$\varepsilon_{yy} = -\nu\frac{\sigma_{xx}}{E} + \frac{\sigma_{yy}}{E} - \nu\frac{\sigma_{zz}}{E},$$

$$\varepsilon_{zz} = -\nu\frac{\sigma_{xx}}{E} - \nu\frac{\sigma_{yy}}{E} + \frac{\sigma_{zz}}{E}.$$

Plugging in the given values of each normal stress component, Poisson's ratio, and E:

$$\varepsilon_{xx} = 25 \times 10^{-6} = \frac{\Delta_a}{a}, \quad \text{so } \Delta_a = (25 \times 10^{-6})(200\,\text{mm}) = 5.0 \times 10^{-3}\,\text{mm}.$$

Similarly,

$$\Delta_b = -9.8 \times 10^{-4}\,\text{mm},$$

$$\Delta_c = -2.1 \times 10^{-3}\,\text{mm},$$

so that the new dimensions of the copper block are: $a' = 200.005\,\text{mm}$, $b' = 119.999\,\text{mm}$, and $c' = 99.998\,\text{mm}$.

EXAMPLE 4.3

A rectangular block is compressed by a uniform stress σ_0 as it sits between two rigid surfaces with the gap a shown in the figure below. Determine

a. The stress σ_{yy} after the gap is closed
b. The change in the length along the x-axis both before and after the gap is closed
c. The minimum value of σ_0 needed to close the gap
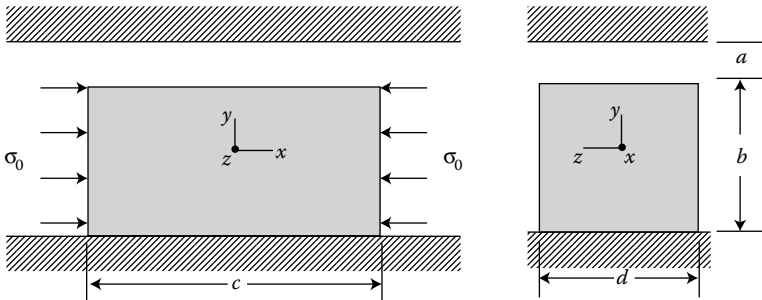
Given: Rectangular block under uniform stress.

Find: Normal stress in the y-direction; deformation in the x-direction; applied stress needed to close gap.

Assume: Material is homogeneous and isotropic; Hooke's law applies.

Solution

1. Before the gap is closed, $\sigma_{xx} = -\sigma_0$ is the only nonzero stress component. After the gap is closed σ_{yy} is not zero. With $\sigma_{zz} = 0$ in both cases, in general

$$\varepsilon_{yy} = -\nu \frac{\sigma_{xx}}{E} + \frac{\sigma_{yy}}{E} = \nu \frac{\sigma_0}{E} + \frac{\sigma_{yy}}{E},$$

then solving for σ_{yy}

$$\sigma_{yy} = E \varepsilon_{yy} - \nu \sigma_0.$$

When the gap is closed, $\varepsilon_{yy} = \Delta L_y / L_y = a/b$, so

$$\sigma_{yy} = E \frac{a}{b} - \nu \sigma_0.$$

2. Generally

$$\varepsilon_{xx} = \frac{\sigma_{xx}}{E} - \nu \frac{\sigma_{yy}}{E} = -\frac{\sigma_0}{E} - \nu \frac{\sigma_{yy}}{E},$$

So

$$\Delta L_x = \varepsilon_{xx} c = -\frac{c}{E} \left(\sigma_0 + \nu \sigma_{yy} \right),$$

and this reduces to $\Delta L_x = -(c/E)\sigma_0$ before the gap is closed.

3. σ_{yy} is zero before and just as the gap closes. With this, re-arranging the result from part (1) gives

$$\sigma_0 = \left(\frac{Ea}{\nu b} \right).$$

EXAMPLE 4.4

For a general case of plane stress, find the out-of-plane normal strain in terms of the in-plane strains.

   Given: Plane stress state.

   Find: Relationship between out-of-plane strain and in-plane strains.

   Assume: Hooke's law applies.

Solution

We start with generalized Hooke's law for the case of plane stress:

$$\varepsilon_{zz} = -\nu \frac{\sigma_{xx}}{E} - \nu \frac{\sigma_{yy}}{E} + \frac{\sigma_{zz}}{E} = -\frac{\nu}{E}(\sigma_{xx} + \sigma_{yy}),$$

and then incorporate the Equation 4.24

$$\sigma_{xx} = \frac{E}{1 - \nu^2} \left(\varepsilon_{xx} + \nu \varepsilon_{yy} \right),$$

$$\sigma_{yy} = \frac{E}{1 - \nu^2} \left(\nu \varepsilon_{xx} + \varepsilon_{yy} \right),$$

to get

$$\varepsilon_{zz} = -\frac{\nu}{E}\left[\frac{E}{1-\nu^2}\left(\varepsilon_{xx} + \nu\varepsilon_{yy} + \nu\varepsilon_{xx} + \varepsilon_{yy}\right)\right] = -\frac{\nu}{1-\nu}\left(\varepsilon_{xx} + \varepsilon_{yy}\right).$$

The negative sign confirms that in-plane stretch corresponds to thinning in the out-of-plane direction. Interestingly, this result shows dependence on Poisson's ratio but not on elastic modulus.

PROBLEMS

4.1 Show that the change in volume of a solid body element whose initial, unstrained volume is $V = l_x l_y l_z$ is given (to first order in the normal strains) by

$$\frac{\Delta V}{V} = \varepsilon_{xx} + \varepsilon_{yy} + \varepsilon_{zz}.$$

4.2 Calculate all of the normal and shear strains for the following displacement field:

$$u(x, y, z) = -z\frac{\partial w(x)}{\partial x}, \quad v(x, y, z) = 0, \quad w(x, y, z) = w(x).$$

Write your answer in a strain tensor. (*Note*: These results will reappear when we study *beams*.)

4.3 Calculate all of the normal and shear strains for the following displacement field:

$$u(x, y, z) = -\alpha yz, \quad v(x, y, z) = \alpha xz, \quad w(x, y, z) = 0.$$

Write your answer in a strain tensor. (*Note*: These results will re-appear when we study *torsion*.)

4.4 Calculate all of the normal and shear strains for the following displacement field:

$$u(x, y, z) = -\alpha yz, \quad v(x, y, z) = \alpha xz, \quad w(x, y, z) = \kappa(x, y).$$

Write your answer in a strain tensor. Compare and contrast these results with those of Problem 4.3.

4.5 Verify that the results $\sigma_{xy} = \sigma_{yx}$, $\sigma_{yz} = \sigma_{zy}$, $\sigma_{xz} = \sigma_{zx}$ are correct by satisfying moment equilibrium for an infinitesimal volume element about each of the three orthogonal axes.

4.6 A circle of diameter d is inscribed on the surface of an unstressed metal (Young's modulus E and Poisson ratio ν) square plate of thickness t and side length l (as pictured below). If the plate is subjected to planar stresses $\sigma_{xx} = 82.7\,\text{MPa}$ and $\sigma_{yy} = 137.8\,\text{MPa}$, and has properties $E = 200\,\text{GPa}, \nu = 0.30, t = 2.00\,\text{cm}$, and $l = 40.0\,\text{cm}$, find the changes in
   a. The length of the diameter AB
   b. The length of the diameter CD

    c. The thickness of the plate

    d. The volume of the plate
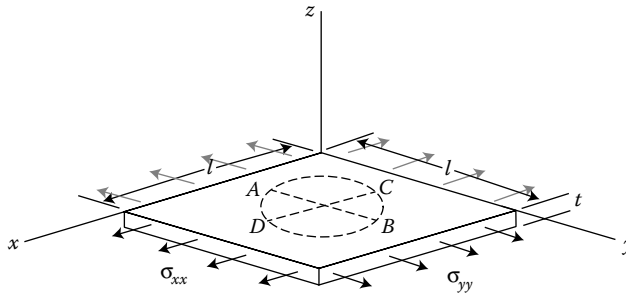
4.7 A piece of $50 \times 200 \times 10$ mm steel plate is subjected to loading along its edges, as shown. (a) If $P_x = 100$ kN and $P_y = 200$ kN, what change in thickness occurs due to the application of these forces? (b) For P_x alone to cause the same change in thickness as in part (a), what must be the magnitude of P_x? Let $E = 200$ GPa and $\nu = 0.25$.

4.8 Two small cubes of equal size but made of different materials are stacked (as shown in the figure below), so they just fit between two rigid surfaces. The bottom cube is subjected to a uniform pressure p on each of its exposed surfaces. Find the *contact* or *interfacial stress* on the connecting plane, expressed in terms of p and the two sets of material properties.
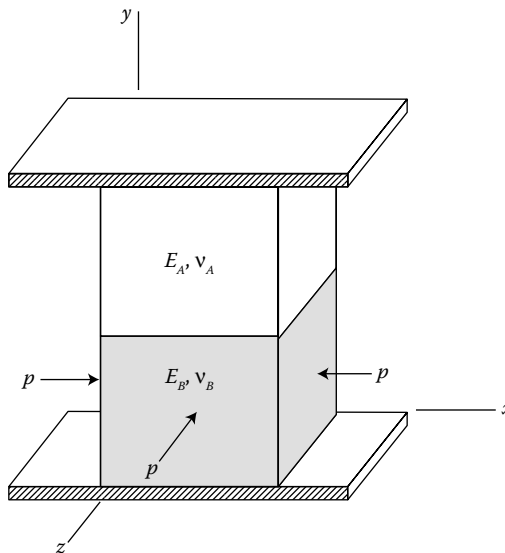
4.9 The two small cubes of Problem 4.8 are each subjected to a separate uniform pressure, p_b on the exposed faces of the bottom cube and p_a on the exposed surfaces of the top cube. What is the ratio of these two pressures, expressed in terms of the two sets of material properties, such that the volume changes of both cubes are the same?

4.10 An isotropic, elastic (modulus E, Poisson's ratio ν), homogenous block of a material with a high coefficient of thermal expansion α is embedded in a mold that has a

cavity open on top and rigid, smooth walls (negligible friction). The coefficient of thermal expansion of the mold is very small, and we can assume its dimensions do not change. The block has original dimensions L_x, L_y, and L_z. If the block temperature is increased by ΔT, what is the change in the height of the block in the z-direction?
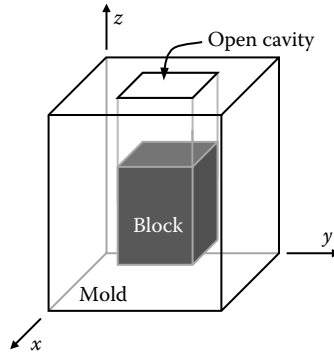
4.11 A prototype bolt shaft (assume a uniform cylinder) that is to be loaded in tension is made of a stainless steel with a yield strength of 450 MPa and has a safety factor of 3 with respect to yielding for the maximum allowable loading. Find two ductile materials that could be used to replace the steel to make the bolt lighter while maintaining the same safety factor. The new bolts will have the same length as the original but may have different diameters. What is the percent weight savings with each of the new materials? What other material properties might be important to consider before a final choice is made?

4.12 Fabric used in hot air balloons (see below) is subjected to biaxial loading that results in a state of plane stress. A particular panel on a balloon that has an x length of 175 cm and a y length of 130 cm is subject to stresses $\sigma_{xx} = 160$ MPa and $\sigma_{yy} = 140$ MPa. The properties of the fabric can be approximated as $E = 87$ GPa and $\nu = 0.34$. Determine (a) the changes in x and y dimensions, and (b) the percent change in thickness of the panel.

4.13 Consider a 4-in square steel bar subjected to transverse biaxial tensile stresses of 20 ksi in the x-direction and 10 ksi in the y-direction. (a) Assuming the bar to be in a state of plane stress, determine the strain in the z-direction and the elongations of the plate in the x- and y-directions. (b) Assuming the bar to be in a state of plane strain, determine the stress in the z-direction and the elongations of the bar in the x- and y-directions. Let $E = 30 \times 10^3$ ksi and $\nu = 0.25$.

4.14 Verify the following equilibrium equations for plane stress in the xz-plane.

$$G\nabla^2 u + \frac{1+\nu}{1-\nu} G \frac{\partial}{\partial x} \left(\frac{\partial u}{\partial x} + \frac{\partial w}{\partial z} \right) = 0,$$

$$G\nabla^2 w + \frac{1+\nu}{1-\nu} G \frac{\partial}{\partial z} \left(\frac{\partial u}{\partial x} + \frac{\partial w}{\partial z} \right) = \rho g.$$

4.15 Verify the following compatibility equation for plane stress in the xz-plane.

$$\nabla^4 \phi = \nabla^2 \nabla^2 \phi = 0.$$

4.16 Derive counterparts for the case of plane strain in the xz-plane of the equilibrium equations shown in Problem 4.14 for plane stress. How do these plane strain results differ from the equilibrium equations for plane stress?

4.17 Derive a counterpart for the case of plane strain in the xz-plane of the compatibility equation shown in Problem 4.15 for plane stress. How does this plane strain result differs from the compatibility equation for plane stress?

4.18 Explain the notation and meaning of Cauchy's formula:

$$t_i = \sigma_{ij} n_j.$$

4.19 Determine, for the following three-dimensional state of stress,

$$\begin{vmatrix} 1000 & 200 & 200 \\ 200 & 1000 & 200 \\ 200 & 200 & 1000 \end{vmatrix} \text{psi}$$

a. The components of the surface traction vector acting on an element of surface that has a normal vector $\hat{\mathbf{n}} = 0.50\hat{\mathbf{i}} + 0.50\hat{\mathbf{j}} + 0.707\hat{\mathbf{k}}$.

b. The component of this surface traction vector in the direction of the unit vector $\hat{\boldsymbol{\lambda}} = 0.25\hat{\mathbf{i}} + 0.935\hat{\mathbf{j}} + 0.25\hat{\mathbf{k}}$.

5

Applying Strain and Stress in Multiple Dimensions

In both one and multiple dimensions, we have now considered how continuum mechanics will help us create and analyze effective designs. We made sure to include (1) kinematics, or strain; (2) stress; (3) constitutive laws, or how strain and stress are related; and (4) equilibrium as we developed general results to help us analyze the internal response of continuous materials to external loading. In Chapter 4, we recognized that strain, stress, and the material stiffness that relates them are each *tensors* (of second-, second-, and fourth-order, respectively). The somewhat involved mathematics of the last parts of Chapter 4 should not have distracted us from our goal: to obtain useful results that we will apply to the design and analysis of structures. In Chapter 5, we will apply the formulations and results of Chapter 4 to several canonical types of external loading, and we will return to the question of how strain and stress depend on the reference coordinate system.

5.1 Torsion

In the previous chapters, we have discussed primarily axial loading conditions and how to determine stresses and deformations under these conditions. We now turn our attention to bodies subjected to a twisting action caused by a torque or a twisting moment. As before, we will be looking at the isolated effects of this one type of loading; we will later be able to combine multiple loading configurations to address more realistic, real-world problems. One example of a twisting external load is in the tightening of a vise grip: the user applies a torque to the threaded screw of the vise, turning it, which in turn causes the jaws to tighten. In practice, rods for transmitting torque, such as motor shafts, are generally circular or tubular in cross section. Most of our examples and applications, therefore, will involve circular sections.

5.1.1 Method of Sections

What happens when a shaft or rod in static equilibrium is subjected to a twisting motion? If the rod is free, this is caused by a pair of externally applied, equal and oppositely directed torques (or couples) acting in parallel planes. If the rod is fixed, this is caused by a single applied external torque and internal resisting torque supplied by the fixed end. The portion of the rod between these two external, or between the external and internal, torques is said to be in *torsion*, or under torsional load. For example, the screw of the bench vise mentioned above is in torsion when the jaws are fully tightened and force is still applied to the handle.

Generally, only one equation of statics will be relevant: $\sum M_x = 0$, where the x-axis is directed along the rod in question. So, when we apply the method of sections, the internal torque must balance the externally applied torque: it must be equal, but have opposite sense. For an example of this, see Figure 5.1.
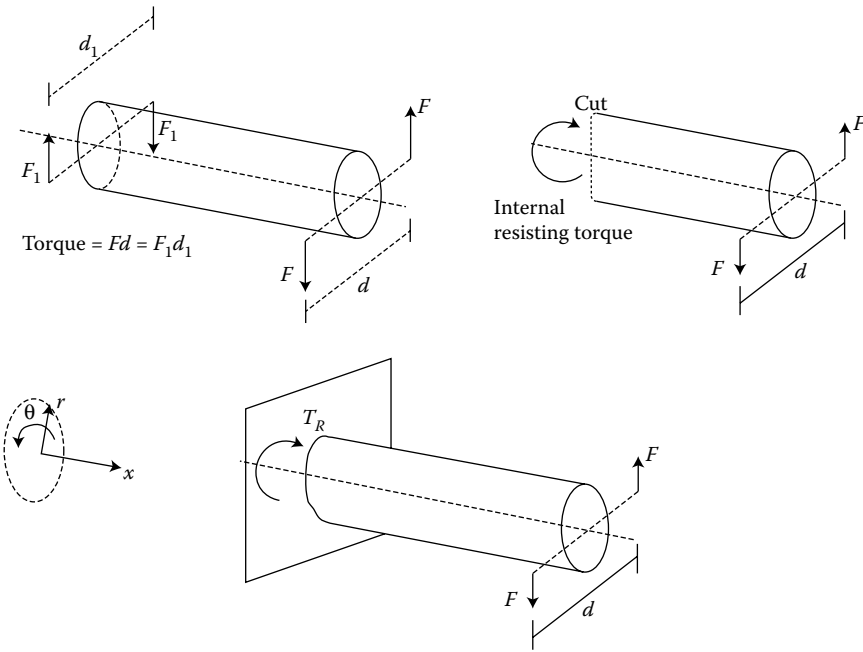
FIGURE 5.1
Sketches showing (clockwise from top left): equal and opposite torques; an FBD of section; rigidly fixed bar.

The torque, being the cross product of lever arm and force, has units of in-lb in U.S. customary system and Nm in SI. Although the terms torque, moment, and couple do have distinct meanings, they are often used interchangeably in modern engineering practice.

In order to relate the internal torque and the stresses it sets up in rods with circular solid and tubular cross sections, we make the following assumptions, all of which are rooted in and validated by copious experimental data:

1. A plane section of material initially perpendicular to the rod's axis remains plane after torques are applied, that is, no warpage or distortion of parallel planes takes place. Imagine a cylinder composed of very thin disks, like a roll of pennies, if the reader will indulge this anachronism. When you twist the roll, the pennies are each displaced, but are not warped out of their planes.

2. Shear strains γ vary linearly from the central axis, reaching γ_{max} at the periphery. That is, shear strain varies linearly with radial coordinate r. The radius itself remains straight. (On any cross section or penny, the outer edges are deformed the most.)

And, if the material composing the rod is linearly elastic, we may apply Hooke's law, from which it follows that

3. Shear stress is proportional to shear strain, as we have seen: $\tau = G\gamma$. Thus, we expect τ, like γ, to increase with r.

5.1.2 Torsional Shear Strain and Stress: Angle of Twist and the Torsion Formula

Consider a torsionally loaded rod like the bottom sketch in Figure 5.1, fixed against rotation at one end and subjected to a torque at the other end. Since torques cause neither direct
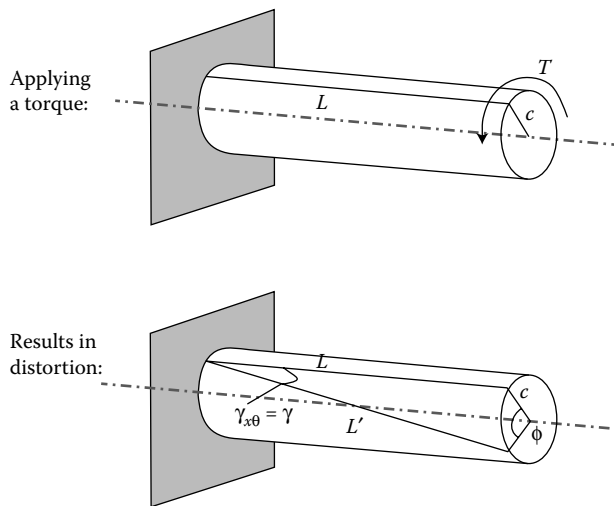
FIGURE 5.2
Circular shaft in torsion.

tension nor compression, this loading develops pure shear stresses on each cross-sectional plane between the applied torque and the fixed end.

If we imagine that the rod is made up of a series of ultra-thin plates (a roll of micropennies), we can visualize each thin plate tending to slide across the contact surface with the adjacent plate. Since the rod is in equilibrium (and does not fracture), some internal resistance must develop that prevents any such slippage. This internal resistance (per unit area) is called the *torsional shear stress*. The resultant of these resisting stresses on any cross-sectional plane is an internal resisting torque.

Since we are by now well aware that all materials have limited (tensile, compressive, and shear) strength, we desire a mathematical relationship between torsional shear stress, applied torque, and the physical properties of the rod. As always, we seek to understand the internal response of a material to (in this case, torsional) loading.

The free end of the rod in Figure 5.1 (bottom) will rotate slightly when a torque is applied. This is shown in Figure 5.2. The shaft radius of length c will be rotated an angle ϕ, called the *angle of twist*, and line length L will become L', actually part of a helical curve. So, the shear distortion of the line is equal to the arc length subtended by this twisting ϕ. We are interested in finding an expression for this arc length, with which we can write the shear strain. The shear strain, like any strain, is defined at each point. However, in the same way that each thin section of a bar loaded in tension by a pair of point forces on its ends stretches by the same amount, each thin section of a rod subject to end torques twists the same amount. Both the normal strain in the bar and the shear strain in the rod do not vary with position along the length (the shear strain also does not vary with position θ around the rod, but as we have said, it does increase linearly with radius). So every point on the rod's outer surface has the same value of shear strain, and we may use the average without loss of information.

If we look closely at the circular front face of the shaft, we can write the arc length corresponding to the shear distortion as ϕc; if we look at the length of the shaft, we see that

(assuming small deformations) the arc length is γL. These two expressions for arc length must be equivalent, so we must have

$$\gamma L = \phi c. \tag{5.1}$$

Remember, this shear strain is at the outer radius, so is the maximum possible shear strain (since shear strain increases linearly with r). In other words, the maximum shear strain γ depends on the angle of twist of the shaft, ϕ:

$$\gamma_{max} = \frac{\phi c}{L}, \tag{5.2}$$

where both γ and ϕ are expressed in radians. In general, the shear strain is given by

$$\gamma(r) = \frac{\phi r}{L}, \tag{5.3}$$

where both γ and ϕ are in radians.

In the previous section, we listed the assumptions made for a circular rod in torsion. The first was that a plane cross section will remain a plane after the shaft has twisted; also, a straight line radius will remain a straight line as the shaft is twisted. Our second assumption that shear strains vary linearly with r tells us that halfway between the center of the shaft and its outer edge, the shear strain will have half its value at the outer surface. We write this statement, which readily follows from Equations 5.2 and 5.3, as

$$\gamma = \frac{r}{c}\gamma_{max}. \tag{5.4}$$

If Hooke's law $\tau = G\gamma$ applies, our third assumption lets us use a similar distribution for shear stress, as shown graphically in Figure 5.3.

Once the stress distribution at a section is established, the resisting torque in the rod can be expressed in terms of stress. Remember that stress is the internal resistance to applied loads. To satisfy equilibrium, this internal resisting torque must balance the externally applied torque T. To best apply this equilibrium relation, we should consider its vector form

$$\int_A d\mathbf{T}_{internal} = \int_A \mathbf{r} \times d\mathbf{F} = \mathbf{T}, \tag{5.5}$$

where the integral sums all torques developed on the section in question by the infinitesimal internal forces acting at some distance r from a rod's axis, over the whole area A of the
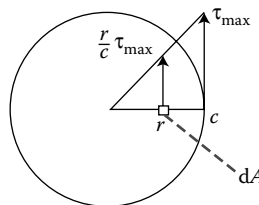
FIGURE 5.3
Shear stress variation on a plane.

cross section. Thinking about this in cylindrical coordinates,* we know that the direction of **r** is always radial and can say the direction of each infinitesimal force d**F** is perpendicular to that, in the local tangential, or θ, direction. Their cross product is in the x-direction along the axis of the beam, as it must be equal to the external torque. Continuing now with magnitudes only, we have

$$\int_A \underbrace{r}_{\substack{\text{moment} \\ \text{arm}}} \underbrace{\underbrace{\frac{r}{c}\tau_{\max}}_{\text{stress}} \underbrace{\mathrm{d}A}_{\text{area}}}_{\text{force}} = T. \tag{5.6}$$

At any given section, $\tau_{\max}$ and c are constant; therefore, we take them out of the integral and write the expression as

$$\frac{\tau_{\max}}{c} \int_A r^2 \, \mathrm{d}A = T. \tag{5.7}$$

The integral $\int r^2 \, \mathrm{d}A$ is called the *polar second moment of area*, denoted by J.† For a circular cross section, $\mathrm{d}A = 2\pi r \, \mathrm{d}r$, and we can calculate J as

$$J = \int_A r^2 \, \mathrm{d}A = \int_0^c 2\pi r^3 \mathrm{d}r = 2\pi \left[\frac{r^4}{4} \right]_0^c = \frac{\pi c^4}{2} = \frac{\pi d^4}{32}, \tag{5.8}$$

where d is the diameter of the solid circular shaft in question. J has dimensions of (length^4). We can now rewrite our expression for the internal torque as

$$\tau_{\max} = \frac{Tc}{J}, \tag{5.9}$$

which is the well-known *torsion formula* for circular shafts, giving us $\tau_{\max}$ in terms of the resisting torque and the rod's dimensions. More generally, we can find the shear stress τ at any point a distance r away from the center of a section from

$$\tau = \frac{r}{c}\tau_{\max} = \frac{Tr}{J}. \tag{5.10}$$

The shear stress we have just derived acts on a circular cross section face, which has its normal in the x-direction, and the local force that causes shear stress acts everywhere in the local θ direction. This shear stress τ can be more specifically designated as $\sigma_{x\theta}$ which must also equal $\sigma_{\theta x}$. Remembering that shear strains γ are two times the shear strains ε that are entered in strain tensors, the corresponding shear strain components are $\varepsilon_{x\theta} = \varepsilon_{\theta x} = \frac{1}{2}\gamma$.

---

* In our previous discussion of the strain and stress tensors, we only discussed Cartesian coordinate systems. Cylindrical coordinates are equally valid.

† J is commonly called the "polar moment of *inertia*," though it is a moment of *area* and not mass, and is more correctly referred to as polar second moment of *area*. Moments of area are geometric properties of certain areas, reflecting how effectively those areas resist deformation. A large J indicates a cross section that will effectively resist torsion. Please see Appendix A for a table of values for common areas.

If our shaft is not solid but a tube of some thickness, similar expressions can be derived. The limits of integration in this case are not 0 and c, but b and c where b marks the inner radius of the tube, so the polar second moment of area becomes

$$J = \int_A r^2 \, dA = \int_b^c 2\pi r^3 \, dr = \frac{\pi c^4}{2} - \frac{\pi b^4}{2}. \tag{5.11}$$

And for very thin tubes, where $b \sim c$, and $c - b = t$, the thickness of the tube, J reduces to

$$J \approx 2\pi R_{av}^3 t, \tag{5.12}$$

where $R_{av} = (b + c)/2$.

If a circular shaft is made from two different materials bonded together as in Figure 5.4, our original *strain* assumption applies. Through Hooke's law, the shear stress distribution will be found to be more like that in Figure 5.4.

Using the torsion formula (Equation 5.9), the angle of twist can now be related to the shear stress, and hence to the applied torque. Recall that $\gamma_{max} = c\phi/L$. If Hooke's law applies, we can use our equation for τ_{max} to write

$$\gamma_{max} = \frac{\tau_{max}}{G} = \frac{Tc}{JG}, \tag{5.13}$$

so equating these two expressions for maximum shear strain, we have

$$\phi = \frac{TL}{JG}. \tag{5.14}$$

This expression suggests the technique used for measuring a material's shear modulus G in a torsion testing machine. In torsion testing, a known torque T is applied, the resulting deformation ϕ measured, and the slope of the plotted data is JG/L. Since the geometric parameters of the sample are known, J and L are known constants, yielding an experimental value of G.
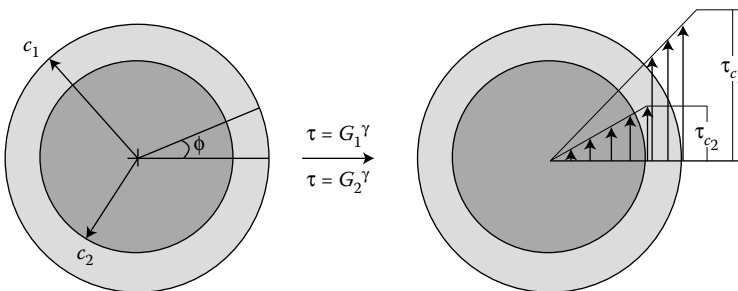
FIGURE 5.4
Elastic behavior of circular rod in torsion having an inner core of flexible material.

Equation 5.14 gives the angle of twist for a rod of uniform J, G, and L. In the case of adjoining sections of differing geometries, we are able to superpose the angles of twist by integrating or merely summing over the different components:

$$\phi = \int_0^L \frac{T(x)}{J(x)G(x)}\mathrm{d}x \quad \text{for continuous changes in torque, diameter, or properties} \quad (5.15)$$

or,

$$\phi = \sum_i \frac{T_i L_i}{J_i G_i} \quad \text{for abrupt changes or stepped shafts.} \quad (5.16)$$

You may find it interesting to compare these results for the twist of a rod with those for the extension of a bar in Section 2.7.

Always remember that we based this derivation of the torsion formula on Hooke's law, so the expressions developed for shear stress and angle of twist in a bar in torsion are only relevant when loads are under the proportional limit. If the yield strength is exceeded somewhere in the rod, or if the material involved has a nonlinear shear constitutive law, these relations are invalidated.

5.1.3 Stress Concentrations

The equations we have so far developed for stresses and strains in circular rods apply to solid and tubular circular rods while the material behaves elastically, and while the cross-sectional area along the rod remains reasonably constant. Stresses calculated from angles of twist determined using Equation 5.15 will also give acceptable results when changes in cross-sectional area are gradual. But for stepped shafts where the diameter changes abruptly, large stress concentrations are possible. In this textbook, we will not be calculating these local stress concentrations, but we will use a torsional stress–concentration factor to estimate their effects. This method is completely analogous to that discussed in Section 2.11 for axially loaded bars, and again the factors depend only on the rod geometry. Figure 5.5 shows the stress–concentration factors for various proportions of stepped round shafts. The factor obtained from the chart is then used to adjust the value of maximum shear stress:

$$\tau_{\max} = K\frac{Tc}{J}, \quad (5.17)$$

where the shear stress Tc/J is obtained for the smaller shaft. It should be clear from the extreme slope at low r in Figure 5.5 that it is desirable to have a large fillet radius r at all sections where a transition in shaft diameter is made.

5.1.4 Transmission of Power by a Shaft

Rotating shafts are commonly used to transmit power. If an applied torque turns a shaft, work is done by the torque. Work, you may recall, is defined as the energy developed by a force acting through a distance against a resistance. When the force is constant, we express the work as force × distance. For a rotating shaft, the applied torque turns the shaft through a circular distance, so work is expressed as torque × angular distance = $T\theta$.
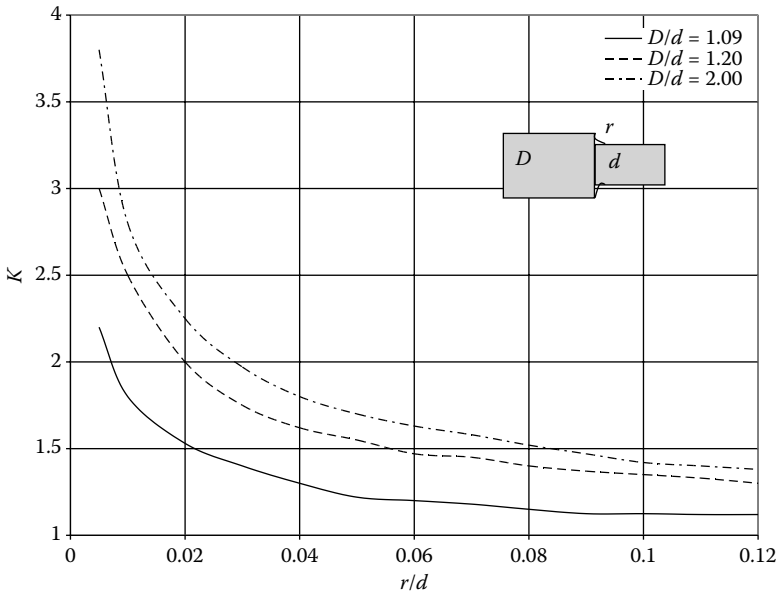
FIGURE 5.5
Torsional stress–concentration factors in circular shafts of two diameters. (After Jacobsen, L.S., Torsional-Stress–Concentrations in Shafts of Circular Cross-Section and Variable Diameter, *Trans. ASME*, 47: 619–638, 1925.)

We will express the rotation angle θ in radians; if a shaft is rotated at constant speed against some resistance, the work done in one revolution will be $2\pi T$. The units of work are (N·m), (ft·lb), or (in·lb).

Power is defined as the work done per unit time. We will therefore want to talk about the shaft rotation per unit time, or the shaft's angular speed. We will use ω to represent the shaft's angular velocity $(d\theta/dt)$ in radians per second. (Often, we will be given a shaft's angular velocity in revolutions per minute, or rpm; to convert this to radians per second, we must multiply by 2π and divide by 60.) Power can then be written

$$P = \omega T. \tag{5.18}$$

The unit conventionally used in the United States is the horsepower (hp). In SI, the unit used to express (N · m/s) is the Watt (W). It was the Scottish inventor James Watt who, having refined the Newcomen pump to create the useful steam engine, needed a standard to which to compare his new technology. The industry standard at the time was what a millhorse could produce, so Watt tested a brewery horse turning a mill wheel, and found that the horse output 33,000 ft-lb/min, a number that became known as 1 horse power (hp). Some useful facts for dealing with these units:

$$1\,\text{hp} = 33{,}000\,\frac{\text{ft} \cdot \text{lb}}{\text{min}} = 550\,\frac{\text{ft} \cdot \text{lb}}{\text{sec}} = 6600\,\frac{\text{in} \cdot \text{lb}}{\text{sec}} = 745.7\,\text{W}.$$

5.1.5 Statically Indeterminate Problems

Just as in the case of axially loaded bars, there are times when we cannot determine the internal torques from statics alone. It is necessary to complement the equilibrium

equations with relations involving the shaft deformations and considering the geometry of the problem. And, as before, several techniques are available to help us.

We can adapt the methods of Section 2.9 directly by substituting torques for forces and twists for displacements. In the force method (we still use this name) for rods in torsion, we introduce an additional equation by writing a geometric compatibility equation that must be satisfied. For example, we might know that the twists of two rods must be equal. Or we might first remove one of the redundant reaction torques and calculate the rotation ϕ_0 at the released support. Then we restore the required boundary conditions by twisting the rod at the released end through an angle ϕ_1 such that the sum $\phi_0 + \phi_1 = 0$.

In the displacement method, the strategy is to consider the torque T_i for the ith shaft component as $T_i = (k_t)_i \phi_i$ and then to write equilibrium equations for each node where shaft segments meet. In these expressions, k_t is the torsional stiffness of a rod, again analogous to a spring constant, and we define it as $(k_t)_i = T_i/\phi_i = G_i J_i/L_i$, with dimensions of [(length · force)/rad]. And, as in the case of axial loads, we can define the reciprocal of stiffness to be the torsional flexibility, which we use in the force method for indeterminate problems.

So just as we did for axially loaded bars which were statically indeterminate, we must ensure (1) equilibrium, (2) geometric compatibility, and (3) consistency of material properties, using constitutive laws such as Hooke's law, in any order we find convenient, until we can solve for all the unknowns in the problem.

5.1.6 Torsion of Solid Noncircular Rods

Everything we have said about torsion has applied to rods with circular cross sections. We assumed early and often that plane sections (i.e., each cross section) remained plane. This assumption depends on the *axisymmetry* of the rod: that it appears the same when viewed from a fixed position and rotated about its axis through an arbitrary angle.

In a square bar, for example, because of the lack of axisymmetry, most lines drawn through a cross section will deform when the bar is twisted, and the cross section itself will be warped out of its original plane. See Figure 5.6 for an illustration of this behavior, or draw an even grid on a rubber eraser and apply a twisting moment to see the irregularity of the grid under torsion.

Disappointingly, then, our equations for strain and stress distribution in elastic circular shafts are nontransferable to noncircular shafts. It would be wrong to assume that shear stress in a square bar varied linearly with distance from the axis of the bar; under this assumption, shear stress would be highest at the corners, and it is actually zero at these points.

The mathematical computation of the stresses and strains in noncircular bars in torsion is quite complex. In fact, it was the French elastician Adhémar Barré de Saint-Venant (of the
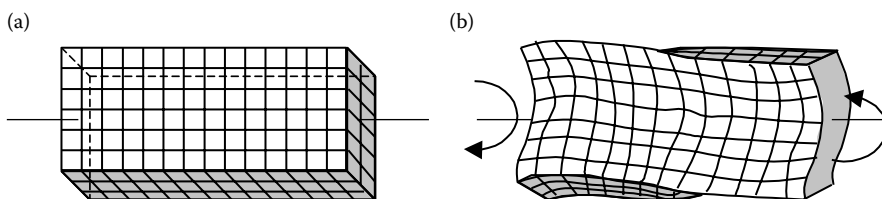
FIGURE 5.6
Rectangular bar (a) before and (b) after a torque is applied.
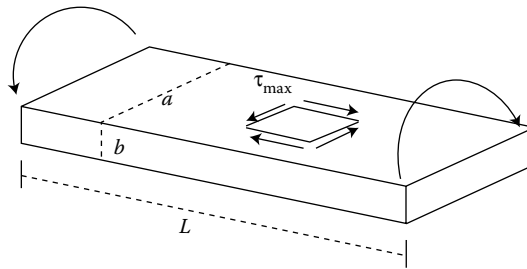
FIGURE 5.7
Generic rectangular bar in torsion.

eponymous principle in Section 2.11) who developed the solution in 1853. This solution is somewhat beyond our scope. However, we can gain some intuition about these problems from the final results of his analysis.

For straight bars with a uniform rectangular cross section of length L and with a and b denoting the wider and narrower sides of the cross section as in Figure 5.7, the maximum shear stress occurs along the center line of the wider face of the bar and is equal to

$$\tau_{\max} = \frac{T}{C_1 a b^2}, \tag{5.19}$$

and the angle of twist may be expressed as

$$\phi = \frac{TL}{C_2 a b^3 G}. \tag{5.20}$$

In these expressions, the coefficients C_1 and C_2 depend only on the ratio a/b and are given in Table 5.1 for a range of values of this ratio. Both these expressions are valid only within the elastic regime. Similar results for different types of cross sections are available in books such as R. J. Roark and W. C. Young's *Formulas for Stress and Strain*.

It is also possible to recast the equation for angle of twist to express the torsional stiffness k_t for a rectangular section:

$$k_t = \frac{T}{\phi} = C_2 a b^3 \frac{G}{L}. \tag{5.21}$$

TABLE 5.1

Coefficients for Rectangular Bars in Torsion

a/b	C_1	C_2
1.0	0.208	0.1406
1.2	0.219	0.1661
1.5	0.231	0.1958
2.0	0.246	0.229
2.5	0.258	0.249
3.0	0.267	0.263
4.0	0.282	0.281
5.0	0.291	0.291
10.0	0.312	0.312
∞	0.333	0.333
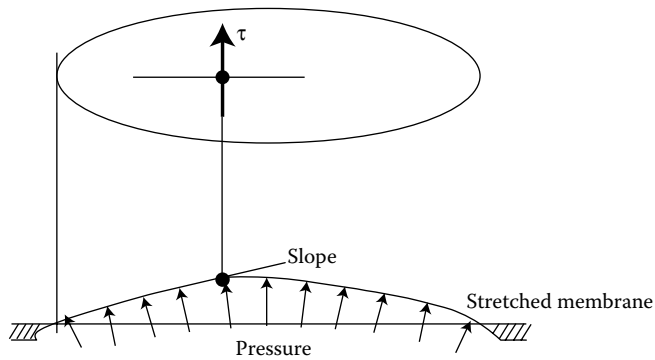
FIGURE 5.8
Membrane analogy for bars in torsion.

An elegant *membrane analogy* provides a way of visualizing the shear stress distribution in noncircular rods. This analogy was introduced by the prolific German scientist Ludwig Prandtl in 1903. The idea comes from the fact that the partial differential equation governing the shear stress in a bar in torsion is the same equation which governs the deformation of an elastic membrane (such as a soap film) attached to a fixed frame and subjected to a uniform pressure on one of its sides. For the equations to be mathematically identical, the frame must be the same shape as the bar cross section. The solution of this equation shows that

1. The shear stress at any point is proportional to the slope of the stretched membrane at the same point, as illustrated in Figure 5.8.
2. The direction of a particular shear stress at a point is normal to the slope of the membrane at the same point, as also illustrated in Figure 5.8.
3. Twice the volume enclosed by the membrane is proportional to the torque carried by the section.

If you simply imagine blowing on a soap film, too gently to detach the film and blow a bubble, you should be able to picture the places at which the film will distort, and where its slope will be greatest. The membrane analogy tells you that these points correspond to the locations of highest shear stress in a cross section in torsion. For example, in Figure 5.9, a circular soap film is shown being deformed by uniform pressure on its lower surface.
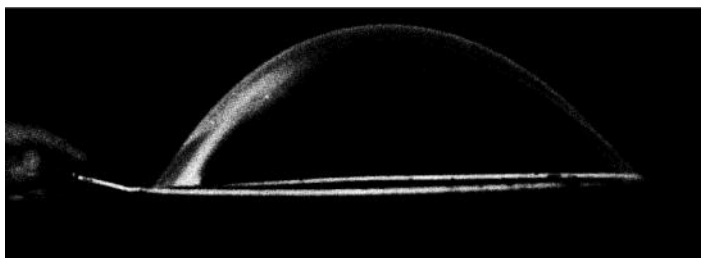
FIGURE 5.9
Soap film on a circular frame. (From Isenberg, C., *The Science of Soap Films and Soap Bubbles*, Dover, 1992. With permission.)

Observe that it is nearly flat at the center, where we know the shear stress to be at its minimum value and that the curvature is very steep at the outer edge, where we already know that due to its radial dependence the shear stress will be maximized.

5.2 Pressure Vessels

Pressure vessels are generally spheres, cylinders, ellipsoids, or some combination of these, with the goal of containing liquids and gases under pressure. Examples of pressure vessels include boilers, fire extinguishers, shaving cream cans, and pipes, as well as the compressed air tanks carried by scuba divers such as those installing the artificial reef components in our motivating example from Chapter 1.

Actual vessels are usually composed of a complete pressure-containing shell with flange rings and fastening devices for connecting and securing mating parts. At this point, we are interested in the stresses developed in the walls of simple spheres and cylinders, two shapes which are widely used in industry. To perform our stress analysis, we will employ a generalized form of Hooke's law.

Thin-walled pressure vessels are those which have a wall thickness t not more than one-tenth of the internal radius r_i of the vessel ($t \leq 0.1r_i$). The walls of an ideal thin-walled pressure vessel act as a membrane, experiencing no bending. The internal pressures within such vessels are relatively low. Thick-walled vessels such as gun barrels or high-pressure hydraulic presses, on the other hand, have $t > 0.1r_i$ and experience dramatic variations in stress from the inner to the outer surface. In this section, we will be considering the simpler thin-walled situation.

Cylindrical and spherical thin-walled pressure vessels are generally subjected to some level of internal fluid (gas and/or liquid) pressure. As a result of the internal pressure, tensile stresses are developed in the vessel walls. These stresses may not exceed specified allowable tensile stresses. Internal pressure tends to rupture the vessel along a joint.

Consider first the cylindrical pressure vessel shown in Figure 5.10a. If we take a section by passing a cutting plane through the pressure vessel, we obtain a slice as in Figure 5.10b, a typical cross section of a cylindrical thin-walled pressure vessel subjected to an internal pressure p. The internal pressure at any point acts equally in all directions and is always perpendicular to any surface on which it acts. This is reflected in Figure 5.10b.

As mentioned above, the radially acting internal pressure is resisted by tensile stresses developed in the walls of the pressure vessel. These are called *circumferential* or *hoop stresses*. In conventional cylindrical coordinates, these are normal stresses on a plane with
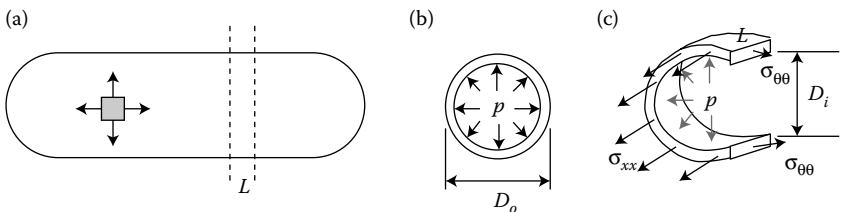
FIGURE 5.10
(a) Cylindrical pressure vessel; (b) cross section; and (c) section of thickness L. As an exercise, label the stresses in (a) as $\sigma_{\theta\theta}$ or σ_{xx}, so that they are in agreement with (c).
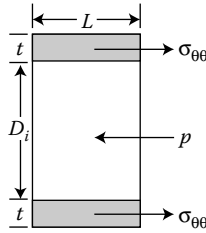
FIGURE 5.11
Projected area of cylindrical pressure vessel half section. Note that arrows to right indicate vectors out of the page; arrows to left indicate vectors into the page.

its area normal in the θ-direction due to forces in the θ-direction, or $\sigma_{\theta\theta}$. If we perform a force balance on the element in Figure 5.10c, where the vessel has been sliced along its length, we can obtain an estimate of these stresses.

In Figure 5.10c, the hoop stress $\sigma_{\theta\theta}$ acting on the two cut surfaces resists the force developed by the internal pressure p. Although this acts perpendicular to the surface at all points, the resulting forces are only unbalanced in the horizontal direction and effectively the pressure acts normal to a projected area $D_i L$. Figure 5.11, which shows only the projected area $D_o L$, should serve to make this even clearer. (Remember that pressure, like stress, is a force per unit area.)

The hoop stress $\sigma_{\theta\theta}$ acts on a combined cut area $2L(r_o - r_i) = 2Lt$. Balancing the forces, we have

$$pD_i L = 2\sigma_{\theta\theta} Lt, \tag{5.22}$$

which neatly simplifies to an expression for hoop stress $\sigma_{\theta\theta}$:

$$\sigma_{\theta\theta} = \frac{pD_i}{2t} = \frac{pr_i}{t}. \tag{5.23}$$

This is an expression for the average circumferential hoop stress and is valid only for thin-walled cylindrical pressure vessels. In these vessels, in fact, it is often estimated that $r_o \approx r_i$, and so the subscript on r is omitted. And incidentally, this expression can also be arrived at by examining an infinitesimal slice of the cylindrical vessel, and integrating over it.

The other normal stress acting in a cylindrical pressure vessel acts *longitudinally* and may be determined by the solution of an axial-force problem. Conveniently, it is called the *longitudinal stress*. In cylindrical coordinates, we call it σ_{xx}. To find its value, we slice the body perpendicular to its axis and obtain the section shown in Figure 5.12.

The pressure acting on the cylindrical length of the cylinder is not shown as it has no component in the x-direction of interest. On the end cap, the pressure acts normal to the surface, but the only net x-direction force, regardless of the nature of the curved shape of
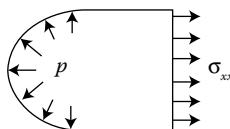
FIGURE 5.12
Longitudinal stress.
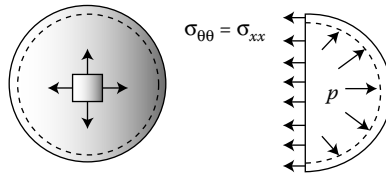
FIGURE 5.13
Spherical pressure vessel.

the end cap, is due to the pressure acting on the projected circular area. This force $p\pi r_i^2$ must be balanced by the force developed by the longitudinal stress σ_{xx} in the wall multiplied by the area on which it acts: $\sigma_{xx}(\pi r_o^2 - \pi r_i^2)$. If we equate these two forces and solve for σ_{xx}:

$$p\pi r_i^2 = \sigma_{xx}(\pi r_o^2 - \pi r_i^2),$$

$$\sigma_{xx} = \frac{pr_i^2}{r_o^2 - r_i^2} = \frac{pr_i^2}{(r_o + r_i)(r_o - r_i)}. \tag{5.24}$$

But, we have $r_o - r_i = t$, the thickness of the cylindrical wall, and since we are considering thin-walled vessels, we take $r_o \approx r_i \approx r$, so we may use

$$\sigma_{xx} = \frac{pr}{2t}, \tag{5.25}$$

and we notice that for thin-walled cylindrical pressure vessels, $\sigma_{xx} \approx \sigma_{\theta\theta}/2$. That the hoop stresses are twice the longitudinal may be appreciated by cooking a hot dog until it "plumps" (deforms by expanding in response to rising internal pressure) and bursts—the tears in its casing will be along the longitudinal direction, because it will fail due to stress in the circumferential or hoopwise direction.

For thin-walled *spherical* pressure vessels, a similar method may be employed. In Figure 5.13, we see a sample vessel and an FBD that combines elements of Figures 5.10 and 5.12. For a sphere, any section we take passing through the center of the sphere will yield the same result, whatever the inclination, and the analysis proceeds just as the case of longitudinal stress for the cylindrical pressure vessel. So, the membrane stress for thin-walled spherical pressure vessels in any plane is

$$\sigma_{\text{sphere}} = \frac{pr}{2t}. \tag{5.26}$$

The complete state of stress in the membrane wall is *biaxial* stress, with an element experiencing σ_{sphere} in two perpendicular directions.

The stresses we have developed for cylindrical and spherical pressure vessels are in the plane of the vessel walls. It is true that the pressure itself acts in a normal direction perpendicular to the wall, but we do not consider this in a thin-walled vessel model. We can see from the stress expressions derived that since $t \leq 0.1 r_i$, the in-plane stresses must be significantly larger than p. The stress tensors therefore are assumed to contain only the two in-plane normal stresses. The plane stress analysis of Chapter 4 is thus applicable.

For either cylindrical or spherical pressure vessels, the effects of internal pressure may be combined with other loading conditions. Just as in the case of thermal effects, the hoop and circumferential stress are simply added to the other stresses in the corresponding positions in the stress tensor. For further discussion of pressure vessels, please see Chapter 6.

5.3 Transformation of Stress and Strain

So far we have considered the isolated effects of normal stresses and shear stresses due to various loading by axial and shear forces and torques. When stresses due to different sources act on an element to cause contributions to the same stress component (such as a pressure vessel's longitudinal normal stress, and the normal stress due to an axial load on the vessel), we can simply add them. Often we will have multiple non-zero stress components due to real loading situations and then we must consider all of the stress tensor components. In some cases, the combinations of stresses produce critical conditions worthy of more detailed examination.

In the previous sections, we have been able to calculate the stress state on a lateral cross section of a component. However, as we remember from our study of axially loaded bars, the stresses on an *inclined* cross section may be quite different. In designing a system, we might prefer to know the stress state at some other orientation, for example, if we were using a material (such as wood or fiber-reinforced concrete) with a grain, or with anisotropic properties, *or* if a weld or bolt were inclined at some angle from our usual axes. Consider the failure of a material under torsion—some materials do fail along the interfaces between the imaginary pennies being twisted, in a "clean break" along the cross section (Figure 5.14a). But more brittle materials tend to fail in a different way, so that the cleavage surface is inclined at an angle of about 45° (Figure 5.14b). Twist a piece of chalk in your hands to see this type of failure. In order to understand these failures, and to create robust designs, we want to develop a way of calculating the stress state on axes that are oriented at an arbitrary angle to our reference axes. We will also be interested to know at what orientation of the axes we can see the largest stresses, and what those stresses are.

We are aware that the most general state of stress at a given point may be represented by six unique components of a stress tensor. Three of these components, σ_{xx}, σ_{yy}, and σ_{zz}, are the normal stresses exerted on the faces of a small cube-shaped element centered at the point, and three are the shear components σ_{xy}, σ_{xz}, and σ_{yz} on the same element. (We remember that the stress tensor is symmetric, and therefore $\sigma_{xy} = \sigma_{yx}$, $\sigma_{xz} = \sigma_{zx}$, and $\sigma_{yz} = \sigma_{zy}$.) If the element is rotated from the standard coordinate axes, we will have to transform the stress components (as shown in Figure 5.15). The same goes for the six independent components of the *strain tensor*.
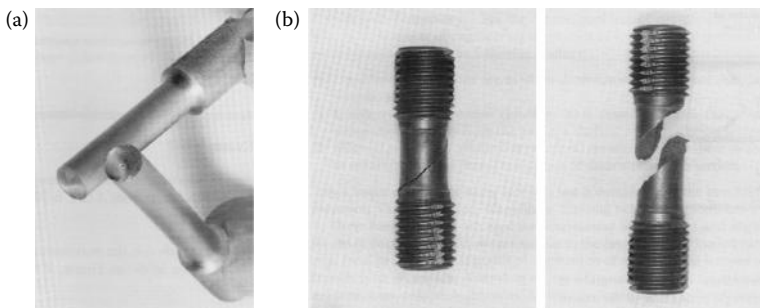
FIGURE 5.14
Failure of circular shafts due to torsion: (a) ductile failure, (b) brittle failure along 45° helix.
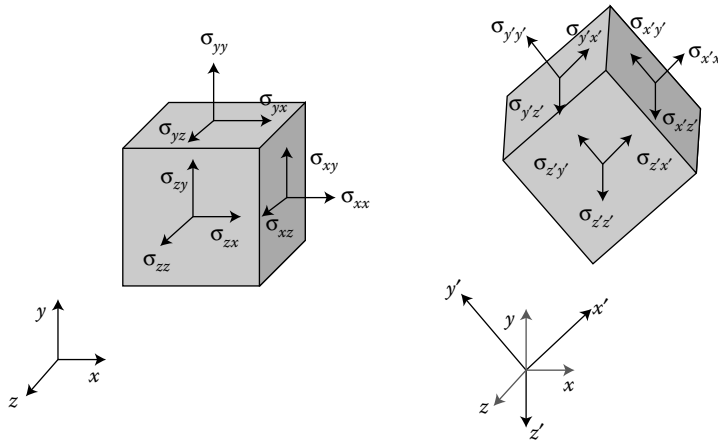
FIGURE 5.15
Stress components on a cubic element. Only the components on faces with positive normal directions are shown; equal and opposite components are present on the negative faces.

In this section, we will focus primarily on *plane stress*, a state in which two faces of the cubic element are stress-free. This two-dimensional case, itself of significant use in practice, is easily extended to three dimensions once it is understood.

5.3.1 Transformation of Plane Stress

In Section 2.6, we considered the stresses on an inclined plane in an axially loaded bar. A similar technique may be used to find the stress state on planes and cubic elements that have been rotated. Let's see that we do in fact know how to transform the stresses on an inclined plane, even now that multiple components of stress are in the picture.

For the state of stress for a cube element shown in Figure 5.16a, we may also express the state of stress on a wedge with a surface at angle α. Because this wedge (ABC) is part of the original element, the stresses on faces AC and BC, which are rectangles with one dimension into the page, are known. They appear again on the wedge in Figure 5.16b. The unknown normal and shear stresses acting on face AB, σ_α and τ_α, are what we want to find. Face AB has area dA. Then the area of face AC is $dA \cos \alpha$ and the area of face BC is $dA \sin \alpha$.

Next we can obtain the forces on the faces, F_i in Figure 5.16c, by multiplying the stresses by their respective areas.

$$F_1 = 3\,\text{MPa} \cos \alpha,$$

$$F_2 = 2\,\text{MPa} \cos \alpha,$$

$$F_3 = 2\,\text{MPa} \sin \alpha,$$

$$F_4 = 1\,\text{MPa} \sin \alpha.$$

To keep the wedge in equilibrium, the unknown forces due to unknown normal and shear stresses must balance these forces:

$$\sum F_N = 0: \qquad N = F_1 \cos \alpha - F_2 \sin \alpha - F_3 \cos \alpha + F_4 \sin \alpha$$

$$= 3 \cos^2 \alpha - 2 \cos \alpha \sin \alpha - 2 \sin \alpha \cos \alpha + 1 \sin^2 \alpha,$$
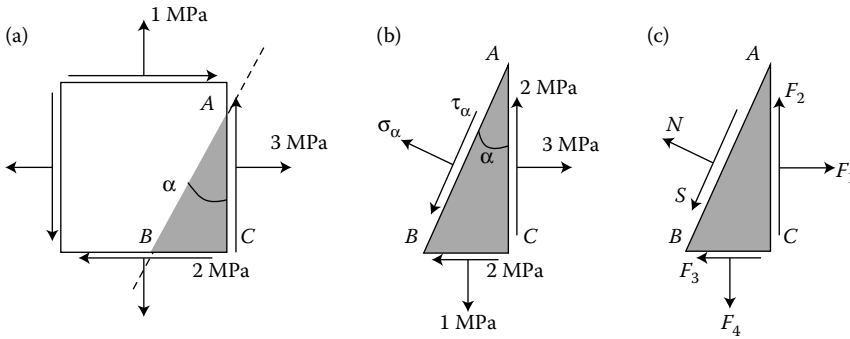
FIGURE 5.16
Finding stresses on an inclined plane. Element has unit depth into the page. (After Popov, E.P., *Engineering Mechanics of Solids*, Prentice Hall, 1998.)

$$\sum F_S = 0: \qquad S = F_1 \sin \alpha + F_2 \cos \alpha - F_3 \sin \alpha - F_4 \cos \alpha$$

$$= 3 \cos \alpha \sin \alpha + 2 \cos^2 \alpha - 2 \sin^2 \alpha - 1 \sin \alpha \cos \alpha.$$

Since forces N and S act on the plane defined by AB, whose area is dA, we divide these forces by dA to find the stresses. We can find the stress values for any angle α, and as an example, with $\alpha = 22.5°$, $\sigma_\alpha = 1.3 \, \text{MPa}$, and $\tau_\alpha = 2.1 \, \text{MPa}$ in the directions shown in Figure 5.16b.

Conceptually, this is all we are doing in this section. This approach is the starting point for all of the seemingly more sophisticated analyses to follow.

We want to generalize the approach of the example to any initial element and any inclined wedge. This is illustrated in Figure 5.17. Again, we want to determine the transformed stresses (in the "prime" directions, as in Figure 5.15); again, we apply the equations of equilibrium to our wedge.
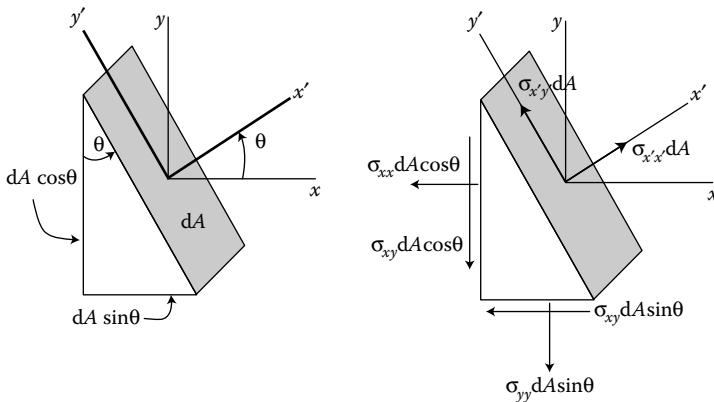
FIGURE 5.17
Derivation of stress transformation on an inclined plane.

Equilibrium in the x'- and y'-directions requires (check these results as an exercise):

$$\sigma_{x'x'} = \frac{\sigma_{xx} + \sigma_{yy}}{2} + \frac{\sigma_{xx} - \sigma_{yy}}{2}\cos 2\theta + \sigma_{xy}\sin 2\theta, \tag{5.27}$$

$$\sigma_{x'y'} = -\frac{\sigma_{xx} - \sigma_{yy}}{2}\sin 2\theta + \sigma_{xy}\cos 2\theta. \tag{5.28}$$

These are the general expressions for the normal and shear stress on any plane located by the angle θ. Clearly, we must know the state of stress in the initial (x, y, z) orientation to find these transformed stresses. The quantities σ_{xx}, σ_{yy}, and σ_{xy} before rotation are initially known.

To find the normal stress on the face perpendicular to the wedge face dA, that is, $\sigma_{y'y'}$, we replace θ by $\theta + 90°$ in the equation for $\sigma_{x'x'}$, and obtain

$$\sigma_{y'y'} = \frac{\sigma_{xx} + \sigma_{yy}}{2} - \frac{\sigma_{xx} - \sigma_{yy}}{2}\cos 2\theta - \sigma_{xy}\sin 2\theta. \tag{5.29}$$

If we add this to the equation for $\sigma_{x'x'}$, we see that $\sigma_{x'x'} + \sigma_{y'y'} = \sigma_{xx} + \sigma_{yy}$, meaning that the sum of the normal stresses remains invariant, regardless of orientation.

In *plane strain* problems where $\varepsilon_{zz} = \varepsilon_{zx} = \varepsilon_{zy} = 0$, a normal stress σ_{zz} can develop. In Section 4.5.3, we saw that this stress is given as $\sigma_{zz} = \nu(\sigma_{xx} + \sigma_{yy})$, where ν is Poisson's ratio. However, the forces resulting from this stress do not enter into the relevant equilibrium equations used to derive in-plane stress transformation relations. The above equations for $\sigma_{x'x'}$ and $\sigma_{y'y'}$ are applicable for *plane stress*, and if corresponding ε terms are substituted for all σ terms, *plane strain*.

We now have general expressions for the normal and shear stresses that we see when a state of plane stress is rotated by any angle θ. Note that since the real, physical state of stress is unchanged, we are merely representing it with respect to different axes.

5.3.2 Principal and Maximum Shear Stresses

As we know, we are often interested in determining the maximum stresses induced in bodies, so that these limiting cases may inform our designs. Now that we have expressions for the stresses at any orientation θ, we can determine the rotations that produce maximum values by setting the derivatives of these expressions to zero, for example,

$$\frac{d\sigma_{x'x'}}{d\theta} = -\frac{\sigma_{xx} - \sigma_{yy}}{2}(2\sin 2\theta) + 2\sigma_{xy}\cos 2\theta = 0, \tag{5.30}$$

which requires that to maximize the stress $\sigma_{x'x'}$,

$$\tan 2\theta_N = \frac{\sigma_{xy}}{(\sigma_{xx} - \sigma_{yy})/2}. \tag{5.31}$$

The N subscript on theta is used to signify its status as the angle defining the plane of maximum or minimum normal stress. The equation for θ_N has two roots [since $\tan 2\beta = \tan(2\beta + 180°)$], 90° apart. One of these roots locates the plane on which the maximum normal stress acts, and the other locates the plane of minimum normal stress.

On these planes corresponding to maximum or minimum normal stresses, there are no shear stresses. These planes are called the *principal planes* of stress, and the (purely normal) stresses acting on them are the *principal stresses*.*

If we substitute θ_N into the equations for normal stresses, we obtain expressions for these extreme stress values. We will denote maximum normal stress by σ_1, and minimum normal stress by σ_2, and find

$$(\sigma_{x'x'})^{\max}_{\min} = \sigma_{1 \text{ or } 2} = \frac{\sigma_{xx} + \sigma_{yy}}{2} \pm \sqrt{\left(\frac{\sigma_{xx} - \sigma_{yy}}{2}\right)^2 + \sigma_{xy}^2}. \tag{5.32}$$

These principal stresses are experienced by an element oriented at θ_N to the original axes.

Turning our attention to the shear stress, we note again that shear stress is zero on the plane defined by θ_N. However, there is a plane on which *shear* stress may be maximized or minimized, which we obtain in the same way that we obtained θ_N. We find that the extreme shear stresses act on planes defined by θ_S, where

$$\tan 2\theta_S = -\frac{(\sigma_{xx} - \sigma_{yy})/2}{\sigma_{xy}}. \tag{5.33}$$

Once again this equation has two roots, 90° apart. Also, the roots of this equation, θ_S, are 45° away from the planes defined by θ_N. Substituting θ_S into our equation for shear stress, we get an expression for the maximum and minimum shear stresses:

$$(\sigma_{x'y'})^{\max}_{\min} = \tau^{\max}_{\min} = \pm\sqrt{\left(\frac{\sigma_{xx} - \sigma_{yy}}{2}\right)^2 + \sigma_{xy}^2}. \tag{5.34}$$

The maximum and minimum values differ only by sign. Physically, this sign has no meaning (except that if it is negative, the shear has the opposite sense from that assumed in Figure 5.17), and so this shear stress regardless of sign is simply called the *maximum 2D shear stress*. However, the magnitude of the maximum shear for the full 3D stress tensor is what we need to know to create robust designs in certain materials, as we will see in Section 5.4. Although the sign of a shear stress component or 2D maximum is not physically significant, note that when we calculate the principal stresses and maximum shear that can be seen by rotation of the coordinate axes in 3D the mathematical sign does affect the result. (Please see Figure 4.7 for a reminder of the shear stress sign convention.)

On the principal axes, the principal stresses were purely normal, with zero shear stress. But the planes where maximum shear stress acts are not necessarily free of normal stresses. If we substitute θ_S into our equation for normal stress, we find that the normal stresses acting on planes of maximum shear stress are

$$\sigma_{\theta_S} = \frac{\sigma_{xx} + \sigma_{yy}}{2}. \tag{5.35}$$

---

* We recognize that the principal stress state, in which an element experiences only normal stresses, signifies that we have in essence diagonalized the symmetric stress tensor. We also note that for pressure vessels, where we found stress components $\sigma_{\theta\theta}$ and σ_{xx}, there was an implicit acknowledgment that the stress state corresponding to conventional cylindrical or spherical coordinates is the principal stress state for a pressure vessel. However, we might still be interested in the stress state under different reference axes to learn the design constraints for a weld used in constructing a pressure vessel from a flat sheet of material. So even when the principal stress state is what we see with our usual coordinates, we will have a motivation to transform the stress state to different axes and orientations.

This stress occurs on both the x'- and the y'-planes, so from it we can confirm that $\sigma_{x'x'} + \sigma_{y'y'} = \sigma_{xx} + \sigma_{yy}$.

5.3.3 Mohr's Circle for Plane Stress

If we look back at our equations for transformed $\sigma_{x'x'}$ and $\sigma_{x'y'}$, we notice that these are the parametric equations of a circle. If we choose a set of rectangular axes and plot points with coordinates $(\sigma_{x'x'}, \sigma_{x'y'})$ for all possible values of θ, all the points will lie on a circle. We can see this more clearly if we rewrite the equations:

$$\sigma_{x'x'} - \frac{\sigma_{xx} + \sigma_{yy}}{2} = \frac{\sigma_{xx} - \sigma_{yy}}{2} \cos 2\theta + \sigma_{xy} \sin 2\theta, \tag{5.36}$$

$$\sigma_{x'y'} = -\frac{\sigma_{xx} - \sigma_{yy}}{2} \sin 2\theta + \sigma_{xy} \cos 2\theta, \tag{5.37}$$

and then square both equations, add them, and simplify to obtain

$$\left(\sigma_{x'x'} - \frac{\sigma_{xx} + \sigma_{yy}}{2}\right)^2 + \sigma_{x'y'}^2 = \left(\frac{\sigma_{xx} - \sigma_{yy}}{2}\right)^2 + \sigma_{xy}^2. \tag{5.38}$$

This equation has the form $(\sigma_{x'x'} - a)^2 + \sigma_{x'y'}^2 = b^2$, where the quantities $a = (\sigma_{xx} + \sigma_{yy})/2$ and $b^2 = [(\sigma_{xx} - \sigma_{yy})/2]^2 + \sigma_{xy}^2$ are constants. We remember that $(x - a)^2 + y^2 = b^2$ is the equation of a circle of radius b with its center at $(+a, 0)$. Hence, we may plot all points $(\sigma, \tau) = (\sigma_{x'x'}, \sigma_{x'y'})$ on a circle. The resulting circle is called *Mohr's circle* of stress, named after Otto Mohr who first proposed its use in 1882.

From Equation 5.38, we can see that the center of this circle will be at $(a, 0)$, or at

$$\left(\frac{\sigma_{xx} + \sigma_{yy}}{2}, 0\right)$$

and that the circle's radius $b = R$ is given by

$$R = \sqrt{\left(\frac{\sigma_{xx} - \sigma_{yy}}{2}\right)^2 + \sigma_{xy}^2}.$$

Using Mohr's circle to graphically display stress transformations will offer a big-picture view of a problem and make certain relationships visually clear. Mohr's circle gives us a way to see all possible stress states at a certain point (i.e., the stress states for all possible axes with their origins at that certain point) at once, as in Figure 5.18. Again, remember that these states are all just different representations of the same physical stress.

Certain observations can be made based on Figure 5.18:

- The largest possible normal stress is σ_1 and the smallest is σ_2. No shear stresses exist together with either one of these principal stresses.
- The largest shear stress $(\sigma_{x'y'})_{\max}$ is equal to the radius R of the circle. A normal stress equal to $(\sigma_1 + \sigma_2)/2$ acts on each of the planes of maximum shear stress. This is σ_{θ_S} as defined in Equation 5.35.
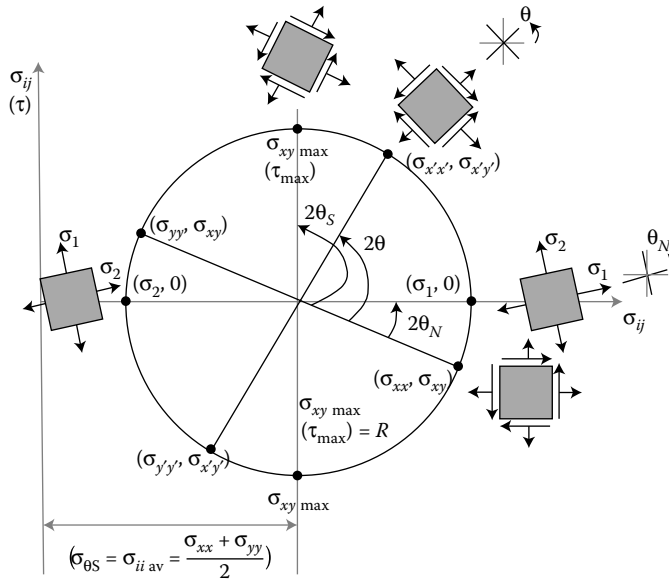
FIGURE 5.18
Mohr's circle.

- If $\sigma_{xx} + \sigma_{yy} = 0$, the center of Mohr's circle coincides with the coordinate origin, and a state of pure shear exists.
- The sum of the normal stresses on any two mutually perpendicular planes is invariant. That is,

$$\sigma_{xx} + \sigma_{yy} = \sigma_1 + \sigma_2 = \sigma_{x'x'} + \sigma_{y'y'} = \text{constant.} \tag{5.39}$$

One tricky aspect of constructing Mohr's circle is whether to plot a given shear stress above or below the σ-axis. There are a variety of conventions used in the literature; the choice of convention is not as critical as is consistency in applying it. The best way to get comfortable with any convention is to work examples, such as Example 5.9.

Mohr's circle also gives us a way to check our earlier results for axial loading and torsional loading. In the case of axial loading, shown in Figure 5.19a, we have already shown that $\sigma_{xx} = P/A$, $\sigma_{yy} = 0$, and $\sigma_{xy} = 0$. The corresponding points X and Y define a circle with radius $R = P/2A$, as in Figure 5.19b. Points D and E yield the orientation of the planes of maximum shearing stress (Figure 5.19c, at $\theta = 45°$, as we already knew; these lines are separated by 2θ on Mohr's circle), and the values of maximum shear stress and corresponding normal stress:

$$\tau_{\max} = R = \frac{P}{2A}. \tag{5.40}$$

In torsional loading, we have $\sigma_{xx} = 0$, $\sigma_{yy} = 0$, and $\sigma_{xy} = \tau_{\max} = Tc/J$ (Figure 5.20a). Points X and Y are on the τ-axis, and Mohr's circle (Figure 5.20b) has radius $R = Tc/J$ and is centered on the origin. Points A and B define the principal planes and the principal stresses:

$$\sigma_{1,2} = \pm R = \pm\frac{Tc}{J}. \tag{5.41}$$
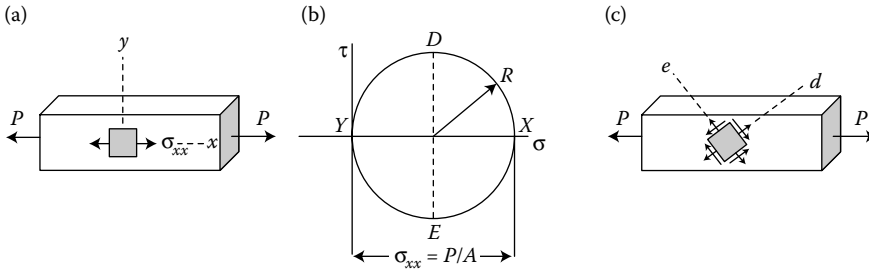
FIGURE 5.19
Mohr's circle for axial loading.
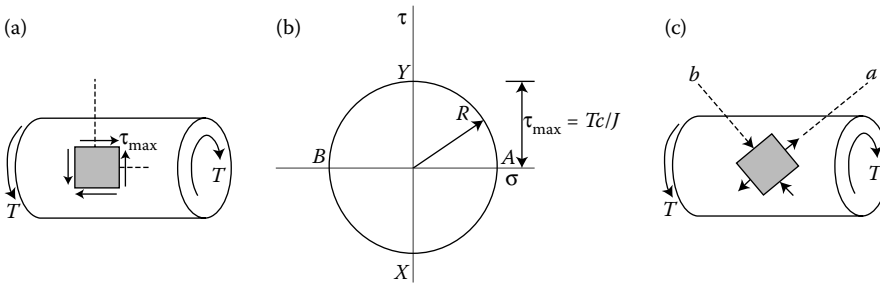
FIGURE 5.20
Mohr's circle for torsional loading.

We also note that for pressure vessels, the standard cylindrical coordinate system (used by us in Section 5.2) is aligned with the principal planes. The stress state given by $\sigma_{\theta\theta}$ and σ_{xx} (and no shear stress $\sigma_{\theta x}$) is the principal stress state; accordingly, it is not unusual to see the hoop stress ($\sigma_{\theta\theta}$) called σ_1, and the longitudinal stress called σ_2.

5.3.4 Transformation of Plane Strain

We recall the existence and form of the *strain tensor*, which like the stress tensor gives us six independent components at each location within a body. We may find ourselves in a situation where the initial *xy*-axes are rotated through some angle θ to axes *x'y'*, and we may need to transform strains associated with *xy* to an equivalent set of strains on the rotated axes. All of the equations in Sections 5.3.1 and 5.3.2 for transformation of plane stress can be used for transformation of plane strain with the substitution of ε terms for σ. However, another approach to getting equivalent results is described here. Of course this result applies just as well to stress tensor transformations, as they are mathematically the same.

We consider first an arbitrary point *A* at point (x, y) in the initial coordinate system. After the rotation through θ, as shown in Figure 5.21, this point *A* is at (x', y'). From the figure, we see that

$$x' = x\cos\theta + y\sin\theta, \tag{5.42a}$$

$$y' = -x\sin\theta + y\cos\theta. \tag{5.42b}$$
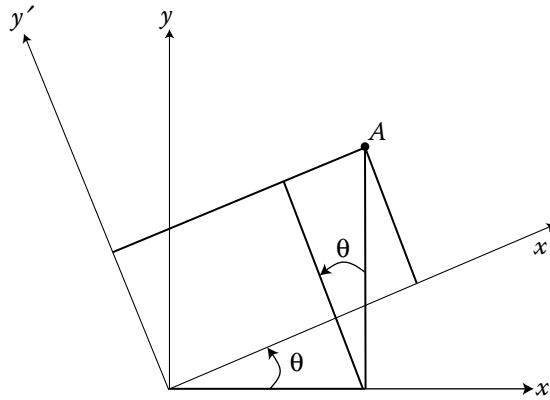
FIGURE 5.21
Coordinate transformation.

These equations may be written in matrix form

$$\begin{pmatrix} x' \\ y' \end{pmatrix} = \begin{pmatrix} \cos\theta & \sin\theta \\ -\sin\theta & \cos\theta \end{pmatrix} \begin{pmatrix} x \\ y \end{pmatrix}.$$

(5.43)

If we want to rearrange this expression, we look at the 2×2 matrix and see that its determinant is unity; hence, its transpose is equal to its inverse. So,

$$\begin{pmatrix} x \\ y \end{pmatrix} = \begin{pmatrix} \cos\theta & -\sin\theta \\ \sin\theta & \cos\theta \end{pmatrix} \begin{pmatrix} x' \\ y' \end{pmatrix}.$$

(5.44)

The same rules of transformation will apply to the small linear displacements u and v:

$$u' = u\cos\theta + v\sin\theta,$$

(5.45a)

$$v' = -u\sin\theta + v\cos\theta.$$

(5.45b)

Next, we recall the definition of normal strain from the previous section. Applying the chain rule, we have the normal strain in the x'-direction:

$$\varepsilon_{x'x'} = \frac{\partial u'}{\partial x'} = \frac{\partial u'}{\partial x}\frac{\partial x}{\partial x'} + \frac{\partial u'}{\partial y}\frac{\partial y}{\partial x'}.$$

(5.46)

If we find the required partial derivatives from Equations 5.44 and 5.45, we will obtain

$$\varepsilon_{x'x'} = \varepsilon_{xx}\cos^2\theta + \varepsilon_{yy}\sin^2\theta + 2\varepsilon_{xy}\sin\theta\cos\theta$$
$$= \frac{\varepsilon_{xx} + \varepsilon_{yy}}{2} + \frac{\varepsilon_{xx} - \varepsilon_{yy}}{2}\cos 2\theta + \varepsilon_{xy}\sin 2\theta,$$

(5.47a)

$$\varepsilon_{y'y'} = \varepsilon_{xx}\sin^2\theta + \varepsilon_{yy}\cos^2\theta - 2\varepsilon_{xy}\sin\theta\cos\theta$$
$$= \frac{\varepsilon_{xx} + \varepsilon_{yy}}{2} - \frac{\varepsilon_{xx} - \varepsilon_{yy}}{2}\cos 2\theta - \varepsilon_{xy}\sin 2\theta.$$

(5.47b)

We may also transform the shear strain, by first writing it in the rotated coordinates as

$$2\varepsilon_{x'y'} = \gamma_{x'y'} = \frac{\partial v'}{\partial x'} + \frac{\partial u'}{\partial y'}. \tag{5.48}$$

And then differentiating and simplifying to obtain

$$\varepsilon_{x'y'} = \frac{\gamma_{x'y'}}{2} = -(\varepsilon_{xx} - \varepsilon_{yy})\sin\theta\cos\theta + \varepsilon_{xy}(\cos^2\theta - \sin^2\theta)$$
$$= -\frac{\varepsilon_{xx} - \varepsilon_{yy}}{2}\sin 2\theta + \varepsilon_{xy}\cos 2\theta. \tag{5.49}$$

We may also construct *Mohr's circle of strain* to determine the principal strains and maximum shear strains. In doing this, we must remember that the shear components of the strain tensor are $\varepsilon_{x'y'}$ (and not $\gamma_{x'y'} = 2\varepsilon_{x'y'}$), and so we plot Mohr's circle of strain as the set of all points $(\varepsilon, \gamma/2)$. The principal (maximum and minimum normal) strains are written as

$$(\varepsilon_{x'x'})_{\substack{\max \\ \min}} = \varepsilon_{1 \text{ or } 2} = \frac{\varepsilon_{xx} + \varepsilon_{yy}}{2} \pm \sqrt{\left(\frac{\varepsilon_{xx} - \varepsilon_{yy}}{2}\right)^2 + \varepsilon_{xy}^2}, \tag{5.50}$$

and they occur on the plane defined by

$$\tan 2\theta_{N_\varepsilon} = \frac{\varepsilon_{xy}}{(\varepsilon_{xx} - \varepsilon_{yy})/2}. \tag{5.51}$$

Compare these to the corresponding stress transformation equations to see that they are mathematically equivalent.

5.3.5 Three-Dimensional State of Stress

The normal and shear stresses acting on a plane through a material depend on the orientation of that plane. We have found both equations and a graphical technique (Mohr's circle) to determine the normal and shear stresses on a variety of planes, but only for the special case of plane stress. If we keep things more general, we obtain the principal stresses in three dimensions.

We remember that our stress tensor is symmetric. From linear algebra, we recall that a symmetric matrix may be diagonalized. This suggests that the symmetric stress tensor may also be diagonalized—that there is a certain coordinate system (x', y', z') for which

$$\begin{pmatrix} \sigma_{x'x'} & \sigma_{x'y'} & \sigma_{x'z'} \\ \sigma_{y'x'} & \sigma_{y'y'} & \sigma_{y'z'} \\ \sigma_{z'x'} & \sigma_{z'y'} & \sigma_{z'z'} \end{pmatrix} = \begin{pmatrix} \sigma_1 & 0 & 0 \\ 0 & \sigma_2 & 0 \\ 0 & 0 & \sigma_3 \end{pmatrix}. \tag{5.52}$$

The axes x', y', z' are called the *principal axes* for this state of stress, and σ_1, σ_2, and σ_3 are the principal stresses, which are the eigenvalues of the matrix. It can be shown[*] that the principal stresses are the roots of the cubic equation

$$\sigma^3 - I_1\sigma^2 + I_2\sigma - I_3 = 0, \tag{5.53}$$

---

[*] For the details of this analysis, first proposed by French mathematician A. L. Cauchy in the 1820s, see Timoshenko, S. P. and Goodier, J. N., *Theory of Elasticity*, McGraw-Hill, 1970, sec. 77.

where

$$I_1 = \sigma_{xx} + \sigma_{yy} + \sigma_{zz} = \text{tr}[\sigma],$$

$$I_2 = \sigma_{xx}\sigma_{yy} + \sigma_{yy}\sigma_{zz} + \sigma_{zz}\sigma_{xx} - \sigma_{xy}^2 - \sigma_{yz}^2 - \sigma_{zx}^2, \tag{5.54}$$

$$I_3 = \sigma_{xx}\sigma_{yy}\sigma_{zz} - \sigma_{xx}\sigma_{yz}^2 - \sigma_{yy}\sigma_{xz}^2 - \sigma_{zz}\sigma_{xy}^2 + 2\sigma_{xy}\sigma_{yz}\sigma_{zx} = \det[\sigma].$$

These quantities I_i are invariants, independent of the orientation of the coordinate system. (The trace of the stress tensor I_1 is the extension of quantity $\sigma_{xx} + \sigma_{yy}$ that we found to be invariant with rotation for the case of plane stress.) We determine the principal stresses by evaluating the coefficients I_i and solving for σ, or using any method that will find the eigenvalues directly.

We determine the maximum shear stress in the same way we did for plane stress and find that the absolute maximum shear stress is the largest of the three values:

$$\max\left(\left| \frac{\sigma_1 - \sigma_2}{2} \right|, \left| \frac{\sigma_1 - \sigma_3}{2} \right|, \left| \frac{\sigma_2 - \sigma_3}{2} \right| \right). \tag{5.55}$$

This absolute maximum shear stress may be visualized by superimposing the Mohr's circles obtained from the three orientations as is shown in Figure 5.22a. Notice from Figure 5.22b that if $\sigma_1 > \sigma_2 > \sigma_3$, the absolute maximum shear stress is $(\sigma_1 - \sigma_3)/2$.

From linear algebra, we know how to perform a general rotation of a stress tensor (or a matrix) from (x, y, z) to (x', y', z') coordinate axes as a change of basis. The transformed stress σ' can be calculated as $\sigma' = A\sigma A^{\mathrm{T}}$, where A is a general orthogonal transformation matrix analogous to the 2×2 matrix of Equation 4.43.

5.4 Failure Prediction Criteria

In Section 2.4, we discussed the need for techniques to predict failure for various materials under various loading. In designing structures, it may be necessary to make compromises and trade-offs, based on material availability, manufacturability, cost, weight, and esthetic issues, but avoiding failure is not negotiable in many contexts. For complex structures subject to general states of stress, various criteria have been proposed for predicting (and so preventing) failure. The applicability of these criteria depends on the nature of the materials and the loading involved. Note that these criteria have been empirically demonstrated to be good predictors of failure, but they are not exact, analytically derived expressions.

In all cases, it is crucial to consider the entire stress tensor, and not just one or several entries, when predicting whether a state of stress will cause failure. To determine whether a structural component will be safe under a given load, we should calculate the stress state at all critical points of the component, and particularly at all points where stress–concentrations are likely to occur.

5.4.1 Failure Criteria for Brittle Materials

We recall from Figure 2.17c that a brittle material subjected to uniaxial tension fails without necking, on a plane normal to the material's long axis. When such an element is under uniaxial tensile stress, the normal stress that causes it to fail is the ultimate tensile strength
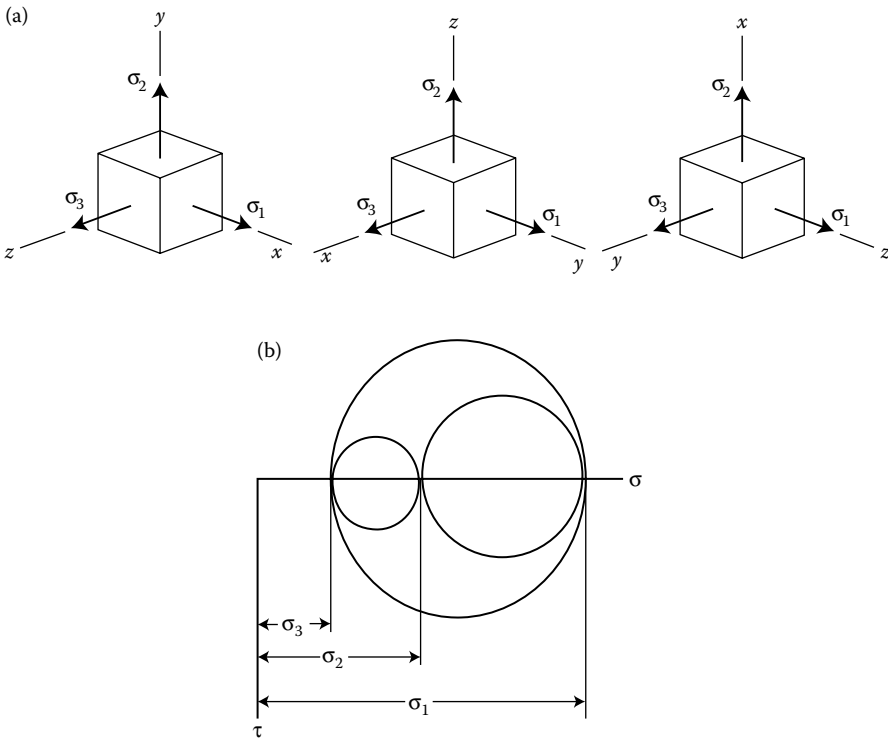
FIGURE 5.22
(a) Different orientations of the coordinate system relative to the element on which the principal stresses act. Only the components on faces with positive normal directions are shown; (b) superimposing the Mohr's circles demonstrates the absolute maximum shear stress.

of the material. However, when a structural element is in a state of plane stress or a three-dimensional stress state, we must determine the principal stresses at any given point and use one of the following criteria.

5.4.1.1 Maximum Normal Stress Criterion

According to this criterion, a given structural element fails when the maximum normal stress in that component reaches the material's ultimate tensile strength. This criterion is appropriate for brittle materials, which do not yield or undergo much plastic deformation, since the implied mechanism for the failure is one of separation rather than sliding or shear. Mathematically, we can represent this criterion using the principal stresses as saying that failure will occur when the maximum positive principal stress reaches the material's ultimate tensile strength. Since for brittle materials the tensile strength is typically much lower than the compressive strength—because tension opens and grows cracks and compression closes them—this criterion is based on the maximum tensile stress. It makes sense to compare the maximum negative principal stress to the material's ultimate compressive strength if failure by compression is also of concern.*

---

* A somewhat more refined version of this is known as Mohr's criterion. It is based on an envelope defined by two Mohr's circles: one constructed for the stress state at failure in a tension experiment, and one constructed

5.4.2 Yield Criteria for Ductile Materials

We observed in Figure 2.17b that a ductile material subjected to uniaxial tension yields and fails by slippage along angled surfaces, primarily due to shear stresses. A uniaxial tension test gives the tensile yield strength for a ductile material, and the compressive yield stress is typically the same. Although ductile materials do not fracture when they reach their yield strengths, at this point permanent deformation can occur and proper function of a structural element may be lost. We, therefore, cast our criteria in terms of *yield* and not of fracture.

5.4.2.1 Maximum Shearing Stress (Tresca) Criterion

Because the plastic deformation initiated at the yield strength takes place through shear deformation, it is natural to expect failure criteria to be expressed in terms of shear stress. Based on this logic, the Tresca criterion says that a given structural component is safe as long as the maximum shear stress value in that component does not exceed the yield shear strength, τ_Y, of the material. Since for axial loading, as we saw in Section 2.6, the maximum shear stress is equal to half the value of the corresponding normal axial stress, we conclude that the maximum shear stress experienced by a uniaxial tensile test specimen is $\tau_Y = \sigma_Y/2$.

We extend this criterion to an arbitrary state of stress by assuming that yielding occurs when the absolute maximum shear stress is equal to τ_Y:

$$\max\left(\left|\frac{\sigma_1 - \sigma_2}{2}\right|, \left|\frac{\sigma_2 - \sigma_3}{2}\right|, \left|\frac{\sigma_3 - \sigma_1}{2}\right|\right) = \tau_Y, \tag{5.56}$$

where σ_1, σ_2, and σ_3 are the principal stresses. Or, using $\tau_Y = \sigma_Y/2$ to recast the criterion in terms of a Tresca equivalent normal stress σ_T,

$$\max(|\sigma_1 - \sigma_2|, |\sigma_2 - \sigma_3|, |\sigma_3 - \sigma_1|) \equiv \sigma_T = \sigma_Y. \tag{5.57}$$

For this criterion, we must consider the full three-dimensional tensor even if the physical state is plane stress. The zero normal stress in the third direction may determine the maximum principal stress difference. For the sake of illustration, however, we can consider a plane stress case where the maximum principal stress is positive and the minimum is negative (so the zero does not contribute to the maximum difference calculation). In this case, our safe region is bounded by the lines $\sigma_1 - \sigma_2 = \pm\sigma_Y$, $\sigma_1 = \pm\sigma_Y$, and $\sigma_2 = \pm\sigma_Y$, which form the hexagon shown in Figure 5.23.

We can also compare the Tresca equivalent stress to the material's yield stress to determine how close the material is to failure. We obtain a *Tresca safety factor*:

$$S_T = \frac{\sigma_Y}{\sigma_T}. \tag{5.58}$$

Failure will occur when $S_T = 1$, and a safe design will ensure that $S_T > 1$.

---

for the stress state at failure in a compression experiment. If the material's ultimate shear strength is known, a third circle may be added. Mohr's criterion says that a general state of stress is safe if its Mohr's circle—based on the maximum and minimum principal stresses—lies entirely within the area bounded by the envelope around the two (or three) circles representing the ultimate failure stresses. This criterion uses a plane stress approach, as it does not consider the intermediate principal stress.
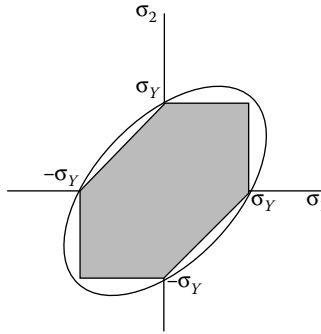
FIGURE 5.23
Failure boundaries for the Tresca (hexagon) and von Mises (ellipse) failure criteria under plane stress.

5.4.2.2 Von Mises Criterion

This criterion for failure of ductile materials is derived from strain energy considerations and states that yielding occurs when

$$\frac{1}{2}\left[(\sigma_{xx} - \sigma_{yy})^2 + (\sigma_{yy} - \sigma_{zz})^2 + (\sigma_{zz} - \sigma_{xx})^2 + 6(\sigma_{xy}^2 + \sigma_{yz}^2 + \sigma_{zx}^2)\right] = \sigma_Y^2, \qquad (5.59)$$

or equivalently in terms of principal stresses,

$$\frac{1}{2}\left[(\sigma_1 - \sigma_2)^2 + (\sigma_2 - \sigma_3)^2 + (\sigma_3 - \sigma_1)^2\right] = \sigma_Y^2. \qquad (5.60)$$

In plane stress, the safe region is bounded by the curve that describes the ellipse in Figure 5.23, but this criterion correctly accounts for the full 3D stress state. We can define a von Mises equivalent stress:

$$\sigma_M \equiv \frac{1}{\sqrt{2}}\sqrt{(\sigma_{xx} - \sigma_{yy})^2 + (\sigma_{yy} - \sigma_{zz})^2 + (\sigma_{zz} - \sigma_{xx})^2 + 6(\sigma_{xy}^2 + \sigma_{yz}^2 + \sigma_{zx}^2)}$$

$$= \frac{1}{\sqrt{2}}\sqrt{(\sigma_1 - \sigma_2)^2 + (\sigma_2 - \sigma_3)^2 + (\sigma_3 - \sigma_1)^2}, \qquad (5.61)$$

and compare this value to the material's yield stress to determine how close the material is to failure. We obtain a *von Mises safety factor*:

$$S_M = \frac{\sigma_Y}{\sigma_M}. \qquad (5.62)$$

Again, failure will occur when $S_M = 1$, and a safe design will ensure that $S_M > 1$.

The Tresca and von Mises criteria do not produce the same safety factors, and a stress state that might just fail by one criterion may produce a small safety factor with the other. Because we design with safety factors of 2 or greater, this difference is not crucial. Both are empirically demonstrated to be effective, but they are not exact analytically derived equations.

5.5 Examples

EXAMPLE 5.1

What must be the length of a 6-mm diameter aluminum ($G = 27\,\text{GPa}$) wire so that it could be twisted through one complete revolution without exceeding a shear stress of $42\,\text{MPa}$?

> **Given:** Cross section of wire, desired deformation, limit on shear stress.
>
> **Find:** Required length of wire.
>
> **Assume:** Hooke's law applies.

Solution

The angle of twist of the wire after one complete revolution will be 2π. The angle of twist is defined:

$$\phi = \frac{TL}{JG}$$

and, using the definition of maximum shear stress, this can also be written as

$$\phi = \frac{\tau_{\text{max}} J}{c} \frac{L}{JG} = \frac{\tau_{\text{max}} L}{cG},$$

which we rearrange to solve for the wire length L:

$$L = \frac{\phi c G}{\tau_{\text{max}}} = \frac{2\pi \cdot (0.003\,\text{m})(27 \times 10^9\,\text{Pa})}{42 \times 10^6\,\text{Pa}},$$

$$L = 12.1\,\text{m}.$$

EXAMPLE 5.2

A solid aluminum alloy ($G_{\text{Al}} = 28\,\text{GPa}$) shaft 60 mm in diameter and 1000 mm long is to be replaced by a tubular steel shaft ($G_{\text{St}} = 84\,\text{GPa}$) of the same outer diameter such that the new shaft will exceed neither (1) twice the maximum shear stress nor (2) the angle of twist of the aluminum shaft. What should be the inner radius of the tubular steel shaft? Which of the two criteria, (1) strength or (2) stiffness, governs?

> **Given:** Dimensions of the aluminum shaft.
>
> **Find:** Dimensions of the steel shaft (same length, same outer diameter) that will meet strength and stiffness requirements.
>
> **Assume:** Hooke's law applies.

Solution

We will design first for strength, then for stiffness.

1. Designing for strength:

$$\tau_{\text{max,St}} \leq 2\tau_{\text{max,Al}},$$

$$\left(\frac{Tc}{J}\right)_{\text{St}} \leq 2\left(\frac{Tc}{J}\right)_{\text{Al}}.$$

Since we are told that the outer diameters of both shafts are equal, and since the applied torque T does not change, we are simply requiring that

$$J_{St} \geq \frac{1}{2} J_{Al},$$

$$\frac{\pi}{2} \left[(0.03 \, \text{m})^4 - r_i^4 \right] \geq \frac{\pi}{4} \left[(0.03 \, \text{m})^4 \right],$$

$$r_i^4 \leq \frac{2}{\pi} \left[\frac{\pi}{2} (0.03 \, \text{m})^4 - \frac{\pi}{4} (0.03 \, \text{m})^4 \right],$$

$$r_i^4 \leq \frac{1}{2} (0.03 \, \text{m})^4 = 405 \times 10^{-9} \, \text{m}^4,$$

$$r_i \leq 25.2 \, \text{mm}.$$

2. Designing for stiffness:

$$\phi_{St} \leq \phi_{Al},$$

$$\frac{TL}{J_{St} G_{St}} \leq \frac{TL}{J_{Al} G_{Al}},$$

$$J_{St} G_{St} \geq J_{Al} G_{Al},$$

$$\frac{\pi}{2} \left[(0.03 \, \text{m})^4 - r_i^4 \right] (84 \times 10^9 \, \text{Pa}) \geq \frac{\pi}{2} \left[(0.03 \, \text{m})^4 \right] (28 \times 10^9 \, \text{Pa}),$$

Solve for $r_i \leq 27.1 \, \text{mm}$.

The inner radius of the steel shaft must be $r_i \leq 25.2 \, \text{mm}$, as strength governs.

EXAMPLE 5.3

Two shafts ($G = 28 \, \text{GPa}$) A and B are joined and subjected to the torques shown. Section A has a solid circular cross section with diameter 40 mm, and is 160 mm long; B has a solid circular cross section with diameter 20 mm, and is 120 mm long.
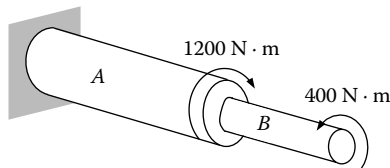
Find (a) the maximum shear stress in sections A and B; and (b) the angle of twist of the rightmost end of B relative to the wall.

Given: Dimensions and properties of composite shaft in torsion.

Find: Shear stresses, angle of twist of free end.

Assume: Hooke's law applies; stress–concentration at the step in the composite shaft is not included.

Solution

Our strategy is to use the method of sections to find the internal torque in each portion of the composite shaft, then find the shear stress and angle of twist induced by this torque.

First, we construct an FBD:
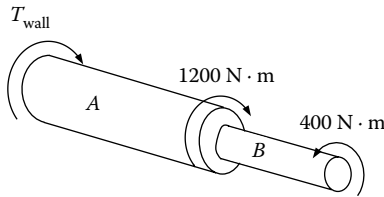
Equilibrium requires that $400\,\text{N} \cdot \text{m} - 1200\,\text{N} \cdot \text{m} - T_{\text{wall}} = 0$.

Therefore, $T_{\text{wall}} = -800\,\text{N} \cdot \text{m}$ (T_{wall} is clockwise, opposite from what is drawn).

Now use the method of sections on segments A and B:
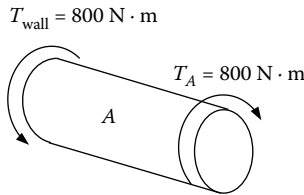
Internal torque $T_A = 800\,\text{N} \cdot \text{m}$, and maximum shear stress occurs at $c_A = 0.02\,\text{m}$. So:

$$\tau_{\text{max},A} = \frac{T_A c_A}{J_A} = \frac{T_A c_A}{\frac{\pi}{2} c_A^4} = 63.7\,\text{MPa}.$$

To find the internal resisting torque in section B, we must look at the whole shaft from the wall to our imaginary section cut:
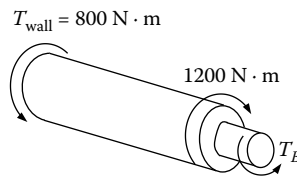
Equilibrium of this section requires that the internal torque $T_B = 400\,\text{N} \cdot \text{m}$. Maximum shear stress occurs at $c_B = 0.01\,\text{m}$, and

$$\tau_{\text{max},B} = \frac{T_B c_B}{J_B} = \frac{T_B c_B}{\frac{\pi}{2} c_B^4} = 255\,\text{MPa}.$$

Next, we will calculate the angles of twist of both A and B, and then find the resultant twist of the free end with respect to the wall: $\phi_A + \phi_B = \phi$.

Taking counterclockwise twists to be positive, as we have taken counterclockwise torques to be

$$\phi_A = \frac{T_A L_A}{J_A G_A} = \frac{(-800\,\text{N} \cdot \text{m})(0.16\,\text{m})}{(2.51 \times 10^{-7}\,\text{m}^4)(28 \times 10^9\,\text{Pa})} = -0.018\,\text{rad}\ (-1.0°),$$

$$\phi_B = \frac{T_B L_B}{J_B G_B} = \frac{(400\,\text{N} \cdot \text{m})(0.12\,\text{m})}{(1.57 \times 10^{-8}\,\text{m}^4)(28 \times 10^9\,\text{Pa})} = 0.109\,\text{rad}\ (6.2°).$$

The total angle of twist of the free end relative to the wall is then

$$\phi = \phi_A + \phi_B = -1.0° + 6.2° = 5.2°\ \text{(counterclockwise)}.$$

EXAMPLE 5.4

Design a hollow steel shaft to transmit 300 hp at 75 rpm without exceeding a shear stress of 8000 psi. Use 1.2:1 as the ratio of the outside to the inner diameter. What solid shaft could be used instead?

   Given: Desired performance of hollow shaft.

   Find: Inner and outer diameters of shaft; dimensions of equivalent solid shaft.

   Assume: Hooke's law applies.

Solution

We can obtain the torque required with

$$T = \frac{P}{\omega},$$

and the conversions, necessary to find a torque in U.S. units of in-lb are built into the following version of this relationship, where N is the number of rotations per minute: $T(\text{in-lb}) = \frac{63,000 \times (\text{hp})}{N(\text{rpm})}$. We have

$$T = \frac{63,000 \times 300\,\text{hp}}{75\,\text{rpm}} = 252,000\,\text{in-lb}.$$

Since the maximum shear stress induced by this torque is given by $\tau_{\max} = Tc/J$, we obtain the value of J/c needed to transmit 600 hp without exceeding the stated stress limit:

$$\frac{J}{c} = \frac{T}{\tau_{\max}} = \frac{252,000\,\text{in-lb}}{8000\,\text{psi}} = 31.5\,\text{in}^3,$$

$$\frac{J}{c} = \frac{\pi}{2}\frac{\left(c^4 - (c/1.2)^4\right)}{c} = 0.813c^3 = 31.5\,\text{in}^3.$$

This has the solution $c = 3.4\,\text{in}$, so the outer diameter necessary is $D_o = 2c = 6.8\,\text{in}$, and the inner diameter is $D_i = D_o/1.2 = 5.6\,\text{in}$.

For a solid shaft, J/c has a simpler form, and we require only

$$\frac{J}{c} = \frac{\pi}{2}c^3 = 31.5\,\text{in}^3,$$

Solving for c, the radius of a solid shaft capable of transmitting 600 hp without exceeding a shear stress of 8000 psi, we have $D = 2c = 5.4\,\text{in}$.

EXAMPLE 5.5

Find the required fillet radius for the juncture of a 6-in-diameter shaft with a 4-in-diameter segment if the shaft transmits 110 hp at 100 rpm and the maximum shear stress is limited to 8000 psi.

   Given: Dimensions of and requirements for shaft performance.

   Find: Fillet radius for connecting two segments of shaft.

   Assume: Hooke's law applies. Transition between segments is only stress–concentration.

Solution

We make use of the relationship between applied torque, power output, and rotational frequency (see also Example 5.4) to find the applied torque:

$$T = \frac{63{,}000 \cdot 110\,\text{hp}}{100\,\text{rpm}} = 69{,}300\,\text{in-lb.}$$

The shear stress in the shaft cannot exceed 8000 psi. We obtain the maximum allowable stress concentration factor, using the smaller segment's radius for c and in J:

$$K = \frac{\tau_{max}J}{Tc} = \frac{8000\,\text{psi}\left[\frac{\pi}{2}(2\,\text{in})^4\right]}{69{,}300\,\text{in-lb}(2\,\text{in})} = 1.45$$

and

$$\frac{D}{d} = \frac{\text{big shaft diameter}}{\text{small shaft diameter}} = \frac{6}{4} = 1.5.$$

From Figure 5.5, we find that this K and this D/d correspond to an r/d ratio of 0.085. This means that the allowable fillet radius is

$$r = (0.085)(4\,\text{in}) = 0.34\,\text{in.}$$

EXAMPLE 5.6

The composite rod with length L consists of an inner core (with shear modulus G_1 and polar second moment of area J_1) and outer tube (with shear modulus G_2 and polar second moment of area J_2) that are firmly bonded to each other. Both parts are also bonded to end plates (not shown) through which a torque T is applied. Determine

a. the maximum shear stress in the core and in the tube

b. the total angle of twist of the composite rod.
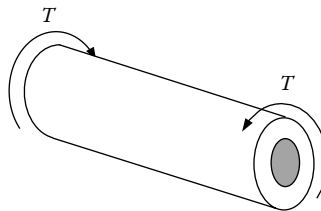
Given: Dimensions and material properties of components of a composite rod.

Find: Stress in each component and total twist.

Assume: Hooke's law applies.

Solution

a. Picking the force method (although the displacement method is equally effective for this problem), we start with an FBD and write the equation of equilibrium:
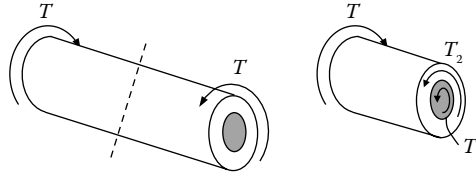
$$T_1 + T_2 - T = 0.$$

The applied torque T is given, leaving one equation for two unknown torques. To gain an additional equation, we enforce geometric compatibility:

$$\phi_1 = \phi_2,$$

where these are the twists of the two rod components. Then with our assumption of elastic (Hookean) behavior, this equation for geometric compatibility becomes

$$\frac{T_1 L_1}{J_1 G_1} = \frac{T_2 L_2}{J_2 G_2}.$$

Recognizing that both components have the same length and solving this pair of equations for the unknown torques

$$T_1 = T \frac{J_1 G_1}{J_1 G_1 + J_2 G_2} \quad \text{and} \quad T_2 = T \frac{J_2 G_2}{J_1 G_1 + J_2 G_2}.$$

b. The total twist is $\phi = \phi_1 = \phi_2$, so plugging in one of the above results:

$$\phi = \phi_1 = \frac{T_1 L}{J_1 G_1} = \frac{T L}{J_1 G_1} \frac{J_1 G_1}{J_1 G_1 + J_2 G_2} = \frac{T L}{J_1 G_1 + J_2 G_2}.$$

These results make sense for torsional elastic elements in parallel.

EXAMPLE 5.7

Calculate the tensile stresses (circumferential and longitudinal) developed in the walls of a cylindrical pressure vessel with inside diameter 18 in and wall thickness 1/4 in. The vessel is subjected to an internal gage pressure of 300 psi and a simultaneous external axial tensile load of 50,000 lb.

Given: Dimensions of and loading on cylindrical pressure vessel.

Find: Hoop and longitudinal normal stresses.

Assume: We will test whether thin-walled theory may be applied to this vessel.

Solution

Does thin-walled theory apply? Is the thickness $t \leq 0.1 r_i$?

$$0.25 \, \text{in} \leq 0.1 \cdot (9 \, \text{in}) = 0.90 \, \text{in} \checkmark$$

We can use thin-walled theory.

The circumferential, or hoop stress, is calculated:

$$\sigma_{\theta\theta} = \frac{pr_i}{t} = \frac{(300\,\text{psi})(9\,\text{in})}{0.25\,\text{in}} = 10.8\,\text{ksi}.$$

The longitudinal stress due to the internal pressure may be combined with the normal stress due to the axial load by straightforward superposition, as these stresses are due to forces in the same direction and act normal to areas with the same orientation:

$$\sigma_{xx} = \frac{pr_i}{2t} + \frac{P}{A} = \frac{(300\,\text{psi})(9\,\text{in})}{0.5\,\text{in}} + \frac{50{,}000\,\text{lb}}{(2\pi r_i)t},$$

$$\sigma_{xx} = 5.4\,\text{ksi} + 3.5\,\text{ksi} = 8.9\,\text{ksi}.$$

Note: the area on which P acts can also be calculated as $\pi r_o^2 - \pi r_i^2$; this gives essentially the same results for thin circular sections.

EXAMPLE 5.8

Aneurysm, a ballooning or dilation of a blood vessel, often afflicts the abdominal aorta, a large vessel supplying blood to the abdomen, pelvis, and legs. While aneurysms can develop and grow gradually, the rupture (rapid expansion and tearing) of an aneurysm is usually catastrophic. Although the healthy abdominal aorta has a diameter of 1.2–2 cm, an aneurismal abdominal aorta may have a diameter up to 6–10 cm. Anatomy textbooks give a range of values for the thickness of artery walls, from which we choose a median value of 0.1 cm. The figure below shows a rough sketch of this anatomy. Using outside references, determine the stresses in the walls of a healthy abdominal aorta and one affected by aneurysm.

(a)   (b)

Kidneys

Iliac arteries
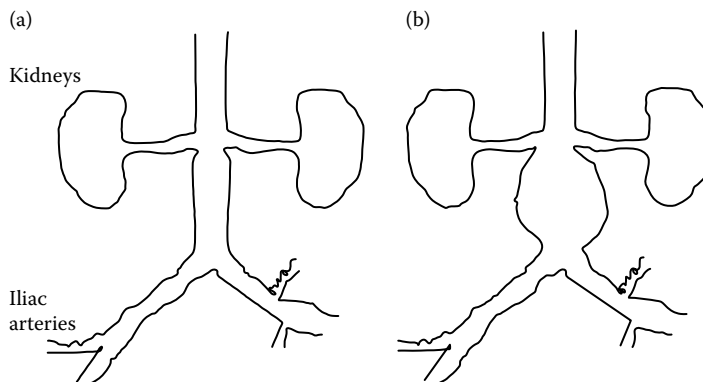
Given: Dimensions of healthy aorta and aneurysm.

Find: Stresses in the aorta walls.

Assume: The healthy aorta is a cylindrical pressure vessel and the aneurysm may be a cylindrical or spherical pressure vessel; thin wall theory applies.

Solution

We would like to model the artery as a pressure vessel, despite the many differences between a physiologically realistic blood vessel and the idealization we have just studied. If we choose a radius of 1.2 cm (or larger) for our model healthy abdominal aorta, we can call our vessel is thin-walled.

The pressure inside the artery varies from a low (diastolic) to high (systolic) value over each heartbeat. Using a typical healthy systolic pressure of 120 mm Hg ($1.6\,\text{N/cm}^2$), we can calculate the peak circumferential or hoop stress in a healthy abdominal aorta:

$$\sigma_{\theta\theta} = \frac{pr}{t} = \frac{1.6\,\text{N/cm}^2 \cdot 1.2\,\text{cm}}{0.1\,\text{cm}} = 19\,\text{N/cm}^2.$$

If the vessel grows to a diameter of 6 cm, the hoop stress in a cylindrical vessel becomes

$$\sigma_{\theta\theta} = \frac{pr}{t} = \frac{1.6\,\text{N/cm}^2 \cdot 3\,\text{cm}}{0.1\,\text{cm}} = 48\,\text{N/cm}^2.$$

If, however, the abdominal aorta remodels itself into a more spherical shape, the hoop stress will be reduced:

$$\sigma_{\theta\theta} = \frac{pr}{2t} = \frac{1.6\,\text{N/cm}^2 \cdot 3\,\text{cm}}{2(0.1\,\text{cm})} = 24\,\text{N/cm}^2.$$

This crude calculation suggests that the aorta may change its shape in part to reduce the stress induced by internal (blood) pressure. It is worth noting again that this pressure pulses, too, resulting in a cyclic loading and unloading of the vessel. Other factors contributing to aneurysm development include elastin degradation, atherosclerosis, and genetics, but continuum mechanics is certainly part of the package.

EXAMPLE 5.9

For the given state of plane stress, construct Mohr's circle, determine the principal stresses, and determine the maximum shearing stress and the corresponding normal stress.
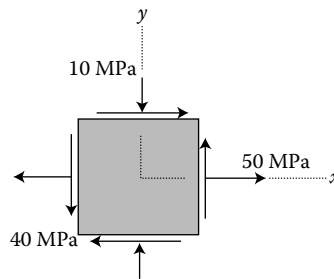
Given: $\sigma_{xx} = 50\,\text{MPa}$, $\sigma_{yy} = -10\,\text{MPa}$, $\sigma_{xy} = 40\,\text{MPa}$.

Find: Extreme stress states.

Assume: Plane stress: $\sigma_{zz} = \sigma_{xz} = \sigma_{yz} = 0$.

Solution

We will outline the steps used to construct Mohr's circle, and make the necessary calculations.

The steps we will follow are

1. Plot point X: $(\sigma_{xx}, \sigma_{xy})$
2. Plot point Y: $(\sigma_{yy}, \sigma_{xy})$

3. Draw line XY, which passes through the circle center: $(\sigma_{av}, 0)$
4. Find radius R and draw in the circle

1. Plot point $X : (\sigma_{xx}, \sigma_{xy})$: We note straight-off that the shear stress given is positive, according to Figure 4.7, but we are not sure how to plot the point $(\sigma_{xx}, \sigma_{xy})$ on Mohr's circle. Finding σ_{xx} on the σ-axis is straightforward—the normal stress sign convention simply says that tensile stresses are positive and compressive are negative, but does τ_{xy} lie above or below that axis? We know that for Mohr's circle to work, we must have points X and Y on the opposite sides of the σ-axis, so that their connecting line XY passes through the center of the circle. Our sign convention must ensure this. We, therefore, make use of a system based on the positive x (and y) faces of our unrotated element.

   Looking at the positive x face of our initial element (right-hand face), we see that the component of shear stress on this face is tending to rotate the element counterclockwise. This tells us to plot point X below the σ-axis. Our convention is that when this component tends to rotate clockwise, X is above the axis; when counterclockwise, below. (This somewhat awkward rule can be remembered by the equally strange mnemonic: "in the kitchen, the clock is above and the counter is below.") We formalize this rule in the figure below. Remember that we will apply this sign convention to points X and Y separately—for Mohr's circle to work, we must have points X and Y on the opposite sides of the σ-axis.

Plotting "positive" shear stress on Mohr's circle:

Below σ_{ii} axis   Above σ_{ii} axis
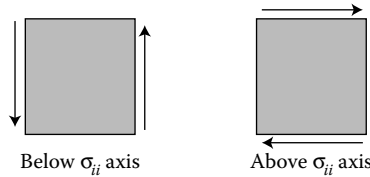
2. Plot point Y: $(\sigma_{yy}, \sigma_{xy})$: Following the same reasoning as for point X, we will plot point Y to the left of the τ-axis, as σ_{yy} is compressive, and above the σ-axis, as the shear stress on the positive y (top) face of the element tends to rotate clockwise.

   These two points may now be plotted on the στ-axes:
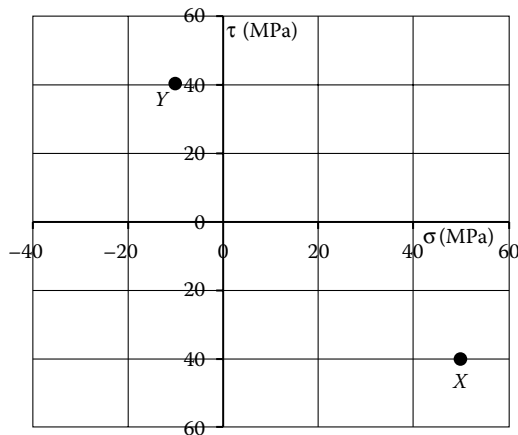
3. Draw line *XY*: This line passes through the σ (horizontal) axis at the center of the circle:

$$(\sigma_{av}, 0) = \left(\frac{\sigma_{xx} + \sigma_{yy}}{2}, 0 \right) = (20\,\text{MPa}, 0).$$
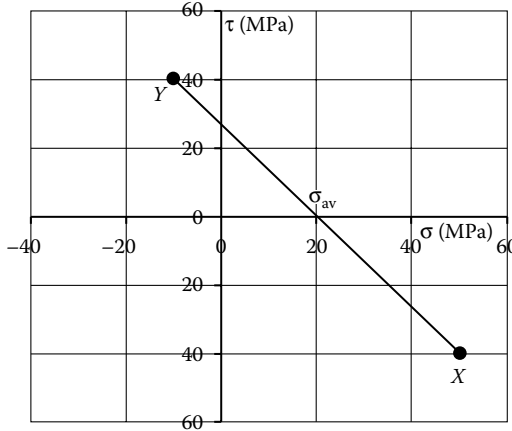
4. Find the radius *R* and draw the circle: We may use the geometry of the first three steps, or the formulas derived in the notes, to calculate the radius of the circle. Graphically, we see that *R* is the hypotenuse of a right triangle whose other legs have length 40 and $50 - 20 = 30$. Thus, $R = ((40)^2 + (30)^2)^{1/2} = 50\,\text{MPa}$.

   Alternatively,

$$R = \sqrt{\left(\frac{\sigma_{xx} - \sigma_{yy}}{2} \right)^2 + (\tau_{xy})^2} = 50\,\text{MPa}.$$

We can now sketch Mohr's circle by hand, using a compass, or using a software package. The circle contains all the information we need about all possible axes, and thus all possible stress states, for the given element.
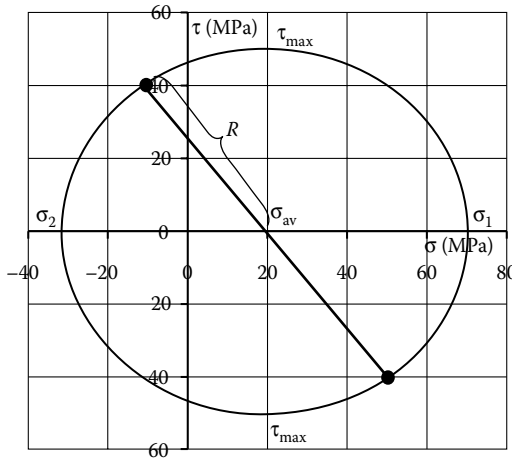
We can find, and label, the principal stresses:

$$\sigma_1 = \sigma_{av} + R = 20\,\text{MPa} + 50\,\text{MPa} = 70\,\text{MPa},$$

$$\sigma_2 = \sigma_{av} - R = 20\,\text{MPa} - 50\,\text{MPa} = -30\,\text{MPa}.$$

This principal stress state (extreme normal stress, no shear stress) occurs when the axes are rotated by θ_N. (Or when the line XY is rotated around Mohr's circle by $2\theta_N$). We can find $2\theta_N$ using a protractor, or we can use our formulas: $\theta_N = \frac{1}{2}\tan^{-1}(2\tau_{xy}/(\sigma_{xx} - \sigma_{yy}))$. At this θ_N, we can calculate that the value of $\sigma_{x'x'}$ (rather than $\sigma_{y'y'}$) is 70 MPa, so we draw our properly oriented element which experiences this principal stress state:
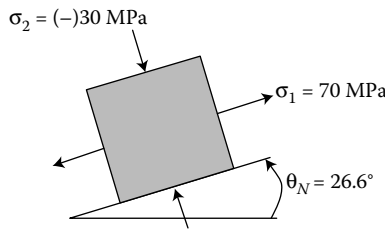
Next, we calculate the maximum shear stress and the corresponding normal stress, which we can see from Mohr's circle is the average normal stress, σ_{av}:

$$\tau_{max} = R = 50\,\text{MPa},$$

$$\sigma_{av} = 20\,\text{MPa}.$$

From the principal stress state, we can see on Mohr's circle that it will take $2\theta = 90°$ to obtain this stress state $(\sigma_{av}, \tau_{max})$. We need, then, to rotate our element's axes 45° counterclockwise past the principal stress orientation. From our initial orientation, this rotation is given by

$$\theta_S = \theta_N + 45° = 26.6° + 45° = 71.6°.$$

We can again draw a properly oriented element experiencing the maximum shear stress, having been rotated by 71.6° counterclockwise from its initial orientation:
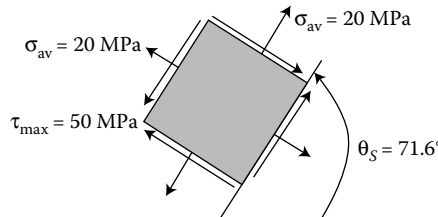
We obtain the proper sense of the shear stress from Mohr's circle. By rotating line XY counterclockwise by $2\theta_S$, we get to a point above the σ-axis. Thus, on the rotated positive x face, we must have a shear stress that tends to rotate the element *clockwise*.

Finally, we can visualize these rotations on Mohr's circle:
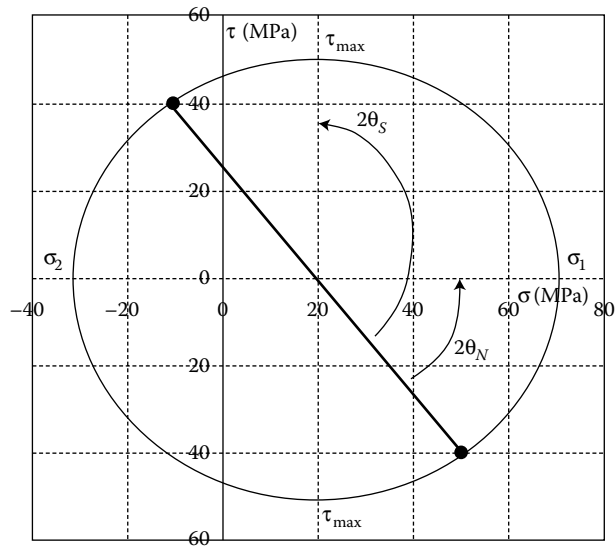
Note: a positive rotation, that is, a positive value in degrees or radians, is counterclockwise, both in physical space and on Mohr's circle.

EXAMPLE 5.10

A compressed air tank is supported by two cradles as shown. Relative to the effects of the air pressure inside the tank, the effects of the cradle supports are negligible. The cylindrical body of the tank has a 30-in outer diameter and is fabricated from a 3/8-in steel plate by welding along a helix that forms an angle of 25° with a transverse (vertical) plane. The end caps are spherical and have a uniform wall thickness of 5/16 in. For an internal gage pressure of 180 psi, determine

a. The normal stresses and maximum shear stresses in the spherical caps
b. The stresses in directions perpendicular and parallel to the helical weld
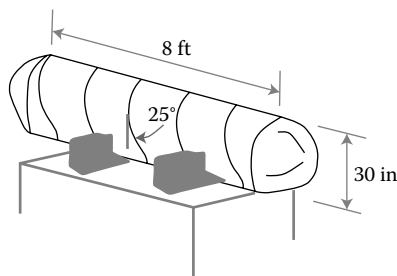
Given: Dimensions of and pressure on compressed air tank.

Find: Stress states in spherical end caps and along welds in cylindrical body.

Assume: Thin-walled pressure vessel theory applies.

Solution

First, we validate our assumption that thin-walled theory will apply in both the spherical end caps and the cylindrical body. We must have $t \leq 0.1r$ in both sections. So:

a. In spherical cap, $t = 5/16$ in and $r = 15 - (5/16) = 14.688$ in. So, $t = 0.0212r$. ✓
b. In cylindrical body, $t = 3/8$ in and inner radius $r = 14.625$ in. So, $t = 0.0256r$. ✓

In a spherical pressure vessel, we have equal hoop and longitudinal stresses:

$$\sigma_{\text{sphere}} = \frac{pr}{2t} = \frac{(180\,\text{psi})(14.688\,\text{in})}{2(0.3125\,\text{in})} = 4230\,\text{psi}.$$
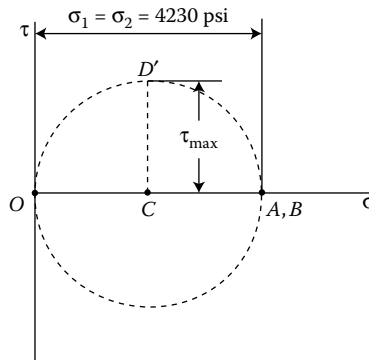
So, in a plane tangent to the cap, Mohr's circle reduces to a point (A, B) on the horizontal (σ) axis, and all in-plane shear stresses are zero. On the surface of the cap, the third principal stress is zero, corresponding to point O. On a Mohr's circle of diameter AO, point D' represents the maximum shear stress; it occurs on planes inclined at $45°$ to the plane tangent to the cap. (This is as we would expect for purely normal loading in the reference axes, as for an axially loaded bar which experiences maximum normal stress on planes inclined at $45°$ to the bar axis.) Hence,

$$\tau_{\text{max}} = \frac{1}{2}(4230\,\text{psi}) = 2115\,\text{psi}.$$

In the cylindrical body of the tank, we have hoop and longitudinal normal stresses:

$$\sigma_{\theta\theta} = \frac{pr}{t} = \frac{(180\,\text{psi})(14.625\,\text{in})}{0.375\,\text{in}} = 7020\,\text{psi},$$

$$\sigma_{xx} = \frac{pr}{2t} = \frac{(180\,\text{psi})(14.625\,\text{in})}{2(0.375\,\text{in})} = 3510\,\text{psi}.$$

Here, the average normal stress is $\sigma_{\text{av}} = \frac{1}{2}(\sigma_1 + \sigma_2) = 5265$ psi, and the radius of Mohr's circle is $R = \frac{1}{2}(\sigma_1 - \sigma_2) = 1755$ psi. We want to rotate our axes from their initial configuration, shown at left below, so that our element has a face parallel to the weld, as shown at right; the transformed $\sigma_{x'x'}$ and $\sigma_{x'y'}$, or σ_w and τ_w, will be the requested stresses.
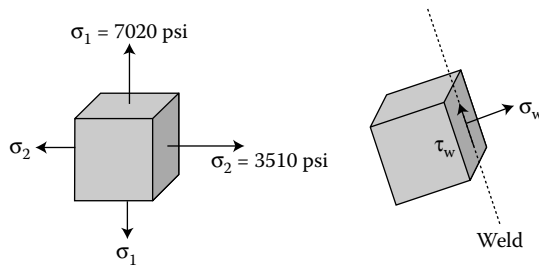
Using the average stress (center) and radius R found above, we construct Mohr's circle and find these transformed stress components.

Since we want to rotate the element by $\theta = 25°$, we rotate around Mohr's circle by $2\theta = 50°$, to arrive at point X'. This point has coordinates:

$$\sigma_w = \sigma_{av} - R\cos 50°$$
$$= 5265 - 1755\cos 50°$$
$$= 4140\,\text{psi (tensile)},$$

$$\tau_w = R\sin 50° = 1755\sin 50°$$
$$= 1344\,\text{psi}.$$

Since point X' is below the horizontal axis, τ_w tends to rotate the element counter-clockwise, as assumed in the sketch below.
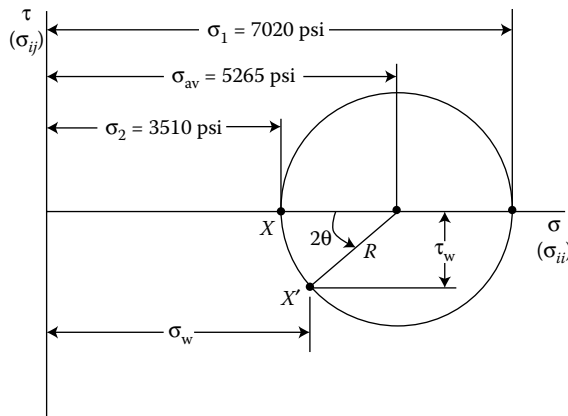
EXAMPLE 5.11

A state of plane stress consists of a tensile stress $\sigma_0 = 8\,\text{ksi}$ exerted on vertical surfaces and unknown shear stresses τ_0. Determine (a) the magnitude of the shear stress τ_0 for which the maximum normal stress is 10 ksi, and (b) the corresponding maximum shear stress.
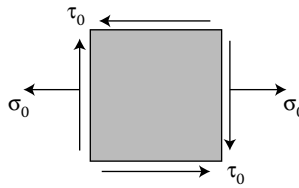
Given: Plane stress state.

Find: Shear stress τ_0; maximum shear stress.

Assume: Plane stress.

Solution

We will assume a sense (sign) for the unknown shear stress, and construct Mohr's circle. The shearing stress τ_0 on faces normal to the x-axis tends to rotate the element clockwise, so we plot point X, whose coordinates are (σ_0, τ_0), above the σ-axis. We see that in our initial state, σ_{yy} is zero and that on faces normal to the y-axis τ_0 tends to rotate the element counterclockwise; thus, we plot point $Y(0, \tau_0)$, below the σ-axis.
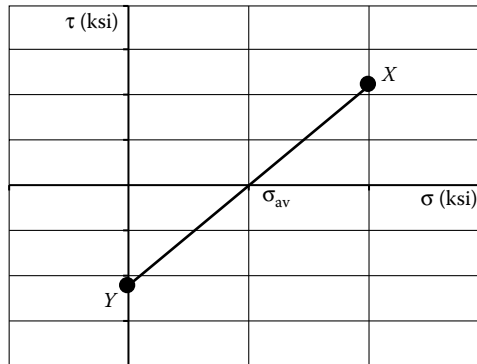
Line XY passes through the center of our circle, at

$$\sigma_{\text{av}} = \frac{1}{2}(\sigma_{xx} + \sigma_{yy}) = \frac{1}{2}(8 + 0) = 4 \, \text{ksi}.$$

We determine the radius R of the circle by observing that the maximum normal stress, given as 10 ksi, appears a distance R to the right of the circle's center:

$$\sigma_1 = \sigma_{\text{av}} + R,$$

$$R = \sigma_1 - \sigma_{\text{av}},$$

$$R = 10 \, \text{ksi} - 4 \, \text{ksi} = 6 \, \text{ksi}.$$
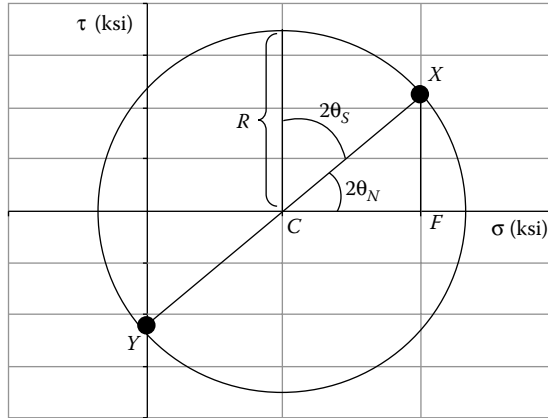
Now we have Mohr's circle to work with. We see that the rotation required to get from our initial stress state (point X) to the principal stress state at $(10\,\text{ksi}, 0)$ is either clockwise $2\theta_N$ as shown, or counterclockwise $360° - 2\theta_N$. We choose to work with the more manageable clockwise rotation, and consider the right triangle CFX.

$$\cos 2\theta_N = \frac{CF}{CX} = \frac{CF}{R} = \frac{4\,\text{ksi}}{6\,\text{ksi}}.$$

$$\theta_N = -24.1°.$$

This rotation, again, is *clockwise*, as reflected by the negative sign. The right triangle CFX also allows us to compute the unknown shear stress, τ_0, which is experienced at point X:

$$\tau_0 = FX = R\sin 2\theta_N = (6\,\text{ksi})\sin 48.2° = 4.47\,\text{ksi}.$$

The maximum shear stress is also apparent from Mohr's circle. It is simply the radius of the circle, R:

$$\tau_{\max} = R = 6\,\text{ksi}.$$

The corresponding normal stress at this stress state is $\sigma_{av} = 4\,\text{ksi}$. Mohr's circle indicates that to get from the initial stress state to the state of maximum shear stress, we must rotate the circle diameter XY counterclockwise by $2\theta_S$, or rotate the element itself by θ_S. It is clear from the circle that $2\theta_S + |2\theta_N| = 90°$. Hence

$$2\theta_S = 90° - |2\theta_N| = 90° - 48.2° = 41.8°.$$

With all this information in hand, we can draw properly oriented elements in each of the identified stress states.
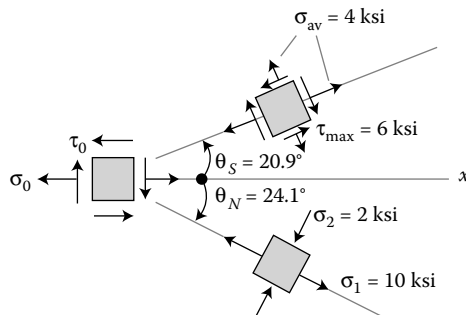
Note: If we had originally assumed the opposite sense of the unknown τ_0, we would have obtained the same numerical answers, but the orientation of the elements would be as shown below.
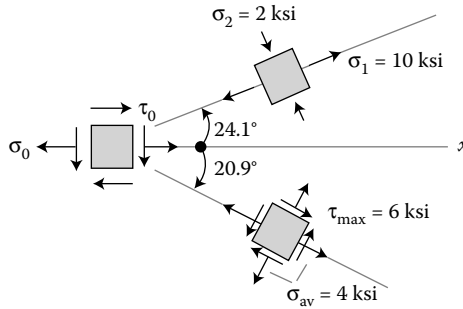
EXAMPLE 5.12

A stress state is described by the tensor $\sigma_{ij} = \begin{pmatrix} 25 & 15 & 5 \\ 15 & 20 & -15 \\ 5 & -15 & -20 \end{pmatrix}$ ksi.

a. Determine the principal stresses.
b. If this state of stress exists in a part made of gray cast iron (a brittle material with ultimate strength in tension of $\sigma_{ult} = 30$ ksi and in compression of $\sigma_{ult} = 120$ ksi), will it fail at this location?
c. If this state of stress exists in a part made of 6061-T6 aluminum (a ductile material with yield strength of $\sigma_{ys} = 35$ ksi). Will the part fail by yielding at this location?

Given: Three-dimensional stress state.

Find: Principal stresses and evaluate failure criteria for two materials.

Assume: Failure criteria apply.

Solution

a. The principal stresses may be found from the roots of the cubic equation in Section 5.3.5 or by finding the eigenvalues of the tensor. Either way the values are: $\sigma_1 = 38.4$ ksi, $\sigma_2 = 13.5$ ksi, and $\sigma_3 = -26.8$ ksi.
b. For brittle materials, the first check should be a comparison of the maximum positive principal stress with the ultimate strength in tension. Since 38.4 ksi is greater than the strength of 30 ksi, we predict that the cast iron will fail at this point. (If we did not predict failure, we would next compare the maximum negative principal stress to the ultimate compressive strength).
c. For ductile materials we have two criteria, and either is valid. For the Tresca criterion, we evalulate

$$\max\left(\left|\frac{\sigma_1 - \sigma_2}{2}\right|, \left|\frac{\sigma_2 - \sigma_3}{2}\right|, \left|\frac{\sigma_1 - \sigma_3}{2}\right|\right) = \frac{38.4 - (-26.8)}{2} = 32.6 \text{ ksi}$$

and compare to $\sigma_Y/2 = 17.5$ ksi to predict that this material, too, will fail due to the given stress state.

The von Mises criterion shows this as well. Since we have already found the principal stresses, we can use the compact form of the von Mises stress:

$$\sigma_M = \frac{1}{\sqrt{2}}\sqrt{(\sigma_1 - \sigma_2)^2 + (\sigma_2 - \sigma_3)^2 + (\sigma_1 - \sigma_3)^2}$$

$$= \frac{1}{\sqrt{2}}\sqrt{(38.4 - 13.5)^2 + (13.5 - (-26.8))^2 + (-26.8 - 38.4)^2}$$

$$= 57\,\text{ksi},$$

which is greater than the yield stress.

PROBLEMS

5.1 A solid circular shaft of 40 mm diameter is to be replaced by a hollow circular tube. If the outside diameter of the tube is limited to 60 mm, what must be the thickness of the tube for the same linearly elastic material working at the same maximum stress? Determine the ratio of weights for the two shafts.

5.2 The propeller of a wind generator is supported by a hollow circular shaft with 0.4 m outer radius and 0.3 m inner radius. The shear modulus of the material is $G = 80\,\text{GPa}$. (a) If the propeller exerts an 840 kN · m torque on the shaft, what is the resulting maximum shear stress? (b) What is the angle of twist of the propeller shaft per meter of length?

5.3 A 100-mm diameter core is bored out from a 200-mm diameter solid circular shaft. What percentage of the shaft's torsional strength is lost due to this operation?

5.4 A solid circular shaft has a slight uniform taper. Find the error committed if the angle of twist for a given length is calculated using the mean radius of the shaft when $b/a = 1.2$.
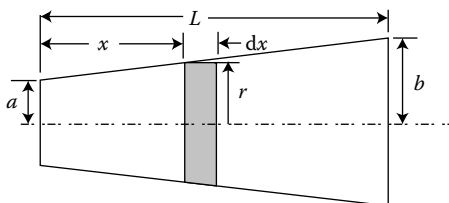
5.5 Calculate the torsional stiffness k_t of the rubber bushing shown. Assume that the rubber is bonded both to the steel shaft and to the outer steel tube, which is in turn attached to a machine housing. Assume that the metal parts do not deform, and that the shear modulus of rubber is G.
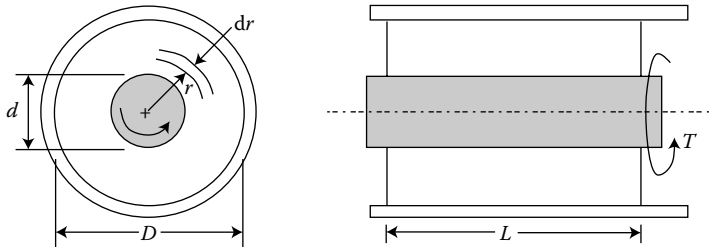
5.6 The stepped shaft rotates at 120 rpm and has a 20 kW input at A. 16 kW is taken off to operate machinery at B, and the remaining 4 kW is used at C. The shaft is stainless steel with yield strength in shear of 300 MPa.

    a. Not including the effect of stress–concentration, what are the minimum allowable diameters for segments AB and BC to achieve a safety factor of 3?

    b. With the minimum shaft radii, and now considering stress–concentration, what is the safety factor if the fillet radius is 1 mm?
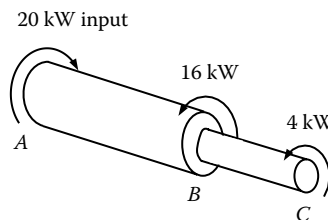
5.7 Determine the reaction torques at the fixed end of the circular shaft shown.
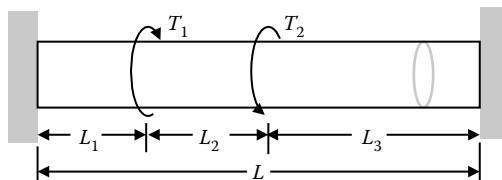
5.8 Two structural steel shafts with flanges forged on their ends are rigidly connected with a circle of bolts. The shafts are meant to rotate in their supports at A and D, however a $100\,\text{N} \cdot \text{m}$ torque is applied to flange B while the shafts are locked and prevented from rotating at A and D. Shaft AB has diameter 20 mm and shaft CD has diameter 30 mm. What is the maximum shearing stress that occurs in a shaft?

$T = 100 \text{ N} \cdot \text{m}$

A   B C   D

0.5 m   0.5 m
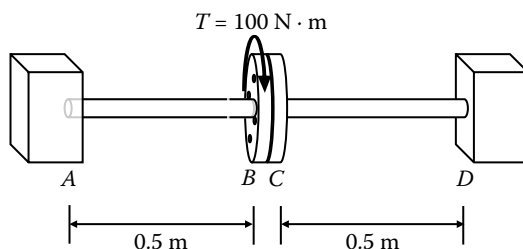
5.9 The wrong size bolts were used to connect the flanges in Problem 5.8, and when the torque is applied to flange B it rotates by 2 degrees (twisting shaft AB) before engaging flange C. Once flange C is engaged both B and C rotate together, twisting both shafts. What is the maximum shearing stress that occurs in a shaft?

5.10 Consider the torsion of a thin-walled tube. Determine an approximate expression for the torque if the shear stress must be less than a given working stress τ_w. Express this result in terms of the tube's mean radius R and its thickness t. (*Hint: The binomial theorem will be useful here*.) Also, derive an approximate expression for the strength-to-weight ratio of the tube in terms of the working stress, its radius, and length L, and its specific weight ρg. This result is widely used in aircraft design.

5.11 A cylindrical pressure vessel of 120 in outside diameter, used for processing rubber, is 36 ft long. If the cylindrical portion of the vessel is made from 1 in thick steel ($E = 29 \times 10^6$ psi, $v = 0.25$) plate and the vessel operates at 120 psi internal pressure, determine the total elongation of the circumference and the increase in the length caused by the operating pressure.

5.12 A closed cylindrical tank of length L, radius R, and wall thickness t contains a liquid at pressure p. If a hole is suddenly made in the cylinder, determine

   a. How much the tank radius R changes
   b. How much the tank length L changes

5.13 An inflatable cylindrical Quonset hut of length L, radius $R = 30$ ft from material with thickness $t = 2.5$ mm, $E = 30.7$ GPa, and $v = 0.24$ has a longitudinal seam that runs the entire length of the hut at its highest point (see figure). The hut is closed at each end by a quarter of a sphere.
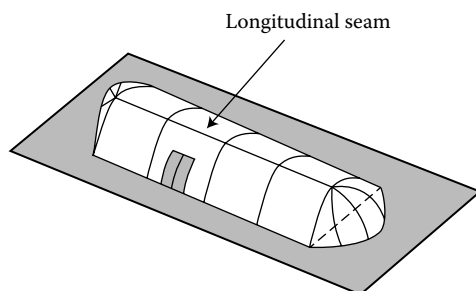
Longitudinal seam

If the hut is inflated to a pressure $p = 3.44\,\text{kPa}$, determine

   a. The maximum tension (force per length along the seam) that the longitudinal seam must withstand with a factor of safety of 2

   b. How much higher the peak of the cylindrical roof gets when the hut is inflated to pressure p

   c. The maximum tension that a seam in the quasi-spherical end cap must withstand to maintain the same safety factor of 2

Note: Quonset huts (see photograph above) were lightweight, prefabricated structures developed to be used as military barracks and offices during World War II. The Quonset hut skeleton was a row of semi-circular steel ribs covered with corrugated sheet metal. The ribs sat on a low steel-frame foundation with a plywood floor. The basic model was 20 feet wide and 48 feet long with 720 square feet of usable floor space. A larger model was 40 by 100 feet. Approximately 170,000 Quonset huts were produced during the war. After the war, the military sold the huts to civilians for about a thousand dollars each.

5.14 A strain gage is installed as shown on an aluminum soda can. The can's radius is 1.3 in and its wall thickness is 0.004 in (sometimes written as 4 mil; 1 mil = 1/1000 in). When the lid of the can is opened, the magnitude of the strain reading changes by 180 μstrain.

To circuit
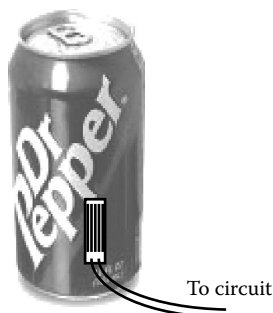
    a. What was the internal pressure p in the can?

    b. When the can was pressurized, what was the factor of safety with respect to yielding in the cylindrical wall?

5.15 For a state of plane stress, examine how the normal and shear stress vary on an inclined section as a function of angle θ (measured from the positive x-axis). Over the range 0–2π, plot normal stress and shear stress as a function of θ—use the particular plane stress example of $\sigma_{yy} = 0.4\sigma_{xx}$ and $\sigma_{xy} = 0.9\sigma_{xx}$ (normalize your vertical plot axis to σ_{xx}). Comment on the significance of key features and points of the curves (e.g., relative positions/values of maxima, minima, and zero crossings). Pick a few angles and draw the rotated square element with the state of stress at that angle.
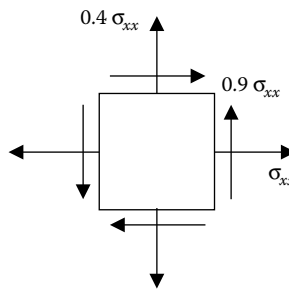
5.16 For the state of stress shown, determine

    a. the principal planes

    b. the principal stresses

    c. the orientation of the planes of maximum shear stress

    d. the extreme shear stresses and any associated normal stresses
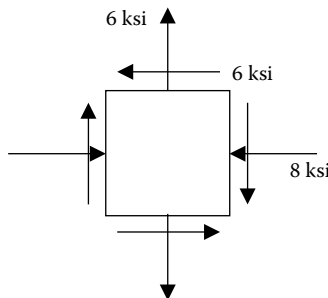
5.17 For the state of stress shown, determine

    a. the principal planes

    b. the principal stresses

    c. the orientation of the planes of maximum shear stress

100 MPa

20 MPa

80 MPa
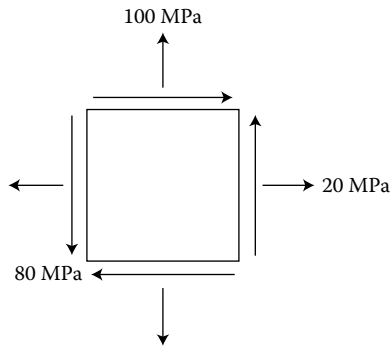
5.18 For the state of stress given in Problem 5.17, determine

    a. the maximum shear stress

    b. the normal stresses on the plane of maximum shear stress

    c. the normal and shear stresses after the element has been rotated through an angle of 30° clockwise

5.19 Using the equations for stress transformation,

    a. confirm the angles that define the planes of maximum and minimum shear stress

    b. determine the maximum and minimum values of the shear stress

5.20 Consider the top part of the balloon to be half of a spherical pressure vessel. What is the ratio of the normal stress across a vertical seam to the normal stress across a seam inclined 45 degrees?

5.21 A weld is oriented at an angle θ (less than 45°) from the horizontal axis in a component loaded in plane stress. All stresses have positive values as shown. If we are concerned that the component might fail due to tensile normal stress across the weld,

which is the safer design—or are they both the same—or does it depend on the magnitudes of the stresses?
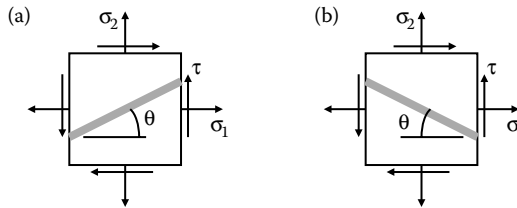
5.22 A solid circular rod of known radius is twisted in a testing machine with a known torque T. Only one strain gage is available. Does each of the test setups below give us enough information to determine the shear modulus of the material?
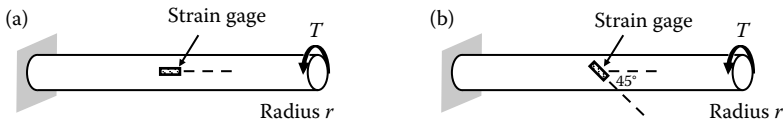
5.23 A rosette composed of three strain gages measures strain at a point on the surface of a flat sheet of annealed stainless steel loaded in plane stress. The strains measured (numbers correspond to strain gages in the figure) are

$$\varepsilon_1 = +280\,\mu\text{strain}, \quad \varepsilon_2 = +720\,\mu\text{strain}, \quad \varepsilon_3 = -120\,\mu\text{strain}.$$

   a. Find the in-plane strains at this point using the xy-axes shown.
   b. Find the in-plane stresses at this point.
   c. What is the percent change in thickness of the plate if this stress state is uniform over it?
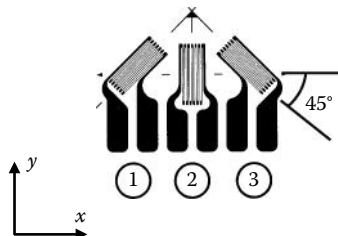
(Courtesy of Micro-Measurements, a brand of VPG, Raleigh, NC, USA.)

5.24 If the strain rosette applied to the plate in Problem 5.23 was instead a delta rosette of the configuration shown, what would the gage readings be?
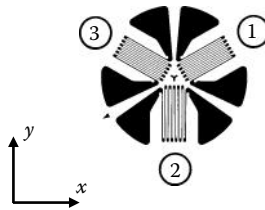
(Courtesy of Micro-Measurements, a brand of VPG, Raleigh, NC, USA.)

5.25 In order to penetrate a workpiece, a tungsten carbide drill bit is subject to a torque of 3.8 Nm and an axial force of 5 kN. Tungsten carbide is very strong (compressive strength 1400 MPa, tensile strength 340 MPa) but also brittle. Assuming the bit is a uniform cylinder with 4 mm diameter, what is the safety factor with respect to failure during this operation?

5.26 You are asked to design a cylindrical scuba tank with a radius $R = 16$ cm to a pressure of $p = 12.0$ MPa at a factor of safety of 2.0 with respect to the yield stress. The relevant tabulated yield values for the steel of which the tank is intended to be made are 290 MPa in tension and 124 MPa in shear.

   a. Explain why the in-plane (in the plane of the cylinder wall) shear stress is not the maximum shear stress?
   b. What wall thickness t would you recommend?

5.27 A cylindrical pressure vessel with hemispherical endcaps has radius $r = 2\,\text{m}$, wall thickness $t = 10\,\text{mm}$, and is made of steel with yield stress $\sigma_y = 1800\,\text{MPa}$. It is internally pressurized at $p = 2\,\text{MPa}$. Compare the Tresca and von Mises safety factors.

5.28 An annealed stainless steel cylindrical pressure vessel has an inner radius of 250 mm and a wall thickness of 10 mm. In addition to an internal pressure of $p = 4\,\text{MPa}$, the vessel is loaded with a torque $T = 200\,\text{kNm}$. Will it fail?
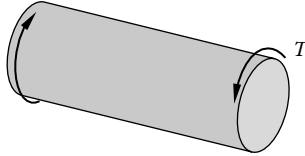
6

Case Study 2: Pressure Vessels

Pressure vessels are structures designed to contain or preclude a significant pressure, that is, a force distributed over the entire surface of the vessel in question. Pressure vessels show up in a variety of settings and typically are in one of two shapes. Some are spherical: balloons of all sorts, gas storage tanks (Figure 6.1a), and basketballs. Many are cylindrical: pressurized cabins in aircraft, rocket motors, scuba tanks, oil-storage tanks, aerosol spray cans, and fire extinguishers. Some of the cylindrical tanks have flat ends or caps, as in spray cans and home heating oil-storage tanks. Often, though, the cylindrical tanks have slightly rounded caps (Figure 6.1b), or spherical caps, as do submarines (Figure 6.1c). Nuclear reactor containment vessels are often cylinders with spherical caps, although newer nuclear plants tend to have spherical containment tanks.

Pressure vessels have given way or exploded in some rather dramatic fashions. Among the most notorious are the explosion of a molasses-storage tank in Boston in 1919 that resulted in 21 deaths and more than 150 injured as 2 million gallons of thick, brown molasses swept through Boston's North End (Figure 6.2, Problem 6.1); the burning of the Hindenburg blimp in Lakehurst, New Jersey in 1937; the rupture of the Apollo 13 oxygen tank in 1970; and the implosion of several submarines, including the USS Thresher in 1963, the USS Scorpion in 1968, and the Russian submarine Kursk in 2001. Though the causes of these catastrophes varied, serious pressure build-ups and the failures of connections or joints or seams were involved in most. Thus, the design and construction of a pressure vessel is at least as important as its shape. In fact, a major piece of regulatory code is the ASME *International Boiler and Pressure Vessel Code* (IBPVC) that governs the design and manufacture of pressure vessels.

6.1 Why Pressure Vessels Are Spheres and Cylinders

Why pressure vessels are curved, rather than flat? Two important reasons become evident when we review the physics of pressure vessels. The first has to do with material properties. As we noted in Sections 2.4 and 2.11, cracks propagate in metals, even in ductile metals. Further, crack propagation is especially likely to propagate from the *stress concentrations* that typically form at corners that subsume an angle less than 90°, termed *re-entrant corners* (see Figure 6.3). That is why, for example, airplane windows have rounded corners. There is a similar increased likelihood of crack propagation when we have structural elements like rectangular tubes that include four corners.

The second reason that pressure vessels are spheres or cylinders is that when such shapes are pressurized, they respond with a set of normal stresses that are distributed uniformly through the thickness and always directed along tangents to the surface enclosed (see Section 5.2). These stress states are called *membrane stresses*. These shapes and their membrane stress states produce much *stiffer* structural forms than their beam counterparts and thus

(a)   (b)   (c)
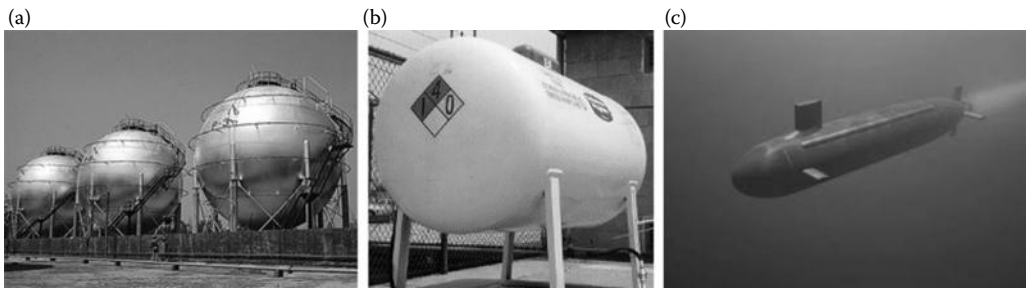
FIGURE 6.1
(a) A *spherical* pressure vessel; (b) a *cylindrical* pressure vessel with a slightly rounded cap; (c) a submarine: a *cylindrical* pressure vessel with a rounded cap.

FIGURE 6.2
A glimpse of the aftermath of the 1919 failure of 5-story-high tank that unleashed 12,000 tons of molasses on Boston's North End. (Photograph by Leslie Jones, *Boston Herald*. With permission.)

(a)   (b)

1620654 ——————— 1 mm   Fillet 3 outside view
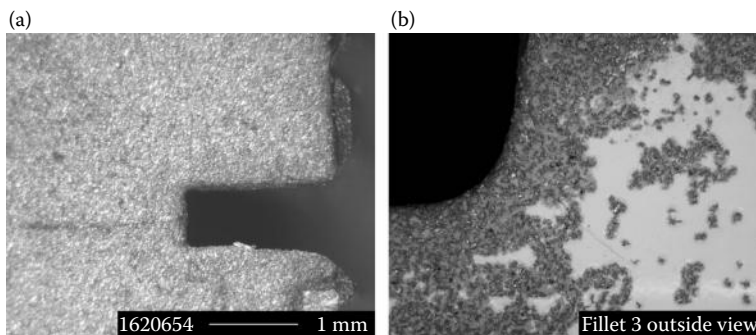
FIGURE 6.3
Cracks emanating (a) from a re-entrant corner inside a groove; (b) from a filleted corner. (Courtesy of J. A. King.)

they deflect or deform much less. Consider the pressurized cylinder originally depicted in Figure 5.10. We have already seen in Section 5.2 that a thin-walled pressure vessel experiences a circumferential stress, the *hoop stress* $\sigma_{\theta\theta}$, of magnitude:

$$\sigma_{\theta\theta} = \frac{pr_i}{t}. \tag{6.1}$$

Remember, too, that the wall thickness of a thin-walled vessel is always significantly smaller than the radius, that is, $t \ll r_i$, so that the stresses induced by the pressure are significantly larger than the pressure itself.

Now consider what happens to the geometry of a cylinder when that cylinder is subjected to this pressure. We would expect it to expand symmetrically, meaning that its radius will become larger (see Figure 6.4). Thus, if we use w to denote the radial motion or deflection of the cylinder, the circle that was originally of mean radius R (which we will use in place of inner radius r_i for simplicity) will become a circle of radius $(R + w)$. So the circumference of the cylinder increases from $2\pi R$ to $2\pi(R + w)$, and the resulting hoop strain $\varepsilon_{\theta\theta}$ is given by

$$\varepsilon_{\theta\theta} = \frac{2\pi(R + w) - 2\pi R}{2\pi R} = \frac{w}{R}. \tag{6.2}$$

For the sake of simplicity, let us assume a one-dimensional stress–strain law, $\sigma = E\varepsilon$ (although we of course know that generalized Hooke's law is really what we need for complete analysis of the strains caused by the biaxial stress state in a pressure vessel wall). This means that we can find (see Problems 6.2 and 6.3) that the radial expansion or deflection is

$$\frac{w}{t} = \frac{p}{E}\left(\frac{R}{t}\right)^2. \tag{6.3}$$

Now imagine that instead of a cylinder of radius R and thickness t, we were using a square tube of dimensions $H \times H$ (and wall thickness t) to contain a gas at the same pressure. We assume that the tube's side lengths H are comparable in magnitude to the cylinder radius R (see Problem 6.3) and that $t \ll H$. How does the shape of this square tube change when the gas is subjected to pressure? As we look at Figure 6.5, we can envision that a given side, say the one marked BC, will move upward or outward due to two effects: the upward movement of points B and C as sides AB and CD are stretched, and the vertical or *transverse* motion of the side BC due to the pressure acting on that surface. The side
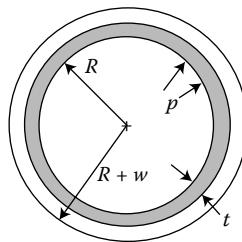
FIGURE 6.4
The development of hoop strain in a pressurized cylinder due to the (greatly exaggerated) axisymmetric radial deflection w.
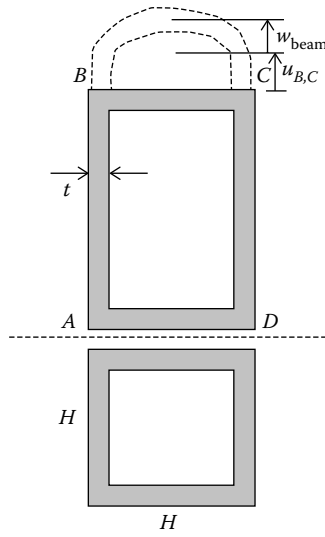
FIGURE 6.5
A pressurized square tube with cross section side dimensions $H \times H$ and wall thickness t. Note that the movement of side BC is due in part to the upward movement of points B and C as sides AB and CD are stretched, and in part due to the bending of the side BC due to the pressure acting on that surface. Deformations are not to scale; $w_{\text{beam}} \gg u_{B,C}$.

stretching is just like the extension of a one-dimensional bar, so the equal vertical movement of points B (from the stretching of AB) and C (from the stretching of CD) can be shown (see Problem 6.4) to be

$$\frac{u_{B,C}}{t} = \frac{p}{2E}\left(\frac{H}{t}\right)^2. \tag{6.4}$$

On the other hand, the transverse motion of the side BC is actually due to the *bending* of that side under the pressure load. As we will see in Chapter 9 when we analyze the deflections of bent beams, the maximum deflection of such a beam occurs at its center and can be modeled as

$$\frac{w_{\text{beam}}}{t} = \frac{5p}{32E}\left(\frac{H}{t}\right)^4. \tag{6.5}$$

Note that this beam deflection is proportional to the ratio (H/t) raised to the *fourth* power. Compare that with the deflection due to the stretching of the sides (Equation 6.4), which is proportional to the same ratio *squared*, which means that the bending deflection of a tube face is going to be much, much larger than movement due to the stretching of the sides (again, see Figure 6.5). Further, compare the beam bending deflection (Equation 6.5) to the radial expansion of a circular cylinder (Equation 6.3) of the same sheet material and under the same pressure:

$$\frac{w_{\text{beam}}/t}{w_{\text{cyl}}/t} = \frac{5p}{32E}\left(\frac{H}{t}\right)^4 \frac{E}{p}\left(\frac{t}{R}\right)^2 = \frac{5}{32}\left(\frac{H}{t}\right)^2\left(\frac{H}{R}\right)^2, \tag{6.6}$$

or, since $H \sim R$ (see Problem 6.4, again),

$$\frac{w_{\text{beam}}}{w_{\text{cyl}}} \sim \left(\frac{H}{t}\right)^2 \gg 1. \tag{6.7}$$

Equation 6.7 clearly shows that the deflections due to the bending of the sides of a rectangular tube are two orders of magnitude larger than the radial motion due to the extension of the walls of a circular cylinder. Thus, a cylinder, like a sphere, responds to pressure as a *stiff* structural form characterized by large membrane forces and stresses and relatively small (compared to the corresponding bending of thin-walled cylinders that are not pressurized) deflections (see Problem 6.6). We will say more about this when we describe beam bending in Chapters 7 and 9.

We have noted that some cylindrical tanks have spherical caps and, while we are on the subject of radial expansion of such tanks, it is interesting to examine another aspect of pressure vessel behavior: can we put a hemispherical cap on the end of a cylinder of the same radius R? For a cylinder of finite length, we noted in Section 5.2 that both axial and hoop stresses result from an internal pressure p:

$$\sigma_{\theta\theta} = \frac{pR}{t} \quad \text{and} \quad \sigma_{xx} = \frac{pR}{2t}. \tag{6.8}$$

The hoop strain for a (two-dimensional) state of plane stress within the cylinder surface would follow from Equation 4.27, rather than the one-dimensional version used above. Thus,

$$\varepsilon_{\theta\theta} = \frac{\sigma_{\theta\theta} - \nu\sigma_{xx}}{E}, \tag{6.9}$$

so that we can eliminate the hoop strain between Equations 6.2 and 6.9, and the hoop stresses from Equation 6.8 to find the radial expansion to be

$$\frac{w_{\text{cyl}}}{t} = \frac{(2-\nu)p}{2E}\left(\frac{R}{t}\right). \tag{6.10}$$

A comparable analysis for the sphere would look much like the cylinder's, with the obvious exception that the stresses in a hemispherical cap were found in Section 5.2 to be

$$\sigma_{\text{sphere}} = \frac{pR}{2t}, \tag{6.11}$$

(using the same mean radius R as an approximation of r_i) so that here the analysis of the sphere's hoop strain yields the following radial deflection for the sphere:

$$\frac{w_{\text{sph}}}{t} = \frac{(1-\nu)p}{2E}\left(\frac{R}{t}\right). \tag{6.12}$$

Clearly both p and R must be the same for the mated cylinder and sphere, and the radial deflections are compatible only if they are equal. If we set the right-hand side of Equation 6.10 to equal that of Equation 6.12, we find that the radial deflections are equal when

$$\frac{(Et)_{\text{cyl}}}{(Et)_{\text{sph}}} = \frac{2-\nu_{\text{cyl}}}{1-\nu_{\text{sph}}}, \tag{6.13}$$

where we have added appropriate subscripts to distinguish the thicknesses and material properties. If the materials are the same, which seems a reasonable assumption, then

$$\frac{t_{\text{cyl}}}{t_{\text{sph}}} = \frac{2 - \nu}{1 - \nu},$$

(6.14)

which suggests that the thickness of the cylinder should be much larger than that of the cap. For typical materials for which $\nu = 0.30$, the ratio (6.14) is about 2.43! Thus, the cylinder should be thicker by a factor of almost 2.5.

What happens in "real life" is, of course, more complicated. The mismatch caused by the mating of spheres and cylinders produces some modest bending effects that are superposed on the basic membrane states caused by the pressure. The bending stresses add a modest amount (~30%) to the membrane stresses, and they decay fairly rapidly as we move away from the joint or intersection of cap and circular tube. As a result, cylinders are tapered near the joints, with locally increased thickness designed to accommodate the added bending stresses. The complete analysis of these *edge effects* allows us to carefully and safely design such intersections and thus avoid a catastrophic failure due to a bad joint.

6.2 Why Do Pressure Vessels Fail?

A gas pressure vessel typically contains a large volume of gas that has been compressed to fit into the vessel's much smaller volume, which produces the constant pressure that acts on the container's inner wall. When such vessels fail, they explode because the pent-up gas wants to return to its initial volume as quickly as it can (see Problems 6.9–6.12). However, pressure vessels containing incompressible liquids also fail, as did the Boston molasses tank mentioned earlier. The common link is that tank failures typically arise because their designers either failed to properly anticipate possible sources of crack propagation or failed to adequately analyze the stresses at connections. For example, the owners of the Boston molasses tank, the Purity Distilling Company, claimed that it failed because of (variously) an explosion, vibration from an adjacent elevated train track, fermentation producing carbon dioxide and raising the pressure inside the tank, and a runaway trolley car colliding with the tank. However, forensic analysis of the tank ruins showed that its joints were inadequately designed and, further, the tank was fabricated with even thinner materials than required by the (already inadequate) design!

The 50-ft high, 90-ft diameter steel molasses tank had been ordered from Hammond Iron Works in 1915 by the Purity Distilling Company on authorization of U.S. Industrial Alcohol. (At the time, molasses was a standard sweetener; it can also be fermented to produce alcoholic beverages.) The treasurer of Purity ordered it without consulting an engineer. The only constraint was that the tank has a factor of safety of 3 for the storage of molasses, which is 50% more dense than water, weighing 12 lb per gallon.

All the steel sheets used in construction of the tank actually proved less thick than shown on the drawings used to obtain the building permit. For instance, the bottom ring—the most stressed part of the structure—was supposed to be 0.687 in; as built, it was only

0.667 in. The steel thicknesses for the other six rings were similarly found to be 5–10% less than the values indicated on the permit plans.

The tank was completed early in 1916 and tested with only 6 in of water. During the tank's 3 years of service, it had on several occasions contained a maximum of around 1.9 million gallons (for periods up to 25 days). At the time of failure, the tank had been near maximum capacity (at 2.3 million gallons) for 4 days. Months later, at the legal proceedings, several recalled that the seams of the tank were leaking molasses before the disaster. It was alleged to discourage neighborhood children from collecting the obvious drippings, the owner had painted the tank brown to hide the leaks.

The detailed design of joints, and of the connections of pipes and gages and doors, is beyond our scope. However, understanding the nature of the stress fields in pressure vessels is not. The estimates of the membrane stresses given for the cylinder (Equation 6.8) and sphere (Equation 6.11) are correct as far as they go, but they are incomplete—and sufficiently incomplete that by themselves they do not form an adequate basis for a comprehensive design. Thus, we will explore the stress states in greater depth to show that *shear* is present in pressure vessels and that Mohr's circle can be used to advantage in the design of joints.

Consider first the sphere. If we establish an x, y-coordinate system tangent to the sphere's surface at any point on the sphere, the equations for stress transformation (5.27) through (5.29) quickly confirm that the stresses in the plane of the sphere are always normal stresses, that is,

$$\sigma_{x'x'} = \sigma_{y'y'} = \frac{pR}{2t} = \sigma_1 = \sigma_2. \tag{6.15}$$

But what happens through the thickness, or in the z-direction? Consider the element shown in Figure 6.6. We see there a stress state

$$\sigma_{yy} = \frac{pR}{2t}, \quad \sigma_{zz} = -p. \tag{6.16}$$
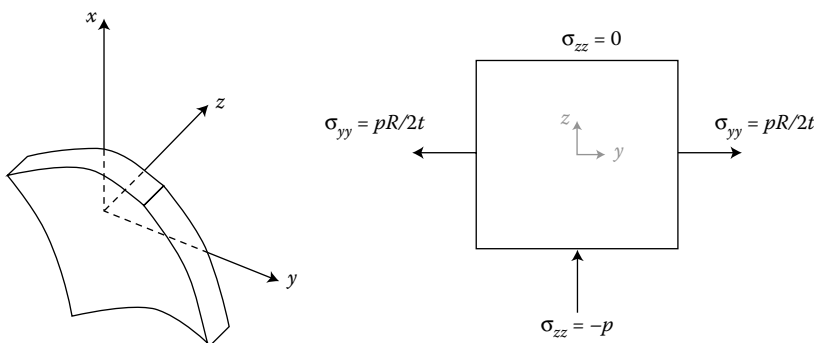
FIGURE 6.6
An element in the skin of a spherical pressure vessel, and a "blow-up" of the y–z-plane showing the stress $\sigma_{zz} = -p$ due to the internal pressure p acting on the sphere's inner wall, and the stress $\sigma_{yy} = pR/2t$, acting as shown.

If we then apply the stress transformation Equations 5.27 through 5.29 to this stress state (see Problem 6.13), we would find that in the *z-y*-plane the stresses vary as

$$\sigma_{z'z'} = \frac{1}{2}\left(-p + \frac{pR}{2t}\right) - \frac{1}{2}\left(p + \frac{pR}{2t}\right)\cos 2\theta, \tag{6.17a}$$

$$\sigma_{z'y'} = \frac{1}{2}\left(p + \frac{pR}{2t}\right)\sin 2\theta, \tag{6.17b}$$

$$\sigma_{y'y'} = \frac{1}{2}\left(-p + \frac{pR}{2t}\right) + \frac{1}{2}\left(p + \frac{pR}{2t}\right)\cos 2\theta. \tag{6.17c}$$

Equation 6.17b shows that there are shear stresses in the wall of a spherical pressure vessel and that the maximum shear stress occurs at $\theta = \pi/4$ and has the value

$$\tau_{max} = \sigma_{x'y'_{max}} = \frac{p}{2}\left(1 + \frac{R}{2t}\right). \tag{6.18}$$

Thus, there is a shear stress that acts through the thickness: its magnitude is the same as the principal membrane stresses and it must be accounted for in the design of spherical tanks (see Problem 6.14).

A similar situation occurs in the case of cylindrical tanks, with an interesting twist that arises because of the different ways that cylindrical tanks are actually made. While hollow reeds and bamboo tubes occur quite naturally, we have to manufacture cylindrical tanks. Typically that means forming flat, rectangular sheets around a rigid form, termed a *mandrel*, and welded together along seams that can be longitudinal, transversely circumferential, or even helically wound around the cylinder's axis (Figure 6.7). This means that the stresses along the seams are of especial interest, and thus the transformation of stresses needs to be considered. In fact, if we identify *x* as the axial coordinate in a cylinder and *y* as the circumferential coordinate, the membrane stress state of a pressurized cylinder is

$$\sigma_{xx} = \frac{pR}{2t}, \quad \sigma_{yy} = \frac{pR}{t}. \tag{6.19}$$
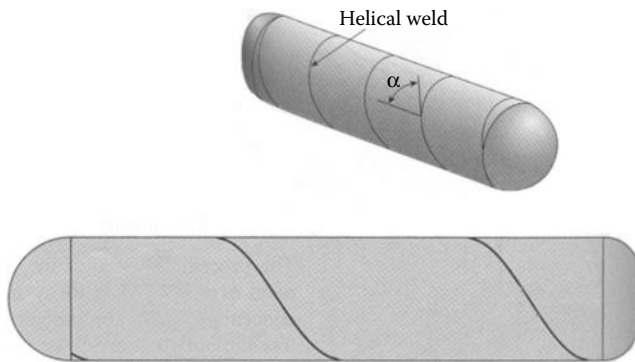
FIGURE 6.7
A cylindrical tank with helical seams. (After J. M. Gere and S. P. Timoshenko, *Mechanics of Materials*, 4th Edition, PWS Publishing Company, Boston, MA, 1997.)

Then this stress state substituted into the stress transformation Equations 5.27 through 5.29 yields the following stresses in the x–y-plane (see Problem 6.15):

$$\sigma_{x'x'} = \frac{3pR}{4t} - \frac{pR}{4t}\cos 2\theta, \tag{6.20a}$$

$$\tau_{x'y'} = -\frac{pR}{4t}\sin 2\theta, \tag{6.20b}$$

$$\sigma_{y'y'} = \frac{3pR}{4t} + \frac{pR}{4t}\cos 2\theta. \tag{6.20c}$$

Equation 6.20 allows us to determine the variation of the stresses with the angle θ. We can thus calculate the in-plane or membrane stresses along any intended seams (see Problems 6.16 and 6.17). Of course, in addition to the membrane stresses just analyzed, cylindrical tanks also have shear stress components that are directed in the thickness or z-direction.

Cylindrical pressure vessels that are made from welded steel sheets are very common, and this is the least expensive way to manufacture cylindrical tubing. It is also common to see cylinders that have been extruded from a solid piece of steel or aluminum, with welding only necessary at the end caps. This extrusion method is preferred for applications requiring higher safety factors than welded tubing, for example, in scuba cylinders. A third manufacturing technique of interest is *spin casting*, which helps to reduce the weight of the pressure vessel and also requires no welds along the length of the vessel. The tank material, generally aluminum, is melted and poured into a rotating cylindrical mold, where it solidifies in the desired vessel shape.

PROBLEMS

6.1 Determine in both US customary and SI units the volume that 12,000 tons of molasses occupies.

6.2 Derive Equation 6.3 by substituting Equations 6.1and 6.2 into the appropriate one-dimensional stress–strain law.

6.3 Is Equation 6.3 dimensionally correct? Explain your answer.

6.4 Determine how much the sides AB and CD of the square tube in Figure 6.7 are stretched due to an upward pressure p acting on the bottom surface of side BC. How does this answer compare to Equation 6.4?

6.5 Develop three scenarios for comparable circular cylinders of radius R and square tubes of side H that allow one to say $R \sim H$. (*Hint*: What geometric attributes of the cylinder and tube might be made equal?)

6.6 If a structural stiffness parameter was defined in terms of the pressure/radial deflection ratio (i.e., p/w), compare the stiffness parameters for a circular cylinder of radius R with that of a square tube of side H. What are the physical dimensions of these stiffness parameters and of their ratio? Assume that $R \sim H$. (*Hint*: Recall Equations 6.3 and 6.5.)

6.7 Given that the hoop strain is likely to be a very small number, estimate the pressure-to-modulus ratio, p/E.

6.8 Given the result of Problem 6.7, estimate the magnitude of the radial deflection of a pressurized cylinder as a fraction of its thickness. (*Hint*: Equation 6.3 might be handy.)

6.9 The adiabatic compression of an ideal gas obeys the following law: $p \, V^\gamma = $ constant, where p is the pressure, V the volume, and $\gamma = 1.4$. Assuming that the ideal law provides a reasonable rough estimate of the gas' behavior, determine the pressure in a tank of $1 \, \text{ft}^3$ volume when it stores $100 \, \text{ft}^3$ of standard atmospheric air.

6.10 For the two scuba cyliners shown, of radii $R = 4 \, \text{in}$ and length $L = 25 \, \text{in}$, estimate the pressure reading if $80 \, \text{ft}^3$ of air was compressed into them.

6.11 For the assumptions stated in Problem 6.9, show that the work done in adiabatically compressing an ideal gas is

$$W_{1-2} = -\int_1^2 p \, dV = \frac{p_1 V_1}{\gamma - 1}\left[\left(\frac{V_1}{V_2}\right)^{\gamma - 1} - 1\right].$$

6.12 Determine how much work was required to undertake the compression specified in Problem 6.9. Is that a lot of work (or energy)? Explain your answer, perhaps by providing a suitable comparison.

6.13 Verify that Equation 6.17 is correct by substituting the stress state of Equation 6.16 into the stress transformation Equations 5.27 through 5.29.

6.14 Determine an appropriate approximation to Equation 6.18 for thin-walled pressure vessels, that is, $t/R \ll 1$. From which of the original components of stress does the dominant, surviving term originate?

6.15 Verify that Equation 6.20 is correct by substituting the stress state of Equation 6.19 into the stress transformation Equations 5.27 through 5.29.

6.16 Determine the maximum in-plane stresses for a cylindrical tank made of steel ($E = 205 \, \text{GPa}$, $\nu = 0.30$), having a mean radius of $2 \, \text{m}$ and a thickness of $20 \, \text{mm}$, and subjected to an internal pressure $p = 1 \, \text{MPa}$.

6.17 Determine the in-plane normal and shear stresses along the seam of the tank of Problem 6.16 if it is helically wound at an angle $\theta = 60°$.

6.18 How much would the maximum stress in the Boston molasses tank have been increased by the reduction in wall thickness from the design spec, 0.687 in, to 0.667 in?

References

ASME *International Boiler and Pressure Vessel Code* (IBPVC), American Society of Mechanical Engineers, New York, 2001.

C. L. Dym, *Introduction to the Theory of Shells*, Hemisphere Publishing, New York, 1990.

J. M. Gere and S. P. Timoshenko, *Mechanics of Materials*, 4th Edition, PWS Publishing Company, Boston, MA, 1997.

H. Petroski, *To Engineer Is Human*, St. Martin's Press, New York, 1982.

N. Schlager (Editor), *When Technology Fails*, Gale Research, Detroit, MI, 1994.

S. P. Timoshenko and S. Woinowsky-Krieger, *Theory of Plates and Shells*, McGraw-Hill, New York, 1959.

7

Beams

The word *beam* is derived from Germanic words meaning *tree* or *structural element*. (One would guess that "tree" came first.) Beams are among the most common structural elements, popping up in the support structures of cars, aircraft, and buildings. A beam carries loads applied at right angles, or transverse, to its longitudinal axis, which cause it to bend. In practice, structural elements may experience complex loading including axial bar loading, torsional rod loading, and transverse beam loading. As we have already examined axial and torsional loading, for now we will consider the isolated effects of beam loading. The fundamental elements of continuum mechanics will serve us well: we will need equilibrium (and stress), constitutive laws, and compatibility (an appreciation of the kinematics of deformation). This time we will start with equilibrium, then develop our definitions of stress and strain, relatable by Hooke's law when deformations are small. We will examine first the internal forces and moments in the beams, and then the resulting stresses on the beams, and finally (in Chapter 9) the beams' deflections due to this loading.

7.1 Calculation of Reactions

Not surprisingly, our first step in analyzing a beam will be to draw an FBD and determine the reactions at its supports. A beam's behavior when subjected to an external load depends on the type of supports and on the type of loading.

There are three basic types of supports for planar structures such as beams: (1) the roller or link, which is capable of resisting a force in only one specific line of action; (2) the pin, which is capable of resisting a force in any direction, and whose reaction force hence has two components in a two-dimensional analysis and three components in a three-dimensional analysis; and (3) the fixed support, which is capable of resisting a force in any direction and is also capable of resisting a moment or a couple. This third type of support is obtained, for example, by building a beam into a wall, casting it into concrete, or welding its end to a main structure. Figure 7.1 shows physical and idealized diagrams of these three types of supports, and the resisting reactions they offer.

In addition to the type of supports, we also take into account the type of loading on the beam. In this book, we have considered a number of concentrated "point" loads; we can also see this type of loading on beams. We will also consider problems where the loads are distributed, either uniformly or not. Figure 7.2 gives an idea of how these load diagrams will look, and what their real-world equivalents might be.

Often when considering equilibrium, we will be able to replace a distributed load by an equivalent concentrated resultant load, acting through the centroid (center of force) of the distributed load. Note that when we consider deflections of beams in Chapter 9 we need to be careful, however, as the resultant load does not produce the same deflection as the distributed load.

Type	Real support	Idealized support	Reactions provided
Roller			
Pin or knife-edge			
Fixed			

FIGURE 7.1
Beam supports.

Concentrated loading		
Evenly distributed loading		
Unevenly distributed loading		

FIGURE 7.2
Types of loading conditions for beams.

We will also be able to classify beam problems, as we have classified axial bar and torsion problems, into statically determinate and statically indeterminate scenarios. And as before, whenever we encounter a statically indeterminate problem, we will supplement the equations of static equilibrium with compatibility (geometric restrictions) and constitutive laws.

Armed with this information about beam supports and loads, we are prepared to calculate beam reaction forces and moments. In statically determinate cases, the equations of static equilibrium will suffice.

7.2 Method of Sections: Axial Force, Shear, Bending Moment

By now we are good friends with the method of sections: the idea that if a whole body is in equilibrium, any part or section of this body is in equilibrium itself. We exploit this method to determine the complete force system of a body, including both external and internal forces and moments. In the particular case of a beam, the externally applied forces and the support reactions keep the entire body in equilibrium. When we make "cuts" to apply the method of sections, equilibrium requires the existence of internal forces at the cut section. These internal resisting forces and moments are what keep the cut sections in equilibrium. At each section, we may find any or all of: a vertical force, a horizontal force, and a moment necessary to maintain equilibrium. In the case of three-dimensional problems, there are additional force and moment reactions to be determined, but the principles remain the same.

7.2.1 Axial Force in Beams

A horizontal force N may be necessary at a beam section to satisfy equilibrium. The magnitude and sense of this force N are obtained from the solution of $\sum F_x = 0$. If the force N acts toward the section, it is a compressive force, sometimes called a *thrust*, as we have already seen; if it acts away from the section, N is called axial tension. Its line of action will always be directed through the centroid* of the beam's cross-sectional area. This loading is as we have seen for bars, and the normal stress may be calculated as in Chapter 2.

7.2.2 Shear in Beams

Typically, to keep a cut section in equilibrium, there must be an internal vertical force V at the cut. Because this internal force acts normal to the beam axis and therefore along the beam's cross-sectional area, it is called a *shear force*. The shear's magnitude is the sum of the vertical components of all the external forces acting on this cut section, and it is in the opposite direction to balance the external forces.

If we look at two adjacent sections, the shear on their shared face is defined as in Figure 7.3. The shear on this face should clearly have the same magnitude no matter which way we choose to look at it; the positive direction of the shear depends on the face. If we are looking at a face that has its outward normal pointing in the positive horizontal direction, a positive shear force acts in the positive vertical direction. On a face with its normal

---

* The *centroid* of an area is defined as its geometric center. Imagine cutting the shape of the cross section out of cardboard; the centroid would be the center of mass of the cutout.
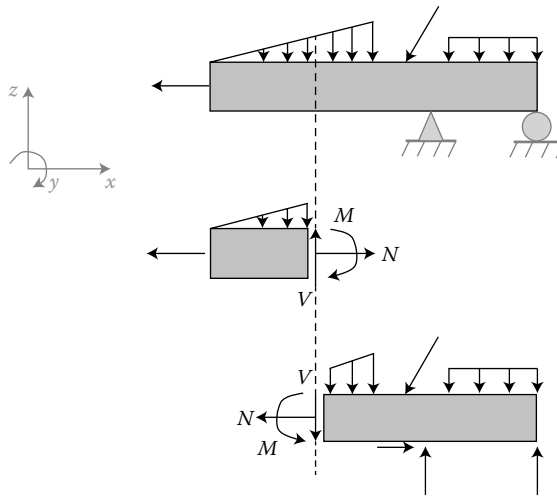
FIGURE 7.3
Application of method of sections.
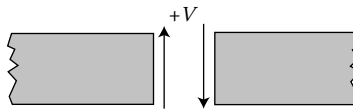
FIGURE 7.4
Definition of positive shear.

pointing in the negative horizontal direction, the corresponding shear—still positive—acts in the negative vertical direction. Looking ahead, this will ensure that the shear stress that this shear force causes matches the sign convention we learned in Chapter 4. Thus, for the typical right-handed coordinate system we will use for beams, shown in Figure 7.3, positive shear involves upward V on the left-hand segment of a cut beam, and downward V on the adjacent right-hand segment, as shown in Figure 7.4. So in addition to specifying the direction of V, it will be important to make sure we have associated it with a particular side of a cut.

7.2.3 Bending Moment in Beams

We have two internal forces, an axial force N and a shear force V, to assist us in satisfying equilibrium equations for a beam. In general, we will have axes defined with x directed along the axis of the beam (positive to the right), z directed vertically (positive upward), and y directed parallel to the beam's cross-sectional surfaces (positive into the page). Clearly, N and V will help out with $\sum F_x = 0$ and $\sum F_z = 0$. The remaining equilibrium equation for a planar problem is $\sum M_y = 0$, and we will generally need an internal resisting moment to help us meet this requirement, to balance the moment caused by external loads. This internal moment is developed within the cross-sectional area of the cut, in a direction opposite to the resultant external moment. The magnitude of the internal resisting moment, it should be apparent, equals the external moment. These moments tend to bend a beam in the plane of the loads, and are hence called *bending moments*.

In the method of sections, this external moment can be defined as the sum of the moments of all the external forces and external moments acting on one side of the cutting
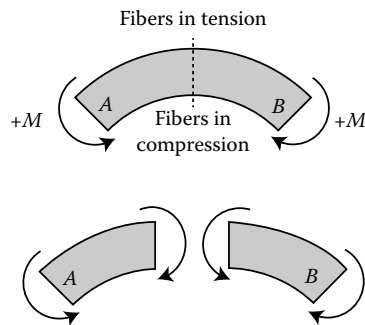
FIGURE 7.5
Definition of positive bending moment.

plane. The sign of the balancing internal moment at the cut follows our consistent convention: on a face that has its outward normal pointing in the positive horizontal direction, a positive internal moment acts in the positive direction determined by the right-hand rule. Of course on the opposite side of the cut, this postive internal moment acts in the opposite direction, as required by equilibrium and sign convention consistency. With our coordinate system, this means that *the bending moment in a beam is positive when the bottom fibers are in compression and the top fibers are in tension. The bending moment is negative when the bottom fibers are in tension and the top fibers are in compression*. An illustration of this convention is shown in Figure 7.5.

7.3 Shear and Bending Moment Diagrams

Now that we have sign conventions for the internal forces and moments in a beam, we have the ability to represent the varying values of internal forces and bending moment throughout the length of the beam. We do this by means of separate diagrams for each quantity. These diagrams are called *axial force, shear*, and *bending moment diagrams*. We will rarely use axial force diagrams since most of the beams we will investigate (and most beams in practice) are loaded by forces acting perpendicular to the beam axis, and for these cases there are no axial forces at any section. Again, any stresses due to axial forces, when they are present, can be calculated just as in Chapter 2.

These diagrams can be quick sketches, typically made just below the FBD of the beam. From a quick glance at such a diagram, a designer can ascertain the type of performance that will be required of a beam at every section.

We will first construct these diagrams by inspection of the FBD; then, we will use integration to evaluate more complex cases. See Section 7.7 for examples implementing the protocols described here for constructing shear and bending moment diagrams.

7.3.1 Rules and Regulations for Shear Diagrams

Protocol:

1. Sketch FBD of beam.

2. Find reactions.

3. Draw V diagram directly below load diagram (FBD).

4. By solving $\sum F_z = 0$ on each section of the beam, find and plot V. The sections should be evaluated with cuts between (not at) points of application of concentrated loads and reactions.

5. Locate point(s) of zero shear.

Fun facts:

- For any part of the beam where there are no external loads, the shear diagram will be a straight horizontal line.
- At the point of application of a concentrated load, there will be a sudden change in the shear. This is why we do not want to make a cut right at the point of application of a load.
- Where there is a uniformly distributed load, the shear diagram will be a straight line with the slope equal to the load intensity.
- For a simply supported beam subjected to vertical loads, the absolute values of the positive and negative areas contained by the shear diagram are equal.

7.3.2 Rules and Regulations for Moment Diagrams

Protocol:

1. Draw M diagram directly below shear diagram.

2. Either (a) calculate areas under the shear diagram between key points,* then calculate moments by adding shear areas beginning at the left end of the beam; or (b) use FBDs of sections beginning at the left end of the beam to compute moment expressions between key points.

3. Plot moment values.

Fun facts:

- For a simply supported, single span beam, bending moment at both ends is equal to zero.
- For a cantilever beam acted on only by vertical downward loads, bending moment is zero at the free end and maximum at the fixed end. (Shear is also maximum at the fixed end.)
- Local maximum bending moment(s) occur at point(s) of zero shear, or where V goes through zero.

---

* Key points: points of application of concentrated loads and reactions; points of zero shear and where the V diagram goes through zero; and the endpoints of all distributed loads.

7.4 Integration Methods for Shear and Bending Moment

To develop a more elegant method for calculating the shear forces and moments (V and M) within a beam, we will derive a few differential relations. To do this, we will imagine using the method of sections on an infinitesimally small section of the beam, say one with length dx. To keep things as general as possible, we will say that this beam is acted on by a distributed force with intensity $q(x)$. q has units of force per unit length and a positive q is defined as a load in the positive z-direction. An FBD of such a segment is shown in Figure 7.6.

The changes in shear and moment from the left face of element dx to the right are denoted by dV and dM, respectively.* Our next step is to write the equations of equilibrium for this element:

$$\sum F_z = -V + q \, dx + (V + dV) = 0, \tag{7.1}$$

which simplifies to

$$\frac{dV}{dx} = -q. \tag{7.2}$$

We also sum the moments about the center of the right face of our element, with clockwise moments positive:

$$(M + dM) - V \, dx - M + (q \, dx)(dx/2) = 0, \tag{7.3}$$

which gives us

$$\frac{dM}{dx} = V - \frac{q \, dx}{2}. \tag{7.4}$$
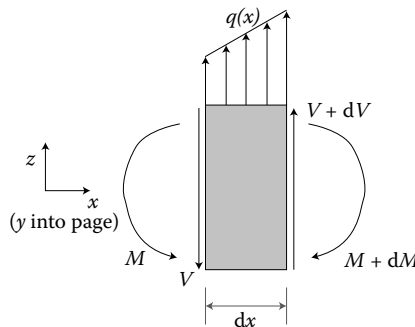
FIGURE 7.6
Differential element.

---

* We do not need to consider any variation of $q(x)$ within dx, because in the limit as $dx \to 0$, the change in q becomes negligibly small. This is not an approximation.

If we take the limit as $dx \to 0$, we see that we have two equations:

$$\frac{dV}{dx} = -q,$$
$$\frac{dM}{dx} = V. \tag{7.5}$$

And furthermore, by substituting $dM/dx = V$ into $dV/dx = -q$, we obtain

$$\frac{d^2M}{dx^2} = -q. \tag{7.6}$$

Equations 7.5 and 7.6 are very useful in the construction of shear and moment diagrams, as we will see.

Integrating the above equation for dV/dx, we obtain an expression for shear at any x:

$$V = -\int q \, dx + C_1. \tag{7.7}$$

From this integral, we can see that the shear at any section is simply a sum (i.e., an integral) of the vertical forces along the beam from the left end of the beam *to the section of interest*, plus a constant of integration C_1. This constant is equal to the shear on the left-hand end of the beam (at $x = 0$). So, between any two sections of a beam, the shear V changes by the amount of vertical force included *between* these two sections. If no force occurs between any two sections, there is no change in the shear (i.e., the shear diagram is a horizontal line). If a concentrated force occurs, a discontinuity or jump in the value of V occurs at the point of application. The *slope* of the shear diagram comes from the load intensity q. If, for example, the applied distributed load is downward (negative) and uniformly distributed ($q = q_0 = $ constant), then the slope of $V(x)$ is positive and also constant. For nonuniform distributed loads, the slope of the shear diagram is determined from the trend of q. Similarly, for a V diagram with positive slope, the corresponding M diagram is concave up, and for $V(x)$ with negative slope, $M(x)$ is concave down (note we are talking about the M diagram here, not the shape of the beam itself). This follows nicely from the differential relations we have just derived: if V goes as $+x$, M goes as $+x^2$; and if V goes as $-x$, M goes as $-x^2$.

Once again, to determine a shear diagram in this way, we must first find the reactions. Then we can start summing vertical forces to calculate the shear at any point. Integrating the dM/dx equation, we obtain a relation for bending moment at any x:

$$M = \int V \, dx + C_2, \tag{7.8}$$

where, again, C_2 is a constant of integration, determined from boundary conditions at $x = 0$. If the ends of the beam are on rollers, pins, or free, the moments at these ends are zero. If an end of the beam is fixed, the moment at this end is known from the reactions. For such cantilever beams, zero moment is felt at the free end.

The term $V \, dx$ represents the area beneath the V diagram over a length dx. The sum of these areas over a length x, according to the above equation, will give us the bending moment $M(x)$. By proceeding from the leftmost ($x = 0$) end of a given beam to the right, we can construct a moment diagram.

7.5 Normal Stresses in Beams and Geometric Properties of Sections

We know now that a system of internal forces may occur in a beam subject to external loads. We have already considered the stresses due to internal axial forces such as N. Now, we want to develop a way to talk about the stresses due to the shear force V and bending moment M. For simplicity, we will begin our discussion of these stresses by focusing on beams with symmetric (left to right) cross sections, and we will first consider a load state known as *pure bending* or *flexure*. In pure bending, only bending moments, not shear forces, are applied to the beam.

We will use a similar approach to the one we used to consider the effects of torsion. First, we make a plausible assumption about the deformation to ensure that we will be able to deal with the problem analytically. Figure 7.7 should help you visualize this assumption for pure bending. In Figure 7.7a, a horizontal beam with a vertical axis of symmetry is shown. The horizontal line parallel to the x-coordinate axis through the cross section centroid will be called the *axis* of the beam. If we look at a segment of this beam when it is subjected to a bending moment, as in Figure 7.7b, the beam bends in the plane of symmetry. Although the planes initially perpendicular to the beam axis slightly tilt, the lines defining their boundaries remain straight. That is, *plane sections through a beam taken normal to its axis remain plane after the beam is subjected to bending.*[*]

This assumption is completely valid for elastic, rectangular elements in pure bending. If shears are also introduced, there are some small corrections to the theory. But, in practice, this theory and assumption are remarkably robust and capable of supporting the stress analysis of all beams even with shear present.

Looking again at Figure 7.7b, we see that the beam axis has deformed into a portion of a circle of radius ρ. For an element (shaded) defined by an infinitesimal segment $d\theta$, the
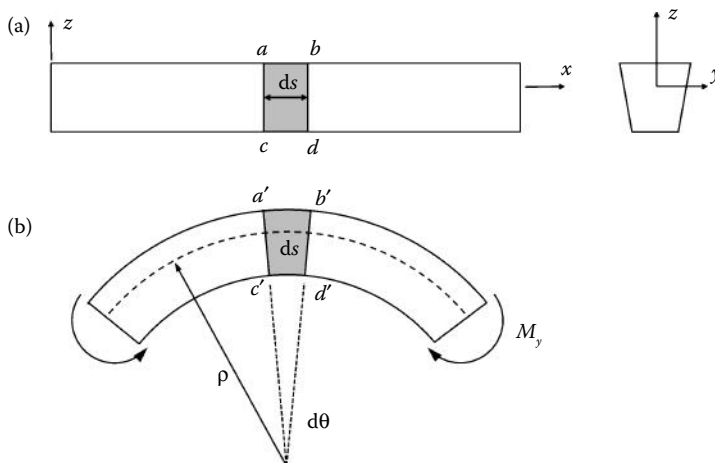
FIGURE 7.7
Behavior of elastic beam (a) in bending (b).

---

[*] In the immediate vicinity of the applied load, the behavior is somewhat more complex; we make use of Saint-Venant's principle to apply the assumption to the whole beam. Incidentally, this "plane sections remain plane" hypothesis for bending was first made (with some mistakes) by influential Swiss mathematician Jacob Bernoulli (1645–1705), whose nephew Daniel was renowned for his work in fluid mechanics.
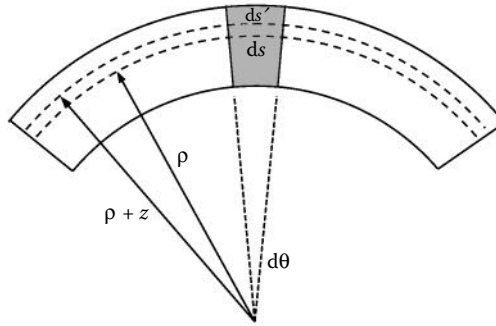
FIGURE 7.8
Nomenclature for deformation of beam in bending.

length ds of the beam axis (an arclength on this circle with radius ρ containing angle dθ) is given by ds = ρ dθ. Rearranging,

$$\frac{d\theta}{ds} = \frac{1}{\rho} \equiv \kappa, \tag{7.9}$$

where the reciprocal of ρ is defined as the axis *curvature* κ. For pure bending of a prismatic beam, that is, a beam with a non-changing cross section along its length, both ρ and κ are constant. In the course of solving the bending problem, we hope to find a way of determining κ.

If we imagine another curve, parallel to the beam axis, at some radius ρ + z, we can find the arclength contained in our shaded segment. We will call this arclength ds', and ds' = (ρ + z)dθ, as shown in Figure 7.8. We write the difference between our two arclengths:

$$ds' - ds = (\rho + z)d\theta - \rho d\theta = z\,d\theta. \tag{7.10}$$

We then divide this difference by the first arclength ds, the initial length of the segment of interest. At some z position, called the *neutral axis*, the segment length does not change under pure bending. In Figure 7.7b, the horizontal lines above the neutral axis have been lengthened, and those below it have been compressed, but the neutral axis has not changed length. ds was in fact the length of all horizontal lines in the shaded segment before the bending moments were applied. Hence, dividing this new change in arclengths, ds' − ds, by the old one, ds, we should get an expression for *strain*. And, we do:

$$\varepsilon_{xx} = \frac{ds' - ds}{ds} = z\frac{d\theta}{ds} = \kappa z. \tag{7.11}$$

This is a normal strain, a measure of how much dimensions in the x-direction have changed under this bending moment. We see that it depends linearly on z.

By using Hooke's law, we obtain a relation for normal longitudinal stress in the beam:

$$\sigma_{xx} = E\varepsilon_{xx} = E\kappa z. \tag{7.12}$$

Note that due to the position of the origin of the z-axis in the beam at the neutral axis, z can have either positive or negative values. We will need to develop a way of determining the location of the origin. How can we find out where the neutral axis is?
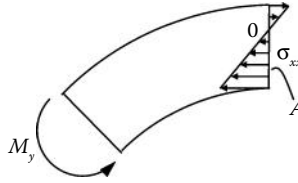
FIGURE 7.9
Internal stress distribution on a cut section of a beam in equilibrium.

To answer this question, we turn to the equations of equilibrium using the free body diagram in Figure 7.9, which shows the linearly varying stress on cut area A. In pure bending, the sum of all forces at a section in the x-direction must vanish, so

$$\sum F_x = 0 \quad \longrightarrow \quad \int_A \sigma_{xx} \, dA = 0, \tag{7.13}$$

where the integration over A represents summation over the entire cross-sectional area A of the beam. Using Hooke's law, we can rewrite this integral as

$$\int_A E \kappa z \, dA = E \kappa \int_A z \, dA = 0. \tag{7.14}$$

Since E and κ are constant, we have taken them outside the integral. By definition, the remaining integral $\int z \, dA = z_c A$, where z_c is the distance from the origin to the centroid of the area. Since the integral must equal zero, this distance z_c must equal zero, and hence the origin must coincide with the centroid. That is, the x-axis must pass through the centroid of the cross section, and this is the location of the neutral axis. A modification of this idea gives us a way to find the centroid. If we set up a temporary set of coordinate axes with a known origin location, we can call z_c the distance from the temporary origin to the centroid of the area and solve for it as

$$z_c = \frac{\int z \, dA}{\int dA} = \frac{\sum z \, dA}{\sum dA}. \tag{7.15}$$

The summation expressions are simpler to use when the cross-sectional geometry can be broken up into simple shapes (see Examples 7.3 and 7.4).

Returning to Equation 7.12, we now see that along the x-axis (where z is zero) both normal strain ε_{xx} and normal stress σ_{xx} equal zero. In bending theory, the name neutral axis indicates that at the level of this axis there is neither tension nor compression.

To finish up our solution of the bending problem, we use the second available equation of equilibrium. The sum of the externally applied and the internal resisting moments on

a section of the beam as shown in Figure 7.9 must vanish, so, using the convention of clockwise moments being positive:[*]

$$\sum M_0 = 0 \quad \longrightarrow \quad \int_A \underbrace{z}_{\text{arm}} \underbrace{\mathrm{d}F}_{\text{force}} - M_y = 0,$$

$$M_y = \int_A \underbrace{z}_{\text{arm}} \underbrace{\sigma_{xx} \, \mathrm{d}A}_{\text{force}} = \int_A z(E\kappa z)\mathrm{d}A. \tag{7.16}$$

Recognizing that E and κ (in this case of pure bending) are constants, we can write

$$M_y = E\kappa \int_A z^2 \, \mathrm{d}A, \tag{7.17}$$

and we now define the *second moment of area* (often and erroneously called the *moment of inertia*[†]) defined with respect to the cross section's neutral (centroidal), or y-axis:

$$I_y = \int_A z^2 \, \mathrm{d}A. \tag{7.18}$$

This is similar to the polar second moment of area that we saw in Section 5.1. There, each bit of area was multiplied by the square of its radial distance from the x-axis. Here, each bit of area is multiplied by the square of its distance from the horizontal y-axis. As with calculation of the centroid location, the integral may be replaced by a summation if the cross section is composed of simple shapes for which I_y has already been calculated. In Appendix A, the second moments of area for shapes are given with respect to their own centroids. As we need the second moment of area of each simple shape *with respect to the centroid of the whole cross section*, we must include a shift term for each area contribution. Thus, the summation form of the second moment is

$$I_y = \sum \left(I_{y_{\text{centroid}}} + Ad^2 \right), \tag{7.19}$$

where $I_{y_{\text{centroid}}}$ is the second moment of area of a shape that is part of the whole cross section, A is the area of that part, and d is the distance from the centroid of the part to the centroid of the whole cross section[‡] (see Examples 7.3 and 7.4).

---

[*] Note that there are two different notions of positive and negative moments and forces at work here. When we are writing equilibrium expressions, all of the forces or moments in one direction must be given the same sign. In this kind of calculation, we are either writing equilibrium equations for an entire beam, or we are writing them for a cut section where the formerly internal forces have been shown explicitly. Thus, in this case everything (for now) is treated as an external force. This is different than when we are considering the method of sections itself, and drawing the forces and moments on a cut internal section. Then, on one side of the cut the forces and moments will be equal and opposite to the other side of the cut (so they cancel when the beam is put back together, as they should because there is no real external force there) but they will both be positive, as defined in Section 7.2.

[†] In fact, this is analogous to the moment of inertia that you may know from dynamics. There, each bit of a body's mass is multiplied by its distance to an axis, squared, and contributions are integrated over the entire body. Here, each bit of area of the cross section is multiplied by its distance to the neutral axis, squared, and contributions are integrated over the entire area. But moment of inertia is not a correct term in this context.

[‡] This may look familiar as it is analogous to the parallel axis theorem for moment of inertia from dynamics.

Beams are commonly composed of multiple simple shapes, either built up from several components or constructed from a single piece of material in a T- or I-shaped beam. Now that we have learned some beam theory, it may seem straightforward to recognize that the T- and I-shaped cross sections commonly used for beams improve upon a basic rectangular cross section in two important ways: (1) reducing weight and (2) increasing the cross section's second moment of area, in order to reduce the stress induced by a particular load, thus increasing the load the beam can withstand.*

If we replace the integral in Equation 7.17 by I_y, we have

$$\kappa = \frac{M_y}{E I_y}. \tag{7.20}$$

And when we substitute this expression for κ back into our equation for normal stress, we obtain the elastic *flexure formula* for pure bending of beams:

$$\sigma_{xx} = \frac{M_y}{I_y} z, \tag{7.21}$$

which, to demonstrate the dependence of normal stress on both x and z positions along and in the beam, we can also write as

$$\sigma_{xx}(x, z) = \frac{M_y(x)}{I_y} z. \tag{7.22}$$

Note that since z is negative at the bottom of the beam and positive at its top edge, under a positive bending moment the normal stress will be negative (reflecting compression) at the bottom of the beam and positive (reflecting tension) at the top. Often we omit the y subscripts in this equation as they are usually correctly implied.

Since we are interested in the limiting behavior of beams, it is valuable to have an expression for the maximum stress occuring anywhere in a beam. For beams with symmetric

---

* By this logic, it is only reasonable that we would find the canonical T- and I-profiles in early railroad rails, and the skeletons of Industrial Revolution-era ships.

  However, like many developments in science and engineering, the adoption of such beams did not follow a linearly logical path. The beam theory developed by Galileo, Mariotte, Coulomb, Navier, and St. Venant, although available, was apparently not utilized by the engineers who empirically developed the I-beam's shape.[†] Instead of being motivated by the equations we have ourselves admired, these engineers responded to manufacturing requirements and limitations, to the careful and systematic experiments they performed, and to their own intuition.

  Design choices are often driven by the available materials. Iron, the dominant structural material when the industrialized world began to need railroads, came in two flavors: cast iron, which resists compression beautifully but is very brittle; and higher purity wrought iron. Improvements in rolling mills made it possible to roll wrought iron into rails for the young British rail system. In 1830, American Robert Stevens visited England and intuitively refined the shape into a T-rail (or T-beam) for American railroads. The shape was also used for building: by the 1850s, New York manufacturer and builder Peter Cooper recognized the utility of the rolled T-shape for fire-resistant building construction. This was an improvement on the standard practice of rolling and heating, then welding flat bars into composite beams that tended to delaminate and fail.

  The T-beam was evolved into the I-beam through the experiments of British engineer William Fairbairn, who was hoping to improve upon the scientific art of ship-building. The empirically developed I-beam was then included in Rankine's[‡] 1868 textbook on ship construction.

[†] The appropriately intrigued reader is directed to Jewett, R. A. "Structural Antecedents of the I-Beam, 1800–1850," *Technology and Culture* **8**(3): 346–362. 1967.

[‡] Yes, *that* Rankine. William Rankine (1820–1872) was a Scottish civil engineer who also helped develop the science of thermodynamics.

cross sections, bent in the plane of symmetry, we designate z_{max} as c, and at a position x along the beam, we obtain

$$\sigma_{max}(x) = \frac{M(x)c}{I}. \tag{7.23}$$

The convention is to dispense with the sign in this expression, because the sense of the normal stresses can be determined by inspection of the beam in question, and with the subscripts. The maximum magnitude of stress in the beam overall is found by using the maximum value of $M(x)$.

Normal stress in the direction of the beam's long axis (here the x-axis) is the *only* stress resulting from pure bending.* The stress tensor's matrix representation at every point in the beam is therefore

$$\sigma = \begin{pmatrix} \sigma_{xx} & 0 & 0 \\ 0 & 0 & 0 \\ 0 & 0 & 0 \end{pmatrix}. \tag{7.24}$$

Remembering Poisson's ratio, we will have normal strains in the y- and z-directions: $\varepsilon_{yy} = \varepsilon_{zz} = -\nu\varepsilon_{xx}$, where ε_{xx} is given by σ_{xx}/E or $Mz/(EI)$.

7.6 Shear Stresses in Beams

We will now consider shear stresses in beams caused by transverse shear. (Remember, transverse here means normal to the beam's long axis.) We will also give some thought to the attachment of separate parts of a beam by bolts, gluing, or welding.

For problems of torsion and pure bending, we began by assuming a strain distribution across the cross section. (In both cases, this distribution followed from the assumption made about "plane sections remaining plane.") We cannot make any analogous assumption about the strain distribution due to shear force. However, we will be able to use the expressions for normal stress that we have developed in the previous section.

By examining the equilibrium of an infinitesimal beam element, we saw in Equation 7.5 that $dM = Vdx$, that is, the shear force V is linked with a *change* in bending moment. So, if a shear and a bending moment are present at one section of a beam, the adjoining section will have a different bending moment, even if the shear remains constant. This variation in moment establishes shear stresses on the conceptual parallel longitudinal planes of the beam. (As when we first defined shear stress in Section 2.2, we can imagine the beam to be composed of thin planes that are allowed to slide with respect to each other.) Even when we seem to be talking about isolated shear forces, we must remember that these forces are linked with a change in the bending moment along the beam's length.

The shear and moment diagrams in Figure 7.10 show this: bending moment varies over sections with constant shear, while in regions of no shear there is no change in the moment. Note that we mean variation in the x-direction.

The distribution of shear stress over the beam cross section, that is, variation in the z-direction, is much different than that of normal stress. The shear stress is zero at those points where the bending normal stress is a maximum. And, maximum shear stress very

---

* That is, the only stress relative to the x-, y-, and z-coordinates as we have defined them. The stress state on a different plane, as we well know, could look different.
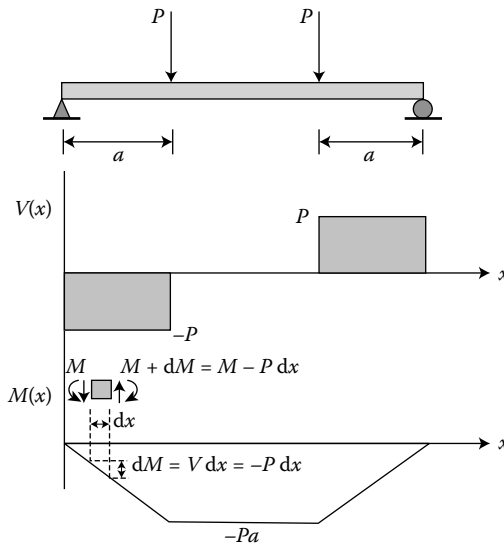
FIGURE 7.10
Shear and bending moment diagrams for the loading shown. (Adapted from Popov, E. P., *Engineering Mechanics of Solids*, Prentice Hall, 1998.)

often occurs at the neutral axis (where normal strain and stress due to bending are both zero). We will now derive an expression for shear stress that shows this. Alternatively, we could derive it using the theory of elasticity from Chapter 4. This is done as an exercise in Example 7.8.

Consider the beam as a long, slender body with rectangular cross section ($b \times h$) and length L, as shown in Figure 7.11. "Slender" beams are those for which b and h are both much less than L. The beam of interest is in plane stress in the y-direction, that is,

$$\sigma_{yy} = \sigma_{yx} = \sigma_{yz} = 0. \tag{7.25}$$

For the purpose of this derivation, consider that our beam is made by stacking five planks as shown in Figure 7.12. If the planks were not adhered to each other and this stack were bent, the planks would slide relative to each other—picture how the pages slide across each other when you bend a paperback book. But if the stack is to act as one built-up beam the planks should be attached, and so consider them to be glued together.
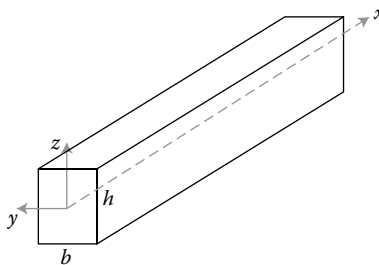
FIGURE 7.11
Rectangular beam.
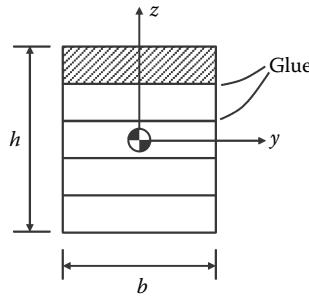
FIGURE 7.12
Cross section of rectangular beam built up by gluing five planks together.

Now when the beam is bent, the glue prevents sliding because it transmits shear force from one plank to the next. Our goal is to determine the shear stress in a layer of glue. The expression we derive will be useful for finding shear stress at any point in solid (not just built-up) beams with general (not just rectangular) symmetric cross sections.

In Figure 7.13, a section of the beam with length dx is isolated. For the general case of bending moment changing over this distance from M to $M + dM$, there is a corresponding change over x in the magnitude of the normal stress distribution (with its z variation, as given in Equation 7.22). Since we are interested in the shear stress in a layer of glue, we use the method of sections to expose a layer by isolating a plank. In Figure 7.14a, the cross section of the plank to be isolated is labeled A', and this same area is indicated on each end of the plank section in Figure 7.14b. The plank is isolated in Figure 7.14c with its free body diagram in Figure 7.14d. Forces F_1 and F_2 are the resultants of the stress distributions on the plank shown in Figure 7.14c, and F_{shear} is the unknown shear force in the glue. Note that it is pointing in the negative x-direction on a face with its normal in the negative z-direction, so by our sign convention the corresponding stress would be positive. This section of the plank must be in equilibrium, so

$$\sum F_x = F_2 - F_1 - F_{\text{shear}} = 0. \tag{7.26}$$
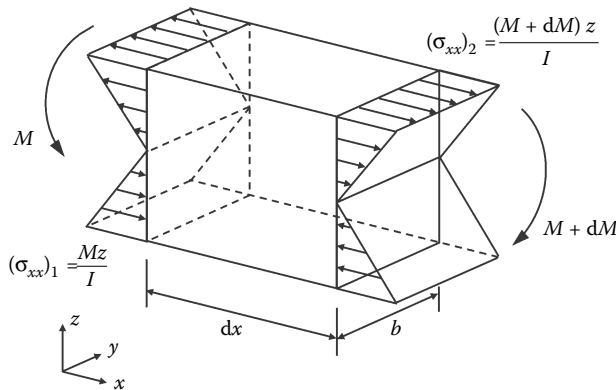
FIGURE 7.13
Normal stress on a section of a bent beam with rectangular cross section. (Adapted from Popov, E. P., *Engineering Mechanics of Solids*, Prentice Hall, 1998.)
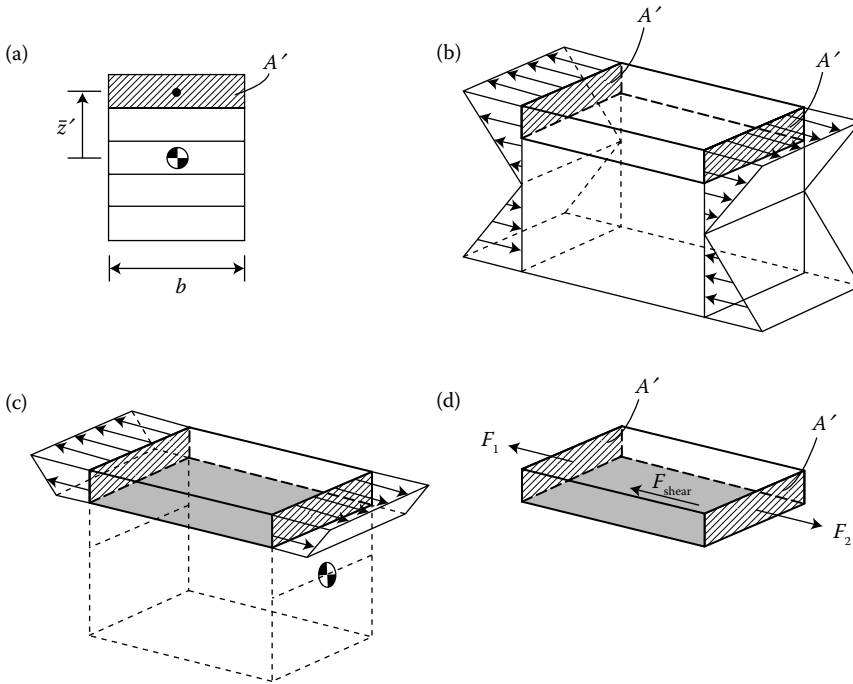
FIGURE 7.14
Elements used in derivation of shear stress in a beam: (a) cross section of plank; (b) stress distribution shown on whole cross section; (c) stress distribution on isolated subsection A' of the cross section; (d) free body diagram of isolated subsection. (Adapted from Popov, E. P., *Engineering Mechanics of Solids*, Prentice Hall, 1998.)

Then

$$
F_{\text{shear}} = F_2 - F_1 = \int_{A'} (\sigma_{xx})_2 \, \mathrm{d}A - \int_{A'} (\sigma_{xx})_1 \, \mathrm{d}A
$$

$$
= \int_{A'} \frac{(M + \mathrm{d}M)z}{I} \, \mathrm{d}A - \int_{A'} \frac{Mz}{I} \mathrm{d}A = \frac{\mathrm{d}M}{I} \int_{A'} z \, \mathrm{d}A.
$$

(7.27)

This indicates that the magnitude of the shear force is proportional to the change in bending moment and also to an integral that is nearly familiar. We have seen the second moment of area, and this integral, now with z and not z^2, is sensibly called the *first moment of area* of area A'. Note that it is not the first moment of area of the whole cross section, just the area A' on one side of the glue layer. Further note that z is still measured from the centroid, even though that point is not within A'. The letter Q is often used to designate first moments of area, so in this case we define

$$
Q' = \int_{A'} z \, \mathrm{d}A,
$$

(7.28)

as the first moment of area of the portion of the cross section that would tend to slide relative to the plane of the glue. As with the integrals in the previous section, this may

be replaced by a sum for an A' composed of simple shapes. Replacing this term in Equation 7.27,

$$F_{\text{shear}} = \frac{\mathrm{d}M}{I}Q'. \tag{7.29}$$

Then the average shear stress is this shear force divided by the area on which it acts:

$$\sigma_{zx} = \sigma_{xz} = \frac{F_{\text{shear}}}{b\,\mathrm{d}x} = \frac{\mathrm{d}M}{\mathrm{d}x}\frac{Q'}{Ib} = \frac{VQ'}{Ib}, \tag{7.30}$$

where we have made use of $V = \mathrm{d}M/\mathrm{d}x$, and b is the width of the layer of glue (or the width of contact where this shear force prevents sliding) as shown in Figure 7.13. This, like the classical bending stress equation, is a well-known and important result. We have derived it by considering an x-directed force on a plane with a z-pointing normal (σ_{zx}), but the symmetry of the stress tensor tells us that this must also be the stress at points on our cut x face due to shearing forces in the z-direction (σ_{xz}).

To emphasize the dependence of this stress on the x- and z-position within the beam, we can explicitly write

$$\sigma_{xz}(x, z) = \frac{V(x)Q'(z)}{Ib(z)}. \tag{7.31}$$

We know well that the shearing force V varies with x, and we have seen that Q', the first moment of area for area A' about the centroidal axis of the original cross section, depends on the level z of the section of interest (the location of the glue). The width b of the beam is constant with z in this case of a rectangular cross section, but in general it need not be. This result is applicable for general cross sections. It is certainly applicable in beams that are solid, as well. The glue we considered was helpful for visualization, but if the beam had a solid rectangular section then we would have found the shear stress in the solid at that same level z. It may be helpful when determining the shear stress in a point in a solid beam to imagine cutting it into two layers at the point of interest, gluing the layers back together, and finding the shear stress in the glue.

If we explicitly write the functional dependence of the shear stress on a rectangular cross section on z, as we will see in Example 7.8, we find that the shear stress is distributed quadratically (and symmetrically) through the thickness, achieving its maximum value at the beam centerline ($z = 0$) and being zero on both the top and bottom surfaces ($z = \pm h/2$). The latter point is consistent with the assumptions we have made about the loading of bent beams. Figure 7.15 allows us to compare the distributions of normal and shear stress along the height of the cross section.
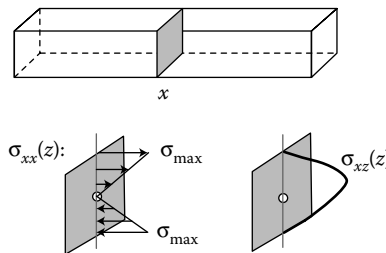
FIGURE 7.15
Stress distributions for rectangular cross section.

7.7 Examples

EXAMPLE 7.1

Find the reactions and determine the axial force P, the shear V, and the bending moment M caused by the applied loads at the specified sections. Also, draw FBDs indicating the sense (direction) of all forces and moments.
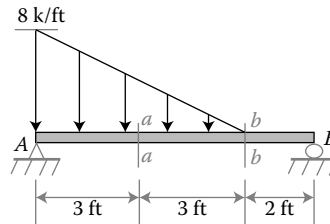
Given: Dimensions of and loading on beam.

Find: Internal forces and bending moment.

Assume: The only assumptions necessary are implicitly made throughout this textbook: Equilibrium, and Saint-Venant's principle.

Solution

Our strategy is to find the reactions at the supports from the whole beam's equilibrium, and then use the method of sections to find the internal forces and moments at the specified locations.

For the purpose of finding reaction forces, we can replace the distributed load by its equivalent concentrated load. The magnitude of this concentrated load is simply the area under the distributed load, in this case $W = \frac{1}{2}(8\,\text{k/ft})(6\,\text{ft}) = 24\,\text{kips}$. It acts at the centroid of the triangular area under the distributed load: one-third of the way from its maximum intensity, or 2 ft from the left end of the beam. We use this load in our free-body diagram:
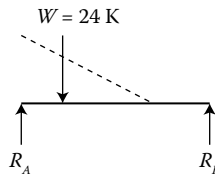
$$\circlearrowleft \qquad \sum M_B = 0 = -R_A(8\,\text{ft}) + (24\,\text{k})(6\,\text{ft}) \rightarrow R_A = 18\,\text{kips},$$

$$\circlearrowleft \qquad \sum M_A = 0 = -(24\,\text{k})(2\,\text{ft}) + R_B(8\,\text{ft}) \rightarrow R_B = 6\,\text{kips},$$

$$\sum F_z = 0 \ \text{is then used as a check:} \ R_A + R_B = 24\,\text{kips.} \ \checkmark$$

Next, we consider sections a–a and b–b. We make an imaginary cut at the specified location, and realize that considering the loading to the left, *or* to the right, of the a–a cut will yield equivalent results:

$$\tfrac{1}{2}(4\,\text{k/ft})(3\,\text{k}) = 6\,\text{k}$$

$R_A = 18\,\text{k}$
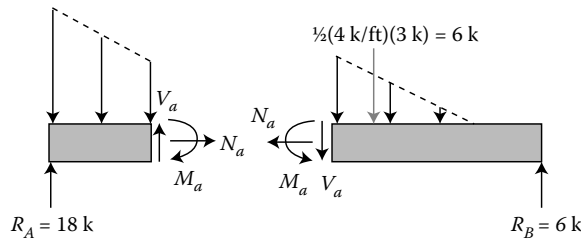
$R_B = 6\,\text{k}$

We choose the simpler side to calculate, in this case the portion of the beam to the right of a–a. We simply apply the equilibrium equations to this section of the beam:

$$\sum F_x = 0 = N_a,$$

$$\sum F_z = 0 = -V_a + R_B - 6\,\text{k} \;\rightarrow\; V_a = 0\,\text{kips},$$

$$\sum M_{\text{about}\,a} = 0 = M_a - (6\,\text{k})(1\,\text{ft}) + R_B\,(5\,\text{ft}) \;\rightarrow\; M_a = -24\,\text{ft-kips}.$$

Next comes the cut at b–b. It is clear that using the portion of the beam to the right of b–b will be easier, and so we construct an FBD and apply equilibrium:

N_b

$M_b \quad V_b$

$R_B = 6\,\text{k}$
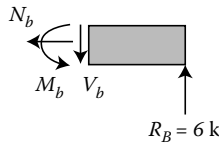
$$\sum F_x = 0 = P_b,$$

$$\sum F_z = 0 = -V_b + R_B \;\rightarrow\; V_b = 6\,\text{kips},$$

$$\sum M_{\text{about}\,b} = 0 = R_B\,(2\,\text{ft}) + M_b \;\rightarrow\; M_b = -12\,\text{ft-kips}.$$

Note: The negative signs on the moments at cuts a–a and b–b indicate that these moments are opposite from the way they are drawn in our FBDs. It is convenient to assume positive shear and bending moment when constructing FBDs, so that a negative sign will always represent negative shear or negative bending moment. Please refer to Figures 7.4 and 7.5 for a reminder of the sign convention for shear and bending moment.

EXAMPLE 7.2

Plot shear and moment diagrams for the beams shown:
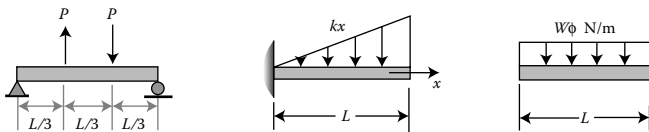
Given: Loading on three beams.

Find: Internal response to this loading.

Assume: The only assumptions necessary are implicitly made throughout: equilibrium, and Saint-Venant's principle.

Solution

In each case, we will first find the external reaction forces and/or moments, then use the method of sections at points of interest along the beam to construct the diagrams of $V(x)$ and $M(x)$.

Starting with the first beam, to find reactions, we need an FBD of the whole beam:
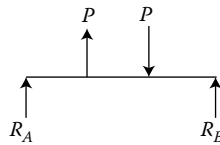
$$\circlearrowleft \qquad \sum M_A = 0 = \frac{PL}{3} - \frac{2PL}{3} + R_B L \quad \rightarrow \quad R_B = \frac{P}{3} \text{ (up)},$$

$$\circlearrowleft \qquad \sum M_B = 0 = \frac{PL}{3} - \frac{2PL}{3} - R_A L \quad \rightarrow \quad R_A = -\frac{P}{3} \text{ (down)}.$$

To construct V diagram, look only at the points where the loading conditions change.

- At the left-hand end of the beam, V must balance R_A, so $V = P/3$.
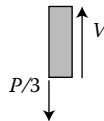
- At the right-hand end, V must balance R_B, so $V = P/3$.
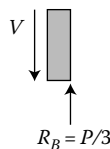
- Just to the right of the upward applied load P, $V = -2P/3$.

To construct *M* diagram:

- $M = 0$ at simply supported ends
- $M = 0$ at center by symmetry
- At upward P, $M = \frac{P}{3}\left(\frac{L}{3}\right) = \frac{PL}{9}$
- At downward P, $M = \frac{P}{3}\left(\frac{2L}{3}\right) - P\left(\frac{L}{3}\right) = -\frac{PL}{9}$

Plot the results.
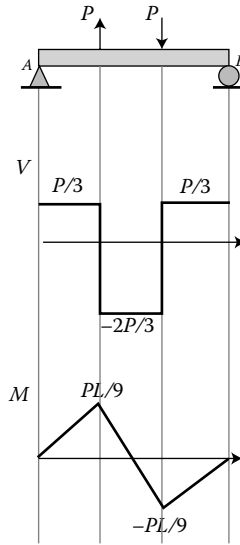
For the second beam, once again, we start with the external reactions, using the equivalent concentrated load in place of the distributed one:
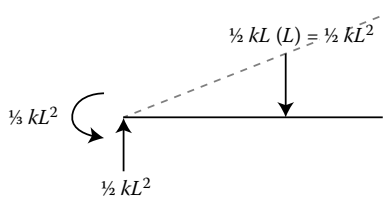
Since the distributed load is linearly distributed, the shear distribution is parabolic, and the moment distribution is cubic. We may proceed either by integrating the distributed load $q(x) = kx$ once for $V(x)$ and twice for $M(x)$, or by making our imaginary cut at some distance x from the end of the beam, and finding the internal shear and moment. Both methods will provide the same results.

Integration:

$$V(x) = -\int q\,dx = -\int -kx\,dx = \frac{1}{2}kx^2 + C_1,$$

$$V(0) = -\frac{1}{2}kL^2 = C_1,$$

$$V(x) = \frac{1}{2}kx^2 - \frac{1}{2}kL^2,$$

$$M(x) = \int V \, dx = \frac{1}{6}kx^3 - \frac{1}{2}kL^2 x + C_2,$$

$$M(0) = \frac{1}{3}kL^3 = C_2,$$

$$M(x) = \frac{1}{6}kx^3 - \frac{1}{2}kL^2 x + \frac{1}{3}kL^3.$$

Method of sections:
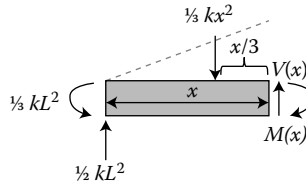
$$\sum F_z = 0 = \frac{1}{2}kL^2 - \frac{1}{2}kx^2 + V(x),$$

$$\text{so} \quad V(x) = \frac{1}{2}kx^2 - \frac{1}{2}kL^2,$$

$$\curvearrowleft \qquad \sum M_x = 0 = M(x) + \frac{1}{3}kL^3 - \frac{1}{2}kL^2 x + \frac{1}{2}kx^2 \left(\frac{x}{3}\right).$$

(We note that the internal shear $V(x)$ does not cause a moment about the cut at x.)

$$\text{so} \quad M(x) = \frac{1}{6}kx^3 - \frac{1}{2}kL^2 x + \frac{1}{3}kL^3.$$

The resulting shear and moment diagrams are as shown below. We can check our results by evaluating $V(x)$ and $M(x)$ at $x = L$. Both are zero there, as they must be at a free end.
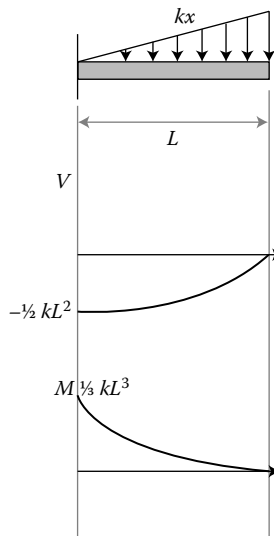
We now consider the third beam. The fixed support can offer both reaction forces and a moment, which are found using an FBD:
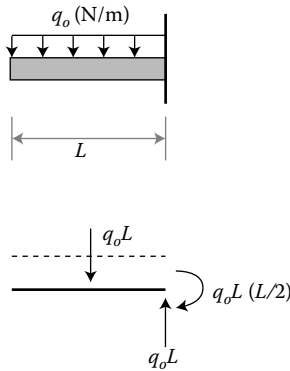
$$\sum F_z = 0 \;\rightarrow\; V(L) = q_0 L,$$

$$\sum M_0 = 0 \;\rightarrow\; M(L) = \frac{1}{2} q_0 L^2.$$

The shear V is zero at the free end of this cantilever beam, and must balance the upward reaction force $q_0 L$ at the fixed end. Since the distributed load is uniformly distributed, the shear distribution is linear.

The moment M is zero at the free end and must balance the reaction moment $q_0 L^2/2$ at the fixed end. Since the shear distribution is linear (proportional to x), the bending moment distribution is parabolic (proportional to x^2). The shear and moment diagrams are shown:
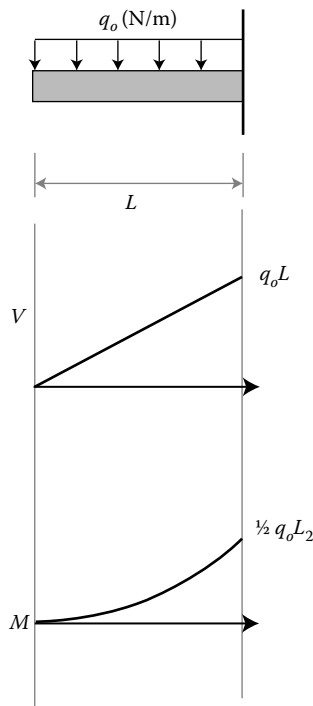
EXAMPLE 7.3

Find the centroid and the second moment of area about the horizontal (y) axis of the cross section shown. All dimensions are in millimeters. If a beam is constructed with the cross section shown from steel whose maximum allowable tensile stress is 400 MPa, what is the maximum bending moment that may be applied to the beam?
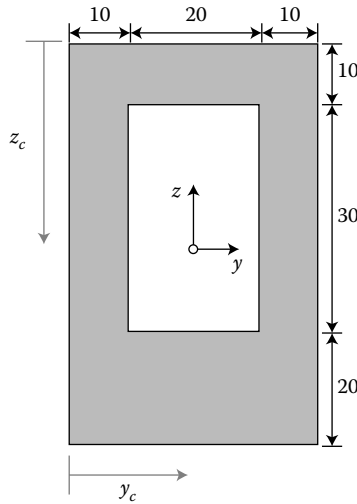
Given: Dimensions of beam cross section; limiting stress.

Find: Location of centroid; maximum applied moment.

Assume: Hooke's law applies.

Solution

The symmetry of the cross section shown suggests that the horizontal coordinate of the centroid will be on the vertical centerline, as sketched. y_c is then 20 cm. We need only locate the vertical location of the centroid (z_c). Several strategies are available to us. We recognize that the cross section is a large rectangle, with an inner rectangular hole. It will thus be possible for us to find the area and second moment of area of the large outer rectangle, and simply subtract off the properties of the inner rectangle.

Recall that $z_c = \int z \, dA / \int dA = \sum z \, dA / \sum dA$, where z and z_c are measured from an arbitrarily chosen reference datum, in this case the top of the cross section. For clarity, results are tabulated as follows:

	A (mm^2)	z (mm)	$A \cdot z$ (mm^3)	
Outer	$40 \times 60 = 2400$	30	72,000	Centroid:
Outer				$z_c = \dfrac{\sum Az}{\sum A} = 31.7\,\text{mm}$
Inner	$-20 \times 30 = -600$	25	$-15,000$	from top (or 28.3 mm from bottom)
Inner				
$\sum$	1800		57,000	

With the location of the centroid known, we can find the second moment of area with respect to that location, starting with the second moment of area of a rectangle about its own centroid from Appendix A.

	$I_{\text{rectangle}} = bh^3/12$ (mm^4)	d (mm)	$A \cdot d^2$ (mm^4)	
Outer	720,000	$31.7 - 30 = 1.7$	6940	Second moment of area:
Outer				$I = \sum \left(\dfrac{bh^3}{12} + Ad^2 \right)$
Inner	$-45,000$	$31.7 - 25 = 6.7$	$-26,940$	$= 655,000\,\text{mm}^4$
Inner				
$\sum$	675,000		$-20,000$	

If the maximum allowable normal stress is 400 MPa, we can find the maximum moment that can be applied using the relationship:

$$\sigma_{\max} = \frac{Mc}{I}.$$

We have found the second moment of area I, and c is the maximum distance from the centroid attainable on the cross section, in this case 31.7 mm. Solving for M:

$$M = \frac{\sigma_{\max} I}{c} = \frac{(400\,\text{N/mm}^2)(655{,}000\,\text{mm}^4)}{31.7\,\text{mm}} = 8.26\,\text{kN\,m}$$

EXAMPLE 7.4

A steel T-beam is used in an inverted position to span 400 mm. If, due to the application of the three forces as shown in the figure, the longitudinal strain gage at A (3 mm down from top of beam and at the x location shown) registers a compressive strain of -50×10^{-5}, how large are the applied forces?
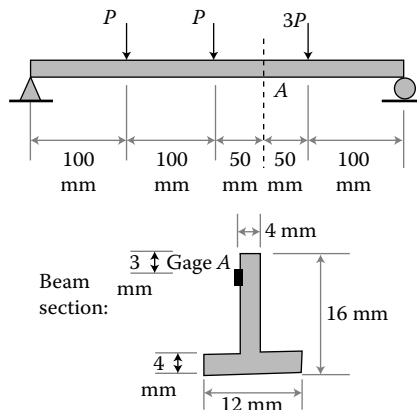
Given: Dimensions of and strain in T beam.

Find: Magnitude of applied force P.

Assume: Hooke's law applies.

Solution

The gage at A, in the upper portion of the cross section, registers a negative strain. This tells us that the bending moment in the beam at A is negative. Using Hooke's law, we will be able to relate this measured strain to a normal stress in the beam at this point, which we can then relate to the local bending moment. To do these calculations, we will need to know the location of the centroid and the second moment of area of the inverted T cross section.

As in Example 7.3, the centroid is clearly on the vertical line of symmetry. We need z_c, which we will calculate relative to the top of the section:
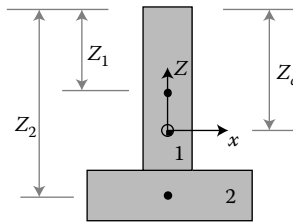
	A (mm^2)	z (mm)	$A \cdot z$ (mm^3)
1	$4 \times 12 = 48$	6	288
2	$12 \times 4 = 48$	14	672
$\sum$	96		960

Hence, $z_c = \sum z A / \sum A = 10$ mm from the top, or 6 mm from bottom. Next comes the second moment of area I:

	$bh^{3}/12$ (mm^4)	d (mm)	Ad^2 (mm^4)
1	576	4	768
2	64	4	768
$\sum$	640		1536

$$I = \sum \left(\frac{bh^3}{12} + Ad^2 \right) = 2176 \, \text{mm}^4.$$

We are now ready to apply Hooke's law and find the stress corresponding to the strain measured at A. The beam is steel, so its Young's modulus is $E = 200$ GPa. In addition,

$$\sigma_{xx_A} = E \varepsilon_{xx_A} = (200 \times 10^9 \, \text{Pa})(-50 \times 10^{-5}) = -10^8 \, \text{Pa}.$$

This is measured at $z_A = 3$ mm from the top of the T, or 7 mm from the neutral axis.

Next, we relate this stress to the internal bending moment at A:

$$\sigma_{xx_A} = \frac{M_A z_A}{I},$$

$$-10^8 \, \text{Pa} = \frac{M_A(0.007 \, \text{m})}{2.176 \times 10^{-9} \, \text{m}^4},$$

$$\text{so} \quad M_A = \frac{(-10^8 \, \text{Pa})(2.176 \times 10^{-9} \, \text{m}^4)}{0.007 \, \text{m}} = -31.1 \, \text{N m}.$$

We then consider the loading on the beam to relate this local bending moment to the applied loads P. To do this, we must construct an FBD:
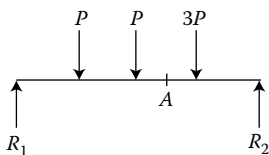
Equilibrium requires that $\sum F_z = 0$, or $R_1 + R_2 = 5P$, and if we also impose $\sum M_1 = 0$ we will have $0.1P + 0.2P + 0.3(3P) - 0.4R_2 = 0$, and solving these two equations we have $R_1 = 2P$ and $R_2 = 3P$. We can then use the method of sections, cutting the beam and ensuring equilibrium of the right half, to find the bending moment at A:
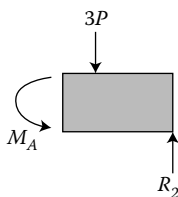
$$\curvearrowleft \qquad \sum M_A = 0 = M_A - 3P \cdot (0.05 \, \text{m}) + 3P \cdot (0.150 \, \text{m}),$$

$$M_{\text{about } A} = -0.450P + 0.150P = -0.3P.$$

So, knowing that $M_A = -31.1 \, \text{N m}$ and that $M_A = -0.3P$, we find that

$$P = \frac{-31.1 \, \text{N m}}{-0.3 \, \text{m}} = 104 \, \text{N}.$$

EXAMPLE 7.5

An I-beam is made by gluing five wood planks together, as shown. At a given axial position, the beam is subjected to a shear force $V = 6000 \, \text{lb}$. (a) What is the average shear

stress at the neutral axis $z = 0$? (b) What are the magnitudes of the average shear stresses acting on each glued joint?
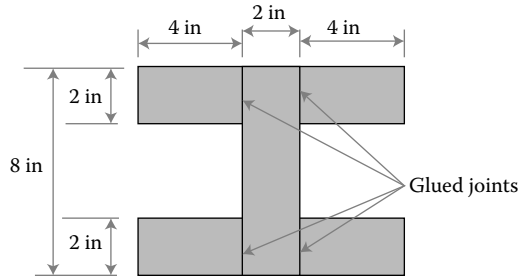
Given: Cross section, local loading.

Find: Average shear stresses.

Assume: Hooke's law applies.

Solution

We obtained a formula for shear stress at a given height, $\sigma_{xz} = VQ'/Ib$, where Q' and b depend on the z position in question. I in this relationship is always the second moment of area of the entire cross section about the z-axis. We have been given V. So, we must calculate I once and then calculate the appropriate values of Q' and b for both parts of this problem.

By inspection of the cross section's symmetry, we see that the centroid is at the geometric center of the I-beam. For the central vertical segment, therefore d, the distance between the centroid of the segment and the centroid of the entire cross section, is zero. The four remaining segments will each have the same second moment of area about their own horizontal bisectors, and the same areas and distances d. Thus, we can write

$$I = I_{\text{vertical}} + 4I_{\text{smaller}} = \left(\frac{1}{12}bh^3\right)_{\text{vertical}} + 4\left[\frac{1}{12}bh^3 + Ad^2\right]_{\text{smaller}},$$

$$I = \frac{1}{12}(2\,\text{in})(8\,\text{in})^3 + 4\left[\frac{1}{12}(4\,\text{in})(2\,\text{in})^3 + (2\,\text{in} \times 4\,\text{in})(3\,\text{in})^2\right] = 384\,\text{in}^4.$$
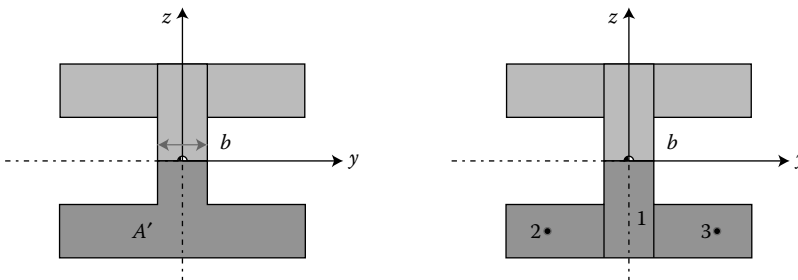
We can calculate Q' at the neutral axis by finding the centroid and area of the shaded area on the left, or by summing the contributions due to the individual planks, as shown at right. The values of z for planks 2 and 3 are the same as their d values used in the I calculation.

$$Q' = \int_{A'} z\,dA = \sum z'A'$$

$$= (2)(2 \cdot 4) + 3(4 \cdot 2) + 3(4 \cdot 2) = 64\,\text{in}^3.$$

So, the average shear stress at the neutral axis is $\sigma_{xz} = VQ'/Ib = (6000\,\text{lb})(64\,\text{in}^3)/$ $(384\,\text{in}^4)(2\,\text{in}) = 500\,\text{psi}$.

As an exercise, verify that each glued joint is subjected to the same average shear stress. We will determine only the average shear stress acting on the lower-right glued joint by using the area A and length of contact b as shown below. The value of Q' is $(3)(4 \cdot 2) = 24\,\text{in}^3$, and the average shear stress is $VQ'/Ib = 188\,\text{psi}$.
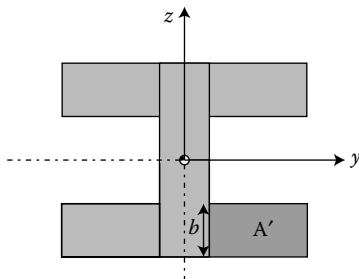
EXAMPLE 7.6

The beam shown is subjected to a distributed load. For the cross section at $x = 0.6\,\text{m}$, determine the average shear stress (a) at the neutral axis and (b) at $z = 0.02\,\text{m}$.
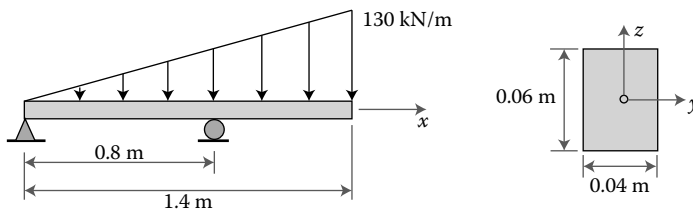
Given: Dimensions of and loading on simply supported beam.

Find: Shear stress at two locations along height of cross section at $x = 0.6\,\text{m}$.

Assume: Hooke's law applies.

Solution

First we need to consult our FBD and find the reactions at the supports.

$$\sum F_y = 0 \;\rightarrow\; R_A + R_B = 91\,\text{kN},$$

$$\sum M_B = 0 = R_A(0.8\,\text{m}) + 91\,\text{kN}(0.133\,\text{m}),$$

½ (130 kN/m)(1.4 m) = 91 kN

⅓ (1.4 m) = 0.467 m
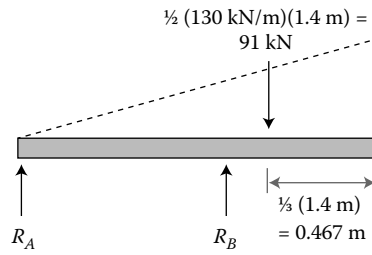
$$\rightarrow \quad R_A = -15.1 \, \text{kN (downward)},$$

$$\rightarrow \quad R_B = 106.1 \, \text{kN (upward)}.$$

We are interested in the cross section at $x = 0.6 \, \text{m}$. We know that the average shear stress depends on the internal shear force in the beam at the point of interest, so we need to calculate the shear $V(x = 0.6 \, \text{m})$. To do this, we will make an imaginary cut at $x = 0.6 \, \text{m}$:
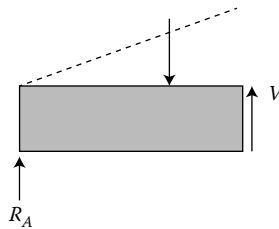
In this 0.6-m-long span, the distributed load has a maximum intensity of $\left(130 \, \frac{\text{kN}}{\text{m}}\right) \frac{0.6 \, \text{m}}{1.4 \, \text{m}} = 55.7 \, \frac{\text{kN}}{\text{m}}$, so the equivalent concentrated load acting on the 0.6-m-long segment is the area under this load: $\frac{1}{2} \left(55.7 \, \frac{\text{kN}}{\text{m}}\right) (0.6 \, \text{m}) = 16.7 \, \text{kN}$.

Equilibrium of our 0.6 m segment:

$$\sum F_y = 0 = V - R_A - 16.7 \, \text{kN},$$

$$\rightarrow \quad V = 16.7 \, \text{kN} + 15.1 \, \text{kN} = 31.8 \, \text{kN}.$$

The second moment of area for the cross section is

$$I = \frac{1}{12}bh^3 = \frac{1}{12}(0.04)(0.06)^3 = 7.2 \times 10^{-7} \, \text{m}^4.$$

At the height of the centroid or neutral axis, Q' is the first moment of area of the area above (or below) the centroid:

$$Q' = z'A' = 0.015(0.03 \times 0.04) = 1.8 \times 10^{-5} \, \text{m}^3.$$

Then the shear stress at the centroid is

$$\sigma_{xz} = \frac{VQ'}{Ib} = \frac{(31.8 \, \text{kN})(1.8 \times 10^{-5} \, \text{m}^3)}{(7.2 \times 10^{-7} \, \text{m}^4)(0.04 \, \text{m})} = 19.9 \, \text{MPa}.$$

At $z = 0.02$ m above the neutral axis

$$Q' = z'A' = 0.02(0.02 \times 0.04) = 1.0 \times 10^{-5}\,\text{m}^3.$$

This is the only change from the calculation at $z = 0$, and the shear stress at this point is 11.0 MPa.

EXAMPLE 7.7

For a thin elastic beam with rectangular cross section ($b \times h$) and loading that causes bending moment $M(x)$, derive Equation 7.22, the expression for the normal stress $\sigma_{xx}(x, z)$ in a beam, starting from the fact that, as we have shown, the normal stress varies linearly through the thickness.

Given: Rectangular beam in bending.

Find: Normal stress starting from an assumption of a linear distribution.

Assume: Hooke's law applies; no axial loading on the beam.

Solution

We begin with a general statement of the fact that the normal stress varies linearly through the thickness:

$$\sigma_{xx}(x, z) = f(x) \cdot z,$$

where $f(x)$ is an (as yet) unknown function of x. Then we can integrate this stress over the area of the cross section to find an expression for the axial resultant on the beam, which is zero:

$$\int_{-h/2}^{h/2} \sigma_{xx}(x, z) b\,dz = f(x) \cdot b \int_{-h/2}^{h/2} z\,dz = 0.$$

Now, let us take the moment (about the y-axis) of the axial normal stress acting on a thin strip of cross-sectional area $b\,dz$ at height z:

$$dM_y = (\sigma_{xx} b\,dz)z.$$

And if we sum this moment for all strips through the thickness, we obtain a positive internal moment, $M(x)$:

$$M(x) = \int_{-h/2}^{h/2} dM_y = \int_{-h/2}^{h/2} z(\sigma_{xx} b\,dz) = f(x) \int_{-h/2}^{h/2} z^2 b\,dz = f(x)I.$$

We recognize the integral as I, the second moment of area for the cross section about the centroid. Solving for $f(x)$, we obtain

$$f(x) = \frac{M(x)}{I}.$$

And we can now write the equation for the normal stress as we have in Equation 7.22:

$$\sigma_{xx}(x, z) = f(x) \cdot z = \frac{M(x)z}{I}.$$

EXAMPLE 7.8

Having confirmed the normal stress equation in Example 7.7, derive the shear stress distribution in a rectangular beam ($b \times h$) subject to loading that causes bending moment $M(x)$ and shear force $V(x)$, starting from the plane stress elasticity equations of equilibrium from Chapter 4:

$$\frac{\partial \sigma_{xx}}{\partial x} + \frac{\partial \sigma_{xz}}{\partial z} = 0,$$

$$\frac{\partial \sigma_{zx}}{\partial x} + \frac{\partial \sigma_{zz}}{\partial z} = 0.$$

Given: Rectangular beam in bending.

Find: Normal stress starting from plane stress elasticity equations.

Assume: Hooke's law applies; no axial loading on the beam.

Solution

The first of the equilibrium equations represents equilibrium in the x-direction. We can rearrange the equation and then substitute the known expression for σ_{xx} and taking the partial derivative with respect to x, recognizing that neither z nor I is a function of x:

$$\frac{\partial \sigma_{xz}}{\partial z} = -\frac{\partial \sigma_{xx}}{\partial x} = -\frac{\partial (M(x)z/I)}{\partial x} = -\frac{z}{I}\frac{\mathrm{d}M}{\mathrm{d}x}.$$

We can now integrate through the beam thickness, from the z location of interest to the top of the beam at $h/2$, to obtain

$$\int_{z}^{h/2} \frac{\partial \sigma_{xz}(x,z)}{\partial z}\,\mathrm{d}z = \int_{z}^{h/2} -\frac{z}{I}\frac{\mathrm{d}M(x)}{\mathrm{d}x}\,\mathrm{d}z = -\frac{1}{I}\frac{\mathrm{d}M(x)}{\mathrm{d}x}\int_{z}^{h/2} z\,\mathrm{d}z,$$

$$\sigma_{xz}(x,\tfrac{h}{2}) - \sigma_{xz}(x,z) = -\frac{1}{2I}\frac{\mathrm{d}M(x)}{\mathrm{d}x}\left(\frac{h^2}{4} - z^2\right),$$

$$\sigma_{x,z}(x,z) = \frac{1}{2I}\frac{\mathrm{d}M(x)}{\mathrm{d}x}\left(\frac{h^2}{4} - z^2\right).$$

We have used the fact that the shear stress must be zero on the top surface of the beam as there is no layer above it to provide a shear force to the surface. Now instead of just stating that $\mathrm{d}M(x)/\mathrm{d}x = V(x)$, we can show this by writing $V(x)$ as the integral of the shear stress over the cross section:

$$V(x) = \int_{-h/2}^{h/2} \sigma_{xz}(x,z)b\,\mathrm{d}z.$$

Then, by substituting the previous result into this equation we find that:

$$V(x) = \frac{1}{2I}\frac{\mathrm{d}M(x)}{\mathrm{d}x}\int_{-h/2}^{h/2}\left(\frac{h^2}{4} - z^2\right)b\,\mathrm{d}z = \frac{1}{2(bh^3/12)}\frac{\mathrm{d}M(x)}{\mathrm{d}x}b\left(\frac{h^2}{4}z - \frac{z^3}{3}\right)\Bigg|_{-h/2}^{h/2} = \frac{\mathrm{d}M(x)}{\mathrm{d}x}.$$

We can now write an explicit expression that shows how a beam carries a resultant shear force $V(x)$ with a spatially varying stress distribution on a section:

$$\sigma_{xz}(x,z) = \frac{1}{2I} V(x) \left(\frac{h^2}{4} - z^2 \right).$$

Now that we have this expression, we can use it to determine maximum value of shear stress on the section. We can see that we have a parabolic distribution of shear stress, with a maximum at $z = 0$, the neutral axis, and at that level

$$\sigma_{xz,\text{max}}(x) = \frac{3V(x)}{2bh} = 1.5 \frac{V(x)}{A}.$$

The maximum shear stress is 1.5 times the average. Remember that these results are only for a rectangular cross section.

EXAMPLE 7.9

An axial load is applied to a solid circular bar that contains an offset in order to fit in a tight space in a machine. Compute the maximum tensile and compressive normal stresses at section a.
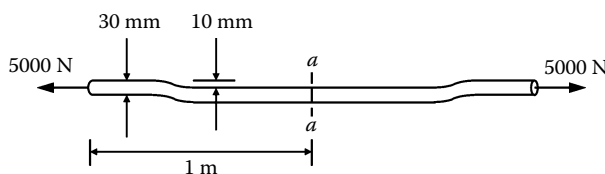
Given: Magnitude of axial force and bent bar geometry.

Find: Maximum normal stresses at specified section.

Assume: Hooke's law applies.

Solution

Although we have learned about bars subject to axial loading, rods subject to torsion, and beams subject to bending in separate chapters, in practice elements are often acted upon by multiple types of loads. In this example, the center section is subject to both axial loading and bending, as we can see by constructing an FBD of the section to the left of a.

Solve for the internal forces and moment at a:

$$\sum F_x = 0 = N_a - 5000\,\text{N} \;\rightarrow\; N_a = 5000\,\text{N},$$

$$\sum F_z = 0 = V_a,$$

$$\sum M_{\text{about}\,a} = 0 = -M_a + (5000\,\text{N})(0.01\,\text{m}) \;\rightarrow\; M_a = 50\,\text{N m}.$$

The normal stress due to N_a is

$$\sigma_{xx} = \frac{N_a}{A} = \frac{5000\,\text{N}}{\pi(0.015\,\text{m})^2} = 7.1\,\text{MPa}.$$

The normal stress due to M_a varies, with the maximum tensile stress at the top surface ($z = +0.015\,\text{m}$) and the maximum compressive at the bottom ($z = -0.015\,\text{m}$). For the circular cross section, Appendix A tells us that $I = \pi r^4/4$.

$$\sigma_{xx} = \frac{M_a\,(\pm z_{\text{max}})}{I} = \frac{(50\,\text{N}\,\text{m})(\pm 0.015\,\text{m})}{\frac{\pi}{4}(0.015\,\text{m})^4} = \pm 18.9\,\text{MPa}.$$

Because both of these stresses contribute to the same component of the stress tensor, in our linear setting we use the principle of superposition to add them. The maximum tensile and compressive stresses are

$$\sigma_{xx,\text{top}} = \frac{N_a}{A} + \frac{M_a\,(+z_{\text{max}})}{I} = 7.1\,\text{MPa} + 18.9\,\text{MPa} = 26\,\text{MPa} \ (\text{maximum tension}),$$

$$\sigma_{xx,\text{bottom}} = \frac{N_a}{A} + \frac{M_a\,(-z_{\text{max}})}{I} = 7.1\,\text{MPa} - 18.9\,\text{MPa} = -11.8\,\text{MPa} \ (\text{maximum compression}).$$

In several of the problems below you are asked to consider superposition of multiple sources of stress. In some cases there will be multiple contributions to a single element of the stress tensor, which may be added as in this example. In others, loads cause contributions to different elements of the stress tensor.

PROBLEMS

7.1 Draw the shear diagram for the following beam:
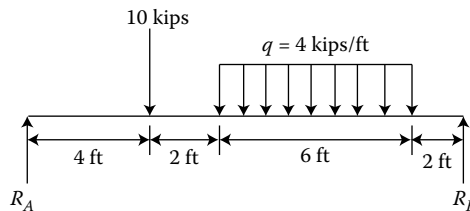
7.2 Draw shear and bending moment diagrams for the following beam:
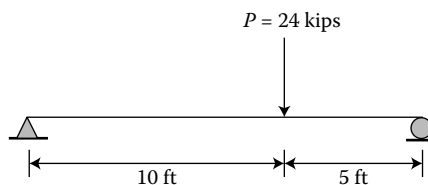
7.3 Draw shear and bending moment diagrams for the following *overhanging* beam:
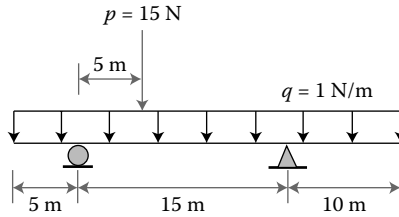
7.4 Draw shear and bending moment diagrams for the following beam:
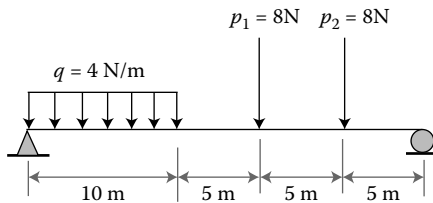
7.5 Construct axial force, shear and bending moment diagrams for the loaded beam shown. Note: drawing is not to scale.
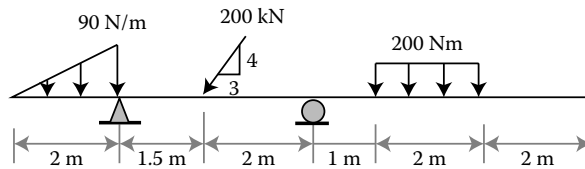
7.6 The shear-force diagram for a beam is shown. Assuming that only forces (not applied moments) act on the beam, determine the beam's loading and draw the bending moment diagram.
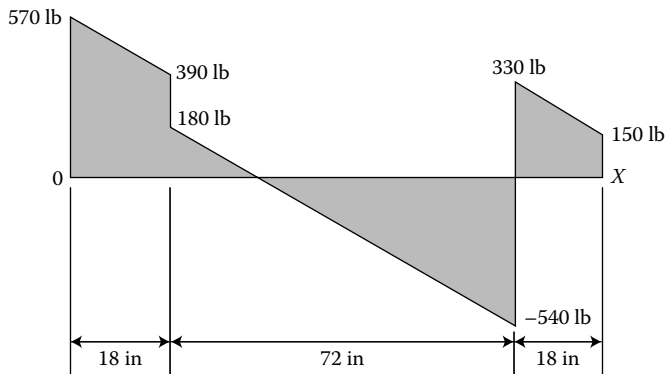
7.7 The force applied to a nut in a nutcracker is larger than the force P applied to the handles. Model the top element of the nutcracker as a beam as shown, and find the forcce on the nut as a function of P and lengths a and b. Draw the shearing force and bending moment diagrams for the beam and find the maximum normal stress in the beam if it has a circular cross section with radius c.

(Photograph courtesy of Dreamstime ID 19388023.
With permission.)
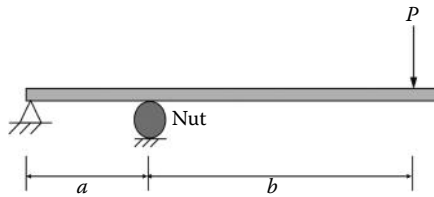
7.8 A uniform cantilever beam with triangular cross section is loaded only due to its own weight (a load uniformly distributed along the length). What is the ratio of the maximum tensile normal stress to the maximum compressive normal stress in the beam?
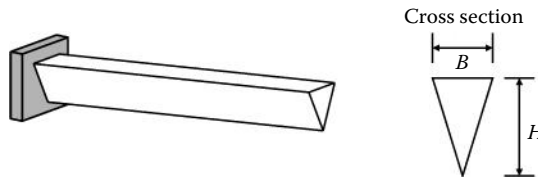
7.9 A hollow structural steel tube is being selected to support traffic lights like those shown. The tube is a uniform cantilever of 30 ft long, with lights mounted 15 ft and 30 ft from the support pole. For this preliminary design, wind loads are not being included, but with a high factor of safety the maximum normal stress in the beam may not exceed 12 ksi. The loads being considered are the 30 lb weight of each light and the self-weight of the tube. The available tubes have 1/2 in wall thickness and outer diameters ranging from 2 to 8 in, in 1/2 in increments. To the nearest 1/2 in, what outer diameter tube is required? Explain why the beam in the picture has a tapered (smaller at the tip) cross section and whether such a taper should be considered in a refinement of this design.

(http://commons.wikimedia.org/wiki/File%3AStampede_Traffic_Signal.JPG)

7.10 Each wood railroad tie supports part of the weight of a train (plus the relatively small weight of a section of rail). This is modeled with two point loads representing the force of the rail on the tie. The reaction from the ground is modeled as uniformly distributed since the railroad tie is supported along its whole length. Determine the smallest allowable dimension s of the square cross section if both of these conditions must be met:

a. The largest normal stress in the railroad tie cannot exceed 9 MPa.

b. The largest shear stress in the railroad tie cannot exceed 1 MPa.

(Photograph courtesy of Lorenzo McGary.
With permission.)
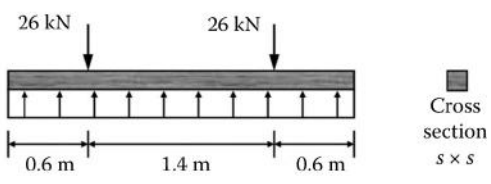
7.11 A laminated plastic beam with a square cross section is built up by gluing together three strips, each $10\,\text{mm} \times 30\,\text{mm}$ in cross section. It must carry a load P at its midpoint.

a. The beam has a total weight W and a length L. Considering the weight of the beam as a distributed load in addition to the applied load P, draw the shearing force and bending moment diagrams, indicating magnitudes in terms of W, L, and P.

b. If the beam has a total weight of 4 N and a length of 400 mm, calculate the maximum permissible load P that may be placed at the midpoint if the maximum allowable tensile stress in the plastic is 8 MPa and the maximum allowable shear stress in the glued joints is 0.3 MPa.
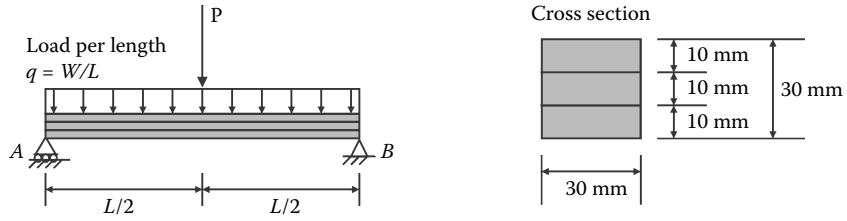
7.12 Derive a general expression for $Q'(z)$ for a rectangular cross section, and use it with Equation 7.31 to confirm the expression for $\sigma_{xz}(x,z)$ from Example 7.8.

7.13 Figure (a) shows a steel I-beam cross section (note, not symmetric about the y axis). Two steel plates with cross section $10\,\text{mm} \times 200\,\text{mm}$ are welded to the beam. Figure (b) and the 3D inset show the configuration of the composite I-beam, plates, and welds. All welds have the same geometry and are continuous in the longitudinal (x)-

direction along the beam. The welds bond to the plates only in the area shown in the inset (from the edge of the original I-beam out to the edge of the plate). What is the average shear stress in a weld/plate interface at the bottom flange if we consider a section where the shear force is 40 kN?
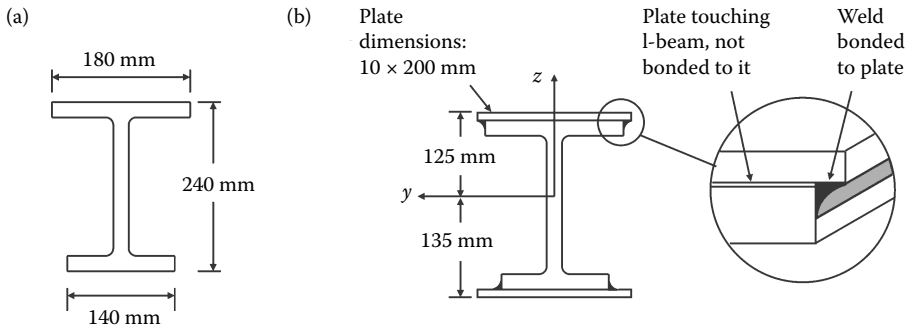
7.14 A steel frame is fabricated with the cross section shown. The centered hole allows cables to be run up to equipment above. The frame supports a load P at a distance d from the centroid of the vertical beam. Bending of the horizontal piece does not need to be included, consider it to be rigid. On the outside of the beam at a distance of 1 m from the ground, two strain gages are installed to measure longitudinal normal strain. The gage at A measures $\varepsilon = 200 \times 10^{-6}$ and the gage at B measures $\varepsilon = -250 \times 10^{-6}$.

  a. What are the magnitudes of the force P and the distance d?

  b. What is the maximum shear stress on the transverse section 1 m from the ground?
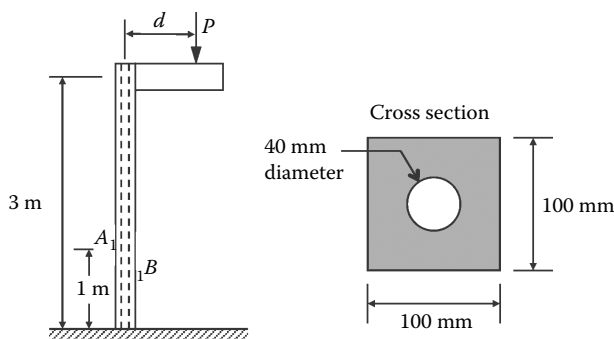
7.15 The maximum force applied to the tip of the allen wrench before the bolt loosened is 60 N. Assume the wrench has a circular cross section with a radius 2 mm. The length of the short segment (touching the screw) is 3 cm and the length of the long segment (to which the force is applied) is 6 cm. Write the stress tensors at points A and B, both of which are on the top (z-facing surface) of the wrench. *Hint*: you will need to use some results from Chapter 5.
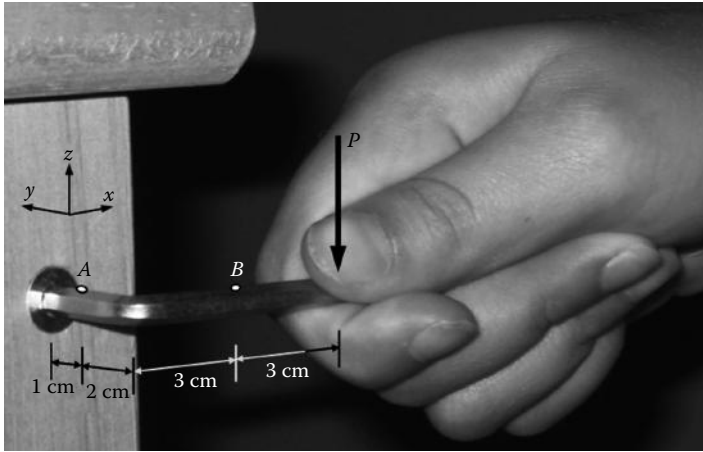
7.16 The solid steel shaft with radius 40 mm has two pulleys B and C, both with radius 0.5 m, rigidly welded to it. The belts on the pulleys produce the loads shown. The torque of 1500 N m is also externally applied. The rectangular supports at A and D do not provide any resistance to rotation about any axis—they act as pin supports. Assuming that the shear stress due to bending is negligible compared to other contributions, what is the factor of safety with respect to yielding in the shaft? *Hint*: you may want to refer back to results from more than one section of Chapter 5.
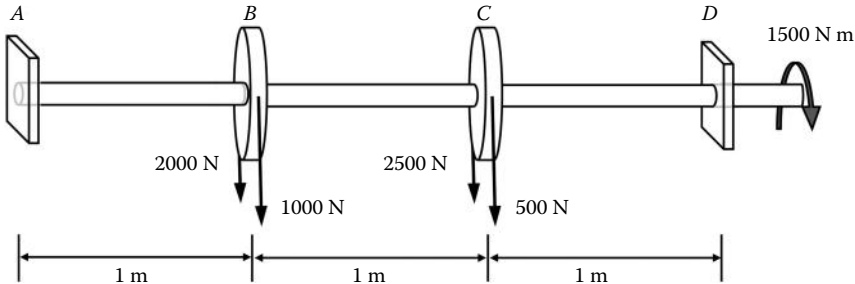
7.17 A heavy rectangular beam is being lifted slowly by a crane that applies force P at $x = \frac{2}{3}L$. The plank is 12 m long and weighs 1.5 kN/m. When $\theta = 30°$, find

a. The shear stress σ_{xz} at point A (on the top surface of the beam at $x = \frac{1}{2}L$).

b. The normal stress σ_{xx} at point A.

c. The normal stress σ_{xx} at point B (on the top surface of the beam at $x = \frac{3}{4}L$).
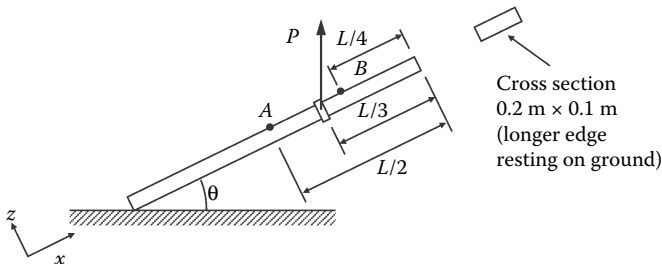
7.18 Airplane fuselages are subject to a variety of complex loads during flight. Consider a Boeing 777 modeled as a cylinder with 1/4 in wall thickness of 2024 aluminum, 209 ft length and 20.3 ft outer diameter. Assume the cylinder is loaded uniformly along the length with total weight (self-weight, passengers, all that luggage, cargo) of 600,000 lb. The load is supported by a lift from the wings, which can be simply modeled as a uniformly distributed load along the 31 ft length of the wingbox as shown. The fuselage is also pressurized for passenger safety and comfort, so that at a cruising altitude of 32,000 ft the internal pressure is atmospheric pressure at 7200 ft, resulting in an internal pressure 7.3 psi higher than the outside air. Aerodynamic loads that cause several modes of bending and twisting are not considered in this problem.

   a. Find the position (x) along the length of the fuselage that experiences the maximum bending moment. At this section, find the normal stress in the fuselage due to the weight and lift loads, as a function of vertical position in the section (z).

   b. Find the stresses due to pressure.

   c. Considering only the stresses determined in parts (a) and (b), that is, neglecting shear due to bending and dynamic loads, what is the factor of safety with respect to yielding in the fuselage? *Hint:* consider points with extreme values of the stress components.
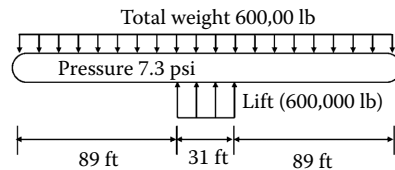
(http://commons.wikimedia.org/wiki/File:ZK-OKQ_%288338658778%29.jpg)

8

Case Study 3: Physiological Levers and Repairs

The human skeletal system is a natural mechanical apparatus. Our beam models can provide useful ways of explaining how the musculoskeletal system works and why it sometimes breaks, as well as provide a basis for repairing broken elements. In the first category, we will extend Problem 2.5 to model the human forearm as a beam. Then we will use a simple beam analysis to design a repair for a broken hip bone.

8.1 The Forearm Is Connected to the Elbow Joint

In Problem 2.5, we performed a very simple equilibrium analysis of the bones and bicep muscle of a human arm. Our single interest there was to find the force exerted by the biceps muscle when it supported a weight through the elbow–biceps–forearm–hand system. A more complete analysis requires a deeper consideration of that system. This is, by the way, a very old problem. Figure 8.1 shows a diagram taken from the treatise *De Motu Animalum*, published in Italy by Giovanni Alfonso Borelli (1608–1679). Note that Borelli's work, whose English title is *On the Movement of Animals*, preceded the 1687 publication of Newton's laws of motion. Working without the benefits of Newton's laws, Borelli discovered that the forces on bones are significantly higher than the forces applied externally. Thus, the skeleton is at a mechanical disadvantage, as the following analysis will show.

We show an anatomical drawing of the elbow–biceps–forearm–hand system in Figure 8.2. The elbow joint is a complicated hinge that allows a bent arm to go straight up and down, to extend away from the body, and to rotate about an axis through the forearm. (The forearm rotations *pronation* and *supination* are much like those experienced by runners when their feet rotate with respect to their ankles and legs.) We restrict our analysis to simple lifting with no extension or rotation. Then we can assume that the three muscles shown in Figure 8.2 act as a single "biceps-brachialis" muscle unit that exerts the force B shown in the free-body diagram in Figure 8.3. The force J is exerted by the joint on the forearm, and W is the supported weight. In this model, the elbow joint clearly acts as a simple planar hinge. The angle θ at which B acts can be determined by anatomical measurement, and the angle ϕ at which J acts is unknown or indeterminate. (The observant reader will note that the arm's own weight is left out altogether; see Problems 8.3 through 8.7.)

We now sum forces in the x- and y-directions, and moments about an axis drawn through the elbow joint (and we ignore the small offset between the application of the muscle force B and the axis of the arm):

$$\sum F_x = B \cos \theta - J \cos \phi = 0, \qquad (8.1a)$$
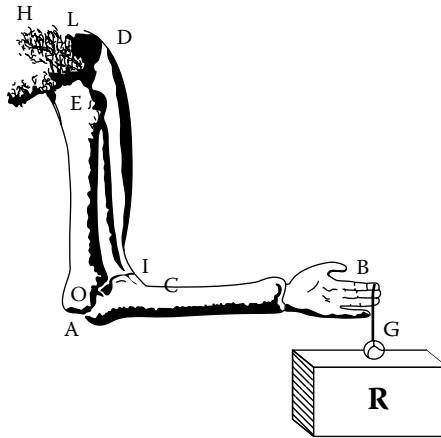
FIGURE 8.1
The *elbow force* problem presented by the mathematician Giovanni Alfonso Borelli (1608–1679) in his treatise, *De Motu Animalum*. (From R. B. Martin, D. B. Burr, and N. A. Sharkey, *Skeletal Tissue Mechanics*, Springer-Verlag, New York, 1998. With permission.)
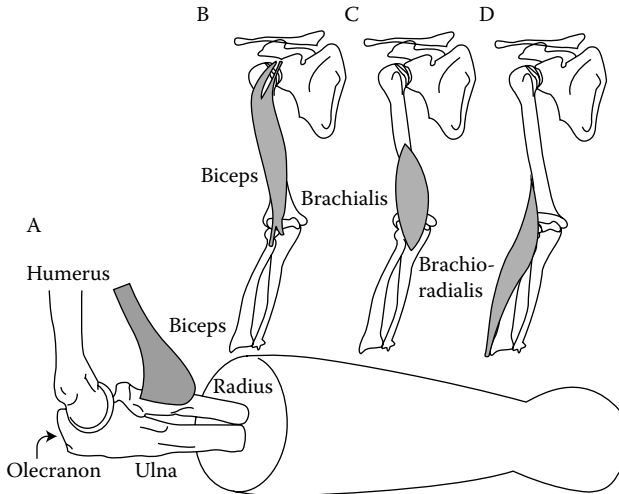
FIGURE 8.2
Anatomical drawings of the elbow–biceps–forearm–hand system, showing some of the muscles and bones that enable the joint to flex up and down, extend in and out, and rotate about the forearm's axis. (From R. B. Martin, D. B. Burr, and N. A. Sharkey, *Skeletal Tissue Mechanics*, Springer-Verlag, New York, 1998. With permission.)

$$\sum F_y = B \sin \theta - J \sin \phi - W = 0, \tag{8.1b}$$

$$\sum M_z = WL - Bb \sin \theta = 0. \tag{8.1c}$$

Equation 8.1 comprises a set of three equations for three unknowns: B, J, and ϕ. They can be straightforwardly solved (Problem 8.1) to yield

$$B = \frac{WL}{b \sin \theta}, \tag{8.2a}$$
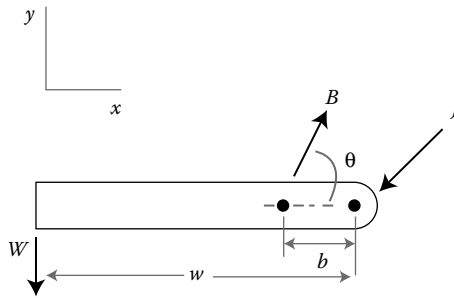
FIGURE 8.3
A FBD of the principal forces acting on a forearm when the elbow acts as a simple (planar) hinge, raising and lowering the hand with respect to the elbow. (Adapted from R. B. Martin, D. B. Burr, and N. A. Sharkey, *Skeletal Tissue Mechanics*, Springer-Verlag, New York, 1998.)

$$J = \sqrt{(B \sin \theta - W)^2 + (B \cos \theta)^2}, \tag{8.2b}$$

$$\phi = \tan^{-1} \frac{B \sin \theta - W}{B \cos \theta}. \tag{8.2c}$$

The FBD in Figure 8.3 shows that the forearm must bend like a beam and that the bending moment will: be zero at the hand carrying the weight; increase (in magnitude) linearly until it reaches its maximum value at the point where B is applied; and then decrease to zero at the hinge. Therefore, the maximum moment carried by the *ulna* and *radius* bones is given by (see Problem 8.2)

$$M_{\text{max}} = -W(L - b). \tag{8.3}$$

Now let us estimate the magnitudes of the internal forces and the moment that result from supporting the weight W. First of all, from our everyday experience, we can approximate $\sin \theta \approx 1$ because the biceps acts almost immediately adjacent to the elbow joint (or hinge). Second, in a similar estimate resulting from inspection of the geometry of the elbow–biceps–forearm–hand system, we can say that $L/b \gg 1$ (see Problem 8.8). The first consequence of these two assumptions follows from Equation 8.2a, and is

$$B \approx W \left(\frac{L}{b} \right) \gg W. \tag{8.4}$$

Thus, the force exerted by the biceps is an order of magnitude larger than the weight supported. The second consequence of our two assumptions follows from Equations 8.2b and 8.4 and states a similar result about the reaction force at the joint:

$$J \approx \sqrt{(B - W)^2 + (B)^2} \approx B \gg W. \tag{8.5}$$

Finally, a corresponding estimate of the maximum moment in the beam resulting from the weight W at its tip follows from Equation 8.3:

$$M_{\text{max}} \approx -WL. \tag{8.6}$$

This result is consistent with what we have already seen about the behavior of beams since in the limit $\sin\theta \approx 1$ the forearm is acting as a cantilever beam.

8.2 Fixing an Intertrochanteric Fracture

The *hip bone* is connected to the *thigh bone* or *femur*. The femur's *neck* and *head* comprise the familiar post-and-ball joint connecting the thigh bone to the hip bone. This ball joint allows the thigh bone to rotate and swivel so we can sit and walk and run. The femur's neck and head are connected to the top of the femur by the *trochanter*, an elaborate bony structure that has several parts (see Figure 8.4). An *intertrochanteric fracture* occurs when the substantial forces transmitted from the hip to the femur cause the trochanter to break. Modeling the repair of an intertrochanteric fracture is a neat application of beam theory.

Figure 8.5 displays a sketch of an intertrochanteric nail plate that has been inserted into the top of the femur. The nail plate transmits the appropriate (and substantial) forces from the hip bone, across the ball joint, to the thigh bone—when the basic trochanteric structure is no longer able to do that because it has cracked. Figure 8.5 also shows that this substantial force of 400 N must be carried at an angle of 20° with the axis of the nail plate, so that the nail plate across the trochanteric structure can be modeled as a beam that also supports an axial load. We need to know the relevant stresses and strains in order to validate the design of this orthopedic device.

The entire nail plate structure is rigidly attached to the femur as shown in Figure 8.5. Thus, the nail plate itself, apart from its vertical attachment to the femur, can be modeled as an axially and transversely loaded cantilever beam. The beam (or nail plate) is made of
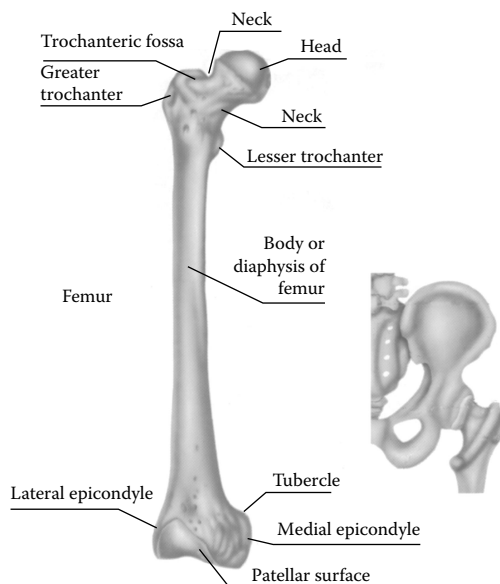
FIGURE 8.4
The skeletal structure of the femur and its connection to the hip bone across the trochanteric structure at the top of the femur. (Adapted from Barron's *Atlas of Anatomy*, Barron's Educational Series, Hauppauge, New York, 1997.)
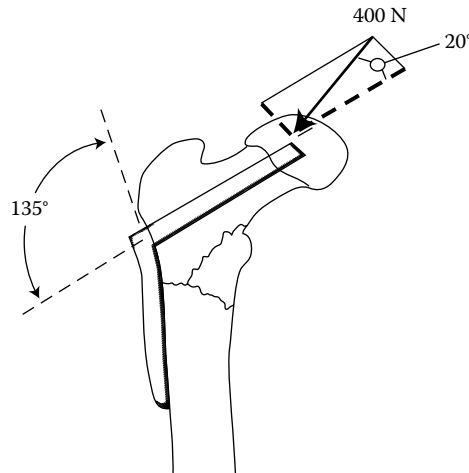
FIGURE 8.5
The nail plate structure showing both the nail plate itself and its rigid, vertical connection to the femur. The nail plate is intended to provide the support needed after an intertrochanteric fracture. (Adapted from J. D. Enderle, S. M. Blanchard and J. D. Bronzino, *Introduction to Biomedical Engineering*, Academic Press, San Diego, 2000.)

stainless steel ($E = 205\,\text{GPa}$) and has the following dimensions: $b = 5\,\text{mm}$, $h = 10\,\text{mm}$, and $L = 60\,\text{mm}$ long. The FBD in Figure 8.6 shows that the beam is subjected to an axial force of $400 \cos 20° = 376\,\text{N}$ and a transverse tip load of $400 \sin 20° = 137\,\text{N}$. The axial and bending behaviors can be considered as two separate issues and combined by superposition; we will focus here on the beam bending (see Problems 8.9 and 8.10).

The bending of the nail plate is modeled simply as that of a tip-loaded cantilever. Thus, with P being the load and x the distance from the tip, the shear and moment in such a beam are, respectively,

$$V(x) = P, \tag{8.7}$$

and

$$M(x) = -Px. \tag{8.8}$$

The shear force and stress are constant over the length of the beam, and the maximum moment and bending stress will occur at the support, located at the *greater trochanter*. The maximum shear and bending stresses in the coordinate frame of the beam are, respectively, τ_{max} or $\sigma_{xz\,max} = 4.11\,\text{MPa}$ and σ_{max} or $\sigma_{xx\,max} = 197\,\text{MPa}$ (see Problems 8.11 and 8.12).
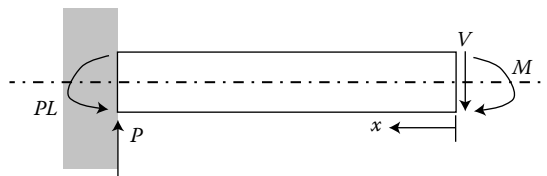
FIGURE 8.6
FBD of the bending model of an intertrochanteric nail plate structure.

Both of these stresses are much smaller than the yield stress for stainless steel, $\sigma_{yield} = 700\,\text{MPa}$, and so the proposed stainless steel nail plate can be considered a satisfactory design *in terms of its mechanical performance*. It is important to keep in mind that we have not considered whether, for example, the nail plate might be rejected by the body in which it was placed. There are important compatibility issues to consider when materials are selected for human implants and biomimetic devices (see Problem 8.13).

PROBLEMS

8.1 Confirm that Equation 8.2 is correct by solving Equation 8.1.

8.2 Draw the moment diagram for the elbow–biceps–forearm–hand system and determine the magnitude and location of the maximum moment.

8.3 How do the magnitudes of the biceps force B and joint reaction J change if the total weight w of the forearm and hand are included in the analysis and are assumed to act at the midpoint of the forearm?

8.4 Draw the moment diagram for the elbow–biceps–forearm–hand system and determine the magnitude and location of the maximum moment if the total weight w of the forearm and hand are included and are assumed to act at the midpoint of the forearm.

8.5 How large (as a fraction of the supported weight W) must the weight w of the forearm and hand be to change the analysis done under the assumption of weightlessness?

8.6 What sort of simple measurement or experiment could be done to determine the total weight w of the human forearm and hand?

8.7 How do the magnitudes of the biceps force B and joint reaction J change if the total weight w of the forearm and hand are included in the analysis and are assumed to be uniformly distributed over the forearm length L?

8.8 Examine and measure the arms of three (or more) of your colleagues and develop average estimates of the distances b and L, and of the L/b ratio.

8.9 Determine the axial stress and strain of the axially loaded nail plate. How much does the nail plate shorten as a result of this axial response?

8.10 What is the maximum shear stress that is caused by the axial force on the nail plate?

8.11 Calculate and confirm the maximum shear stress due to the bending of the stainless steel nail plate given above.

8.12 Calculate and confirm the maximum bending stress of the stainless steel nail plate given above.

8.13 Research and identify the major materials compatibility issues that arise when devices such as the nail plate are inserted or implanted in a human being.

References

Barron's *Atlas of Anatomy*, Barron's Educational Series, Hauppauge, New York, 1997.

P. Brinckmann, W. Frobin, and G. Leivseth, *Musculoskeletal Biomechanics*, Thieme, New York, 2002.

J. D. Enderle, S. M. Blanchard, and J. D. Bronzino, *Introduction to Biomedical Engineering*, Academic Press, San Diego, 2000.

R. B. Martin, D. B. Burr, and N. A. Sharkey, *Skeletal Tissue Mechanics*, Springer-Verlag, New York, 1998.

9

Beam Deflections

Knowing the accurate deflection of a beam under certain loading conditions is of interest to us as designers. In some designs, for example, when we design for stiffness, we will be seeking to *minimize* deflection (strain). Floorboards, roof supports, and bookshelves are some examples of beams whose deflections are ideally minimized. In other cases, a functional design may *rely* on the deflections of beams; examples of this include diving boards, leaf springs, and atomic force microscope cantilevers. Both situations require that we be able to predict the deflection behavior of a beam under loading (and more prudently than is suggested in Figure 9.1).

9.1 Governing Equation

We will model the deflected shape of a beam in terms of the vertical movement of the beam's neutral axis. Once again, we will make use of the premise that during bending, plane cross-sections normal to this axis through a beam remain plane. For simplicity, we will first consider bending only about one of the principal axes of the cross-section. All of this should sound familiar from the previous section's explanation of *pure bending*, but now we will include an added generality: we will discuss variation of the radius of curvature ρ of the neutral axis along the span (x).

In Figure 9.2, we see a segment of a beam with a greatly exaggerated z-direction deflection w, measured from the x-axis. We note that the slope of the beam's neutral axis at point A is $dw/dx = -\tan\theta$. Since we are assuming small deformations, we say $\tan\theta \approx \theta$ in radians. The change in slope between points A and B, which were originally dx apart on the horizontal beam axis, is $-d\theta$. The curvature of the beam, or the *rate* of change of the slope with respect to x, is

$$\frac{d}{dx}\left(\frac{dw}{dx}\right) = \frac{d}{dx}(-\theta),\tag{9.1}$$

or,

$$\frac{d^2w}{dx^2} = -\frac{d\theta}{dx}.\tag{9.2}$$

In Figure 9.2, we remind ourselves that the neutral axis can be thought of as a segment of a very large circle with radius ρ. The angle $d\theta$ between A (deflection w) and B (deflection $w + dw$) is the change in θ from x to $x + dx$. In terms of ρ, this angle may be written

$$d\theta = \frac{1}{\rho}\,ds,\tag{9.3}$$
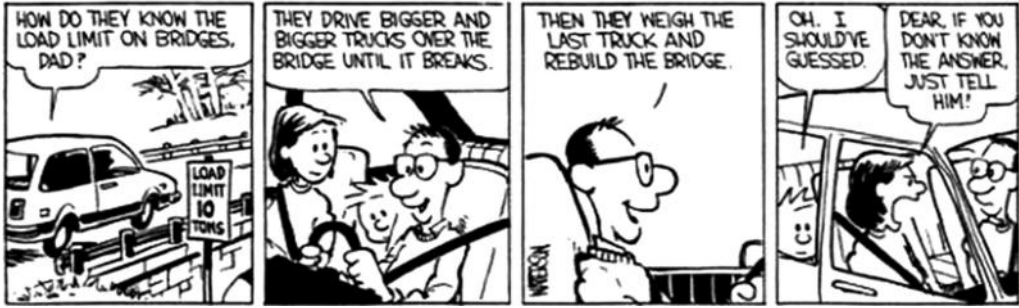
FIGURE 9.1
Inspiration from Bill Watterson, *Calvin and Hobbes*. (Used by permission of Universal Press Syndicate.)
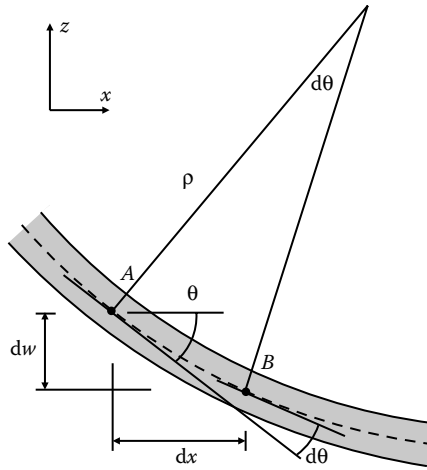
FIGURE 9.2
Beam deflected by pure bending; points *A* and *B* lie on the beam's neutral axis. A line with the slope of the neutral axis at *A* is extended past *B* to show the change in slope, $-\mathrm{d}\theta$, between *A* and *B*.

where ds is the arc length given by

$$\mathrm{d}x = \mathrm{d}s\cos\theta = \mathrm{d}s\left(1 - \tfrac{1}{2}\theta^2 + \cdots\right),\tag{9.4}$$

and again, since we are restricting ourselves to small angles θ, the higher-order terms drop out and we have

$$\mathrm{d}x \approx \mathrm{d}s,\tag{9.5}$$

and hence

$$\frac{\mathrm{d}\theta}{\mathrm{d}x} = \frac{1}{\rho}.\tag{9.6}$$

If we substitute Equation 9.2 into this expression, we have

$$\frac{\mathrm{d}^2 w}{\mathrm{d}x^2} = -\frac{1}{\rho}.\tag{9.7}$$

Recalling from Equation 7.20 that the radius of curvature can be related to the bending moment and the beam's flexural rigidity as

$$\kappa = \frac{1}{\rho} = \frac{M}{EI}, \tag{9.8}$$

we obtain a new relationship between the beam's deflection and the bending moment:

$$\frac{d^2 w}{dx^2} = -\frac{M}{EI}. \tag{9.9}$$

Here, $M = M_y$ and $I = I_y$ as in Chapter 7. With this equation, we will be able to calculate the deflections of beams. Our basic strategy will be to determine the bending moment $M(x)$ in a beam, then integrate this new equation twice to determine $w(x)$.

We also observe that if the EI product is constant, as it is for many beams, the governing equation for deflection can be recast in terms of the moment, shear, or load:

$$EI \frac{d^2 w}{dx^2} = -M(x), \tag{9.10a}$$

$$EI \frac{d^3 w}{dx^3} = -V(x), \tag{9.10b}$$

$$EI \frac{d^4 w}{dx^4} = q(x). \tag{9.10c}$$

Fewer constants of integration are necessary in the lower-order equations. No matter which of these equations we choose to use, we will need to use boundary conditions to determine the constants of integration.

9.2 Boundary Conditions

As we have seen when obtaining shear $V(x)$ and moment $M(x)$ by the integration methods of Section 7.4, the conditions at the beam ends are significant. We know that the type of support at a boundary helps to determine the internal forces and moments at this location, and it follows that the type of support also affects the deflection $w(x)$.

- At a *fixed* or *clamped support*, the displacement w and its slope dw/dx (negative of rotation θ as explained in the previous section) must vanish. If this support is at $x = 0$ as shown in Figure 9.3a, we must have

$$w(0) = 0,$$
$$\left. \frac{dw}{dx} \right|_{x=0} = 0. \tag{9.11}$$
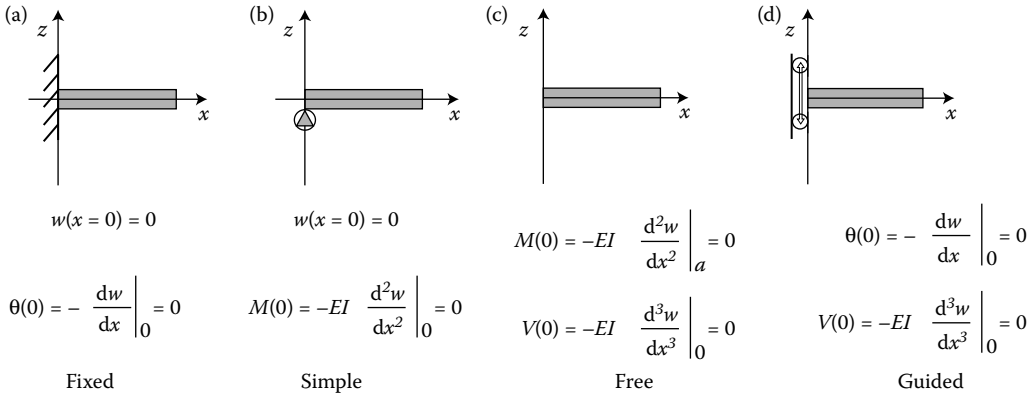
FIGURE 9.3
Homogeneous boundary conditions for beams with constant EI. In (a) both conditions are kinematic; in (c) both are static; and in (b) and (d), conditions are mixed.

- At a *roller* or *pinned support*, aka a "simple support," neither deflection w nor moment M can exist. So, if this support is at $x = 0$ as in Figure 9.3b, we must have

$$w(0) = 0,$$

$$M(0) = -EI \left. \frac{\mathrm{d}^2 w}{\mathrm{d}x^2} \right|_{x=0} = 0. \tag{9.12}$$

- At a *free end*, the beam experiences neither moment nor shear. If $x = 0$ is free (Figure 9.3c), we have

$$M(0) = -EI \left. \frac{\mathrm{d}^2 w}{\mathrm{d}x^2} \right|_{x=0} = 0,$$

$$V(0) = -EI \left. \frac{\mathrm{d}^3 w}{\mathrm{d}x^3} \right|_{x=0} = 0. \tag{9.13}$$

- At a *guided support* like that sketched in Figure 9.3d, free vertical movement is permitted, but rotation of the end is prevented. This type of support cannot resist shear. In addition,

$$\left. \frac{\mathrm{d}w}{\mathrm{d}x} \right|_{x=a} = 0,$$

$$V(a) = -EI \left. \frac{\mathrm{d}^3 w}{\mathrm{d}x^3} \right|_{x=a} = 0. \tag{9.14}$$

The boundary conditions pertaining to force quantities (V or M) are known as *static* boundary conditions. Those that describe geometrical or deformational behavior of an end (w or $\mathrm{d}w/\mathrm{d}x$) are known as *kinematic* boundary conditions.

The boundary conditions listed above are all *homogeneous* boundary conditions (i.e., something must equal zero). It is also possible to encounter *nonhomogeneous* boundary conditions, where a specified non-zero shear, moment, rotation, or displacement is prescribed. In this case, the prescribed quantity simply replaces 0 in the above conditions.
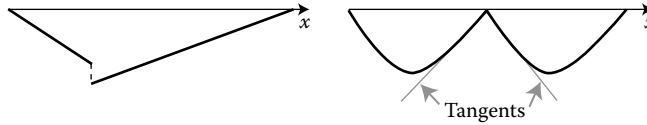
FIGURE 9.4
Discontinuous configurations of the neutral axis' deflection which would have to be corrected by enforcing continuity boundary conditions.

In some calculations, we will uncover discontinuities in the mathematical functions for either load or stiffness along a given beam's length. These discontinuities occur at concentrated forces or moments and at abrupt changes in cross-sectional areas. When this happens, we supplement our boundary conditions with the physical requirement of *continuity of the neutral axis*.[*] Anywhere a discontinuity occurs, we must ensure that deflection and the tangent to the neutral axis remain the same when this discontinuity's point is approached from either direction. Figure 9.4 illustrates two unacceptable geometries that would have to be corrected by imposing this requirement.

This requirement is expressed as a continuity boundary condition: at a place d where two solutions meet, we must have continuity of deflection w and its tangent or slope dw/dx:

$$w_1(d) = w_2(d),$$

$$\frac{dw_1}{dx}\bigg|_{x=d} = \frac{dw_2}{dx}\bigg|_{x=d}. \tag{9.15}$$

We now have sufficient information to solve our differential equation for deflection. In practice, using the method described in Section 9.4 is more efficient than implementing continuity boundary conditions directly.

9.3 Beam Deflections by Integration and by Superposition

If we start with the equation $EI\,d^4w/dx^4 = q(x)$, we must integrate this expression four times to obtain the solution for deflection $w(x)$. Assuming the product EI is constant:

$$EI\frac{d^4w}{dx^4} = EI\frac{d}{dx}\left(\frac{d^3w}{dx^3}\right) = q(x),$$

$$EI\frac{d^3w}{dx^3} = \int q(x)\,dx + C_1,$$

$$EI\frac{d^2w}{dx^2} = \int\int q(x)\,dx + C_1x + C_2,$$

---

[*] The shape of the neutral axis is sometimes called the *elastic curve*; hence some texts call this requirement *continuity of the elastic curve*.

$$EI\frac{dw}{dx} = \int\int\int q(x)\,dx + \frac{1}{2}C_1x^2 + C_2x + C_3,$$

$$EIw(x) = \int\int\int\int q(x)\,dx + \frac{1}{6}C_1x^3 + \frac{1}{2}C_2x^2 + C_3x + C_4.$$

The constants C_i have physical meanings. The second of these five equations is equivalent to $V = -\int q\,dx + C_1$, since we know that $-EId^3w/dx^3 = V$; the third equation should also look familiar. We have worked with these equations and seen that the constants C_1 and C_2 come from the end conditions on V and M; hence, these two constants come from *static boundary conditions*. When we continue onto the fourth and fifth equations, we obtain two more constants of integrations, C_3 and C_4, which describe the slope and deflection of the neutral axis. These constants come from the *kinematic boundary conditions*.

If we begin our integration at a point further down this chain, starting with $-EI\,d^2w/dx^2 = M(x)$, we will obtain after two integrations:

$$-EIw = \int\int M(x)\,dx + C_3x + C_4. \tag{9.16}$$

We will once again find C_3 and C_4 from the kinematic boundary conditions.

Any one of these five equations may be used as a starting point for finding beam deflection. The choice depends entirely on the available data.

It is important to note that distributed loads should not be replaced by their resultants for determining deflections. Although two loadings may be statically equivalent (e.g., cause the same reaction forces) they will not cause the same deflected shapes.

As long as the beam behaves elastically, it is possible to *superpose* solutions to determine the deflection $w(x)$ in a complex loading situation. Tables 9.1 and 9.2 offer deflections $w(x)$ for many isolated loads. Although some might appear to be in a different form, these are exactly the same as the results obtained from integrating. Using such a table and our previous results, we can simply add the solutions for the various loads, as in Figure 9.5. This is also an excellent way to resolve the problem of statically indeterminate beams, as we will see in Section 9.6.

In Section 9.4, we will discuss a mathematically rigorous and very convenient technique that can be used to analyze more complex situations. The method uses discontinuity functions, and it is especially useful in resolving discontinuities in loading along the beam's axis.
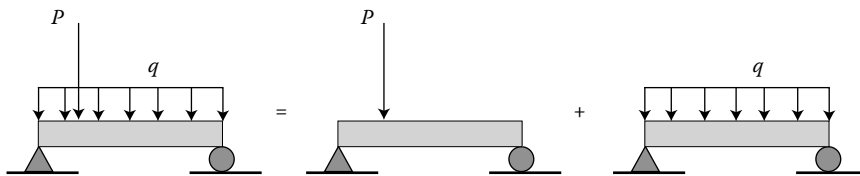
FIGURE 9.5
Finding deflection by superposition.

TABLE 9.1

Deflections and Slopes of Neutral Axes for Variously Loaded Cantilever Beams
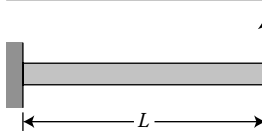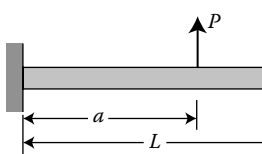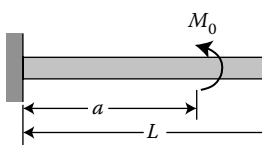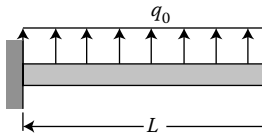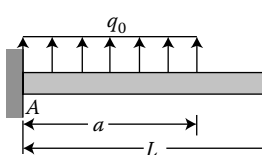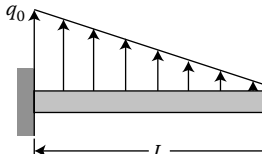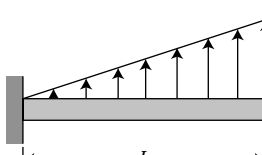
$$w(x) = \frac{PL^3}{6EI}\left[3\left(\frac{x}{L}\right)^2 - \left(\frac{x}{L}\right)^3\right]$$

$$w(x) = \frac{Pa^3}{6EI}\left[3\left(\frac{x}{a}\right)^2 - \left(\frac{x}{a}\right)^3\right], \quad 0 \le x \le a$$

$$w(x) = \frac{Pa^3}{6EI}\left[3\left(\frac{x}{a}\right) - 1\right], \qquad a \le x \le L$$

$$w(x) = \frac{M_0 a^2}{2EI}\left(\frac{x}{a}\right)^2, \qquad 0 \le x \le a$$

$$w(x) = \frac{M_0 a^2}{2EI}\left[2\left(\frac{x}{a}\right) - 1\right], \quad a \le x \le L$$

$$w(x) = \frac{q_0 L^4}{24EI}\left[6\left(\frac{x}{L}\right)^2 - 4\left(\frac{x}{L}\right)^3 + \left(\frac{x}{L}\right)^4\right]$$

$$w(x) = \frac{q_0 a^4}{24EI}\left[6\left(\frac{x}{a}\right)^2 - 4\left(\frac{x}{a}\right)^3 + \left(\frac{x}{a}\right)^4\right], \quad 0 \le x \le a$$

$$w(x) = \frac{q_0 a^4}{24EI}\left[6\left(\frac{x}{a}\right) - 1\right], \qquad a \le x \le L$$

$$w(x) = \frac{q_0 L^4}{120EI}\left[10\left(\frac{x}{L}\right)^2 - 10\left(\frac{x}{L}\right)^3 + 5\left(\frac{x}{L}\right)^4 - \left(\frac{x}{L}\right)^5\right]$$

$$w(x) = \frac{q_0 L^4}{120EI}\left[20\left(\frac{x}{L}\right)^2 - 10\left(\frac{x}{L}\right)^3 + \left(\frac{x}{L}\right)^5\right]$$

TABLE 9.2

Deflections and Slopes of Neutral Axes for Variously Loaded Simply Supported Beams

$$w(x) = \frac{PbL^2}{6EI}\left[\left(1 - \left(\frac{b}{L}\right)^2\right)\left(\frac{x}{L}\right) - \left(\frac{x}{L}\right)^3\right], \quad 0 \le x \le a$$

$$w(x) = \frac{M_0 L^2}{6EI}\left[\left(6\left(\frac{a}{L}\right) - 3\left(\frac{a}{L}\right)^2 - 2\right)\left(\frac{x}{L}\right) - \left(\frac{x}{L}\right)^3\right], \quad 0 \le x \le a$$

$$w(x) = \frac{q_0 L^4}{24EI}\left[\left(\frac{x}{L}\right) - 2\left(\frac{x}{L}\right)^3 + \left(\frac{x}{L}\right)^4\right]$$

$$w(x) = \frac{q_0 L^4}{24EI}\left[\left(\left(\frac{a}{L}\right)^4 - 4\left(\frac{a}{L}\right)^3 + 4\left(\frac{a}{L}\right)^2\right)\left(\frac{x}{L}\right) + \left(2\left(\frac{a}{L}\right)^2 - 4\left(\frac{a}{L}\right)\right)\left(\frac{x}{L}\right)^2 + \left(\frac{x}{L}\right)^3\right],$$

$$0 \le x \le a$$

$$w(x) = \frac{q_0 L^4}{24EI}\left[-\left(\frac{a}{L}\right)^4 + \left(4\left(\frac{a}{L}\right)^2 + \left(\frac{a}{L}\right)^4\right)\left(\frac{x}{L}\right) - 6\left(\frac{a}{L}\right)^2\left(\frac{x}{L}\right)^2 + 2\left(\frac{a}{L}\right)^2\left(\frac{x}{L}\right)^3\right],$$

$$a \le x \le L$$

$$w(x) = \frac{q_0 L^4}{360EI}\left[7\left(\frac{x}{L}\right) - 10\left(\frac{x}{L}\right)^3 + 3\left(\frac{x}{L}\right)^5\right]$$

9.4 Discontinuity Functions

Determining the deflection and slope of a beam using the integration method is straightforward when we can represent the bending moment within the beam by a single analytical function $M(x)$. *Discontinuity functions* (frequently but inexactly called *singularity functions*) make it possible to characterize the shear V and bending moment M by single mathematical expressions even when the loading is discontinuous. This method is most effective for beams with a constant product EI. Discontinuity functions are particularly valuable in computational techniques.

   Using discontinuity functions to describe the beam deflections was first suggested in 1862 by German mathematician A. Clebsch (1833–1872), though the notation of Equation 9.17 was introduced somewhat later by W. H. Macaulay (1853–1936), a British

mathematician and engineer. The angle brackets ⟨⟩ used to write discontinuity functions are often called "Macaulay's brackets."*

In general, unit discontinuity functions are defined:

$$\langle x - a \rangle^n = \begin{cases} (x - a)^n, & \text{when } x \geq a, \\ 0, & \text{when } x < a, \end{cases} \quad \text{for } n \geq 0. \tag{9.17}$$

The discontinuity functions corresponding to $n = 0$, 1, and 2 are graphed in Figure 9.6a. These are useful for representing $M(x)$ functions because a load that occurs (or a distributed load that begins) at a point a contributes to $M(x)$ only when x is greater than a. Figure 9.7 shows how discontinuity functions can be used to express $M(x)$ on four representative beams by scaling the unit discontinuity functions. Note that the expressions are for the bending moment caused by the single load shown and that multiple loads, including those provided by support forces, can be represented using superposition. A complete $M(x)$ expression for a beam may then be used in Equation 9.10a.

We have seen from Equation 9.10 that we have the choice of starting with expressions for bending moment, shear force, or load. If we want to use discontinuity functions to represent the load $q(x)$ directly we need some additional Macaulay bracket notation because the definition in Equation 9.17 can represent distributed loads for which $q(x)$ contributions are polynomials but not point loads. For concentrated applied point loads and moments, we use negative integer values of n with the angle bracket notation. As shown in Figure 9.6b, these are not conventional continuous functions, and the values of n are not exponents. They instead indicate the type of singularity that the discontinuity function represents. For $n = -1$, the notation indicates the Dirac delta, or unit impulse function. We have seen this in Section 2.5, where it was used to represent axial point loads on bars, but now we represent the same idea with Macaulay bracket notation. When $n = -2$, the notation indicates a unit doublet. This may be used for representing a concentrated moment.
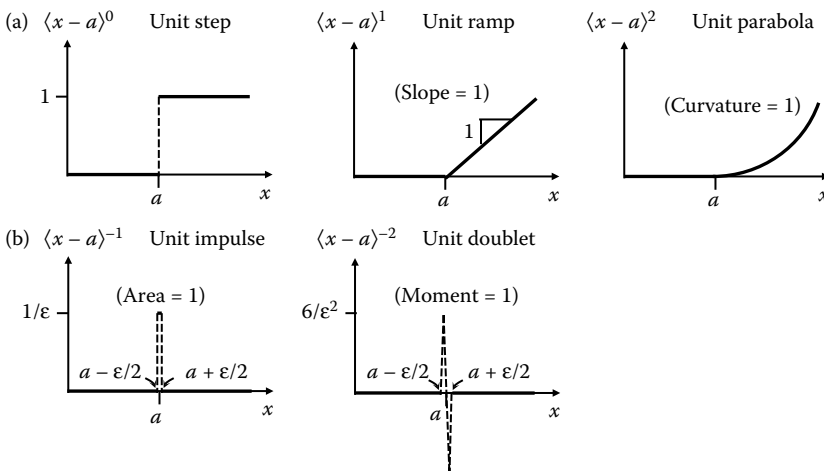
FIGURE 9.6
(a) Unit discontinuity functions with $n = 0$, 1, and 2. (b) Unit discontinuity (singularity) functions with $n = -1$ and -2. These are represented by limits as $\varepsilon \to 0$.

---

* W. H. Macaulay, "Note on the Deflection of Beams," *Messenger of Mathematics*, vol. 48, pp. 129–130, 1919.

$$q(x) = M\langle x - a\rangle^{-2}$$

$$M(x) = -M\langle x - a\rangle^{0}$$

$$q(x) = P\langle x - a\rangle^{-1}$$

$$M(x) = -P\langle x - a\rangle^{1}$$

$$q(x) = q_0\langle x - a\rangle^{0}$$

$$M(x) = -\frac{1}{2}q_0\langle x - a\rangle^{2}$$

$$q(x) = k\langle x - a\rangle^{1}$$

$$M(x) = -\frac{1}{6}k\langle x - a\rangle^{3}$$

$$q(x) = c\langle x - a\rangle^{2}$$

$$M(x) = -\frac{1}{24}c\langle x - a\rangle^{4}$$

$$q(x) = q_0\langle x - a\rangle^{0} - q_0\langle x - b\rangle^{0}$$

$$M(x) = -\frac{1}{2}q_0\langle x - a\rangle^{2} + \frac{1}{2}q_0\langle x - b\rangle^{2}$$
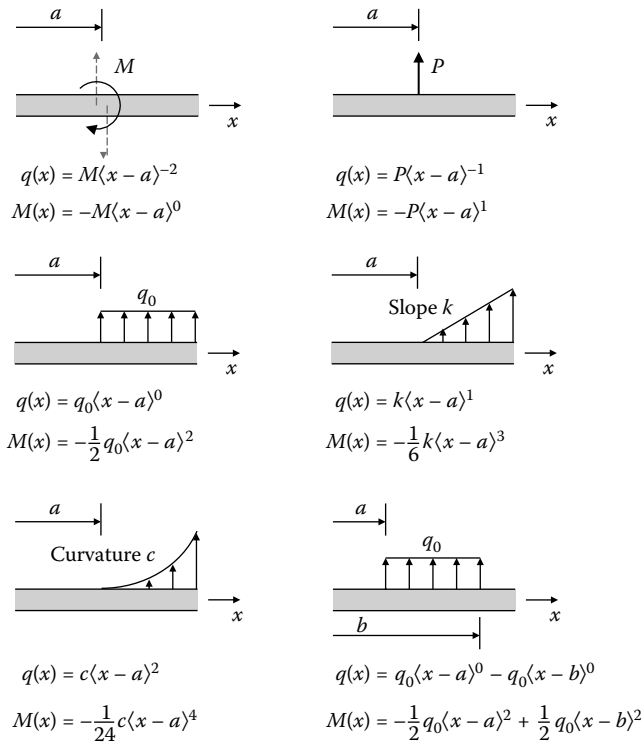
FIGURE 9.7
Basic beam loadings expressed in terms of discontinuity functions.

Figure 9.7 shows how discontinuity functions can be used to express the loadings and moments on representative beams. The expressions for $M(x)$ may be found directly using equilibrium or via the integration method of Section 7.4. Note that when an expression containing a Macaulay bracket term is integrated, the terms within the angle brackets stay within the angle brackets, unchanged. When $n \geq 0$, these terms otherwise integrate like regular polynomial terms. The integral of the unit doublet is the unit impulse, and the integral of the unit impulse is the unit step. Finally, it is important to reinforce the idea that for $x < a$, the location of the start of the loading, the value of any of these discontinuity functions is zero.

Like many problem-solving approaches, the use of discontinuity functions is best learned by applying the technique. Practice solving the worked examples in this chapter using the method of discontinuity functions to confirm that the solutions obtained are equivalent to those arrived at by other methods.

9.5 Beams with Non-Constant Cross Section

In practice, we often encounter beams whose cross-sectional areas vary *and* whose loading is complex. This is the typical situation with machine shafts, which have variations in shaft diameter to accommodate rotors, bearings, collars, etc., and it is also common in

aircraft and bridge construction. In such cases, the product EI is no longer constant, as we assumed it was in the preceding sections. Equation 9.10 must then be replaced with a more general form:

$$EI\frac{d^2w}{dx^2} = -M(x), \tag{9.18a}$$

$$\frac{d}{dx}\left(EI\frac{d^2w}{dx^2}\right) = \frac{d(-M(x))}{dx} = -V(x), \tag{9.18b}$$

$$\frac{d^2}{dx^2}\left(EI\frac{d^2w}{dx^2}\right) = \frac{d(-V(x))}{dx} = q(x). \tag{9.18c}$$

9.6 Statically Indeterminate Beams

In Section 2.9, we learned that structures are statically indeterminate when there are more reactions than are needed to maintain equilibrium and hence more unknowns than we can determine using the fixed number of equations of static equilibrium. As we did for bars, we can gain the additional needed equations by enforcing geometric compatibility for deformed parts of the body and at its boundaries (compatibility) and including a stress–strain relationship such as Hooke's law for elastic materials (constitutive law).

While analogs of both the force method and the displacement method of Section 2.9 can be developed for beams, the force method is particularly practical as it allows us to use tabulated results like those in Tables 9.1 and 9.2. The list of steps in Section 2.9.1 for implementing the force method may be directly applied here.

For example, consider a uniformly loaded beam for which the left end is fixed, but the right end is supported with a roller (as shown in Figure 9.8a). Either the moment reaction at the left end may be considered redundant (a pin support would be sufficient for equilibrium) or the roller at the right end may be (the cantilever is in equilibrium without it). Taking the second option, we remove the right hand support, which permits the system to deform as in Figure 9.8b. We can use the fourth entry in Table 9.1 to evaluate the tip deflection Δ_{tip/q_0} due only to the externally applied load (q_0 in the negative z-direction):

$$\Delta_{\text{tip}/q_0} = \frac{-q_0 L^4}{24EI}\left[6\left(\frac{x}{L}\right)^2 - 4\left(\frac{x}{L}\right)^3 + \left(\frac{x}{L}\right)^4\right]\Bigg|_{x=L} = -\frac{q_0 L^4}{8EI}. \tag{9.19}$$

But this deformation violates the geometric condition that is actually imposed at the right end, where the deflection is known to be zero. To comply with geometric compatibility, we must find the deflection $\Delta_{\text{tip}/R}$ that would be caused by R at the right end, as shown in Figure 9.8c. Thus,

$$\Delta_{\text{tip}/R} = \frac{RL^3}{6EI}\left[3\left(\frac{x}{L}\right)^2 - \left(\frac{x}{L}\right)^3\right]\Bigg|_{x=L} = \frac{RL^3}{3EI}. \tag{9.20}$$

Just as in Section 2.9.1, we may then achieve compatibility by requiring that

$$\Delta_{\text{tip}/q_0} + \Delta_{\text{tip}/R} = 0, \tag{9.21}$$
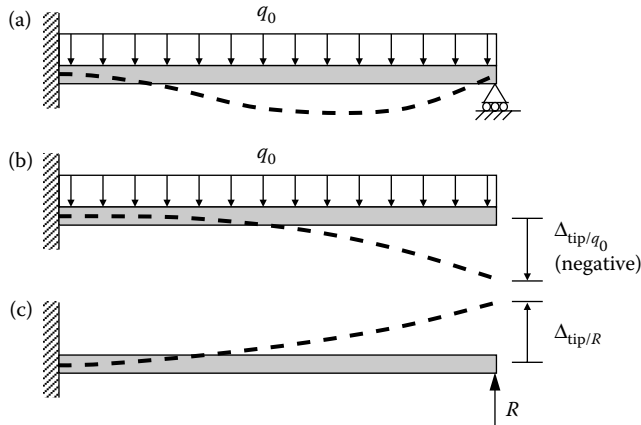
FIGURE 9.8
Decomposition of indeterminate beam by force method: (a) indeterminate beam subject to distributed load q and effect of pin support; (b) beam subjected only to distributed load q; (c) beam subjected only to pin reaction force.

enforcing the condition that there is no real displacement of the tip of the beam. Note that we knew to compute displacements at the tip because this was the point of application of the redundant load. From this expression, we find an expression for R:

$$R = \frac{q_0 L^4}{8EI} \frac{3EI}{L^3} = \frac{3}{8} q_0 L. \tag{9.22}$$

If the real physical displacement was some known non-zero value, the right-hand side of Equation 9.21 would be set to this value and a different value of R would be obtained. In Section 9.7, we consider the case where the deflection at the support is not a fixed known value.

We can extend our understanding of statically indeterminate problems using an example that has two more supports than are needed for equilibrium (Figure 9.9). This is called a second-degree indeterminate problem.

We approach the problem using the method of *flexibility coefficients*, an extension of the force (flexibility) method. We decompose the indeterminate problem into three determinate ones. To keep terms straight, the displacement Δ at a point on the beam is given a subscript denoting the location and a superscript identifying the position of the load. Thus, the deflection at $x = x_1$ due to a load P applied at x_2 is denoted by $\Delta_1^{P_2}$.
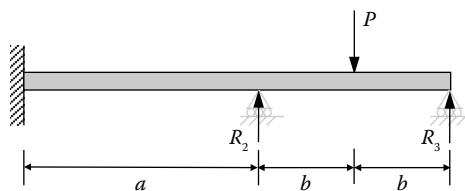
FIGURE 9.9
Cantilever with two supports: statically indeterminate.

For the loading in Figure 9.9, using decomposition (considering the applied load P and the reaction forces R_2 and R_3 one load at a time using Table 9.1, with b eliminated by replacement with $(L - a)$, we find that

$$\Delta_2^P = \left(\frac{Pa^2}{12EI}\right)(3L + a), \qquad \Delta_3^P = \left(\frac{P}{48EI}\right)(5L^3 + 9L^2a + 3La^2 - a^3), \quad (9.23a,b)$$

$$\Delta_2^{R_2} = \left(\frac{a^3}{3EI}\right)R_2, \qquad \Delta_3^{R_2} = \left(\frac{a^2(3L - a)}{6EI}\right)R_2, \qquad (9.24a,b)$$

$$\Delta_2^{R_3} = \left(\frac{a^2(3L - a)}{6EI}\right)R_3, \qquad \Delta_3^{R_3} = \left(\frac{L^3}{3EI}\right)R_3. \qquad (9.25a,b)$$

The principle of compatibility requires that when we re-assemble our component problems into the original beam, that is, apply superposition, the structure must hold together without violating any geometric or other constraints. Since we are applying compatibility at the two (redundant) supports, this means that

$$\Delta_2 = \Delta_2^P + \Delta_2^{R_2} + \Delta_2^{R_3} = 0, \qquad (9.26a)$$

$$\Delta_3 = \Delta_3^P + \Delta_3^{R_2} + \Delta_3^{R_3} = 0. \qquad (9.26b)$$

From this pair of equations, we can now determine the two redundant reactions.

This approach can be extended to any number of redundant reactions, but keeping track of terms could get confusing. So let us write the equations in matrix form, and in so doing we will introduce the idea of a matrix of *flexibility coefficients*. Flexibility coefficients relate deflection to applied load: the deflection at location i due to forces P_j applied at points j can be expressed in terms of flexibility coefficients f_{ij} as $\Delta_i = f_{ij}P_j$. This expression uses the indicial notation summation convention that we learned in Chapter 1.

First, the flexibility coefficients corresponding to the unknown reaction forces are extracted from Equations 9.24a,b through 9.25a,b, that is,

$$\begin{pmatrix} f_{22} & f_{23} \\ f_{32} & f_{33} \end{pmatrix} = \begin{pmatrix} \dfrac{a^3}{3EI} & \dfrac{a^2(3L - a)}{6EI} \\ \dfrac{a^2(3L - a)}{6EI} & \dfrac{L^3}{3EI} \end{pmatrix}. \qquad (9.27)$$

This expression shows the property of symmetry, which we could also have seen in the prior component results, namely $\Delta_2^{R_3} = \Delta_3^{R_2}$. We note now the general principle that $f_{ij} = f_{ji}$.

The matrix form of the dependence of deflections on the applied loads can now be written as

$$\begin{pmatrix} \Delta_2 \\ \Delta_3 \end{pmatrix} = \begin{pmatrix} \Delta_2^P \\ \Delta_3^P \end{pmatrix} + \begin{pmatrix} \Delta_2^{R_2} \\ \Delta_3^{R_2} \end{pmatrix} + \begin{pmatrix} \Delta_2^{R_3} \\ \Delta_3^{R_3} \end{pmatrix}$$

$$= \begin{pmatrix} \Delta_2^P \\ \Delta_3^P \end{pmatrix} + \begin{pmatrix} f_{22} & f_{23} \\ f_{32} & f_{33} \end{pmatrix} \begin{pmatrix} R_2 \\ R_3 \end{pmatrix} = \begin{pmatrix} 0 \\ 0 \end{pmatrix}, \qquad (9.28)$$

because we know that the true deflections at the support points are zero. Rearranging,

$$\begin{pmatrix} R_2 \\ R_3 \end{pmatrix} = - \begin{pmatrix} f_{22} & f_{23} \\ f_{32} & f_{33} \end{pmatrix}^{-1} \begin{pmatrix} \Delta_2^P \\ \Delta_3^P \end{pmatrix}. \tag{9.29}$$

Problem 9.18 asks you to complete this solution with specific numerical values.

We now have extended the force (flexibility) method to include an arbitrary number of redundants, formulated a structural problem in matrix notation, and found that the (structural) flexibility coefficients form a symmetric matrix. This representation is very powerful for numerical work and it is utilized in the finite-element method (FEM) for structural computation.

9.7 Beams with Elastic Supports

What happens in the case of a support that is not rigid? How does a flexible or elastic support affect a beam's deflection? Consider a modification of the example from the previous section, with the right end supported by a spring of stiffness k_s as in Figure 9.10a, instead of a rigid support.

This problem is indeterminate as in the previous section because the magnitude of the reaction force applied through the spring is unknown, and the beam deflection at that point is also unknown. This problem can be decomposed, so that the respective moments and tip deflections may be found. However, our consistency or compatibility condition for this application of the force method requires we recognize the unknown deflection at $x = L$ due to the spring. Thus, the present compatibility condition requires that

$$\Delta_{\text{tip}/q_0} + \Delta_{\text{tip}/R} = \Delta_s,$$
$$-\frac{q_0 L^4}{8EI} + \frac{RL^3}{3EI} = \frac{-R}{k_s}, \tag{9.30}$$

(a)

(b)
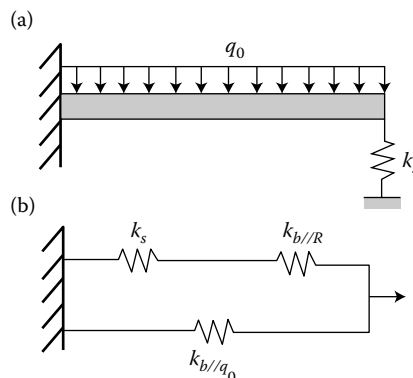
FIGURE 9.10
An indeterminate beam with elastic support (a) and its equivalent mechanical circuit (b).

where the negative sign on the right-hand side comes from drawing the reaction force R in equal and opposite directions on the beam and the spring as is required by the method of sections. An equation for the redundant R emerges as

$$R\left(\frac{1}{k_s} + \frac{L^3}{3EI}\right) = \frac{q_0 L^4}{8EI}. \tag{9.31}$$

Note that this equation for the redundant (spring) force requires that we add the flexibility coefficients for both the spring and the tip-loaded cantilever. It is also interesting to observe that if we define the following two stiffness coefficients,

$$k_{b/q_0} = \frac{q_0 L}{\Delta_{\text{tip}/q_0}} = \frac{8EI}{L^3}, \tag{9.32}$$

$$k_{b/R} = \frac{R}{\Delta_{\text{tip}/R}} = \frac{3EI}{L^3}, \tag{9.33}$$

then the equation for the redundant can be cast as

$$R\left(\frac{1}{k_s} + \frac{1}{k_{b/R}}\right) = q_0 L\left(\frac{1}{k_{b/q_0}}\right). \tag{9.34}$$

This result is just what we would expect from an *equivalent mechanical circuit* for this problem (shown in Figure 9.10b). The load carried by the discrete spring at the tip of the cantilever is found to be

$$R = q_0 L\left(\frac{k_{b/R}}{k_{b/q_0}}\right)\left(\frac{k_s}{k_s + k_{b/R}}\right). \tag{9.35}$$

Clearly, if there is no discrete spring at the tip, there will be no reaction at the tip. Further, if the discrete spring is allowed to become infinitely stiff, we can take the appropriate limit in the above equation and use the prior definitions to show that there will be a reaction whose magnitude is

$$\lim_{k_s \to \infty} R = q_0 L\left(\frac{k_{b/R}}{k_{b/q_0}}\right) = \frac{3q_0 L}{8}, \tag{9.36}$$

which is the result of Equation 9.22.

Elastic supports arise fairly often in practice, so it is useful to have the capacity to model their behavior. Two simple examples are pictured in Figure 9.11, and their corresponding stiffness coefficients for a supporting cantilever (Figure 9.11a) and for cable support (Figure 9.11b) are, respectively,

$$k_{\text{cantilever}} = \frac{3E_1 I_1}{L_1^3}, \tag{9.37}$$

and

$$k_{\text{cable}} = \frac{A_2 E_2}{L_2}. \tag{9.38}$$

In practice, of course, elastic or yielding supports may be more complicated, but they can often be modeled as simple extensional or rotational springs.
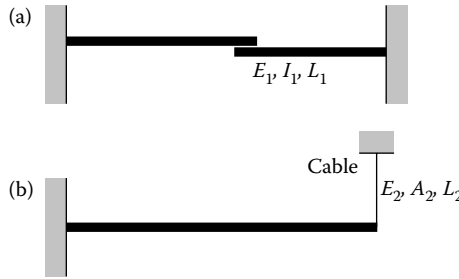
FIGURE 9.11
Examples of elastic supports: beam (a) resting on cantilever beam, and (b) held by cable subject to axial deformation.

9.8 Strain Energy for Bent Beams

As we remember from our discussion in Section 2.12, strain energy represents the energy absorbed by a material during a loading process. This is sometimes referred to as "internal work," or "potential energy." Strain energy is a useful concept for determining the response of structures to static (and dynamic) loads. We begin our discussion of strain energy in beam bending by restating results for a simply supported, uniformly loaded beam and extending them to reinforce the validity of our basic assumptions. First of all, the deflected shape of this simple beam may found to be (as in Table 9.2)

$$w(x) = \frac{q_0 L^4}{24 E I} \left[\left(\frac{x}{L}\right) - 2\left(\frac{x}{L}\right)^3 + \left(\frac{x}{L}\right)^4 \right]. \tag{9.39}$$

We can now "go backwards," and use this result to calculate the moment and shear force:

$$M(x) = -E I \frac{d^2 w}{dx^2} = \frac{q_0 L^2}{2} \left[\left(\frac{x}{L}\right) - \left(\frac{x}{L}\right)^2 \right], \tag{9.40}$$

$$V(x) = -E I \frac{d^3 w}{dx^3} = \frac{q_0 L}{2} \left[1 - 2\left(\frac{x}{L}\right) \right], \tag{9.41}$$

and the normal and shear stresses (see Example 7.8) due to bending for this problem with a beam of rectangular cross-section $(b \times h)$ are

$$\sigma_{xx} = \frac{M(x)z}{I} = \frac{q_0 L^2 z}{2I} \left[\left(\frac{x}{L}\right) - \left(\frac{x}{L}\right)^2 \right], \tag{9.42}$$

$$\sigma_{xz} = \frac{V(x)}{2I} \left(\frac{h^2}{4} - z^2\right) = \frac{q_0 L}{4I} \left(\frac{h^2}{4} - z^2\right) \left[1 - 2\left(\frac{x}{L}\right) \right]. \tag{9.43}$$

Note first of all that we can compare the maximum values of the bending and shear stresses:

$$(\sigma_{xx})_{\max} = \sigma_{xx} \left(\frac{L}{2}, \frac{h}{2}\right) = \frac{q_0 L^2 h}{16I}, \tag{9.44}$$

$$(\sigma_{xz})_{\max} = |\sigma_{xz}(0,0)| = \frac{q_0 L h^2}{16I}, \tag{9.45}$$

from which it follows that

$$\frac{(\sigma_{xz})_{\text{max}}}{(\sigma_{xx})_{\text{max}}} = \frac{h}{L}, \tag{9.46}$$

so that for slender beams, with $h \ll L$, the shear stress is much smaller than the normal stress. We can then infer that the shear strain is also much smaller than the normal strain, so the fact that our kinematics assumptions include zero shear strain should not bother us too much.

However, we can go one step further to confirm this result. In the same way that we can calculate the energy stored in a simple spring, we can calculate the energy stored in an elastic beam due to different kinds of deformation. More specifically, we can calculate the energy stored due to bending deformation and the energy stored due to shear deformation. In general, as an extension to the strain energy density (energy per unit volume) for a one-dimensional bar shown in Section 2.12, the strain energy density at a point in a general elastic solid is

$$U_0 = \tfrac{1}{2}\sigma_{ij}\varepsilon_{ij}, \tag{9.47}$$

where the repeated indices indicate summation (as usual) over all of the elements of the tensors. The dimensions of this expression are those of work per volume, as they should be, and the details of this calculation result from a straightforward analysis of the work done on a volumetric element $dx\,dy\,dz$ by a set of stresses σ_{ij} acting through the corresponding gradients of deformation, or strain, ε_{ij}. To find the total stored strain energy U, we can integrate this expression over the volume V of the elastic body:

$$U = \frac{1}{2}\int_V \sigma_{ij}\varepsilon_{ij}d\,V. \tag{9.48}$$

For our beam problem, there are only two non-zero terms to examine. Bringing in Hooke's law, due to normal stress,

$$U_{\text{normal}} = \frac{1}{2}\int_V \sigma_{xx}\varepsilon_{xx}b\,dx\,dz = \frac{1}{2}\int_V \frac{\sigma_{xx}^2}{E}b\,dx\,dz, \tag{9.49}$$

while for shear,

$$U_{\text{shear}} = \frac{1}{2}\int_V (\sigma_{xz}\varepsilon_{xz} + \sigma_{zx}\varepsilon_{zx})b\,dx\,dz = \frac{1}{2}\int_V \frac{\sigma_{xz}^2}{G}b\,dx\,dz. \tag{9.50}$$

If we substitute the stresses into the strain energy expressions, we can then do some algebra to find that

$$U_{\text{normal}} = \frac{q_0^2 L^5}{240EI}, \tag{9.51}$$

$$U_{\text{shear}} = \frac{q_0^2 L^5}{240EI}\left[2(1+\nu)\left(\frac{h}{L}\right)^2\right], \tag{9.52}$$

so that the ratio of these two strain energy terms is

$$\frac{U_{\text{shear}}}{U_{\text{normal}}} = 2(1 + \nu)\left(\frac{h}{L}\right)^2. \tag{9.53}$$

The ratio of the energy stored in shear to that stored in bending is proportional to the square of the thickness-to-length ratio. Since the work done by loads on beams is stored as strain energy, and since the shear component of this energy is very small for long, slender beams, the assumption we make when neglecting deformation due to shear when we are modeling the bending of beams is sound.

9.9 Deflections by Castigliano's Second Theorem

Strain energy is also used directly in methods for finding the deflections of structures. Although most are subjects for separate courses on structural mechanics, we can get a taste of such methods here by introducing *Castigliano's second theorem*.* This famous theorem from 1879 says

> The deflection of a structure at any point where a load is applied can be obtained from the partial derivative of the strain energy function with respect to that load.

We will not prove this theorem, but we can write out its useful form for beams here and demonstrate it in Example 9.6. Starting with the expression for strain energy that was developed in Equation 9.49, which includes only the energy due to normal stress (because we established that it is much larger than that due to shear stress in long, slender beams), we can write $\mathrm{d}V$ as $\mathrm{d}A\,\mathrm{d}x$ and replace the expression we know for σ_{xx}:

$$U = \frac{1}{2}\int_V \sigma_{xx}\varepsilon_{xx}\mathrm{d}V = \frac{1}{2}\int_V \frac{\sigma_{xx}^2}{E}\,\mathrm{d}V$$

$$= \frac{1}{2}\int_0^L \int_A \frac{1}{E}\left[\frac{M(x)z}{I}\right]^2\mathrm{d}A\,\mathrm{d}x. \tag{9.54}$$

Then because $M(x)$ and I do not vary in the cross-section A,

$$U = \frac{1}{2}\int_0^L \frac{1}{E}\frac{[M(x)]^2}{I^2}\left[\int_A z^2\,\mathrm{d}A\right]\mathrm{d}x = \frac{1}{2}\int_0^L \frac{[M(x)]^2}{EI}\mathrm{d}x, \tag{9.55}$$

where we have recognized that the integral over A is the definition of second moment of area, I, about the y-axis. If we use Equation 9.55 to get an expression for U, by squaring

---

* Castigliano's *first* theorem makes a similar case for the forces being calculated as the partial derivatives of strain energy with respect to the appropriate deflections.

the polynomial (or other) function $M(x)$, we can implement Castigliano's second theorem with

$$\Delta_i = \frac{\partial U}{\partial P_i},\tag{9.56}$$

which is an elegant mathematical form relating the load at point i, P_i, to the deflection of the structure at that position, Δ_i, through the strain energy U. This is useful on its own as shown in Example 9.6, but it can also be used to generate one or more compatibility equations for solving statically indeterminate problems, as shown in Example 9.7.

9.10 Examples

EXAMPLE 9.1

A bending moment M_1 is applied at the free end of a cantilever of length L and constant flexural rigidity EI. Find an expression for $w(x)$.
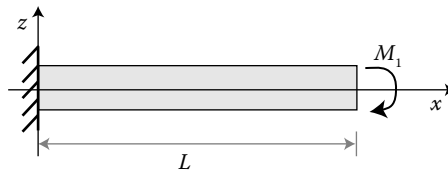
Given: Load applied to beam.

Find: Deflection, or "equation of elastic curve."

Assume: Hooke's law applies; long, slender beam.

Solution

We start with an FBD and the external reaction forces and/or moments. In this case, this procedure is straightforward: the fixed support exerts a reaction moment equal and opposite to M_1 on the beam. If we made an imaginary cut at any x and used the method of sections to find the local internal bending moment, we would similarly find that at each x, the internal bending moment was M_1. $M(x) = M_1 =$ constant, as shown in the bending moment diagram.
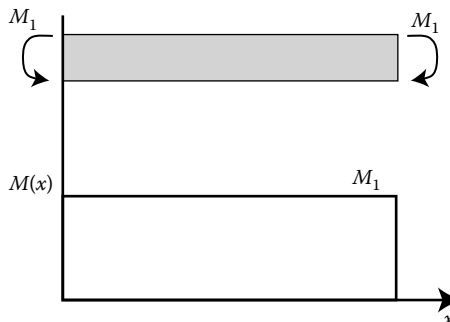
At the fixed end $(x = 0)$, we know that deflection and slope are both zero; at the free end $(x = L)$, we know the moment is M_1 and the shear is zero. We can thus begin integrating the second-order equation for deflection $w(x)$:

$$EI\frac{\mathrm{d}^2w(x)}{\mathrm{d}x^2} = -M(x) = -M_1,$$

Integrate: $\qquad EI\frac{\mathrm{d}w(x)}{\mathrm{d}x} = -M_1 x + C_3,$

Apply BC: $\qquad \left.\frac{\mathrm{d}w}{\mathrm{d}x}\right|_{x=0} = 0 \;\rightarrow\; C_3 = 0 \text{ (fixed end)},$

Integrate: $\qquad EI\,w(x) = -\frac{1}{2}M_1 x^2 + C_4,$

Apply BC: $\qquad w(0) = 0 \;\rightarrow\; C_4 = 0 \text{ (fixed end)}.$

So,

$$w(x) = -\frac{M_1 x^2}{2EI}.$$

This deflection is negative, which means that the deflection due to M_1 is downward. The maximum deflection is at $x = L$, and the neutral axis has the general shape sketched here.
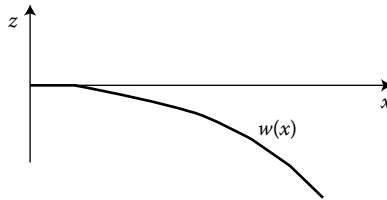
EXAMPLE 9.2

A simple beam supports a concentrated downward force P at a distance a from the left support. The flexural rigidity EI is constant. Find $w(x)$.
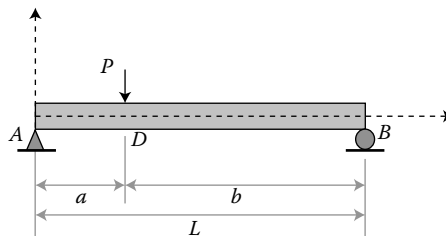
Given: Loading conditions, reaction forces, length of beam.

Find: Deflection $w(x)$.

Assume: Hooke's law applies; long, slender beam.

Solution

We want to integrate the internal moment to find the deflection $w(x)$. We have simple supports, so we know that at A, $w(x = 0) = 0$ and $M(x = 0) = 0$, and at B, $w(x = L) = 0$ and $M(x = L) = 0$. We use the method of sections to find $M(x)$:
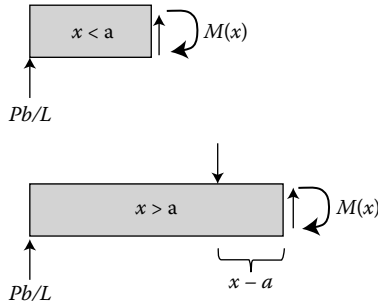
$$M_1(x) = -\frac{Pb}{L}x,$$
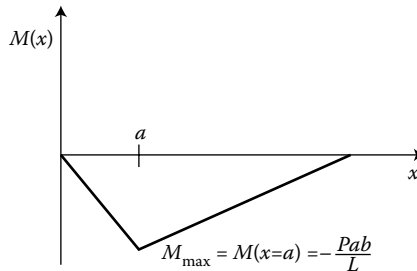
$$M_2(x) = -\frac{Pb}{L}x + P(x - a) = -\frac{P(L - a)}{L}x + P(x - a) = \frac{Pa}{L}(x - L).$$

We note that there is a discontinuity at $x = a$, so we have two distinct $M(x)$ expressions. Although $M(x)$ may be discontinuous in this way, neither the slope nor the deflection is allowed to be discontinuous. We can, therefore, integrate the two distinct $M(x)$ expressions for the deflections of the two portions of the beam, and match the two solutions at $x = a$.

For $0 \leq x \leq a$,

$$EI\frac{d^2 w_1}{dx^2} = -M_1 = \frac{Pb}{L}x,$$

Integrate:
$$\frac{dw_1}{dx} = \frac{Pb}{2EIL}x^2 + A_1.$$

Integrate:
$$w_1(x) = \frac{Pb}{6EIL}x^3 + A_1 x + A_2.$$

For $a \leq x \leq L$,

$$EI\frac{d^2w_2}{dx^2} = -M_2 = -\frac{Pa}{L}(x-L) = Pa - \frac{Pax}{L},$$

Integrate:
$$\frac{dw_2}{dx} = \frac{Pax}{EI} - \frac{Pax^2}{2EIL} + B_1.$$

Integrate:
$$w_2(x) = \frac{Pax^2}{2EI} - \frac{Pax^3}{6EIL} + B_1x + B_2.$$

To find the constants of integration A_i and B_i, we will apply the end BCs as well as the continuity condition: both w and dw/dx must be continuous at $x = a$, so that $w_1(a) = w_2(a)$ and $\frac{dw_1}{dx}\big|_{x=a} = \frac{dw_2}{dx}\big|_{x=a}$. Beginning with the end conditions, we have

$$w_1(0) = 0 = A_2,$$

$$w_2(L) = 0 = \frac{PaL^2}{3EI} + B_1L + B_2,$$

$$w_1(a) = w_2(a) \;\rightarrow\; \frac{Pa^3b}{6EIL} + A_1a = \frac{Pa^3}{2EI} - \frac{Pa^4}{6EIL} + B_1a + B_2,$$

$$\frac{dw_1}{dx}\bigg|_{x=a} = \frac{dw_2}{dx}\bigg|_{x=a} \;\rightarrow\; \frac{Pa^2b}{2EIL} + A_1 = \frac{Pa^2}{EI} - \frac{Pa^3}{2EIL} + B_1.$$

Here we have three equations for three unknown constants, so we can solve the equations simultaneously and obtain the remaining constants:

$$A_1 = -\frac{Pb}{6EIL}(L^2 - b^2) \quad \text{and} \quad B_1 = -\frac{Pa}{6EIL}(2L^2 + a^2),$$

so

$$A_2 = 0 \quad \text{and} \quad B_2 = \frac{Pa^3}{6EI}.$$

So the deflection of the beam (after some esthetic rearrangements) is given by

$$0 \leq x \leq a: \qquad w_1(x) = \frac{Pbx}{6EIL}(x^2 + b^2 - L^2),$$

$$a \leq x \leq L: \qquad w_2(x) = -\frac{Pax^3}{6EIL} + \frac{Pax^2}{2EI} - \left[\frac{Pa}{6EIL}(2L^2 + a^2)\right]x + \frac{Pa^3}{6EI}.$$

Note: the deflection at the point of application of force P may be determined by substituting $x = a$ into either of the above expressions and is $Pa^2b^2/3EIL$.

An alternative method, which does not require the need to explicitly enforce the continuity conditions at a, is to use discontinuity functions. Writing one expression for $M(x)$ that works for the entire beam can be done with Macaulay brackets. There is no need to use the Macaulay bracket notation for $x = 0$, but it may be done for consistency of notation:

$$M(x) = -\frac{Pb}{L}\langle x - 0\rangle^1 + P\langle x - a\rangle^1.$$

We then carry on with the two integration steps:

$$EI\frac{\mathrm{d}^2w}{\mathrm{d}x^2} = -M = \frac{Pb}{L}\langle x-0\rangle^1 - P\langle x-a\rangle^1,$$

Integrate:
$$\frac{\mathrm{d}w}{\mathrm{d}x} = \frac{Pb}{2EIL}\langle x-0\rangle^2 - \frac{P}{2EI}\langle x-a\rangle^2 + C_1.$$

Integrate:
$$w(x) = \frac{Pb}{6EIL}\langle x-0\rangle^3 - \frac{P}{6EI}\langle x-a\rangle^3 + C_1 x + C_2.$$

The BCs we need are just end conditions:

$$w(0) = 0 = C_2,$$

$$w(L) = 0 = \frac{Pb}{6EIL}L^3 - \frac{P}{6EI}(L-a)^3 + C_1 L.$$

So

$$C_1 = -\frac{PbL}{6EI} + \frac{P}{6EIL}(L-a)^3,$$

$$w(x) = \frac{Pb}{6EIL}\langle x-0\rangle^3 - \frac{P}{6EI}\langle x-a\rangle^3 + \left[-\frac{PbL}{6EI} + \frac{P}{6EIL}(L-a)^3\right]x,$$

which looks different but is the same as the result obtained above. Plotting both solutions for arbitrary values of P, EI, a, and b is an easier way to demonstrate this than manipulating the expressions further. Remember that the second Macaulay bracket term does not get included until $x > a$.

EXAMPLE 9.3

For the beam with the given loading, with a maximum load intensity of q_0, find (a) the reaction at A, (b) the equation of the elastic curve $w(x)$, and (c) the slope at A.
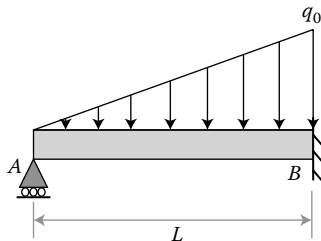
Given: Loading and support conditions, length of beam.

Find: Reactions, deflection $w(x)$, slope of neutral axis at A.

Assume: Hooke's law applies; long, slender beam.

Solution

We start with an FBD of the system:

$$\sum F_y = 0 = R_A + R_B - \tfrac{1}{2}q_0L,$$

$$\curvearrowright \qquad \sum M_{\text{about } A} = 0 = -M_B + R_BL - \left(\tfrac{1}{2}q_0L\right)\left(\frac{2L}{3}\right),$$

$$\curvearrowright \qquad \sum M_{\text{about } B} = 0 = -M_B - R_AL + \left(\tfrac{1}{2}q_0L\right)\left(\frac{L}{3}\right).$$
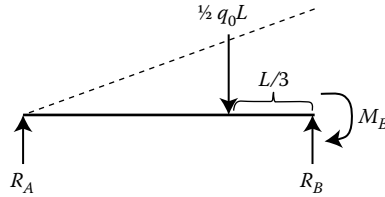
We have three unknowns (R_A, R_B, and M_B) and only two relevant equilibrium equations, so this problem is statically indeterminate. We will proceed with the solution for $w(x)$, leaving the reactions as unknowns, and hope that our boundary conditions for V, M, dw/dx, and w may help us out. First, we will make an imaginary cut at some x to determine the form of $M(x)$.
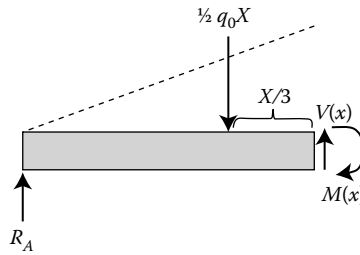
We require moment equilibrium about our point x, that is, $-M(x) + \left(\tfrac{1}{2}q_0x^2/L\right)(x/3) - R_Ax = 0$. Thus, $M(x) = -R_Ax + q_0x^3/6L$. Having this expression for internal bending moment as a function of x allows us to integrate the second-order equation for deflection $w(x)$:

$$EI\frac{d^2w(x)}{dx^2} = -M(x) = R_Ax - \frac{q_0x^3}{6L}.$$

Integrate: $\qquad\qquad EI\frac{dw(x)}{dx} = \frac{1}{2}R_Ax^2 - \frac{q_0x^4}{24L} + C_1.$

Integrate: $\qquad\qquad EIw(x) = \frac{1}{6}R_Ax^3 - \frac{q_0x^5}{120L} + C_1x + C_2.$

Note that the numbering scheme for our constants of integration is not tied to the numbered C_i cited in Section 9.3. Although this scheme was followed in Example 9.1, there is no need to stick to it. In working problems, we will most often be integrating

the second-order equation and so will have only two constants to find, so they may be named in any manner the problem solver deems appropriate.

We now need some boundary conditions to find the constants C_1 and C_2 above. At A, where $x = 0$, we have a pin support, at which we are sure both moment and deflection are zero. Then one of these that helps us is $w(x = 0) = 0$. At B, or $x = L$, we have a fixed support, where deflection and slope must both be zero. Applying these three BCs gets us

$$w(x = 0) = 0 \quad \rightarrow \quad C_2 = 0,$$

$$w(x = L) = 0 \quad \rightarrow \quad \frac{1}{6}R_A L^3 - \frac{q_0 L^4}{120} + C_1 L = 0,$$

$$\left.\frac{\mathrm{d}w}{\mathrm{d}x}\right|_{x=L} = 0 \quad \rightarrow \quad \frac{1}{2}R_A L^2 - \frac{q_0 L^3}{24} + C_1 = 0.$$

At last, we have two equations and two unknowns, a soluble system. We choose arbitrarily to solve for R_A first, and do this by multiplying the slope boundary condition by L and then subtracting the deflection condition:

$$\left(\frac{1}{2}R_A L^3 - \frac{q_0 L^4}{24} + C_1 L\right) - \left(\frac{1}{6}R_A L^3 - \frac{q_0 L^4}{120} + C_1 L\right) = 0.$$

So,

$$\frac{1}{3}R_A L^3 - \frac{q_0 L^4}{30} = 0.$$

This allows us to solve for $R_A = \frac{1}{10}q_0 L$, which is an upward force as assumed in the FBD, and which we note is independent of EI. By substituting this R_A into either condition at $x = L$, we are able to find that the constant $C_1 = -\frac{1}{120}q_0 L^3$. Putting both of these into our expression for the deflection of the neutral axis, we have

$$EIw(x) = \frac{1}{6}\left(\frac{1}{10}q_0 L\right)x^3 - \frac{q_0 x^5}{120L} + \left(-\frac{1}{120}q_0 L^3\right)x,$$

or

$$w(x) = \frac{q_0/L}{120EI}\left(-x^5 + 2L^2 x^3 - L^4 x\right).$$

We could then find a general expression for the slope $\mathrm{d}w/\mathrm{d}x$ of the neutral axis along the beam, and find the slope at A as requested in part (c):

$$\frac{\mathrm{d}w}{\mathrm{d}x}(x = 0) = -\frac{q_0 L^3}{120EI}.$$

Note: We could also have solved this complex problem by recognizing the loading on the beam as the superposition of two more straightforward conditions:
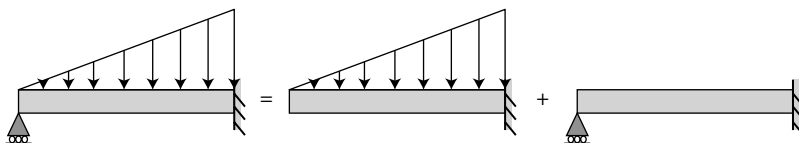
The superposition of $w(x)$ for both these loading conditions is exactly the result achieved above. Superposition is quite a useful technique for finding the deflections of beams.

EXAMPLE 9.4

The beam shown has uniform elastic modulus E and second moment of area I. Determine

1. The reactions at the left wall.
2. The beam's deflection w as a function of x.
3. The maximum allowable value of load intensity q_0 if the beam has a square cross-section with sides of 4 in and length $L = 96$ in, and is made from a material with $E = 15 \times 10^6$ psi and maximum allowable normal stress 110 ksi.
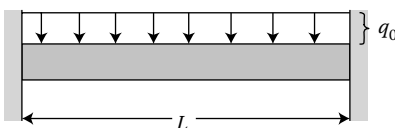
Given: Loading conditions; properties of beam.

Find: Reactions, deflection, maximum allowable intensity q_0.

Assume: Hooke's law applies; long, slender beam.

Solution

Since there are no applied axial loads we know that the supports exert equal and opposite axial forces, which may occur due to the sagging of the beam, but we do not have a method to find them and they are not considered in this problem. An FBD of the system can thus be constructed:
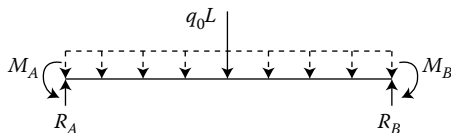
And, summing forces and moments, we have

$$\sum F_z = 0 = -q_0L + R_A + R_B,$$

$$\circlearrowleft \qquad \sum M_A = 0 = M_A - M_B + R_B L - \frac{q_0 L^2}{2}.$$

By symmetry, we can reasonably assume that $R_A = R_B$ and $M_A = M_B$; however, this assumption will not help us solve the equations of statics for the reaction moments. We will need more than just statics to find all four reactions. As in Example 9.3, we will proceed with the solution for deflection $w(x)$ and hope that the boundary conditions will help us identify our unknowns. At the two fixed supports, we know that both deflection and slope must equal zero, that is, $w(0) = w(L) = 0$ and $dw/dx|_{x=0} = dw/dx|_{x=L} = 0$.

We use the method of sections and make a cut at a distance x to find the internal bending moment $M(x)$:
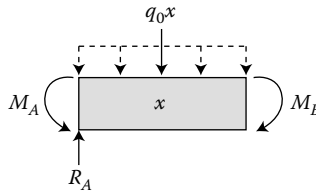
Balancing moments on this x-long segment, we have

$$M(x) = M_A - R_A x + \frac{q_0 x^2}{2}.$$

Next, we integrate for the deflection $w(x)$:

$$EI\frac{d^2 w}{dx^2} = -M(x) = -M_A + R_A x - \frac{q_0 x^2}{2},$$

$$EI\frac{dw}{dx} = -M_A x + \frac{R_A x^2}{2} - \frac{q_0 x^3}{6} + C_1,$$

$$EI\,w(x) = -\frac{M_A x^2}{2} + \frac{R_A x^3}{6} - \frac{q_0 x^4}{24} + C_1 x + C_2.$$

Applying our BCs we have

$$w(0) = 0 \;\rightarrow\; C_2 = 0,$$

$$\left.\frac{dw}{dx}\right|_{x=0} = 0 \;\rightarrow\; C_1 = 0,$$

$$w(L) = 0 \;\rightarrow\; -\frac{M_A L^2}{2} + \frac{R_A L^3}{6} - \frac{q_0 L^4}{24} = 0,$$

$$\left.\frac{dw}{dx}\right|_{x=L} = 0 \;\rightarrow\; -M_A L + \frac{R_A L^2}{2} - \frac{q_0 L^3}{6} = 0.$$

We solve these last two equations together with the two equilibrium equations for our four unknowns, and find

$$R_A = R_B = \frac{q_0 L}{2},$$

$$M_A = M_B = \frac{q_0 L^2}{12}.$$

We can now substitute these values into the expression for $w(x)$ above:

$$EI\,w(x) = -\frac{M_A x^2}{2} + \frac{R_A x^3}{6} - \frac{q_0 x^4}{24} + C_1 x + C_2,$$

$$w(x) = \frac{1}{EI}\left[-\frac{q_0 L^2 x^2}{24} + \frac{q_0 L x^3}{12} - \frac{q_0 x^4}{24} \right],$$

or

$$w(x) = \frac{q_0 x^2}{24EI}\left[-L^2 + 2Lx - x^2\right].$$

To find the maximum allowable load intensity q_0 based on the given normal stress limitation, we must calculate the maximum normal stress induced in the beam in terms of q_0. Because normal stress is linearly proportional to bending moment, we will do this by finding the maximum internal bending moment in the beam. We return to our general equation for $M(x)$ and now put in the known values for the reactions.

$$M(x) = M_A - R_A x + \frac{q_0 x^2}{2} = \frac{q_0 L^2}{12} - \frac{q_0 L x}{2} + \frac{q_0 x^2}{2}.$$

The maximum $M(x)$ will occur where $dM/dx = 0$: $dM/dx = -q_0\frac{L}{2} + q_0 x = 0$ at $x = \frac{L}{2}$. We must consider the end points of the beam, which also have zero slope, as well. The bending moment at the center of the beam is

$$M\left(\frac{L}{2}\right) = -\frac{q_0 L^2}{24}.$$

This has a lower magnitude than the bending moment $q_0 L^2/12$ at the ends of the beam, so the ends are the critical points.

Below, we sketch the form of $M(x)$.
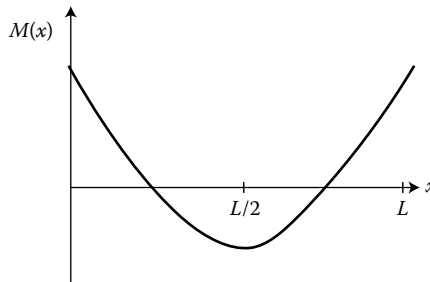
The second moment of area of the given cross-section is $I = bh^3/12 = (4\,\text{in})^4/12 = 21.3\,\text{in}^4$. The maximum normal stress is given by

$$\sigma_{\text{max}} = \frac{M_{\text{max}}c}{I} \leq \sigma_{\text{allow}}.$$

So working with the magnitude of M_{max} only since there are equal and opposite tensile and compressive stresses at each x location in the beam,

$$|M_{\text{max}}| = \frac{q_0 L^2}{12} \leq \frac{\sigma_{\text{max}} I}{c},$$

$$q_0 \leq \frac{(110\,\text{ksi}) \cdot (21.3\,\text{in}^4)}{2\,\text{in}}\frac{12}{(96\,\text{in})^2} = 1.53\,\text{kips/in}.$$

Note that this result is independent of the Young's modulus of the beam, E.

EXAMPLE 9.5

Before the distributed load q_0 is applied, there is a gap s between the ends of the cantilevers. Determine the reactions provided by the walls at A and C when the load is applied, assuming that the load is more than large enough to close the gap. Both beams have the same E and I.
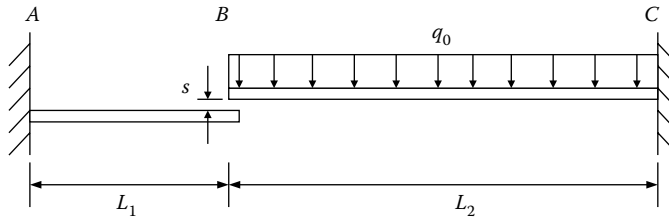
Given: Cantilever that will act as a flexible support for another cantilever when gap is closed.

Find: Reaction forces at the walls.

Assume: Hooke's law applies; long slender beams with constant cross-section; the load causes the gap to close.

Solution

If the load is not sufficient for the gap to close, then each beam may be analyzed separately. The problem is more interesting, and statically indeterminate, when the gap does close. When the beams are in contact, they exert equal and opposite forces F_B on each other, so the beams are supported by three unknown forces, R_A, R_C, and F_B and two moment reactions M_A and M_C but there are only four equilibrium equations available, two from each beam:

$$R_A = F_B, \qquad\qquad M_A = F_B L_1,$$

$$R_C = -F_B + q_0 L_2, \qquad\qquad M_C = -F_B L_2 + \frac{1}{2} q_0 L_2^2.$$
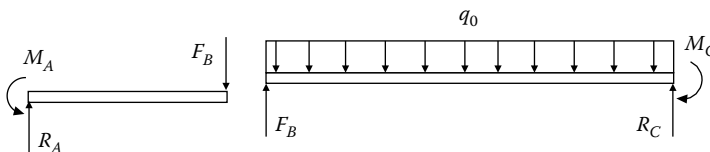
To plan our implementation of the force method, we start by constructing the compatibility relationship to become the fifth needed equation. Since the beams end up touching, we know that the difference between the tip deflections must be s. Also, using superposition we can say that the deflection of the tip of the upper beam is the sum of the deflections due to the applied load and the unknown reaction force F_B. Note that all terms are drawn and will be computed using the convention of positive deflection being up. So

$$\Delta_{1/F_B} + s = \Delta_{2/F_B} + \Delta_{2/q_0}.$$

Table 9.1 gives us the information we need to calculate the tip deflections. For the lower beam,

$$w_1(x) = \frac{-F_B L_1^3}{6EI}\left[3\left(\frac{x}{L_1}\right)^2 - \left(\frac{x}{L_1}\right)^3\right],$$

so

$$\Delta_{1/F_B} = w_1(L_1) = \frac{-F_B L_1^3}{3EI}.$$

Similarly for the upper beam, considering x going right to left, the point reaction force causes deflection

$$\Delta_{2/F_B} = w_2(L_2) = \frac{F_B L_2^3}{3EI}.$$

And for the distributed load,

$$w_2(x) = \frac{-q_0 L_2^4}{24EI}\left[6\left(\frac{x}{L_2}\right)^2 - 4\left(\frac{x}{L_2}\right)^3 + 4\left(\frac{x}{L_2}\right)^4\right],$$

so

$$\Delta_{2/q_0} = w_2(L_2) = \frac{-q_0 L_2^4}{8EI}.$$

Now enforcing compatibility

$$\Delta_{1/F_B} + s = \Delta_{2/F_B} + \Delta_{2/q_0},$$

becomes

$$-\frac{F_B L_1^3}{3EI} = \frac{F_B L_2^3}{3EI} - \frac{q_0 L_2^4}{8EI} - s.$$

Solving for the unknown force, we obtain

$$F_B = \frac{q_0 L_2^4/8EI + s}{L_1^3/3EI + L_2^3/3EI} = \frac{3q_0 L_2^4 + 24sEI}{8\left(L_1^3 + L_2^3\right)}.$$

Then from the equilibrium relations

$$R_A = \frac{3q_0 L_2^4 + 24sEI}{8\left(L_1^3 + L_2^3\right)}, \qquad M_A = \frac{\left(3q_0 L_2^4 + 24sEI\right)L_1}{8\left(L_1^3 + L_2^3\right)},$$

$$R_C = -\frac{3q_0 L_2^4 + 24sEI}{8\left(L_1^3 + L_2^3\right)} + q_0 L_2, \qquad M_C = -\frac{\left(3q_0 L_2^4 + 24sEI\right)L_2}{8\left(L_1^3 + L_2^3\right)} + \frac{1}{2}q_0 L_2^2.$$

EXAMPLE 9.6

Use Castigliano's second theorem to find the deflection of the beam at points B and C due to the load P at B. The beam has a constant EI.
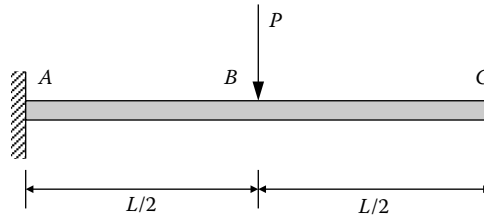
Given: Cantilever beam with a point load.

Find: Deflection at point of applied load and at the tip.

Assume: Hooke's law applies; long slender beam.

Solution

Castigliano's second theorem lets us find the deflection at B in a straightforward manner. We find the strain energy in the beam, take the partial derivative of it with respect to force P, and the result is the deflection at B, the point of application of force P. It pays to think ahead to the other deflection that is requested before beginning, however. There is no point load at C, so how can we find the deflection there? We can cleverly add a "dummy" force Q at C, and then the partial derivative of strain energy with respect to Q is the deflection at C. We then set the value of Q to its real value, zero.

To use Castigliano's second theorem, we need the function $M(x)$ which we can write using Macaulay bracket notation. Starting with the load $q(x)$ and including the reaction force R_1 and moment M_1 at the left end,
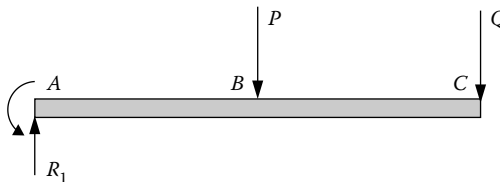
$$q(x) = -M_A\langle x - 0\rangle^{-2} + R_A\langle x - 0\rangle^{-1} - P\langle x - \tfrac{1}{2}L\rangle^{-1} - Q\langle x - L\rangle^{-1}.$$

The final term is always zero and is dropped in the following expressions. Integrating twice and remembering the negative sign in $dV/dx = -q$, we obtain

$$V(x) = M_A\langle x - 0\rangle^{-1} - R_A\langle x - 0\rangle^{0} + P\langle x - \tfrac{1}{2}L\rangle^{0},$$

$$M(x) = M_A\langle x - 0\rangle^{0} - R_A\langle x - 0\rangle^{1} + P\langle x - \tfrac{1}{2}L\rangle^{1}.$$

Using equilibrium, we can eliminate $M_A = PL/2 + QL$ and $R_A = P + Q$. And we recognize that the Macaulay brackets are not needed on the first two terms:

$$M(x) = \tfrac{1}{2}PL + QL - Px - Qx + P\langle x - \tfrac{1}{2}L\rangle^{1}.$$

Now the strain energy can be broken up into two integrals:

$$U = \frac{1}{2} \int_0^L \frac{[M(x)]^2}{EI} \, dx$$

$$= \frac{1}{2EI} \int_0^{\frac{1}{2}L} \left[\tfrac{1}{2}PL + QL - Px - Qx\right]^2 dx + \frac{1}{2EI} \int_{\frac{1}{2}L}^L [QL - Qx]^2 \, dx$$

$$= \frac{L^3}{48EI}(P^2 + 5PQ + 7Q^2) + \frac{L^3}{48EI}Q^2 = \frac{L^3}{48EI}(P^2 + 5PQ + 8Q^2).$$

Implementing Castigliano's second theorem,

$$\Delta_B = \frac{\partial U}{\partial P} = \frac{L^3}{48EI}(2P + 5Q),$$

$$\Delta_C = \frac{\partial U}{\partial Q} = \frac{L^3}{48EI}(5P + 16Q).$$

These deflections are both downward, the direction of P and Q. Now setting Q to its real value, zero, we get the final result:

$$\Delta_B = \frac{PL^3}{24EI} \quad \text{and} \quad \Delta_C = \frac{5PL^3}{48EI}.$$

EXAMPLE 9.7

Use Castigliano's second theorem to find the reaction force in the support at C due to the load P at B. The beam has a constant EI.
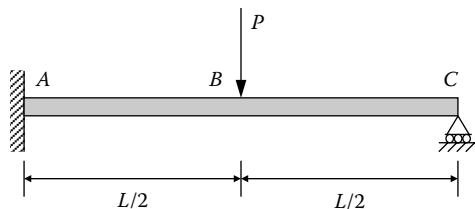
Given: Statically indeterminate cantilever beam with a point load.
Find: Reaction force at redundant support.
Assume: Hooke's law applies; long slender beam.

Solution

The work we have done in Example 9.6 allows us to quickly solve this problem. There is now a real force at C, so we can consider the force Q to be $-R_C$ (noting Q was pointing

down and R_C is pointing up). Our intermediate result from Example 9.6 for Δ_C can be set to equal the real, physical deflection at C, which due to the support is zero:

$$\Delta_C = \frac{\partial U}{\partial Q} = \frac{L^3}{48EI}(5P + 16Q) = 0.$$

From this compatibility equation, we find that $R_C = -Q = 5P/16$.

The problem does not ask for the deflection at B, but we could find it with other equations from Example 9.6 now that R_C is known.

PROBLEMS

9.1 The beam shown has modulus E and second moment of area I. The load per length increases linearly in the right half of the beam and has a maximum value of q_0.

  a. Use the method of sections to find $M(x)$, and then use integration method with the second-order differential equation to find the expression for the deflection $w(x)$.

  b. Find the deflection $w(x)$ again using the integration method with the fourth-order equation. That is, start by writing $q(x)$.

  c. Determine the maximum deflection and the point at which it occurs.
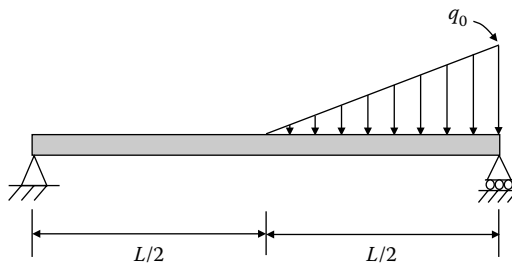
9.2 Beam $ABCDE$ has simple supports at B and D and symmetrical overhangs at each end, as shown. The center span has length L and each overhang has length b. A uniform load of intensity q acts on the beam.

  a. Determine the ratio b/L such that the deflection Δ_C at the midpoint of the beam is equal to the deflections Δ_A and Δ_E at the ends.

  b. For this value of b/L, what is the deflection Δ_C at the midpoint?
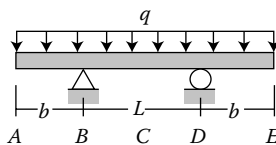
9.3 This atomic force microscope probe is a silicon beam and tip. The beam is 40 μm wide, 4 μm thick, and 130 μm long. The tip is set back 15 μm from the end of the cantilever.

The deflection of the tip is 1 µm for every 42 µN of force applied to the tip. What is the elastic modulus of the silicon?

(Courtesy of Ted Pellea.)

9.4 For the allen wrench of Problem 7.15, what is the deflection of the tip of the wrench when the maximum load of 60 N is applied, just before the bolt loosens?

9.5 A cantilever beam AB supports a uniform load of intensity q acting over part of the span and a concentrated load P acting at the free end, as shown. Determine the deflection and slope at end B of the beam. The beam has length L and constant flexural rigidity EI.
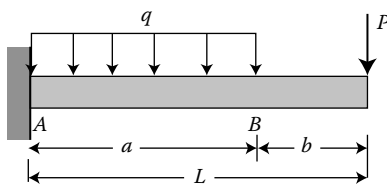
9.6 A beam with a constant EI is loaded as shown. (a) Determine the length a of the overhang such that the elastic curve would be horizontal over support B. (b) Determine the maximum deflection between the supports.
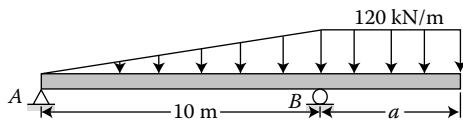
9.7 A simply supported beam 5 m long is loaded with a 20 N downward force at a point 4 m from the left support. The second moment of area of the cross-section of the beam is $4I_1$ for segment AB and I_1 for the remainder of the beam. Determine the deflection $w(x)$ of the neutral axis.
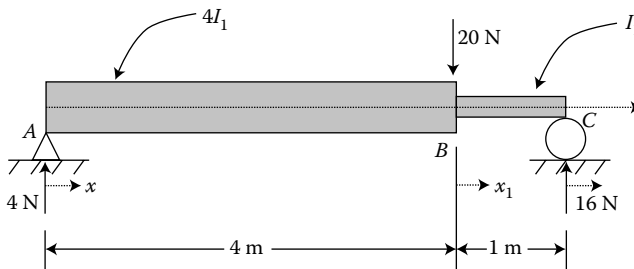
9.8 Consider an aluminum cantilever beam 1600 mm long, with a 10-kN force applied 400 mm from the free end. For a distance of 600 mm from the fixed end, the beam

has $I_1 = 50 \times 10^6$ mm^4. For the remaining 1000 mm of its length, the beam has $I_2 = 10 \times 10^6$ mm^4. Find the deflection and the angular rotation of the free end. Neglect the weight of the beam, and use $E = 70$ GPa.
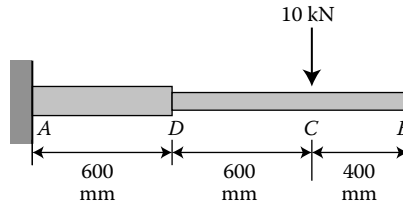
9.9 Determine the tip deflection of a beam with linear varying width $b(x)$, constant height h, length L, and elastic modulus E due to tip load P. Write the answer in terms of the maximum width $b_L = b(L)$. Also determine the normal stress as a function of x. On the same axes, plot this normal stress, as well as the normal stress in a cantilever of the same length with a constant width $b_L/2$. Both beams have the same volume of material—which can carry a higher load P?
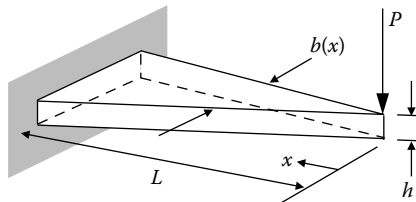
9.10 A cantilever beam AB has a rigid (i.e., its deformation is negligible relative to that of the beam) bracket AC attached to its free end and a vertical load P applied at point C. Find the ratio a/L required so that the deflection at point A will be zero. E and I are constant along the beam.
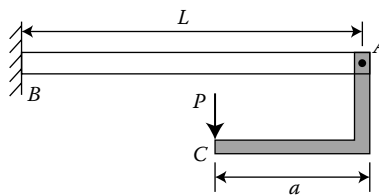
9.11 A 1 in $\times$ 10 in plank on a redwood deck has $L = 48$ in long and supported on three joists that rest on the ground and so do not bend. The joists act as pin/roller supports for the plank. If a 130 lb person stands on the plank in the location shown, what is the reaction force on each of the joists?
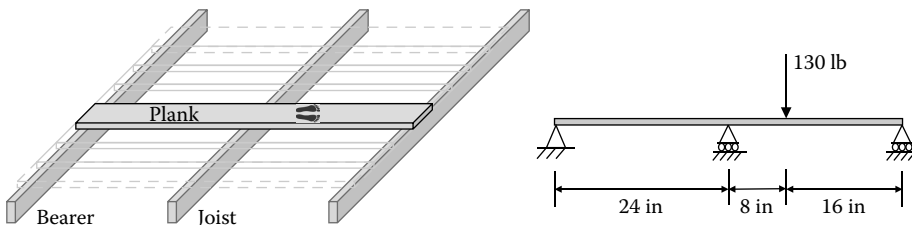
9.12 An aluminum ($E = 70\,\text{GPa}$) cantilever must carry an end load of 1.4 kN as shown. However, in this design, when the beam is loaded the end of the cantilever A has to have the same elevation as point C (i.e., the net deflection of A must be zero). A hydraulic jack may be used to raise point B to achieve this. Determine the amount that B should be raised and the reaction at B (when the load is applied and B has been raised). Do not consider the weight of the beam. The cross-section of the beam is *half* of an I-beam as shown. The properties given in the box below are for the *whole* I-beam. The position of the centroid of the half-section (relative to the top of the section) is shown in the figure.
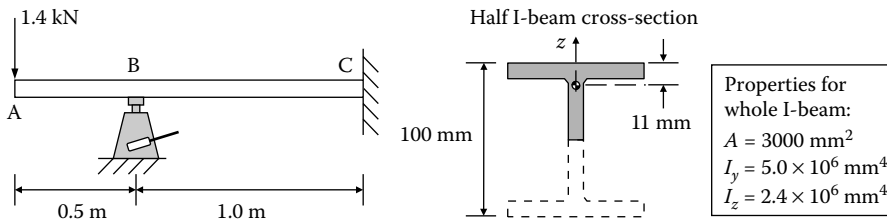
9.13 A cable with a length H, a cross-sectional area A, and modulus E is attached to the end of a cantilever beam with length L, second moment of area I, and modulus E (same modulus as the cable). The beam is loaded with a force per length of q_0, which includes the weight of the beam itself. Determine the force in the cable.
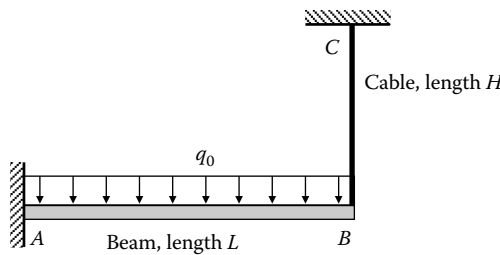
9.14 When the deck from Problem 9.11 is raised off of the ground and installed on the side of a house, the two outer joists are reinforced and remain rigid, but the center joist bends under the load of the 130 lb person (standing in the same place), providing a flexible support at the plank center. If the joist is a 2 in (width) × 8 in (depth) simply supported redwood beam 10 ft long, loaded at its center, what is the reaction force on each of the three plank supports?
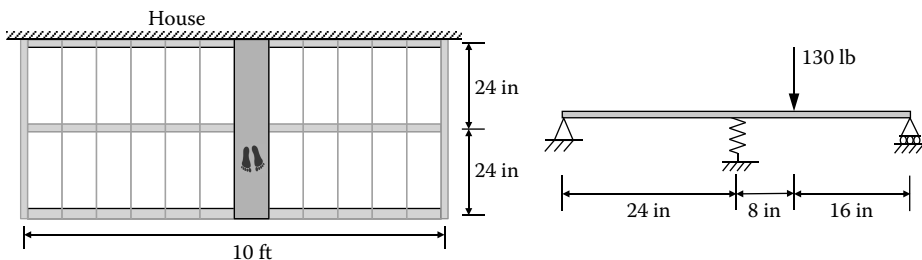
9.15 The deck of Problems 9.11 and 9.14 is not wide enough, and another $2\,\text{in} \times 8\,\text{in}$ joist is required to extend the planks to $72\,\text{in}$ long. What is the reaction force in each of the four plank supports when the person is standing at the location of one of them? The joists are both loaded at their centers.
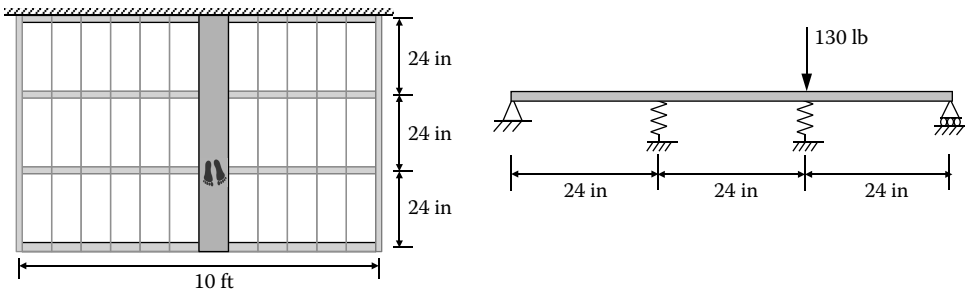
9.16 A simply supported beam of length L is subjected to loads that produce a symmetric deflection curve with maximum deflection at the midpoint of the span. How much strain energy U is stored in the beam if the deflection curve is (a) a parabola, or (b) a half wave of a sine curve?

9.17 Use Castigliano's second theorem to determine the tip deflection of this cantilever with a length L, a constant EI, and a linearly increasing load with a maximum force/length q_0. Confirm your result using Table 9.1.
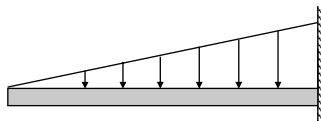
9.18 For the beam in Section 9.6 with two redundant supports, shown again here, determine the reaction forces (a) from the matrix equation in Section 9.6 and (b) using Castigliano's second theorem. For both, use $a = 3\,\text{ft}$, $L = 5\,\text{ft}$, and $P = 7\,\text{kips}$ to simplify expressions.
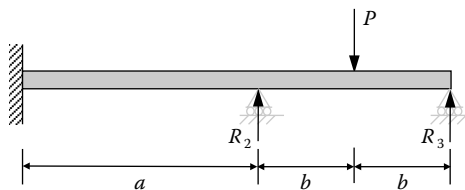
10

Case Study 4: Truss-Braced Airplane Wings

This case study provides a glimpse of the history of flight, as it considers how we can use elementary beam theory to explain one aspect of how airplanes work. We are all familiar with the Wright Brothers' famous Wright Flyer (Figure 10.1a), and we have likely seen similar early-twentieth-century planes in the movies or at air shows (Figure 10.1b). Note that these aircraft are *biplanes*: each has a pair of wings arrayed one above the other, with the wings connected by struts and cables that keep their respective wing spans in (relative) place. The bottom wing functions as a beam cantilevered from the bottom of the fuselage, while the top wing is connected to the bottom wing by the aforementioned struts and cables, but not to the fuselage itself. Note also in Figure 10.1b showing the Boeing Model 40 biplane, just how much shorter and stubbier (relative to the lengths of the fuselages) the wings of the biplane are, compared to those of the 787.

This marked change in appearance stems from two advances in technology. Biplanes like the Boeing 40 had evolved from the Wright Flyer in that pilots were no longer required to lie prone on an open, exposed platform—as Orville and Wilbur had done. Instead, there were enclosed fuselages made of steel tubular frames, covered first by fabric and later by metal panels, to provide aerodynamic smoothness and efficiency, as well as an indoor cargo space. Two technological advances enabled the transition from the Boeing 40 to the Boeing 707, 737, and 747, and to the composite 787: (1) the ability to make thin sheets of aluminum that could serve as aerodynamic surfaces; and (2) the ability to analyze, design, and manufacture *monocoque*[*] aircraft structures in which the framing and the surfaces were connected in a single coherent structure. Of course, we are focusing on the structural aspects only here and are ignoring parallel advances such as those in aircraft propulsion. The earliest monocoque aircraft, like the cargo and passenger DC3s and the famed British Spitfires, were driven by propellers well before the advent of the jet engine. And the Boeing 787 recognizes another advance in materials, namely the introduction of composites as the main structural material for the modern jetliner. For more on that subject, please see Chapter 15.

For the moment we will focus on wings and how we can use beam theory to model their behavior. When such cantilevered wings are subject to loads along their spans or lengths, they bend either upward or downward, depending on whether the net pressure exerted is upward or downward. In fact, we show in Figure 10.2 an extreme and telling version of such wing-beam behavior, namely, the shape of a B52 wing during a static deflection test. This dramatic photograph shows just how much a wing bends under flight loading, as it ranges from a maximum upward deflection of 6.7 m (22 ft) through a downward maximum of 3.6 m (12 ft). So we might think of this B52 wing as an exceptionally large and springy diving board! Both the picture and the behavior shown clearly suggest that even such a complex wing structure appears to act like—and so might be modeled as—a basic cantilever beam.

---

[*] This term combines the Latin word *mono* (for one) and the French word *coque*, meaning shell. It refers to a structural approach allowing an object's external "skin" to support loads.

(a)   (b)
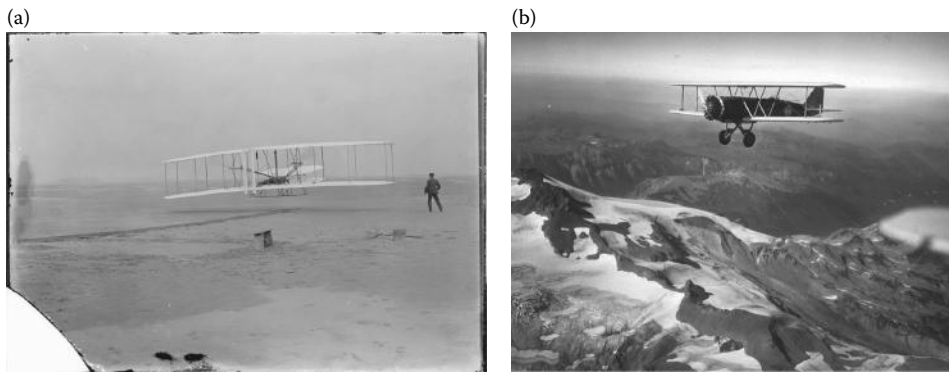
FIGURE 10.1
Two early biplanes: (a) the famed Wright Flyer in 1903 in Kitty Hawk, North Carolina. (Courtesy of the US Library of Congress.); and (b) the Boeing Model 40 flying over mountains, likely the Cascade Range, in the 1930s. Note the wing structure in 1940s is typical of aircraft during flying's formative years in the early part of the previous century. (Accessed from Seattle Municipal Archives via Wikipedia Commons on 6 April 2013.)
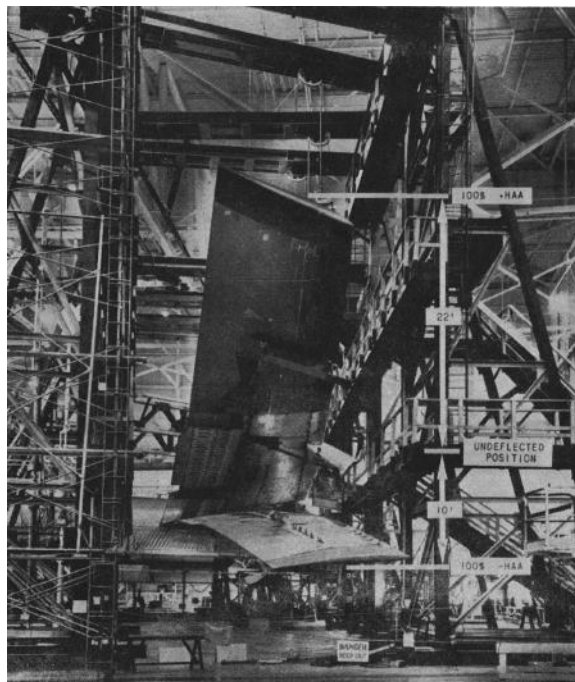
FIGURE 10.2
The deflected shapes, upward and downward, of a B52 wing show just how much an airplane wing can bend or deflect. (From R. L. Bisplinghoff and H. Ashley, Principles of Aeroelasticity, 1962, New York. Copyright Wiley-VCH Verlag GmbH & Co. KGaA. Reproduced with permission. Republished by Dover Publications, Mineola, New York, 1975, 2013. With permission.)

Of course, actual wing structures are not really as simple as the cantilevers we studied in Chapters 7 and 9: they have more complex cross sections and, more importantly, they are comprised of many moving parts. Anyone who has sat by the window of a modern jet, especially during take-off and landing, will have seen the flaps and ailerons that change the shape of the wings to provide the aerodynamic form appropriate to the particular flight regime. A truly discerning observer will also have noted that the wings themselves bend or flex during flight, just as cantilever beams do. In fact, for many purposes, we can treat an airplane's wings as simple cantilevers. This is the crux of what we do as engineers: we determine the appropriate level of detail needed to accurately model the behavior of a physical device or system, depending on the behavior we are trying to predict.

There is a limit to how long a simple cantilever can be before it bends or deflects too much. This deflection limit also limits the amount of lift that can be generated by the airflow around the wing, because that lift is proportional to the wing's (or cantilever's) surface area. If there is a limit to the lift generated, then there is a limit on how much weight, in terms of passengers and/or cargo, the plane can carry. That is an incentive to make the wing as long as we can without exceeding those deflection limits. Another incentive: a longer wing has greater lift efficiency. (To be technically correct, the lift efficiency increases with the wing's aspect ratio, but if we regard our wing model as having a constant effective width, we can increase the wing's aspect ratio and thus its lift efficiency by making it longer.) We can make the wing longer by providing it with additional support beyond its cantilever base or root. So can we make a wing significantly longer by adding a truss element to support the wing? If we did that, would the supporting base moment of the truss-supported wing be noticeably smaller than that of the unsupported wing? Further, would the bending deflection of the wing be noticeably smaller than that of its unsupported counterpart?

10.1 Modeling and Analysis

The aim of our modeling is to determine whether providing an additional intermediate support to a cantilever beam standing in for a real airplane wing will significantly reduce the clamping moment at its base, and so also its maximum bending stress, as well as its maximum deflection at its tip. For an elementary cantilever of original length L_0 subjected to a uniform load q_0 (see Table 9.1), the moment at the base and the deflection at the tip are, respectively, given by

$$M_0 = \frac{q_0 L_0^2}{2} \quad \text{and} \quad \Delta_{\text{tip}} = \frac{q_0 L_0^4}{8EI}. \tag{10.1}$$

We can use Equation 10.1 to generate simple estimates of how an unsupported wing might behave.

In order to use our model to predict the behavior of a truss-supported wing, we could insert a truss member between the fuselage and some point on the wing. In Figure 10.3, we show a wind-tunnel scale model of such a configuration which is being developed in a NASA technology demonstration project aimed at developing a greener aircraft. In Figure 10.4, we see a sketch of a beam-and-truss member model of the truss-braced wing concept. This truss-supported beam is statically indeterminate to the first degree because of the unknown force transmitted by the truss element in supporting the beam. We also
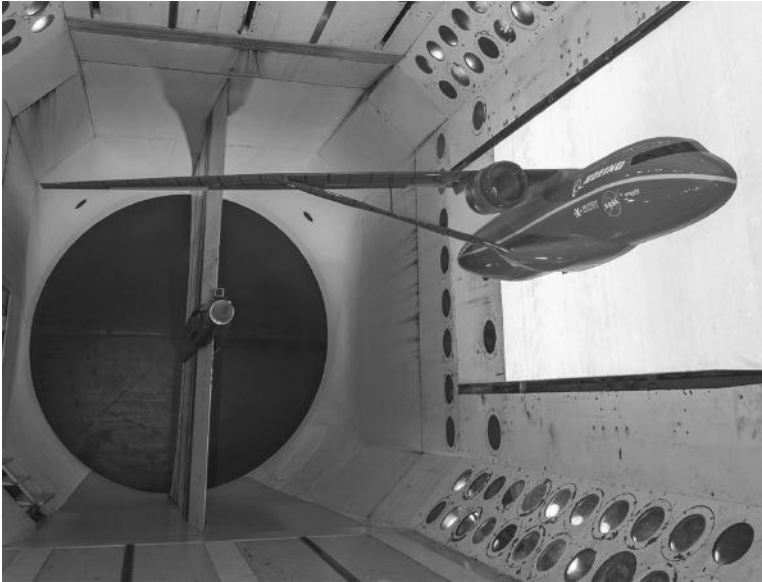
FIGURE 10.3
A wind tunnel scale model of a conceptualization of a truss-braced airplane wing. (Courtesy of NASA Langley/Sandie Gibbs.)

note that this supporting can be resolved into two components at its interesection with the beam or wing: one acts normal to the beam's centerline, and the other acts along the beam's axis. Since we presume beams to be much more flexible (i.e., much less stiff) when loaded normal to their axes than along their axes, we can then assume that the axial component of the truss support force will be carried without much noticeable axial deformation by the (relatively) high axial stiffness of the beam. This allows us to simplify our model still further to consider only an elementary cantilever supported by a vertical supporting spring, as shown in Figure 10.5. This spring-supported cantilever is still indeterminate to the first degree, but we can now focus only on its transverse (in level flight, vertical) deflection.

We can determine the *redundant* or unknown truss force for the configuration just as we did for the spring-supported beam in Figure 9.10a, only here we must recognize that the
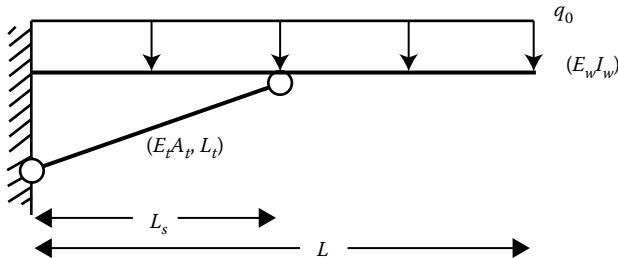
FIGURE 10.4
A cantilever beam simulating a wing of length $L_0 = L_w$ that has been increased to a new length $L = L_0 + \Delta L_0$. It has a bending stiffness $E_w I_w$ and is subject to a uniform load q_0 and supported by a truss element (i.e., a bar) of length L_t, extensional stiffness $E_t A_t$, and transmitting a supporting force F_t ($F_t > 0$ in tension).
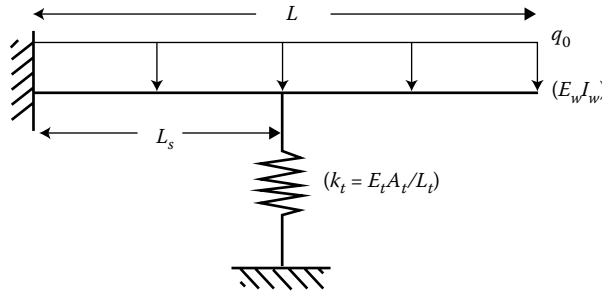
FIGURE 10.5
A cantilever beam simulating a wing of length $L_0 = L_w$ that has been increased to a new length $L = L_0 + \Delta L_0$. It has a bending stiffness $E_w I_w$ and is subject to a uniform load q_0 and supported by a transverse (i.e., vertical) spring with a spring stiffness $k_t = E_t A_t / L_t$ that encapsulates the stiffness of the truss element it is modeling.

spring occurs at a distance L_s from the base, where, obviously, $0 \leq L_s \leq L$, and where L is the new length of the now-spring-supported beam $L = L_0 + \Delta L_0$. Then the unsupported cantilever's deflection at that point is, from Table 9.1,

$$w(L_s) = \frac{q_0 L^4}{24 E I} \left(\frac{L_s}{L}\right)^2 \left(\left(\frac{L_s}{L}\right)^2 - 4\left(\frac{L_s}{L}\right) + 6\right), \qquad (10.2a)$$

or, in terms of the dimensionless length ratio $\alpha = L_s/L$,

$$w(L_s) = \frac{q_0 L^4}{24 E I} \alpha^2 \left(\alpha^2 - 4\alpha + 6\right). \qquad (10.2b)$$

Using Equation 10.2b, we can then relate this deflection to the total load $q_0 L$ on the beam in terms of a stiffness parameter for the uniform load on the beam (or wing):

$$k_{wq_0} = \frac{24 E_w I_w}{L_s^3} \left(\frac{\alpha}{\alpha^2 - 4\alpha + 6}\right), \qquad (10.3)$$

so that

$$q_0 L = k_{wq_0} w(L_s) \quad \text{and/or} \quad q_0 L_s = \alpha k_{wq_0} w(L_s). \qquad (10.4)$$

We also introduce the axial stiffness of the truss member that forms the support

$$k_t = \frac{E_t A_t}{L_t}, \qquad (10.5)$$

and the bending stiffness of that length of the beam (i.e., wing) that is within the support (which is obtained from the tip deflection of a cantilever of length L_s),

$$k_{wb} = \frac{3 E_w I_w}{L_s^3}. \qquad (10.6)$$

Now we can use the shorthand of the three stiffnesses just defined to calculate the redundant truss force R_t by enforcing compatibility as we did in Equation 9.34. We require that

the net bending deflection of the beam under the downward uniform load q_0 and the upward support force R_t be compatible with (i.e., the same as) the extension of its truss member support:

$$R_t \left(\frac{1}{k_t} + \frac{L_s^3}{3EI} \right) = q_0 L \left(\frac{1}{k_{wq_0}} \right). \tag{10.7}$$

We then solve for the redundant force:

$$R_t = \frac{q_0 L}{8} \left(\frac{\alpha^2 - 4\alpha + 6}{\alpha(1 + k_{wb}/k_t)} \right) = \frac{q_0 L_s}{8} \left(\frac{\alpha^2 - 4\alpha + 6}{\alpha^2(1 + k_{wb}/k_t)} \right). \tag{10.8}$$

There are several limiting cases of Equation 10.8 that can be demonstrated to verify this result (see Problems 10.4 and 10.8).

Finally, having made our statically indeterminate beam into a determinate system by virtue of Equation 10.8, it is now a straightforward matter to calculate the moment at the cantilever base and the deflection at the free tip of the supported cantilever. That moment and deflection are, respectively,

$$M_L = \frac{q_0 L^2}{2} \left(\frac{1 - (k_t/4k_{wb})(\alpha^2 - 4\alpha + 2)}{1 + k_t/k_{wb}} \right) \tag{10.9}$$

and

$$\Delta_{\text{tip}} = \frac{q_0 L^4}{8 E_w I_w} \left(1 - \frac{(3\alpha - \alpha^2)(\alpha^2 - 4\alpha + 6)}{6(1 + k_{wb}/k_t)} \right). \tag{10.10}$$

Note that the stiffness ratio k_t/k_{wb} appears directly in Equation 10.9, while that ratio's reciprocal appears in Equation 10.10.

Equations 10.9 and 10.10 can be compared with their counterparts for the elementary unsupported cantilver given in Equation 10.1. However, in order to assess whether the added support makes a difference, or estimate how much of a difference it might make, we will use these results in a somewhat more refined way. Recall that the argument we proposed was that the support would allow a longer wing, so we can use Equations 10.1 and 10.9 to calculate the increase we would achieve in the beam length if we required only that the moment (and so the bending stress) remained the same. That length change ΔL_0 that can be added to the original wing length L_0 is found to be

$$\frac{\Delta L_0}{L_0} = \left[\frac{1 + k_t/k_{wb}}{1 - (k_t/4k_{wb})(\alpha^2 - 4\alpha + 2)} \right]^{1/2} - 1. \tag{10.11}$$

In a similar manner, we can approximate the change in the value of the tip deflection from Equations 10.1 and 10.10 as (see Problem 10.8):

$$\Delta(\Delta_{\text{tip}}) \approx -\frac{q_0 L_0^4}{8 E_w I_w} \left(1 + 4\frac{\Delta L_0}{L_0} \right) \left[\frac{(3\alpha - \alpha^2)(\alpha^2 - 4\alpha + 6)}{6(1 + k_{wb}/k_t)} \right]$$

$$\approx -\frac{q_0 L_0^4}{8 E_w I_w} \left[\frac{(3\alpha - \alpha^2)(\alpha^2 - 4\alpha + 6)}{6(1 + k_{wb}/k_t)} \right]. \tag{10.12}$$

10.2 What Does Our Model Tell Us?

Equations 10.11 and 10.12 show the potential for both increasing the wing length (i.e., $\Delta L_0/L_0 \geq 0$) and decreasing the tip deflection (i.e., $\Delta(\Delta_{\text{tip}}) \leq 0$) by adding the truss support, although there are some limits. In particular, the dimensionless location of the truss support must be in the range $0 \leq \alpha \leq 1$.* The polynomial $\alpha^2 - 4\alpha + 2$ vanishes at $\alpha \approx 0.586$ and changes sign as it passes through that point, being positive for $\alpha < 0.586$ and negative for $\alpha > 0.586$. Consequently, the added support serves to increase the length *only* when $\alpha < 0.586$, and the *smallest* increase in wing length occurs with the support placed at $\alpha = 0.586$, for which $\alpha^2 - 4\alpha + 2 = 0$ (and $\alpha^2 - 4\alpha + 6 \approx 4$). Thus, the "optimized" changes in wing length and tip deflection when the truss suport is placed at that location are, respectively,

$$\frac{\Delta L_0}{L_0}\bigg|_{\alpha=0.586} = \sqrt{1 + k_t/k_{wb}} - 1 \tag{10.13}$$

and

$$\Delta(\Delta_{\text{tip}})\bigg|_{\alpha=0.586} \approx -\frac{q_0 L_0^4}{8 E_w I_w}\left[\frac{0.943}{1 + k_{wb}/k_t}\right]. \tag{10.14}$$

Consider the implications of the foregoing results. This rough calculation suggests that the truss bar should supply a stiffness such that $k_t < 4k_{wb}/(\alpha^2 - 4\alpha + 2)$ in order for the additional length estimate in Equation 10.13 to be real. Given what we just noted about the magnitude of the polynomial in Equation 10.11, this effectively means that the truss bar stiffness must be positive and finite. If, for example, the truss bar provided one-half of the bending stiffness of the supported part of the beam (i.e., $k_t = 0.50k_{wb}$), then the resulting length (and thus lift area) gain is about 22%, and the corresponding tip deflection is reduced some 31%.

The real question is, just how big should the stiffness ratio k_t/k_{wb} be to make a difference in an actual plane? From Equations 10.5 and 10.6, we see that

$$\frac{k_t}{k_{wb}} = \frac{1}{3}\left(\frac{E_t}{E_w}\right)\left(\frac{A_t L_s^3}{I_w L_t}\right). \tag{10.15}$$

Since it seems reasonable to expect that the truss and wing would be made of the same material(s), then we really need to know or estimate the value of

$$\frac{k_t}{k_{wb}}\bigg|_{E_t=E_w} = \frac{1}{3}\left(\frac{A_t L_s^3}{I_w L_t}\right). \tag{10.16}$$

Consider the Boeing 737–800. It has an initial wing length $L_0 = 75\,\text{ft} = 22.86\,\text{m}$, with a second area moment that drops from $1.2635\,\text{ft}^4$ at the root to $0.00085\,\text{ft}^4$ at the tip,

---

* It may seem from Equation 10.11 that we should be attentive to the case of $\alpha^2 - 4\alpha + 2 = -4$, which would make $\Delta L_0 = 0$ and control the sign of $\Delta(\Delta_{\text{tip}})$. However, since $0 \leq \alpha \leq 1$, this case is not physically possible.

with an average value $I_{w/av} = 0.2980\,\text{ft}^4 = 0.00863\,\text{m}^4$. If we take $k_t/k_{wb} = 0.50$ again, then Equation 10.13 states that the length increase due to a truss support is

$$\Delta L_0\big|_{\alpha=0.586} = \left(\sqrt{1 + k_t/k_{wb}} - 1\right) L_0 = (0.2247)(75) = 16.86\,\text{ft}. \qquad (10.17)$$

This means that we would take our wing length as $L_w = L = L_0 + \Delta L_0 = (75 + 16.86) = 91.86\,\text{ft}$. Since we assumed $\alpha = 0.586$ for the minimum length benefit, the supported wing length is $L_s = 53.83\,\text{ft}$ and the truss dimensions must then be

$$\frac{A_t}{L_t} = 3\left(\frac{0.2980}{(53.83)^3}\right)\left(\frac{k_t}{k_{wb}}\bigg|_{E_t=E_w}\right)\text{ft} = 5.734 \times 10^{-6}\left(\frac{k_t}{k_{wb}}\bigg|_{E_t=E_w}\right)\text{ft}. \qquad (10.18)$$

Figure 10.4 shows that $L_t > L_s$, so taking $L_t = 57.42\,\text{ft}$ (which amounts to assuming a fuselage height just over 20 ft), we see that Equation 10.18 suggests that our stiffening bar needs to have a very small area:

$$A_t = 5.734 \times 10^{-6}(57.42)(0.50)\,\text{ft}^2 = 1.624 \times 10^{-4}\,\text{ft}^2 = 0.153\,\text{cm}^2. \qquad (10.19)$$

Thus, a tiny truss member produces a 22% increase in our model wing length and a corresponding increase in the wing's aspect ratio, without accounting for potential penalties due to the truss' additional weight or its added aerodynamic drag.

We can also use the above model results differently. Rather than seeking values of $\Delta L_0/L_0$ for a specified k_t/k_{wb}, we can ask what truss stiffness (or stiffness ratio) we need to achieve a specified increase in wing length. We look at this by rewriting Equation 10.13 as

$$\frac{k_t}{k_{wb}} = \left(1 + \frac{\Delta L_0}{L_0}\right)^2 - 1. \qquad (10.20)$$

To achieve a 22% increase in length, we would thus need a truss $k_t = 0.49k_{wb}$, which basically confirms our earlier calculation. To achieve a 50% increase in length, we require $k_t = 1.25k_{wb}$, a much larger stiffness that does seem unreasonable, within the scope of this model.

10.3 Conclusions

It is important to keep in mind that the analysis we have just presented is not only an incomplete model of the actual behavior of a real truss-braced wing, but it is also not even a remotely complete analysis of the structural mechanics of such a wing. We did not study the effects of a truss' additional weight or its extra drag, or the possibility that the truss bar might buckle. We only exercised a simple model in a "back of the envelope" calculation intended to answer only one question: From an elementary structural mechanics view, is a significant increase in wing length—and lift area— physically plausible with a truss-braced wing? If this simple model had shown that there would be no appreciable gain realizable with such a brace, we might ask whether it could be worth investing resources in further exploration. But having found some noticeable positive

gain, we found that in principle such a truss-based wing is realizable, which suggests that a truss-supported wing does warrant further exploration. (We also developed a simple calculator that can be used to validate any numbers we might generate with more complex computer models.) But we must always keep in mind that the design of any serious engineering artifact requires mediating among competing objectives and making compromises. So while there may be a clear structural advantage, we should expect drawbacks (e.g., additional drag from the truss element) that must be balanced against perceived gains.

PROBLEMS

10.1 Determine the support reactions of a simple beam of length L under both a counter-clockwise moment M_0^* at the left support ($x = 0$) and a uniform load q_0 applied over its length.

10.2 What would the magnitude of the applied moment M_0^* in Problem 10.1 have to be in order to make the slope at $x = 0$ vanish?

10.3 What would be the support reaction at $x = L$ for the beam in Problem 10.2? Does that compare—and if so, how—with the result given in Equation 10.7?

10.4 What is the value of R_t in Equation 10.8 when $\alpha \to 0$?

10.5 What is the value of R_t in Equation 10.8 when $\alpha \to 1$?

10.6 What are the values of M_L and Δ_{tip} in Equations 10.9 and 10.10, respectively, when $\alpha \to 0$?

10.7 What are the values of M_L and Δ_{tip} in Equations 10.9 and 10.10, respectively, when $\alpha \to 1$?

10.8 Identify and estimate the approximations being made in the two forms of Equation 10.12.

References

R. L. Bisplinghoff and H. Ashley, *Principles of Aeroelasticity*, John Wiley & Sons, New York, 1962. Republished by Dover Publications, Mineola, New York, 1975, 2013.

M. K. Bradley and C. K. Droney, *Subsonic Ultra Green Aircraft Research: Phase 1 Report*, NASA Contractor Report CR-2011-216847, Boeing Research and Technology, Huntington Beach, CA, April 2011.

D. Stinton, *The Anatomy of the Aeroplane*, American Elsevier Publishing Company, New York, 1966.

G. Warwick, "NASA, Boeing Test Low-Drag Truss-Braced Wing Concept," *Aviation Week and Space Technology*, 2014.

P. P. Wegener, *What Makes Airplanes Fly?: History, Science and Applications of Aerodynamics*, Springer-Verlag, New York, 1991.

11

Instability: Column Buckling

In our analysis of the internal response to external loading on bars, beams, pressure vessels, and shafts in torsion, we have had two primary concerns: the *stiffness* and the *strength* of the structure. By strength, we mean the ability of our structure to support the required loads without experiencing excessive stress; by stiffness, we mean its ability to support the required loads without undergoing excessive deformations. In practice, we have a third concern: the *stability* of our structure, by which we mean its ability to support the required loads without experiencing a sudden change in configuration.

The instability known as *buckling* typically occurs when forces much lower than those necessary to exceed material yield stresses are applied. Buckling can occur whenever a slender* structural member is subjected to compression. These forces are applied axially, as shown in Figure 11.1. Here, by holding a metal ruler between his palms, a man has been able to induce instability, and the ruler fails as a structural element.

The most common occurrence of this kind of loading, and of buckling instability, is in columns. Figure 11.2 shows some examples of structural columns: the ancient Greek Parthenon contained columns that were constructed of stacked stones, *not* single slender supports; the nineteenth-century use of iron as a structural material led to slender metal compressive members such as those on the Welsh viaduct shown, and these members are susceptible to buckling, as are the concrete columns of Markle Hall. Figure 11.3 shows failed columns.

11.1 Euler's Formula

Consider a column of length L supported by pin supports at both ends, subjected to a compressive axial load P that acts through the centroid of the cross section, as in Figure 11.4a. We would like to determine the critical value, P_{cr}, for which the initial position is no longer stable. Once P exceeds P_{cr}, any small perturbation or misalignment causes the column to buckle, taking on the sort of curvature illustrated in Figure 11.4b. Our method of finding P_{cr} is to determine the conditions under which the geometry of Figure 11.4b is possible. We will find that unlike the problems we have solved so far, the solution involves nonlinearity.

We approach this column as a vertical beam subjected not to a transverse load (as we may have come to expect), but instead to an axial load. We use x to denote the distance from the top, along the beam's initial elastic curve (the shape of the neutral axis). The column's deflection w in the z-direction denotes the lateral deflection of the elastic curve from its original position, just as it did for beams. We make an imaginary cut at some point

---

* We have just developed a theory of beam bending and deflection that applies to slender beams, for which the cross-sectional dimensions are much less than the axial length; for columns, we continue to work under this assumption, and we quantify a measure of slenderness.
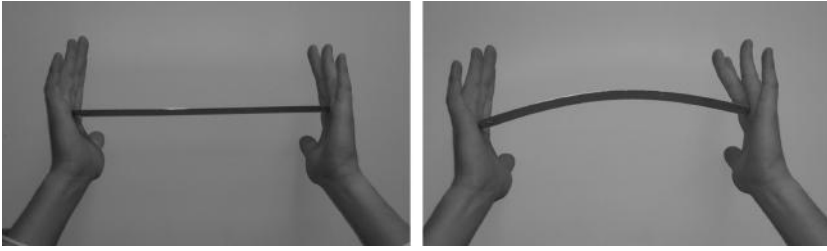
FIGURE 11.1
At left, application of compressive axial force to metal ruler. At right, a small compressive load causes the ruler to "buckle."

FIGURE 11.2
Examples of columns: Parthenon (left); Crymlyn Viaduct (middle); Markle Hall, Lafayette College (right).

FIGURE 11.3
Examples of column failure by buckling, *top row*: Columns in Salisbury cathedral; freeway supports damaged in 1971 San Fernando, CA earthquake; *Bottom row*: Box beam column damage in 1985 Mexico City earthquake; Wind turbine column failure; and buckling of thin-walled pressure vessel, which is not described by the models in this chapter.
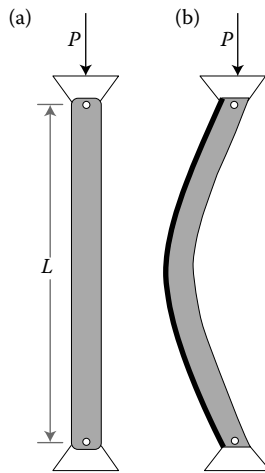
FIGURE 11.4
(a) Beam/column under compression; (b) buckled geometry.

C along this curve, as in Figure 11.5, and observe that at this point the internal axial force is P and the internal bending moment is $M = Pw$.

We understand that this internal bending moment—which is unusual for us because it is a function of the deflection w of the column's axis—also may be related to the deflection w using Equation 9.9:

$$\frac{\mathrm{d}^2 w}{\mathrm{d}x^2} = -\frac{M}{EI} = -\frac{P}{EI}w. \tag{11.1}$$
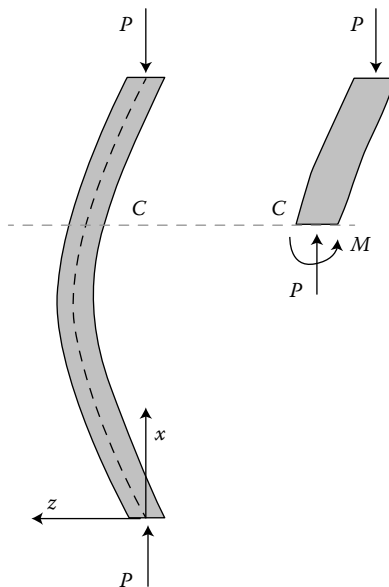
FIGURE 11.5
Method of sections on buckling column.

We note that the second moment of area I of the cross section in this case may be I_y or I_z and will discuss how to choose the appropriate I once we have derived an expression for P_{cr}.

We rearrange Equation 11.1 as

$$\frac{d^2 w}{dx^2} + \frac{P}{EI} w = 0, \tag{11.2}$$

and find that it is an ordinary differential equation with whose solution we are likely familiar:

$$w(x) = A \sin \sqrt{\frac{P}{EI}} x + B \cos \sqrt{\frac{P}{EI}} x. \tag{11.3}$$

To move from this general solution to a specific expression for the buckling column, we apply the relevant boundary conditions. These are specific to the column supports, which for our column (Figure 11.4a) are pins at both ends. At the bottom of our beam, $x = 0$, and we have $w = 0$ since the pin support does not allow any deflection. We also have $w = 0$ at the top support, where $x = L$. The first condition, $w(x = 0) = 0$, requires that $B = 0$. To have $w(x = L) = 0$, we require

$$A \sin \sqrt{\frac{P}{EI}} L = 0. \tag{11.4}$$

This statement holds if either $A = 0$, or $\sin \sqrt{(P/EI)} L = 0$. If $A = 0$, the general solution is $w = 0$, and the column remains straight. Since we are modeling the buckling phenomenon, we are concerned with satisfying the second condition. Due to the periodic nature of $\sin x$, this requires that

$$\sqrt{\frac{P}{EI}} L = n\pi,$$

where n is any integer. Solving for the force P that will make this happen, we find

$$P = \frac{n^2 \pi^2 EI}{L^2}. \tag{11.5}$$

This suggests that there are many *modes* of buckling, each with a different value of n, as shown in Figure 11.6. We are particularly interested in the first mode, the smallest load that can cause buckling, which corresponds to $n = 1$. Therefore, the critical load P_{cr} for the pinned–pinned column of Figures 11.4 and 11.5 is

$$P_{cr} = \frac{\pi^2 EI}{L^2}. \tag{11.6}$$

This result is known as *Euler's formula*, as Swiss mathematician Leonhard Euler first derived it in 1744. Applying this force makes it possible for the shape of the neutral axis of the column to be described by $w = A \sin \frac{\pi x}{L}$. Note that we have not determined the value of the coefficient A, which is the column's maximum deflection w_{max}. We will not be able to solve for this deflection, but our goal was only to determine the force that would cause this type of instability to occur.
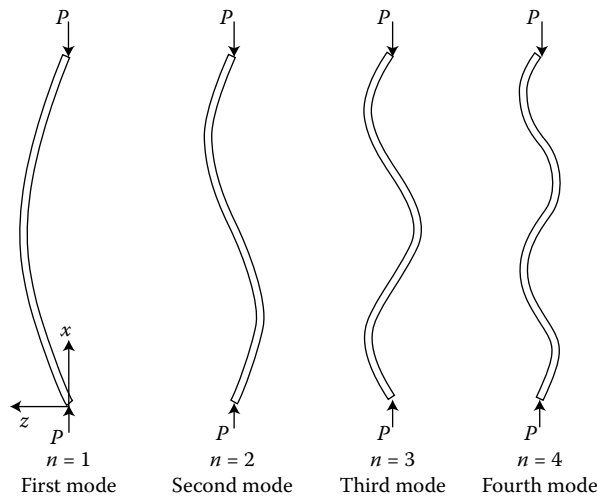
FIGURE 11.6
Deflection distributions in the first four buckling modes.

The second moment of area I in Euler's formula should be taken about the axis around which the column bends. This is often apparent from the way the column is supported; when it is not, we recognize that a buckling column bends about the principal axis of its cross section with the smaller second moment of area and make our calculations accordingly. When calculating the critical buckling load, one should first determine whether I_y or I_z is the smaller second moment of area I for the cross section.

We note that Euler's formula (Equation 11.6) as just derived applies to the particular case of a column with two pinned ends. The column ends are thus free to rotate at the ends where the loads P are applied; in other words, there are no reactions at the ends other than P. This affected the boundary conditions we used in obtaining P_{cr}. For different supports, and thus different boundary conditions, the value of P_{cr} is different. We codify these differences by using an *effective length* L_e in the place of L in Euler's formula, where the relationship between L_e and L depends on the end supports:

$$P_{cr} = \frac{\pi^2 E I}{L_e^2}. \tag{11.7}$$

Values of the effective length for a variety of supports are tabulated in Table 11.1.

TABLE 11.1

Effective Length L_e for Different End Supports

End Conditions	Effective Length
Fixed–free	$2L$
Pinned–pinned	L
Fixed–pinned	$0.7L$
Fixed–fixed	$0.5L$

The value of normal stress corresponding to the critical load is called the critical stress, σ_{cr}. We divide Euler's formula by the column's cross-sectional area:

$$\sigma_{cr} = \frac{P_{cr}}{A} = \frac{\pi^2 E I}{L_e^2 A}. \tag{11.8}$$

Next, we set the second moment of area $I = Ar^2$, where r is the cross-sectional area's *radius of gyration*. We obtain the radius of gyration of various shapes using its definition, $r = (I/A)^{1/2}$:

$$\sigma_{cr} = \frac{\pi^2 E Ar^2}{L_e^2 A} = \frac{\pi^2 E r^2}{L_e^2} = \frac{\pi^2 E}{(L_e/r)^2}. \tag{11.9}$$

The quantity L_e/r is known as the column's *slenderness ratio*. The critical stress is proportional to the elastic modulus of the material used and is inversely proportional to the square of this ratio. For sufficiently slender columns, σ_{cr} can be much lower than the material's yield stress, and the column almost certainly fails due to buckling. If this critical buckling stress is greater than the material's yield stress, the column in question likely yields in compression before it has the opportunity to buckle—this is often true for short, stubby columns.

In practice, loads are rarely applied as we have modeled our P—a perfectly aligned axial load. To more realistically assess the likelihood of buckling, we must develop a model that includes the effects of load eccentricity.

11.2 Effect of Eccentricity

The lines of action of applied forces P are generally not through the cross section's centroid, as we had optimistically modeled them in the previous section. We now analyze the potential for buckling when an *eccentric*, or off-center, load is applied, again beginning with a beam/column that is free to rotate at pinned ends. We see that this off-center load P applies a moment to the column even when it is straight. As illustrated in Figure 11.7, the force P has a moment arm equal to its eccentricity e. We can thus replace the off-center P by a centric load, also with magnitude P, and a moment $M = Pe$, as shown in Figure 11.7. No matter how small either P or e is, this moment M will cause some bending of the column. In a sense, we are calculating not how to make the column stay straight but how much bending is permissible to maintain a normal stress $\sigma < \sigma_{cr}$ and a tolerable deflection w_{max}. As expected from the previous section, the solution to this question comes from a nonlinear expression. This means that we cannot use superposition and add the effect of M to our understanding of the solution for P alone, we must start from the beginning with both loads considered together.

Note that an eccentrically loaded column *will* deflect, unlike a centrically loaded column which *may* deflect. While the loading in Section 11.1 could potentially cause the instability of buckling, in eccentric loading we are certain to observe deflection.

Again, we want to obtain the equation of the column's elastic curve. We begin with the method of sections in an effort to find the internal bending moment at some arbitrary position x. Figure 11.8 indicates that the internal bending moment necessary to keep this
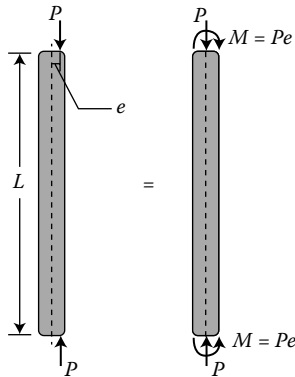
FIGURE 11.7
Modeling an eccentric load P.

section in equilibrium is $M(x) = Pw + Pe$. We proceed with the second-order equation for the column's deflection $w(x)$:

$$\frac{\mathrm{d}^2 w}{\mathrm{d}x^2} = -\frac{M}{EI} = -\frac{P}{EI}w - \frac{P}{EI}e, \tag{11.10}$$

or

$$\frac{\mathrm{d}^2 w}{\mathrm{d}x^2} + \frac{P}{EI}w = -\frac{P}{EI}e. \tag{11.11}$$
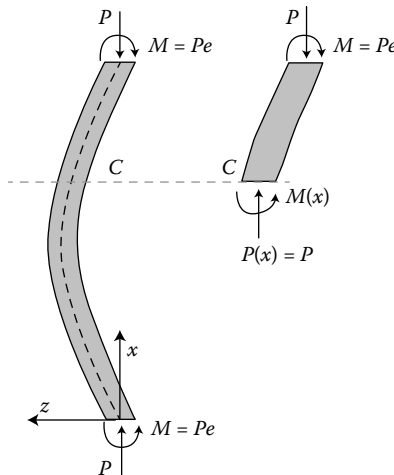
FIGURE 11.8
Method of sections for eccentric P.

The left-hand side of this equation is the same as the homogeneous ordinary differential equation we solved for centric loading, whose solution we already know. We add to this general solution the constant $-e$ that solves the nonhomogeneous equation, and have

$$w(x) = A \sin \sqrt{\frac{P}{EI}} x + B \cos \sqrt{\frac{P}{EI}} x - e. \tag{11.12}$$

Again, we make use of the boundary conditions to identify the unknown constants. At $x = 0$, we have $w = 0$, which requires that $B = e$. At $x = L$, we also have $w = 0$, so that

$$A \sin \sqrt{\frac{P}{EI}} L = e \left(1 - \cos \sqrt{\frac{P}{EI}} L \right). \tag{11.13}$$

We make use of the trigonometric identities

$$\sin \sqrt{\frac{P}{EI}} L = 2 \sin \sqrt{\frac{P}{EI}} \frac{L}{2} \cos \sqrt{\frac{P}{EI}} \frac{L}{2} \quad \text{and} \quad 1 - \cos \sqrt{\frac{P}{EI}} L = 2 \sin^2 \sqrt{\frac{P}{EI}} \frac{L}{2}$$

to write

$$A = e \tan \sqrt{\frac{P}{EI}} \frac{L}{2}, \tag{11.14}$$

which allows us to write the equation of the elastic curve:

$$w(x) = e \left(\tan \sqrt{\frac{P}{EI}} \frac{L}{2} \sin \sqrt{\frac{P}{EI}} x + \cos \sqrt{\frac{P}{EI}} x - 1 \right). \tag{11.15}$$

We obtain the value of the maximum deflection $w_{\max}$ by evaluating this expression at $x = L/2$:

$$w_{\max} = e \left[\sec \left(\sqrt{\frac{P}{EI}} \frac{L}{2} \right) - 1 \right]. \tag{11.16}$$

The nature of the secant curve tells us that the value of $w_{\max}$ becomes infinite when

$$\sqrt{\frac{P}{EI}} \frac{L}{2} = \frac{\pi}{2}.$$

While the column deflection does not actually become infinite, it becomes unacceptably large at this condition. We can therefore find the critical force P_{cr} that satisfies the expression:

$$\sqrt{\frac{P_{\text{cr}}}{EI}} \frac{L}{2} = \frac{\pi}{2}.$$

It is

$$P_{\text{cr}} = \frac{\pi^2 EI}{L^2}, \tag{11.17}$$

which is Euler's formula for the buckling of a column under centric loading. Knowing this allows us to recast the maximum deflection in terms of this critical load:

$$w_{\max} = e \left[\sec \left(\frac{\pi}{2} \sqrt{\frac{P}{P_{\mathrm{cr}}}} \right) - 1 \right].$$ (11.18)

The form of Equation 11.18 is useful, since it expresses deflection as a function of the ratio of the applied load P to the critical load P_{cr}, and if this ratio is 1, then the column has surely failed. Of course, as mentioned before, we are certain that an eccentrically loaded column will deflect in this manner—it is not just a possibility as for a normally loaded column. Therefore, the notion of a critical stress is not as relevant as our old friend the material's yield stress. The maximum normal stress in the column occurs where the bending moment is maximized, that is, at $x = L/2$. We obtain this stress by superposing the stress due to P with the bending stress,

$$\sigma_{\max} = -\frac{P}{A} + \frac{M_{\max} c}{I},$$ (11.19)

where $M_{\max}$ is $Pw_{\max} + Pe = P(w_{\max} + e)$. We plug in our expression for $w_{\max}$ and have

$$\sigma_{\max} = -\frac{P}{A} \left[1 + \frac{ec}{r^2} \sec \left(\sqrt{\frac{P}{EI}} \frac{L}{2} \right) \right],$$ (11.20)

or

$$\sigma_{\max} = -\frac{P}{A} \left[1 + \frac{ec}{r^2} \sec \left(\frac{\pi}{2} \sqrt{\frac{P}{P_{\mathrm{cr}}}} \right) \right].$$ (11.21)

Since the applied force P is compressive, the maximum normal stress is compressive, as reflected by the negative sign in the previous expressions. Just as for centric loading, the second moment of area I also used to calculate the column's radius of gyration is the smaller of I_y and I_z for the column cross section.

If the end conditions for a particular column differ from the pinned–pinned supports assumed in this model, then L should be replaced by the appropriate effective length L_{e}.

11.3 Examples

EXAMPLE 11.1

An aluminum column of length L and rectangular cross section has a fixed end B and supports a centric axial load at A. Two smooth and rounded fixed plates restrain end A from moving in one of the vertical planes of symmetry but allow it to move in the other plane. (1) Determine the ratio a/b of the two sides of the cross section corresponding to the most efficient design against buckling. (2) Design the most efficient cross section for the column, knowing that $L = 50\,\mathrm{cm}$, $E = 70\,\mathrm{GPa}$, $P = 22\,\mathrm{kN}$ and that a safety factor of 2.5 for buckling is required.
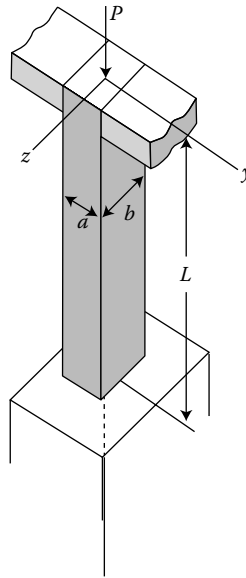
Given: Loading and support conditions for column; safety factor; length and elastic modulus.

Find: Optimal rectangular cross section of column.

Assume: Hooke's law applies (we have assumed constant E in derivations).

Solution

Figure on next page indicates that we must consider buckling in both the xy- and xz-planes and that due to the nature of the support at A, the critical load and the prospect of buckling will be different in the two planes. As the supports allow end A to move freely in the z-direction, for buckling in the xz-plane we have a fixed–free support combination; the supports constrain motion in the y-direction but do not provide a reaction moment so that in the xy-plane we have a fixed–pinned support.

1. For buckling in the xy-plane, due to the fixed–pinned support combination, we find from Table 11.1 that the effective length of the column with respect to buckling in this plane is $L_e = 0.7L$. And we have

$$I_z = \frac{1}{12}ba^3.$$

   For buckling in the xz-plane, the column sees a fixed–free support situation, so the effective length is $L_e = 2L$. And

$$I_y = \frac{1}{12}ab^3.$$

   The most efficient design is that for which the critical buckling loads corresponding to the two possible modes of buckling are equal; neither mode is preferred. This is the case if

$$\frac{\pi^2 E \left(1/12ba^3\right)}{(0.7L)^2} = \frac{\pi^2 E \left(1/12ab^3\right)}{(2L)^2}.$$

From which we determine the ratio $a/b = 0.35$.

2. A safety factor of 2.5 means that for our design with specific parameters we must have a critical load that is 2.5 times the load P that will actually be applied. So $P_{cr} = 2.5P = 2.5(22\,\text{kN}) = 55\,\text{kN}$.

Using the ratio a/b found above, and the buckling criterion for the xz-plane (xy is the same), we have

$$P_{cr} = 55\,\text{kN} = \frac{\pi^2 E \left((1/12)(0.35b)b^3 \right)}{(2L)^2}.$$

With the given values for E and L, we can solve for $b = 4.1\,\text{cm}$ and $a = 0.35b = 1.4\,\text{cm}$.

EXAMPLE 11.2

An 8-ft length of structural tubing has the illustrated cross section and geometric properties. Using Euler's formula and a safety factor of 2, determine the allowable centric load for the column and the corresponding normal stress. Assuming that this allowable load is applied as shown at a point 0.75 in from the geometric axis of the column, determine the horizontal deflection of the top of the column and the maximum normal stress in the column. Use $E = 29 \times 10^6$ psi.
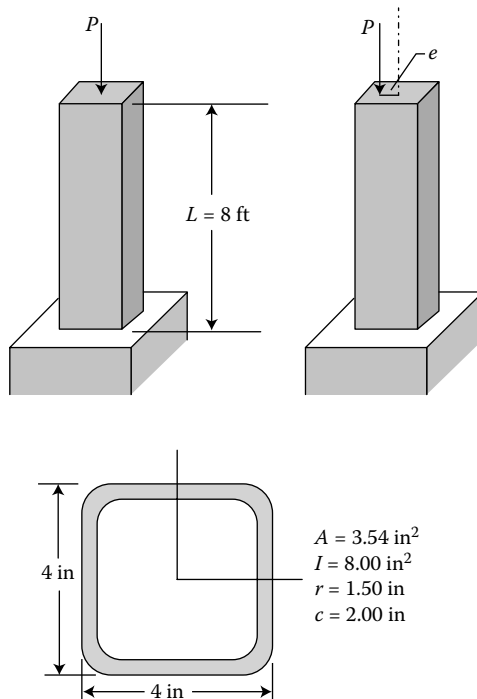
Given: Geometry of column, including second moment of area; safety factor.

Find: P_{cr} and σ_{cr}; w_{max} and σ_{max} if $P_{cr}/2$ applied eccentrically.

Assume: Hooke's law applies.

Solution

Since the column has one fixed and one free end, the effective length is $L_e = 2L = 16\,\text{ft} = 192\,\text{in}$. Using Euler's formula, we find the critical load to be

$$P_{cr} = \frac{\pi^2 E I}{L_e^2} = \frac{\pi^2 (29 \times 10^6\,\text{psi})(8.00\,\text{in}^4)}{(192\,\text{in})^2} = 62\,\text{kips}.$$

Since we are asked to use a safety factor of 2, our allowable centric load is then $P_{cr}/2 = 31\,\text{kips}$. The corresponding normal stress is

$$\sigma = \frac{P_{\text{allow}}}{A} = \frac{31\,\text{kips}}{3.54\,\text{in}^2} = 8.8\,\text{ksi}.$$

We have been asked for the horizontal deflection at the top of the column, which, given the supports, is the maximum deflection w_{max}. As long as we have used the correct L_e to obtain P_{cr}, we are able to use the secant formulas for eccentric loading on columns with any type of supports:

$$w_{\text{max}} = e\left[\sec\left(\frac{\pi}{2}\sqrt{\frac{P}{P_{cr}}}\right) - 1\right] = (0.75\,\text{in})\left[\sec\left(\frac{\pi}{2}\sqrt{\frac{1}{2}}\right) - 1\right]$$

$$= (0.75\,\text{in})(2.252 - 1) = 0.94\,\text{in}.$$

The maximum normal stress is calculated as

$$\sigma_{\text{max}} = -\frac{P}{A}\left[1 + \frac{ec}{r^2}\sec\left(\frac{\pi}{2}\sqrt{\frac{P}{P_{cr}}}\right)\right]$$

$$= -\frac{31\,\text{kips}}{3.54\,\text{in}^2}\left[1 + \frac{(0.75\,\text{in})(2\,\text{in})}{(1.50\,\text{in})^2}\sec\left(\frac{\pi}{2\sqrt{2}}\right)\right]$$

$$= -(8.8\,\text{ksi})[1 + 0.667(2.252)]$$

$$= -22\,\text{ksi}.$$

The sign correctly indicates that this is a compressive stress.

EXAMPLE 11.3

A 3-m long fixed–fixed ended column of square cross section is to be made of wood in which the maximum allowable stress is 16 MPa and with $E = 13\,\text{GPa}$. Using a safety factor with respect to buckling of 2.5, determine the required size of the cross section if the column is to safely support centric loads of (1) 100 kN and (2) 200 kN.

Given: Geometry of column, safety factor.

Find: Size of square cross section for given applied loads.

Assume: Hooke's law applies; the anisotropy in the wood may be neglected.

Solution

1. Since we are asked to use a safety factor of 2.5, to support an actual load of 100 kN, we must have $P_{cr} = 250\,\text{kN}$. Designating the length of the side of the square cross section

as s and with $L_e = 0.5L = 1.5\,\text{m}$,

$$P_{cr} = \frac{\pi^2 E I}{L_e^2} = \frac{\pi^2 (13 \times 10^9\,\text{Pa})(1/12 s^4)}{(1.5\,\text{m})^2} = 250\,\text{kN}.$$

Then $s = 8.5\,\text{cm}$. We must also check that the allowable stress criterion is satisfied:

$$\sigma = \frac{P}{A} = \frac{100\,\text{kN}}{(0.085\,\text{m})^2} = 13.8\,\text{ksi}.$$

It is, so the size we have selected is sufficient.

2. Now to support an actual load of 200 kN, we must have $P_{cr} = 500\,\text{kN}$.

$$P_{cr} = \frac{\pi^2 E I}{L_e^2} = \frac{\pi^2 (13 \times 10^9\,\text{Pa})(1/12 s^4)}{(1.5\,\text{m})^2} = 500\,\text{kN}.$$

So $s = 10.1\,\text{cm}$. Checking the allowable stress,

$$\sigma = \frac{P}{A} = \frac{200\,\text{kN}}{(0.101\,\text{m})^2} = 19.5\,\text{ksi}.$$

The size that is sufficient to prevent buckling does not meet the strength criterion for this load. We must redesign a larger column that will meet both criteria using

$$\sigma_{\text{allow}} = 16\,\text{MPa} = \frac{200\,\text{kN}}{s^2},$$

which gives $s = 11.2\,\text{cm}$.

PROBLEMS

11.1 An I-beam with the proportions shown is to be used as a long column. There is a concern about buckling, so two reinforcing plates are to be welded along the length of the column. Two options for the resulting cross section are shown. Which will increase the critical buckling load? Will it have a large or small effect? Explain why.

(a)   (b)
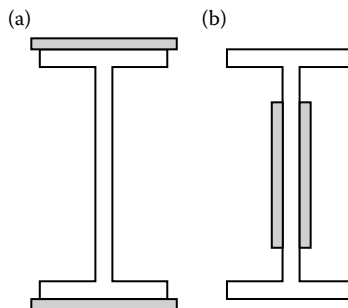
11.2 A W10 × 45 beam is made of structural steel and used as a column with a length 15 ft. If its ends are fixed, can the column support the critical load without yielding? (The

designation W10 × 45 provides specifications about the cross-sectional shape of this column (or beam). Specifically, each flange is 8.02 in wide and 0.62 in thick; the web is 0.35 in wide; and the total height of the cross section is 10.10 in.)

11.3 A slender vertical bar AB with pinned ends and length L is held between immovable supports. What increase ΔT in the temperature of the bar will produce buckling?

11.4 A W2 × 87 structural steel column has a length of 12 ft. (Look up the geometric properties of the W2 × 87 cross section.) If its bottom end is fixed, while its top is free, and it is subjected to an axial load of $P = 380$ kip, determine the safety factor with respect to buckling.

11.5 The A36 steel bar AB has a square cross section. If it is pin-connected at its ends, determine the maximum allowable load P that can be applied to the truss. Use a safety factor with respect to buckling of 2.
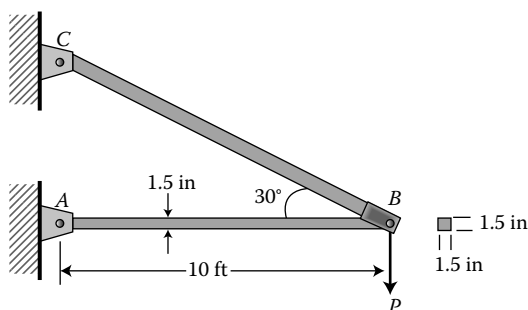
11.6 In more than one paragraph but less than a page, discuss some of the failure modes experienced in the collapse of the World Trade Center and how they might have been prevented.

11.7 A truss ABC supports a load W at joint B as shown. The length L_1 of member AB is fixed, but the length of strut BC varies as the angle θ is changed. Strut BC has a solid circular cross section. Assuming that collapse occurs by buckling of the strut, determine the angle θ for minimum weight of the strut.
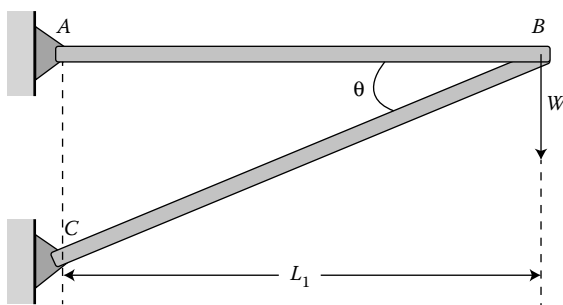
11.8 For a deck, supports of length 3.25 m are proposed to be built from aluminum with a Young's modulus of 72 GPa and a yield stress of 480 MPa. A cylindrical design is proposed with outer diameter $d = 100$ mm and wall thickness t to be specified. If the

design specs require that each column support a load of 100 kN with a safety factor of 3, find the necessary column thickness t.

11.9 A rectangular brass column is loaded with a load of $P = 1500\,\text{lb}$ applied 0.45 in off its centroidal axis. Find the longest permissible length L of the column if the deflection of its free end cannot exceed 0.12 in.
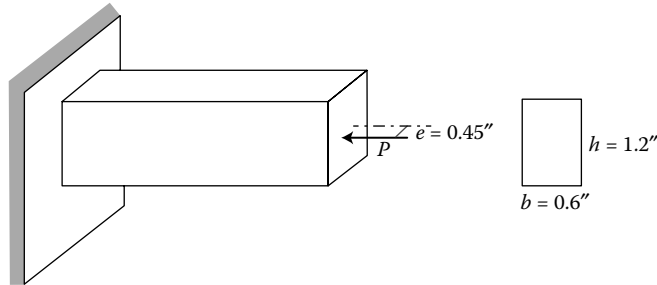
11.10 Consider Equation 11.16, giving the maximum deflection for eccentric loading. Make a graph that illustrates the relationship between deflection and load. What happens when the load is P_{cr}?

11.11 It has been observed that the most effective way to crush an empty aluminum beverage can is to apply an eccentric compressive load. Use buckling theory to explain this phenomenon. The can wall thickness is 80 μm, and the radius-to-thickness ratio is 200. The can is 12.2 cm high. How does the effect of eccentric compression compared with the likelihood of crushing (buckling) the empty can with normal loading?

11.12 A steel bar with the cross section shown and effective length $L = 2.5\,\text{m}$ is subjected to a compressive load $P = 200\,\text{kN}$ with a eccentricity $e = 0.00625\,\text{m}$. Find (a) the beam's maximum deflection, and (b) the maximum normal stress.
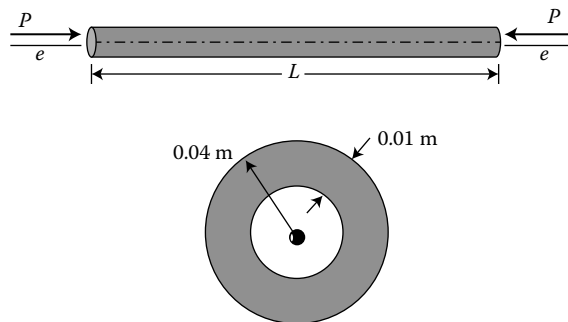
11.13 For the bar in Problem 11.12, find the largest allowable value of P if the allowable compressive stress is 250 MPa.

12

Case Study 5: Hartford Civic Arena

A new arena in Hartford, Connecticut, was approved in 1970 and built in 1973. The facility suffered a catastrophic failure in January 1978, when its roof collapsed only hours after a large crowd had attended a UConn hockey game. The resulting damage is seen in Figure 12.1. The center of the roof appears sunken in, while the corners have been thrust upward.

Tasked with saving money for the city of Hartford, the architect and engineering firm created an innovative design for the arena's roof. The proposed roof consisted of two main layers arranged in 30 by 30-ft grids composed of horizontal steel bars 21 ft apart. A set of 30-ft diagonal bars connected the nodes of the upper and lower layers, and, in turn, were braced by a middle layer of horizontal bars. The 30-ft bars in the top layer were also braced at their midpoint by intermediate diagonal bars, so they were *frame* elements subject to both axial and transverse bending loads. The space frame (meaning a frame structure that is three-dimensional, as opposed to a two-dimensional plane frame), shown in Figure 12.2, looks like a set of linked pyramid-shaped trusses.

This was not a conventional space frame roof design. Many of its unique features contributed to the vulnerability of the structure. In particular, the cross section of the bars did not provide good resistance to buckling. The cross section was composed of four structural steel angles (bars with L-shaped cross sections themselves) arranged in a composite cross-shaped section. This configuration has a much smaller radius of gyration than either an I-section or a tube section arrangement of the same angles (Figure 12.3). Also, the top horizontal bars intersected at a different point than the diagonal bars rather than at the same point, making the roof especially susceptible to buckling as this load eccentricity induced bending stresses. And, the space frame was not cambered (slightly arched upward). Computer analysis predicted a downward deflection of 13 in at the midpoint of the roof and an upward deflection of 6 in at the corners due only to the roof's dead load.

To save time and money, the roof frame was assembled on the ground. While it was on the ground, the inspection agency notified the engineers that inspectors had measured excessive deflections. No changes or repairs were made. Hydraulic jacks were used to lift the completed roof into position. Once the frame was in its final position but before the roof deck (which would support the final roofing material) was installed, the roof frame's deflection was measured to be twice that predicted by computer analysis, and the engineers were notified. However, they expressed little concern and responded that such discrepancies between the actual and the theoretical values should be expected. The subcontractor fitting the steel frame supports for fascia panels onto the outside of the truss ran into difficulties due to the excessive deflections of the frame, but as directed by the contractor, he reshaped some panels with his coping saw, and re-made others so that they would all fit.

The engineers, contractor, and members of the Hartford City Council made public statements attesting to the safety of the structure. And the roof survived for 5 years before the heavy snow of January 1978 triggered its catastrophic failure. At 4:15 am on January 18th, witnesses reported hearing a loud crack and seeing the center of the roof begin to sink in
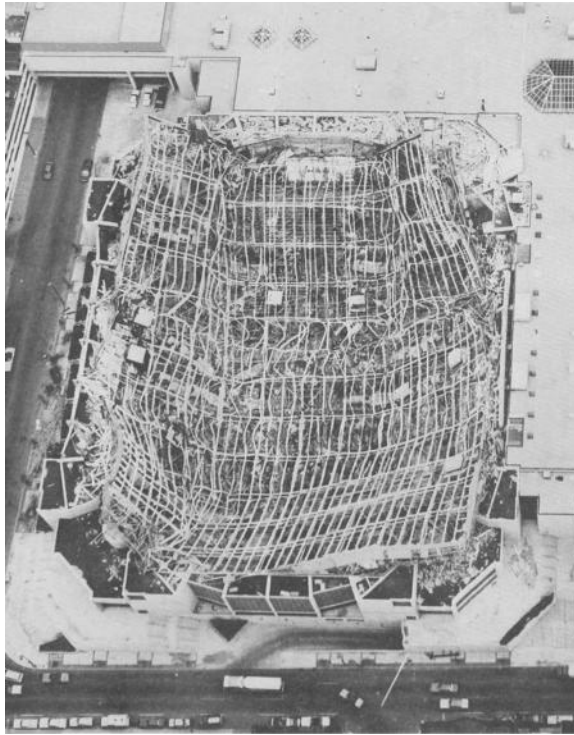
FIGURE 12.1
Damage at the Hartford Civic Arena, 1978. (Feld, Jacob and Carper, Kenneth, *Construction Failure*, Wiley & Sons, New York, 1997.)

before the explosive chaos of the rapid collapse. Because the hockey crowd had left hours earlier, no one was hurt in the collapse.

In the subsequent investigation (performed by an appointed panel and an outside failure analysis agency), it was determined that the roof of the Hartford Arena had begun failing as soon as it was completed due to an underestimation of the "dead load"* the roof
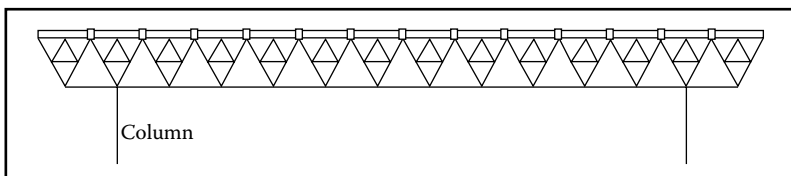
FIGURE 12.2
Sketch of roof design. (After M. Levy and M. Salvadori, *Why Buildings Fall Down*, Norton, New York, 1992.)

---

* Structures we design must withstand both "dead" and "live loads"; the sum of these is sometimes called the "design load." The dead load is simply the weight of the structure itself; live load is the anticipated weight it must also be able to support. For example, bridges must be able to support a predicted traffic load of cars and trucks; buildings must support the weight of the people and furniture in them; and all structures must also withstand loading due to wind, rain, and snow.
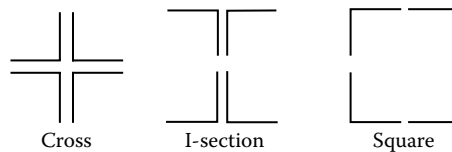
FIGURE 12.3
Cross-shaped member cross section, as used in the Hartford Arena roof frame; more conventional I-section and tube cross section shapes.

would need to support and three design errors that resulted in a significant overloading of structural components. In particular:

- The top layer's exterior compression members on the east and the west faces were overloaded by 852%.
- The top layer's exterior compression members on the north and the south faces were overloaded by 213%.
- The top layer's interior compression members in the east–west direction were overloaded by 72%.

In addition, the support braces in the middle layer had been installed at 30-ft intervals, rather than the designed 15 ft, reducing the structure's ability to withstand loading, particularly such dramatic overloading. The most overstressed members in the top layer buckled under the added weight of the snow, causing the other members to buckle. This changed the forces acting on the lower layer from tension to compression, causing them to buckle as well.

The investigators also determined that several departures from the engineers' design contributed to, but did not cause, the collapse: (1) the slenderness ratio of the built-up cross-shaped elements violated the American Institute of Steel Construction (AISC) code provisions; (2) elements with bolt holes exceeding 85% of the total area violated the AISC code; (3) spacer plates that joined the four angles of a cross section were placed too far apart in some elements, allowing individual angles to buckle; (4) some of the steel did not meet material property specifications; and (5) there were misplaced diagonal elements.

A second investigation blamed the failure not on lateral buckling, but on torsional buckling of diagonal elements that could not support the live load of the heavy snowfall.* A third investigation pinned the blame on a faulty weld securing the scoreboard to the roof.

It was noted that the roof, despite its many flaws, had apparently survived for 5 years before its dramatic failure. One study analyzed the *progressive failure* of the roof, which was a 5-year-long process. When an element of a frame structure buckles, it transfers its load to adjacent bars. These bars eventually buckle under the increased load and continue the load-transferring domino effect until the entire roof structure cannot withstand any greater load and begins to give way. This sort of progressive failure can be triggered by even a minor structural flaw unless the design includes *redundancy*—as Levy and Salvadori put it, "structural insurance." Analyses have shown that relatively few additional braces in the Hartford roof would have prevented bar buckling.

---

* Several other roof collapses in the Northeast were attributed to heavy snows in 1978, including the roof of the auditorium at C. W. Post College on Long Island.

The assessment of responsibility for the collapse was as complicated as determining the reasons. The fact that five independent subcontractors constructed the arena made assessing responsibility especially tricky. Lack of ownership and oversight by the contractors toward the entire project had resulted in creating a fragmented system, in which no one examined the "big picture." Six years after the collapse, all the involved parties reached an out-of-court settlement.

It is also worth noting that potential problems with the Hartford arena design were brought before the engineers several times during the construction of the arena. The engineers, confident in their designs (and, perhaps willfully unaware that what was built might not be precisely what they would designed) and in their computations (from which they would reportedly omitted buckling as a possible failure mode), did not heed warnings or re-examine their work. In fact, unanticipated deformations can indicate a flawed design and are generally worth investigating.

References

"Collapsed Roof Design Defended." *Engineering News-Record* [*ENR*], June 29, 1978.

"Collapsed Space Truss Roof Had a Combination of Flaws." *ENR*, June 22, 1978.

"Design Flaws Collapsed Steel Space Frame Roof." *ENR*, April 6, 1978.

The Education Committee of the Technical Council on Forensic Engineering of the American Society of Civil Engineers [ASCE]. Shepherd, Robin and David Frost (Eds.). *Failures in Civil Engineering: Structural, Foundation, and Geoenvironmental Case Studies*. New York: The Society, 1995.

Feld, Jacob and Carper, Kenneth, *Construction Failure*, Wiley & Sons, New York, 1997.

"Hartford Collapse Blamed on Weld." *ENR*, June 24, 1979.

M. Levy and M. Salvadori, *Why Buildings Fall Down*, Norton, New York, 1992.

R. Martin and N. Delatte, "Another look at the Hartford Civic Center Coliseum Collapse," *Journal of Performance of Constructed Facilities*, Vol. 15, No. 1, February 2001, pp. 31–36

"New Theory on Why Hartford Roof Fell." *ENR*, June 14, 1979.

H. Petroski, *To Engineer Is Human*. St. Martins Press, New York, 1995.

S. Ross et al., *Construction Disasters*. McGraw-Hill Book Co, New York, 1984.

"Space Frame Roofs Collapse Following Heavy Snowfalls." *ENR*, January 26, 1978.

13

Connecting Solid and Fluid Mechanics

We are now familiar with the response of solids to external loading. We have learned about the stress tensor, the strain tensor, and the individual components of these measures of "internal response to external loads." Time and again, we have returned to the essence of continuum mechanics:

- Kinematics of deformation (including geometric compatibility)
- Definition of stress
- Constitutive law (stress–strain relationship)
- Equilibrium

Solids, we remember, are *continua*—their densities may be mathematically defined. Fluids—gases and liquids—may also satisfy this definition, and so these concepts of stress and strain also apply to them. As we have done for solids, we would now like to contemplate the response of fluids to loading and to consider how stress may be related to the material's deformation.

Remember that a fluid may be called a *continuum* if the Knudsen number, *Kn*, is less than about 0.1. The Knudsen number is defined as

$$Kn = \frac{\lambda}{L},$$ (13.1)

where L is a problem-specific characteristic length, such as a diameter or width, and λ is the material's "mean free path." We have already considered in Chapter 1 what *is* and what *is not* a continuum at some length.

When this assumption of a material's continuity is made, the properties of a material—solid or fluid—may be assumed to apply uniformly in space and time. That is, the density ρ may vary in space and time, but it is always definable and is a continuous function of x, y, z, and t.

Fluids are usually defined, and distinguished from solids, as materials that deform continuously under shear stress. This is true no matter how small the applied shear stress is. Also, when normal stress is applied—when a fluid is squeezed in one direction—the fluid flows in the other two directions. This can be observed when you squeeze a hose in the middle and see water flow from its ends. Fluids cannot offer permanent resistance to these kinds of loads.

If we now consider fluid mechanics with the ideas of solid mechanics fresh in our minds, we will see many connections and analogies between the two fields. Fluids have their own measures of *elasticity*, *resistance* to loads, and *deformation*. In the following sections, we will discuss some of the important properties of fluids. If density variation or heat transfer is significant, these fluid properties must be supplemented with additional information.

Once again we will rely on the fundamentals listed above. Put another way, also by now familiar, we will ensure equilibrium (or Newton's second law), compatibility, and a

constitutive law are satisfied at all times. In this chapter, we will first consider the kinds of stress that may be experienced by a volume of fluid; next, we will discuss a fluid's constitutive law. Finally, we will develop a way to talk about the kinematics of deformation of a fluid, this time using strain *rate* rather than strain as we did for solids. In Chapter 16, we will use these three definitions to enforce equilibrium.

13.1 Pressure

In fluids, pressure results from a normal compressive force acting on an area, as shown in Figure 13.1.

It is written as

$$p = \lim_{\Delta A \to 0} \frac{\Delta F_n}{\Delta A}, \tag{13.2}$$

and has units of N/m^2 or psi.

We recognize that this is also the definition of a normal stress. In fact, if this compression were the only force acting on an element of the fluid, the element's stress tensor could be written as

$$\sigma_{ij} = \begin{pmatrix} -p & 0 & 0 \\ 0 & -p & 0 \\ 0 & 0 & -p \end{pmatrix}, \tag{13.3}$$

where the negative sign is present because positive pressure is compressive, and compression is represented by negative normal stress. We will see that in reality a variety of forces may act on a fluid element, but that pressure will always be an important part of its stress state.

As in our discussion of pressure vessels, we will generally speak of a *gage pressure* that is measured relative to local atmospheric pressure, that is $p_{\text{gage}} = p_{\text{absolute}} - p_{\text{atm}}$.

Pressure, as shown in Figure 13.1, is a *surface force*, acting on boundaries of a fluid through direct contact. Shear forces and stresses also fit this description. Fluids may also be acted on by *body forces*, which are applied without physical contact and distributed over the entire fluid volume. The total body force is in fact proportional to the fluid volume. Gravitational and electromagnetic fields impart body forces to fluids.
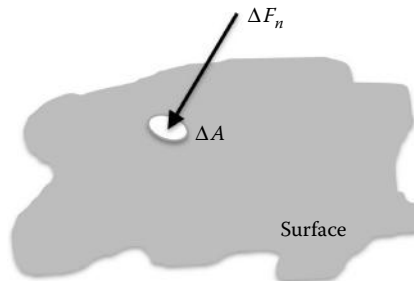
FIGURE 13.1
Definition of pressure.

13.2 Viscosity

A fluid's viscosity can be thought of as a measure of how well the fluid *flows*. Water and maple syrup, for example, flow differently, at different rates; the difference is reflected in their viscosities.

The rate of deformation of a fluid is directly linked to the fluid's viscosity. If we consider a fluid element of area $dx \times dy$ under application of a shearing stress τ, as in Figure 13.2, we see that the shear strain angle $d\theta$ grows continuously as long as τ is maintained. (Remember that this is what differentiates fluids from solids: that they deform *continuously* under shear. There is therefore a time dependence in their constitutive law. The *rate* at which this deformation occurs depends on many factors, and particularly on the fluid's properties.)

In Figure 13.2, we see that a plate sliding with speed du over our initially rectangular fluid element induces some angular deformation $d\theta$ in a time dt. When this experiment is performed on common fluids like water, oil, and air, the experimenters observe that the shear stress τ (which is σ_{yx}) is proportional to the rate of angular deformation $d\theta/dt$. The constant of proportionality is the fluid's viscosity μ.

We use the geometry of Figure 13.2 to manipulate this experimentally observed relationship into its more useful form:

$$\sigma_{yx} \propto \frac{d\theta}{dt}, \tag{13.4a}$$

$$\tan d\theta = \frac{du \, dt}{dy}. \tag{13.4b}$$

For small angles, $\tan d\theta \approx d\theta$, and we can rearrange this to have $d\theta \, dt = du/dy$. Finally, we have

$$\tau = \sigma_{yx} = \mu \frac{du}{dy}. \tag{13.5}$$

Fluids for which this linear proportionality exists, for which viscosity μ does not itself depend on the strain rate, are called *Newtonian*, and we see that this is analogous to the behavior of a *Hookean* solid. Newton first referred to the "slipperiness" of fluids and wrote down the essence of Equation 13.5, in his *Principia* in 1687. In both cases, we have *stress = (constant) · (strain* or *strain rate)*, whether this constant is E, G, or μ. The dimensions of viscosity are time · force/area, or Pa · s (N · s/m^2) in the SI system. The viscosity of a fluid,
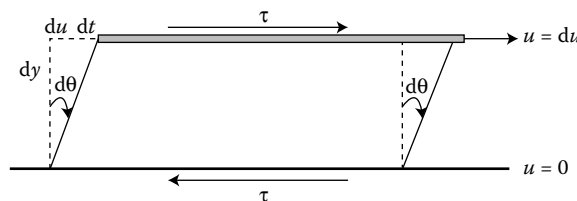
FIGURE 13.2
Sliding plate inducing shear stress τ. Note that this is σ_{yx}.
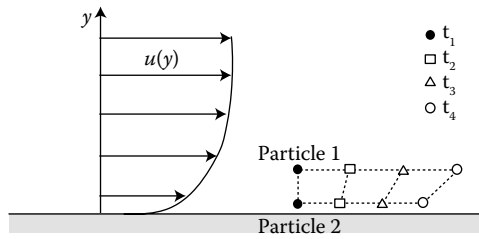
FIGURE 13.3
Relative motion of two fluid particles in the presence of shear stress.

we see, measures its ability to resist deformation due to shear stress, or to resist flow. In a sense, it measures the fluid's stiffness, just as E and G did for solids.

Although we are struck by the analogy between the constitutive laws for solids and fluids, we also note the key difference: the dependence on strain for solids, and on strain *rate* for fluids. Remembering Hooke's initial source of inspiration—the extension of a spring—we arrive at another comparison:

Component	Constitutive Law	Material	Constitutive Law
–⋀⋀–	$F = kx$	Solid	$\tau = G\gamma$
–⊏⊐–	$F = c\dfrac{\mathrm{d}x}{\mathrm{d}t}$	Fluid	$\tau = \mu\dfrac{\mathrm{d}u}{\mathrm{d}y}$

If we think of solids as behaving more like springs, and fluids behaving more like dashpots (or dampers), we can relate these constitutive laws to ones with which we are familiar. We can also foresee the introduction of other materials whose behavior is neither purely solid nor purely fluid—non-Newtonian fluids, for example—which may be modeled by the series or parallel combination of these spring and dashpot elements. We can even visualize the gamut of constitutive behavior as a spectrum with springs (Hookean elastic solids) at one end, and dashpots (Newtonian fluids) at the other, with myriad variations between.* Please see Chapter 14 for a discussion of the many types of material behavior possible in between these two idealized extremes.

The $\mathrm{d}u/\mathrm{d}y$ term that appears in the definition of viscosity (Equation 13.5) was derived in terms of the angular deformation, or shear strain, of the fluid element per time, that is, the *strain rate*. It also represents a *gradient of velocity*, as shown in Figure 13.3. Note that if a fluid is not flowing, shear stresses cannot exist, and only normal stress (pressure) is considered.

Viscosity varies with temperature, as shown in Figure 13.4. For a liquid, the temperature dependence can be approximated by an exponential equation, $\mu(T) = c_1 \exp[c_2/T]$, where the constants c_1 and c_2 are determined from measured data. In liquids, the shear stress is due in greater part to intermolecular cohesive forces, and these cohesive forces decrease with increasing T. Figure 13.4 demonstrates that the viscosity of a gas, which is due to the thermal motion of molecules, is much less dependent on temperature.

---

* We should pause again to empathize with Robert Hooke, whose work was suppressed by the bitterly competitive Isaac Newton, but who now finds himself facing his rival on the opposite end of the material behavior spectrum.
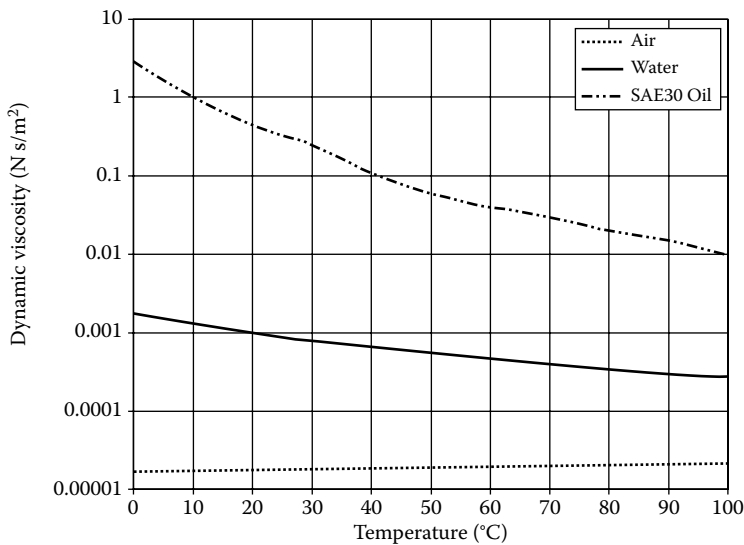
FIGURE 13.4

Viscosity versus temperature for representative liquids and gases. (Fox, R. W. and McDonald, A. T., Introduction to Fluid Mechanics, 1978. Copyright Wiley-VCH Verlag GmbH & Co. KGaA. Reproduced with permission.)

For non-Newtonian fluids, the viscosity may also depend on the type or rate of loading applied to the fluid. *Dilatants* such as quicksand or slurries become more resistant to motion as the strain rate increases. A mixture of corn starch and water is a dilatant and, as you can experimentally verify, feels harder the harder (faster) you pound it. *Pseudoplastics* become less resistant to motion with increased strain rates. Examples of this include ketchup and latex paint. *Bingham plastics*, or viscoplastics, require a minimum shear stress to cause motion, but after this threshold behave like Newtonian fluids. Toothpaste is a Bingham plastic.* Figure 13.5 illustrates the constitutive behavior for these classes of fluids.

Viscosity causes fluids to adhere to surfaces; this is called the *no-slip condition* and it means that the fluid adjacent to any surface moves with the same velocity as the surface itself.

Incidentally, μ is more formally called the *dynamic viscosity* of a given fluid. We may also wish to think in terms of a fluid's *kinematic viscosity*, denoted by ν:

$$\nu \equiv \frac{\mu}{\rho}, \tag{13.6}$$

which is of special interest as it reflects a fluid's tendency to *diffuse* velocity gradients. The SI units of kinematic viscosity are m^2/s.

---

* The materials scientist Eugene Bingham (1878–1945) was a professor of chemistry at Lafayette College. He coined the term *rheology* for the study of fluid deformation and flow, that is, for the continuum mechanics of fluids. Bingham chose a quote from Heraclitus, "*panta rei*"—"everything flows"—as a suitable motto for the Society of Rheology he helped found in 1929. He and the chemical engineer Markus Reiner proposed the Deborah number as a fundamental quantity of rheology, with larger Deborah numbers resulting in material behavior further toward the "solid" end of the spectrum. It was named for the prophetess Deborah who sang, "The mountains flowed," to the defeated Philistines. We refer readers to Reiner's text, *Deformation, Strain, and Flow: An Elementary Introduction to Rheology*, New York: Interscience, 1960.
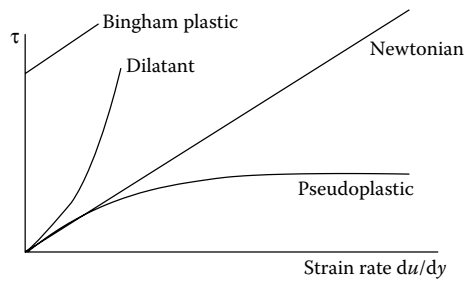
FIGURE 13.5
Representative constitutive behavior for Newtonian and non-Newtonian fluids. The slope of the stress–strain rate diagram, representing the viscosity or resistance to deformation, is constant for a Newtonian fluid.

13.3 Surface Tension

The attractive forces between fluid molecules result in *surface tension*. Molecules deep within the fluid are closely packed, and bound by cohesive forces. But the molecules at surfaces are less densely packed, and—because half their neighbors are missing—have nothing to balance their cohesive forces. The result is an inward force, or contraction, at the surface.

Surface tension is generally represented with a lower-case sigma, but to avoid confusion with components of the stress tensor, we will denote surface tension with s. It is measured in (N/m) or in (lb/ft), and depends on the two fluids in contact and on their temperature.

The scale of a given problem determines which forces (inertia, pressure, viscosity, or surface tension) are involved in its physics. Though in traditional fluid mechanics textbooks, the importance of this last force, surface tension, is often minimized, it has enormous relevance in emerging micro- and nano-scale applications.

Because inertia (the $m\mathbf{a}$ term in $\mathbf{F} = m\mathbf{a}$) scales as the volume of an object, when objects get smaller, inertia decreases by a power of 3. But the force due to surface tension only goes as the length of a given surface, so that the same reduction in size causes it to decrease by only a power of 1. This scaling means that surface tension dominates the micro-scale physics, and inertia hardly enters the picture. However, the importance of surface tension has not always been well understood. Surface tension was seen as a major problem when researchers first began designing MEMS devices. The slightest amount of moisture beneath a miniature cantilever beam would pull the beam down to the substrate, welding it in place. The first micromotors could be rendered inoperable by the moisture in a single drop of water. Now that it is better understood, surface tension can be harnessed to create motion if it is increased locally and decreased somewhere else. Researchers do this by adding a surfactant (such as soap, which lowers surface tension), raising the temperature at one point (which decreases surface tension), or by applying an electrical potential.

13.4 Governing Laws

Newton's laws of motion apply to fluids, just as they do to solids. Newton's second law, $\mathbf{F} = m\mathbf{a}$, will be especially useful to us as we consider the combined effects of all

forces—due to pressure, viscosity, surface tension, etc.—on a fluid and require their resultant to equal $m\mathbf{a}$. We will develop this further in Chapter 18.

13.5 Motion and Deformation of Fluids

The motion and deformation of a fluid element depend on the velocity field. The relationship between this motion and the forces causing the motion depends on the acceleration field (via $\mathbf{F} = m\mathbf{a}$). We will use an *Eulerian* description, in which we concentrate on a spatial point (x, y, z) and consider the flow through and around this point, rather than the *Lagrangian* method of description sometimes used to track individual fluid particles.

13.5.1 Linear Motion and Deformation

If all points in a given fluid element have the same velocity, the element simply translates from one point to the next. However, we typically have *velocity gradients* present, so that the element is deformed and rotated as it moves. We will write the velocity $\mathbf{V} = (u, v, w)$ in Cartesian (x, y, z) coordinates. You may wonder about the fact that we are using the same letters for the components of the velocity vector as we used for the components of the displacement vector in our discussion of solids. We will discuss the reasoning behind this choice at the end of Section 13.5.2. A sample fluid element, a cube with infinitesimal volume $d\mathcal{V} = dx\,dy\,dz$, is shown in Figure 13.6. This element is part of a flow with velocity gradient $\partial u/\partial x$—that is, the x velocity is varying with x. In a time interval dt, the change in the element's volume is given by

$$\left(\frac{\partial u}{\partial x} dx\, dt\right)(dy\, dz) = \frac{\partial u}{\partial x}\, dt\, d\mathcal{V}. \tag{13.7}$$

The *rate* at which the volume $d\mathcal{V}$ is changing, per unit volume, due to $\partial u/\partial x$ may be written

$$\frac{1}{d\mathcal{V}}\frac{d(d\mathcal{V})}{dt} = \lim_{dt\to 0}\left[\frac{\partial u/\partial x\, dt}{dt}\right] = \frac{\partial u}{\partial x}. \tag{13.8}$$
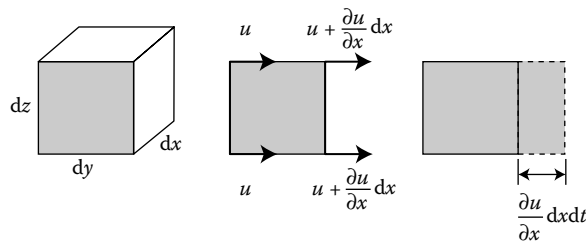
FIGURE 13.6
Linear deformation of fluid element by $\partial u/\partial x$.

And if velocity gradients $\partial v / \partial y$ and $\partial w / \partial z$ are also present, we will have the rate of change in volume (per unit volume):

$$\frac{1}{\mathrm{d}\mathcal{V}}\frac{d(\mathrm{d}\mathcal{V})}{dt} = \frac{\partial u}{\partial x} + \frac{\partial v}{\partial y} + \frac{\partial w}{\partial z} = \nabla \cdot \mathbf{V}, \tag{13.9}$$

where we have recognized the sum of the partial derivatives of the velocity vector $\mathbf{V}$'s components as the *divergence* of $\mathbf{V}$.

Notice that the isolated effect of each of these velocity gradients causes a one-dimensional, normalized change in length per time, or *normal strain rate*, which can be written in the same way:

$$\varepsilon_{xx} = \frac{\partial u}{\partial x}, \tag{13.10a}$$

$$\varepsilon_{yy} = \frac{\partial v}{\partial y}, \tag{13.10b}$$

$$\varepsilon_{zz} = \frac{\partial w}{\partial z}. \tag{13.10c}$$

The quantity $\nabla \cdot \mathbf{V}$ derived above for the entire volume is known as the *volumetric strain rate*. For an incompressible fluid, the volume of a fluid element cannot change, and we must have $\nabla \cdot \mathbf{V} = 0$.

13.5.2 Angular Motion and Deformation

In addition to undergoing normal strain rates, a fluid element may experience angular motion and deformation. We will measure this with a *shear strain rate*, derived from the change in shape of the fluid element in Figure 13.7. The figure shows the position of an element with initial area $\mathrm{d}x\,\mathrm{d}y$ at time t, and its subsequent position at time $t + \mathrm{d}t$.

We see that the initially horizontal side (initial length $\mathrm{d}x$) has undergone a rotation $\mathrm{d}\alpha$, and the initially vertical side (initial length $\mathrm{d}y$) has been rotated $\mathrm{d}\beta$.
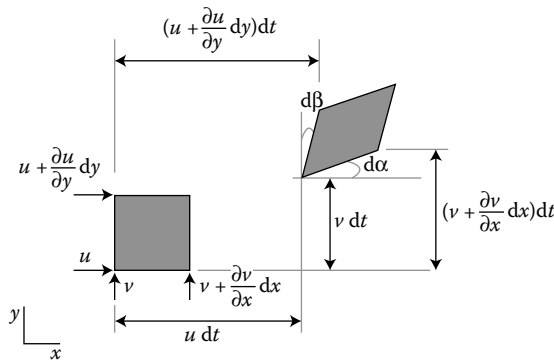
FIGURE 13.7
Translation and angular deformation of a fluid element.

We can calculate these angles and then find an expression for the *shear strain rate*, defined as $(d\alpha + d\beta)/dt$. We will also assume that the angles are small, so $\tan d\alpha \approx d\alpha$. From the figure, we see

$$\tan d\alpha \approx d\alpha = \frac{(\partial v/\partial x)\,dx\,dt}{dx} = \frac{\partial v}{\partial x}dt. \tag{13.11}$$

(We note that if $\partial v/\partial x > 0$, the rotation of this side is counter-clockwise.) Similarly we find

$$d\beta = \frac{\partial u}{\partial y}dt \tag{13.12}$$

(seeing that if $\partial u/\partial y > 0$, the rotation of this side is clockwise)—and thus we find the *shear strain rate*:

$$\frac{d\alpha + d\beta}{dt} = \frac{\partial v}{\partial x} + \frac{\partial u}{\partial y}. \tag{13.13}$$

And extending this to the other two dimensions, we see that in general the ij component of shear strain rate may be written as

$$\gamma_{ij} = \frac{\partial u_i}{\partial x_j} + \frac{\partial u_j}{\partial x_i}. \tag{13.14}$$

However, as before, when we compose the *strain rate tensor*, these shear components must be divided by 2 in order to make the tensor behave like a tensor. Now, a general form for the ij component of the strain rate tensor, including both normal and shear components, may be written

$$\varepsilon_{ij} = \frac{1}{2}\left(\frac{\partial u_i}{\partial x_j} + \frac{\partial u_j}{\partial x_i}\right) = \frac{1}{2}\left(u_{i,j} + u_{j,i}\right). \tag{13.15}$$

So that the matrix form of the tensor itself looks like

$$\varepsilon_{ij} = \begin{pmatrix} \varepsilon_{xx} & \varepsilon_{xy} = \dfrac{\gamma_{xy}}{2} & \varepsilon_{xz} = \dfrac{\gamma_{xz}}{2} \\ \varepsilon_{yx} = \dfrac{\gamma_{xy}}{2} & \varepsilon_{yy} & \varepsilon_{yz} = \dfrac{\gamma_{yz}}{2} \\ \varepsilon_{zx} = \dfrac{\gamma_{xz}}{2} & \varepsilon_{zy} = \dfrac{\gamma_{yz}}{2} & \varepsilon_{zz} \end{pmatrix}$$

$$= \begin{pmatrix} \dfrac{\partial u}{\partial x} & \dfrac{1}{2}\left(\dfrac{\partial u}{\partial y} + \dfrac{\partial v}{\partial x}\right) & \dfrac{1}{2}\left(\dfrac{\partial u}{\partial z} + \dfrac{\partial w}{\partial x}\right) \\ \dfrac{1}{2}\left(\dfrac{\partial u}{\partial y} + \dfrac{\partial v}{\partial x}\right) & \dfrac{\partial v}{\partial y} & \dfrac{1}{2}\left(\dfrac{\partial w}{\partial y} + \dfrac{\partial v}{\partial z}\right) \\ \dfrac{1}{2}\left(\dfrac{\partial u}{\partial z} + \dfrac{\partial w}{\partial x}\right) & \dfrac{1}{2}\left(\dfrac{\partial w}{\partial y} + \dfrac{\partial v}{\partial z}\right) & \dfrac{\partial w}{\partial z} \end{pmatrix}. \tag{13.16}$$

All of these components of the strain rate tensor should look strikingly similar to the components of the strain tensor derived for a solid in Section 4.2. This similarity, while undeniably wondrous, should not be surprising: both fluids and solids are *continua*, and

their deformations can be written mathematically in the form of a nine-component tensor, which we have seen can be related to the nine components of stress. The difference between this strain rate tensor and the strain tensor in Section 4.2 is simply that for solids, strain is a dimensionless quantity measuring percent length change, while for fluids, we measure *rate* of strain so that (u, v, w) here are velocities rather than lengths.

13.5.3 Vorticity

To quantify the rotation of fluid elements due to a given flow, we again consider the angles $d\alpha$ and $d\beta$ as shown in Figure 13.7. We want to find an expression for the average rotation *rate* of this element. Again we consider both $d\alpha$ and $d\beta$, the rotations of two mutually perpendicular lines. (This is because the average of these two rotation rates will be independent of the initial orientation of the pair.) To combine these two, we must remember that $d\alpha$ is a counterclockwise rotation, while $d\beta$ was clockwise—so we will find the combined effect to be:

Angular velocity of element about the z-axis $= \dfrac{1}{dt}\left[\dfrac{1}{dy}\left(-\dfrac{\partial u}{\partial y}\,dy\,dt\right) + \dfrac{1}{dx}\left(\dfrac{\partial v}{\partial x}\,dx\,dt\right)\right].$

Or

$$\omega_z = \frac{\partial v}{\partial x} - \frac{\partial u}{\partial y}. \tag{13.17}$$

This angular velocity could also be computed for rotation about the x- and y-axes, with similar results, giving us three components

$$\omega_x = \frac{\partial w}{\partial y} - \frac{\partial v}{\partial z}, \tag{13.18a}$$

$$\omega_y = \frac{\partial u}{\partial z} - \frac{\partial w}{\partial x}, \tag{13.18b}$$

$$\omega_z = \frac{\partial v}{\partial x} - \frac{\partial u}{\partial y}, \tag{13.18c}$$

of what is known as the *vorticity* vector. We recognize that the vorticity may be written as the *curl* of the velocity field, or

$$\boldsymbol{\omega} = \nabla \times \mathbf{V}. \tag{13.19}$$

If a flow has $\nabla \times \mathbf{V} = 0$, the flow is called *irrotational*. For such flows, the velocity vector $\mathbf{V}$ can be written as the gradient of a scalar potential function $[\mathbf{V} = \nabla \phi]$, since the curl of a gradient must be zero.

13.5.4 Constitutive Equation for Newtonian Fluids

We recall that the relationship between stress and deformation in a continuum is known as a *constitutive equation*. We now seek an equation linearly relating the stress to the rate of strain in a fluid, a counterpart to the generalized form of Hooke's law for solids that we saw in Section 4.4.

We have already seen that pressure is a normal stress on the surface of a fluid element. This contribution to the stress tensor may be written as a diagonal matrix with eigenvalues

$-p$. We make use of the tensor equivalent of the identity matrix, known as the *Kronecker delta*, introduced in Section 1.5. The Kronecker delta is a second-order, isotropic tensor whose matrix representation is

$$\delta_{ij} = \begin{pmatrix} 1 & 0 & 0 \\ 0 & 1 & 0 \\ 0 & 0 & 1 \end{pmatrix}. \tag{13.20}$$

And so we can write the pressure's contribution to the fluid's stress state as

$$\sigma_{ij} = -p\delta_{ij}, \tag{13.21}$$

where δ_{ij}, and hence σ_{ij}, is only nonzero when $i = j$.

Knowing that we can superpose these components of normal stress with any normal components that arise due to fluid motion, as described in Section 13.5.1, we simply add on the stress tensor that is developed by fluid motion, so that the complete stress picture is given by

$$\sigma_{ij} = -p\delta_{ij} + \sigma_{ij}^d, \tag{13.22}$$

where σ_{ij}^d, the part of the stress tensor due to fluid motion, is known as the *deviatoric stress tensor*. It is related to the velocity gradients, as we have seen through the construction of the strain rate tensor. We now know

$$\varepsilon_{ij} = \frac{1}{2}\left(\frac{\partial u_i}{\partial x_j} + \frac{\partial u_j}{\partial x_i} \right), \tag{13.23}$$

and we assume a linear relationship between stress and strain rate:

$$\sigma_{ij}^d = K_{ijmn}\varepsilon_{mn}, \tag{13.24}$$

where K_{ijmn} is a fourth-order tensor with 81 components, very much like the large tensor invoked in our discussion of the generalized form of Hooke's law (Section 4.4). We recall that for solids, this large tensor depended on E and G and Poisson's ratio ν. For fluids, K turns out to depend on viscosity μ, and to have a very simple form for most fluids. We need only assume that the fluid is isotropic and that the stress tensor is symmetric to reduce K to a matter of only two (not 81) elements.[*] In fact, the whole mess can be reduced quite nicely to

$$\sigma_{ij} = -\left(p + \frac{2}{3}\mu\nabla \cdot \mathbf{V} \right)\delta_{ij} + 2\mu\varepsilon_{ij}, \tag{13.25}$$

which for an incompressible fluid ($\nabla \cdot \mathbf{V} = 0$) reduces still further to

$$\sigma_{ij} = -p\delta_{ij} + 2\mu\varepsilon_{ij}. \tag{13.26}$$

---

[*] For the details of this, please see Kundu, P. K., *Fluid Mechanics*, Academic Press, 1990, pp. 89–93. For the mathematical justification, see Aris, R., *Vectors, Tensors, and the Basic Equations of Fluid Mechanics*, Dover, 1962.

This is the constitutive law for an incompressible, Newtonian fluid. As we did for solids, we will be able to consider a few components of this relationship at a time. But again, it is useful to see the big picture.

13.6 Examples

EXAMPLE 13.1

In the center of a hurricane, the pressure can be very low. Find the force acting on the wall of a house, measuring 10 ft by 20 ft, when the pressure inside the house is 30 in Hg and the pressure outside is 26.3 in Hg. Express the answer in both pounds and Newtons.
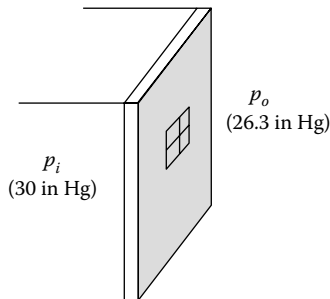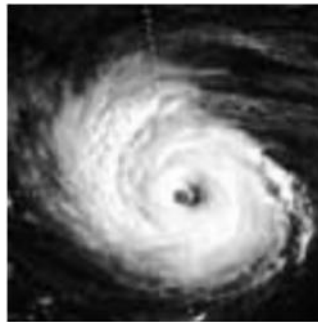
Given: Pressure on both sides of wall; wall dimensions.

Find: Resultant force on the wall.

Assume: Uniform pressure distributions on both sides of the wall. Negligible pressure contributions from inside the wall.

Solution

A mercury barometer measures the local atmospheric pressure. A standard atmosphere has a pressure of 14.7 psi, or 101.3 kPa. A mercury barometer reads this standard atmospheric pressure as 760 mm Hg, or 29.92 in Hg. Since we are asked for a result in two different units, we must be mindful of these conversion factors.

The resultant force on the wall is simply the net pressure applied to it, times its area. A quick free-body diagram of the wall will be of use:
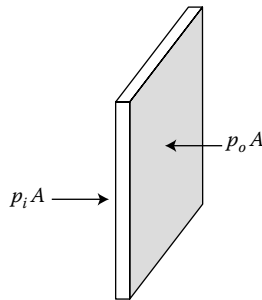
We see that the net force on the wall will be directed outward, and that it is

$$F = (p_i - p_o)A$$

$$= (30.0 - 26.3)(\text{in Hg})\frac{14.7\,\text{psi}}{29.92\,\text{in Hg}} \cdot (120\,\text{in})(240\,\text{in})$$

$$= 52{,}300\,\text{lb}$$

$$= 52{,}300\,\text{lb}\frac{9.8\,\text{N}}{2.205\,\text{lb}}$$

$$= 233\,\text{kN}.$$

This outward force is very large, and if the wall has not been adequately strengthened, the force can explode the wall outward. If you know a hurricane is coming, it is therefore a good idea to open as many windows as possible, to equalize the pressure inside and outside.

EXAMPLE 13.2

The flow between two parallel plates, one of which is moving with a constant speed U, is known as *Couette flow*. If the fluid between the two plates is Newtonian, develop an expression for the velocity distribution in the fluid layer. If the fluid is SAE oil at $20°$C, which has a viscosity of 0.26 Pas, and if the top plate moves with a speed $U = 3$ m/s and the gap thickness is $h = 2$ cm, what shear stress is applied to the fluid?
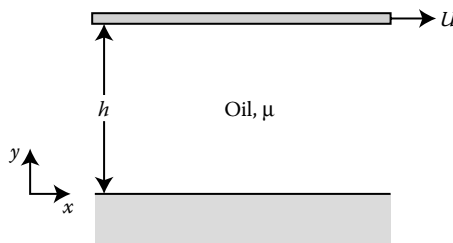
Given: Couette flow.

Find: Fluid velocity distribution, shear stress.

Assume: Newtonian fluid; any transient effects due to initiation of plate motion have died out and flow is steady; negligible gravity; one-dimensional flow; $u = u(y)$ only.

Solution

We know that, for a Newtonian fluid, the definition $\sigma_{yx} = \mu(\mathrm{d}u/\mathrm{d}y)$ is a linear relationship with a constant viscosity μ. This is a differential equation we can solve for velocity $u(y)$.

Due to equilibrium, the shear stress will be constant throughout the layer of fluid.
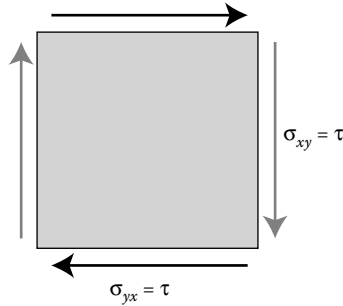
This is because there are no other forces on the fluid, so to keep a fluid element in equilibrium we must have $\sigma_{yx}(= \sigma_{xy}) = \text{constant} = \tau$. So

$$\tau = \mu\frac{\mathrm{d}u}{\mathrm{d}y},$$

$$\frac{\mathrm{d}u}{\mathrm{d}y} = \frac{\tau}{\mu} = \text{constant}.$$

If we call this constant C and then integrate, we find that the velocity must have the form

$$u(y) = Cy + D.$$

To complete the solution, we will use boundary conditions. We have discussed an important property of viscous fluids: that the fluid adjacent to a solid surface moves with the same speed as that surface. This is known as the *no-slip* condition. At the lower plate, which is at rest, we have $u(y = 0) = 0$; at the upper plate which slides with speed U we have $u(y = h) = U$. Applying these boundary conditions:

$$u(y = 0) = 0 \rightarrow D = 0,$$

$$u(y = h) = U \rightarrow C = \frac{U}{h}.$$

We, therefore, must have

$$u(y) = \frac{U}{h}y.$$
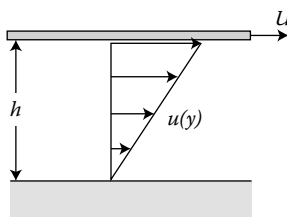
For the given numerical values, we find the shear stress:

$$\tau = \mu \frac{du}{dy} = \mu \frac{U}{h} = (0.26\,\text{Pa}\cdot\text{s})\frac{(3\,\text{m/s})}{(0.02\,\text{m})} = 39\,\text{Pa}.$$

EXAMPLE 13.3

A 5-kg cube with sides 12 cm long slides down an oil-coated incline. If the incline makes a $10°$ angle with the horizontal and the oil layer is 0.2 mm thick, estimate the constant speed with which the block slides down the incline. The viscosity of the oil is 0.1 Pa s.
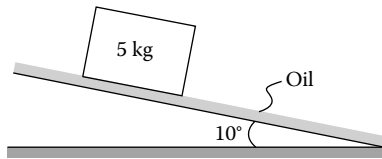
Given: Dimensions of cube and fluid layer.

Find: Cube's terminal velocity.

Assume: Newtonian fluid; flow is steady; negligible end effects; one-dimensional fluid flow in thin layer can be modeled as Couette flow.

Solution

We begin with an FBD of the cube.
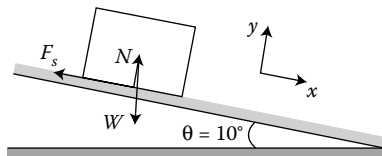
This contains the weight of the cube itself, a normal force upward, and a frictional resistance from the oil. This shear force F_s is simply the fluid shear stress acting over the area of contact between cube and fluid. (An equal and opposite shear force acts on the layer of oil.)

The cube is not accelerating—we are seeking its *terminal velocity*. So, the cube is in static equilibrium. We must have the sum of forces in both x- and y-directions equal zero. The x-direction is more useful to us:

$$\sum F_x = 0,$$

$$0 = W\sin\theta - F_s.$$

In the layer of oil, we have a top surface (the bottom of the cube) that is moving with a constant velocity, say V, in the x-direction, and a bottom surface (the inclined plane) which is at rest. The oil is therefore in Couette flow. We make use of our result from Example 13.2 to express the shear force:

$$F_s = \tau A = \mu \frac{V}{h} A.$$

So,

$$0 = W \sin \theta - \mu \frac{V}{h} A.$$

Rearranging, we have

$$V = \frac{Wh \sin \theta}{\mu A}.$$

Plugging in the given values,

$$V = \frac{(5\,\text{kg})(9.8\,\text{m/s}^2)(0.2 \times 10^{-3}\,\text{m}) \sin(10°)}{(0.1\,\text{Pa} \cdot \text{s})(0.12\,\text{m})^2} = 1.18\,\text{m/s}.$$

EXAMPLE 13.4

The steady flow of an incompressible fluid has the x and y velocity components:

$$u = x^2 + y^2 + z^2,$$

$$v = xy + yz + z.$$

What form does the z component of velocity have?

Given: u, v for steady, incompressible flow.
Find: w.
Assume: Steady flow.

Solution

We know that the volumetric strain rate can be written as the divergence of the velocity field, and that for an incompressible fluid or flow, this must equal zero:

$$\nabla \cdot \mathbf{V} = \frac{\partial u}{\partial x} + \frac{\partial v}{\partial y} + \frac{\partial w}{\partial z} = 0.$$

For the given velocity components,

$$\frac{\partial u}{\partial x} = 2x,$$

$$\frac{\partial v}{\partial y} = x + z.$$

Hence

$$2x + x + z + \frac{\partial w}{\partial z} = 0.$$

Or

$$\frac{\partial w}{\partial z} = -3x - z.$$

Integrating both sides in z:

$$w = -3xz - \frac{1}{2}z^2 + k(x, y),$$

where $k(x, y)$ may be a constant, or any function of x and/or y. The precise nature of $k(x, y)$ cannot be determined from what is known.

PROBLEMS

13.1 A beaker has the shape of a circular cone of diameter 7 in and height 9 in. When empty, it weighs 14 oz; full of liquid, it weighs 70 oz. Find the density of the liquid in both SI and U.S. customary units.

13.2 Some experimental data for the viscosity of argon gas at 1 atm are provided: Fit these data to a power law.

$T(K)$	300	400	500	600	700	800
μ (Ns/m^2)	2.27×10^{-5}	2.85×10^{-5}	3.37×10^{-5}	3.83×10^{-5}	4.25×10^{-5}	4.64×10^{-5}

13.3 Some experimental data for shearing stress τ and shear strain rate γ obtained for a particular non-Newtonian fluid at 80°F are shown below. Please plot these data and fit a second-order polynomial to the data using graphing software. Estimate the apparent viscosity of this fluid when the shear strain rate is $70\,\mathrm{s}^{-1}$, and compare this value with the viscosity of water at the same temperature.

τ (lb/ft^2)	0	2.11	7.82	18.5	31.7
γ (s^{-1})	0	50	100	150	200

13.4 The space between two very long parallel plates separated by a distance h is filled with a fluid with viscosity

$$\mu = \mu_0 \left(\frac{du}{dy} \right)^n,$$

where μ_0 is a constant and n is a constant exponent. The top plate slides to the right with a constant speed V_0, as shown.
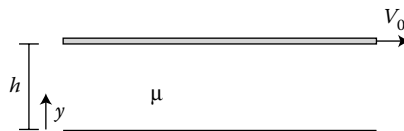
a. Find the velocity distribution between the plates, and an expression for the shear stress τ.

b. Graph the shear stress versus the shear strain rate V_0/h for several values of $n > 0$ (dilatant), $n = 0$ (Newtonian), and $n < 0$ (pseudoplastic).

13.5 Many devices have been developed to measure the viscosity of fluids. One such device, known as a *rotational viscometer*, involves a pair of concentric cylinders with radii r_i and r_o, and total length L. The inner cylinder rotates at a rate of Ω rad/s when a torque T is applied. Derive an expression for the viscosity of the fluid between the cylinders, μ, as a function of these parameters.

13.6 A thin plate is separated from two fixed plates by viscous liquids with viscosity values μ_1 and μ_2. The plate spacings are h_1 and h_2 as shown. The contact area between the center plate and each fluid is A. Assuming a linear velocity distribution in each fluid, find the force F required to pull the thin plate at velocity V.
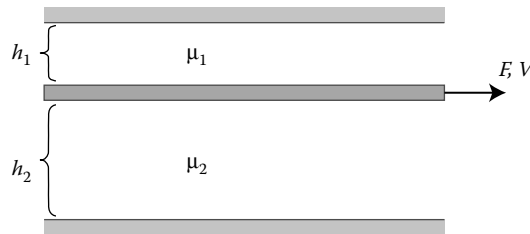
13.7 Magnet wire is single-strand wire with a thin insulation layer (of enamel, varnish, glass, etc.) to prevent short circuits. In a production facility, copper ($E = 120\,\text{GPa}$, $\sigma_{ys} = 70\,\text{MPa}$) magnet wire is to be coated with varnish by pulling it through a circular die (i.e., a cylindrical tube) of 0.35 mm diameter. The wire diameter is 0.30 mm and it is centered in the die. The varnish ($\mu = 0.020\,\text{Pas}$) completely fills the space between the wire and the die for a length of 30 mm. Determine the maximum speed with which the wire can be pulled through the die while ensuring a factor of safety of 3.0 with respect to yielding.

13.8 A solid cylindrical needle of diameter d, length L, and density ρ_n is able to float in liquid of surface tension s. Assuming a contact angle of $0°$, derive an expression for the maximum diameter d_{max} that will be able to float in the liquid. If the needle is steel and the liquid is water, what is the value of d_{max}?

13.9 A flow is described (in Cartesian coordinates) by the velocity vector $\mathbf{V} = 2xy\hat{\mathbf{i}} - 3y^2\hat{\mathbf{j}}$. Is the flow incompressible?

13.10 A flow is described (in Cartesian coordinates) by the velocity vector $\mathbf{V} = (2x^2 + 6z^2x)\hat{\mathbf{i}} + (y^2 - 4xy)\hat{\mathbf{j}} - (2z^3 + 2yz)\hat{\mathbf{k}}$. Is the flow incompressible?

13.11 For the given fluid stress tensor, calculate the following quantities.

$$\sigma = \begin{pmatrix} \sigma_{xx} & \sigma_{xy} & \sigma_{xz} \\ \sigma_{yx} & \sigma_{yy} & \sigma_{yz} \\ \sigma_{zx} & \sigma_{zy} & \sigma_{zz} \end{pmatrix} = \begin{pmatrix} -2Az & 0 & Ax \\ 0 & -2Az & Ay \\ Ax & Ay & -2Az \end{pmatrix}.$$

a. The stress divergence
b. The component of the surface force acting on a cube of edge length α in the y-direction
c. The total surface force acting on a cube of edge length α
d. The appropriate dimensions for the constant A

13.12 Is the velocity field $\mathbf{V} = (x^2 - y^2)\hat{\mathbf{i}} - 2xy\hat{\mathbf{j}}$ physically possible for a constant density flow?

13.13 The velocity distribution for a Newtonian constant density fluid is given by

$$\mathbf{V} = (6xy^2 - 3x^3)\hat{\mathbf{i}} + (9x^2y - 2y^3)\hat{\mathbf{j}}.$$

Determine the stress tensor for this flow.

13.14 A sled slides along a thin horizontal layer of water between an icy surface and the sled's runners. The horizontal force that the water applies to the runners is 5 N when the sled's speed is 15 ft/s. The total area of contact between both runners and the water is 74 cm^2. Determine the thickness of the water layer under the runners.

13.15 A piston with a diameter of 5.5 in and a length of 9.5 in slides downward with a velocity V through a vertical pipe. The downward motion is resisted by an oil film between the piston and the pipe wall. The film thickness is 0.002 in, and the cylinder weighs 0.5 lb. Estimate the piston velocity V if the oil viscosity is 0.016 lbs/ft^2.

14

Case Study 6: Mechanics of Biomaterials

We have discussed the properties and behavior of Hookean solids and Newtonian fluids: materials that are special cases, on either extreme of the spectrum of material behavior. These materials and most applications fit our favorite simplifying assumptions (homogeneity, isotropy, linearity, small deformations), nicely. While a great number of engineering materials are well-served by these assumptions and models, the increasingly important category of biomaterials demands that we consider the more complex behaviors between these two idealized extremes.

Biomaterials may be natural (blood vessels, bone, cartilage, or the cornea) or artificial (joint replacements, blood vessel shunts and stents, or the results of tissue engineering). Scientific interest in biomaterials is not an exclusively modern phenomenon: ancient technology relied on horn, tendon, and various woods and fibers. However, we are now able to analyze the biological role of biomaterials, and how these complex behaviors contribute to the species that rely on them. This helps us to understand the relationship between properties and applications, or between structure and function. Since engineers often seek to replace or mimic biological materials, we must understand both the material behavior and the biological reasons for it.

It is critical for engineers to understand how such materials will respond to loading, to mechanical stresses, and to biochemical and electrical stimuli, as well. In his pioneering texts on Biomechanics, Y. C. Fung outlines a systematic approach to problems in biomechanics: the first step is studying organism morphology, organ anatomy, tissue histology, and structure of materials. The second is *determining the mechanical properties of the materials involved*, before later steps—deriving the governing equations, developing boundary conditions, solving the problems, and performing experiments—follow. As Fung notes, determining the mechanical properties of biomaterials can be difficult, because "we cannot isolate the tissue for testing, or the size of available tissue specimens is too small, or it is difficult to keep the tissue in the normal living condition. Furthermore, biological tissues are often subjected to large deformations, and the stress–strain relationships are usually nonlinear and history dependent."

Tensile testing of the sort described in Chapters 2 and 4 has yielded an extensive array of properties for biomaterials. Values of elastic (Young's) modulus are tabulated in Table 14.1; values of the shear modulus and Poisson's ratio are shown in Table 14.2. These values come with strong disclaimers, though, as they are only as valid as the assumptions behind them. While these parameters have familiar meanings, and while biomaterials obey many of the equations we have already derived, we must be cautious. Remember well the assumptions implicit in many results of engineering mechanics, and consider how well such assumptions describe the material of interest. Remember the handy equation that could be used to relate E, G, and ν—Equation 4.2? It does not hold for biomaterials. The measured G and E tabulated for bone would suggest a Poisson's ratio of 0.8, which is twice the measured value and larger than the maximum theoretical value of 0.5 for isotropic materials; and tree trunks and bamboo stalks would have Poisson's ratios of 6 or 7. The modeling challenge is that those assumptions we have begun to make almost implicitly about

TABLE 14.1

Modulus of Elasticity for Various Biomaterials

Material	Elastic Modulus *E* (MPa)
Aorta, cow	0.2
Aorta, pig	0.5
Nuchal ligament (mainly elastin)	1.0
Dragonfly tendon (mainly resilin)	1.8
Cartilage	20
Tendon (mainly collagen)	2000
Tree trunks	6400
Wood, dry, with grain	10,000
Teeth (dentine)	15,000
Bone (large mammal)	18,000
Teeth (enamel)	60,000
Kevlar (synthetic fiber)	130,000
Steel	200,000

Source: S. Vogel, *Comparative Biomechanics: Life's Physical World*, Princeton: Princeton University Press, 2003.

Note: These values should be regarded as rough approximations, with wide variations depending on the rate of stretching, on the amount and orientation of deformation, and on the natural biological diversity of each material.

TABLE 14.2

Shear Modulus and Poisson's Ratio for Various Biomaterials

Material	Shear Modulus *G*	Poisson's Ratio ν (MPa)
Aorta (at 100 mm Hg)	0.15	0.24
Cartilage (rabbit)	0.35	0.30
Tendon (mainly collagen)	1 (huge variation)	0.40
Tree trunks	450	0.33
Bone (large mammal)	3300–5000	0.40
Teeth (enamel)	65,000	0.3
Kevlar (synthetic fiber)	30,000	–
Steel	77,000	0.33

Source: S. Vogel, *Comparative Biomechanics: Life's Physical World*, Princeton: Princeton University Press, 2003.

Note: These values should be regarded as rough approximations, with wide variations depending on the rate of stretching, on the amount and orientation of deformation, and on the natural biological diversity of each material.

materials—homogeneity, isotropy, linearity, and small deformations—often do not apply to biomaterials.

Material testing of biomaterials to obtain the values shown in Table 14.1 is also a challenge. The properties, microstructure, and behavior of natural biomaterials change in response to the physiological environment. This makes determining decisive experimental results or developing detailed constitutive models very difficult. (The interdependence of structure and function for biological materials also means that "bone" or "muscle" may

have very different behavior and properties depending on its physiological location and purpose. For example, human bone consists of both dense, very stiff cortical bone, which is much stiffer and stronger in the direction subjected to greater loads, as well as a porous trabecular or cancellous bone.) The bulk of elastomechanical testing of natural biomaterials has been conducted *in vitro* in an experimental simulacrum of *in vivo* conditions, including thermal conditions and ionic concentrations which affect smooth muscle activity. Proper specimen preparation and conditioning is vital to maintaining the integrity of the material. Debes and Fung first proposed a preconditioning of very low-frequency cyclic loading for a few cycles, suggesting that the internal structure of the tissue would respond to this loading until it reached a steady state that would allow consistent mechanical response to loading.

14.1 Nonlinearity

We may have begun to take for granted the linear elasticity of most engineering materials. When working problems, we may even have been tempted to construct a rubber stamp saying "Hooke's law applies" for the Assumptions section of our solutions. It is time, however, to re-examine that assumption. Many biomaterials have stress–strain curves that are not linear but are "J-shaped," that is, curves that get increasingly steep. An example is shown in Figure 14.1. This sort of curve signifies that the elastic modulus or stiffness of the material increases with extension. For materials with nonlinear behavior, the elastic modulus, cited in Table 14.1, is calculated from low-strain, quasi-linear "toe" region of the stress–strain curve.

In our discussion of pressure vessels, we considered an abdominal aortic aneurysm (Example 5.8), positing that the aneurysm exposed to high fluid pressures might remodel itself into a more spherical shape to reduce the induced stresses. The aortic wall, however, is not a Hookean material. And good thing, too: artery walls must expand and contract
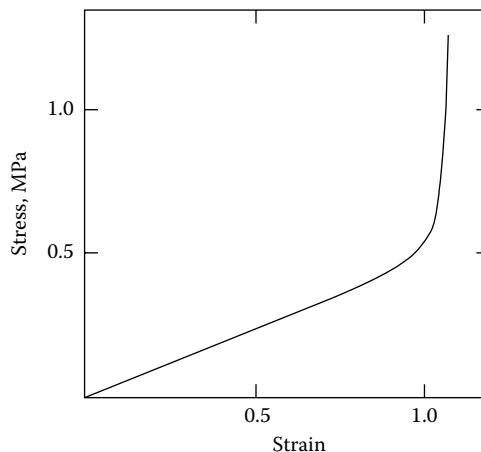
FIGURE 14.1
Exemplary J-shaped stress–strain curve for nuchal ligament of deer. (After S. Vogel, *Comparative Biomechanics: Life's Physical World*, Princeton: Princeton University Press, 2003.)

with each heartbeat, to accommodate the heart's pressure pulse. A Hookean material would be a poor choice for a cylinder meant to have a compliant wall, because already dilated portions of the cylinder would tend to expand further just as much as areas that had not expanded, thus creating regions of dangerously high stress.

Although Hookean linearity is the "best-case scenario" for many of our analyses, there are many reasons that *nonlinearity* is an advantage for biomaterials. Getting stiffer as it gets closer to the failure point can make a structure safer, because it then requires a disproportionate force to break. Additionally, the stress–strain curve's upward concavity reduces the area under the curve (compared to a Hookean material with the same limits), meaning less energy will be released on failure of the biomaterial. Energy release drives crack propagation, and for a biomaterial (e.g., skin), we would prefer cracks not to propagate.

14.2 Composite Materials

One way to keep cracks from propagating dramatically, and disastrously, through materials is to construct composites from materials with different properties. A well-known engineering trick is to use carbon fibers (which are very strong and stiff) to reinforce other materials, such as concrete (which is stronger in compression than in tension) or plastic (carbon fiber-reinforced plastic, widely known as "carbon fiber," is widely used in modern bicycles and racecars). This addition of a strong component allows the matrix materials (concrete or plastic) to be used in a wider array of applications and to be more durable. For more on engineered composite materials, please see Chapter 15.

Nature has made good use of composite materials, in wood and leaves of grass, and in tendons (which are collagen fiber-reinforced) and bone (in which cells form osteons that reinforce the longitudinal direction against compressive loads). Table 14.3 shows some natural composites and their components.

Blood vessels are soft tissue comprised of elastin and collagen fibers, smooth muscle, and a single layer of endothelial cells lining the vessel lumen. The proportions of the fibrous proteins and vascular smooth muscle depend on the type of blood vessel and the loading it must withstand. The two types of protein fibers have important consequences for the material behavior of vessels. Elastin is a very elastic fiber with a large Hookean region in

TABLE 14.3

Natural Composite Biomaterials

Material	Strong Component	Matrix
Wood	Cellulose (polysaccharide)	Lignin, hemicelluloses
Sponge body wall	Calcareous, siliceous spicules, collagen	Miscellaneous organic
Stony corals	Aragonite ($CaCO_3$) crystals	Chitin fibril network
Mollusk shell	Calcite ($CaCO_3$), aragonite	Protein, sometimes chitin
Bird eggshell	Calcite crystals	Protein, some polysaccharide
Cartilage	Collagen fibrils	Mucopolysaccharide
Bovid horn	Keratin fibers	Wet, amorphous keratin
Bone	Hydroxyapatite ($Ca_5(PO_4)_3(OH)$)	Collagen, other organic
Tooth enamel	Hydroxyapatite	Organic
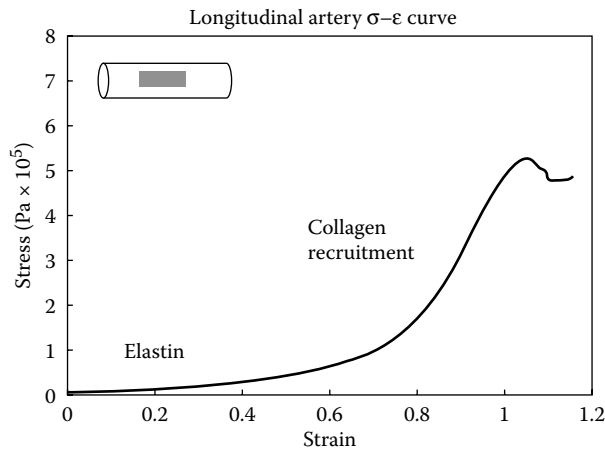
FIGURE 14.2
Experimental stress–strain diagrams for a bovine artery, showing two distinct regimes of material stiffness and the J-shaped overall curve. (Data from J. S. Rossmann, Elastomechanical properties of bovine veins, *Journal of Mechanical Behavior of Biomedical Materials* 3(2) (2010): 201–205.)

its stress–strain behavior. It provides blood vessels with the ability to expand (or *distend*) to accommodate the pressure pulse of the heartbeat. Vessels that are too stiff will not expand, which will result in high blood pressure or hypertension. Collagen fibers form a network outside the elastin. Collagen has a very high elastic modulus and a very high ultimate strength: its stiffness provides a *limit* to the vessel walls' distensibility. The collagen fibers are typically arranged with some slackness or "give;" in tendons, this is known as "crimp." This crimp means that each collagen fiber must be stretched taut before it begins to resist additional deformation, so that the material gradually stiffens as it is stretched. In this way, each collagen fiber in turn is "recruited" to contribute to the overall behavior of the vessel. This behavior creates a J-shaped stress–strain curve, as shown in the experimental data in Figure 14.2.

Figure 14.2 shows a stress–strain curve for a bovine artery with two identifiable regions: a long "toe" region of linear behavior dominated by elastin, in which large deformations result in only small stresses; and an increasingly steep region illustrating the recruitment of collagen fibers to stiffen the composite material.

Blood vessels also exhibit behavior called *cylindrical orthotropy*—different mechanical properties in the circumferential and longitudinal directions. Since we know from our study of pressure vessels that arteries and veins will experience different stresses in these two directions, it is only logical that arteries and veins have responded to directionally dependent pressure loading by having directionally dependent properties. The different stiffness values in circumferential and longitudinal directions are evident from the slopes of the experimentally obtained stress–strain diagrams shown in Figure 14.3.

Because of the difficulty associated with obtaining valid and generalizable experimental data for biomaterials, it is desirable to develop constitutive models (like the generalized form of Hooke's law useful for less complex materials). The gradual recruitment of collagen fibers has been included in constitutive models in a "neo-Hookean" fashion. In such a model, each collagen fiber can be thought of as a "linear" spring activated differently, with all the fibers (springs) acting in parallel, with this combination in parallel with the elastin component, in order to comprise the artery wall's bulk behavior.
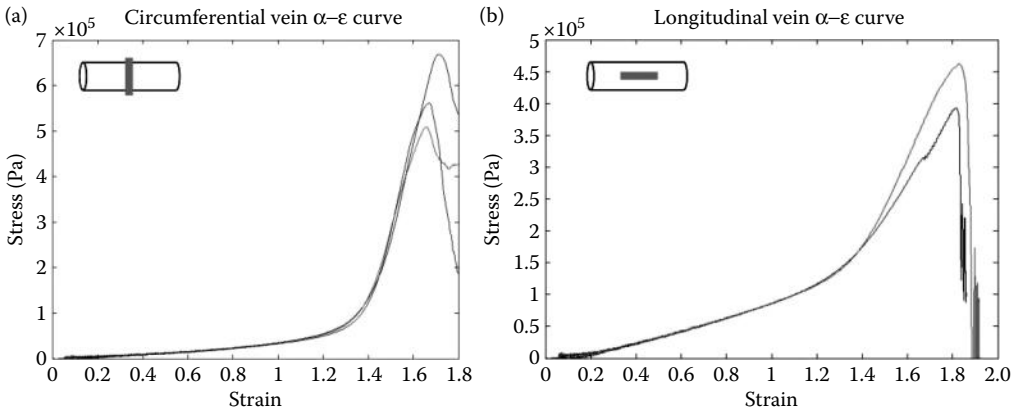
FIGURE 14.3
Experimental data for bovine veins in the (a) circumferential and (b) longitudinal directions. The slopes of the toe (elastin-dominated) regions are $E_{\text{circ}} = 30\,\text{kPa}$ and $E_{\text{long}} = 100\,\text{kPa}$.

14.3 Viscoelasticity

Recall the material behavior spectrum, and the special cases at its extrema: Hookean solids, for whom shear stress equals the product of a shear modulus and shear strain; and Newtonian fluids, for whom shear stress is viscosity times shear strain *rate*. At these extremes, these constitutive relationships are linear. We have already recognized that Hookean solids may be modeled as springs—as is the extension, so is the force; and that Newtonian fluids behave like dampers or dashpots. A spring is an elastic element, a dashpot a viscous one—so we will be able to fill in the middle of the material behavior spectrum with combinations of these two elements. Materials whose behavior is best described by such a combination are known as viscoelastic materials.

For viscoelastic materials, both how much they deform *and* how fast they deform are important. Many, biomaterials exhibit some degree of viscoelasticity. The two primary characteristics of viscoelastic behavior are *creep* and *stress relaxation*. *Creep* occurs when a material is exposed to a constant load for a long time and the material deforms increasingly: it is why a rubber band used to suspend a weight will gradually lengthen, and why you will find that you are measurably shorter at the end of an active day during which your intervertebral cartilage has been subjected to constant compressive loading. *Stress relaxation* means that when a constant deformation is applied to a material, over time it will resist that deformation less, so that the experienced loading decreases with time.

Another key feature of viscoelastic materials is *hysteresis*. This is the term used to describe the tendency of viscoelastic materials to dissipate energy, rather than to store all of the energy of deformation as linearly elastic solids do. A schematic of this behavior is shown on a stress–strain diagram in Figure 14.4a; the area between the loading and unloading curves represents dissipated or lost energy. (For a Hookean solid, the loading and unloading curves are the same for small deformations.) Figure 14.4b shows an experimentally obtained hysteresis curve for bovine veins in which it becomes clear that for these vessels, the amount of energy dissipated increases with increasing strain rate. This energy dissipation is what makes viscoelastic materials well suited to absorbing or cushioning shock.
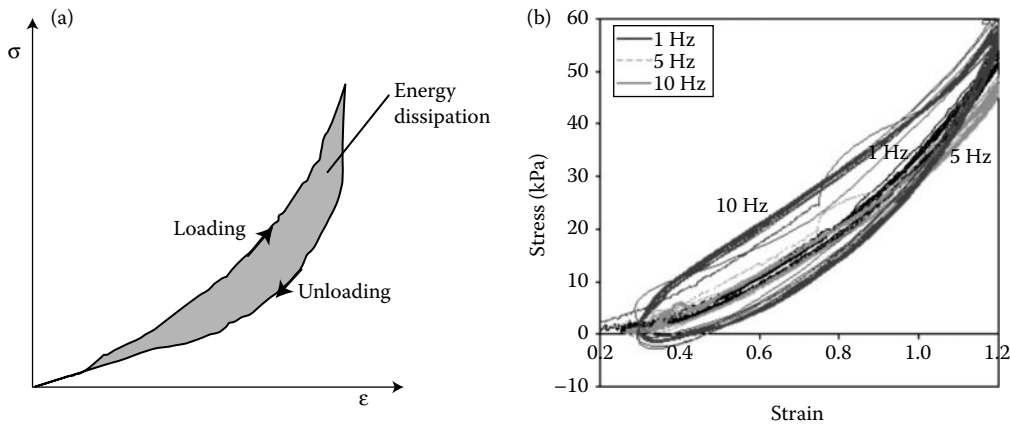
FIGURE 14.4
Hysteresis of viscoelastic materials: (a) representative stress–strain diagram; and (b) experimentally obtained stress–strain diagram for bovine veins. (Data from J. S. Rossmann, Elastomechanical properties of bovine veins, *Journal of Mechanical Behavior of Biomedical Materials* 3(2) (2010): 201–205.)
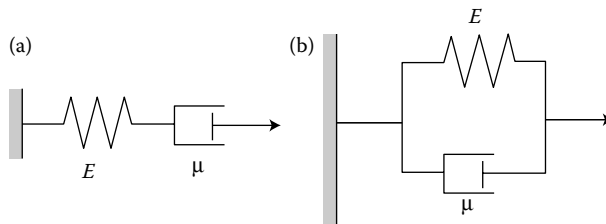
FIGURE 14.5
Schematics of the two most common mechanical models for viscoelastic material behavior: (a) Maxwell and (b) Kelvin–Voigt materials.

The classical models for viscoelasticity represent different combinations of the spring (elastic) and dashpot (viscous) elements, as shown in the schematics of Figure 14.5. Other combinations are possible, of course; but these two models proved remarkably effective for many materials.

For a Maxwell material, because the elastic and viscous elements are in series, they experience the same load ($\sigma_s = \sigma_d = \sigma$), and the net deformation of the material is the sum of the deformation of each element ($\varepsilon_s + \varepsilon_d = \varepsilon$).* The resulting constitutive law relating stress and strain is thus written as

$$E\mu\frac{d\varepsilon}{dt} = \mu\frac{d\sigma}{dt} + E\sigma, \tag{14.1}$$

where E is the elastic modulus or spring stiffness of the elastic element and μ is the dynamic viscosity of the viscous element of the material.

---

* The elements experiencing the same load translates to experiencing the same stress because the spring and dashpot are modeling two behavioral aspects of the same tissue, so they can be considered to have the same area. Similarly, since strain involves a reference (undeformed) length, and since both elements have a common reference, any relationships we would normally use for changes in displacement x also hold for strains.
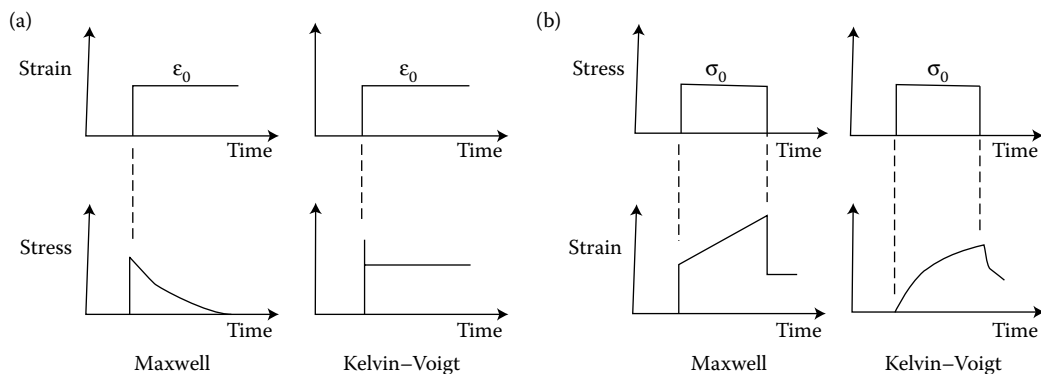
FIGURE 14.6
Characteristic (a) stress relaxation and (b) creep responses of the Maxwell and Kelvin–Voigt models. (After J. D. Humphrey and S. L. Delange, *Biomechanics*, New York: Springer, 2003.)

In a Kelvin–Voigt material, the elements in parallel share the same deformation ($\varepsilon_s = \varepsilon_d = \varepsilon$), and the total stress is the sum of that experienced by each element ($\sigma_s + \sigma_d = \sigma$). The constitutive law for the viscoelastic material is therefore

$$E\varepsilon + \mu\frac{\mathrm{d}\varepsilon}{\mathrm{d}t} = \sigma. \tag{14.2}$$

The ability of these models to capture viscoelastic behavior such as stress relaxation and creep varies, as you will see in Problems 14.2–14.4. The response of each model to a step input in load or deformation, which can be deduced from the constitutive equations, is shown in Figure 14.6.

A brief historical note: these models are attributed to James Clerk Maxwell (1831–1879), a prolific Scottish theoretical physicist who developed the Maxwell model of viscoelasticity in order to mathematically describe the viscous behavior of air; Woldemar Voigt (1850–1919), a German physicist notable for his work in crystallography; and William Thomson (Lord Kelvin, 1824–1907), an Irish thermodynamicist whose interest in modeling mechanical behavior was rooted in his interest in irreversibility, a.k.a. the second law of thermodynamics.

PROBLEMS

14.1 Show that the constitutive law for a Maxwell body must have the form given in Equation 14.1.

14.2 For the Kelvin–Voigt model of viscoelastic behavior, (a) find the solution of Equation 14.2, $\varepsilon(t)$, due to a step input in stress (a constant stress of magnitude unity applied beginning at $t = 0$), and (b) the solution $\sigma(t)$ due to a step input in strain. Sketch both solutions.

14.3 For the Maxwell model of viscoelastic behavior, (a) find the solution of Equation 14.1, $\varepsilon(t)$, due to a step input in stress (a constant stress of magnitude unity applied beginning at $t = 0$), and (b) the solution $\sigma(t)$ due to a step input in strain. Sketch both solutions.

14.4 Compare your results for Problems 14.2 and 14.3 to the sketches in Figure 14.6. Which of the two models represents creep behavior well, and which better represents stress relaxation?

References

J. C. Debes and Y. C. Fung, Biaxial mechanics of excised canine pulmonary arteries, *American Journal of Physiology* **269**(2) (1995): H433–H442.

Y. C. Fung, *Biomechanics: Mechanical Properties of Living Tissues*, New York: Springer, 1993.

M. R. Hill, X. Duan, G. A. Gibson, S. Watkins, and A. M. Robertson, A theoretical and non-destructive experimental approach for direct inclusion of measured collagen orientation and recruitment into mechanical models of the artery wall, *Journal of Biomechanics* **45** (2012): 762–771.

J. D. Humphrey and S. L. Delange, *Biomechanics*, New York: Springer, 2003.

J. S. Rossmann, Elastomechanical properties of bovine veins, *Journal of Mechanical Behavior of Biomedical Materials* **3**(2) (2010): 201–205.

S. Vogel, *Comparative Biomechanics: Life's Physical World*, Princeton: Princeton University Press, 2003.

15

Case Study 7: Engineered Composite Materials

In Chapter 14, we noted that some biological materials are "composites," comprised of multiple materials with significantly different physical properties. The resulting combined materials have characteristics that are different from any of their component materials. Many engineered composite materials are designed with similar objectives, often yielding materials that are stronger, lighter, or less expensive than traditional materials. We characterize the components as "matrix" and "reinforcement;" composite materials should have at least one of each. The matrix material surrounds and supports the reinforcement materials by maintaining their relative positions. The reinforcements impart their particular mechanical and physical properties to enhance the matrix properties. Like biological materials, engineered composites are often anisotropic, due to the orientation of the reinforcements. Engineered composite materials include concrete (and its steel-reinforced form as well), fiber-reinforced plastic (including fiberglass), metal composites, and ceramic composites.

15.1 Concrete

Concrete itself is a "composite," in the sense that it results from the combination of several materials. It is composed of (1) coarse granular aggregate sometimes called filler, embedded in (2) a hard matrix (cement or another binder) that fills the spaces among the aggregate particles and binds them together with the aid of (3) water. The ancient Roman architect/engineer Vitruvius* first wrote down a recipe for concrete—his version included volcanic ash as the binder. The Roman Colosseum was constructed from concrete; more recently, the Hoover Dam and Panama Canal have made good use of this material. It is now the most widely used structural material worldwide.

We often use steel bars (which are very strong) to reinforce concrete (which is stronger in compression than in tension). The resulting material is known as "rebar" due to the reinforcement provided by the bars. The bars may be arranged in any direction, to withstand anticipated loading, or in multiple directions when arranged in a mesh as in Figure 15.1. The addition of a reinforcing component allows concrete to be used in a wider array of applications, as the combined material is stronger, and able to withstand a wider range of loading types, than either component.

---

* Vitruvius was a Roman civil engineer during the first-century BC whose multi-volume book *De Architectura* records the building practices of Roman aqueducts, roads, and other structures. Vitruvius prized proportion and symmetry, and held dear three principles of effective design: utility, durability, and beauty. His work was rediscovered during the Renaissance and celebrated in Leonardo Da Vinci's image of the proportional ideal of the "Vitruvian man."

FIGURE 15.1
The Nine Bowl skateboarding facility in Troy, Michigan, uses rebar to provide strength and structural support. (Photo courtesy of Davo Scheich.)

15.2 Plastics

In the 1967 film *The Graduate*, the recent college graduate played by Dustin Hoffman is told that one word fully encompasses the future: "plastics" are said to be synonymous with progress, and the young graduate is directed to neglect them at his peril. Although the movie's sympathy with Hoffman's character painted the plastics enthusiast in a less than glowing light, from our contemporary perspective, it is true that plastics have transformed much of modern society.

Plastics are composed of organic polymers, which may be synthetic (often derived from petrochemicals) or natural. The vast majority of these polymers are based on chains of carbon atoms alone or with oxygen, sulfur, or nitrogen. This backbone links a large number of repeating units together. The properties of a plastic are affected by the different molecular groups hanging from the backbone, and may be fine-tuned by intentionally hanging side chains of artfully chosen structure.

Many commercially produced composites use a polymer matrix material often called a resin solution. There are many different polymers available depending upon the starting raw ingredients. There are several broad categories, each with numerous variations. The most common are known as polyester, vinyl ester, epoxy, phenolic, polyimide, polyamide, and polypropylene. The reinforcement materials are generally fibers or ground minerals.

In 1932, a researcher at Owens-Illinois accidentally pointed a jet of compressed air toward molten glass and produced glass fibers. Owens joined forces with the Corning Company in 1935, and the company soon patented "fiberglas" (with one 's'). However, the new material was very brittle, and refinements were made to its manufacturing process at Owens Corning before it began to be widely used in cars, airplanes, and boats.

We often use carbon fibers (which are very strong) to reinforce plastic: carbon fiber-reinforced plastic, widely known as "carbon fiber," is widely used in modern bicycles and racecars. Due to the orientation of the fibers, glass and carbon fiber-reinforced plastics are

typically anisotropic, but they can be designed to have strength in exactly the directions required by an application.

Polymer-based composites are now ubiquitous in modern society, beloved for their moldability into a wide variety of shapes, for their ability to be optimized for certain properties, and for their lightness and seeming indestructibility.

15.2.1 3D Printing

A particularly interesting application of plastics has been in the development of rapid prototyping or 3D Printing technology. In this process, a material—often ABS plastic—is heated until it flows from a printer head following toolpaths derived from computer-aided engineering drawings. The toolpaths describe successive layers of the designed object, building the object layer by layer. Adjacent layers cool and harden together. A second material, often a dissolvable plastic, is also used to support the object as it is being "printed." This is an additive manufacturing technique, as opposed to CNC manufacturing in which material is removed by the computer-controlled tool or printer head.

3D Printing is appealing because it enables designers to quickly and inexpensively move from drawing to prototype and to perform the iterations of the prototype and testing phases of design processes. It also permits complex shapes to be created much more easily than they could be machined with traditional manufacturing tools.

The resulting objects, however, are anisotropic, with different properties in the plane of printed layers than in other directions. While this is not what we typically mean by composite materials, the toolpaths of material that provides inner support to the object may be specified to provide reinforcement.

15.3 Ceramics

Ceramic matrix composites—in which fibers of ceramic are embedded in a ceramic matrix material—were engineered to combat a weakness of standard ceramics: their very low crack resistance (or fracture toughness). The most frequently used materials for both fiber and matrix are carbon, silicon carbide, alumina, and mullite. These new materials are of great interest in the aerospace industry, where the desirably low thermal conductivity of ceramics has sometimes been compromised by ceramics' brittleness and susceptibility to crack propagation.

Novel composite materials played a prominent role in the development of Boeing's 787 Dreamliner airplane (Figure 15.2), whose use of composites permitted a new robust single-barrel fuselage design and reduced aircraft weight. The 787 uses 50% composites by weight; by comparison, Boeing's 777 uses only 12% composites by weight and is 50% aluminum. Carbon fiber technology has also revolutionized the design of prosthetic limbs, including innovative designs using carbon-reinforced polymer (e.g., Figure 15.3) that have enabled double amputee athletes to compete in the Olympic Games.

The nature of the anisotropy in physical properties of composites depends on a range of factors. For example, the stiffness of a composite panel will depend upon the orientation of the applied loads and on the design of the panel: the fiber reinforcement and matrix used, the method of panel build, thermoset versus thermoplastic, type of weave, and orientation of fiber axis to the primary force. While the fibers do indeed provide "reinforcement" in their primary axis, composite materials are weak in the direction perpendicular to the fibers.

Materials used in 787 body
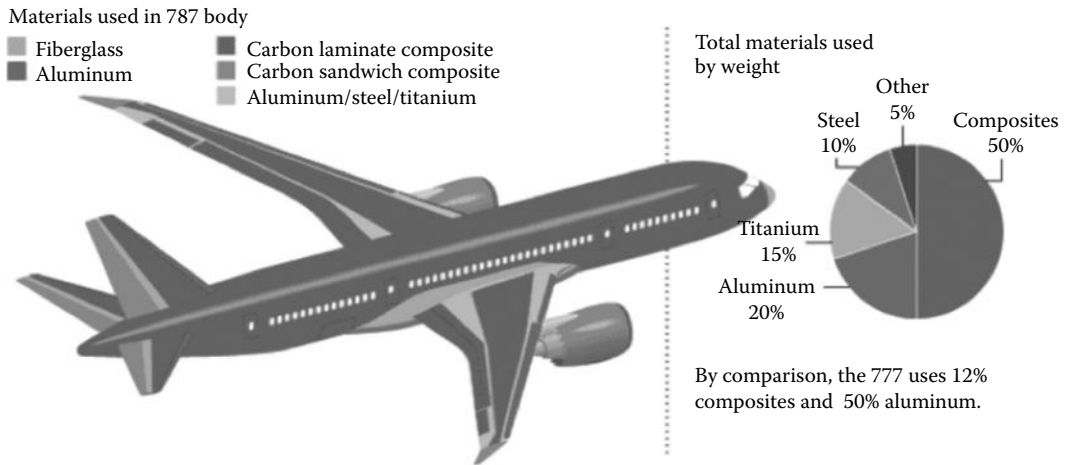
FIGURE 15.2
The Boeing 787 Dreamliner contains significantly more composite material than competitive aircraft. (Image courtesy of Boeing.)

FIGURE 15.3
Ossur's Flex Foot Cheetah prosthetics in action. (Image courtesy of Elvar Pálsson.)

For a composite material to be effectively strengthened and stiffened, the fibers must be longer than a critical fiber length. This critical length l_c depends on the fiber diameter d and its ultimate (typically tensile) strength σ_f^*, and on the smaller of the matrix's yield shear strength or the fiber–matrix bond strength, τ_c, according to

$$l_c = \frac{d\sigma_f^*}{2\tau_c}. \tag{15.1}$$

For many glass and carbon fiber–matrix combinations, this critical length is in the order of 1 mm, which is between 20 and 150 times the fiber diameter. When fibers are much longer than this critical fiber length ($l \gg l_c$, generally $> 15 l_c$), they are known as "continuous fibers" and are effective in transferring stress from the matrix and reinforcing the material. When fibers are much shorter than the critical length, the matrix deforms significantly and is not as effectively reinforced. However, sometimes the relative ease and expense of "discontinuous fiber" or particulate reinforcement may justify settling for less effective strengthening; short-fiber composites may achieve elastic modulus and tensile strength values near 90 and 50% of comparable continuous-fiber materials.*

When dealing with engineered *or* natural composite materials, we must remember that the material stiffness in our generalized form of Hooke's law (Equation 4.15) permits us to take into account different behavior in different directions: often, composite materials have stiffness or compliance matrices that are much more interesting than those of isotropic materials!

PROBLEMS

15.1 A continuous-fiber composite is loaded axially, in the direction of fiber alignment. In this case, we may model the fiber and matrix as two materials in parallel: the two materials "share" the applied load F, so that $F = F_f + F_m$; and the two materials experience the same normal strain in the direction of the applied load. Develop an expression for the effective elastic modulus of the composite material in terms of the moduli and volume fractions of its fiber and matrix constituents.

15.2 For the material and loading described in Problem 15.1, what is the ratio of the load carried by the fibers to that carried by the matrix?

15.3 A continuous-fiber composite is loaded transversely, in the direction normal to the fiber alignment. We may model the fiber and matrix as two materials in series: the two materials experience the same stress; and "share" the deformation in the transverse direction, so that the material's net deformation is the sum of the deformation of each element. Develop an expression for the effective elastic modulus of the composite material in terms of the moduli and volume fractions of its fiber and matrix constituents.

15.4 Wrapped carbon tubes are often used for fishing rods, tail booms for helicopters and gliders, and drive shafts for small vehicles. In the roll-wrapping process, a resin pre-impregnated fiber cloth (Pre-Preg) is wrapped around a mandrel; tubes may be manufactured in a variety of woven patterns. Provide an explanation for why either a helical or a square weave might be selected.

15.5 Research the controversy surrounding the eligibility of athletes with prosthetic limbs to compete in the Olympic Games. Propose at least three calculations that can be made using concepts in this textbook to determine whether prosthetic limbs comprise an "unfair advantage" for an athlete. Please specify to which sport(s) and which event(s) your proposed calculations are most relevant.

---

* Please see W. D. Callister, *Materials Science and Engineering: An Introduction*, Wiley, for further discussion.

16

Fluid Statics

When there is no relative motion between fluid particles, no shearing stresses exist, and the only stress present is a normal stress, the pressure. Hence $\mathbf{F} = m\,\mathbf{a}$ (or more properly, $\sum \mathbf{F} = m\,\mathbf{a}$) is a balance between the forces due to pressure and the inertia of the fluid. Our fluid, like the solids we studied in Chapters 2 to 11, is in *equilibrium*.

16.1 Local Pressure

We have defined fluid pressure as an infinitesimal normal force divided by the infinitesimal area it acts on. From our study of solid mechanics, we may suspect that the value of p will change if the orientation of this planar area changes—that we will have a different p if the xy-plane is rotated to $x'y'$. However, this is *not* the case, as we can show by a simple analysis of a now-familiar inclined plane.

If we write the equations of motion ($\sum \mathbf{F} = m\,\mathbf{a}$) in the y- and z-directions for the element shown in Figure 16.1, we have

$$\sum F_y = p_y\,dx\,dz - p_s\,dx\,ds\,\sin\theta = \rho\frac{dx\,dy\,dz}{2}a_y, \tag{16.1a}$$

$$\sum F_z = p_z\,dx\,dy - p_s\,dx\,ds\,\cos\theta - \rho g\frac{dx\,dy\,dz}{2} = \rho\frac{dx\,dy\,dz}{2}a_z, \tag{16.1b}$$

noting the geometry of the problem, $dy = ds\cos\theta$ and $dz = ds\sin\theta$, we can rewrite these equations as

$$p_y - p_s = \rho a_y\frac{dy}{2}, \tag{16.2a}$$

$$p_z - p_s = (\rho a_z + \rho g)\frac{dz}{2}. \tag{16.2b}$$

And, since our real interest is in what is happening at a *point*, we shrink this element, taking the limit as dx, dy, and dz go to zero (while maintaining θ), and hence we must have $p_y = p_s$ and $p_z = p_s$, or

$$p_s = p_y = p_z. \tag{16.3}$$

Since θ was an arbitrary angle, this must be true for any θ, so that we may say *the pressure at a point at a fluid is independent of direction as long as there are no shearing stresses present*. In other words, in a fluid at rest, pressure at a point is the same in all directions. This result is due to the French mathematician Blaise Pascal (1623–1662) and is known as *Pascal's law*.
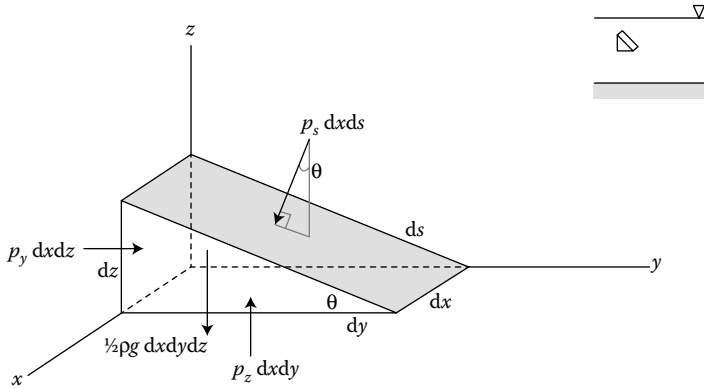
FIGURE 16.1
Forces on an arbitrary wedge-shaped element of fluid.
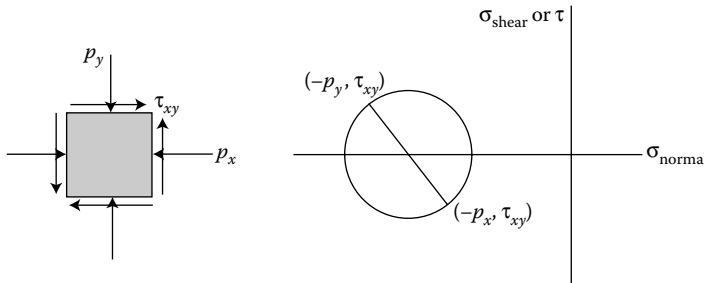
FIGURE 16.2
Mohr's circle.

We could also consider the Mohr's circle of stress for a fluid with no relative motion between fluid particles. A general Mohr's circle is sketched in Figure 16.2. When shear stress is absent, Mohr's circle degenerates to a point and $p_i = p_j$. Hence using Mohr's circle, we could have beaten Pascal to the punch.

16.2 Force due to Pressure

We would like to be able to determine the pressure variation within a fluid. Certainly, Pascal's law will help us do this. We will consider another small fluid element, this time in the shape of a cube (the shape is ours to choose since Pascal's law tells us that p at the center of an element is independent of the orientations of the element's faces, and choosing a cube simplifies the geometry). This element is shown in Figure 16.3. We will write Newton's second law for this element, first finding an expression for the force due to pressure $p(x, y, z)$.

The pressure is p at the center of our element, a point with coordinates (x, y, z). Since p varies in x, y, and z, we can write the pressures at each of the element's faces using the chain rule:
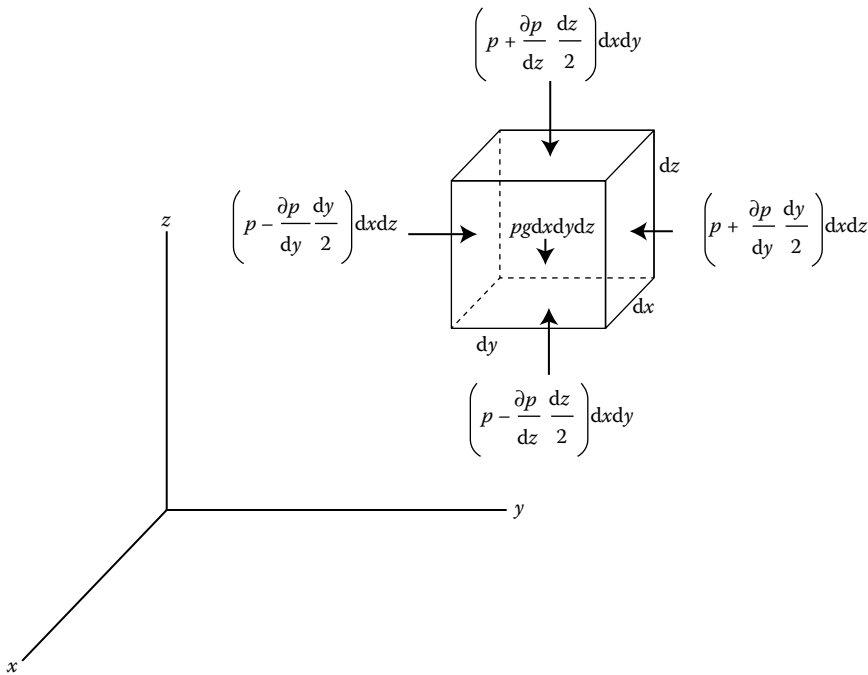
FIGURE 16.3
Forces acting on a small fluid element (x forces, not shown, have similar form).

$$\mathrm{d}p = \frac{\partial p}{\partial x}\,\mathrm{d}x + \frac{\partial p}{\partial y}\,\mathrm{d}y + \frac{\partial p}{\partial z}\,\mathrm{d}z, \tag{16.4}$$

so that the pressure at a distance $(\mathrm{d}x/2)$ from the element's center is written as

$$p\left(x + \frac{\mathrm{d}x}{2}, y, z\right) = p(x, y, z) + \frac{\partial p}{\partial x}\frac{\mathrm{d}x}{2}. \tag{16.5}$$

The same reasoning gives us expressions for the pressure on all six faces of the element in Figure 16.3.

The resultant forces on the element are the differences between those on top and bottom, right and left, or front and back faces. For example, the resultant force due to pressure in the y-direction is

$$\mathrm{d}F_y = -\frac{\partial p}{\partial y}\,\mathrm{d}x\,\mathrm{d}y\,\mathrm{d}z. \tag{16.6}$$

And the resultant surface force on the element can be written in vector form as $\mathrm{d}\mathbf{F} = \mathrm{d}F_x\hat{\mathbf{i}} + \mathrm{d}F_y\hat{\mathbf{j}} + \mathrm{d}F_z\hat{\mathbf{k}}$, or

$$\mathrm{d}\mathbf{F} = -\left(\frac{\partial p}{\partial x}\hat{\mathbf{i}} + \frac{\partial p}{\partial y}\hat{\mathbf{j}} + \frac{\partial p}{\partial z}\hat{\mathbf{k}}\right)\mathrm{d}x\,\mathrm{d}y\,\mathrm{d}z. \tag{16.7}$$

The group of terms in parentheses is the vector form of the *pressure gradient*, or grad p. We can thus write the resultant surface force on the element using the notation:

$$\frac{d\mathbf{F}}{dx\,dy\,dz} = -\nabla p. \tag{16.8}$$

Something very interesting has happened: the force on the element due to pressure has been shown to depend only on the *gradient* of pressure, or on how pressure varies in x, y, and z.

To complete $\sum \mathbf{F} = m\,\mathbf{a}$, we combine this resultant surface force with the body force (gravity) acting on the element and set these forces equal to the inertia of the element. The body force is written as $-\rho g\,dx\,dy\,dz\,\hat{\mathbf{k}}$, and $m\mathbf{a}$ is written as $\rho\,dx\,dy\,dz\,\mathbf{a}$. The element volume, $dx\,dy\,dz$, appears in all terms and may be divided out of the equation, leaving in vector form

$$-\nabla p - \rho g\hat{\mathbf{k}} = \rho\mathbf{a}. \tag{16.9}$$

This is the general equation of motion for a fluid in which there are no shear stresses. It is an equation per unit volume of the fluid, since we have divided through by $dx\,dy\,dz$, and each term in Equation 16.9 hence has dimensions of force-per-volume.

16.3 Fluids at Rest

In the special case of a fluid at rest, acceleration $\mathbf{a} = \mathbf{0}$ and the governing equation reduces to

$$-\nabla p - \rho g\hat{\mathbf{k}} = 0. \tag{16.10}$$

With three component equations:

$$\frac{\partial p}{\partial x} = 0, \tag{16.11a}$$

$$\frac{\partial p}{\partial y} = 0, \tag{16.11b}$$

$$\frac{\partial p}{\partial z} = -\rho g. \tag{16.11c}$$

The x and y components show that the pressure in this special case does not depend on x or y. The pressure $p = p(z)$ only, and its dependence is given by

$$\frac{dp}{dz} = -\rho g. \tag{16.12}$$

To use this equation to calculate pressure throughout a fluid, it is necessary to specify how the product (ρg) varies with z. In most engineering applications, variation in g is negligible, and so we concern ourselves primarily with the variation of density ρ.

An *incompressible* fluid is defined as one which requires a *very large* pressure change to effect a small change in volume. This threshold is so high that in most cases, the fluid's

volume and therefore its density are constant. Most liquids satisfy this requirement. When ρg can be taken to be constant, the equation for p is easily integrated:

$$\int_{p_1}^{p_2} \mathrm{d}p = -\rho g \int_{z_1}^{z_2} \mathrm{d}z. \tag{16.13}$$

So,

$$p_1 - p_2 = \rho g (z_2 - z_1), \tag{16.14}$$

or, if $h = z_2 - z_1$, then $p_1 - p_2 = \rho g h$ or

$$p_1 = p_2 + \rho g h. \tag{16.15}$$

This equation describes what is called a *hydrostatic* pressure distribution. The distance $h = z_2 - z_1$ is measured downward from the location of p_2. Equation 16.15 is sometimes written in the shorthand form:

$$\Delta p = \rho g \Delta h. \tag{16.16}$$

While Equation 16.16 is handy, we must be mindful of the physical significance of these "deltas." Hydrostatic pressure increases linearly with depth, as the pressure increases to "hold up" the weight of the fluid above it. This is familiar knowledge to anyone who has lingered near the bottom of a deep swimming pool, or gone SCUBA diving.

Many devices exploit the hydrostatic pressure distribution. The hydraulic brakes in an automobile take advantage of the fact that pushing on a column of fluid with a certain force (by pressing on a foot pedal) transmits the pressure by moving brake fluid through the car's brake lines. A hydraulic lift in a mechanic's shop allows a small force to be applied to a small piston area, then transmitted as fluid pressure to a larger area in order to lift a heavy vehicle (whose weight is much greater than the small force applied).* Similar hydraulic pistons are often used to reduce the force required to move or lift heavy loads.

For a *compressible* fluid—typically a gas—the fluid density can change significantly due to relatively small changes in pressure and temperature. For these fluids, the product ρg is typically quite small—for air at sea level at 60°F, ρg is 0.0763 lb/ft³, compared with 62.4 lb/ft³ for water at the same conditions. It, therefore, requires very large elevation changes h to make much difference in the pressure of compressible fluids. To account for the variation in ρg, we make use of the ideal gas law, $p = \rho R T$, to write

$$\frac{\mathrm{d}p}{\mathrm{d}z} = -\frac{gp}{RT}. \tag{16.17}$$

Separating variables and integrating, we get

$$\int_{p_1}^{p_2} \frac{\mathrm{d}p}{p} = \ln\left(\frac{p_2}{p_1}\right) = -\frac{g}{R} \int_{z_1}^{z_2} \frac{\mathrm{d}z}{T}, \tag{16.18}$$

where g and R are assumed constant over the elevation change from z_1 to z_2.

---

* Readers concerned that this might violate the energy conservation principle should note that the distance the large piston is moved is much less than the throw of the smaller piston, and thus breathe more easily.
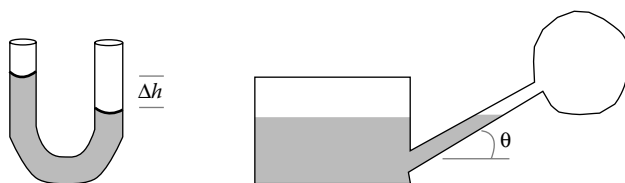
FIGURE 16.4
Types of manometers: left, U-tube; right, inclined-tube.

Pressure is often measured using liquid columns in vertical or inclined tubes, or *manometers*. These devices make use of the information we have just obtained: that pressure increases with depth and that (therefore) two points at the same elevation in a continuous length of the same fluid must have the same pressure. The three most common types of manometers are U-tube and inclined-tube manometers, and piezometers. Examples of manometers are shown in Figure 16.4.

As you might expect, manometers are not particularly well suited for the measurement of very high pressures (since they must then include a very very long tube), or of pressures which vary rapidly in time. Some other devices have thus been developed—and they are of special interest to us as students of continuum mechanics. This other class of measurement devices makes use of the idea that when a pressure acts on an elastic structure the structure will deform, and this deformation can be related to the magnitude of the pressure. A Bourdon tube is one example of this; it consists of a calibrated hollow, elastic curved tube that tends to straighten when the pressure inside it increases. A *pressure transducer* as in Figure 16.5 converts the reading from a Bourdon tube or other measurement device into an electrical output.
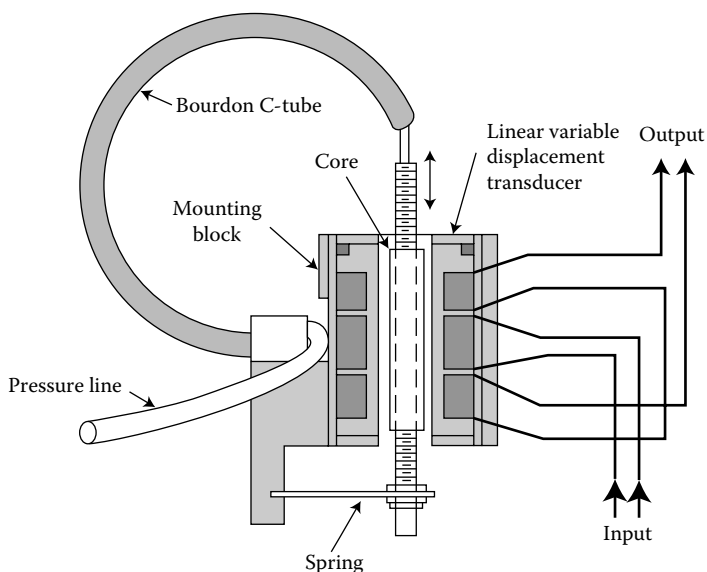
FIGURE 16.5
Bourdon tube pressure transducer. (After B. R. Munson, D. F. Young, and T. H. Okiishi, *Fundamentals of Fluid Mechanics*, 1998. Copyright Wiley-VCH Verlag GmbH & Co. KGaA. Reproduced with permission.)

Another example of this type of device is shown in Figure 16.6. In this case, the sensing element is a thin, elastic diaphragm that is in contact with the fluid. Fluid pressure causes the diaphragm to deflect, and its deflection is measured and converted into an electrical voltage. Strain gages are attached to the reverse side of the diaphragm or to an element attached to the diaphragm. Figure 16.6a shows two different sized strain-gage pressure transducers, both made by Viggo-SpectraMed (now Ohmeda), commonly used to measure physiological pressures within the human body. Pressure-induced deflection of the diaphragm is measured using a silicon beam on which strain gages and a bridge circuit have been deposited (as shown in Figure 16.6b).
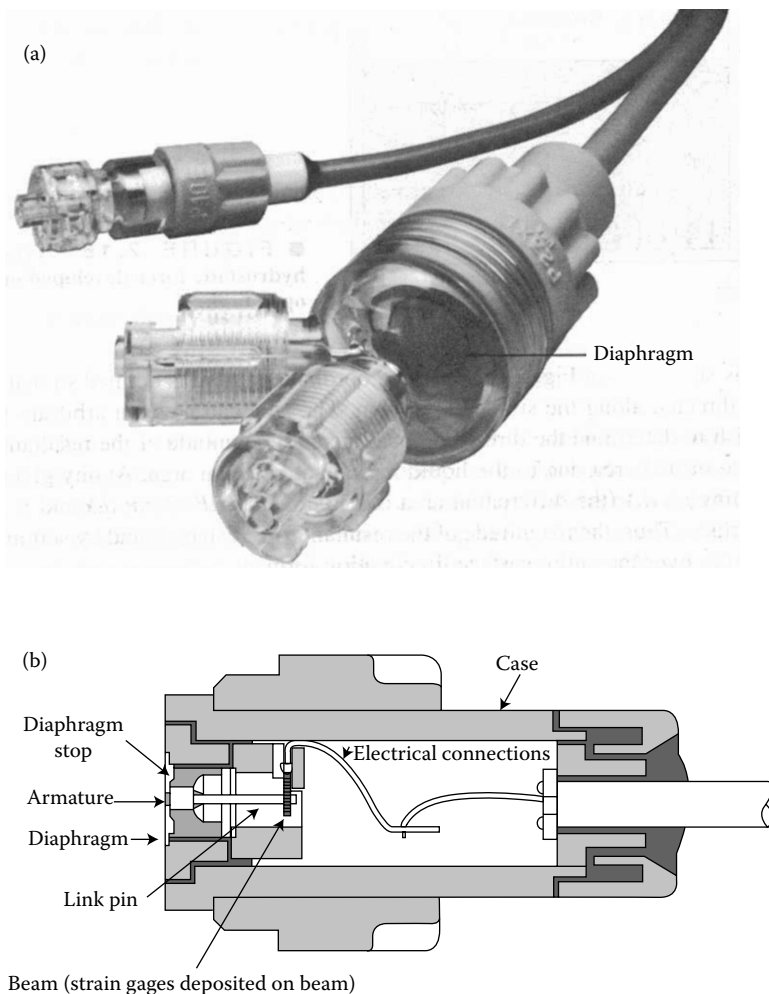
FIGURE 16.6
(a) Photographs and (b) schematic of strain-gage pressure transducers used for biological flows. (B. R. Munson, D. F. Young, and T. H. Okiishi, *Fundamentals of Fluid Mechanics*, 1998. Copyright Wiley-VCH Verlag GmbH & Co. KGaA. Reproduced with permission.)

16.4 Forces on Submerged Surfaces

When we design devices and objects that are submerged within a body of fluid, such as dams, ships, holding tanks, bridge supports, and artificial reefs, we must consider the magnitudes and locations of forces acting on both plane and curved surfaces due to the fluid. If the fluid is at rest, we know that this force will be perpendicular to the surface (normal stress) since there are no shearing stresses present. If the fluid is also incompressible, we know that the pressure will vary linearly with depth.

For a horizontal surface, such as the bottom of a tank, the force due to fluid pressure is easily calculated. The resultant force is just $F = pA$, where p is the uniform pressure and equals $\rho g h$ and A is the area of the surface. Since the pressure is constant and uniformly distributed over the bottom, the resultant force acts through the centroid of the area.

In the case of a vertical surface, the pressure is not constant, but varies linearly with depth along the submerged surface. This is sketched in Figure 16.7b, and reminds us very much of the distributed loading we have seen acting on beams, as in Figure 16.7a. In our analysis of such beams, we found that the equivalent concentrated force (by which we replaced the distributed load to calculate reactions and internal forces) acted through the centroid of the area between the force profile and the beam surface. For example, for a linearly increasing load as in Figure 16.7a, the shape created is a triangle, and the resultant concentrated load acts at $h/3$ from the right end, the centroid of that triangle. The same is true for submerged surfaces. In Figure 16.7b, a hydrostatic pressure is drawn as a distributed load on a vertical wall. This creates a triangular shape, known as a "pressure prism," whose centroid is at $h/3$ from the deepest point. This is the "center of pressure" (the point at which the resultant force acts, y_R) for this load. The resultant force F_R is simply the pressure integrated over this vertical surface:

$$F_R = \int_A dF = \int_A p\, dA = \int_A \rho g y\, dA = \rho g h_c A, \qquad (16.19)$$

where $h_c = h/2$ is the depth of the centroid of the submerged surface itself (as opposed to the centroid of the load distribution) and A is the area of the vertical surface.

We would like to move beyond the idealizations of horizontal and vertical surfaces to more realistic geometries. It will be useful to formulate a method for calculating the force due to pressure on an *inclined* surface, at an angle θ to the horizontal fluid surface as shown in Figure 16.8. This general formulation can then be applied to a wide range of problems.
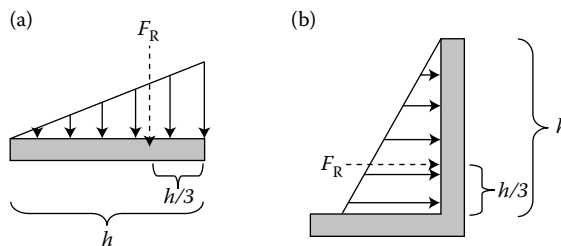
FIGURE 16.7
Pressure prisms for (a) distributed beam loading and (b) hydrostatic pressure.
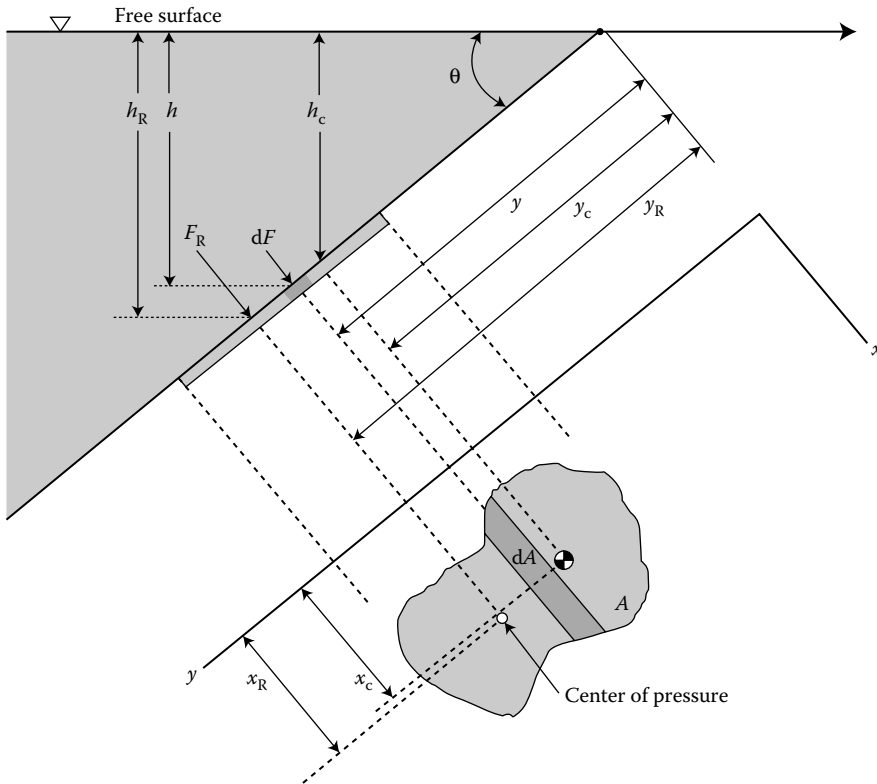
FIGURE 16.8
Hydrostatic force on an inclined plane surface of arbitrary shape.

Essentially, we are once again considering the effect of a distributed force, and in order to deal with the equivalent concentrated load, we must find the "center of pressure" at which this equivalent load acts. We choose coordinates, as shown in Figure 16.8, that are convenient for the surface in question, and we must find the point (x_R, y_R)—the center of pressure, at which the resultant force acts.

The total force exerted on the plane surface by the fluid is simply the integral of the fluid pressure over the surface's entire area:

$$F_R = \int_A dF = \int_A p\, dA, \qquad (16.20)$$

where p is the gage pressure. For a fluid at rest, the pressure distribution is hydrostatic, and $dF = \rho gh = \rho gy \sin\theta$. For constant ρg and θ, we thus have

$$F_R = \rho g \sin\theta \int_A y\, dA, \qquad (16.21)$$

and we recognize that the integral $\int y\, dA = y_c A$, where y_c is the position of the centroid of the entire submerged surface. So, the resultant force is simply

$$F_R = \rho g A y_c \sin\theta = \rho g h_c A, \qquad (16.22)$$

where h_c is the vertical distance from the fluid surface to the centroid of the area. We notice that this force's magnitude is independent of the angle θ and depends only on the fluid's specific weight, the total area, and the depth of the centroid.

Although we might suspect that this resultant force passes through the centroid of the surface, if we remember that pressure is increasing with increasing depth, we realize that the center of pressure must actually be below the centroid. We can find the coordinates of the center of pressure by summing moments around the x-axis, forcing the moment of the resultant force to balance the moment of the distributed force due to pressure, so that

$$y_R = \frac{\int_A y^2 \, dA}{y_c A} = \frac{I_x}{y_c A}. \tag{16.23}$$

Please note that the xy-axes are now playing the same role for our submerged surface that the yz-axes did for beam cross sections, so that I_y in the context of beams is the same as I_x in this new context. Since I_{xc} (about the centroid) is typically the easiest second moment of area to calculate, and the one tabulated in handy places,* we use the parallel axis theorem to make sure we are considering the second moment of area with respect to our x-axis as drawn in Figure 16.8:

$$I_x = I_{xc} + A y_c^2, \tag{16.24}$$

so that

$$y_R = \frac{I_{xc}}{y_c A} + y_c. \tag{16.25}$$

This expression demonstrates that the resultant force acts on a point *below* the centroid, since $I_{xc}/y_c A > 0$. In a similar way, we determine the x-coordinate of the center of pressure:

$$x_R = \frac{I_{xyc}}{x_c A} + x_c. \tag{16.26}$$

The second moment of area I_{xy} that appears in this expression is the second moment of area with respect to the x- and y-axes, and equals $\int xy \, dA$. For symmetric (about their x-axes) shapes, I_{xyc} is 0 and the resultant force acts at x_c.

When the submerged surface in question is *curved*, our work is somewhat more complicated. The resultant force due to pressure acts *normal* to the surface, which did not affect our integration over the surface area for a plane surface as the surface had only one outward normal vector. However, for a curved surface, the outward normal changes continuously all along the surface, making our integration less easily simplified.

Rather than accounting for this variation in the outward normal, most analyses simply separate the resultant force on the surface F_R into its horizontal (F_H) and vertical (F_V) components. Each of these has a straightforward physical interpretation that becomes clear when it is calculated. As an example, let us consider a parabolic dam as shown in Figure 16.9. The shape of the curved dam surface is described by $z/z_0 = (x/x_0)^2$.

The gage pressure at any height z is given by

$$p = \rho g(h - z). \tag{16.27}$$

---

* For example, in Appendix A of this book!
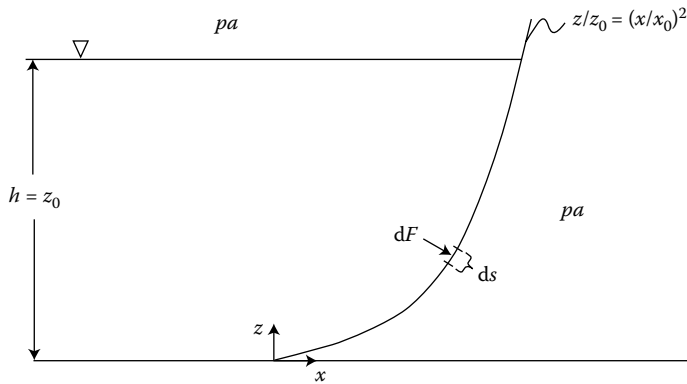
FIGURE 16.9
Curved surface of a parabolic dam.

So, the infinitesimal force at any height z, acting on an infinitesimal area element dA, is

$$dF = \rho g(h - z)\, dA. \tag{16.28}$$

And the area dA at any z is simply the width w of the dam into the page times the infinitesimal length ds along the curved surface, as shown in Figure 16.10.

We want to find the horizontal and vertical components of this vector $d\mathbf{F}$, so we begin with the horizontal force:

$$dF_H = dF \sin\theta \tag{16.29}$$

$$= \rho g(h - z)w\, ds \sin\theta. \tag{16.30}$$

From Figure 16.10, we see that $ds \sin\theta$ is just dz, so we have

$$dF_H = \rho g(h - z)w\, dz, \tag{16.31}$$
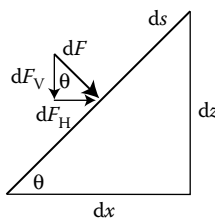
FIGURE 16.10
Infinitesimal segment of a curved surface.

and we proceed by integrating in z to find the resultant horizontal force on the surface.

$$F_H = \rho g \int_0^h (h - z) w \, dz \tag{16.32a}$$

$$= \rho g w \left[hz - \frac{z^2}{2} \right]_0^h \tag{16.32b}$$

$$= \frac{1}{2} \rho g w h^2. \tag{16.32c}$$

We can rearrange this horizontal force as

$$F_H = \left(\rho g \frac{h}{2} \right) w h, \tag{16.33}$$

and recognize that wh would be the area of a vertical projection of our parabolic curved surface and that $\rho g(h/2)$ would be the resultant force on this vertical projection. We can thus physically interpret the horizontal component of force on a curved submerged surface as the resultant force that would act on a vertical projection (same depth into page, same height) of the curved surface.

Next, we look for the vertical component F_V, integrating $dF_V = dF \cos \theta$ over the surface:

$$dF_V = dF \cos \theta \tag{16.34}$$

$$= \rho g(h - z) w \, ds \cos \theta, \tag{16.35}$$

In Figure 16.10, we see that $ds \cos \theta$ is just dx, so we have

$$dF_V = \rho g(h - z) w \, dx. \tag{16.36}$$

To integrate this expression in x, we will need to express z as a function of x, using the equation of the curved surface. Here, when substituting z in terms of x, we use $z_0 = h$.

$$F_V = \rho g \int_0^{x_0} \left(h - \frac{h}{x_0^2} x^2 \right) w \, dx$$

$$= \rho g h w \left[x - \frac{x^3}{3x_0^2} \right]_0^{x_0}$$

$$= \frac{2}{3} \rho g h w x_0. \tag{16.37}$$

We recognize that $\frac{2}{3} x_0 z_0$ is the area contained by a parabolic section with maximum height z_0 and maximum width x_0. (In our case, $z_0 = h$.) Since w is the width of this section

into the page, the vertical force component is the fluid density ρ times the acceleration of gravity g times the volume of fluid, that is, this force is equal to the weight of fluid above the curved surface.

To find the center of pressure at which the resultant of these components acts, we first consider where each component force must act. For the inclined plane surface, these components must induce the same *moment* about a reference point as does the distributed force. Because F_H is the force that would act on a vertical projection of the curved surface, it acts where the equivalent force due to pressure would act on that vertical projection: at $h/3$ up from the base of the surface, the centroid of the pressure prism. Because F_V is the weight of the fluid supported by the surface, it acts at the x-coordinate of the centroid of that volume of fluid. These coordinates come naturally out of the moment calculation. Taking our reference point as the origin of the x, z axes, we require

$$\underbrace{F_H z_H}_{\substack{\text{moment due to concentrated} \\ \text{horizontal force component}}} = \rho g w \underbrace{\int_0^h z(h - z) \mathrm{d}z.}_{\substack{\text{sum of all moments due to all} \\ \text{infinitesimal forces } \mathrm{d}F_H, \text{ each} \\ \text{with moment arm } z}} \tag{16.38}$$

For any curved surface (since the shape of the curve, $x(z)$ does not enter into the integral), this moment equivalence requires that $z_H = \frac{1}{3}h$. We must also have

$$\underbrace{F_V x_V}_{\substack{\text{moment due to concentrated} \\ \text{vertical force component}}} = \rho g w \underbrace{\int_0^{x_0} x(h - z) \mathrm{d}x.}_{\substack{\text{sum of all moments due to all} \\ \text{infinitesimal forces } \mathrm{d}F_V, \text{ each} \\ \text{with moment arm } x}} \tag{16.39}$$

For our parabolic surface, we plug in $z = (h/x_0^2)x^2$, and we get $x_V = \frac{3}{8}x_0$. This is in fact the x-coordinate of the centroid of a parabolic section. The line of action of the resultant force $F_R = \sqrt{(F_H^2 + F_V^2)}$ passes through the point (x_V, z_H) with slope $= \tan^{-1}(F_V/F_H)$.

16.5 Buoyancy

An object that is submersed in fluid is subjected to hydrostatic pressure over its entire surface area. In the previous section, we limited ourselves to the consideration of simple surfaces—walls, gates, and dams. However, if we recognize that the hydrostatic pressure acts on *all* surfaces, we see clearly how a resultant *buoyancy* force arises. The sketch in Figure 16.11 illustrates this.

Archimedes (287–212 BC) was a Greek mathematician who invented the lever, fine-tuned the definition of *pi*, and "discovered" buoyancy. Though some details of this story have taken on the distinct patina of apocrypha, it is still a cracking-good yarn. Archimedes' close friend, King Hiero of Syracuse, suspected that the gold crown he had recently received
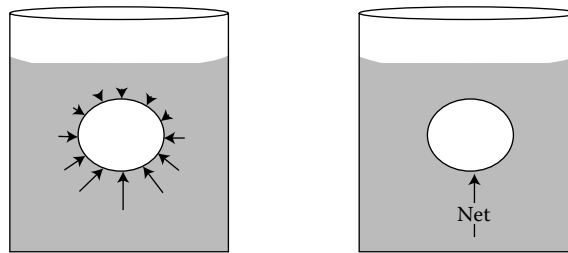
FIGURE 16.11
Distributed force due to hydrostatic pressure on a submerged object. Left, distributed; right, net resultant upward vertical buoyancy force.

from the goldsmith did not include all of the gold he had supplied. He shared his suspicions with Archimedes, who (it is said) went home to ruminate in the bathtub. Archimedes, ever observant, noticed that his body displaced the bathwater—when he got into the tub, the water level rose. He quickly calculated that the weight of displaced water balanced his own weight, and celebrated this discovery by running through the streets shouting "*Eureka* (I have found it)," so intoxicated by hydrostatics that he neglected to dry off or don a bathrobe. The next day, so the story goes, Archimedes dunked his friend's crown, as well as a lump of gold equal to what he had provided to the goldsmith, and found that they did not displace equal amounts of water. The crown did, in fact, contain less gold than the King had specified. The goldsmith, unable to produce the remainder of the gold, was beheaded posthaste.

Archimedes' principle states that the buoyant force on an object equals the weight of the volume of fluid the object displaces.

The force on a submerged object due to the fluid's hydrostatic pressure tends to be an upward vertical force, as the pressure in the fluid increases with depth and the resultant force is upward. Refer to Figure 16.11 to visualize this. If this buoyancy force exactly balances the weight of the object, the object is said to be neutrally buoyant.

The line of action of the buoyancy force acts through the centroid of the displaced fluid volume. The stability of an object designed to float on or maneuver in a fluid depends on the moments due to the buoyancy and weight forces on the object, and whether the resultant moment will tend to right or to capsize the craft. For submerged vessels that operate at a range of depths, mechanisms that allow active control of these forces are necessary. Tanks that can be flooded or filled with air to adjust the vessel's weight mimic the swim bladder in fish to allow vessels to maintain the proper force balance.

16.6 Examples

EXAMPLE 16.1

Determine the pressure difference between the benzene at A and the air at B.

   Given: Manometer geometry and gage fluids; heights of fluid columns.
   Find: Pressure difference between A and B.

Assume: No relative motion of fluid elements (hydrostatics); fluids have constant, uniform density, and it is appropriate to evaluate densities at 20°C.
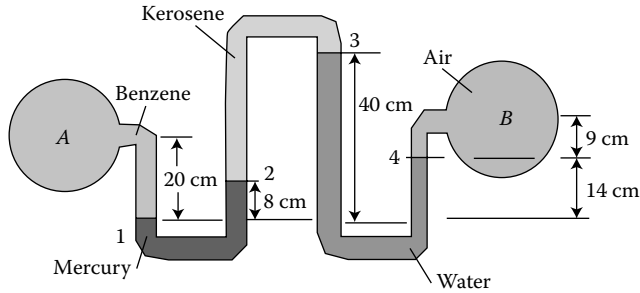
Solution

We look up the properties of the fluids used in our manometer at 20°C and find that

Fluid	Density ρ (kg/m^3)
Water	998
Mercury	13,550
Air	1.2
Benzene	881
Kerosene	804

We know that in a fluid at rest, the pressure depends only on the elevation in the fluid. Thus, in any continuous length of the same fluid, two points at the same elevation must be at the same pressure. Manometers are based on this principle. We find the requested pressure difference by starting at point A and working our way through the manometer, noting that the pressure increases when the fluid level drops and that pressure decreases when the fluid level rises.

$$
\begin{aligned}
\text{Point 1:} &\quad P_1 = P_A + \rho_B g h_1 \\
\text{Point 2:} &\quad P_2 = P_1 - \rho_M g h_2 \\
\text{Point 3:} &\quad P_3 = P_2 - \rho_K g h_3 \\
\text{Point 4:} &\quad P_4 = P_3 + \rho_W g h_4 \\
\text{At } B: &\quad P_B = P_4 - \rho_A g h_5.
\end{aligned}
$$

So, $P_B = P_A + \rho_B g h_1 - \rho_M g h_2 - \rho_K g h_3 + \rho_W g h_4 + \rho_A g h_5$. Factoring out g, we have $P_B - P_A = g(\rho_B h_1 - \rho_M h_2 - \rho_K h_3 + \rho_W h_4 + \rho_A h_5)$:

$$
\begin{aligned}
P_B - P_A = (9.8\,\text{m/s}^2)[&(881\,\text{kg/m}^3)(0.2\,\text{m}) - (13{,}550\,\text{kg/m}^3)(0.08\,\text{m}) \\
&- (804\,\text{kg/m}^3)(0.32\,\text{m}) \\
&+ (998\,\text{kg/m}^3)(0.26\,\text{m}) \\
&- (1.2\,\text{kg/m}^3)(0.09\,\text{m})] = -8885\,\text{Pa},
\end{aligned}
$$

or, $P_A - P_B = 8.9\,\text{kPa}$.

EXAMPLE 16.2

Panel ABC in the slanted side of a water tank is an isosceles triangle with the vertex at A and the base $BC = 2\,\mathrm{m}$, as shown. Find the force on the panel due to water pressure, and this force's line of action.
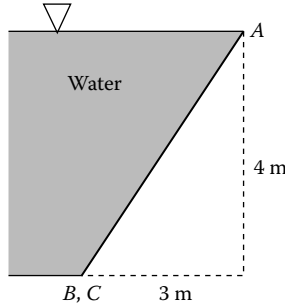
Given: Dimensions of panel in water tank.

Find: Resultant force on panel, location of center of pressure.

Assume: No relative motion of fluid elements (hydrostatics); water has constant, uniform density, equal to its tabulated value at $20\,^\circ\mathrm{C}$ ($998\,\mathrm{kg/m^3}$).

Solution

We first want to understand the geometry of the triangular panel. We are given a side view of the tank, and the height of the triangle ABC. In a head-on view, we would see the panel as sketched below at left.
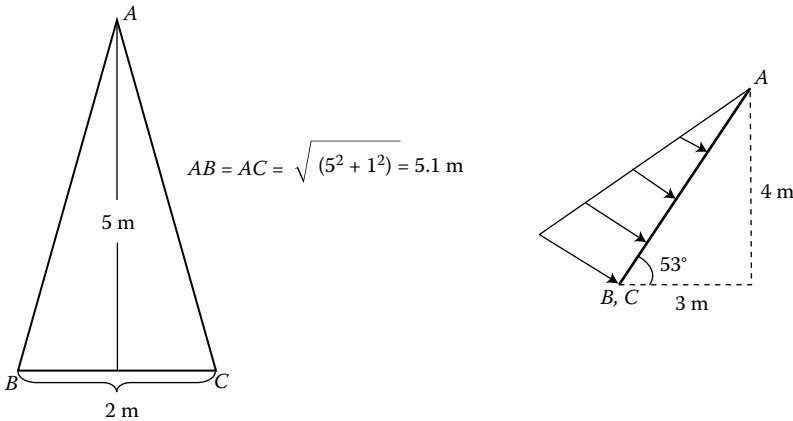
The water pressure has a hydrostatic distribution, as sketched above at right, and the resultant force is found by integrating this pressure over the panel area. This is equivalent to the formula:

$$F_\mathrm{R} = \rho g h_\mathrm{c} A,$$

where h_c is the depth of the centroid of the submerged surface, the triangular panel ABC. The depth of point A is zero; the depth of points B and C is $4\,\mathrm{m}$. The depth of the centroid of the triangular gate ABC is 2/3 of the way down. (*Note*: This is because

the submerged surface is a triangle, *not* because the pressure has a triangular pressure prism.)

$$h_c = \frac{2}{3}(4\,\text{m}) = 2.67\,\text{m},$$

$$A = \frac{1}{2}bh = \frac{1}{2}(2\,\text{m})(5\,\text{m}) = 5\,\text{m}^2.$$

So,

$$F_R = \rho g h_c A = (998\,\text{kg/m}^3)(9.8\,\text{m/s}^2)(2.67\,\text{m})(5\,\text{m}^2),$$

$$F_R = 131{,}000\,\text{N} = 131\,\text{kN}.$$

This force acts at the center of pressure of the submerged panel ABC. Due to the symmetry of the panel, this is on the centerline ($x_R = 0$), and we are only required to calculate the y-coordinate y_R.
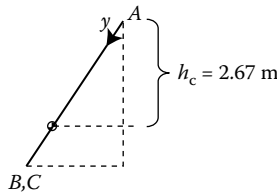
Similar triangles:
$$\frac{4}{5} = \frac{2.67}{y_c}$$
$$y_c = 3.33\,\text{m}$$

$$y_R = y_c + \frac{I_{xc}}{y_c A} = y_c + \frac{I_{xc}\sin\theta}{h_c A}$$

$$= y_c + \frac{(1/36)bh^3\sin\theta}{h_c A}$$

$$= 3.33\,\text{m} + \frac{(1/36)(2\,\text{m})(5\,\text{m})^3\sin 53°}{(2.67\,\text{m})(5\,\text{m}^2)}$$

$$= 3.33\,\text{m} + 0.417\,\text{m}$$

$$= 3.75\,\text{m}.$$

Note that this y_R is measured down from A, along the panel surface, as shown in the sketch.
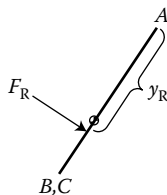
EXAMPLE 16.3

Gate *AB* has an evenly distributed mass of 180 kg, and is 1.2 m wide "into the page." The gate is hinged at *A* and rests on a smooth tank floor at *B*. For what water depth *h* will the force at point *B* be zero?
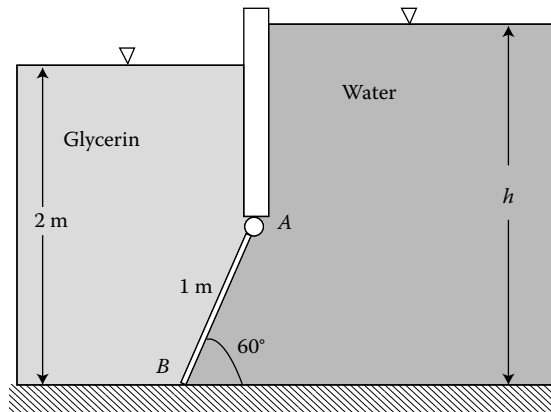
Given: Gate dimensions and mass; fluids on either side.

Find: Water depth *h* required for $R_B = 0$.

Assume: No relative motion of fluid elements (hydrostatics); fluids have constant, uniform density, and it is appropriate to evaluate densities at 20°C. Looking up these values, we find that the densities of water and glycerin are 998 kg/m^3 and 1260 kg/m^3, respectively.

Solution

We start with a FBD of gate *AB*.
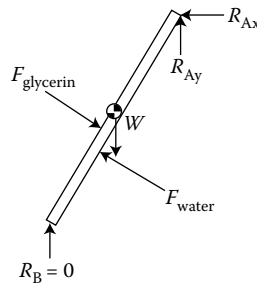
We intend to apply the equations of equilibrium to the gate, to ensure the proper relationships between forces and meet the constraint that R_B must be equal to 0. To do this, we will first need to evaluate all the forces in the FBD. The weight of the gate is simply *mg*, or $W = (180 \text{ kg})(9.8 \text{ m/s}^2) = 1766 \text{ N}$, and this force acts at the centroid of the gate.
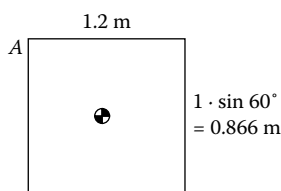
Next, we must find the forces on the gate due to fluid pressure, and where they act. We begin with glycerin. Since we would prefer not to have to find the reaction forces at *A*, we plan to sum moments about this point. We will need to know the depth of the centroid of the gate, h_c, measured from the surface of glycerin. The gate is a rectangle, as shown above, and due to its symmetry, its centroid is simply 0.433 m down from the hinge at *A*. The depth of the centroid is thus $2\,\text{m} - 0.433\,\text{m} = 1.567\,\text{m}$ below the glycerin surface.

$$F_{\text{glycerin}} = \rho_{\text{glycerin}} g h_c A$$
$$= (1260\,\text{kg/m}^3)(9.8\,\text{m/s}^2)(1.567\,\text{m})(1.2\,\text{m}^2)$$
$$= 23.2\,\text{kN}.$$

This force acts at $y_R = y_c + I_{xc}/(y_c A) = y_c + I_{xc}\sin\theta/(h_c A)$, and since we intend to sum moments about *A*, we would like to know the moment arm from F_{glycerin} to point *A*. Thus, we are most concerned with how much deeper y_R is than y_c, as y_c is clearly 0.5 m from point *A*.

$$y_R - y_c = \frac{I_{xc}\sin\theta}{h_c A} = \frac{(1/12)bh^3\sin\theta}{h_c A} = \frac{(1/12)(1.2\,\text{m})(1\,\text{m})^3\sin 60^\circ}{(1.567\,\text{m})(1.2\,\text{m}^2)} = 0.0461\,\text{m}.$$

We now know that $F_{\text{glycerin}} = 23.2\,\text{kN}$ has a moment arm of 0.5461 m relative to point *A*.

What remains to be found is the force due to the water on the other side of the gate. Both the magnitude of this force and its moment arm (where it acts) will depend on the depth of water, *h*. For the moment, we will leave both these values in terms of the depth of the centroid of the gate, h_c, measured from the water surface—the depth $h = h_c + 0.433\,\text{m}$.

$$F_{\text{water}} = \rho_{\text{water}} g h_c A$$
$$= (998\,\text{kg/m}^3)(9.8\,\text{m/s}^2)h_c(1.2\,\text{m}^2)$$
$$= (11.75 h_c)\,\text{kN}.$$

And this force acts at y_R, where

$$y_R - y_c = \frac{I_{xc}\sin\theta}{h_c A} = \frac{(1/12)bh^3\sin\theta}{h_c A} = \frac{(1/12)(1.2\,\text{m})(1\,\text{m})^3\sin 60^\circ}{h_c(1.2\,\text{m}^2)} = \frac{0.0722}{h_c}.$$

So, $F_{\text{water}} = 11.75 h_c$ kN has a moment arm of $(0.5 + 0.0722/h_c)$ m relative to point *A*.
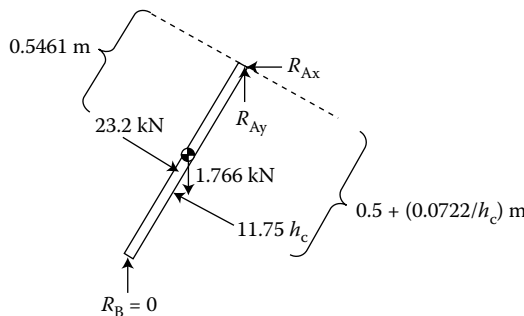
We choose to sum moments about point A to avoid having to solve for the hinge reaction forces, and require that the gate be in equilibrium:

$$\circlearrowleft \quad \sum M_A = 0 = (23{,}200\,\text{N})(0.5461\,\text{m}) + (1766\,\text{N})(0.5\cos 60^\circ) - (11{,}750 h_{\text{c}})\left(0.5 + \frac{0.0722}{h_{\text{c}}}\right).$$

Solving this expression for h_{c}, we find

$$h_{\text{c}} = 2.09\,\text{m}.$$

The depth of the water is then $h = h_{\text{c}} + 0.433\,\text{m} = 2.52\,\text{m}$.

EXAMPLE 16.4

The bottle of champagne shown is under pressure, as indicated by the mercury-manometer reading. Compute the net vertical force on the 2-in radius hemispherical end cap at the bottom of the bottle.
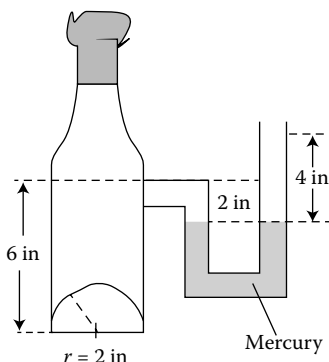
Given: Pressure measurement; bottle geometry.

Find: Net vertical force on hemispherical surface.

Assume: No relative motion of fluid elements (hydrostatics); fluids have constant, uniform density, and it is appropriate to evaluate densities at $68\,^\circ$F. We look up values for champagne and mercury at this temperature and find that $(\rho g)_{\text{C}} = 59.9\,\text{lbf/ft}^3$, and $(\rho g)_{\text{M}} = 847\,\text{lbf/ft}^3$.

Solution

We have a manometer that gives us the champagne pressure at a height of 6 in (We will denote values at this position by the subscript $*$), if we work through the U-tube as we did in Example 16.1:

$$p_* + (\rho g)_{\text{C}}\left(\frac{2}{12}\,\text{ft}\right) - (\rho g)_{\text{M}}\left(\frac{4}{12}\,\text{ft}\right) = p_{\text{atm}} = 0 \quad \text{(gage)}.$$

So,

$$p_* = (\rho g)_{\text{M}}(0.333\,\text{ft}) - (\rho g)_{\text{C}}(0.167\,\text{ft})$$

$$= (847\,\text{lbf/ft}^3)(0.333\,\text{ft}) - (59.9\,\text{lbf/ft}^3)(0.167\,\text{ft})$$

$$= 272\,\text{lbf/ft}^2 = 272\,\text{psf}.$$

This pressure p_* acts on the circular cross-sectional area of the champagne bottle at a height of 6 in, imparting a resultant force of $p_* A = (272\,\text{psf})(\frac{\pi}{4}(\frac{4}{12}\,\text{ft})^2) = 23.74\,\text{lbf}$ on the champagne below it. In addition, the champagne below this 6 in height imparts its own force on the hemispherical surface. The vertical component of this force, which we are looking for, can also be interpreted as the weight of this champagne above the surface. The net vertical force on the endcap will thus be the $p_* A$ force already calculated, *plus* the weight of the fluid below $*$ and above the hemispherical surface. Since we know the specific weight of the champagne, we need only to find the volume between $*$ and the endcap.
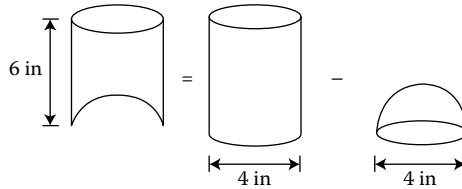
$$F_V = p_* A + \text{weight of champagne}$$

$$= p_* A + (\rho g)_C \left[\pi(0.167)^2(0.5) - \frac{2\pi}{3}(0.167)^3 \right]$$

$$= 23.74\,\text{lbf} + [2.61 - 0.58]\,\text{lbf}$$

$$= 25.8\,\text{lbf}.$$

EXAMPLE 16.5

A parabolic dam's shape is given by $z/z_0 = (x/x_0)^2$, where $x_0 = 10\,\text{ft}$ and $z_0 = 24\,\text{ft}$. The dam is 50 ft wide (into the page). Find the resultant force on the dam due to the water pressure, and its line of action.
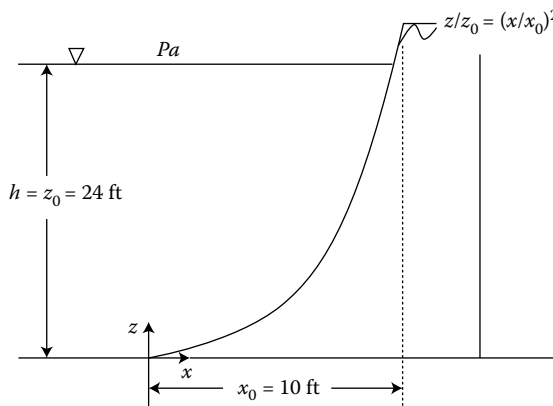
Given: Geometry of dam; water depth.

Find: Resultant force due to pressure; line of action.

Assume: No relative motion of fluid elements (hydrostatics); fluids have constant, uniform density, and it is appropriate to evaluate densities at $68°\text{F}$.

Solution

We look up the density of water at this temperature and find that $\rho g = 62.4\,\text{lbf/ft}^3$. We will find separately the horizontal and vertical components of the resultant force on the dam surface. To find the horizontal component F_H, we consider the vertical projection of the curved dam surface, a rectangle which is 24 ft high and 50 ft wide (into the page). This projected surface has an area $A = (24)(50) = 1200\,\text{ft}^2$, and its centroid is halfway down, at a depth of $h_\text{c} = 12\,\text{ft}$. So,

$$F_\text{H} = \rho g h_\text{c} A$$
$$= (62.4\,\text{lbf/ft}^3)(12\,\text{ft})(1200\,\text{ft}^2)$$
$$= 899{,}000\,\text{lbf}$$
$$= 899\,\text{kips}.$$

This force acts at the centroid of the pressure prism on the projected vertical surface, at $z_\text{H} = h/3 = 8$ ft from the bottom.

The vertical component F_V can be interpreted as the weight of fluid above the curved surface. We consider the properties of a parabolic section, as shown in the sketch, to find this value.
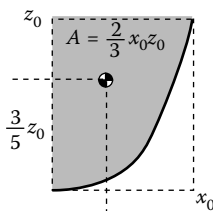
$$F_\text{V} = \rho g \,\mathcal{V}$$
$$= \rho g \left(\frac{2}{3} x_0 z_0 \right) (50\,\text{ft})$$
$$= (62.4\,\text{lbf/ft}^3) \left[\frac{2}{3}(24\,\text{ft})(10\,\text{ft}) \right] (50\,\text{ft})$$
$$= 499{,}000\,\text{lbf}$$
$$= 499\,\text{kips}.$$

This force acts at the x-coordinate of the centroid of the volume of fluid, $\mathcal{V}$. From our sketch, we see that this is $3x_0/8 = 3.75$ ft from the origin indicated above.

The resultant normal force on the surface of the parabolic dam is

$$F_\text{R} = \sqrt{F_\text{H}^2 + F_\text{V}^2}$$
$$= \sqrt{(899\,\text{k})^2 + (499\,\text{k})^2}$$
$$= 1028\,\text{kips}.$$

The line of action of this force passes through the point $(x_V, z_H) = (3.75\,\text{ft}, 8\,\text{ft})$, and has slope equal to $\tan^{-1}(F_V/F_H) = \tan^{-1}(499/899) = 29°$.

$z = 0.24x^2$

$F_R = 1028\,\text{k}$

499

899

8 ft

Center of pressure

3.75 ft
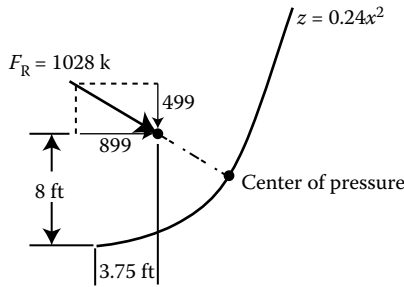
PROBLEMS

16.1 In 1646, the French scientist Blaise Pascal put a long vertical pipe in the top of a barrel filled with water and poured water in the pipe. He found that he could burst the barrel (not just make it leak a bit like the picture shows) even though the weight of the water added in the pipe was only a small fraction of the force required to break the barrel. Briefly explain his finding.
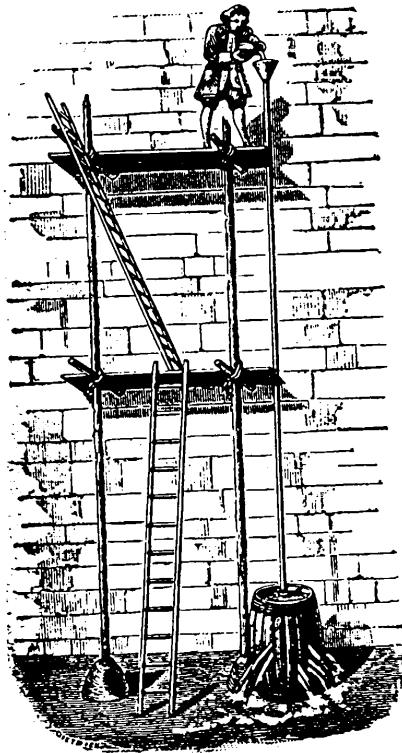
16.2 In each of the gates shown, the top of the gate is supported by a frictionless hinge. Each has a rectangular overhang that sticks out or in a distance a from the gate (a is small relative to the depth h). A stop at the bottom of each wall prevents it from opening in a counterclockwise direction. When the water is at the same depth h in

both cases, what is the ratio of the horizontal force exerted on stop (a) to the horizontal force exerted on stop (b)? Please draw appropriate FBDs.
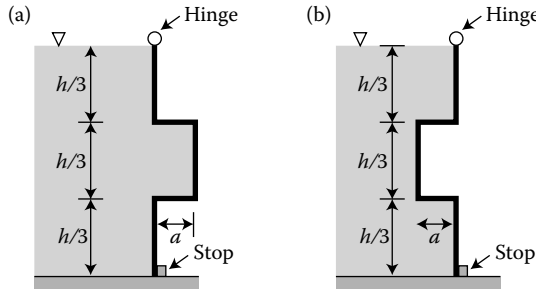
16.3 The wood ($\sigma_{ys} = 8\,\text{ksi}$, $E = 1.5 \times 10^6\,\text{psi}$) forms for a concrete wall that is to be 8 ft high are sunk into the ground at the bottom (fixed support) and held in place at the top (10 ft from the ground) by 0.5-in diameter tie rods that permit negligible horizontal deflection at that height. Each plank in the form may be modeled as an individual beam.

(End view)
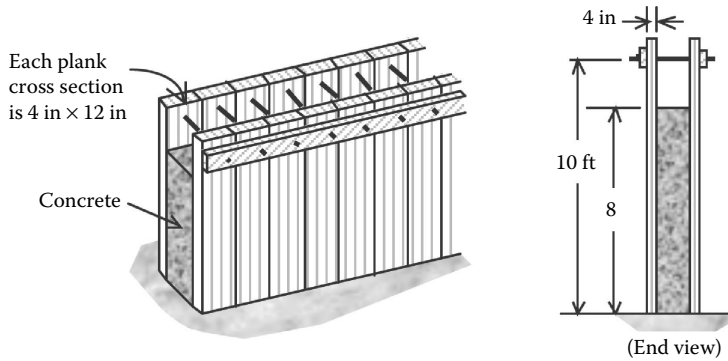
Assuming that concrete behaves as a liquid (specific gravity = 2.5) just after it is poured, determine

a. The resultant force on a plank due to the concrete, and its corresponding center of pressure (height as measured from the ground)

b. The normal stress in a tie rod using the *actual distributed load*

c. The maximum normal stress due to bending in a plank using the *actual distributed load*

16.4 For wall A shown, what is the magnitude and line of action of the horizontal component of the hydrostatic force of the water on the wall (an arc of a circle)?

If you were to compare the maximum normal stress due to bending in walls A and B, (induced by the hydrostatic loading), would B's be lower, the same, or greater than A's? (Explain briefly in a complete sentence.)
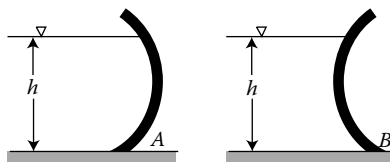
16.5 A tall standpipe with an open top, as shown, has diameter $d = 2$ m and wall thickness $t = 5$ mm.
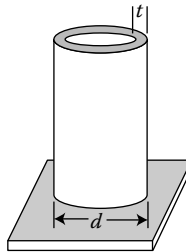
a. If a circumferential stress of 32 MPa is measured in the wall at the bottom of the standpipe, what is the height h of water in the standpipe?

b. What is the axial stress in the standpipe wall due to the water pressure?

c. What is the maximum shear stress induced in the standpipe wall, and where does it occur?

16.6 A closed tank contains 1.5 m of SAE 30 oil, 1 m of water, 20 cm of mercury, and an air gap on top. The absolute pressure at the bottom of the tank is 60 kPa. What is the pressure in the air?

16.7 Consider a circular cylinder of radius R and length L, and in inverted cone (point/tip up) with base radius R and height L. Both cylinder and cone are filled with water and open to the atmosphere. Write a concise, coherent paragraph that explains the *hydrostatic paradox*: Both containers have the same downward force on the bottom since those bases have the same surface area, even though the cone's volume is only one-third of the cylinder's volume.

16.8 The Three Gorges Dam (三峡大坝) is 2309 m long, 185 m tall, and 115 m wide at the base.

a. Determine the horizontal component of the hydrostatic force resultant on the dam exerted by water 175 m deep.

b. If all of the people in China (approximately 1.3 billion) were to somehow simultaneously push horizontally against the dam, could they generate enough force to hold it in place with the water at this depth? Support your answer with appropriate calculations.

16.9 What force P is needed to hold the 4-m-wide gate shown closed?
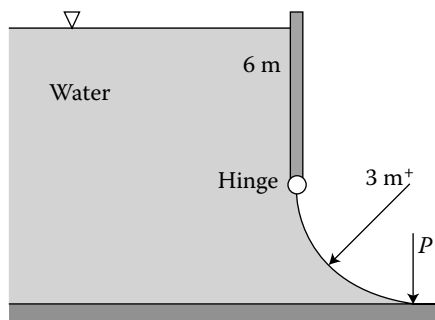
16.10 Suppose you have three spheres of cork, aluminum, and lead, each with diameter 1.5 cm. You drop all three spheres into a cylinder of water. Explain the different behavior of the three spheres upon their release.

16.11 A solid brass sphere of diameter 11.0 in is lowered into the ocean to a depth of 10,000 ft. Determine the change in diameter, the change in volume, and the strain energy of the sphere due to hydrostatic pressure.

16.12 Sometimes when you are driving into the mountains, or even riding an elevator, your ears "pop" as the pressure difference between the inside and outside of the ear is equalized. (As you ascend and ambient air pressure decreases, the air trapped in your inner ear pushes your eardrums outward; this expansion is uncomfortable, and also makes it harder to hear. Your body equalizes the pressure by venting some of the trapped air through your Eustachian tubes, two small channels that connect the inner ears to the throat.) Estimate the pressure difference (in Pa) associated with this phenomenon if it occurs during a 50 m elevation change.

16.13 A water-filled U-tube manometer is used to measure the pressure inside an air tank. The water level in the U-tube on the side connected to the tank is 5 ft above the base of the tank. The water level in the other side of the U-tube, open to the atmosphere, is 2 ft above the base. What is the pressure inside the tank?

16.14 A hydraulic press is shown below. The plunger has an area of $1\,\text{in}^2$, and a force, F_1, can be applied to the plunger through a lever with a mechanical advantage of 8 to 1. If the large piston has an area of $150\,\text{in}^2$, what load F_2 can be raised by a force of 30 lbf applied to the lever?
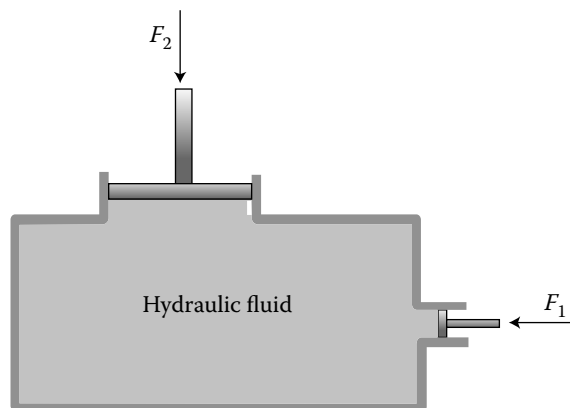
16.15 A square gate, 4 m by 4 m, is located on the 45° face of a dam. The top edge of the gate is 8 m below the water surface. Determine the resultant force of the water on the gate, and the point through which it acts.

16.16 A long, vertical wall separates seawater from fresh water. If the seawater is 7 m deep, what depth of freshwater is required to yield a zero resultant force on the wall? When the resultant force is zero, will the net moment on the wall due to fluid forces also be zero? Explain.

16.17 In the vessels shown in the figure below, the amount of liquid is not constant, but the height of the fluid surface is the same for each vessel. In which vessel is the pressure of the fluid on the bottom of the vessel the greatest?

A   B   C   D   E
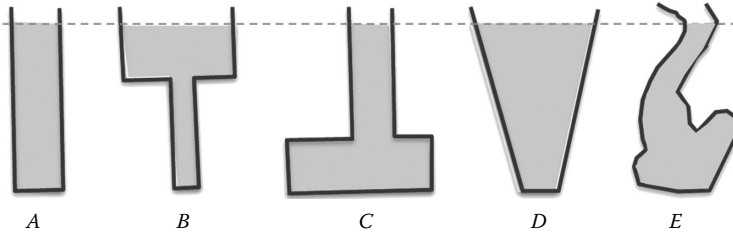
17

Case Study 8: St. Francis Dam

At 3 min before midnight, March 12, 1928, the St. Francis Dam—built to supply water to the growing city of Los Angeles—collapsed (Figure 17.1). During the early morning hours of March 13th, more than 38,000 acre-feet of water surged down from 1650 ft above sea level. At its highest, the wall of water was said to be 78 ft high; by the time it hit Santa Paula, 42 miles south of the dam, the water was 25 ft deep. Almost everything in the water's path was destroyed: livestock, structures, railways, bridges, and orchards. Ultimately, parts of Ventura County lay under 70 ft of mud and debris. Over 500 people were killed, and damage estimates topped $20 million.

William Mulholland, an Irish immigrant who had risen through the ranks of the city's water department* to the position of chief engineer, had proposed, designed, and supervised the construction of the 238-mile Los Angeles Aqueduct, which brought water from the Owens Valley to the city. The St. Francis Dam had been one of the more controversial aspects of his plans. Still, the charismatic Mulholland had the full support of the Department of Water and Power (DWP) and city leaders. The dam was violently opposed by Owens Valley residents, who sabotaged its construction and often un-built portions overnight. The Aqueduct itself had been dynamited in 1924. The St. Francis Dam was Mulholland's 19th, and final, dam. Figure 17.2 shows Mulholland surveying its wreckage.

The St. Francis was a curved gravity concrete dam, designed to be 62 m high. During construction, the height was increased by 7 m to allow more water to be stored in the reservoir. No change was made to the other dimensions of the dam. In the days before the dam collapsed, the water level in the reservoir was only inches below the top of the dam.

At the subsequent inquest, it was demonstrated that the dam was leaking as late as the day before the collapse, and it was brought into evidence that the Department of Water and Power—and more importantly, Mulholland himself—knew it. Mulholland testified that he had been at the dam the day before the break, but said that he hadn't noticed anything unusual. A muddy leak had so worried the resident dam keeper that he'd called Mulholland out to investigate, but Mulholland and his deputy pronounced the leak safe before returning to the city. Leaks, he pointed out in his testimony, were not particularly unusual in dams, especially dams as large as the St. Francis.

Although the assignation of cause and culpability is still a contentious subject among modern analysts, the 1928 jury ruled that the disaster was caused by the failure of a fault and rock formations on which the dam was built. Even so, the public held the DWP, and particularly William Mulholland, responsible. This included Mulholland himself, who uttered unforgettably, "I envy the dead." Mulholland attempted to resign from his post as Chief Engineer, but his board refused, stating: "The board hereby declines to grant such a request and urges the chief to remain on the job he has so faithfully filled for half a century."

---

* Mulholland's first job with the DWP was as a "Zanjero," digging wells and maintaining the aque-ditches, called "zanjas," that lined Los Angeles streets to distribute water from the Los Angeles River.

FIGURE 17.1
St. Francis Dam before and after the collapse. (Photographs courtesy of Santa Clarita Valley Historical Society.)

FIGURE 17.2
Mulholland and H. Van Norman, inspecting wreckage at the St. Francis Dam, March 15, 1928. (Photograph courtesy of Santa Clarita Valley Historical Society.)

Still, Mulholland insisted, "Fasten [the blame] on me. If there was any error of judgment—human judgment—I was the human." The Coroner's inquest cleared Mulholland and the LADWP of any crimes, but stated unequivocally that the disaster had been caused by an error in engineering judgment and recommended:

> *The construction and operation of a great dam should never be left to the sole judgment of one man, no matter how eminent.*

Although no criminal charges were brought against Mulholland, he retired from the DWP soon after the jury's verdict, and lived in self-imposed exile until he died in 1935, at 79 years old.

Recent investigations into the St. Francis Dam disaster have revealed that the ground on which it was built was indeed unstable; it was constructed on the site of an ancient

landslide, which 1920s engineers could not have detected, and tunnels created during the construction process may have further weakened the foundation. Even so, its design has been shown to be inadequate (as we will see in even the simplified analyses of Problems 17.1–17.4), and out of step with the contemporary understanding of concrete gravity dam requirements. In response to the disaster, the California legislature updated its dam safety program and eliminated the exemption of municipal engineering departments from regulations. Having determined that the unregulated design of construction projects constituted a hazard to the public, the California legislature passed laws to regulate civil engineering and, in 1929, created the state Board of Registration for Civil Engineers (now the Board for Professional Engineers, Land Surveyors, and Geologists).

PROBLEMS

17.1 For a dam of height $H = 62\,\text{m}$, thickness b, and width into the page $w = 75\,\text{m}$ as shown, made of concrete with a density of $2300\,\text{kg/m}^3$, retaining a body of water that is 60 m deep, find the net moment about point A and the minimum thickness of the dam that will prevent this moment from overturning the dam.
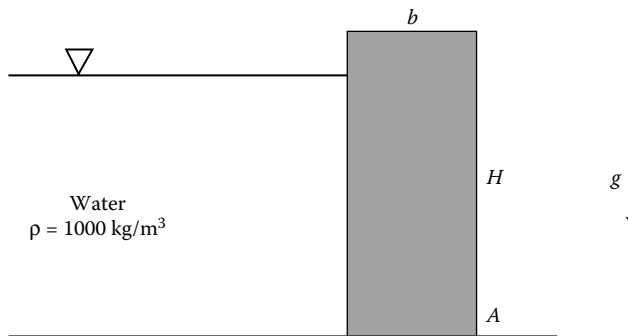
17.2 If the dam's height is increased to 70 m, and the water depth rises to 68 m, what thickness b is required to prevent tipping?

17.3 The St. Francis dam (with dimensions as in Problem 17.2) was observed to be leaking muddy water at its base, indicating that water was seeping under and around its supports. If water is allowed to penetrate freely under our model dam to point A, what thickness b is necessary to prevent the dam from tipping?

17.4 If we refined our model to more accurately represent the geometry of the St. Francis dam, including the curvature of the surface, would you expect the required thickness b to increase or decrease? Why?

References

M. Davis, "How the Hero Who Brought Water to L.A. Abruptly Fell from Grace," *Los Angeles Times*, July 25, 1993, p. M3.

N. Hundley and D. C. Jackson, *Heavy Ground: William Mulholland and the St. Francis Dam Disaster*, Huntington Library Press in association with the University of California Press, 2014.

D. C. Jackson and N. Hundley, "William Mulholland and the St. Francis Dam Disaster (Privilege and Responsibility)," *California History*, September, 2004.

"L.A. Then and Now: An Avalanche of Water Left Death and Ruin in Its Wake." *Los Angeles Times*, February 16, 2003.

M. Leslie, *Rivers in the Desert: William Mulholland and the Inventing of Los Angeles*. New York: HarperCollins, 1993.

R. Mattson, *William Mulholland: A Forgotten Forefather*. Stockton: Pacific Center for Western Studies, 1976.

"Mulholland Unflinching," *Los Angeles Times*, March 28, 1928.

"Water board to demand grand jury quiz on dam," *Los Angeles Times*, March 22, 1928.

18

Fluid Dynamics: Governing Equations

In Chapter 17, we considered cases in which there was no relative motion of fluid particles—no velocity gradients, and thus no shear stress. Now we will consider the somewhat more interesting flows in which velocity gradients and accelerations do appear.

18.1 Description of Fluid Motion

You have probably seen the car companies' ads featuring this year's models in wind tunnels, with smoke tracing the flow of air over the cars' streamlined curves. There is a mathematical way to define the equations of these smoke traces, and a physical interpretation of them, that we will find quite useful in our discussion of fluid dynamics.

The velocity field specifies the instantaneous speed and direction of the motion of all points in the flow. A *streamline* is everywhere tangent to the velocity field and so reflects the character of the flow field. Streamlines are instantaneous, being based on the velocity field at one given time. The smoke traces mentioned above and illustrated in Figure 18.1 are *streaklines*, which include all the fluid particles that once passed through a certain point. We may also describe a flow field with *pathlines*, which represent the trajectory traced out by a given fluid particle over time. When the flow is steady, or independent of time t, the streamlines, streaklines, and pathlines coincide.

For a two-dimensional flow field, we can find the equations of streamlines by applying their definition. Since streamlines are tangent to velocity, the slope of a streamline must equals the tangent of the angle that the velocity vector makes with the horizontal, as shown in Figure 18.2. In mathematical language, this is

$$\frac{\mathrm{d}y}{\mathrm{d}x} = \frac{v}{u}, \quad \text{or } \frac{\mathrm{d}x}{u} = \frac{\mathrm{d}y}{v}, \tag{18.1}$$

so that if the velocity field is known as a function of x and y (and t, if the flow is unsteady), we simply integrate the above expression to find the equation of the streamline.

For a three-dimensional flow, we write

$$\frac{\mathrm{d}x}{u} = \frac{\mathrm{d}y}{v} = \frac{\mathrm{d}z}{w} = \mathrm{d}s. \tag{18.2}$$

And we can integrate these expressions with respect to s, holding time constant and using the initial condition (x_0, y_0, z_0, t_0) at $s = 0$, then eliminate s to find the equation of the streamline.

FIGURE 18.1
Smoke-traced streaklines of flow around a car. (From DaimlerChrysler. With permission.)
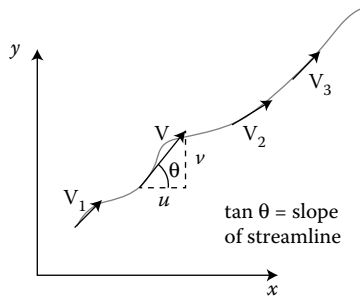
FIGURE 18.2
Streamlines are tangent to the velocity field.

For the two-dimensional flow of an incompressible* fluid, an even lovelier method of finding streamlines exists. We need only remember that for incompressible flow, $\nabla \cdot \mathbf{V} = 0$, or

$$\frac{\partial u}{\partial x} + \frac{\partial v}{\partial y} = 0. \tag{18.3}$$

We can then define a *stream function* ψ by the following:

$$u = \frac{\partial \psi}{\partial y}, \tag{18.4a}$$

and

$$v = -\frac{\partial \psi}{\partial x}. \tag{18.4b}$$

Lines of constant ψ are the streamlines for the flow with $\mathbf{V} = (u, v)$.

Streamlines can give us important information about the pattern and relative speed of flow. Closely spaced streamlines reflect faster flow than widely spaced streamlines. There is no flow *across* or *through* streamlines, since the velocity field is purely tangential to these lines. Streamlines can hence be thought of as boundaries for the flow. Fluid particles on one side of a streamline will never cross it. Solid boundaries of resting solids are always streamlines, since flow does not penetrate them.

───────────────────

* A similar stream function may be derived for compressible flows, though this is outside the scope of this book.

18.2 Equations of Fluid Motion

Although the physics of fluid mechanics is certainly familiar—neither mass conservation nor $\mathbf{F} = m\mathbf{a}$ is a new concept—fluid particles are much harder to keep track of than the solid bodies we have considered previously. It is very difficult to follow a prescribed amount of fluid mass around. We will therefore need some new tools with which to apply the same old physics.

Rather than following the flow of a fixed fluid mass, which would be quite challenging, we will keep track of a prescribed *volume* through which fluid may flow. This volume may be thought of as an imaginary "cage" for fluid, though it is more commonly known as a *control volume*. We may choose to have a "cage" of finite size, in which case we will use the integral governing equations of Section 18.3, or of infinitesimally small size, in which case our equations will be the partial differential equations of Section 18.4.

18.3 Integral Equations of Motion

We will first apply our "old physics" to a control volume or "cage" of finite size. This approach is particularly useful when we are interested in the large-scale behavior of the flow field, and the effect of a flow on devices such as nozzles, turbine blades, or heart valves.

In our study of solid mechanics we often used a free-body diagram, in which we isolated an object from its surroundings, replaced these surroundings by the actions they had on our object, then applied Newton's laws of motion. The fluid mechanics equivalent of this free-body or object would be a fluid element, a specific quantity of matter composed of many fluid particles. This is the so-called *system* approach. However, fluids move and deform in such a way that it is difficult to keep track of a specific quantity of matter. It is easy to follow a branch moving on the surface of a river, but it is hard to follow a particular portion of water in the river. This is why we consider the flow *through* set boundaries (in this section, finite *control volumes*) instead of the mass once contained in these boundaries.

18.3.1 Mass Conservation

When a fluid is in motion, it moves in such a way that mass is conserved. This principle, known as mass conservation, places restrictions on the fluid's velocity field. To see this, we consider the steady (i.e., not changing in time) flow of fluid through a duct. A relevant control volume (CV) is shown in Figure 18.3.

In this simple example, both inflow and outflow are one-dimensional, so that the velocity V_i and density ρ_i distributions are constant over the inlet and outlet areas. Applying conservation of mass to this control volume means that whatever mass flows into the CV must flow out. In some time interval Δt, a volume of $A_1 V_1 \Delta t$ flows into the CV, and a volume of $A_2 V_2 \Delta t$ flows out. These volumes are shaded in Figure 18.3. We multiply these volumes by the fluid density at each control surface so that we will have the amount of mass flowing in and out ($\rho_1 A_1 V_1 \Delta t$ and $\rho_2 A_2 V_2 \Delta t$). We then balance mass in with mass out, canceling the Δt that appears in both terms, and have

$$\rho_1 A_1 V_1 = \rho_2 A_2 V_2. \tag{18.5}$$
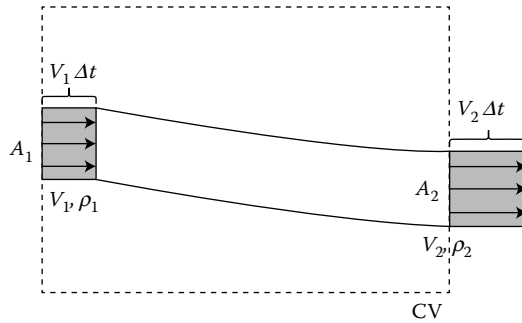
FIGURE 18.3
CV for a steady, one-dimensional fluid through a duct.

These terms are now mass flow *rates*, a.k.a. mass fluxes, as we have divided by Δt. This mathematically states that mass flow rate entering the control volume is balanced by mass flow rate leaving it. For a more general CV with N inlets and outlets, we would write

$$\sum_{i=1}^{N} \rho_i\, A_i\, V_i = 0, \tag{18.6}$$

with inflows negative and outflows positive.

We now move beyond this simple case of one-dimensional, steady flow. To conserve mass, we require *no net change of mass* in our volume. In the previous example, the amount of mass in our control volume changed only due to flow in and flow out. The amount of mass may also change in time due to the flow's unsteadiness. In a more general equation, we must account for both.

Total rate of change of property	=	Time rate of change in property	+	Flux of property across CV surfaces

In our earlier example, this was easy to do: because it was a steady flow, there was no time rate of change, and because the flow was one-dimensional and uniform, the flux was easily computed. We need a more general mathematical statement of mass conservation.

The time rate of change of mass in our control volume is the time derivative of the total product of CV fluid density and the volume (integrated over the volume, since density of fluid can vary spatially)

$$\text{Time rate of change} = \frac{\partial}{\partial t} \int_{CV} \rho\, d\mathcal{V}. \tag{18.7}$$

The flux of mass across a control surface is the amount of mass per unit time that is transported across the surface's area with outward unit normal vector $\hat{\mathbf{n}}$. Hence for a CV with N inlets and outlets

$$\text{Flux across surfaces} = \sum_{i=1}^{N} \rho_i \left(\mathbf{V} \cdot \hat{\mathbf{n}} \right)_i A_i. \tag{18.8}$$
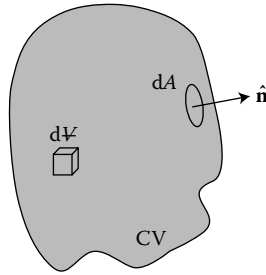
FIGURE 18.4
Standard potato-shaped control volume (CV).

The dot product $(\mathbf{V} \cdot \hat{\mathbf{n}})_i$ is simply the normal component of velocity across the ith control surface, and since $\hat{\mathbf{n}}$ is an outward normal vector, product $(\mathbf{V} \cdot \hat{\mathbf{n}})_i$ is negative for flows into the control volume, and positive for flows out of it. More generally, when we do not have discrete areas with constant density, velocity, and normal vectors:

$$\text{flux across surfaces} = \int_{\text{CS}} \rho(\mathbf{V} \cdot \hat{\mathbf{n}}) \, dA. \tag{18.9}$$

We sum, or integrate, the fluxes across all the control surfaces, as shown in Figure 18.4.

Mass conservation requires that the total change in mass in the control volume, which must equal the sum of the time rate of change of mass in the CV plus the flux of mass across all control surfaces, is equal to zero:

$$0 = \frac{\partial}{\partial t} \int_{\text{CV}} \rho \, d\mathcal{V} + \int_{\text{CS}} \rho(\mathbf{V} \cdot \hat{\mathbf{n}}) \, dA. \tag{18.10}$$

This is how we write mass conservation for a finite-sized control volume.

18.3.2 Newton's Second Law, or Momentum Conservation

In order to write down Newton's second law, $\sum \mathbf{F} = m\mathbf{a}$ for a finite control volume, we must consider (1) all forces on the fluid in the CV that may cause an acceleration, and (2) how to express the fluid's $m\mathbf{a}$, or the total rate of change of its linear momentum.

Forces on a fluid, just like those acting on a solid, may be either surface (acting through direct contact, on control surfaces) or body forces (acting on the entire control volume without contact, and sometimes called "field" forces). We will begin with surface forces. We are already familiar with the notion that a difference in pressure imparts a force. Indeed, a pressure gradient can cause a fluid to move toward the region of lower pressure. The force on a fluid due to pressure variation must be included in $\sum \mathbf{F} = m\mathbf{a}$. When there is relative motion of fluid particles, a frictional force (i.e., a viscous stress) is developed and acts on the fluid. Because of the complex form of the constitutive law for fluids, this can be the hardest term to construct; fortunately, it is often possible to *neglect* viscous effects relative to pressure gradients, inertia, and other forces. We will add only a rather vague "F_{visc}" to the equation at this time. The primary body force acting on fluids is gravity. We may also include external reaction forces (from ducts or other surfaces) that act on the fluid.
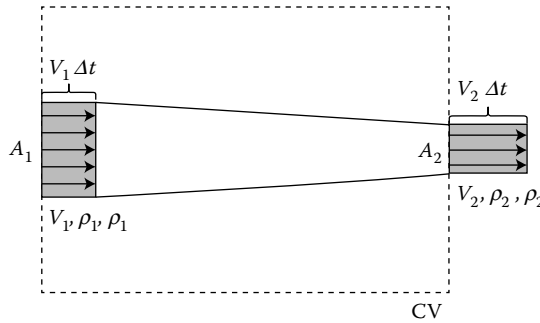
FIGURE 18.5
CV for a steady, one-dimensional fluid through a duct.

The total change in linear momentum of fluid in the control volume, like the total change in mass, must be written as its time rate of change plus the flux of it across control surfaces. We will again start with a fairly simplistic example: steady, one-directional flow through a duct, as in Figure 18.5.

Because $V_2 \neq V_1$, we know the fluid is accelerating between the inlet and outlet surfaces—even though the velocity is not changing in *time*, there is acceleration due to *spatial* variation in velocity. This fluid acceleration must equals the net force on the fluid in the control volume. The resultant force on the fluid, as we have just discussed, must consist of forces: (1) due to pressure variation, (2) due to viscous stresses, (3) due to gravity, and (4) exerted by the duct on the fluid, that is, reaction forces. To preserve the simplicity of the example, we will neglect both viscous and gravitational effects. The resultant force on the fluid in the CV is thus

$$\underset{\substack{\text{pressure force}\\ \text{on left CS, in}\\ +x\text{-direction}}}{p_1 A_1} \; - \; \underset{\substack{\text{pressure force}\\ \text{on right CS, in}\\ -x\text{-direction}}}{p_2 A_2} \; + \; \underset{\substack{\text{reaction}\\ \text{on fluid}\\ \text{from duct}}}{R_x} \; = F_x, \qquad (18.11)$$

and is in the x-direction (as reflected by its subscript). It is a good practice to draw a free body diagram, or FBD, of your control volume, indicating the relevant forces and their orientations, as we do in Figure 18.6.

Having written down the resultant force F_x on the fluid, we must now write an expression for the total rate of change in the fluid's x-momentum, to balance F_x. Because the flow is steady, the x-momentum does not change in time; we simply need to account for the flow of x-momentum into and out of the control volume. The difference between inflow
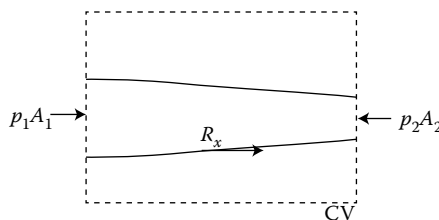
FIGURE 18.6
FBD of fluid in CV.

and outflow, or the *net change in x-momentum*, will balance F_x. In some time interval Δt, an amount of x-momentum of $(\rho_1 A_1 V_1 \Delta t) V_1$ flows into the CV, and an amount $(\rho_2 A_2 V_2 \Delta t) V_2$ flows out. (Note that the x-momentum is simply the mass flux, already found in Section 18.3.1, times the x component of velocity at the given control surface.) Again, outflow is positive, so the net rate of change of momentum is the difference between these terms, divided by the time Δt: $\rho_2 A_2 V_2^2 - \rho_1 A_1 V_1^2$. We can write the x-component of $\sum \mathbf{F} = m\mathbf{a}$:

$$p_1 A_1 - p_2 A_2 + R_x = \rho_2 A_2 V_2^2 - \rho_1 A_1 V_1^2. \tag{18.12}$$

We want to generalize this, so we can apply our physics to less simplistic problems. The forces are easy to generalize: the net pressure force can be written as the pressure p acting on a given control surface, times the area of that control surface: $p\hat{\mathbf{n}}\,dA$. We must sum over all the control surfaces of our CV, and we will write this as an integral: $-\int_{CS} p\hat{\mathbf{n}}\,dA$, where the negative sign reflects the fact that a positive p compresses our fluid. The force due to gravity is also easy to write: $\int_{CV} \rho \mathbf{g}\,d\Psi$, since it acts on the whole control volume. Next we write a more general expression for the total rate of change of fluid linear momentum. Again, the momentum is just mass times velocity, so this extends naturally from our expressions for mass conservation:

$$\text{Time rate of change} = \frac{\partial}{\partial t} \int_{CV} \rho \mathbf{V}\,d\Psi, \tag{18.13}$$

$$\text{Flux across surfaces} = \int_{CS} \rho \mathbf{V}\left(\mathbf{V} \cdot \hat{\mathbf{n}}\right) dA. \tag{18.14}$$

Note that $\mathbf{V}$ is a vector [$\mathbf{V} = (u, v, w)$], and hence there are three components of each of these expressions. We can now write the vector form of our general equation:

$$\mathbf{F} = \mathbf{F}_{\text{visc}} + \mathbf{F}_{\text{external}} + \int_{CV} \rho \mathbf{g}\,d\Psi - \int_{CS} p\hat{\mathbf{n}}\,dA = \frac{\partial}{\partial t} \int_{CV} \rho \mathbf{V}\,d\Psi + \int_{CS} \rho \mathbf{V}\left(\mathbf{V} \cdot \hat{\mathbf{n}}\right) dA. \tag{18.15}$$

As well as the form of its three component equations in Cartesian coordinates:

$$F_x = (F_{\text{visc}})_x + (F_{\text{external}})_x + \int_{CV} \rho g_x\,d\Psi - \int_{CS} p\hat{\mathbf{i}} \cdot \hat{\mathbf{n}}\,dA = \frac{\partial}{\partial t} \int_{CV} \rho u\,d\Psi + \int_{CS} \rho u(\mathbf{V} \cdot \hat{\mathbf{n}})\,dA, \tag{18.16a}$$

$$F_y = (F_{\text{visc}})_y + (F_{\text{external}})_y + \int_{CV} \rho g_y\,d\Psi - \int_{CS} p\hat{\mathbf{j}} \cdot \hat{\mathbf{n}}\,dA = \frac{\partial}{\partial t} \int_{CV} \rho v\,d\Psi + \int_{CS} \rho v(\mathbf{V} \cdot \hat{\mathbf{n}})\,dA, \tag{18.16b}$$

$$F_z = (F_{\text{visc}})_z + (F_{\text{external}})_z + \int_{CV} \rho g_z\,d\Psi - \int_{CS} p\hat{\mathbf{k}} \cdot \hat{\mathbf{n}}\,dA = \frac{\partial}{\partial t} \int_{CV} \rho w\,d\Psi + \int_{CS} \rho w(\mathbf{V} \cdot \hat{\mathbf{n}})\,dA, \tag{18.16c}$$

Note that in the final term, $\mathbf{V} \cdot \hat{\mathbf{n}}$ is a scalar quantity and so does not vary for the component equations. This is how we write $\sum \mathbf{F} = m\mathbf{a}$ for a finite-sized control volume.

18.3.3 Reynolds Transport Theorem

As we have said, the big difference between the forms of the governing equations for fluids and solids is that fluids may flow across the surfaces of a control volume. (For a solid, a control volume *is* a fixed mass of the solid!) The idea of the Reynolds transport theorem is that we can relate these two approaches by accounting for the *flow* across control surfaces.

It is possible to obtain the equations for both mass and momentum conservation using the Reynolds transport theorem, which says that the total rate of change of some quantity η (a *specific* quantity, some parameter H per unit mass) is equal to the time rate of change of η for the contents of the control volume plus a contribution due to the flow of η through the control surface. For our purposes, H may be the mass of fluid in our control volume ($\rho \, d V$), or the fluid momentum ($\mathbf{V} \rho \, d V$). The Reynolds transport theorem has the general form

$$\underbrace{\frac{D}{Dt} \int_{\substack{\text{mass} \\ \text{(system)}}} \eta \, dm}_{\substack{\text{Time rate of change of } \eta \\ \text{for the coincident system} \\ \text{(if we were to follow a } \textbf{mass})}} = \underbrace{\frac{\partial}{\partial t} \int_{\text{CV}} \rho \eta \, d V}_{\substack{\text{Time rate of change of } \eta \\ \text{of the contents of the} \\ \text{coincident control volume}}} + \underbrace{\int_{\text{CS}} \rho \eta \mathbf{V} \cdot \hat{\mathbf{n}} \, dA.}_{\substack{\text{Net rate of flux of } \eta \\ \text{through control surface}}} \qquad (18.17)$$

We typically use D/Dt in this expression rather than d/dt, to represent the time rate of change in a property (our η or H) subjected to a velocity field that varies in space and time. The property can simply change in time, and it can also be affected by the motion of flowing fluid. The operator D/Dt is sometimes called the "material derivative." It has the same meaning as the total derivative d/dt we learned in mathematics classes, requiring the chain rule to fully characterize, but it is the convention to use material derivative terminology and capital D's in fluid mechanics.

Once again, to conserve mass, we must have "flow in" balancing "flow out," and the Reynolds transport theorem with $H = $ mass, thus $\eta = H/$mass $= \rho \, d V / \rho \, d V = 1$ gives us:

$$0 = \frac{\partial}{\partial t} \int_{\text{CV}} \rho \, d V + \int_{\text{CS}} \rho \mathbf{V} \cdot \hat{\mathbf{n}} \, dA, \qquad (18.18)$$

where the left-hand side is zero since, by definition, $D(\text{mass})/Dt$ for a system is zero. For the special case of a steady flow, the first term on the right-hand side drops out, and we must have

$$\int_{\text{CS}} \rho \mathbf{V} \cdot \hat{\mathbf{n}} \, dA = 0. \qquad (18.19)$$

To obtain the control volume form of momentum conservation, we apply the Reynolds transport theorem to $H = m\mathbf{V} = \rho \, d V \, \mathbf{V}$, or $\eta = H/m = \rho \mathbf{V} \, d V / \rho \, d V = \mathbf{V}$, and get

$$\mathbf{F} = \frac{\partial}{\partial t} \int_{\text{CV}} \rho \mathbf{V} \, d V + \int_{\text{CS}} \rho \mathbf{V} \left(\mathbf{V} \cdot \hat{\mathbf{n}} \right) dA, \qquad (18.20)$$

where the left-hand side is $\sum \mathbf{F}$ since Newton's second law tells us that $\sum \mathbf{F} = m\mathbf{a} = d(m\mathbf{V})/dt$. In other words, this equation tells us that the time rate of change of momentum

contained in a fixed volume plus the net flow rate of momentum through the surfaces of this volume, are equal to the sum of all the forces acting on the volume. (We have developed the form of this sum, resultant force **F** in the previous section.)

18.4 Differential Equations of Motion

We can also construct useful expressions of mass conservation and $\sum \mathbf{F} = m\mathbf{a}$ for "cages" or volumes that are infinitesimally small. This is useful when we want to know detailed information about the flow at very small scales, at high resolution.

18.4.1 Continuity, or Mass Conservation

The principle of mass conservation is fundamental to the study of mechanics. It states that mass is neither created nor destroyed; hence, the mass of a system remains constant as the system moves through the flow field.

By considering the flow through an imaginary, very small cage in the flow field, we can derive a useful mathematical expression of this principle. (Though this "cage" has the same dimensions as our frequently discussed fluid element, with volume $d\,V = dx\,dy\,dz$, it is stationary.) The fluid has velocity $\mathbf{V} = (u, v, w)$ when it is at the center of the cage. Its mass flow rate per unit area may then be written as $(\rho u, \rho v, \rho w)$.

We want to obtain an expression for the mass flow across the cage faces (control surfaces), to see what is flowing in and out of the cage (control volume). This is shown for one direction of flow in Figure 18.7. We must multiply the face-specific expressions by the appropriate areas ($dx\,dz$ in both cases), and we can then combine them to get mass flow rate in the y-direction:

$$\left(\frac{dm}{dt}\right)_y = m_y = \left[\rho v + \frac{\partial(\rho v)}{\partial y}\frac{dy}{2}\right]dx\,dz - \left[\rho v - \frac{\partial(\rho v)}{\partial y}\frac{dy}{2}\right]dx\,dz = \frac{\partial(\rho v)}{\partial y}dx\,dy\,dz.$$

(18.21)
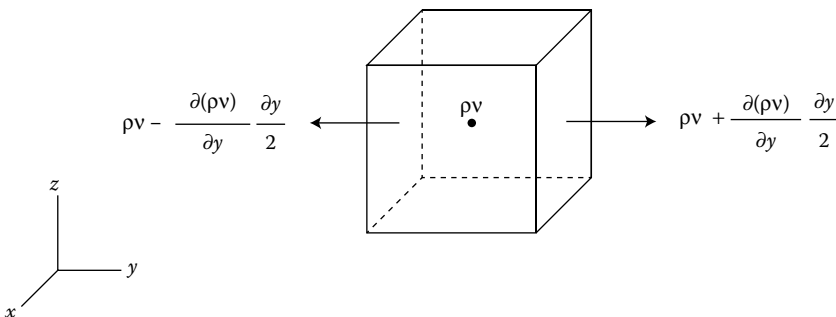
FIGURE 18.7
Mass flow through a cage with volume $dx\,dy\,dz$. We have used Taylor expansions in order to express the values of mass flow at all faces, just as we did for the pressure field.

We repeat this in the x- and z-directions to have an expression for total mass flow rate through the cage:

$$\frac{dm}{dt} = m = \left[\frac{\partial(\rho u)}{\partial x} + \frac{\partial(\rho v)}{\partial y} + \frac{\partial(\rho w)}{\partial z} \right] dx\, dy\, dz. \tag{18.22}$$

To satisfy mass conservation, this mass flow rate must balance the rate of mass decrease within the element, $-\frac{\partial \rho}{\partial t} dx\, dy\, dz$. Balancing these terms and canceling $dx\, dy\, dz$, we obtain

$$\frac{\partial \rho}{\partial t} + \frac{\partial(\rho u)}{\partial x} + \frac{\partial(\rho v)}{\partial y} + \frac{\partial(\rho w)}{\partial z} = 0. \tag{18.23}$$

This is the mass conservation equation, also known as the *continuity equation*, for fluids. It is valid for steady or unsteady flow, and for incompressible or compressible fluids. We remember that the last three terms, the sum of partials of the vector $\rho \mathbf{V}$, represent the divergence of this vector, and we can rewrite the equation in vector form as

$$\frac{\partial \rho}{\partial t} + \nabla \cdot (\rho \mathbf{V}) = 0. \tag{18.24}$$

In vector form, this equation is independent of coordinate choice and will work in cylindrical, spherical, or polar coordinates in addition to our Cartesian (x, y, z) friends.

We note that for steady flows, $\partial \rho / \partial t = 0$. For incompressible ($\rho \approx$ constant) fluids, the continuity equation reduces to $\nabla \cdot \mathbf{V} = 0$, as we saw in Section 13.5.1.

18.4.2 Newton's Second Law, or Momentum Conservation

Just as for solids, the governing equation for fluid mechanics is Newton's second law. We have inched toward expressing this mathematically for fluids by writing out the forces due to pressure, gravity, and viscosity. All that remains is to formulate the *acceleration* of a fluid element, and since we know the effects of these forces, we can write $\sum \mathbf{F} = m\mathbf{a}$.

Although the vast majority of problems we have seen have dealt with non-accelerating solids, we are familiar with the idea that a solid's acceleration is simply the rate of change of its velocity. This is also true for fluids. We must consider the rate of change of the velocity field, remembering that this "change" may be in time t, and also in x, y, and z.

Given a velocity field $\mathbf{V} = (u, v, w)$, where each component is allowed to vary in space and time, so that $u_i = f(x, y, z, t)$, we know that the acceleration is the change in this velocity field in a time interval dt. The velocity of some fluid particle L is $\mathbf{V}_L$ at time t, and at some later time $t + dt$, as shown in Figure 18.8, has evolved:

$$\mathbf{V}_L\big|_t = \mathbf{V}(x, y, z, t), \tag{18.25a}$$

$$\mathbf{V}_L\big|_{t+dt} = \mathbf{V}(x + dx, y + dy, z + dz, t + dt), \tag{18.25b}$$

so the change in $\mathbf{V}_L$ may be written as the difference between these two, or

$$d\mathbf{V}_L = \mathbf{V}(x + dx, y + dy, z + dz, t + dt) - \mathbf{V}(x, y, z, t)$$

$$= \frac{\partial \mathbf{V}}{\partial x}dx + \frac{\partial \mathbf{V}}{\partial y}dy + \frac{\partial \mathbf{V}}{\partial z}dz + \frac{\partial \mathbf{V}}{\partial t}dt, \tag{18.26}$$
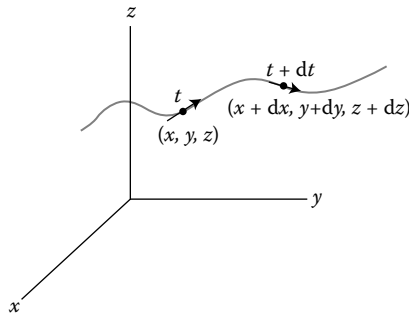
FIGURE 18.8
Evolution of point L and its velocity $\mathbf{V}_L$.

so that the *rate* of change in $\mathbf{V}_L$, or $d\mathbf{V}_L/dt$, is

$$\mathbf{a}_L = \frac{d\mathbf{V}_L}{dt} = \frac{\partial \mathbf{V}}{\partial x}\frac{dx}{dt} + \frac{\partial \mathbf{V}}{\partial y}\frac{dy}{dt} + \frac{\partial \mathbf{V}}{\partial z}\frac{dz}{dt} + \frac{\partial \mathbf{V}}{\partial t}, \tag{18.27}$$

or more generally

$$\mathbf{a} = \underbrace{\frac{\partial \mathbf{V}}{\partial t}}_{\text{local}} + \underbrace{\frac{\partial \mathbf{V}}{\partial x}u + \frac{\partial \mathbf{V}}{\partial y}v + \frac{\partial \mathbf{V}}{\partial z}w}_{\text{convective}} \equiv \frac{D\mathbf{V}}{Dt}. \tag{18.28}$$

This expression is defined as the *material derivative* of the velocity $\mathbf{V}$. It may also be written in vector form as

$$\mathbf{a} = \frac{D\mathbf{V}}{Dt} = \frac{\partial \mathbf{V}}{\partial t} + (\mathbf{V} \cdot \nabla)\mathbf{V}. \tag{18.29}$$

The material derivative is, in a sense, a derivative "following the fluid," as it considers the movement of the fluid particle in question. This way of writing the acceleration takes into account the change in flow velocity in time *and* space, and equips us to write $\sum \mathbf{F} = m\mathbf{a}$ for a fluid element. Notice that it expresses the total change in velocity as the time rate of change, plus a reflection of spatial variation, of velocity.*

We have the above expression for acceleration and we know that $m\mathbf{a}$ is $\rho\, dx\, dy\, dz\, \mathbf{a}$. We know that both surface and body forces can act on a fluid, and we know how to write the forces due to gravity, pressure, and viscous effects. We also know about surface tension—and because surface tension will come into play only at boundaries between fluids, it affects the boundary conditions but not the governing equations themselves.

If viscous effects are neglected, we can write $\sum \mathbf{F} = m\mathbf{a}$ for a fluid element $d\mathcal{V}$:

$$\rho\, d\mathcal{V} \frac{D\mathbf{V}}{Dt} = -\nabla p\, d\mathcal{V} + \rho \mathbf{g}\, d\mathcal{V}, \tag{18.30}$$

or, dividing through by $d\mathcal{V}$,

$$\rho \frac{D\mathbf{V}}{Dt} = -\nabla p + \rho \mathbf{g}, \tag{18.31}$$

---

* Again, we note that for a solid, whose mass could be vigilantly monitored, and which would not flow in response to shear, this flux term would not be necessary.

where typically $\mathbf{g} = -g\hat{\mathbf{k}}$. This equation is Newton's second law for an effectively invis-cid fluid, first derived by Euler in 1755 and henceforth known as the *Euler equation*. It is also known as the inviscid momentum equation, as it expresses the conservation of linear momentum. Please note that the only assumption made in its derivation is that of *inviscid* behavior—this equation holds for both compressible and incompressible flu-ids, and steady and unsteady flows. Viscous effects are generally negligible far from flow boundaries, allowing us to rely on Euler's inviscid momentum equation in good faith.

If we include viscous effects, we must write the force on the fluid element due to the viscous stress tensor, which was discussed in Section 13.5.4. In that discussion, the stress tensor was shown to be composed of a portion due to pressure (already included in the inviscid equation) and another portion that is proportional to the *strain rate tensor*, which itself depends on the velocity gradients in the flow. The force due to stress tensor $\boldsymbol{\sigma}$ on an element $d\mathcal{V}$ may be written as $\nabla \cdot \boldsymbol{\sigma}$. (This requires the recollection of Gauss' theorem, to change the surface force $\int_A \boldsymbol{\sigma} \, d\mathbf{A}$ to a force on the entire volume $\int_V \nabla \cdot \boldsymbol{\sigma} \, d\mathcal{V}$. Physically, we could derive this in the same way we determined the force due to pressure on a fluid element $d\mathcal{V}$.) For a viscous, incompressible Newtonian fluid,* $\sum \mathbf{F} = m\mathbf{a}$ is written

$$\rho \frac{D\mathbf{V}}{Dt} = -\nabla p + \rho \mathbf{g} + \mu \nabla^2 \mathbf{V}, \tag{18.32}$$

where μ is the fluid's viscosity, and the del-squared operator on $\mathbf{V}$ may be written in index notation:

$$\nabla^2 u_i \equiv \frac{\partial^2 u_i}{\partial x_j \partial x_j} = \frac{\partial^2 u_i}{\partial x_1^2} + \frac{\partial^2 u_i}{\partial x_2^2} + \frac{\partial^2 u_i}{\partial x_3^2}. \tag{18.33}$$

Equation 18.32 (as well as its variants with the fuller stress tensor) is known as the Navier-Stokes equation. This name is somewhat interesting since Claude Navier got it wrong. He misunderstood viscosity and the dependence of the stress tensor on veloc-ity gradients, and published a flawed derivation of $\sum \mathbf{F} = m\mathbf{a}$ for viscous fluids in 1822. Though his results were correct, his reasoning was flawed. George Stokes later got the derivation of the viscous terms right, and so his name was added to the marquee. How-ever, in 1843, two years before Stokes' results were published, a paper appeared by Jean Claude Saint-Venant in which this equation was correctly derived and interpreted. It is a mystery why the equation does not bear his name today. As students of continuum mechanics, we are already grateful to Saint-Venant for his discovery that the details of force application are only relevant in the immediate neighborhood of application, allow-ing us to use spatially averaged stress relations, and now we have another reason to thank him, and to condemn the injustice that leaves his name out of most discussions of the Navier–Stokes equation. Incidentally, Navier was no slouch, despite his errors here—he was a great builder of bridges and did important work in elasticity and solid mechanics.

---

* The student chafing under the restrictions of incompressibility and Newtonian behavior is encouraged to take further courses in fluid mechanics, and to refer posthaste to Kundu's *Fluid Mechanics*. She will find that the full form of the stress tensor makes things quite a bit more interesting.

18.5 Bernoulli Equation

Equation 18.32 for the conservation of momentum is a vector equation, with component equations in each direction of motion. These directions may be (x, y, z), (r, θ, z), or (r, θ, φ). If we remember that *streamlines* are everywhere tangent to the velocity vector, we can also think of a set of coordinates defined relative to the streamlines—for two-dimensional flow, one coordinate s directed along the streamline, and n defined normal to the streamline. We could then write the component equations of motion in the s and n directions. The resulting equation in the s direction, which states $\sum \mathbf{F} = m\mathbf{a}$ along a streamline, may be integrated to yield the following equation:

$$\frac{p}{\rho} + gz + \frac{1}{2}V^2 = \text{constant along a streamline}, \tag{18.34}$$

where we have assumed that gravity acts in the negative z-direction, and where V is the velocity in the s direction, simply the magnitude of the velocity vector since $\mathbf{V}$ is in the s direction. This equation is known as the *Bernoulli equation*, and it is true for steady flow of an incompressible fluid under inviscid conditions. For convenience, we write the equation together with its restrictions:

$$\frac{p}{\rho} + gz + \frac{1}{2}V^2 = \text{constant}$$

- On a streamline
- For steady flow
- For incompressible fluid
- If viscous effects neglected

Many problems can be solved using the Bernoulli equation, allowing us to dodge having to solve the full Euler or Navier–Stokes equations. It should not escape our notice that the Bernoulli equation, derived from $\sum \mathbf{F} = m\mathbf{a}$, looks like an energy conservation equation. This is even easier to see if we multiply through by the (assumed constant) density: Equation 18.34 becomes

$$p + \rho gz + \frac{1}{2}\rho V^2 = \text{constant}, \tag{18.35}$$

and we can think of pressure p as a measure of flow work, ρgz as a gravitational potential energy, and $\frac{1}{2}\rho V^2$ as a kinetic energy, all per unit volume of fluid. Daniel Bernoulli actually first arrived at Equation 18.34 by performing an energy balance, even though the concept of energy was still a bit fuzzy in 1738.

One of the most useful applications of the Bernoulli equation is a device known as a Pitot* tube, and its cousin the Pitot-static tube, used to measure flow velocities. The tube (Figure 18.9a) contains a column of air. When an oncoming fluid flow impinges on the nose of the Pitot tube, it displaces this air. As we know from hydrostatics, the displacement will be proportional to the pressure at the stagnation point on the Pitot tube nose. The

---

* The Pitot tube is named for Henri Pitot (1695–1771), a French hydraulic engineer who invented it by intuition when measuring the flow in the River Seine in 1732.
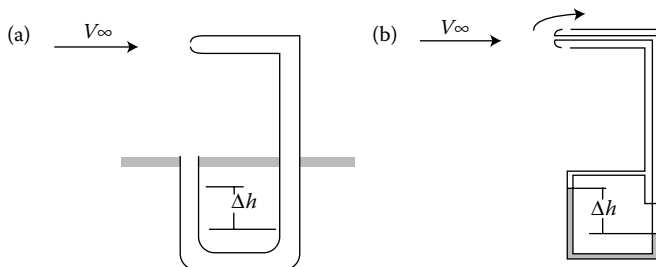
FIGURE 18.9
Pitot tube with differential manometer to measure flow speed: (a) standard arrangement of Pitot tube and static pressure tap, and (b) Pitot-static tube.

stagnation point is at the divide between the flow that goes up-and-over and that which goes down-and-under (imagining a flow in the plane of the page for simplicity) and there the velocity must be zero. The difference between this "stagnation pressure" (where the fluid has speed $V = 0$) and the "static pressure" elsewhere in the flow (where the fluid has average speed V_∞), by Bernoulli's equation, is

$$p_{\text{stagnation}} - p_{\text{static}} = \frac{1}{2}\rho V_\infty^2. \tag{18.36}$$

A Pitot-static tube, as illustrated in Figure 18.9b, contains static pressure ports along the nose to measure the static fluid pressure as well as the stagnation pressure. It is clear from Equation 18.36 and Figure 18.9 that the assumptions of steady, incompressible flow are made when a Pitot tube is used. The flow is also assumed to be inviscid, so that there are no boundary layers near tube or other walls to reduce the bulk flow speed from V_∞.

18.6 Examples

EXAMPLE 18.1

Find the equation of, and sketch, the streamline that passes through $(1, -2)$ for the velocity field given by $\mathbf{V} = xy\hat{\mathbf{i}} - 2y^2\hat{\mathbf{j}}$ m/s.

Given: Velocity vector $\mathbf{V}$.

Find: Streamline through $(x = 1, y = -2)$.

Assume: No assumptions are necessary.

Solution

By definition, a streamline is everywhere tangent to the velocity field. So, the streamline through $(1, -2)$ is tangent to the velocity $\mathbf{V}$ at this point. We state this relationship mathematically as

$$\text{slope } \frac{dy}{dx}\bigg|_{\text{streamline}} = \frac{v}{u},$$

$$\frac{dy}{dx} = \frac{-2y^2}{xy} = \frac{-2y}{x}.$$

Separating variables:

$$\frac{dy}{-2y} = \frac{dx}{x}.$$

Integrating both sides:

$$\int \frac{dy}{-2y} = \int \frac{dx}{x},$$

$$-\frac{1}{2} \ln y = \ln x + C_1.$$

We have absorbed the constants of integration from both sides into this new constant C_1. Or

$$\ln x + \frac{1}{2} \ln y = C_2.$$

This new C_2 is simply $-C_1$ from the previous expression. To get rid of the natural logs and find a graphable function $y(x)$, we take the exponent of the entire expression:

$$x\sqrt{y} = C_3, \text{ or}$$

$$x^2 y = C.$$

This C may no longer bear much resemblance to our initial constant C_1, but the product $x^2 y$ must equal some constant.

At point $(1, -2)$, $x^2 y = (1)^2(-2) = -2$, so the equation of the streamline through $(1, -2)$ is

$$x^2 y = -2.$$

We plot this streamline below.
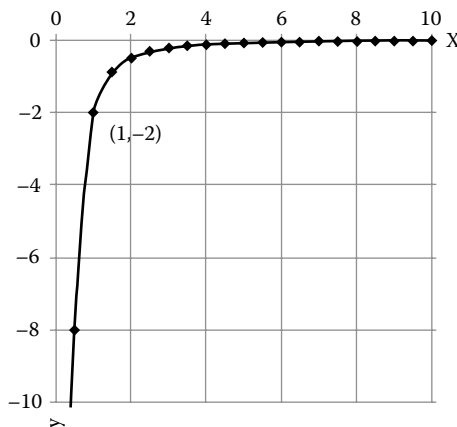
EXAMPLE 18.2

The open tank shown contains water at 20°C and is being filled through Section 1. Assume incompressible flow. First derive an analytic expression for the water-level change dh/dt in terms of arbitrary volume flows Q_1, Q_2, Q_3, and tank diameter d.

Then, if the water level h is constant, determine the exit velocity V_2 for the given data $V_1 = 3\,\text{m/s}$ and $Q_3 = 0.01\,\text{m}^3/\text{s}$.
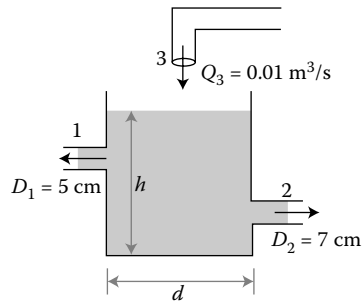
Given: Tank inlet and outlet information.

Find: $\mathrm{d}h/\mathrm{d}t$, unknown exit velocity.

Assume: Inlet and outlet velocity profiles are uniform, one-dimensional. Fluid is incompressible; density is uniform.

Solution

We intend to consider the fluid in the tank as the contents of a control volume.
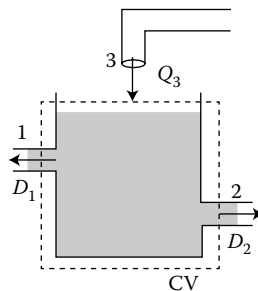
We must have mass conservation:

$$0 = \frac{\partial}{\partial t} \int_{\text{CV}} \rho\,\mathrm{d}V + \int_{\text{CS}} \rho \mathbf{V} \cdot \mathrm{d}\mathbf{A},$$

which for this CV can be written as

$$\frac{\mathrm{d}}{\mathrm{d}t}\left[\rho \frac{\pi d^2}{4} h \right] + \rho\left(Q_2 - Q_1 - Q_3\right) = 0,$$

where we have changed the partial derivative to a total one, as time is the only dependence of the quantity in brackets, and where the signs of various flow rates depend on whether they are into or out of the CV: Q_2 is outflow, and thus positive, while Q_1 and Q_3 are both inflow and negative. We further simplify by canceling the common density,

and by removing the constants from the time derivative:

$$\frac{\pi d^2}{4}\frac{dh}{dt} + (Q_2 - Q_1 - Q_3) = 0,$$

$$\frac{dh}{dt} = \frac{4\left(Q_1 + Q_3 - Q_2\right)}{\pi d^2},$$

If h is constant, $dh/dt = 0$ and we must have $Q_1 + Q_3 - Q_2 = 0$. Each $Q_i = V_i A_i$. We can thus solve for the requested value of V_2 which corresponds to $dh/dt = 0$:

$$Q_2 = V_2 A_2 = Q_1 + Q_3 = 0.01\,\mathrm{m}^3/\mathrm{s} + \frac{\pi}{4}(0.05\,\mathrm{m})^2(3\,\mathrm{m/s}) = 0.0159\,\mathrm{m}^3/\mathrm{s},$$

$$V_2 = \frac{Q_2}{A_2} = \frac{0.0159\,\mathrm{m}^3/\mathrm{s}}{(\pi/4)(0.07\,\mathrm{m})^2} = 4.13\,\mathrm{m/s}.$$

EXAMPLE 18.3

A steady jet of water is redirected by a deflector, as shown. The jet has a mass flow rate of 32 kg/s, cross-sectional area of 2 cm × 40 cm, and speed V_1 when it encounters the deflector. What force per unit width of the deflector (into the page) is needed to hold the deflector in place?
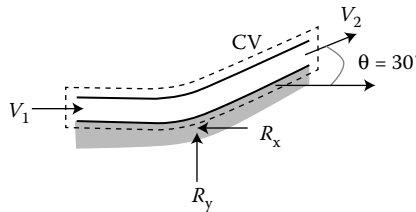
Given: Geometry of flow deflector.

Find: Reaction forces from deflector support on fluid in CV.

Assume: Jet has constant cross-sectional area, even after being deflected. Flow is steady and incompressible. Density of water is constant, uniformly 1000 kg/m³. Gravity and viscous effects may be neglected.

Solution

The flow of water imparts a force to the deflector. Reaction forces from the deflector balance these forces, and act on the fluid in the CV drawn. We are asked for these reactions, R_x and R_y, if the deflector has width of 1 m into the page.

We begin by finding the inlet velocity V_1. We are given the mass flow rate of the jet, $\dot{m}$, which is $\rho V_1 A_1$. As the cross-sectional area A_1 is also given, we use this to find V_1:

$$V_1 = \frac{\dot{m}}{\rho A_1} = \frac{32\,\mathrm{kg/s}}{(1000\,\mathrm{kg/m}^3)(0.02\,\mathrm{m})(0.40\,\mathrm{m})} = 4\,\mathrm{m/s}.$$

If the flow is steady, we must have a constant mass flow rate (what flows into our CV must flow back out again), or $\rho V_1 A_1 = \rho V_2 A_2$. Since we have an incompressible flow and since the jet's cross-sectional area does not change, we must have $V_2 = V_1 = 4\,\mathrm{m/s}$.

In order to find the requested reaction forces, we must apply the conservation of linear momentum, or $\mathbf{F} = m\mathbf{a}$, in both x- and y-directions. These equations are

$$F_x = \left(F_{\text{visc}}\right)_x + \left(F_{\text{external}}\right)_x + \int_{\text{CV}} \rho g_x \, \mathrm{d}V - \int_{\text{CS}} p\hat{\mathbf{i}} \cdot \hat{\mathbf{n}} \, \mathrm{d}A = \frac{\partial}{\partial t} \int_{\text{CV}} \rho u \, \mathrm{d}V + \int_{\text{CS}} \rho u \mathbf{V} \cdot \hat{\mathbf{n}} \, \mathrm{d}A,$$

$$F_y = \left(F_{\text{visc}}\right)_y + \left(F_{\text{external}}\right)_y + \int_{\text{CV}} \rho g_y \, \mathrm{d}V - \int_{\text{CS}} p\hat{\mathbf{j}} \cdot \hat{\mathbf{n}} \, \mathrm{d}A = \frac{\partial}{\partial t} \int_{\text{CV}} \rho v \, \mathrm{d}V + \int_{\text{CS}} \rho v \mathbf{V} \cdot \hat{\mathbf{n}} \, \mathrm{d}A.$$

Since our jet is steady, with negligible contributions from gravity, viscosity, and pressure gradients, these equations simplify greatly:

$$-R_x = \int_{\text{CS}} \rho u \mathbf{V} \cdot \hat{\mathbf{n}} \, \mathrm{d}A,$$

$$R_y = \int_{\text{CS}} \rho v \mathbf{V} \cdot \hat{\mathbf{n}} \, \mathrm{d}A.$$

The x-momentum flux therefore balances the reaction force R_x, negative as it is in the negative x-direction. Writing out the flux at each of the two control surfaces, we have

$$-R_x = \int_{\text{CS}} \rho u \mathbf{V} \cdot \hat{\mathbf{n}} \, \mathrm{d}A = -\rho V_1 V_1 A_1 + \rho (V_2 \cos \theta) V_2 A_2.$$

(Note that $V_2 \cos \theta$ is the x-component of velocity at surface A_2, and that V_2 is $\mathbf{V} \cdot \hat{\mathbf{n}}$ at A_2.)

$$R_x = \dot{m} \, (V_1 - V_2 \cos \theta)$$
$$= (32 \, \text{kg/s})(4 \, \text{m/s})(1 - \cos 30^\circ)$$
$$= 17.2 \, \text{N}.$$

In the y-direction, we have

$$R_y = \int_{\text{CS}} \rho v \mathbf{V} \cdot \hat{\mathbf{n}} \, \mathrm{d}A = 0 + \rho (V_2 \sin \theta) V_2 A_2,$$
$$R_y = \dot{m} \, V_2 \sin \theta$$
$$= (32 \, \text{kg/s})(4 \, \text{m/s}) \sin 30^\circ$$
$$= 64 \, \text{N}.$$

EXAMPLE 18.4

Uniform air flow with speed $U = 1.5 \, \text{m/s}$ approaches a cylinder as shown. The velocity distribution at the location shown downstream in the wake of the cylinder may be approximated by

$$u(y) = 1.25 + \frac{y^2}{4}, \quad -1 < y < 1,$$

where $u(y)$ is in meter per second and y is in meters. Determine (a) the mass flux across the surface AB per meter of depth (into the page) and (b) the drag force per meter of length acting on the cylinder.
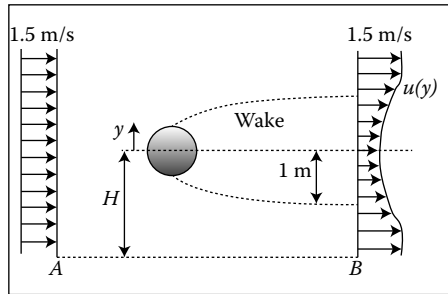
Given: Flow over cylinder; upstream and downstream velocity profiles.

Find: Mass flux across surface AB, drag force on cylinder.

Assume: Air has constant, uniform density 1.23 kg/m^3. Flow is symmetrical and steady. Pressure differences, gravity, and viscous effects may be neglected.

Solution

We first select a control volume. It is generally wisest to choose control volumes on whose surfaces we have information about the flow. It is also useful to take advantage of symmetry, to simplify our calculations.

Our choice of control volume is shown below.
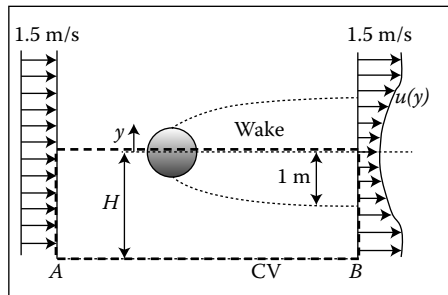
At its left surface, the normal velocity is $U = 1.5$ m/s, into the CV. Its top surface is a plane of symmetry for the flow, so there is no mass flux across it. At the right, the wake velocity profile is given by $u(y)$ above, and outside the wake, the velocity is 1.5 m/s, out of the CV. We have a steady flow, so the conservation of mass is written as

$$0 = \int_{CS} \rho \mathbf{V} \cdot \hat{\mathbf{n}} \, dA,$$

$$0 = \int_{\substack{\text{left}\\CS}} \rho \mathbf{V} \cdot \hat{\mathbf{n}} \, dA + \int_{AB} \rho \mathbf{V} \cdot \hat{\mathbf{n}} \, dA + \int_{\substack{\text{right}\\CS}} \rho \mathbf{V} \cdot \hat{\mathbf{n}} \, dA.$$

Since we are not given the length of the cylinder into the page, we assume a unit cylinder length of 1 m. The areas of our control surfaces are thus $l\,dy$, with a unit length

$l = 1$. Hence the "area" of the left control surface is simply H (m^2). The desired mass flow rate will be the mass flux across *AB per meter of cylinder length*. We now have

$$0 = -\rho U H + \dot{m}_{AB} + \int_0^H \rho u(y)\, \mathrm{d}y. \tag{18.37}$$

This is nearly an expression we can rearrange to solve for the desired mass flow rate. H, however, is not known. To complete the solution we must investigate the flow field further. Outside the wake region, which is 1 m wide at the control surface, the flow out of the right CS has speed 1.5 m/s. The left control surface has a uniform inflow of 1.5 m/s. Hence, more than 1 m away from the cylinder axis, the flow is unaffected by the cylinder and simply proceeds with a constant speed 1.5 m/s. We can therefore assess the amount of mass flux forced across *AB* by integrating only from 0 to 1 m, instead of 0 to H

$$0 = -\rho U(1) + \dot{m}_{AB} + \int_0^1 \rho u(y)\, \mathrm{d}y,$$

$$\dot{m}_{AB} = \rho U(1) - \int_0^1 \rho \left(1.25 + \frac{y^2}{4} \right) \mathrm{d}y,$$

$$\dot{m}_{AB} = (1.23\,\mathrm{kg/m^3}) \left\{ 1.5\,\mathrm{m^3/s} - \left[1.25 y + \frac{y^3}{12} \right]_0^1 \right\},$$

$$\dot{m}_{AB} = 0.205\,\mathrm{kg/s}\ \text{per meter of cylinder length.}$$

To address part (b) of this problem, we will conserve linear momentum in the x-direction. We may either continue with the same control volume as in part (a), multiplying the fluxes by two to obtain the force on the whole cylinder, or we may now use a CV that consists of all the fluid between $-H$ and $+H$, or equivalently -1 and 1. The drag force on the cylinder is in the $+x$-direction; hence, there is an equal and opposite force on the fluid in the $-x$-direction. Conserving x momentum, we have

$$F_x = \left(F_{\mathrm{visc}} \right)_x + \left(F_{\mathrm{external}} \right)_x + \int_{\mathrm{CV}} \rho g_x\, \mathrm{d}\mathcal{V} - \int_{\mathrm{CS}} p\hat{\mathbf{i}} \cdot \hat{\mathbf{n}}\, \mathrm{d}A = \frac{\partial}{\partial t} \int_{\mathrm{CV}} \rho u\, \mathrm{d}\mathcal{V} + \int_{\mathrm{CS}} \rho u (\mathbf{V} \cdot \hat{\mathbf{n}})\, \mathrm{d}A.$$

Under the assumptions of steady flow, with negligible contributions from pressure gradients, gravity, and viscous effects, this becomes

$$-F_x = \int_{\mathrm{CS}} \rho u (\mathbf{V} \cdot \hat{\mathbf{n}})\, \mathrm{d}A.$$

We evaluate the flux at all three control surfaces of the initial CV, and multiply each by two due to symmetry:

$$-F_x = 2 \int\limits_{\substack{\text{left} \\ \text{CS}}} \rho u (\mathbf{V} \cdot \hat{\mathbf{n}}) \, dA + 2 \int\limits_{AB} \rho u (\mathbf{V} \cdot \hat{\mathbf{n}}) \, dA + 2 \int\limits_{\substack{\text{right} \\ \text{CS}}} \rho u (\mathbf{V} \cdot \hat{\mathbf{n}}) \, dA$$

$$= -2 \int\limits_0^1 \rho U U (1 \, dy) + 2 \int\limits_{AB} \rho u (\mathbf{V} \cdot \hat{\mathbf{n}}) \, dA + 2 \int\limits_0^1 \rho u(y) u(y) (1 \, dy).$$

We have again assumed a unit cylinder length into the page, so that the area of both right and left control surfaces is $1 \, dy$. We next recognize that the second integral contains the mass flux we just solved for, $\dot{m}_{AB} = \int\limits_{AB} \rho \mathbf{V} \cdot \hat{\mathbf{n}} \, dA$, and differs from this only by the value of u, the x-component of velocity at the surface AB. The surface AB is at a distance of H from the cylinder axis, where, as we have discussed, the cylinder does not influence the x-directional flow. The velocity u is therefore $U = 1.5 \, \text{m/s}$ on AB. We thus get something even simpler:

$$-F_x = -2\rho U^2 (1)^2 + 2U \dot{m}_{AB} + 2 \int\limits_0^1 \rho \left[1.25 + \frac{y^2}{4} \right]^2 1 \cdot dy,$$

$$-F_x = -2\rho U^2 + 2U \dot{m}_{AB} + 2\rho \left[1.25^2 y + \frac{2.5}{12} y^3 + \frac{y^5}{80} \right]_0^1,$$

$$-F_x = -2(1.23 \, \text{kg/m}^3)(1.5 \, \text{m/s})^2 + 2(1.5 \, \text{m/s})(0.205 \, \text{kg/s}) + 2(1.23 \, \text{kg/m}^3)(1.783 \, \text{m}^2/\text{s}^2),$$

$$F_x = 0.53 \, \text{N per meter of cylinder length.}$$

EXAMPLE 18.5

For the given water siphon, find(a) the speed of water leaving as a free jet at point 2 and (b) the water pressure at point A in the flow. State all assumptions. Heights $h_1 = 1 \, \text{m}$, and $h_2 = 8 \, \text{m}$. Drawing is not to scale.
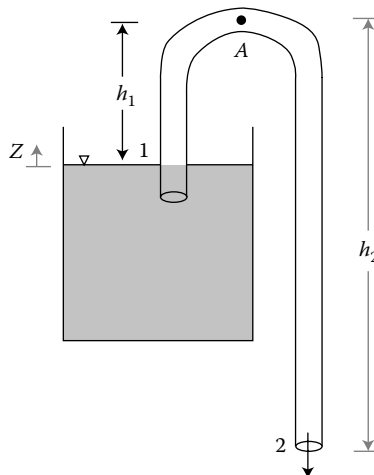
Given: Length of siphon used to remove water from large tank.

Find: Speed at 2 and pressure at *A*.

Assume: Steady flow (all transient effects associated with flow initiation have died down), incompressible (water has constant, uniform density, equal to $1000\,\text{kg/m}^3$), and negligible viscous effects.

Solution

We would like to use the Bernoulli equation to relate the flow quantities between the labeled points. The conditions necessary for the Bernoulli equation to apply have been reasonably assumed. (We feel least confident in our assumption of negligible viscous losses in the siphon, and in Chapter 20 we will discuss a way to characterize the importance of viscosity in a given flow.)

We must have a streamline on which to apply the Bernoulli equation, and so we assume that the one sketched below exists. This streamline connects points 1 and *A*, and *A* and 2.
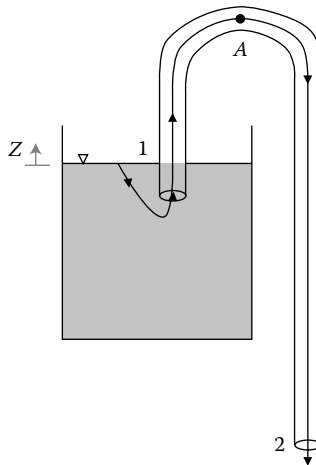
We will make one more assumption in order to solve this problem. By inspection, the reservoir is much larger than the siphon diameter. That is,

$$A_1 \gg A_2.$$

So, if we conserve mass from point 1 to point 2, we will have

$$\rho V_1 A_1 = \rho V_2 A_2.$$

And, with $A_1 \gg A_2$, we must have $V_1 \ll V_2$. We approximate this very small velocity at 1 by saying $V_1 \approx 0$.

We can now apply Bernoulli's equation between points 1 and 2, to find the unknown V_2:

$$\frac{p_1}{\rho} + \frac{V_1^2}{2} + gz_1 = \frac{p_2}{\rho} + \frac{V_2^2}{2} + gz_2,$$

where, as we have just said, $V_1 \approx 0$, and where $p_1 = p_2 = p_{atm}$. (If we are using gage pressures, this means $p_1 = p_2 = 0$.) We note from the figure that $z_1 = 0$, and $z_2 = -7$ m, so

$$gz_1 = \frac{V_2^2}{2} + gz_2,$$

$$V_2^2 = 2g(z_1 - z_2),$$

$$V_2 = \sqrt{2(9.8\,\text{m/s}^2)(7\,\text{m})} = 11.7\,\text{m/s}.$$

Our assumed streamline also goes through point A, so that the Bernoulli equation is

$$\frac{p_1}{\rho} + \frac{V_1^2}{2} + gz_1 = \frac{p_A}{\rho} + \frac{V_A^2}{2} + gz_A.$$

If we conserve mass within the constant-area siphon, we must have

$$\rho V_A A_A = \rho V_2 A_2.$$

Or, since $A_A = A_2$, $V_A = V_2 = 11.7$ m/s. We are now equipped to solve the Bernoulli equation for the unknown p_A:

$$\frac{p_1}{\rho} + gz_1 = \frac{p_A}{\rho} + \frac{V_2^2}{2} + gz_A,$$

$$p_A = p_1 + \rho \left(gz_1 - \frac{V_2^2}{2} - gz_A \right)$$

$$= p_{atm} + \rho g(z_1 - z_A) - \rho \frac{V_2^2}{2}$$

$$= p_{atm} + (1000\,\text{kg/m}^3)(9.8\,\text{m/s}^2)(0 - 1\,\text{m}) - (1000\,\text{kg/m}^3)\frac{(11.7\,\text{m/s})^2}{2},$$

$$p_A = 22.8\,\text{kPa (abs)}$$

$$= -78.5\,\text{kPa (gage)}.$$

We have used standard atmospheric pressure, $p_{atm} = 101.325$ kPa.

EXAMPLE 18.6

A person holds her hand out of an open car window while the car drives through still air at 65 mph. Under standard atmospheric conditions, what is the maximum pressure on her hand? What would be the maximum pressure if the car were traveling at 130 mph?

   Given: Speed of airflow past hand; standard atmospheric conditions.

   Find: Maximum pressure on hand.

   Assume: Flow is steady and incompressible, with negligible viscous effects; air has constant, uniform density, equal to its tabulated value at 20°C (1.23 kg/m^3). Standard atmospheric pressure $p_{atm} = 101.325$ kPa.

Solution

We put ourselves in the frame of the person's hand, so that the hand is still and the air moves with speed 65 mph (or 130 mph). We can visualize the airflow as sketched below:
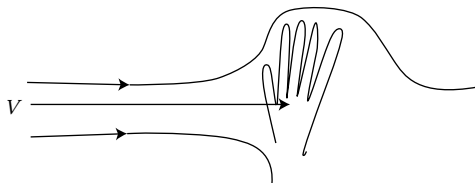
Note that there is a dividing streamline that impinges on the hand at a stagnation point. (Airflow either goes above this streamline, up and over the hand, or below it.) At this stagnation point, the air will be at its maximum pressure, the stagnation pressure. (Recall that pressure and velocity are inversely proportional.) If we assume that this stagnation streamline is level, so that gravitational effects are easily neglected, we can apply the Bernoulli equation on this streamline to find the stagnation pressure. The Bernoulli equation has the form

$$\left(p + \frac{1}{2}\rho V^2\right)_{\text{upstream}} = \left(p + \frac{1}{2}\rho V^2\right)_{\text{SP}},$$

or

$$p_{\text{atm}} + \frac{1}{2}\rho V^2 = p_{\text{max}}.$$

Plugging in the atmospheric pressure, air density, and $V = 65$ mph, we have

$$p_{\text{max}} = 101{,}325\,\text{Pa} + \frac{1}{2}(1.23\,\text{kg/m}^3)\left(65\,\text{mph}\frac{0.447\,\text{m/s}}{1\,\text{mph}}\right)^2 = 101.8\,\text{kPa (abs)}$$

$$= 520\,\text{Pa (gage)}.$$

If the car (and hence the air, in the frame of the hand) moves with speed $V = 130$ mph:

$$p_{\text{max}} = 101{,}325\,\text{Pa} + \frac{1}{2}(1.23\,\text{kg/m}^3)\left(130\,\text{mph}\frac{0.447\,\text{m/s}}{1\,\text{mph}}\right)^2 = 103.4\,\text{kPa (abs)}$$

$$= 2.08\,\text{kPa (gage)}.$$

PROBLEMS

18.1 A two-dimensional fluid velocity field is given by $u = x(1 + 2t)$, $v = y$. Find the equation of the time-varying streamlines which all pass through the point (x_0, y_0) at some time t. Sketch some of the streamlines at various times t.

18.2 A velocity field is given by $\mathbf{V} = ax\hat{\mathbf{i}} + by\hat{\mathbf{j}} - (a + b)z\hat{\mathbf{k}}$, where a and b are constants with dimensions of inverse time. Please find the acceleration in this flow.

18.3 For the following velocity field: (a) determine the acceleration, noting the local and convective components; and (b) determine the location of the maximum acceleration:

$$\mathbf{V} = (C \sin \omega t)[x\hat{\mathbf{i}} - y\hat{\mathbf{j}}].$$

18.4 For the three-dimensional, time-varying velocity field $\mathbf{V} = 3t\hat{\mathbf{i}} + xz\hat{\mathbf{j}} + ty^2\hat{\mathbf{k}}$, find the acceleration of a fluid element.

18.5 Consider a two-dimensional velocity field in Cartesian coordinates:

$$(u, v) = \left(\frac{-ky}{x^2 + y^2}, \frac{kx}{x^2 + y^2} \right),$$

where k is a positive constant. Sketch the velocity profiles along the x-axis and the line $x = y$. Determine the equation of the streamline passing through $(x, y) = (1, 1)$. What are the velocity and acceleration at this point? Sketch both vectors. Is the flow incompressible?

18.6 Consider the velocity field $\mathbf{u} = C_1 tx\hat{\mathbf{i}} + C_2 txy\hat{\mathbf{j}} + C_3 tz\hat{\mathbf{k}}$, where the constants $C_1 = 1\,\mathrm{s}^{-2}$, $C_2 = 2\,\mathrm{m}^{-1}\mathrm{s}^{-2}$, and $C_3 = -2\,\mathrm{s}^{-2}$. For the region described by $[\,0 < x < 1\,\mathrm{m}, 0 < y < 2\,\mathrm{m}$, and $0 < z < 3\,\mathrm{m}\,]$, determine whether this flow satisfies mass conservation for a constant density fluid.

18.7 An inflatable backyard swimming pool is being filled from a garden hose with a flowrate of $0.12\,\mathrm{gal/s}$.
   a. If the pool is 8 ft in diameter, determine the time rate of change of the depth of water in the pool.
   b. Suppose that the pool has a drain port with a diameter 0.5 in. Immediately after the drain is opened, the rate of change of the depth of the water in the pool is observed to decrease to 80% of the value calculated in part (a). Determine the average fluid velocity at the drain port.

18.8 A new jet engine is being tested in a wind tunnel, as illustrated in the following figure. Air, with standard properties at an altitude of 6000 m, enters the engine at a velocity of 275 m/s through a circular intake port of radius 0.5 m. Fuel enters the engine at a mass flowrate of 2.5 kg/s. If the exhaust gas leaves the engine with an average velocity of 300 m/s through an exit port of radius 0.4 m, calculate the density of the exhaust gas. How would your solution to this problem change if the engine were attached to the wing of an airplane flying through still air at a velocity of 900 km/h?
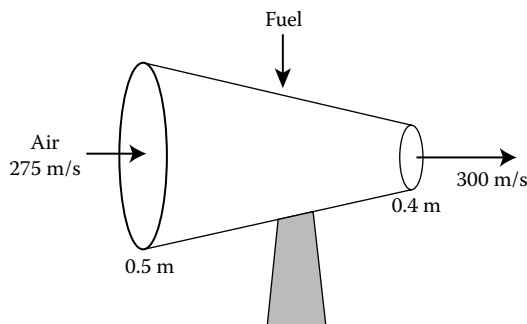
18.9 Based on test results for the prototype jet engine in Problem 18.8, the engine is redesigned. During the next stage of testing, it is desirable to determine the thrust generated by the engine, using the setup shown in the following figure. The air and fuel inlet conditions are the same as in Problem 18.8. If the exhaust gas leaves the

engine with an average velocity of 300 m/s at atmospheric pressure, calculate the magnitude and direction of the force exerted on the support structure.
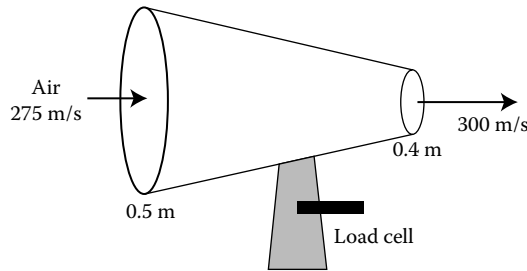
18.10 The horizontal nozzle shown has $D_1 = 0.3$ m and $D_2 = 0.15$ m, with inlet pressure of the operating fluid (water at 20°C) $p_1 = 262$ kPa (absolute) and $V_2 = 17$ m/s. Compute the normal stress induced in the flange bolts (diameter 1 cm) by keeping the nozzle fixed.
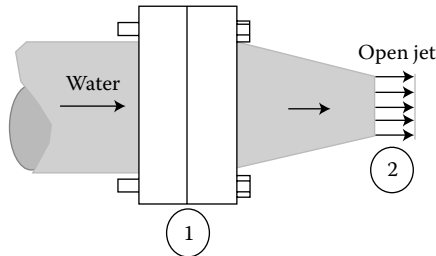
18.11 Water from a stationary nozzle strikes a flat plate (directed normal to the plate as shown in the figure). The velocity of the water leaving the nozzle is 15 m/s and the nozzle area is 0.01 m². After the water strikes the plate, subsequent flow is parallel to the plate.
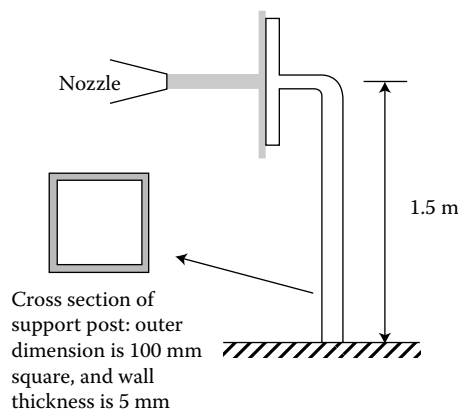
   a. Find the horizontal force that must be provided to the plate by the support.
   b. Find the maximum longitudinal normal tensile stress in the support post if it is a hollow square cross section as shown. Model the force due to the water as a point load.
   c. Find the maximum transverse shearing stress in a cross section of the post.

18.12 Observations show that it is not possible to blow the table tennis ball out of the funnel shown on the left. In fact, the ball can be kept in an inverted funnel, like the one on the right, by blowing through it. The harder one blows through the funnel, the harder the ball is held within the funnel. Explain this phenomenon.
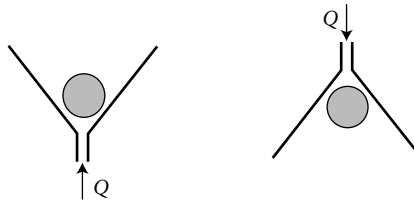
18.13 An open-circuit wind tunnel draws in sea-level standard air and accelerates it through a contraction into a 1 m-by-1 m test section. A differential pressure trans-ducer mounted in the test section wall measures a pressure difference of 45 mm of water between the inside and outside. Estimate (a) the test section velocity in miles/h and (b) the absolute pressure on the front nose of a small model mounted in the test section.

18.14 Blood, an incompressible fluid with density $\rho = 1060\,\text{kg/m}^3$, flows through vessels which often branch. Using the given model for a branching arteriole, and assuming that at the point of interest flow is steady, with negligible contributions from gravity and viscosity, calculate the pressure differences:

a. $P_C - P_A$

b. $P_B - P_A$
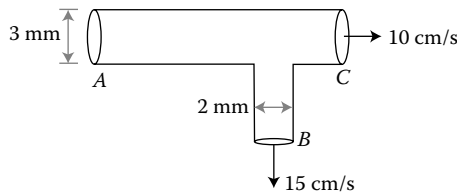
18.15 Five holes are punched in the side of a can of liquid. Which figure shown below best illustrates the velocity profile that would result from liquid leaving the five holes?
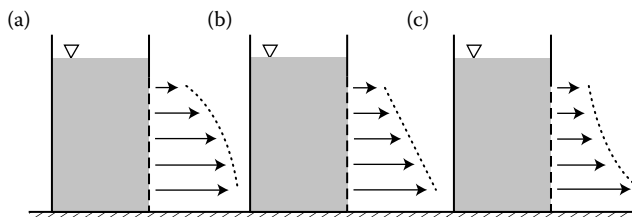
18.16 You have been contracted to build a cylindrical brick chimney of height H, weigh-ing $a = 850\,\text{lb/ft}$ and fixed securely in a concrete foundation. The inner and outer diameters are $d_1 = 3\,\text{ft}$ and $d_2 = 4\,\text{ft}$, respectively. The chimney must be designed to withstand a distributed load due to a 60 mph (88 ft/sec) wind that we will assume is constant at any height from the ground.

  a. Find the static pressure at a stagnation point on the chimney. Assume that this pressure acts over the whole projected area (a rectangle $H \times d_2$) for calculation of the force on the chimney by the wind, but this is only an approximation. Find the force/ft of height on the chimney due to the wind.

  b. You have a strict design requirement: considering the weight of the chimney and the wind load together, there is to be no tensile normal stress in the brickwork (because it is brittle and a poor carrier of tensile stress). What is the maximum allowable height H?

18.17 Two very large tanks of water have smoothly contoured openings of equal cross-sectional area. A jet of water flows from the left tank. Assume the flow is uniform and unaffected by friction/viscous effects. The jet impinges on a flat plate (and departs the plate in a flow parallel to the surface of the plate) that also covers the opening of the right tank. In terms of the height H, determine the minimum value for the height h to keep the plate in place over the opening of the right tank.
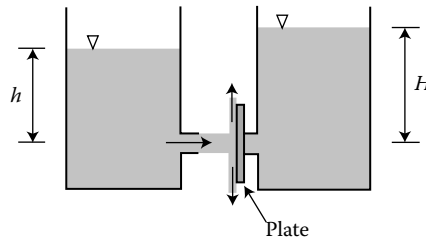
19

Case Study 9: China's Three Gorges Dam,
三峡大坝

China's Yangtze River flows 6400 km (almost 4000 miles) across the country—from mountain glaciers in Tibet through steep gorges and farmland all the way to Shanghai, on the East China Sea. The river supports substantial trade in its Delta region amounting to a fifth of China's economy, and is habitat to many animals, including some endangered species. Flooding of the Yangtze in its lower course has been a pernicious problem, particularly since deforestation has made the region more susceptible to the effects of heavy rains. Ironically, the dams and dikes built in the 1950s to reduce flooding and irrigate farmland actually exacerbated the flood risk by cutting off lakes that had served as natural flood control. (See Chapter 21 for further discussion of flood management approaches.) The Three Gorges region of the Yangtze is shown in Figure 19.1. Xiling Gorge is 75 km long and includes the new Three Gorges Dam near the eastern end. Before construction of the dam, it was known for its treacherous rapids.

The notion of a dam on the Yangtze for flood control and hydroelectric power generation was first proposed by Sun Yat-Sen in 1919. While some survey work and planning was performed, the Chinese Civil War and other complications delayed the project. After the 1954 Yangtze flooding, the Communist leader Mao Zedong wrote a poem, "Swimming," expressing support for a dam on the Yangtze, but prioritized other infrastructure projects, as well as the Great Leap Forward and the Cultural Revolution. In 1992, the National People's Congress approved the dam, and construction finally began in late 1994.

One goal of the Three Gorges Dam project was to reduce China's reliance on coal-burning power plants, which contributed to carbon dioxide emissions and air pollution. The Three Gorges Project included a hydroelectric generation system; hydroelectric power from the dam as built can produce up to one-ninth of China's energy needs.

Hydroelectric plants like the turbines at the Three Gorges Dam produce electrical power through the energy of falling or flowing water. A simple equation to estimate the electrical power production P in Watts, is

$$P = \rho h Q g \eta, \tag{19.1}$$

where ρ is the density of water in SI dimensions (kg/m^3), h is the depth of water (or height of waterfall) (in m), Q is the volumetric flow rate in m^3/s, g is the acceleration of gravity (9.8 m/s^2), and η is the efficiency of energy conversion—a value between 0 and 1.

In the case of a dam-based hydroelectric plant, the high-pressure water kept in the reservoir behind the dam is released by a control gate, and the water then spins a turbine, whose mechanical energy is converted into electrical power by a transformer. Figure 19.2 shows a simple schematic of this process.

The dam was not a particularly popular idea with the public. The government endeavored to persuade them of its virtues with information about the reduced risk of flooding, and the improvement in air quality that could be achieved by replacing coal plants with hydroelectric power.

FIGURE 19.1
Xiling Gorge, China.

The construction of the dam required the planned flooding of sites along the Yangtze. Villages lining the river were designated to be flooded, and their residents relocated to newly planned and built communities on higher ground. Citizens were offered "relocation payments" and new housing in these new communities. This gradual flooding affected sites of natural and cultural historical significance, and some 1.3 million people.
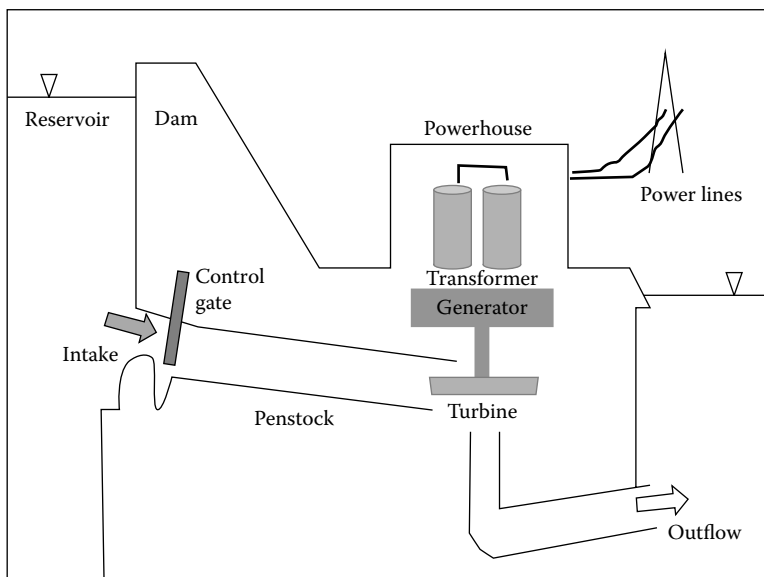
FIGURE 19.2
Schematic of a hydroelectric power plant.

FIGURE 19.3
Completed Three Gorges Dam. (© istock.com/Prill Mediendesign & Fotographie. With permission.)

In his short story, "Village 113," writer Anthony Doerr depicts residents of a village slated for submergence, including a woman who is reluctant to leave her longtime home and her son, an engineer who is helping with the dam-related logistics. Doerr lyrically portrays the sense of imminent loss as preparations are made: "Memory is a house with ten thousand rooms; it is a village slated to be inundated." Doerr also shows the son's enchantment with the scale of the project: he "recites numbers. The dam will be made from eleven million tons of concrete: Its parapet will be a mile long; its impoundment will swallow a dozen cities, a hundred towns, a thousand villages. The river will become a lake and the lake will be visible from the moon." He cannot understand his mother's failure to appreciate the dam, and his own contributions.

As engineers, we must be cautious not to let the technical advantages of a technological enterprise, and astounding specifications of size, power, or capabilities, overwhelm our empathy for human stakeholders. As built, the Three Gorges Dam is indeed a wonder: it is 2335 m long, 185 m high, and 130 m wide at the bottom, tapering to 18 m wide at the top. The dam raised the river to 175 m above sea level, creating a 600 km long reservoir with a storage capacity of 39.9 billion cubic meters. The completed dam (whose final turbine was installed in June, 2012) is the world's largest power station, with a capacity of 22,500 MW—this is about eight times the output of the Hoover Dam on the Colorado River. The completed Three Gorges Dam is shown in Figure 19.3.

This technical achievement has had significant social impacts, reaching beyond the reduced risk of Yangtze flooding and the addition of hydroelectric power as an alternative to coal.

The farmland lost in the submergence process had provided 40% of China's grain and 70% of rice crops. Farmers that were relocated to the hillsides of the dam have struggled to grow crops, and so far the only viable crop able to be produced on such steep terrain has been oranges.

The more than 1300 archeological sites flooded included that of the ancient Ba civilization that settled in the Three Gorges area over 4000 years ago. Only some of the artifacts of these sites have been preserved; the rest are lost beneath the 175-plus meter depth of the

reservoir behind the dam. Some archeological organizations and scholars petitioned for funding and time to remove the artifacts, but these requests were denied by the Chinese government.

Relocated Chinese citizens have had varying degrees of success adjusting to their forced transplantation to new homes and communities. Although few of their individual stories are publicly available, economic analyses have shown that younger citizens adapt more readily and achieve greater financial success than older citizens forced to relocate. The government is moving ahead with a widespread "urbanization" plan, in which millions more will be forced to relocate from rural villages to cities, even in areas not affected by the dam.

The dam has induced erosion and contributed to increased earthquake activity and landslides in the region. The reduction in forested land around the Yangtze has affected wildlife, including a critically endangered crane, and the dam's turbines are harmful to fish.

Fan Xiao, a geologist at the Bureau of Geological Exploration and Exploitation of Mineral Resources in Sichuan province, described to *Scientific American* the tradeoffs and competing objectives of the project. "For the economic interests and profit of the Three Gorges Project Development Corporation," he says, "that's very important. But the function of any river, including the Yangtze, is not only to produce power. At the very least, [a river] is also important for shipping, alleviating pollution, sustaining species and ecosystems, and maintaining a natural evolutionary balance." Moreover: "The Yangtze doesn't belong to the Three Gorges Project Development Corporation," Fan adds. "It belongs to all of society."

References

D. Chethem, *Before the Deluge: The Vanishing World of the Yangtze's Three Gorges*. United States of America: Palgrave Macmillan, 2002.

A. Doerr, "Village 113," in *Memory Wall*, New York: Scribner, 2010.

B. Handwerk, "China's Three Gorges Dam, by the Numbers." *National Geographic News*, 2006.

M. Hvistendahl, "China's Three Gorges Dam: An Environmental Catastrophe?" *Scientific American*, March 25, 2008.

"Three Gorges Project," Chinese National Committee on Large Dams.

S. Winchester, *The River at the Center of the World*. New York: Henry Holt & Co., 1998.

M. Wines, "China admits problems with Three Gorges Dam," *New York Times*, May 19, 2011.

20

Fluid Dynamics: Applications

> That we have written an equation does not remove from the flow of fluids its charm or mystery or its surprise.
>
> **Richard Feynman, 1964**

We have found two distinct ways to apply the fundamental concepts of mass conservation and $\sum \mathbf{F} = m\,\mathbf{a}$ to fluids. We now want to identify some canonical problems of fluid mechanics, their historical context, and their relevance to us. Both solid and fluid mechanics are enormous fields, with many rich details; in this book, we have been necessarily brief with both of them. We encourage further study of both areas, and of the field of continuum mechanics; please consult the References listed at the end of this book.

20.1 How Do We Classify Fluid Flows?

The Navier–Stokes equation contains terms corresponding to several possible forces on a fluid element. If we look at it again, we can name the source of each of these forces:

$$\rho \underbrace{\frac{\mathrm{D}\mathbf{V}}{\mathrm{D}t}}_{\text{inertia}} = \underbrace{-\nabla p}_{\text{pressure}} + \underbrace{\rho \mathbf{g}}_{\substack{\text{gravity} \\ \text{(body force)}}} + \underbrace{\mu \nabla^2 \mathbf{V}}_{\substack{\text{viscous} \\ \text{stress}}}. \tag{20.1}$$

We would like to have a way to quantify the relative effects of these forces, and of other factors, on a given flow; this way, when faced with an intriguing fluid mechanics problem, we could decisively say whether *viscosity* or *inertia* was the more dominant effect, and *how much more* dominant. The most useful result would be a dimensionless parameter—that way, it would not matter whether we were dealing with SI or US units; a certain numerical value of this parameter would represent the same type of flow in either unit system.

It is apparent that by taking the ratio of the inertial and viscous terms of the Navier–Stokes equation, we could obtain this quantification. This ratio will clearly go as ρ/μ. Unfortunately, this ratio ρ/μ has dimensions of time/length^2. To make it dimensionless, we need to multiply it by something with units of length^2/time. The easiest way to construct this "something" is to multiply the velocity $\mathbf{V}$ by a characteristic length scale of the problem, say L. It turns out that this is also correct physically, as we can see by a scaling argument:

$$\text{Inertial force} = m\,\mathbf{V}\frac{\mathrm{d}\mathbf{V}}{\mathrm{d}s} \sim \rho L^3 V \frac{V}{L} = \rho L^2 V^2, \tag{20.2}$$

$$\text{Viscous force} = \tau A = \mu \frac{\mathrm{d}u}{\mathrm{d}y} A \sim \mu \frac{V}{L} L^2 = \mu V L, \qquad (20.3)$$

$$\text{Ratio of inertial to viscous forces} = \frac{\rho L^2 V^2}{\mu V L} = \frac{\rho V L}{\mu}. \qquad (20.4)$$

This ratio is known as the Reynolds number, abbreviated *Re*.[*] When *Re* is large, inertial effects dominate the flow, and when *Re* is small, viscous effects dominate. This lets us know what terms we can drop out of the Navier–Stokes equation when we are at the far ends of the *Re* spectrum. As expected, *Re* also tells us something about the character of the flow. Generally, lower *Re* flows are smooth, with parallel streamlines because viscosity tends to diffuse more complex flow patterns. These flows are known as *laminar*. At higher *Re*, viscosity is not strong enough to diffuse eddies and other rotational flow patterns, and the flow tends to be more disorderly. These higher *Re* flows are called *turbulent*. A critical value of Reynolds number, Re_{crit}, is a threshold separating laminar from turbulent flows. The value of Re_{crit} depends on the type of flow being considered, as we will see.

Other non-dimensional parameters serve to measure the relative effects of other forces on a particular flow. For example, the Euler number *Eu* compares pressure drop to inertial forces. The Euler number and a few other relevant parameters are listed in Table 20.1.

The Reynolds, Euler, Froude, and Weber numbers, among others, allow us to quantify the relative importance of different forces on the flow in question; they are also useful in planning experiments. Two flows, with the same *Re*, have very similar flow patterns and characteristics—inertia and viscosity have the same relationship in both flows. To build an experimental model of a flow whose real dimensions are unwieldy, it is sufficient to match the appropriate nondimensional parameters. It is much more economical to study the influence of *Re* on a given flow than to have to independently vary the density ρ and viscosity μ of a fluid, the size of the model L, and the flow speed V!

TABLE 20.1

Relevant Non-Dimensional Parameters

Reynolds number	*Re*	$\dfrac{\text{Inertia}}{\text{Viscosity}}$	$\dfrac{\rho V L}{\mu}$
Euler number	*Eu*	$\dfrac{\text{Pressure}}{\text{Inertia}}$	$\dfrac{\Delta p}{\rho V^2}$
Froude number	*Fr*	$\dfrac{\text{Inertia}}{\text{Gravity}}$	$\dfrac{V}{\sqrt{Lg}}$
Weber number	*We*	$\dfrac{\text{Inertia}}{\text{Surface tension}}$	$\dfrac{V^2 L \rho}{s}$
Mach number	*M*	$\dfrac{\text{Velocity}}{\text{Local speed of sound}}$	$\dfrac{V}{a}$

[*] The Reynolds number is named after Osborne Reynolds, the son of an Anglican priest who became a noted fluid mechanician (becoming especially active in fluids after 1873). He was particularly influential in the study of pipe flow and the transition from laminar to turbulent flow. He also established the course of study in applied mathematics at the University of Manchester, though sadly, as one biographer reports, *"Despite his intense interest in education, he was not a great lecturer. His lectures were difficult to follow, and he frequently wandered among topics with little or no connection."* (Anderson, J. D., *A History of Aerodynamics*, Cambridge, 1997.)

20.2 What Is Going on Inside Pipes?

Pipelines, blood vessels, hallways, and ink-jet printers all contain examples of *internal flows*. A fluid's "stiffness," viscosity, has a significant effect on the flow of an incompressible fluid through a pipe or between parallel plates. The critical Reynolds number in a pipe is about 2000; for $Re < 2000$, pipe flow is laminar.

Pipe flow is said to be *fully developed* when it does not change in the flow direction; as in Figure 20.1, the velocity profile $u(x,r)$ becomes independent of axial length x. At the pipe inlet, flow is uniform [$u(x,r) = U_0$ = constant]; as x increases, a very thin layer near the walls slowly grows outward. Viscous effects dominate these thin *boundary layers*, but viscosity does not yet affect the inner core of the flow. We continue along the pipe length x until viscosity affects the entire cross section. Finally, the thin layers all merge and the flow becomes fully developed.

For a laminar flow, we can determine the entrance length L_E necessary for a pipe flow to become fully developed if we know the Reynolds number:

$$\frac{L_E}{D} = 0.065Re, \tag{20.5}$$

where Re is based on the average velocity ($V = \bar{u}$) and the diameter of the pipe ($L = D$).

Now that we know to expect the flow to become independent of axial length x, we would like to be able to determine the shape of the velocity profile $u(y)$, or $u(r)$ for a circular pipe. We will assume steady flow, to simplify our lives a bit. Figure 20.2 shows a cylindrical fluid element for which we can now write $\sum \mathbf{F} = m\mathbf{a}$.

Once the flow is fully developed, it experiences no acceleration. (The local acceleration, $\partial u/\partial t = 0$, and the convective acceleration, $u(\partial u/\partial x) = 0$, since u is a function of r only.) Every part of the fluid moves with constant velocity, although neighboring particles have different velocities and this velocity gradient, as we well know, gives rise to shear stress.

For this simple analysis, we will neglect gravity, assuming that pressure and viscous effects are much more significant. The pressure is constant across vertical cross sections (with no hydrostatic effect due to gravity), though it changes in x. So if pressure is $p = p_1$ at section (1) as shown, it is $p_2 = p_1 - \Delta p$ at section (2). We anticipate that pressure decreases in the direction of flow, so that $\Delta p > 0$.* A shear stress τ acts on the surface of the fluid cylinder. This shear stress is a function of radius r, $\tau = \tau(r)$.
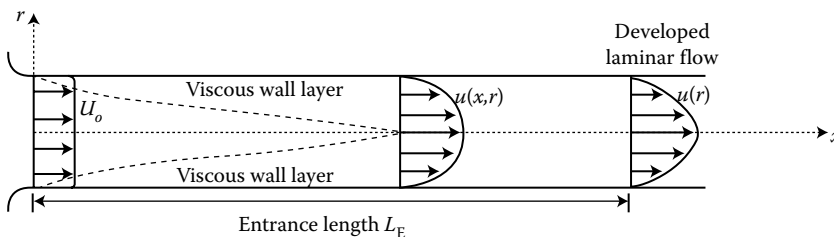
FIGURE 20.1
Laminar flow developing in a pipe or a wide rectangular channel.

---

* Fluids tend to flow from high-pressure toward lower-pressure regions, just as mass tends to flow from regions of high to low concentrations.

(a)

(b)
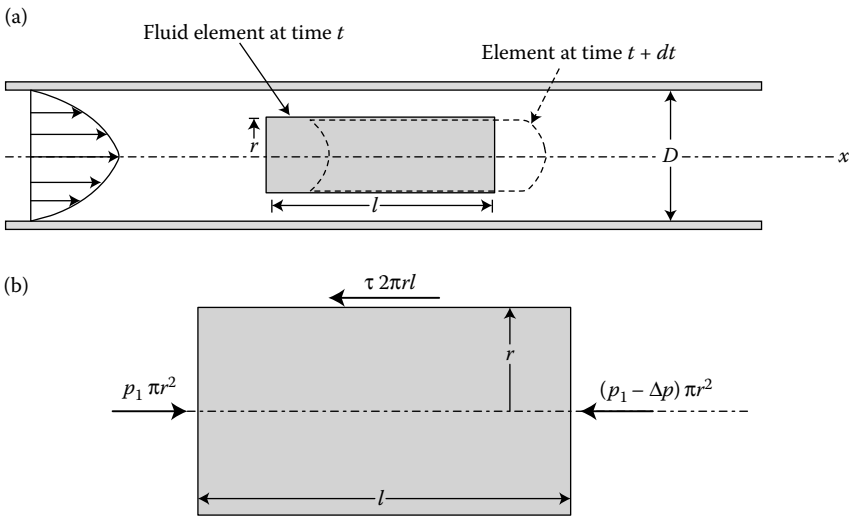
FIGURE 20.2
(a) Motion of a cylindrical fluid element within a pipe flow; (b) FBD of a cylindrical fluid element.

Once again, we need to look at this FBD (Figure 20.2b) and write out $(\sum \mathbf{F} = m\mathbf{a})_x$ for this cylindrical fluid element. We have $a_x = 0$, and the remaining terms of the force balance are

$$p_1 \pi r^2 - (p_1 - \Delta p)\pi r^2 - \tau 2\pi r l = 0. \tag{20.6}$$

This expression can be simplified, yielding

$$\frac{\Delta p}{l} = \frac{2\tau}{r}. \tag{20.7}$$

This balance of forces is necessary to drive each fluid particle down the pipe with a constant velocity. Since neither Δp nor l depends on the radial coordinate r, the right-hand-side term, $2\tau/r$, must not depend on r. That is, $\tau = Cr$, where C is a constant. At $r = 0$, that is, the pipe centerline, there is no shear stress. At r's maximum value of $D/2$, the shear stress has its maximum value, called τ_w, the *wall shear stress*. (Note that this is σ_{rx}.) This boundary condition lets us determine the value of C, which must be $C = 2\tau_w/D$:

$$\tau(r) = \frac{2\tau_w r}{D}. \tag{20.8}$$

From the force balance, then, we must have

$$\Delta p = \frac{4l\tau_w}{D}. \tag{20.9}$$

We see that a small shear stress can produce a large pressure difference if the pipe is relatively long. We also note that if viscosity were zero, there would be no shear stress and the pressure would be constant throughout the pipe. To get further with this analysis, we need to know how the shear stress is related to the velocity.

We could proceed by integrating the full Navier–Stokes equation for this steady, incompressible, viscous flow of a Newtonian fluid, or we could simply remember that for a Newtonian fluid, shear stress is proportional to velocity gradient. For our pipe flow, this is

$$\tau = -\mu \frac{\mathrm{d}u}{\mathrm{d}r}, \tag{20.10}$$

where we have included the negative sign in order to have $\tau > 0$ for $\mathrm{d}u/\mathrm{d}r < 0$, since the velocity decreases from the centerline to the outer wall and shear stress is maximum at the pipe wall; it is more intuitive to keep track of positive τ's. If we combine this equation (the definition of a Newtonian fluid) with the force balance ($\sum \mathbf{F} = m\mathbf{a}$), and eliminate τ, we obtain

$$\frac{\mathrm{d}u}{\mathrm{d}r} = -\left(\frac{\Delta p}{2\mu l}\right) r, \tag{20.11}$$

which we integrate to find the velocity profile:

$$u(r) = -\left(\frac{\Delta p}{4\mu l}\right) r^2 + C_1 \tag{20.12}$$

and use the no-slip boundary condition ($u(r = D/2) = 0$) to find $C_1 = (\Delta p/16\mu l) D^2$, so that

$$u(r) = \frac{\Delta p D^2}{16\mu l}\left[1 - \left(\frac{2r}{D}\right)^2\right] = V_c\left[1 - \left(\frac{2r}{D}\right)^2\right], \tag{20.13}$$

where V_c is the centerline velocity, defined by $\Delta p D^2/16\mu l$. We can also express the velocity profile in terms of the wall shear stress, and in terms of $R = D/2$, as

$$u(r) = \frac{\tau_w D}{4\mu}\left[1 - \left(\frac{r}{R}\right)^2\right]. \tag{20.14}$$

This velocity profile is *parabolic* in the radial coordinate r and has a maximum value, V_c at the centerline, and minimum values (zero) at the pipe wall. We can next find the volume flowrate Q through the pipe. We integrate over a series of very small rings of radius r and thickness $\mathrm{d}r$ to find Q:

$$Q = \int u \, \mathrm{d}A = \int_{r=0}^{r=R} u(r) 2\pi r \, \mathrm{d}r = 2\pi V_c \int_0^R \left[1 - \left(\frac{r}{R}\right)^2\right] r \, \mathrm{d}r, \tag{20.15}$$

$$Q = \frac{\pi R^2 V_c}{2}. \tag{20.16}$$

The average velocity is defined as the flowrate divided by the cross-sectional area, so for this flow we have

$$V_{av} = \frac{\pi R^2 V_c}{2\pi R^2} = \frac{V_c}{2} = \frac{\Delta p D^2}{32\mu l}, \tag{20.17}$$

and

$$Q = \frac{\pi D^4 \Delta p}{128 \mu l}. \tag{20.18}$$

We have found that the average velocity is half the centerline velocity for our laminar parabolic velocity profile. Our results also confirm that the flowrate is

- Directly proportional to the pressure drop
- Inversely proportional to the viscosity
- Inversely proportional to pipe length
- Proportional to the diameter to the fourth power

Equation 20.18 for Q is commonly known as Poiseuille's law, so named for a French physician who performed the first analysis of laminar pipe flow with the goal of learning about blood flow.* Fully developed laminar pipe flow, with its parabolic velocity profile, is generally known as *Poiseuille flow*.

20.3 Why Can an Airplane Fly?

A body, such as a wing or an airfoil, experiences a resultant force due to the inter-action between the body and the moving fluid surrounding it. Figure 20.3 shows a two-dimensional airfoil and the forces on it due to the surrounding fluid: (a) pressure distribution, (b) viscous force distribution, and (c) resultant forces, lift and drag.

You are probably already familiar with the idea that the pressure distribution is respon-sible for lift. The basic idea is that pressure is lower on the upper surface of a wing, so a net upward force keeps the wing aloft. We could show this using the Bernoulli equation: the flow over the smooth upper surface is much faster (therefore exerts lower pressure) than that past the lower surface.

Knowing that drag D and lift L are the x and y resultants of the pressure and viscous stress forces, we could obtain expressions for D and L by integrating these pressure and viscous forces over the body's surface:

$$D = \int \mathrm{d}F_x = \int p \cos\theta \, \mathrm{d}A + \int \tau_{\mathrm{w}} \sin\theta \, \mathrm{d}A, \tag{20.19}$$

$$L = \int \mathrm{d}F_y = -\int p \sin\theta \, \mathrm{d}A + \int \tau_{\mathrm{w}} \cos\theta \, \mathrm{d}A, \tag{20.20}$$

where θ is the degree of inclination (with respect to horizontal) of the outward normal at any point along the body surface. To carry out this integration, we must know the body shape, including θ as a function of position along the body, and the distribution of τ_{w} and p. This is quite difficult to do for realistic geometries. As we have seen when finding

---

* Jean Poiseuille (1799–1869) made the same assumptions we have made: he modeled blood flow as steady, incompressible flow of a non-Newtonian fluid in rigid circular pipes. Although these are spectacularly inap-propriate assumptions for blood flow as it is now understood, Poiseuille flow theory has proved robust in its ability to relate flow rate and fluid mechanical forces for many internal flows. It is even a reasonable ballpark predictor of blood flow, as we will see in Problem 20.8.
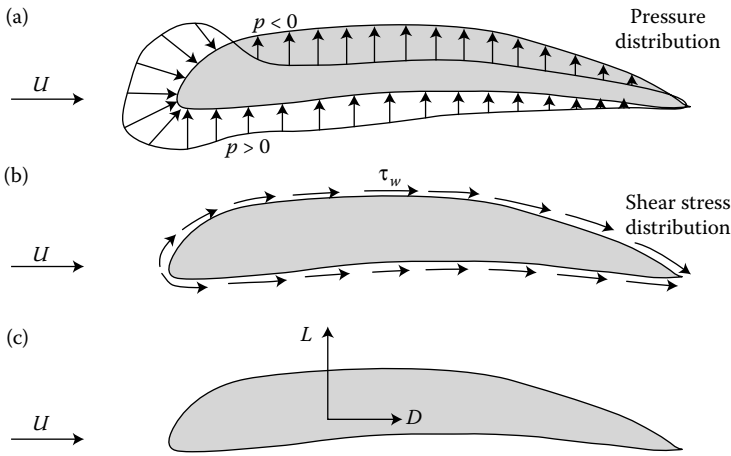
FIGURE 20.3
Forces on two-dimensional airfoil: (a) pressure force, (b) viscous force, and (c) resultant lift and drag forces.

the resultant pressure forces on submerged curved surfaces, there are sometimes ways to get around messy integrations involving changing orientations. This is also the case for lift and drag.

In the simplest force analysis of an airplane, the four important forces are lift, drag, thrust (forward propulsion provided by engines), and weight of the plane. Lift must exceed weight, and thrust must exceed drag, in order for flight to be possible. We can calculate the lift and drag forces for a certain shape in a certain flow using the following formulas:

$$L = C_L \frac{1}{2} \rho U^2 A, \tag{20.21}$$

$$D = C_D \frac{1}{2} \rho U^2 A, \tag{20.22}$$

where A is a characteristic area of the object, typically taken to be the *frontal area*, the projected area that would be seen by an observer riding along with the onrushing flow, parallel to the upstream velocity U; or the *planform area* whose outward normal points in the direction of the lift force. It is important to specify which A one is using in a calculation, and why, when citing lift and drag results. The coefficients C_L and C_D for most common shapes have been determined from experimental data and are tabulated as functions of Reynolds number, as shown in Figure 20.4 for a sphere and a circular cylinder.

We notice in Figure 20.4 that the drag coefficient decreases sharply at a Reynolds number of about 5×10^5. This corresponds to the value of Re_{crit} at which flow transitions from laminar to turbulent. Turbulent flow is characterized by higher fluid momentum, thinner boundary layers, and higher viscous stresses at solid surfaces than laminar flow. For flows over cylinders and spheres, the fluid's higher momentum causes it to more readily follow the body surface without "separating" into a wake region. Turbulent wakes behind cylinders and spheres are therefore generally smaller than laminar wakes. This reduction in the pressure drag on the object overwhelms any increase in viscous drag, and therefore we see a sharp "drag drop" corresponding to the transition to turbulent flow. This phenomenon is sometimes exploited, for example, vortex generators on airplane wings serve to trip flow into turbulent behavior at lower Re than Re_{crit}.
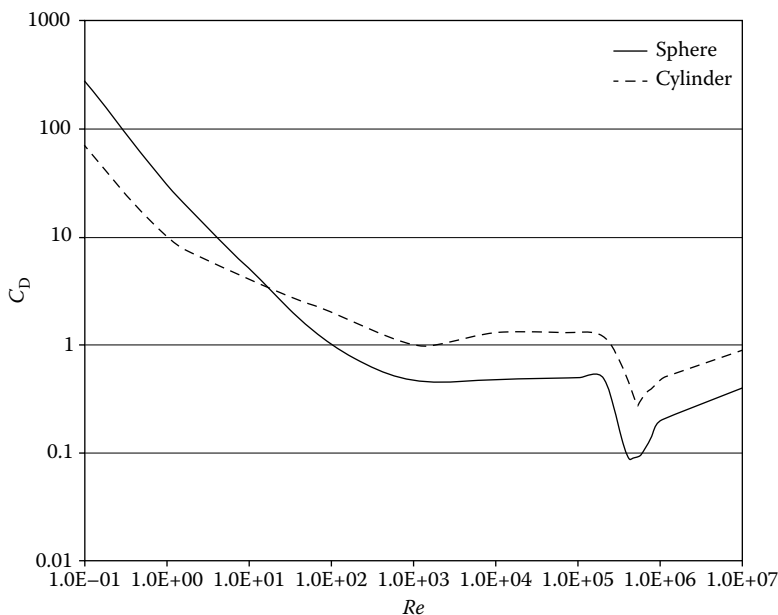
FIGURE 20.4
Drag coefficients for smooth cylinder and sphere, as functions of *Re*.

20.4 Why Does a Curveball Curve?

Baseballs and other objects moving through fluids leave *wakes* behind them. These wakes can be either laminar (relatively smooth flow, viscosity damping out disorderly structures) or turbulent (much more disordered, lots of whorls and eddies with no viscosity to wipe them out). Even in laminar flow, obstructions and protrusions such as wings and flaps on airplanes and rocks in streams can cause some rotational flow behind them. Zones of rotational flow are called *vortices*. Figure 20.5 shows the vortices behind several spheres, for a range of Reynolds numbers.

There is much that could be said about these flow patterns—a semester's worth—but for now, we are interested in baseballs. A typical pitch has a speed of 75–90 mph. A regulation MLB ball must have a circumference between 9 and 9.25 in, or a diameter of about 2.9 in. Using the properties of still air at standard atmospheric conditions, we can calculate a typical Reynolds number:

$$Re = \frac{\rho V D}{\mu} = \frac{(1.2\,\text{kg/m}^3)(37\,\text{m/s})(0.0737\,\text{m})}{1.83 \times 10^{-5}\,\text{N}\cdot\text{s/m}^2} = 1.79 \times 10^5.$$

For a smooth sphere, the transition to turbulence begins at a critical Reynolds number of about $Re_\text{crit} \sim 5 \times 10^5$. The main difference between a baseball and the smooth spheres in Figure 20.5 is the raised stitching. This unevenness on the ball surface makes the transition to turbulence happen at lower *Re*. This is actually a favorable condition for sports balls—as we saw in Figure 20.4, turbulent drag coefficients are lower than laminar ones. So catalyzing the transition to turbulence can decrease the drag on a ball. This is another
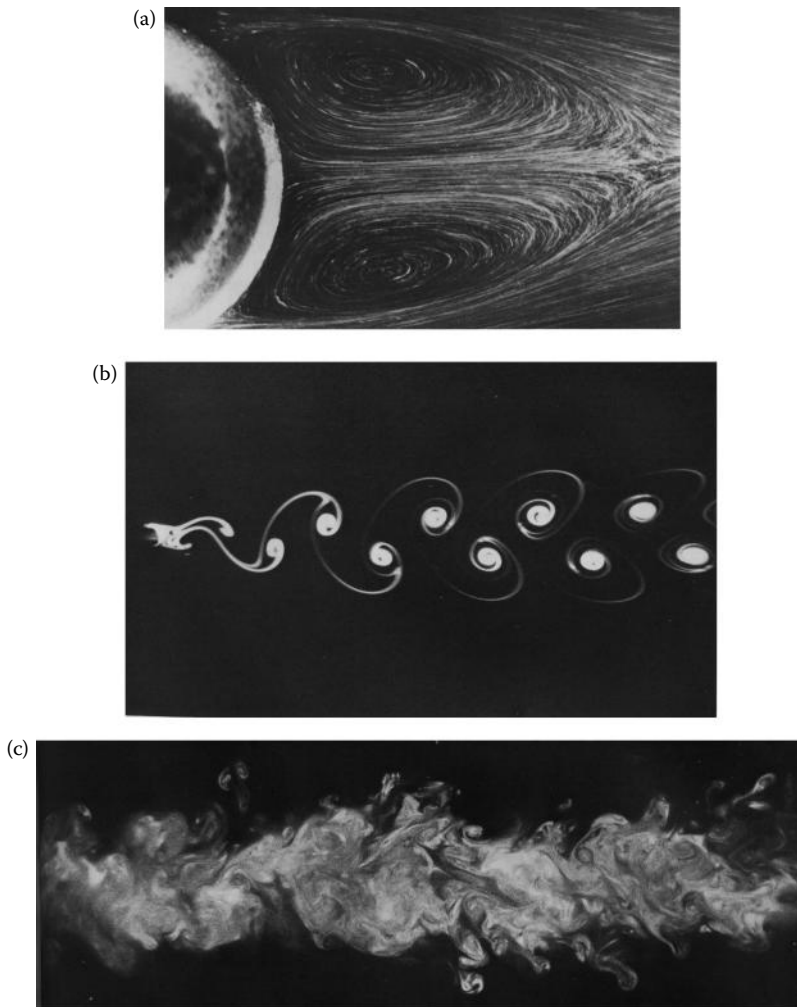
FIGURE 20.5
Wakes behind smooth bodies. Note dependence on Reynolds number. (a) Sphere at $Re = 118$. Recirculating regions behind sphere still attached. (b) Cylinder at $Re = 200$. Wake develops into two parallel rows of staggered vortices. (c) $Re = 1770$. Turbulent wake behind cylinder. Instantaneous flow patterns shown by oil fog. (From Van Dyke, M. 1982. *An Album of Fluid Motion*, Parabolic Press, Stanford. With permission.)

way of exploiting the drag drop, and it is why golf balls are dimpled. The dependence of a baseball's drag coefficient on its speed is shown in Figure 20.6.

If a baseball is thrown without any backspin or topspin imparted by the pitcher, the orientation of the seam causes an asymmetry in the wake, which in turn causes an irregular trajectory. This delivery is commonly known as a *knuckleball*. If, on the other hand, the pitcher *does* impart some spin to the ball as he or she hurls it, the right amount of spin will stabilize this irregularity and help the trajectory follow a predictable path. This is shown in Figure 20.7, as we see the streamlines over a spinning baseball. The streamlines are crowded near the bottom of the ball (representing faster flow), and the wake is deflected
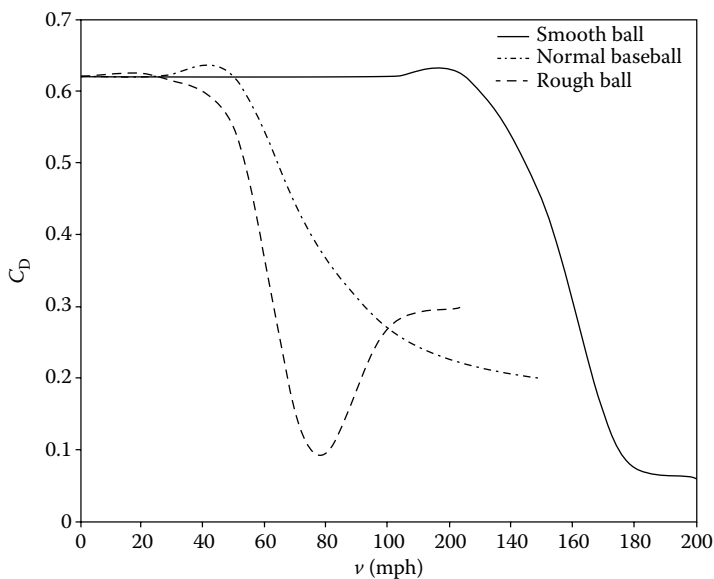
FIGURE 20.6
Drag coefficient as function of speed v for various spheres. (After R. K. Adair, *The Physics of Baseball*, 1994.)

upward by the spin. This deflection is linked to a net downward force on the ball, which is why a pitch thrown in this way will drop or sink as it approaches the batter.

Other types (different in magnitude and direction) of spin can alter the baseball's path in different ways. This effect, known as the Magnus effect, has motivated considerable research into the aerodynamics of baseball. The types of spin imparted for a range of pitch deliveries are sketched in Figure 20.8.
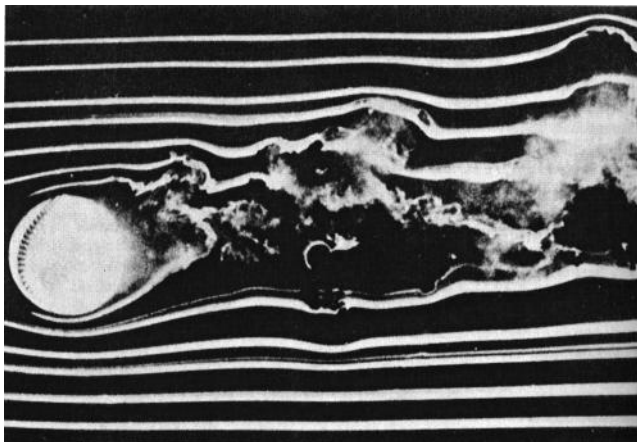
FIGURE 20.7
Smoke photograph of flow around a spinning baseball. Flow is from left to right, flow speed is 21 m/s, and ball is spinning counterclockwise at 15 m/s ($=\omega r$). (Photograph courtesy of F. N. M. Brown, University of Notre Dame.)

Fast ball   Curve ball   Slider   Screw ball
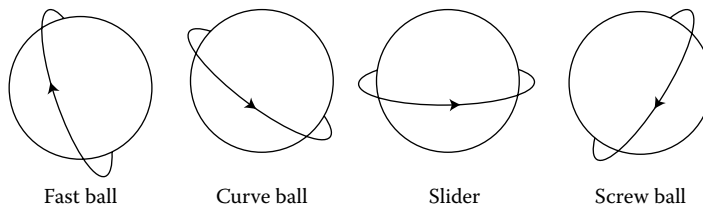
FIGURE 20.8
Ball rotation directions, as seen by the batter, for pitches thrown overhand by a right-handed pitcher. Arrow indicates the direction of rotation. (After R. K. Adair, *The Physics of Baseball*, 1994.)

PROBLEMS

20.1 Typical values of the Reynolds numbers for several animals moving through air or water are listed below. In which cases is the fluid inertia important? In which cases do viscous effects dominate? Do you expect the flow in each case to be laminar or turbulent? Explain.

Animal	Speed	Re
Large whale	10 m/s	300,000,000
Flying duck	20 m/s	300,000
Large dragonfly	7 m/s	30,000
Invertebrate larva	1 mm/s	0.3
Bacterium	0.01 mm/s	0.00003

20.2 The velocity distribution in a fully developed laminar pipe flow is given by

$$\frac{u}{U_{CL}} = 1 - \left(\frac{r}{R}\right)^2,$$

where U_{CL} is the velocity at the centerline and R is the pipe radius. The fluid density is ρ, and its viscosity is μ.
   a. Find the average velocity U_{av} over the cross section.
   b. State the Reynolds number for the flow based on average velocity and pipe diameter. At what approximate value of this Reynolds number do you expect the flow to become turbulent? Why is this value only approximate?
   c. Assume that the fluid is Newtonian. Find the wall shear stress τ_w in terms of μ, R, and U_{CL}.

20.3 A wing generates a lift L when moving through sea-level air with a velocity U. How fast must the wing move through the air at an altitude of 35,000 ft if it is to generate the same lift? (Assume the lift coefficient is constant.)

20.4 The drag on a 2-m-diameter satellite dish due to an 80 km/h wind is to be determined through wind tunnel testing on a geometrically similar 0.4-m-diameter model dish.
   a. At what air speed should the model test be performed?
   b. If the measured drag on the model was determined to be 170 N, what is the predicted drag on the full-scale prototype?

20.5   The viscous, incompressible flow between the parallel plates shown is caused by
       both the motion of the bottom plate and a pressure gradient, $\partial p/\partial x$. Determine the
       relationship between U and $\partial p/\partial x$ such that the shear stress on the fixed plate is
       zero.
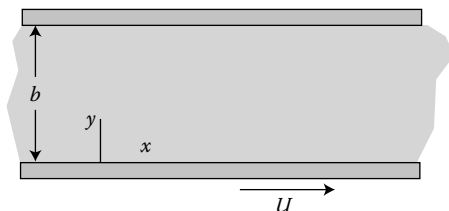
20.6   Water exits a reservoir at 30 m depth to enter the 150 mm diameter inlet of a turbine,
       as shown. The turbine outlet is also 150 mm in diameter. The exit flow is then ejected
       to the atmosphere at 9 m/s through a nozzle with diameter 75 mm. What power is
       developed by the turbine? What horizontal force is required to anchor the turbine if
       the inflow and outflow are horizontal?
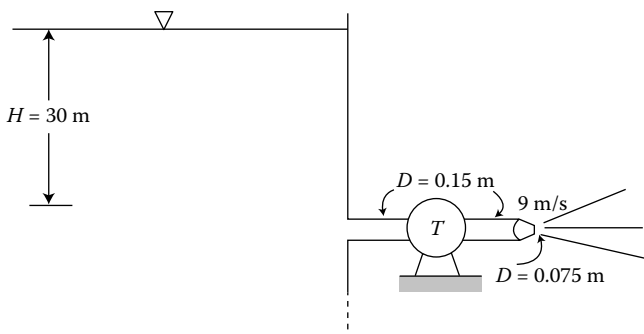
20.7   Crude oil flows through a level section of the Alaskan pipeline at a rate of 1.6 mil-
       lion barrels per day (1 barrel = 42 gallons). The pipe inside diameter is 120 cm, and
       its roughness has a characteristic dimension of 1.5 mm. The maximum allowable
       pressure is 8300 kPa, and the minimum pressure required to keep dissolved gases in
       solution in the crude oil is 350 kPa. The crude oil has SG = 0.93, and its viscosity at
       the pumping temperature is $\mu = 0.017\,\mathrm{Ns/m^2}$. For these conditions, determine the
       maximum possible spacing between pumping stations.

20.8   Blood is a very interesting fluid: a suspension of red and white blood cells and
       platelets in a liquid plasma. We would like to be as optimistic as Jean Poiseuille in
       modeling blood flow, but we know that these cells in the plasma can cause blood's
       viscosity to be dependent on the shear rate, that is, blood's composition can cause
       it to behave like a *non-Newtonian* fluid. Especially in regions of very low shear rate,
       blood's red blood cells have been shown to aggregate and form clumps that cause
       blood to require a certain yield stress to be applied before it flows smoothly again.
           You are given the following data for an "average" person. This person's cardiac
       output is 5 l/min; heart rate is 60 bpm; and at a hematocrit of 40%, blood density
       is $1.06\,\mathrm{g/cm^3}$, and blood viscosity is 3.5 centiPoise (named for Jean Poiseuille, and
       abbreviated cP; 1 cP = 1 mPa s). Also:

	Internal Diameter (mm)	Wall Thickness (mm)	Percentage of Heart Q	Typical Pressures (mm Hg)
Ascending aorta	20	2	100	100
Abdominal aorta	12	1.5	50	90
Femoral artery	8	0.8	10	80
Random arteriole	0.1	0.02	0.001	60

Note that the vessels downstream from the heart receive only a portion of its volumetric output, due to branching of vessels. The percentages given here are ballpark estimates.

Based on these parameters, calculate the following in each of the measured vessels:

a. Pressure drop

b. Mean velocity

c. Shear rate at vessel wall

d. Reynolds number

e. Percent cross-sectional area change due to pulse pressure, assuming small strain $\varepsilon_{\theta\theta} = \sigma_{\theta\theta}/E$

20.9 Based on the values you calculated in Problem 20.8, answer and explain the following:

a. In which vessels should elasticity of the vessel be considered?

b. In which vessels should the non-Newtonian behavior of blood be considered?

c. Where in the body might turbulence develop?

d. Why does most of the pressure drop in the arterial system occur in the arterioles?

20.10 Wind tunnel testing of the concrete reef balls used in artificial reefs is proposed. A typical reef ball (e.g. Figure 1.2) has a diameter of 6 ft, and is immersed in sea water. A scale model is prepared with diameter of 6 in.

a. At what range of velocities should wind tunnel tests be performed to ensure that the experimental data are relevant to the real reef balls?

b. What effect do you believe that the holes in the reef ball will have on the flow, if any?

20.11 The pressure drop through an oil pipeline is to be modeled by using the flow of water through an identical length of tubing. The required oil velocity in the prototype pipeline is known to be 35 cm/s. In order for the experimental model to be relevant and yield transferable results, the Re and the Eu of the model must match those of the pipeline.

a. Use the Reynolds number to determine the required velocity of the model fluid.

b. Use the Euler number to predict the pressure drop in the model, if the pressure drop measured in the prototype pipeline was 0.05 psi.

20.12 A streamlined support strut has thickness $t = 1$ in and drag coefficient $C_D = 0.02$. Calculate the drag force per unit length of the strut if it is moving at $V = 10$ mph in water. Compare this result to the force per unit length of a 1 in diameter circular strut.

20.13 Could you reduce friction in a pipe by coating the pipe wall with Teflon? Why or why not?

20.14 The flow of water in a 4 mm diameter pipe must remain laminar. Plot a graph of the maximum allowable flowrate as a function of temperature for $0 < T < 100°C$.

20.15 For fully developed laminar pipe flow in a circular pipe, the velocity profile is given by $u(r) = 2(1 - r^2/R^2)$ in m/s, where R is the inner radius of the pipe. If the pipe's inner diameter is 4 cm, find the maximum and average velocities in the pipe as well as the volume flow rate.

21

Case Study 10: Living with Water, and the Role of Technological Culture

Recent American history includes severe flooding in two major metropolitan areas: in New Orleans, due to Hurricane Katrina in 2005, and in the greater New York area, due to 2012's Hurricane Sandy. In both regions, the floods caused devastating damage and triggered calls for increased protections for citizens living in at-risk regions.

The levees in place in New Orleans were breached by Katrina's unusually high surge. In fact, the levees on the lower Mississippi River actually funneled more water upstream, enhancing the surge size and exacerbating damage. Levees (also known as dikes) are built along rivers and low-lying coastlines and are intended to help prevent flooding by containing rising waters. However, by confining water they also result in higher and faster flow. The levee system along the Mississippi River now comprises over 5600 km (2500 miles) of levees.

Levees may fail due to gradual erosion or sudden rupture, allowing water to flood the surrounding land. When the water level is higher than the levee, sometimes referred to as "overtopping," this will also cause flooding, but is less disastrous as it generally does not damage the levee itself.

Some were shocked that the New Orleans region incurred such damage after Hurricane Katrina, despite the levee system. By comparison, it was noted that in the Netherlands, large parts of the country exist below sea level. Dutch coastal engineers have accomplished many technological feats, largely in response to their country's own devastating flood, the 1953 storm surge known as *De Ramp*, or "The Disaster." The immediate response of coastal engineers was to implement the *Deltaplan*, which involved closing two rivers' tidal outlets, and subsequently building a storm gate for a third river that does not impede shipping or induce environmental hazards: this gate, the Maeslantkering, is typically left open, but slides closed when a surge is predicted (Figure 21.1). The complete system of dikes or levees, dams, sluices, and locks built is known as the Delta Works.

In the United States, the primary response to a series of powerful hurricanes in the 1950s was to develop warning systems and protective measures, including surge prediction models. As Bijker (2007) notes, the differences among these models and their predictions result from the different needs of the modelers: protection (USACE), warning (Weather Service), or insurance (FEMA).

The risk criteria used in both countries are significantly different. The United States emphasizes "flood hazard mitigation," accepting that major storms will occur and endeavoring to predict them accurately enough to minimize loss of life and property, and designs levees and other coastal defenses to the technical norm of the "hundred year flood," or a 1:100 chance. In the Netherlands, the criterion of 1:10,000 was specified for the *Deltaplan* and for levees in central Holland. Rather than mitigating the hazards of the inevitable 1:100, the Dutch Deltaplan aspired to simply keeping the water out.

It is interesting to note that the technological cultures of these two countries are distinct, with differences in the overall geography, political landscape, and the general public's
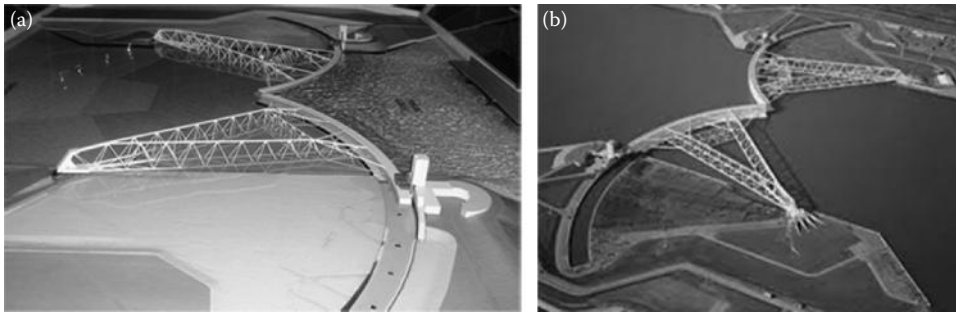
FIGURE 21.1
The Maeslantkering storm surge gate closes when a sea level rise of 3 m is predicted. (a) An engineering model; (b) the constructed gate in place. (Images courtesy of the Rijkswaterstaat Ministry of Infrastructure and the Environment.)

technical literacy. For example, the Netherlands is almost entirely lowlands, with no mountains, deserts, or great plains. The lack of diversity in the geography means that almost everyone in the Netherlands is at risk of flooding[*]; this contrasts with an American tendency to disdain those "foolish" enough to live in a region at greater risk of whatever natural disaster has just occurred. This shared geography and risk in the Netherlands is compounded by the nation's politics, which emphasize a central government role in healthcare, education, infrastructure, and coastal defense; while in America, without a shared sense of common good as something government should define and protect, we are more likely to privatize and individualize such functions (Mukherji, 2007). And as fiction writer Jim Shepard puts the Dutch perspective in his 2011 short story "The Netherlands Lives with Water," "Either we pulled together as a collective or got swept away as individuals."

Neither approach is infallible, of course. Each country's coastal engineers could certainly learn things of value from the other's and thus strengthen both defenses. Recently, the Dutch government relocated several farmers to create river spillways, as if to acknowledge that sea barriers are insufficient (in the face of rising seas and rivers) as well as ecologically suboptimal. Rather than fighting nature, the new Dutch approach combines gates and dikes with spillways to accommodate nature. A new $3 billion dollar water management project, Room for the River, consists of nearly 40 interlinked infrastructure projects throughout the Netherlands. In Rotterdam, a floating pavilion has been constructed as a model of sustainable (the structures are solar powered) adaptation. The Dutch have created an approach that splits the difference between the American fixation on evacuation and the prior Dutch focus on prevention. The middle way is to focus on: "what to do with the water once it's there."

The devastation in the New Orleans delta region, and in New York and New Jersey, is not an example of technology's failing the culture; in many ways, it represents the culture having failed the technology. Bijker (2007) concludes that "changing a water management

---

[*] Many of us remember the childhood story *Hans Brinker, or the Silver Skates*, in which its American author Mary Mapes Dodge relates the "Dutch folk tale" of a nameless hero who saved a city by plugging a leaky dike (levee) with his finger. This tale appears to have been invented by Dodge and has been refuted by many Dutch scholars as improbable—Dutch culture, they insist, would not have created a singular hero in this way, but would have been more likely to honor a communal effort. See Russell Shorto's *Amsterdam* for a more thoughtful analysis than is permitted here.

style also calls for changing the relevant political culture, and . . .for a much more active engagement of civil society."

New York governor Andrew Cuomo seemed to recognize this when he engaged a Dutch firm to reshape Governors Island in New York City using many of the techniques employed in the Room for the River projects. New York is now pursuing both a Dutch-designed barrier as well as relatively inexpensive measures such as restoring wetlands and planting oyster beds. While the technology is readily transferrable and effectively balances proven techniques of both prevention and accommodation, Cuomo and other politicians must work hard to provide affected residents with adequate knowledge and agency.

Engineers must balance the needs of a range of stakeholders when proposing flood prevention and protection techniques and must communicate clearly with the governments and the public we work with and for. When possible, we should also influence the technological culture in which we operate, to ensure that citizens understand the value of social, as well as technical, infrastructure in community resilience. Our most effective and sustainable products will both mitigate the damage of disasters *and* strengthen our communities' social networks and sense of shared responsibility.

References

Bijker, W. E. 2007. American and Dutch Coastal Engineering: Differences in Risk Conception and Differences in Technological Culture, *Social Studies of Science* **37**(1): 143–151.

Kerr, P. C. et al., 2013. Surge Generation Mechanisms in the Lower Mississippi River and Discharge Dependency. *Journal of Waterway, Port, Coastal, and Ocean Engineering* **139**(4): 326–335.

Kimmelman, M. 2013 Going with the Flow, *New York Times*, February 17, 2013.

Kleinenberg, E. 2013 Adaptation, *The New Yorker*, January 7, 2013.

Mukherji, C. 2007. "Levees, Seawalls, and State Building in 17th Century France: Stewardship Politics and the Control of Wild Weather," *Social Studies of Science* **37**(1): 127–133.

Shepard, J. 2011. *You Think That's Bad*, Knopf.

Shorto, R. 2013. *Amsterdam: A History of the World's Most Liberal City*, Doubleday.

22

Solid Dynamics: Governing Equations

In Chapters 1 to 11, we considered the equilibrium of solids. By examining the isolated effects of various types of loading, and then the methods of combining these effects in more realistic situations, we have come to understand many problems for which $\sum \mathbf{F} = \mathbf{0}$. However, although external forces often balance each other, causing a solid to be in equilibrium, it is also possible for unbalanced external forces to result in the solid's *motion*. In Chapters 13 to 20, we have developed our understanding of the forces on fluids, as well. Because both solids and fluids can be treated as continua, and because they are governed by mass conservation and Newton's second law, we expect their equations of motion to markedly resemble each other. In this chapter, we will briefly consider the governing equations for the motion of solids, and some examples of their solution.

The key concepts in the dynamics of deformable solids are continuity, compatibility, and the relevant constitutive law. In the problems we have considered thus far, we have rarely had to check these conditions (and the constitutive law, either Hooke's or Newton's, has most often been a straightforward one); we have been able to implicitly assume they were met. However, as our study of mechanics continues, we will encounter more general, less constrained problems. In this section, we will discuss the "next level" of continuum mechanics in the context of these three C's. We will begin by briefly defining each of them. As you may recall from Chapters 2 and 4,

Continuity signifies that density is a definable, continuous function

Compatibility implies that all displacements (u, v, w) must be continuous

A *Constitutive law* relates deformation (strain) to loading (stress)

22.1 Continuity, or Mass Conservation

If a material is a "continuum," we are able to ignore the fundamentally discrete composition of matter—all those atoms dancing about—and to assume that the substance of material bodies is continuously distributed. As has been discussed in Section 1.4, this is possible when the behavior of interest is on a much larger scale than that of molecular interactions: lengths much larger than atomic mean free paths; and time scales much larger than characteristic times of atomic bond vibration. This continuum model allows us to divide matter into smaller and smaller portions, each of which has the physical properties of the original body. So, we can assign quantities such as density and velocity to each point of the space occupied by the body.*

---

* This is the starting-off point for George Mase's *Continuum Mechanics for Engineers*, an excellent transitional text to move from the mechanics analyses of this textbook to the level of graduate continuum mechanics.

Recall that for a continuum we are able to mathematically define a mass density:

$$\rho = \lim_{\Delta V \to 0} \frac{\Delta m}{\Delta V}, \tag{22.1}$$

and that this density, like other properties of the continuum, is a continuous function of position and time: $\rho = \rho(\mathbf{x}, t)$. We can thus describe the mass of an entire body (of total volume V) by

$$m = \int_V \rho(\mathbf{x}, t) \mathrm{d}V. \tag{22.2}$$

Since mass is neither created nor destroyed, we require that the mass of the body remains invariant under motion. Its total derivative must be zero:

$$\dot{m} = \frac{\mathrm{d}}{\mathrm{d}t} \int_V \rho(\mathbf{x}, t) \mathrm{d}V = \int_V \left(\frac{\partial \rho}{\partial t} + v_i \frac{\partial \rho}{\partial x_i} + \rho \frac{\partial v_i}{\partial x_i} \right) \mathrm{d}V = 0, \tag{22.3}$$

where we have, in a sense, used the chain rule to construct a "total" or "material derivative" of the fluid mass $\rho(\mathbf{x}, t) V$. Note that v_i is the ith component of the vector velocity field $\mathbf{V}$. Previously, we have used u_i to indicate displacements for solids and velocities for fluids, but this is the first time we have written velocities for solids.

Since the above expression must hold for any $\mathrm{d}V$ of the body, we must have

$$\frac{\partial \rho}{\partial t} + v_i \frac{\partial \rho}{\partial x_i} + \rho \frac{\partial v_i}{\partial x_i} = 0, \tag{22.4}$$

or

$$\frac{\partial \rho}{\partial t} + \frac{\partial}{\partial x_i}(\rho v_i) = 0, \tag{22.5}$$

where the repeated i index, we remember from Chapter 1, represents a summation over i. In vector notation, we could write the conservation of mass as

$$\frac{\partial \rho}{\partial t} + \nabla \cdot (\rho \mathbf{V}) = 0. \tag{22.6}$$

We note that if the density is constant in $\mathbf{x}$ and t, the material is said to be *incompressible*, and in this case our continuity equation requires that

$$\frac{\partial}{\partial x_i} v_i = 0 \quad \text{or} \quad \nabla \cdot \mathbf{V} = 0, \tag{22.7}$$

for incompressible continua. Equations 22.6 and 22.7 are exactly how we have written mass conservation for a fluid in Section 18.4.1.

22.2 Newton's Second Law, or Momentum Conservation

Newton's second law of motion states that $\mathbf{F} = m\mathbf{a}$: the resultant force on an object balances this object's inertia—its mass times its acceleration. An object's mass times acceleration can also be viewed as the time rate of change of that object's linear momentum. We already understand how to state the resultant force on a body: so far we have been writing $\sum \mathbf{F} = \mathbf{0}$ for a variety of systems. The stress tensor for a given body reflects its response to all external loads and so by writing the stress tensor we have effectively written the resultant surface force on the body. We may also consider the effects of a "body force" such as gravity or the force due to an electromagnetic field; we will use $\mathbf{B}$ to represent such forces per unit volume, just as we did in Section 2.5. A sample tuberous body with resultant surface and body forces is shown in Figure 22.1.

Hence we understand that the ith component of the total resultant force $\mathbf{F}$ on a body is written

$$F_i = \int_V \rho B_i \, dV + \int_S \sigma_{ij} n_j \, dS, \tag{22.8}$$

All that remains is then to write the change in momentum for the same body, or $m\mathbf{a}$. Again, we will write only the ith component of the body's acceleration:

$$\int_V \rho \frac{dv_i}{dt} dV, \tag{22.9}$$

where we have taken the total derivative of the momentum per volume, $(\rho \mathbf{V})$, and then used the conservation of mass to eliminate the derivatives of density. $\mathbf{F} = m\mathbf{a}$ is then simply the balance of the resultant force and the inertia:

$$\int_V \rho B_i \, dV + \int_S \sigma_{ij} n_j \, dS = \int_V \rho \frac{dv_i}{dt} dV. \tag{22.10}$$
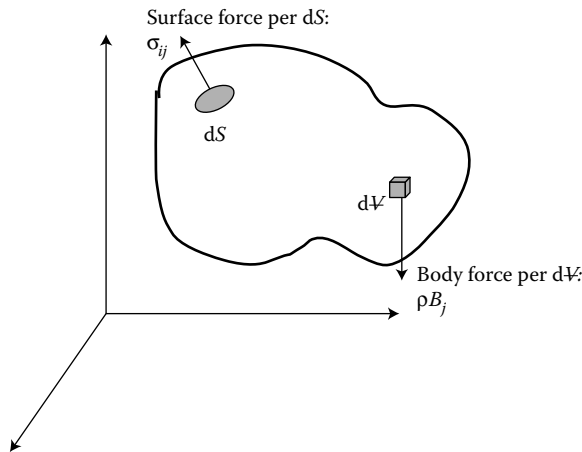
FIGURE 22.1
Forces on a body.

It only remains for us to convert the surface area integral to a volume integral, which we may do by Gauss' theorem, and obtain

$$\int_V \rho B_i \, dV + \int_V \frac{\partial}{\partial x_j} \sigma_{ij} \, dV = \int_V \rho \frac{dv_i}{dt} dV. \tag{22.11}$$

As this must be true for any volume, we truly have

$$\rho B_i + \frac{\partial}{\partial x_j} \sigma_{ij} = \rho \frac{dv_i}{dt}. \tag{22.12}$$

Or, in vector form,

$$\nabla \sigma + \rho \mathbf{B} = \rho \frac{d\mathbf{V}}{dt}. \tag{22.13}$$

For solids in equilibrium, as we have already seen, the resultant forces sum to zero. The x component of the governing equation for such a solid would be

$$\frac{\partial \sigma_{xx}}{\partial x} + \frac{\partial \sigma_{xy}}{\partial y} + \frac{\partial \sigma_{xz}}{\partial z} + \rho B_x = 0. \tag{22.14}$$

Equation 22.13, as expected, looks strikingly like the Navier–Stokes equation developed for fluids in Section 18.4.2. Here, the viscous force and the pressure force (previously known as F_{visc}, or $\mu \nabla^2 \mathbf{V}$, and $-\nabla p \, dV$, respectively) have been combined, as the pressure (a.k.a. normal stress) and viscous stresses are combined into one stress tensor σ. But the form of $\sum \mathbf{F} = m\mathbf{a}$ looks awfully familiar.

22.3 Constitutive Laws: Elasticity

The behavior of the material in question provides us with our third governing equation. We can then analyze solids in motion by solving these three equations. If a material behaves "elastically," this means two things to us: (1) the stress is a unique function of the strain and (2) the material is able to fully recover to its "natural" shape after the removal of applied loads. Although elastic behavior can be either linear or nonlinear, in this textbook we are concerned primarily with *linearly elastic* materials to which Hooke's law applies. The constitutive law for linearly elastic behavior is simply

$$\sigma_{ij} = C_{ijkm}\varepsilon_{km} \quad \text{or} \quad \sigma = \mathbf{C}\varepsilon, \tag{22.15}$$

where, as we discussed in Section 4.4, $\mathbf{C}$ is a fourth-order tensor whose 81 components reduce to 36 unique components due to the symmetry of both the stress and strain tensors.

For isotropic materials, we are able to find the exact form of $\mathbf{C}$. If the material is isotropic, then its elastic tensor $\mathbf{C}$ must be a fourth-order, isotropic tensor. An isotropic tensor is one whose components are unchanged by any orthogonal transformation from one set of Cartesian axes to another. This requirement guides the form that $\mathbf{C}$ must take

$$C_{ijkm} = \lambda \delta_{ij}\delta_{km} + \mu(\delta_{ik}\delta_{jm} + \delta_{im}\delta_{jk}) + \beta(\delta_{ik}\delta_{jm} - \delta_{im}\delta_{jk}), \tag{22.16}$$

where λ, μ, and β are scalars. We remind ourselves that the Kronecker deltas are simple second-order identity tensors ($\delta_{ij} = 1$ if $i = j$, but $\delta_{ij} = 0$ if $i \neq j$). Due to the symmetry of both the stress and strain tensors, we must have $C_{ijkm} = C_{jikm} = C_{ijmk}$. This requires that $\beta = -\beta$, and thus that $\beta = 0$. Hooke's law—here's the important part—then takes the form

$$\sigma_{ij} = [\lambda \delta_{ij} \delta_{km} + \mu(\delta_{ik} \delta_{jm} + \delta_{im} \delta_{jk})]\varepsilon_{km}, \tag{22.17}$$

or, using the Kronecker delta's substitution property,

$$\sigma_{ij} = \lambda \delta_{ij} \varepsilon_{kk} + 2\mu \varepsilon_{ij}. \tag{22.18}$$

This is Hooke's law for isotropic elastic behavior. If we rearrange this to make it an expression for strain ε_{ij}, we can obtain the following relations for Young's modulus and the Poisson's ratio (the shear modulus $G = \mu$) and finally the generalized form of Hooke's law, for linearly elastic materials:

$$E = \frac{\mu(3\lambda + 2\mu)}{\lambda + \mu},$$

$$\nu = \frac{\lambda}{2(\lambda + \mu)}, \tag{22.19}$$

$$\varepsilon_{ij} = \frac{1}{E}\big[(1 + \nu)\sigma_{ij} - \nu \delta_{ij} \sigma_{kk}\big]. \tag{22.20}$$

As long as the material in question does not split apart or overlap itself, its displacements must be continuous. This compatibility requirement is guaranteed by a displacement field that is single-valued and continuous, with continuous derivatives. The strain tensor is composed of the derivatives of the displacement field, as we have seen. So in two dimensions, we may write the compatibility condition in the form:

$$\frac{\partial^2 \varepsilon_{xx}}{\partial y^2} + \frac{\partial^2 \varepsilon_{yy}}{\partial x^2} = \frac{\partial^2 \gamma_{xy}}{\partial x \partial y}. \tag{22.21}$$

Alas, in three dimensions we have six unique strain components to keep track of, and there are five additional compatibility conditions.

Using these governing equations, it is possible to fully describe the equilibrium or motion of a continuum. Often, a constitutive law will be experimentally obtained for a given material, and it is the job of the continuum mechanician to express the governing equations appropriately and solve them. In most cases, it is not possible to obtain analytical solutions of these equations; generally, it is necessary to solve them numerically.

By integrating the differential equations of equilibrium, we will obtain results that agree with our simpler calculations, since our new partial differential equations are simply saying what we have said all along: for a body in equilibrium, the sum of the forces acting on the body is zero. This is the same statement whether we say it by means of a FBD and average stresses, or whether we solve complex partial differential equations.

In general, "continuum mechanics" is a field that emphasizes generality and abstraction, but is based on physical material behavior. The tensor mathematics introduced in this book support the general applicability of continuum mechanics, and they complement the more concrete diagrams and physical intuition of an engineer.

References

Adair, R.K., *The Physics of Baseball*, Harper Perennial, 1994.

Anderson, J.D., *A History of Aerodynamics*, Cambridge, MA: Cambridge University Press, 1997.

Aris, R., *Vectors, Tensors, and the Basic Equations of Fluid Mechanics*, Dover, 1962.

Bassman, L. and Swannell, P., *Engineering Statics Study Book*, University of Southern Queensland, 1994.

Bedford, A. and Liechti, K.M., *Mechanics of Materials*, Prentice Hall, 2000.

Beer, F.P. and Johnston, E.R., *Mechanics of Materials*, McGraw Hill, 2nd Edition, 1992.

Chadwick, P., *Continuum Mechanics*, Dover, 1976.

Cook, R.D. and Young, W.C. *Advanced Mechanics of Materials*, Prentice Hall, 2nd Edition, 1999.

Crowe, M.J., *A History of Vector Calculus*, Mineola, NY: Dover, 1967.

Dym, C.L., Little, P., and Orwin, E., *Engineering Design: A Project-Based Introduction*, 3rd Edition, New York: Wiley and Sons, 2014.

Enderle, J.D., Blanchard, S.M., and Bronzino, J.D., *Introduction to Biomedical Engineering*, San Diego, CA: Academic Press, 2000.

Fung, Y.C., *Biomechanics*, Springer, 1998.

Fung, Y.C., *A First Course in Continuum Mechanics,* Prentice Hall, 1994.

Gere, J.M. and Timoshenko, S.P., *Mechanics of Materials*, PWS Publishing, 4th Edition, 1997.

Gordon, J.E., *The New Science of Strong Materials, or Why You Don't Fall through the Floor*, Princeton, NJ: Princeton University Press, 1988.

Gordon, J.E., *Structures: Why Things Don't Fall Down*, DaCapo, 2003.

Humphrey, J.D. and Delange, S.L., *Biomechanics*, New York: Springer, 2003.

Isenberg, C., *The Science of Soap Films and Soap Bubbles*, Dover, 1992.

Jacobsen, L.S., *Trans. ASME*, 47: 619–638, 1925.

Kuethe, A.M. and Chow, C-Y., *Foundations of Aerodynamics*, Wiley, 4th Edition, 1986.

Kundu, P.K., *Fluid Mechanics*, Academic Press, 1990.

Levy, M. and Salvadori, M., *Why Buildings Fall Down: How Structures Fail*, W.W. Norton, 1994.

Malvern, L.E. *Introduction to the Mechanics of a Continuous Medium*, Prentice Hall, 1969.

Mase, G.T. and Mase, G.E., *Continuum Mechanics for Engineers*, CRC Press, 2nd Edition, 1999.

Munson, B.R., Young, D.F., and Okiiski, T.H., *Fundamentals of Fluid Mechanics*, Wiley, 3rd Edition, 1998.

Petroski, H., *To Engineer Is Human*, New York: St. Martin's Press, 1982.

Popov, E.P., *Engineering Mechanics of Solids*, Prentice Hall, 2nd Edition, 1998.

Potter, M.C. and Wiggert, D.C., *Mechanics of Fluids*, Prentice Hall, 2nd Edition, 1997.

Reiner, M., *Deformation, Strain, and Flow: An Elementary Introduction to Rheology*, New York: Interscience, 1960.

Sabersky, R.H., Acosta, A.J., Hauptmann, E.G., and Gates, E.M., *Fluid Flow*, Prentice Hall, 4th Edition, 1999.

Schey, H.M., *Div, Grad, Curl, and All That*, W.W. Norton, 1973.

Smits, A.J., *A Physical Introduction to Fluid Mechanics*, Wiley, 2000.

Spiegel, L. and Limbrunner, G.F., *Applied Statics and Strength of Materials*, 3rd Edition, 1999.

Van Dyke, M., *An Album of Fluid Motion*, Parabolic Press, Stanford, 1982.

Vogel, S., *Comparative Biomechanics: Life's Physical World*, Princeton, NJ: Princeton Universtity Press, 2003.

Wylie, C.R. and Barrett, L.C., *Advanced Engineering Mathematics*, New York: Mc-Graw-Hill, 1982.

Additional references are cited in Case Studies and footnotes.

Appendix A: Second Moments of Area

The second moment of area I, sometimes less accurately called the area moment of inertia, is a property of a shape that describes its resistance to deformation by bending. The polar second moment of area J, often called the polar moment of inertia, describes the resistance of a shape to deformation by torsion. Since the coordinate axes used to obtain the I's and J's listed here run through the centroid of each shape, all second moments of area cited here may be thought of as having an additional subscript "c" denoting that they are taken relative to the centroid. Centroid positions are indicated on the figures.
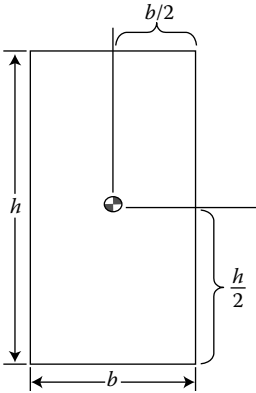
Remember,

$$I_y = \int z^2 \, dA,$$

$$I_z = \int y^2 \, dA,$$

$$J = \int r^2 \, dA.$$

Note that $I_y + I_z = J$. Here, the axes originate at the area's centroid, with y horizontal and positive right and z vertical and positive up.

	Area (A)	Second Moment of Area (I)	Polar Second Moment of Area (J)
	bh	$I_y = bh^3/12$ $I_z = hb^3/12$	$(bh/12)(h^2 + b^2)$

	Area (A)	Second Moment of Area (I)	Polar Second Moment of Area (J)
	$bh/2$	$I_y = bh^3/36$ $I_z = (hb^3 - b^2hd + bhd^2)/36$	$I_y + I_z$
	πr^2	$I_y = I_z = \pi r^4/4$	$J = \pi r^4/2$
	$\pi(r_o^2 - r_i^2)$	$I_y = I_z = \pi(r_o^4 - r_i^4)/4$	$J = \pi(r_o^4 - r_i^4)/2$
	$\pi r^2/2$	$I_y = (\pi/8 - 8/9\pi)r^4$ $I_z = \pi r^4/8$	$J_c = (\pi/4 - 8/9\pi)r^4$
	$\pi r^2/4$	$I_y = I_z = (\pi/16 - 4/9\pi)r^4$	$J_c = (\pi/8 - 8/9\pi)r^4$

The geometrical properties of some standard beam cross sections may be found in published tables. For example, in contemporary practice, steel I-beams are described by a standard terminology that encodes information about their dimensions, generally expressed as

$$W \text{ or } S \text{ depth (inches)} \times \text{weight per unit length (pound force per foot)},$$

where "W" or "S" is used depending on whether the flanges are rectangular or tapered, and "depth" is the total height (in the z-direction) of the beam's cross section. The dimensions of the flanges and extent of the cross section in the y-direction are incorporated into the weight per unit length, assuming structural steel's nominal density.

Appendix B: A Quick Look at the del Operator

We use the *del operator* to take the gradient of a scalar function, say $f(x, y, z)$:

$$\nabla f = \hat{\mathbf{i}}\frac{\partial f}{\partial x} + \hat{\mathbf{j}}\frac{\partial f}{\partial y} + \hat{\mathbf{k}}\frac{\partial f}{\partial z}.$$

If we "factor out" the function f, the gradient of f looks like

$$\nabla f = \left(\hat{\mathbf{i}}\frac{\partial}{\partial x} + \hat{\mathbf{j}}\frac{\partial}{\partial y} + \hat{\mathbf{k}}\frac{\partial}{\partial z}\right) f.$$

The term in parentheses is called *del* and is written as

$$\nabla = \hat{\mathbf{i}}\frac{\partial}{\partial x} + \hat{\mathbf{j}}\frac{\partial}{\partial y} + \hat{\mathbf{k}}\frac{\partial}{\partial z}.$$

By itself, ∇ has no meaning. It is meaningful only when it acts on a scalar function. ∇ *operates* on a scalar function by taking partial derivatives and combining them into the gradient. In indicial or index notation, we can write ∇_i to mean "take the partial derivative of what follows with respect to the i direction." We say that ∇ is a vector operator acting on scalar functions, and we call it the *del operator*.

Since ∇ resembles a vector, we will consider all the ways that we can act on vectors and see how the del operator acts in each case.

Vectors		**Del**	
Operation	*Result*	*Operation*	*Result*
Multiply by a scalar a	$\mathbf{A}a$	Operate on a scalar f	∇f
Dot product with another vector $\mathbf{B}$	$\mathbf{A} \cdot \mathbf{B}$	Dot product with a vector $\mathbf{F}(x, y, z)$	$\nabla \cdot \mathbf{F}$
Cross product with another vector $\mathbf{B}$	$\mathbf{A} \times \mathbf{B}$	Cross product with a vector $\mathbf{F}(x, y, z)$	$\nabla \times \mathbf{F}$

B.1 Divergence

Let us first compute the form of the divergence in regular Cartesian coordinates. If we let a random vector $\mathbf{F} = F_x\hat{\mathbf{i}} + F_y\hat{\mathbf{j}} + F_z\hat{\mathbf{k}}$, then

$$\text{div}\,\mathbf{F} = \nabla \cdot \mathbf{F} = \left(\hat{\mathbf{i}}\frac{\partial}{\partial x} + \hat{\mathbf{j}}\frac{\partial}{\partial y} + \hat{\mathbf{k}}\frac{\partial}{\partial z}\right) \cdot \left(F_x\hat{\mathbf{i}} + F_y\hat{\mathbf{j}} + F_z\hat{\mathbf{k}}\right) = \frac{\partial F_x}{\partial x} + \frac{\partial F_y}{\partial y} + \frac{\partial F_z}{\partial z}.$$

In inidicial notation, this is: $\text{div}\,\mathbf{F} = \nabla_i F_i = F_{i,i}.$

Like any dot product, the divergence is a scalar quantity. Also note that, in general, div **F** is a function and will change in value from point to point.

B.2 Physical Interpretation of the Divergence

The divergence quantifies how much a vector field "spreads out," or diverges, from a given point P. For example, in Figure B.1 the figure on the left has positive divergence at P, since the vectors of the vector field are all spreading as they move away from P. The figure in the center has zero divergence everywhere since the vectors are not spreading out at all. This is also easy to compute, since the vector field is constant everywhere and the derivative of a constant is zero. The field on the right has negative divergence since the vectors are coming closer together instead of spreading out.

In the context of continuum mechanics, the divergence has a particularly interesting meaning. For solids, if the vector field of interest is the displacement vector **U**, the divergence of this vector tells us about the overall *change in volume* of the solid. See Equation 4.5 and Problem 4.1. When we have $\nabla \cdot \mathbf{U} = 0$ we know that the volume of a given solid body remains constant, and we can call the solid "incompressible." For fluids, we use the velocity vector **V** to talk about the deformation kinematics. The divergence of the velocity vector tells us about the volumetric strain rate, and when we have $\nabla \cdot \mathbf{V} = 0$ we say that the flow is incompressible. This, generally, allows us to neglect changes in fluid density and say that density remains constant. See Equation 13.9.

EXAMPLE B.1

Calculate the divergence of $\mathbf{F} = x\hat{\mathbf{i}} + y\hat{\mathbf{j}} + z\hat{\mathbf{k}}$.

$$\nabla \cdot \mathbf{F} = \frac{\partial}{\partial x}(x) + \frac{\partial}{\partial y}(y) + \frac{\partial}{\partial z}(z) = 1 + 1 + 1 = 3.$$

This is the vector field shown on the left in Figure B.1. Its divergence is constant everywhere.
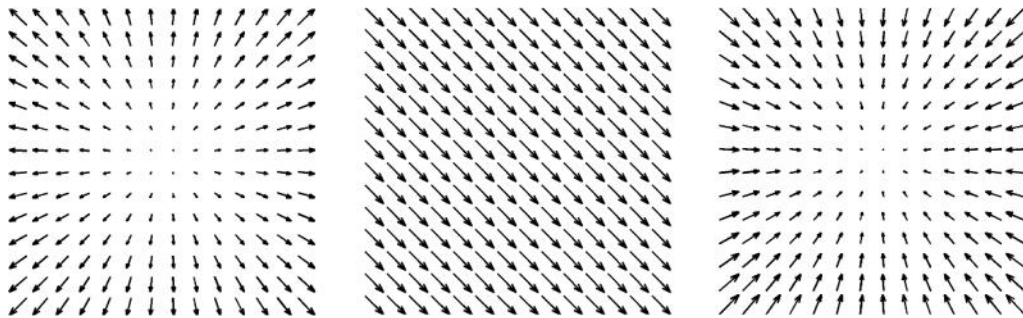
FIGURE B.1
Three vector fields.

B.3 Curl

We can also compute the curl in Cartesian coordinates. Again, let $\mathbf{F} = F_x\hat{\mathbf{i}} + F_y\hat{\mathbf{j}} + F_z\hat{\mathbf{k}}$, and calculate

$$\text{curl } \mathbf{F} = \nabla \times \mathbf{F} = \begin{vmatrix} \hat{\mathbf{i}} & \hat{\mathbf{j}} & \hat{\mathbf{k}} \\ \dfrac{\partial}{\partial x} & \dfrac{\partial}{\partial y} & \dfrac{\partial}{\partial z} \\ F_x & F_y & F_z \end{vmatrix} = \hat{\mathbf{i}}\left(\dfrac{\partial F_z}{\partial y} - \dfrac{\partial F_y}{\partial z}\right) + \hat{\mathbf{j}}\left(\dfrac{\partial F_x}{\partial z} - \dfrac{\partial F_z}{\partial x}\right) + \hat{\mathbf{k}}\left(\dfrac{\partial F_y}{\partial x} - \dfrac{\partial F_x}{\partial y}\right).$$

Not surprisingly, the curl is a vector quantity. In inidicial notation, it can be written as $\text{curl } F = \varepsilon_{ijk}\nabla_j F_k.$*

B.4 Physical Interpretation of the Curl

The curl of a vector field measures the tendency of the vector field to swirl. Consider the illustrations below. The field on the left, called $\mathbf{F}$, has curl with positive $\hat{\mathbf{k}}$-component. To see this, use the right-hand rule. Place your right hand at P. Point your fingers toward the tail of one of the vectors of $\mathbf{F}$. Now curl your fingers around in the direction of the tip of the vector. Stick your thumb out. Since it points toward the $+z$ axis (out of the page), the curl has a positive $\hat{\mathbf{k}}$-component.

The second vector field $\mathbf{G}$ has no visible swirling tendency at all, so we would expect $\nabla \times \mathbf{G} = \mathbf{0}$. The third vector field does not look like it swirls either, so it also has zero curl.

> **EXAMPLE B.2**
>
> Compute the curl of $\mathbf{F} = -y\hat{\mathbf{i}} + x\hat{\mathbf{j}}$.
>
> $$\nabla \times \mathbf{F} = \begin{vmatrix} \hat{\mathbf{i}} & \hat{\mathbf{j}} & \hat{\mathbf{k}} \\ \dfrac{\partial}{\partial x} & \dfrac{\partial}{\partial y} & \dfrac{\partial}{\partial z} \\ -y & x & 0 \end{vmatrix} = 2\hat{\mathbf{k}}.$$
>
> This is the vector field on the left in Figure B.1. As you can see, the analytical approach demonstrates that the curl is in the positive $\hat{\mathbf{k}}$-direction, as expected.
>
> **EXAMPLE B.3**
>
> Compute the curl of $\mathbf{H} = x\hat{\mathbf{i}} + y\hat{\mathbf{j}} + z\hat{\mathbf{k}}$, or $\mathbf{H}(\mathbf{r}) = \mathbf{r}$.
>
> $$\nabla \times \mathbf{H} = \begin{vmatrix} \hat{\mathbf{i}} & \hat{\mathbf{j}} & \hat{\mathbf{k}} \\ \dfrac{\partial}{\partial x} & \dfrac{\partial}{\partial y} & \dfrac{\partial}{\partial z} \\ x & y & z \end{vmatrix} = \mathbf{0}.$$
>
> This, as you have probably guessed, is the vector field on the far right in Figure B.1.

---

* This equation in index notation includes the Levi–Civita symbol, ε_{ink}. This is not strain, but a mathematical symbol that indicates a $3 \times 3 \times 3$ array of permutations of 0, $+1$, and -1.

B.5 Laplacian

The divergence of the gradient appears so often that it has been given a special name: the Laplacian. It is written as ∇^2 or Δ and, in Cartesian components, has the form

$$\nabla^2 f = \frac{\partial^2 f}{\partial x^2} + \frac{\partial^2 f}{\partial y^2} + \frac{\partial^2 f}{\partial z^2}.$$

It operates on scalar functions and produces a scalar result. When we take the Laplacian of a vector field, $\mathbf{F} = F_x \hat{\mathbf{i}} + F_y \hat{\mathbf{j}} + F_z \hat{\mathbf{k}}$, we obtain

$$\nabla^2 \mathbf{F} = (\nabla^2 F_x)\hat{\mathbf{i}} + (\nabla^2 F_y)\hat{\mathbf{j}} + (\nabla^2 F_z)\hat{\mathbf{k}}.$$

Suggested Reading

Crowe, M. J., *A History of Vector Calculus*. Dover, 1967.
Schey, H. M., *Div, Grad, Curl, and All That*. W. W. Norton, 1973.
Wylie, C. R. and Barrett, L. C., *Advanced Engineering Mathematics*. McGraw-Hill, 1982.

Appendix C: Property Tables

This appendix contains tabulated values for the properties of engineering materials (Tables C.1 and C.2) and fluids (Tables C.3 and C.4). Exact values of these properties vary widely with changes in composition, heat treatment, and mechanical working. The natural (and some engineered) materials listed have properties that are strongly influenced by the humidity, temperature, and other conditions of the local environment. Composite and anisotropic materials exhibit different properties in different directions, as well. In some cases, missing entries in these tables are due to the large range of values; more precise data are available from manufacturers. Other entries are blank because the values are not meaningful, for example, brittle materials do not have yield strengths.

TABLE C.1
Typical Properties of Engineering Materials (SI)

Material	Density (kg/m³)	Yield Strength (MPa)		Ultimate Strength (MPa)			Moduli (GPa)		Coefficient of Thermal Expansion α (10⁻⁶/°C)	Poisson's Ratio ν
		Tension	Shear	Tension	Compression	Shear	E	G		
Metals										
Steel										
Structural A36 (hot-rolled)	7850	250	145	400	400	–	200	79	12.4	0.27
Stainless AISI 1020 (cold-rolled)	7920	350	–	420	420	–	205	80	11.7	0.29
Stainless (annealed)	7920	260	150	585	585	–	193	77	17.3	0.25
Gray Cast Iron (ASTM A25)	7200	–	–	179	669	–	79	32	12.1	0.2–0.3
Malleable Cast Iron	7300	230	65	345	372	331	172	69	12.1	0.25
Aluminum										
1100-H14	2710	95	76	110	110	–	70	26	21.8	0.35
6061-T6	2710	255	131	290	290	186	70	26	23.6	0.35
7075-T6	2800	500	331	572	572	–	72	27	23.4	0.33
Copper										
Annealed NICLAL 1300	8650	150	–	425	425	–	130	44	16.0	0.34
Yellow-brass, annealed (65% Cu, 35% Zn)	8470	97	220	315	315	–	105	35	20.3	0.33
Red-brass, annealed (85% Cu, 15% Zn)	8740	70	–	270	270	–	115	44	18.7	0.31
Tin bronze (UNS C90700)	8800	150	–	305	305	–	105	38	18.0	0.38
Magnesium alloy AZ31	1770	200	130	260	260	–	45	17	25.2	0.32
Titanium (6% Al, 4% V)	4430	924	–	1000	1000	–	120	44	9.4	0.36
Timber (parallel to grain)										
Douglas fir	470	–	50	108	108	–	13	–	Varies	0.29
Red oak	740	–	–	112	112	–	12	–	Varies	–
Redwood	415	–	–	–	–	–	9	–	Varies	–
Plastics										
Nylon (molding compound)	1140	45	–	75	95	–	2.8	–	144	0.4
Polycarbonate	1200	35	–	65	85	–	2.4	–	122	0.37
Polyester, PBT	1340	55	–	55	75	–	2.4	–	135	–
Polystyrene	1030	55	–	55	90	–	3.1	–	135	0.34–0.35
Vinyl, rigid PVC	1440	45	–	40	70	–	3.1	–	135	0.4
Other										
Rubber	910	–	–	15	–	–	–	–	162	0.44–0.5
Concrete (high strength)	2380	–	43	–	–	–	30	13	6	0.1–0.2
Granite (average)	2770	–	–	20	240	35	70	4	7.2	0.2–0.3
Sandstone (average)	2300	–	–	7	85	14	40	2	9.0	~0.2
Glass (soda-lime)	2500	–	–	–	50	–	72	30	9	0.2–0.27
Kevlar	1450	–	–	717	483	20.3	131	–	–	0.34
Human tendon	–	–	–	50	50	–	1	–	–	–

TABLE C.2
Typical Properties of Engineering Materials (US)

Material	Specific Weight (lbf/in³)	Yield Strength (ksi) Tension	Shear	Ultimate Strength (ksi) Tension	Compression	Shear	Moduli (10⁶ psi) E	G	Coefficient of Thermal Expansion α (10⁻⁶/°F)	Poisson's Ratio ν
Metals										
Steel										
Structural A36 (hot-rolled)	0.283	36	21	59	59	–	29	11.0	6.9	0.27
Stainless AISI 1020 (cold-rolled)	0.285	50.8	–	60.9	60.9	–	29.7	11.6	6.5	0.29
Stainless (annealed)	0.285	37.7	22	84.8	84.8	–	28	11.2	6.5	0.25
Gray Cast Iron (ASTM A25)	0.260	–	–	26	97	–	11.5	4.6	6.7	0.2–0.3
Malleable Cast Iron	0.263	33	9.4	50	54	48	25	10	6.7	0.25
Aluminum										
1100-H14	0.098	14	11	16	16	–	10.1	3.8	12.1	0.35
6061-T6	0.098	37	19	42	42	27	10.1	3.8	13.1	0.35
7075-T6	0.101	73	48	83	83	–	10.4	3.9	13.0	0.33
Copper										
Annealed NICLAL 1300	0.311	21.8	–	61.6	61.6	–	18.9	6.4	9.0	0.34
Yellow-brass, annealed (65% Cu, 35% Zn)	0.305	14.1	31.9	45.7	45.7	–	15.2	5.1	11.3	0.33
Red-brass, annealed (85% Cu, 15% Zn)	0.315	10.0	–	39	39	–	16.7	6.4	10.4	0.31
Tin bronze (UNS C90700)	0.317	22	–	44	44	–	15.2	5.5	10	0.38
Magnesium alloy AZ31	0.064	29	19	38	38	–	6.5	2.5	14	0.32
Titanium (6% Al, 4% V)	0.160	134	–	145	145	–	17.4	6.4	5.2	0.33
Timber (parallel to grain)										
Douglas fir	0.017	–	7.3	15.7	15.7	–	1.9	–	Varies	–
Red oak	0.027	–	–	16.2	16.2	–	1.7	–	Varies	–
Redwood	0.015	–	–	–	–	–	1.3	–	Varies	–
Plastics										
Nylon (molding compound)	0.041	6.5	–	10.9	13.8	–	0.4	–	80	0.4
Polycarbonate	0.043	5.1	–	9.4	12.3	–	0.35	–	68	0.37
Polyester, PBT	0.048	8	–	8	10.9	–	0.35	–	75	–
Polystyrene	0.037	8	–	8	13.1	–	0.45	–	70	0.34–0.35
Vinyl, rigid PVC	0.052	6.5	–	5.8	10.1	–	0.45	–	75	0.4
Other										
Rubber	0.033	–	–	2.2	–	–	–	–	90	0.44–0.5
Concrete (high strength)	0.086	–	6.2	–	–	–	4.3	1.9	5.5	0.1–0.2
Granite (average)	0.100	–	–	2.9	34.8	5.08	10	0.58	4	0.2–0.3
Sandstone (average)	0.083	–	–	1.0	12.3	2.03	6	0.29	5	0.2
Glass (soda-lime)	0.09	–	–	–	7.3	–	10.4	4.3	44	0.2–0.27
Kevlar	0.052	–	–	104	70.1	2.9	19	–	–	0.34
Human tendon	–	–	–	7.2	7.2	–	0.15	–	–	–

The American Society for Testing Materials (ASTM) numbering system for gray cast iron is established such that the numbers correspond to the minimum tensile strength in ksi (sometimes denoted kpsi.) Thus, an ASTM no. 20 cast iron has a minimum tensile strength of 20 ksi.

TABLE C.3

Typical Properties of Common Fluids (SI)

Material	Temperature T ($S°C$)	Density ρ (kg/m^3)	Viscosity μ (N s/m^2)	Surface Tension s (N/m)
Water	0	1000	1.75×10^{-3}	0.0757
	10	1000	1.30×10^{-3}	0.0742
	20	998	1.00×10^{-3}	0.0727
	30	996	7.97×10^{-4}	0.0712
	40	992	6.51×10^{-4}	0.0696
	50	988	5.44×10^{-4}	0.0679
	60	983	4.63×10^{-4}	0.0662
	70	978	4.00×10^{-4}	0.0645
	80	972	3.51×10^{-4}	0.0627
	90	965	3.11×10^{-4}	0.0608
	100	958	2.79×10^{-4}	0.0589
Air	0	1.29	1.72×10^{-5}	
	10	1.25	1.77×10^{-5}	
	20	1.21	1.81×10^{-5}	
	30	1.17	1.86×10^{-5}	
	40	1.13	1.91×10^{-5}	
	50	1.09	1.95×10^{-5}	
	60	1.06	2.00×10^{-5}	
	70	1.03	2.04×10^{-5}	
	80	1.00	2.09×10^{-5}	
	90	0.973	2.13×10^{-5}	
	100	0.947	2.17×10^{-5}	

TABLE C.4

Typical Properties of Common Fluids (US)

Material	Temperature T ($°F$)	Density ρ (slug/ft^3)	Viscosity μ (lbf s/ft^2)	Surface Tension s (lbf/ft)
Water	32	1.94	3.66×10^{-5}	0.00519
	40	1.94	3.19×10^{-5}	0.00514
	50	1.94	2.72×10^{-5}	0.00509
	60	1.94	2.34×10^{-5}	0.00503
	70	1.93	2.04×10^{-5}	0.00498
	80	1.93	1.79×10^{-5}	0.00492
	90	1.93	1.59×10^{-5}	0.00486
	100	1.93	1.42×10^{-5}	0.00480
	212	1.86	5.83×10^{-6}	0.00404
Air	40	0.00247	3.63×10^{-7}	
	50	0.00242	3.69×10^{-7}	
	60	0.00237	3.75×10^{-7}	
	70	0.00233	3.80×10^{-7}	
	80	0.00229	3.86×10^{-7}	
	90	0.00225	3.91×10^{-7}	
	100	0.00221	3.97×10^{-7}	
	200	0.00187	4.48×10^{-7}	

Properties of air are obtained at standard atmospheric pressure.

Appendix D: All the Equations

	Solids	**Fluids**
Kinematics (What is the vector (u, v, w) everything depends on?)	Displacement $\mathbf{u}$	Velocity $\mathbf{V}$, that is, displacement rate
Volume change/volume change rate	$\nabla \cdot \mathbf{u} = \dfrac{\partial u}{\partial x} + \dfrac{\partial v}{\partial y} + \dfrac{\partial w}{\partial z} = u_{i,i}$	$\nabla \cdot \mathbf{V} = \dfrac{\partial u}{\partial x} + \dfrac{\partial v}{\partial y} + \dfrac{\partial w}{\partial z} = V_{i,i}$
Strain/strain rate	$\varepsilon = \varepsilon_{ij} = \dfrac{1}{2}\left(\dfrac{\partial u_i}{\partial x_j} + \dfrac{\partial u_j}{\partial x_i} \right)$	$\varepsilon = \varepsilon_{ij} = \dfrac{1}{2}\left(\dfrac{\partial u_i}{\partial x_j} + \dfrac{\partial u_j}{\partial x_i} \right)$
1D constitutive law Hookean/Newtonian	$\sigma = E\,\varepsilon$ $\tau = G\gamma$	$\tau = \mu\gamma$
3D ideal constitutive law[a]	$\sigma_{ij} = \lambda\varepsilon_{kk}\delta_{ij} + 2G\,\varepsilon_{ij}$ $\lambda = \dfrac{E\nu}{(1+\nu)(1-2\nu)}$	$\sigma_{ij} = -p\delta_{ij} + 2\mu\varepsilon_{ij}$
General constitutive law	$\sigma_{ij} = K_{ijkm}\,\varepsilon_{km}$	$\sigma_{ij} = K_{ijkm}\,\varepsilon_{km}$
Conservation of mass	$\rho = \text{constant}$	$\dfrac{\partial \rho}{\partial t} + (\rho u_i)_{,i} = 0$
Conservation of linear momentum ($\Sigma\mathbf{F} = m\,\mathbf{a}$ for an infinitesimal element)	$\sigma_{ij,j} + B_i = \rho a_i$	$\sigma_{ij,j} + B_i = \rho a_i$
	B_i represents the total body force on the element in question, most often represented by ρg in the vertical direction. a_i is the acceleration, which was zero in most of this book	
Conservation of angular momentum for an infinitesimal element	$\sigma_{ij} = \sigma_{ji}$	$\sigma_{ij} = \sigma_{ji}$

[a] Although it looks different because of the index notation and the fact that it is stress in terms of strain and not vice versa, the expression for solids is the same as the generalized Hooke's law of Section 4.4.

Mechanical Engineering

Integrated Mechanics Knowledge Essential for Any Engineer

Introduction to Engineering Mechanics: A Continuum Approach, Second Edition uses continuum mechanics to showcase the connections between engineering structure and design and between solids and fluids and helps readers learn how to predict the effects of forces, stresses, and strains. The authors' "continuum checklist" provides a framework for a wide variety of problems in solid and fluid mechanics. The essence of continuum mechanics, the internal response of materials to external loading, is often obscured by the complex mathematics of its formulation. By gradually building the formulations from one-dimensional to two- and three-dimensional, the authors help students develop a physical intuition for solid and fluid behavior and for the very interesting behavior of those materials including many biomaterials, between these extremes. This text is an accessible first introduction to the mechanics of all engineering materials and incorporates a wide range of case studies highlighting the relevance of the technical content in societal, historical, ethical, and global contexts. It also offers a useful perspective for engineers concerned with biomedical, civil, chemical, mechanical, or other applications.

New in the Second Edition:

The latest edition contains significantly more examples, problems, and case studies than the first edition.

The 22 chapters in this text:

- Define and present the template for the continuum approach
- Introduce strain and stress in one dimension, develop a constitutive law, and apply these concepts to the simple case of an axially loaded bar
- Extend the concepts to higher dimensions by introducing the Poisson's ratio and strain and stress tensors
- Apply the continuum sense of solid mechanics to problems including torsion, pressure vessels, beams, and columns
- Make connections between solid and fluid mechanics, introducing properties of fluids and strain rate tensor
- Address fluid statics
- Consider applications in fluid mechanics
- Develop the governing equations in both control volume and differential forms
- Emphasize real-world design applications

Introduction to Engineering Mechanics: A Continuum Approach, Second Edition provides a thorough understanding of how materials respond to loading: how solids deform and incur stress and how fluids flow. It introduces the fundamentals of solid and fluid mechanics, illustrates the mathematical connections between these fields, and emphasizes their diverse real-life applications. The authors also provide historical context for the ideas they describe and offer hints for future use.